ASME STANDARDS TECHNOLOGY, LLC

STP-PT-077

DEVELOPMENT OF WELD STRENGTH REDUCTION FACTORS AND WELD JOINT INFLUENCE FACTORS FOR SERVICE IN THE CREEP REGIME AND APPLICATION TO ASME CODES

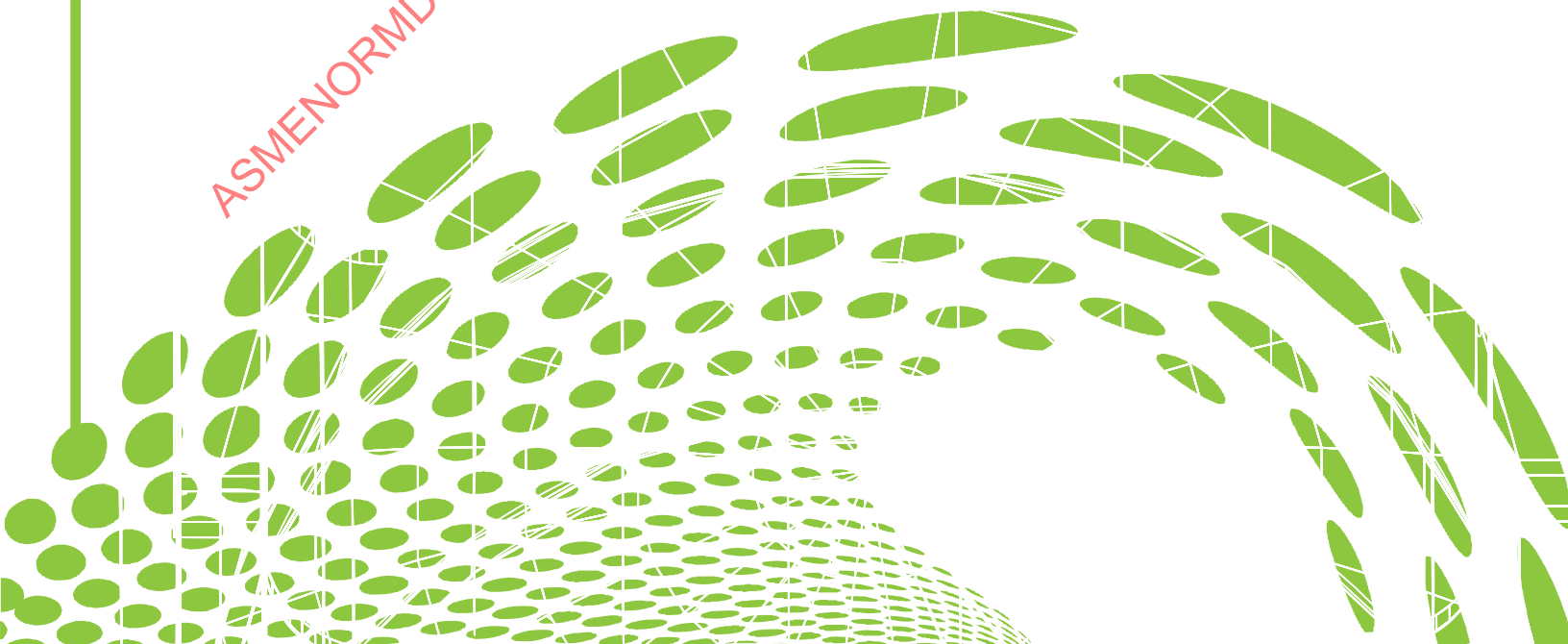

STP-PT-077

DEVELOPMENT OF WELD STRENGTH REDUCTION FACTORS AND WELD JOINT INFLUENCE FACTORS FOR SERVICE IN THE CREEP REGIME AND APPLICATION TO ASME CODES

Prepared by:

J. Shingledecker, Electric Power Research Instiitute
B. Dogan, Electric Power Research Instiitute
J. Foulds, Clarus Consulting, LLC
R. Swindeman, Cromtech, Inc.
D. Marriott, Stress Engineering Services
P. Carter, Stress Engineering Services

ASME STANDARDS TECHNOLOGY, LLC

Date of Issuance: June 26, 2017

This publication was prepared by ASME Standards Technology, LLC ("ASME ST-LLC") and sponsored by The American Society of Mechanical Engineers ("ASME") and the Electric Power Research Institute ("EPRI").

ASME Standards Technology, LLC
Two Park Avenue, New York, NY 10016-5990

ISBN No. 978-0-7918-7126-3

TABLE OF CONTENTS

Foreword ix
PART 1: Development and Application of Weld Strength Reduction Factors Guideline 1
1 APPLICATION GUIDELINE 2
1.1 Overview 2
1.2 Application Guideline 4
1.2.1 Step 1: Develop Database 5
1.2.2 Step 2: Analyze Data 6
1.2.3 Step 3: Base Material Strength Factor 7
1.2.4 Step 4: Application to Welded Structure 8
1.2.5 Step 5: Design Strength Ratio 9
1.3 New Materials 10
1.3.1 Comments on Specimen Size 10
1.3.2 Data Requirements 11
2 APPLICATION TO CHROMIUM-MOLYBDENUM LONGITUDINAL SEAM WELDS 13
2.1 Step 1: Grade 22 Database & Step 2 Pre-Analysis 13
2.1.1 Base Metal 13
2.1.2 Weld Metal 13
2.1.3 Cross-Weld Data 13
2.2 Step 2: Grade 22 Data Analysis 16
2.2.1 Base Metal Data Analysis 16
2.2.2 Weld Metal Data Analysis 16
2.2.3 Cross-Weld Specimen Data Analysis 18
2.2.4 Summary 20
2.3 Step 3: Extracting the Base Metal Strength Factor from Cross-Weld Tests 21
2.4 Step 4: Testing Assumptions 25
2.5 Step 5: Application to Seam Weld Structure 25
2.6 Step 6: Summary and Implications for WSRFs 30
3 APPLICATION TO SUBCRITICALLY HEAT-TREATED GRADE 91 SEAM WELDS 32
3.1 Step 1: (Database) & Step 2 Pre-Analysis (Analyze Data) 32
3.2 Step 2: (Analyze Data) Development of Trend Curves 38
3.3 Step 3: Extracting the Base Material Strength Factor 44
3.4 Step 4: Testing Assumptions Against Non-Standard Specimens 47
3.4.1 Masuyama Specimens 47
3.4.2 EPRI Large Specimens 50
3.5 Step 5: Application to Welded Structures 52
3.6 Step 6: (Design Strength Ratio) Summary & Implications for WSRFs 57
4 OVERALL PROJECT SUMMARY AND FINDINGS 59
References – Part 1 62
PART 2: Literature Review, Industry Approach, and Data Compilation in Support of WSRF Development 63
1 INTRODUCTION 64
2 CREEP FAILURES IN SEAM-WELDED COMPONENTS 65
2.1 CrMo Power Plant Seam-Welded Piping Experience 65
2.1.1 Failures and Major Cracking 65

2.1.2 Cracking and Damage from Inspections 69
2.2 Creep Strength Enhanced Ferritic Steels Long-Seam Experience 69
2.3 Process Plant Long-Seam Experience 71
2.3.1 Refinery Catalytic Reformer Piping Failure 71
2.3.2 Comment 72
2.4 Implications to WSRF 72
2.4.1 Damage and Failure Rate 73
2.4.2 Perspective on CrMo Failure Experience 75
3 CURRENT DESIGN PRACTICES FOR WELD STRENGTH REDUCTION FACTORS 77
3.1 ASME Approach: Section III N-H 77
3.1.1 Section III N-H 77
3.2 ASME Approach: Section I and B31 78
3.2.1 Background on Universal 'Presumptive' Factor 78
3.2.2 Development of WSRFs for Section I, B31.1, and B31.3 79
3.3 European Practices 82
3.3.1 Practices of Determination and Use of WSRF in European Countries 82
3.3.2 The ECCC Approach on Determination of WSRF 85
3.3.3 WSRF in European Codes 86
4 DATABASE OF WELD AND WELDMENT CREEP-RUPTURE PROPERTIES 90
4.1 Carbon Steel 90
4.1.1 Summary of Data 90
4.1.2 Qualitative Observations 91
4.1.3 Analysis of Data 91
4.1.4 Weld Metal Behavior 94
4.1.5 Summary 95
4.2 Chromium-Molybdenum Steels (Gr. 11 & 22) 96
4.2.1 Database 96
4.2.2 Summary of Observations 97
4.3 308 Stainless Steel Weld Metal and 304/308 Stainless Steel Weldment Stress-Rupture Data 97
4.3.1 Review of Studies 97
4.3.2 Summary of the Database on the Stress-Rupture of 304H/308 Stainless Steel Filler Metals and Weldments 102
4.4 316H & 16-8-2 Weld Metal 112
4.4.1 Review of Research on the Stress-Rupture of 316 and 16-8-2 Stainless Steel Filler Metals and Weldments 112
4.4.2 Review of the Database on the Stress-Rupture of 316 and 16-8-2 Stainless Steel Filler Metals and Weldments 114
4.4.3 A Brief Review of the Determination of Stress Rupture Factors for 316 and 16-8-2 116
4.5 Alloy 800/800H 116
4.5.1 Identification of Alloy 800/800H Filler Metals and Weldment Stress-Rupture Data 116
4.5.2 Review of Research on the Stress-Rupture of Filler Metals and Weldments 118
4.5.3 Assembly of the Stress-Rupture Database 120
4.6 Review of 9Cr-1Mo-V (Grade 91) Steel Weld Metal and Weldments Creep-Rupture Data and Weld Strength Reduction Factors 121
4.6.1 Background and Data Sources 121
4.6.2 Characteristics of the Gr. 91 Weld and Weldment Database 122
4.6.3 Review of Reports and Papers on WSRFs for Grade 91 124
5 SUMMARY 127

References – Part 2 228
PART 3: Development of Weld Joint Influence Factors 239
Summary 240
1 INTRODUCTION 241
2 DESCRIPTION OF WORKSCOPE 243
2.1 Weldment Model Development 243
2.2 Computation of Weld Joint Influence Factors 243
2.3 Assessment of Test Specimen Geometry 244
3 DETAILS OF WORK PERFORMED 245
3.1 Weldment Model Development 245
3.1.1 Subtask 2-1: Review the Prior History on Weldment Modeling 245
3.1.2 Subtask 2-2: Selection of Suitable Material Constitutive and Failure Models 245
3.1.3 Subtask 2-3: Synthesis of Weld Sub-Region Properties 247
3.1.4 Subtask 2-4: Methodology for the Analysis of Weldment Deformation and Failure 248
3.1.5 Methodology Development in Summary 251
3.2 Computation of Weld Joint Influence Factors 251
3.3 Cross-Weld Tests 253
4 RESULTS 255
4.1 Concepts 255
4.2 Numerical Predictions 256
4.2.1 WJIF Calculations 256
5 CONCLUSIONS 259
References – Part 3 364

LIST OF FIGURES

Figure 1: Summary of the Ratio of Stress to Cause Rupture to the Calculated Minimum Stress from ASME Section III-NH (formerly N-47) Rules as a Function of Rupture Time for Structural Feature Tests on 316, 304, and 2 1/4Cr-1Mo Showing All Ratios, Regardless Of Material and Rupture Time, Are Greater Than 1, i.e. the Calculated Stresses Are Conservative [2] .3
Figure 2: Box Chart Describing the Application of the Data and Methods in This Project for Developing the Information Needed by ASME Code Sections for Determining Weld Strength Reduction Factors 5
Figure 3: Information Required for Development of a Database 5
Figure 4: Details of Pre-Analysis in Step 2 with Highlighted Data Used for the First Analysis 7
Figure 5: Detail of Process to Determine the Inherent Material Strength Factor From Cross-Weld Tests 8
Figure 6: Minimum Proposed Data Requirements for Weld Metal and Weldment Test Data to Facilitate Analysis for This Project 12
Figure 7: Grade 22 Base Metal Stress Rupture Data from EPRI TR-110807 [10] 14
Figure 8: Grade 22 Weld Metal Stress Rupture Data from EPRI TR-110807 [10] 15
Figure 9: Grade 22 Cross-Weld (X-W) Specimen Stress Rupture Data from EPRI TR-110807 [10].15
Figure 10: Grade 22 Base Metal (BM) Specimen Stress Rupture Data at ≤ 20 ksi from EPRI TR-110807 [10] and the Corresponding Spera Function Curve-Fit 17
Figure 11: Grade 22 Weld Metal (WM) Specimen Stress Rupture Data at ≤ 20 ksi from EPRI TR-110807 [10] and the Corresponding Spera Function Curve-Fit 18

Figure 12: Grade 22 Cross-Weld (X-W) Data and Best-Fit Spera Curve for Specimens Exhibiting Failure in WM, FL, WM/FL and the HAZ 19
Figure 13: Grade 22 Cross-Weld (X-W) Data and Best-Fit Spera Curve for Specimens Exhibiting Failure in WM, FL, WM/FL and the HAZ and Tested at ≤ 20 ksi 20
Figure 14: Grade 22 BM, WM and Cross-Weld (X-W) Best-Fit Behavior as Derived from the EPRI Database 21
Figure 15: Maximum Principal Stress Distribution for 2:1 Weak Zone : Specimen Diameter Ratio (Assumed Cross-Weld Sample Geometry) 23
Figure 16: Maximum Principal Stress Distribution for 1:1 Weak Zone : Specimen Diameter Ratio ..23
Figure 17: Results of Matching Cross-weld and Base Metal Rupture Data 24
Figure 18: Predicted Sample Size Effect Showing Strengthening and Weakening Behavior 24
Figure 19: Comparison of Factored Base Metal, Cross-weld and Weld Metal Strength Trend Lines 25
Figure 20: Seamweld model: Pipe OD = 762 mm, ID = 457 mm, weld semi-angle = 50 26
Figure 21: Distribution of Plastic Strain Prior to Collapse 27
Figure 22: Distribution of MPS Prior to Collapse 27
Figure 23: Development of Max. Weld MPS to OD with Inelastic Strain and Time 28
Figure 24: Calculation of Joint WSRF: Single Sided "U" Weld 28
Figure 25: "X-Groove" Weld Geometry in 20" OD x 0.76" Thick Pipe 29
Figure 26: Distribution of Maximum Principal Stress Due to Inelastic Strain in Weld Metal 29
Figure 27: Calculation of Joint WSRF: "X-Groove" Configuration 29
Figure 28: Summary Plot of CrMo Steel Weldment Reduction Factors 31
Figure 29: Failure Locations as a Function of Test Stress and Temperature for Grade 91 Weld/Weldment Creep-Rupture Database 33
Figure 30: Failure Locations as a Function of Rupture Life and Temperature for Grade 91 Weld/Weldment Creep-Rupture Database 34
Figure 31: Suggested Regions Where Type IV/HAZ Failures Occur for Grade 91 Weldments 34
Figure 32: Larson-Miller Parameter (C=28.944) Comparison of Grade 91 Base Metal Average and Minimum Curves to Cross-Welds with Base Metal Cross-Weld Failures Identified 35
Figure 33: Larson-Miller Parameter (C=28.944) Comparison of Grade 91 Base Metal Average and Minimum Curves to Cross-Welds with Weld Metal Failures and All Weld Metal Test Data Identified 36
Figure 34: Larson-Miller Parameter (C=28.944) Comparison of Grade 91 Base Metal Average and Minimum Curves to Cross-Welds with Fusion Line Failures Identified 37
Figure 35: Larson-Miller Parameter (C=28.944) Comparison of Grade 91 Base Metal Average and Minimum Curves to Cross-Welds with Type IV/HAZ Failures Identified 38
Figure 36: LMP Plot for Grade 91 Base Metal Average and Minimum Curves with the Weld Metal Fit Curve Plotted 39
Figure 37: Comparison of Expected and Measured Rupture Life for Fit of HAZ/Type IV Failures ..40
Figure 38: LMP Plot (Optimized C=24.859) of the HAZ/Type IV Data Curve-Fit Result 40
Figure 39: Regression Constants for Equation (1) Time-Temperature Analysis for Grade 91 Developed by Evaluation of the Database 41
Figure 40: Comparison of Predictions in Figure 39 Plotted with Data at 550°C 42
Figure 41: Comparison of Predictions in Figure 39 Plotted with Data at 593°C 42
Figure 42: Comparison of Predictions in Figure 39 Plotted with Data at 600°C 43
Figure 43: Comparison of Predictions in Figure 39 Plotted with Data at 649/650°C 44
Figure 44: Stress (MPa) for 100,000 Hour Predicted Average Rupture Life for Grade 91 Base Metal and HAZ-Type IV Failures 44
Figure 45: Distribution of Maximum Principal Stress (MPS) in the Weak HAZ of the 0.25"Diameter Cross-weld Tensile Specimen for 66 MPa Tension 45
Figure 46: Comparison of Average HAZ and Other Trendlines with Predicted Cross-weld Behavior (550°C) Using a Base Metal Strength Factor =0.95 46

Figure 47: Comparison of Average HAZ and Other Trendlines with Predicted Cross-weld Behavior (600°c) Using a Base Metal Strength Factor =0.85. 46
Figure 48: Comparison Of Average HAZ And Other Trendlines With Predicted Cross-weld Behavior (650°C) Using A Base Metal Strength Factor =0.82 47
Figure 49: Large U and X-Groove Specimens Evaluated by Masuyama [17]....48
Figure 50: Test Results for Large Cross-Weld Specimens Tested at 650°C-66MPa [17]....49
Figure 51: Limit Analysis of Masuyama 32 mm x 40 mm Tensile Specimen Showing the Predicted Weak Zone MPS Failure Location on the Center (Symmetry) Plane 49
Figure 52: Calculated Changes in Stress for the Two Cross-weld Specimens Considered 50
Figure 53: Table of Comparison of Time to Rupture and Estimated Time to Rupture for Grade 91 Large Specimen Cross-Weld Tests 50
Figure 54: Sketch of Cross-Weld Specimen Configuration for EPRI Tests [18] 51
Figure 55: Limit Analysis Maximum Principal Stress Plots on Symmetry Planes of EPRI 37.5^0 and 10^0 Samples 51
Figure 56: Comparison of Time to Rupture and Estimated Time to Rupture for EPRI Grade 91 Cross-Weld Tests [18]....51
Figure 57: Predictions of Grade 91 Cross-weld Tests Show Strengthening Effect of Constraint for a Wide Range of Stress for Both Sets of Non-Standard Samples Analyzed 52
Figure 58: Seamweld HAZ Model Pipe OD = 762 mm, ID = 427 mm, Weak HAZ Width = 2 mm, Weld Semi-Angle = 10^0 53
Figure 59: Distribution of Inelastic Strain Prior to Collapse. High Strain is Localized in Bore....54
Figure 60: Distribution of MPS Prior to Collapse 54
Figure 61: Development of HAZ Stress Near OD with Creep Strain and Time....55
Figure 62: Calculation of Joint WSRF: Single Sided "U" Weld 55
Figure 63: "X-groove" Weld Geometry in 20" OD x 0.76" Thick Pipe....55
Figure 64: Position of Maximum HAZ Maximum Principal Stress 56
Figure 65: Calculation of Joint WSRF: "X-Groove" Configuration 57
Figure 66: Comparison of Reduction Factors Calculated From This Work (Ratio Between Standard Specimen Type IV-HAZ and BM Curves, BMSF, and WSRFs Calculated for Two Pipe Geometries) Compared to ASME Section I/B31.1 Seam-Weld WSRFs, and Japanese (Yoshida et al.) Analysis....58
Figure 67: Table of EPRI Database of Select Incidents of Major Cracking and Failure of Long Seam-Welded Piping....68
Figure 68: Table of Estimates of Strength Reduction Factors Reflected in the Best-Fit Average Larson-Miller Behavior of Laboratory Cross-Weld Data of Yoshida et al. [15] Compared with Approximate Average Behavior of Base Metal* 71
Figure 69: Table of Exposure Parameters Estimated for Long Seam-Welded Piping in Fossil Power Plants....74
Figure 70: Table of Estimation of Failure Rates....74
Figure 71: Table of Points of Interest on the Grade 22 Statistical Rupture Strength Distribution of Ref. [24]....75
Figure 72: Table of Stress Level, σ, in the Distribution of Grade 22 Rupture Strength, Corresponding to the Estimated Failure Rates of Figure 70....76
Figure 73: Basis for Universal 'Presumptive' Weld Factor from [37] 79
Figure 74: Weld Strength Reduction Factors and Applicable Notes for ASME Section I PG-26 [38]81
Figure 75: Table of Weld Strength Reduction Factors for 316L(N) SS as Recommended by RCC-MR Code 87
Figure 76: Table of Weld Joint Coefficient and Corresponding Testing Group....88
Figure 77: Summary Table of Published Data Analyzed....90

Figure 78: As-Reported C-Steel Weldment and Base Metal Rupture Data [40], [41], [42], [43], [44] on a Larson-Miller Parameter (LMP) Plot Along with the ASTM DS 11S1 Plate [39] and the Curve-Fits to That Data....92
Figure 79: Reproduction of Figure 78 Without the ASTM Data....93
Figure 80: Base Metal and Cross-Weld Test Data Linear Fits Compared for Ex-Service Material Rupture Tests from Ray et al. [43] and Wilson WRC 32 [44]....94
Figure 81: All Weld Metal Data from B&W [45] and the Ex-Service Weld Metal Data of Ellis et al. [40] in Comparison with the ASTM DS 11S1 Plate Data and Curve-Fits on a Larson-Miller Parametric Plot, SR: Stress-Relieved....95
Figure 82: Summary Table of Grade 11 Weld and Weldment Data from Ref [46]....96
Figure 83: Summary Table of Grade 22 Weld and Weldment Data from Ref [46]....96
Figure 84: Summary Table of 304H/308 Filler Metal & Weldment Creep-Rupture Data Sources...103
Figure 85: Summary Table of 304H/308 Filler Metal & Weldment Creep-Rupture Data....105
Figure 86: Summary Table of 16-8-2 Filler Metal Data....114
Figure 87: Summary Table of 316 Filler Metal Data....116
Figure 88: Comparison Table of Chemistries for Coated Filler Metal Electrodes Used to Join the Three Grades of Alloy 800....117
Figure 89: Comparison Table of Chemistries for Bare Filler Metal Electrodes Used to Join Three Grades of Alloy 800....118
Figure 90: Summary Table of 800H Weld and Weldment Data....120
Figure 91: The Distribution of the ORNL Rupture Data for Filler Metal (a), Weld Process (b), Test Temperature (c) and PWHT Temperature (d)....123
Figure 92: Project Outline....241
Figure 93: Temperature Shift for Equivalent Material Properties....248
Figure 94: Table of Temperatures Used to Shift Creep Properties in Gr. 22 Material Zones for the Baseline Case to Demonstrate the Methodology and Sensitivity of Various Parameters to WJIF's....256
Figure 95: Summary of WJIF Solutions (Solid Lines) Compared to Relative Strengths of the Weak Zones (Dashed Lines)....257

FOREWORD

This publication was prepared by ASME ST-LLC and sponsored by ASME and EPRI. The project was conducted by EPRI under a cost-sharing agreement with ASME ST-LLC.

Longitudinal seam-welded, high-temperature piping, given its susceptibility to premature failure with sometimes catastrophic consequences, continues to be of concern. In an effort to provide additional safeguards at the construction phase, the ASME Board on Pressure Technology Codes and Standards (BPTCS) formed a project team to address the concern. To develop a consistent set of Code requirements on long seam-welded piping construction, the project team identified specific needs relating to laboratory data, field experience data, and methods for structural evaluation that could be used in developing the safeguards for use in the Boiler and Pressure Vessel Code and the B31 Power Piping Codes. These needs have been defined as (a) weld strength reduction factors that can be considered inherent to the materials and methods of construction; (b) weld joint influence factors that capture specifics of the structure; and (c) guidance for application of the weld strength reduction factor and the weld joint influence factor in design rules. Consistent with these needs as identified in ASME ST-LLC's request for proposal, this document is presented in three separate parts (reports) as follows.

Part 1: Development and Application of Weld Strength Reduction Factors Guideline (Task 1b/3 project report)
This report ties the elements of Parts 2 and 3 into an application guideline. The guideline includes description of a framework for analyzing laboratory data and using the weld joint influence factor development methods. The Part 1 report provides examples of application to two weld/weldment databases for longitudinal seam welds, illustrating the usefulness of the methodology. The examples are for Grade 91 steel that is susceptible to weld heat-affected zone failure, and Grade 22 steel that has and continues to be used in long seam-welded piping construction. The results are compared with current Code rules, literature findings, and experience.

Part 2: Literature Review, Industry Approach, and Data Compilation in Support of WSRF Development (Task 1a project report)
This report includes a compilation of laboratory and experience data on weldments for select materials of common use and interest – carbon steel, low alloy CrMo steels, austenitic stainless steels, Alloy 800/800H, and Grade 91. A critical part of this extensive database development was collecting relevant information not available to the ASME Code committees when allowable stresses were set for some of these materials. Also given in this report is a summary of approaches that have been taken in establishing weld strength reduction factors worldwide.

Part 3: Development of Weld Joint Influence Factors (Task 2 project report)
The report describes an analysis tool to evaluate the creep rupture strength of a weldment relative to that of base metal, benchmarked against select cases of field experience and laboratory component testing. The methodology can be used for calculating weld joint influence factors for any practical combination of materials and weldment geometries in a relatively quick and computationally efficient manner, also allowing for use of relatively simple materials models readily available to designers.

This publication references the original project task reports that have been reproduced here in the three parts as identified above: Part 1-Tasks 1b and 3; Part 2-Task 1a; Part 3-Task 2.

(EPRI is acknowledged for supporting this publication. EPRI conducts research and development relating to the generation, delivery and use of electricity for the benefit of the public. An independent, non-profit organization, EPRI brings together its scientists and engineers as well as experts from academia and industry to help address challenges in electricity, including reliability, efficiency, affordability, health,

safety and the environment. EPRI's members represent approximately 90 percent of the electricity generated and delivered in the United States, and international participation extends to more than 30 countries.

Established in 1880, the ASME is a professional not-for-profit organization with more than 135,000 members and volunteers promoting the art, science and practice of mechanical and multidisciplinary engineering and allied sciences. ASME develops codes and standards that enhance public safety, and provides lifelong learning and technical exchange opportunities benefiting the engineering and technology community. Visit (https://www.asme.org/) for more information.

ASME ST-LLC is a not-for-profit Limited Liability Company, with ASME as the sole member, formed in 2004 to carry out work related to new and developing technology. The ASME ST-LLC mission includes meeting the needs of industry and government by providing new standards-related products and services, which advance the application of emerging and newly commercialized science and technology, and providing the research and technology development needed to establish and maintain the technical relevance of codes and standards. Visit (http://asmestllc.org/) for more information.

PART 1: DEVELOPMENT AND APPLICATION OF WELD STRENGTH REDUCTION FACTORS GUIDELINE

1 APPLICATION GUIDELINE

1.1 Overview

The purpose of the ASME-EPRI research project is to develop the methodology and data to help establish weld strength reduction factors (WSRF) for service in the creep regime for a wide range of materials with applicability to various sections of ASME Boiler & Pressure Vessel Codes. A review of how various codes address creep behavior of welded structures and pressure vessels in the Task 1a literature review [1] showed that no clear consensus exists between or even within various sections of codes around the world. The range of approaches include: no rules, requirements to follow 'good engineering practice,' simple factors on design irrespective of material, and factors on design which may depend on material, class/group of material, time, or combination of material and weld metal (based primarily on assessments of weld metal only data). ASME Section III-NH contains the most extensive set of rules for welded components based on design life, material and weld metal combination, and temperature. The origins of the strength factors applied in Section III-NH are primarily based, for stainless and nickel-based alloys, on the ratio of weld metal strength to base metal strength, the source for the chromium-molybdenum steels is not known, and the grade 91 values are biased on some cross-weld data with more recent data showing the assessment to be non-conservative at higher-temperatures and/or longer-times [1]. The applicability of these rules has been assessed for a few of the material-weld metal combinations by Corum [2] for a large body of structural 'feature' tests, and the results are provided in Figure 1. The figure shows that in all cases, the application of the Section III-NH rules to welds produced conservative lifetimes relative to measured life in the test, suggesting a material/material class grouping approach is appropriate for design purposes.

Figure 1: Summary of the Ratio of Stress to Cause Rupture to the Calculated Minimum Stress from ASME Section III-NH (formerly N-47) Rules as a Function of Rupture Time for Structural Feature Tests on 316, 304, and 2 1/4Cr-1Mo Showing All Ratios, Regardless Of Material and Rupture Time, Are Greater Than 1, i.e. the Calculated Stresses Are Conservative [2]

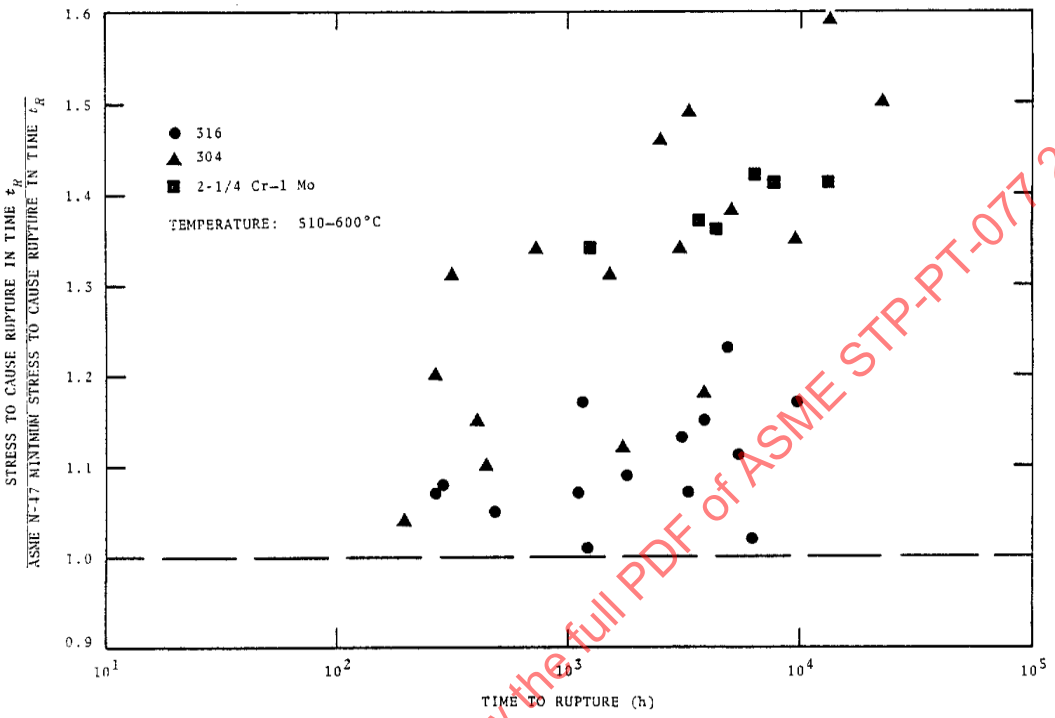

Most weld strength reduction factors (WSRFs) have been based on a relatively simple comparison of laboratory-measured material properties, but the application of these factors are to components or designs. How the weld affects the performance of the structure is critical to the success of any approach for developing and applying WSRFs. It should be also understood that the cross-weld creep-rupture test that has been employed for much of the recent laboratory testing around the world can be viewed as not only a material property test but a structural test as well. Therefore, specimen configuration can have an important impact on the test results. If cross-weld data are to be analyzed, the structural analysis used to evaluate the cross-weld data should ideally be the same as that to develop the WSRFs. Based on this discussion, it is clear that a modeling methodology/tool was necessary for this project.

In Task 2, a brief review of modeling method for creep of welded structures was provided [3]. Detailed finite element analysis (FEA) methods are routinely used for high-temperature creep assessment of structures. When applied to welded structures, the amount of input data is very high, often requiring material constitutive models for the various zones of the weldment such as: base metal, weld metal, coarse-grained heat-affected zones (HAZ), etc. Obtaining such data requires testing of materials heat-treated to simulate the zone processes or by specialized techniques. Therefore, very limited data exist for limited materials and test conditions. Considering the variability in material creep properties and welding processes, the suitability of broadly applying such data, which are not necessarily produced to recognized standards, is questionable. For cases involving life assessments of specific components, detailed FEA modeling with constitutive equations has been successfully employed. For design purposes, however, this type of FEA modeling is not easy to implement within current design codes, especially those based on design by rule approaches.

Realizing the application limitation of a detailed FEA approach, Task 2 investigated simplified methods of FEA analysis, including a decoupling of the stress and creep damage analysis. The decoupled approach identifies 'local damage initiation' as failure of the structure. This has good technical basis within other design codes and was shown in the Task 2 work (and by other researchers) that the conservatism inherent in the decoupled approach was generally less than a factor of 2 in failure time either by measured laboratory results or detailed FEA modeling. Thus for stress-based design, the approach has good technical merit and is not overly conservative. The principle advantages of the Task 2 method/tool are: shortened computational time for quick investigation of a nearly infinite number of variables in the geometry of welded structures, the ability to use rupture data when no creep-strain rate data are available, and the potential to extract material data from simple cross-weld tests.

The global issue of the safe design of welded structures operating in the creep regime for a large number of material, weld metal, and heat-treatment combinations with a nearly infinite number of geometric and loading conditions is a complex problem. The databases collected on this project and available within the literature rarely contain the level of detail necessary to construct detailed constitutive models for a wide array of materials, welds, welding processes, and heat-treatments. However, the databases do often contain a good cross-section of welding processes, testing conditions, and specimen configurations. Based on the problem statement, it is believed that the data assembled in Task 1a and the methodology/tool from Task 2 can be utilized to provide a good technical basis for developing weld strength reduction factors for use within ASME B&PV code. The concept of drawing on large databases of materials, conducting global analysis, and factoring in experience is, in fact, the basis for many of the rules and stress-allowables in the ASME B&PV code today. In this spirit, the following section is an application guide to utilizing the data and methodologies in the project. In the following chapters, this guide is put to use for two examples that show varying levels of input data and analysis.

1.2 Application Guideline

To provide the information necessary for Code sections to develop weld strength reduction factors, a five step process is proposed as follows:

1. Develop Database
2. Analyze Data
3. Base Material Strength Factor(s) (a measure of inherent strength change due to weld, exclusive of structurally-influenced constraint)
4. Application to Welded Structures
5. Design Strength Ratios

These steps, their inputs and logic, and the options within each for testing and refinement are provided schematically in Figure 2. The following sections provide the salient features and actions within each step.

Figure 2: Box Chart Describing the Application of the Data and Methods in This Project for Developing the Information Needed by ASME Code Sections for Determining Weld Strength Reduction Factors

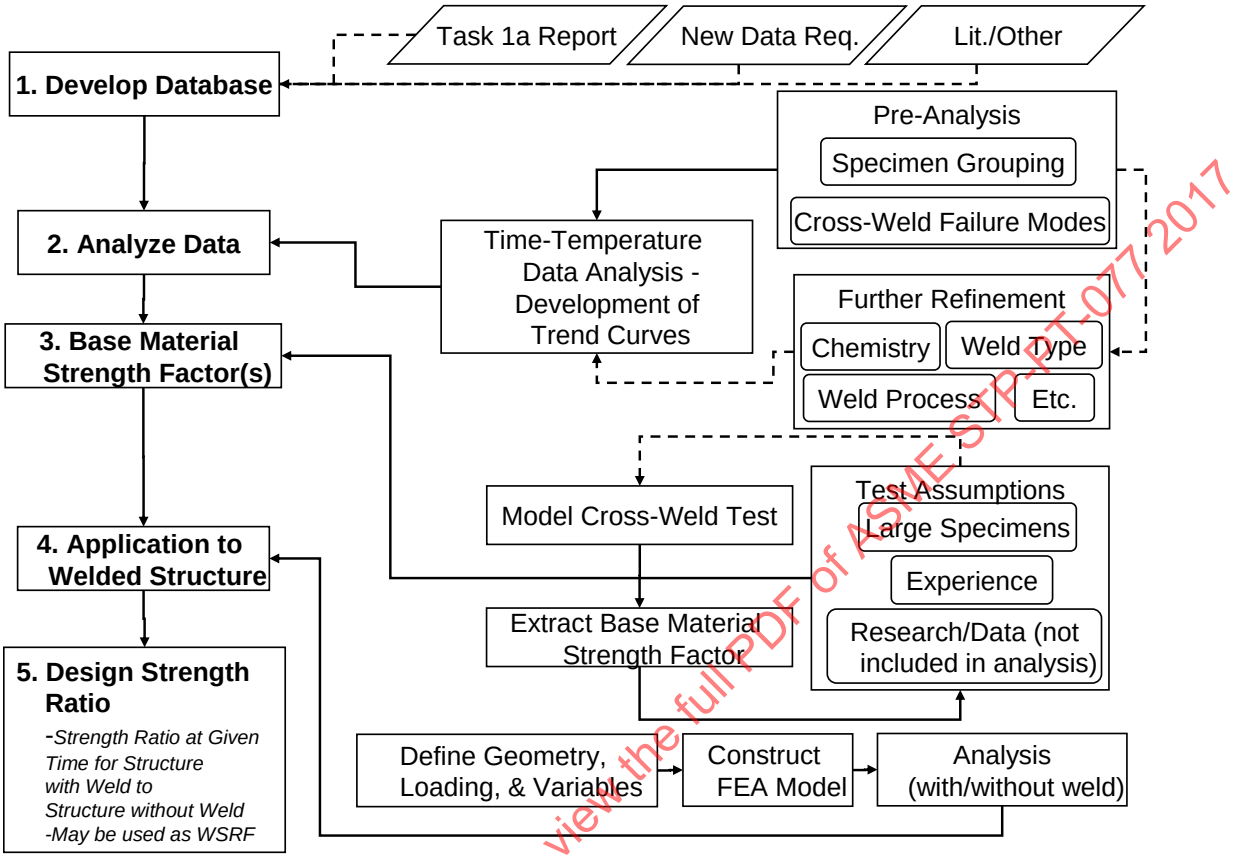

1.2.1 Step 1: Develop Database

A number of databases are available in the Appendix of the Task 1a report. Censoring of the data is not a necessary part of the database development because the data analysis step (Step 2) should remove any data not appropriate for analysis. However, from the development of the Task 1a databases and through the analyses provided in the following chapters, a number of features that are necessary in a database have become apparent. The type of data and requirements are provided in Figure 3 at three levels. The 'Minimum Required' represents the information needed to conduct a coarse global analysis which may lead to over conservatism for welds in the creep regime, the '+' column are the additional data which should allow the analyst reasonable refinement of the dataset to improve accuracy and reduce conservatism in the analysis, and the '++' column are the data in addition to the + column which offers the greatest opportunity for the analyst to refine the data and analysis. It should be noted that the data provided in the ++ column include variables that if found significant are not necessarily addressed in typical qualification of welds in ASME Section IX.

Figure 3: Information Required for Development of a Database

Data Type	Minimum Required (allows for coarse global analysis, may lead to over conservatism)	+ Minimum Desired (allows for reasonable refinement of dataset, can improve accuracy and reduce conservatism)	+ + Ideal (allows for extensive analysis of variables that may or may not be beyond the current ASME Section IX requirements)

Material /weld information	Base metal and weld metal identification, weld process (SAW, SA, GTAW, etc.), heat-treatment	Weld/joint angle/geometry	BM & WM chemistry, welding process detail (heat-flux, etc.)
Specimen Information	Specimen type (BM, WM, Cross-weld)	Specimen size (diameter, cross-section, gauge length)	Specimen orientation/location from joint (orientation to fusion line, location in weld – root, etc.)
Test Conditions	Temperature, stress	Applicable testing standards	
Test Results	Rupture time, failure location (e.g., WM, BM, HAZ)	Elongation, reduction of area, creep strain data (WM & BM tests), minimum creep-rate	Failure location/mode as refined from metallurgical analysis (microstructural cross-sectioning for e.g., fine-grain HAZ, etc.)

1.2.2 Step 2: Analyze Data

The goal of Step 2 (Analyze Data) is to produce trend curves that describe the creep strength (rupture life) of the available data. If possible, data that describes the creep strain-rate behavior can be analyzed to potentially improve the analysis. The use of time-temperature parameters to represent the data, construct trend curves, and extrapolate creep data to longer times is not the subject of this report per se, but a separate ASME S&T, LLC project is currently being undertaken to produce an Excel™-based tool to perform a time-temperature parameter analysis which has been used within ASME Section II for a number of years to develop stress allowables. At the time of this work, the tool was not available, so the analysis performed in the examples in the following chapters utilized optimized Larson-Miller parameters with different stress functions.

To separate the data for analysis, a pre-analysis grouping is first conducted. This is identified in Figure 2 and expanded in Figure 4. Specimens are culled into three main groups: base metal, weld metal, and cross-weld. The cross-weld data are further segmented into standard specimen sizes and non-standard sizes. Unless a large database exists for the non-standard sizes, these data are not included in the initial analysis but are used for Step 3. For the standard size cross-weld specimens (typically 0.2 to 0.5" diameter standard size specimens with a weld in the center of the gauge or the weld fusion line in the center of the gauge), the data are further segmented by failure location. If failure location is not provided for cross-weld tests, the cross-weld data cannot be used in the analysis, leaving a large uncertainty in any assessment that is performed. After this first pre-analysis, and based on the available data in each 'bin' (highlighted in Figure 2), trend curves should be developed for each set of data.

The analyst can then assess the accuracy and goodness of the fits as well as comparisons between the developed trend curves. Depending on the size of the database and the level of information available (+ columns in Figure 3), further refinement can be attempted. Restricting or sorting the data may include:

- Time or stress censoring of datasets where short-time high-stress data that are not representative of low-stress long-time data are effecting the goodness of fit
- Sorting by weld type Figure 3 weld process
- Sorting by base metal or weld metal chemistry
- Segmenting or sorting data within standard cross-weld specimen sizes for fusion line angle to minimize range of geometric variables with the standard specimen sizes
- Segmenting or refining cross-weld data by failure mode. In the best case, the failure location may include failure mode data such as fine-grained versus coarse-grained heat affected zone (HAZ)

from metallurgical evaluations, failure characteristics (necking, shear, etc.), and/or reduction of area measurements which give clues to the failure mode.

If possible, refined trend curves can be compared to the trend curves developed after the pre-analysis to determine the best representations of the data for Step 3. The critical trend curves for use in Step 3 should be the best representations for failure locations/modes in standard cross-weld data.

Figure 4: Details of Pre-Analysis in Step 2 with Highlighted Data Used for the First Analysis

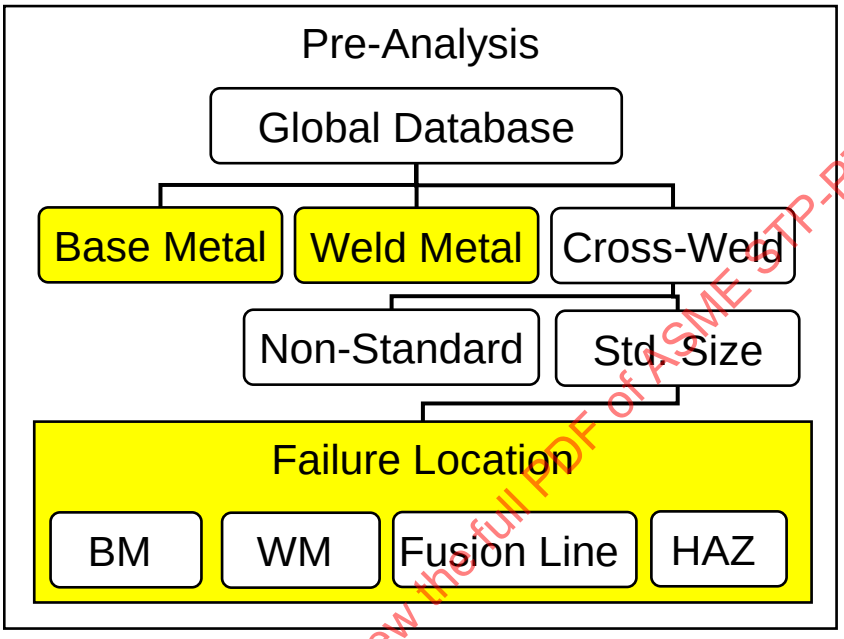

1.2.3 Step 3: Base Material Strength Factor

The Base Material Strength Factor represents a measure of the inherent strength change due to the weld, exclusive of any structurally-influenced constraint. The time-temperature strength relationships for base metal, weld metal, and cross-weld failure locations/modes (possibly a function of additional variables) have been used to set WSRFs by comparing the relative strengths of these trend curves. However, as discussed in the overview, this does not take into account how a weld performs in a structure. Based on the Task 2 work, the ability to back-out a 'base material strength factor' is proposed in this work. The concept is based on the assumption that a standard specimen cross-weld test has a structural component. From Step 2, the behavior of the base metal and standard cross-weld is known, so a simple FEA model of the standard weldment can be constructed with basic knowledge of failure location/mode. By a trial and error approach, the relative strength of the weak zone can be backed out by applying a material strength factor to the base metal and applying this to the cross-weld test and matching the data.

When the Task 2 methodology is applied to the cross-weld test data, one basic assumption that has to be made, which is new to this work, is a transition from effective stress (von Mises stress) controlled 'ductile' failure at "high" stresses to maximum principal stress (MPS) controlled 'brittle' failure at lower stresses. This methodology can explain apparently contradictory phenomena such as strengthening of cross-weld tests with specimen size, and the details of long-term field weld joint failures. In this report, the procedure is to use cross-weld data to infer the reduction in material creep strength (compared with parent material data) and the transition between the effective stress and MPS mechanisms, which explain the average cross-weld failure trendline. Note that the inhomogeneity of crossweld tests means that it would be exceptional to find rupture data that was not affected (positively or negatively) by some degree of constraint. This

constraint has a strengthening effect in the effective stress regime, and often, but not always, a weakening effect in the MPS regime. Thus a model of the cross-weld specimen with the likely "weak" zone is essential to obtain corresponding material properties. Some independent confirmation of these properties is desirable. The following data and sources of test data have been used to obtain and confirm the methods and material strength properties used in this project (Task 2 and Chapters 2 & 3):

- Conventional (0.25" – 0.5" dia) cross-weld rupture trendlines
- Base metal and weld metal rupture trend data
- "Large" cross-weld specimens test results
- Selected failure case studies

In this view, a number of options are available as testing tools. Any large or non-standard specimen data extracted/removed from the original analysis may be particularly useful for this activity as an independent check of the assumption. For the case of large specimens with properly documented geometry, a FEA model of the specimen and the material inputs (including the base material strength factor) can be evaluated. If gross differences exist between prediction and experiment, it may be necessary to revisit the assumptions in the cross-weld model, but if the behavior of the non-standard specimens is properly represented, then this Step is completed.

In lieu of test data, for cases of weak weld metal, the weld metal trend curves (or weld metal data) may be a good check of the data. For cases where no debit on properties (weakness) is found, it may be good to evaluate service experience. If the material is new, no service experience exists, and no non-standard specimen tests are available, an assumption of principal stress control for all conditions can be made that has been shown to best match long-term data or may be conservative depending on test condition. Figure 5 provides a simple representation of the processes. The dashed line indicates a repeat path if the data do not support the initial strength factor analysis.

Figure 5: Detail of Process to Determine the Inherent Material Strength Factor From Cross-Weld Tests

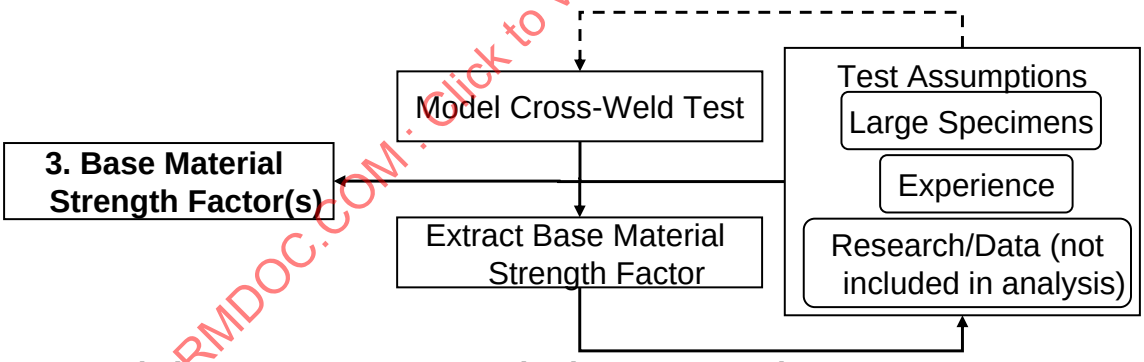

Notes: Dashed Line Represent a Repeat Path Where Prior Strength Factor Derivation is Not Supported by Available Data.

1.2.4 Step 4: Application to Welded Structure

With the completion of Steps 1-3, the model/tool can be used to examine structures for the purpose of developing rules including WSRFs. The first step is to define the geometry and loading of the structure, that may be done by the relevant construction code committee. For the examples in the following chapters, the chosen geometry was a long seam-welded pipe under internal pressure loading. Other welded structures that could be addressed include girth welds (without bending), penetrations, saddle welds, etc. The second step is to define the boundary conditions or number of different structures. For the simple case of seam

welds, one option could be to address minimum and maximum thickness in typical production today. Other options include weldment angle, double-V versus J-groove geometry, peaking, ovality, etc.

With this matrix of structures and boundary conditions, the model can be run for the structure with and without the weldments for given conditions. The committee will again be potentially needed for this exercise because the difference or ratio between the two structures may be a function of stress, time, and temperature. One pragmatic solution to this problem is to evaluate the structure(s) only for temperatures in the time-dependent stress controlled range as defined in Section II-D, Tables 1a and 1b. Thus, the temperature range would only explore the creep-dependent regime. A number of loading (stress) conditions will also be necessary. At first glance, the design stress for the structure appears to be a good value to use, but aside from limited thermally accelerated test data, there is little or no data at design stress levels since test durations at these levels are exceedingly long. So, loading conditions should be chosen such that resulting lives vary from some minimum time (depends on needs of code committee) to a maximum time that exceeds 100,000 hours. This will allow for developing 100,000-hour rupture strength estimates which are in line with current Code practice for setting allowable stresses.

1.2.5 Step 5: Design Strength Ratio

The analyses of Step 4 provide the basis for estimating the design strength ratio. The design strength ratio is the calculated (per Code rule or formula) stress for local damage initiation in a welded structure divided by the calculated stress for local damage initiation in the same structure without a weld. The ratio can be a function of time and temperature, depending on the material behavior and structural constraint effects for a given welded structure. In the examples provided in the following chapters, cases where this ratio changes with time and temperature are presented. The three main variables for any analysis are material, loading conditions, and geometry. Under what conditions these variables are constants or are evaluated for a range of conditions directly relates to applicability to a specific Code section and allows for determination of WSRFs. Given the design strength ratios for the full range of structures of interest would be impossible to determine, as described below, select cases involving combinations of material, loading conditions and geometry may be analyzed to develop an aggregate assessment of strength ratios from which WSRFs may be established for a particular range of variables. Two situations envisaged for such an approach are as follows.

1.2.5.1 Defined material and loading with variable geometry

In this example analysis, a specific material (or material class) is evaluated under specific loading conditions for a range of potential geometric considerations. The current WSRFs for seam welds in Section I and B31.1 are examples where such an analysis could be utilized. For WSRFs that will be directly applied to allowable stress values from Section II-D, Table 1a and 1b, it is recommended that the design strength ratio at 100,000 hours be utilized for analysis. Even with design strength ratios at 100,000 hours for a structure, translating this data into a WSRF requires a final analysis. For the case of seam welds, the bounding conditions to consider for this case would include:

- Material (Constant): one material
- Loading (Constant): internal pressure to produce 100,000-hour rupture in structure without weld
- Geometry (Constant): longitudinal seam weld, no peaking, no ovality
- Geometry (Variable): multiple diameter/thickness ratios, weld geometry

Based on the results for the minimum and maximum expected diameter to thickness ratios, a number of strength ratios will be developed at each temperature. If all these values are close to the same number, universal WSRFs may be applied. If these values only depend on temperature, a temperature-specific WSRF may be developed, and if these values also depend on the geometry, the minimum or average strength ratio can be used to set the WSRF.

1.2.5.2 Defined geometry and loading with variable material (weld deposit and quality) and fabrication-related geometric features

In this analysis, a specific geometric feature relating to fabrication, peaking for this example analysis, is considered for a range of materials under specific loading conditions. In general, the analysis set can include variations in material related to weld process and to quality (e.g., flux type and oxygen content). Design codes seeking to put limits or impose penalties on peaking, ovality, etc. could use such an approach to improve rules or impose WSRFs. For the following:

- Material (Variable): multiple materials
- Loading (Constant): internal pressure to produce 100,000-hour rupture in structure without weld
- Geometry (Constant): longitudinal seam weld
- Geometry (Variable): range of peaking

For a specific seam weld, a range of materials and peaking angles are assessed. The effect of peaking on the performance of each material may exhibit trends for decreased life with increased peaking (suggested in Task 2 work on this subject using a general set of material strength ratios). Option for the Code committees may be to limit peaking or penalize peaking with an additional WSRF as a function of peaking.

Other examples where material, loading, and geometry are either constants or variables can be conceived, but laying out this simple foundation provides a roadmap to take design strength ratios and develop weld strength reduction factors or impose rules limiting fabrication.

1.3 New Materials

A general outcome of this project and the proposed Task 1b application guideline for applying the Task 2 methodology for developing WSRFs is what data should be requested for new material or should be searched for beyond the scope of the databases assembled in Task 1a. Before addressing this issue, some comments on the use of 'large' specimens for determining welds strength reduction factors should be noted based in part on this research.

1.3.1 Comments on Specimen Size

There is considerable disagreement on the design of cross-weld specimens and their use for determining WSRFs. Because some studies have shown that cross-weld creep-rupture life is a function of specimen size [4], [5], it has been suggested that the data derived from 'large' specimens are representative of 'actual components' and the results from these tests can be used to directly calculate WSRFs. There are three main reasons which suggest such an approach to developing WSRFs may be limited, flawed, or potentially non-conservative. Hence, the current application guideline in this chapter is based on an initial analysis of standard cross-weld data.

The first argument for the limitation of using 'large' specimens to directly set WSRFs is based on the methodology proposed in this chapter. The transition from 'ductile' to 'brittle' behavior (effective stress to maximum principal stress controlled local damage initiation) proposed in this chapter clearly indicates that shorter-time data at higher-stresses may not represent long-term behavior of the component. Thus, potentially significant effects or trends for large specimens versus standard specimens may be a function of testing time and temperature. This same argument applies to using the standard specimen size cross-weld data, which is why using these data to back-out a base material strength factor is a critical step in the analysis. In other words, neither 'large' non-standard or standard specimens should be used to directly infer a WSRF without a structural analysis. To add to this point, there is not a guarantee that a 'large' cross-weld specimen will accurately reflect the behavior of a structure, even if thicknesses are similar. In Chapters 2 and 3, different trends were in fact observed for two different classes of materials.

Secondly, not all studies have determined that a clear trend exists between specimen size and rupture life. A review of Type IV failures cited conflicting research on specimen size effects [6], a recent examination of Grade 91 showed no effect of specimen configuration [7], while another study suggested differences in failure mode with specimen size but no difference in rupture times [8]. For the studies that have found differences in life with specimen size, it has generally been proposed that with increasing specimen size for a fixed weak narrow material zone such as a HAZ region, constraint increases resulted in increased rupture life. Rarely is this greater than a factor of 3 in time. Thus, even based on the data that do show increased life with increased specimen size, the effect is minor and conservative for a stress-based design. Creep-rupture data typically have a scatter on the order of one order of magnitude (10X in life), which is far greater than any research has found for specimen size effects.

A third reason for utilizing standard specimen data is the results of Corum already presented in Figure 1. The results show that rules based on standard specimens (formerly N-47, now ASME Section III-NH) are conservative for a wide array of structure tests and multiple materials that fail in different manners. Therefore, the importance of 'large' specimen tests may not be in setting WSRFs but instead as good tests to confirm or refute simplified model assumptions. In Chapters 2 and 3, this approach is evaluated for two separate cases.

1.3.2 Data Requirements

ASME Section II, Part D Appendix 5 requires for new materials: "sufficient time-dependent data shall be provided for weldments and filler metals to allow ASME to assess the properties in comparison with the base material [9]." It requires stress-rupture data in excess of 6,000 hours at each temperature and for each welding process and minimum creep rate data on new filler metals. This work suggests additional information is necessary to properly assess the necessity for WSRFs when a new material is being proposed for service in the time dependent regime. Of particular importance is not only creep and rupture data, but what information is reported with the data. Any data analysis based on cross-weld needs to take into account information (Step 2 in the Application Guideline) including: weld configuration, specimen orientation, specimen size, failure location, failure mode, etc. If these data are unknown, the applicability of the approach proposed in this chapter is of limited value. Based on this work, reporting of cross-weld data should, at a minimum, be covered in the I column in Figure 3.

In general, the database should facilitate a data assessment of standard cross-weld tests to estimate rupture in 100,000 hours. Weld metal data should include both rupture and creep-rate to facilitate estimation of an average creep-rate of 10^{-5}%/hr over the range of time-dependent temperatures. Such testing requirements are in line with the goals of the current base metal requirements in the Code. For base metal, three heats are required and the data is analyzed on a lot basis. Current requirements are for testing of all weld processes, which if not followed, will potentially restrict certain weld processes. Another issue that is not clearly defined is weld metal composition. Unless restricted in the code case, any weld metal can be used to qualify the joint to Section IX, which is based on room temperature requirements and is not necessarily representative of high-temperature behavior. Because of the myriad of potential combinations of weld metals, weld processes, and heat-treatments, the database requirements for welds and weldments (per the current rules) should result in databases that are larger than the base metal databases and likely impractical. Therefore, one solution proposed to this dilemma is to identify weld metal and weldments on a lot basis, as defined in Figure 6. Upon review of this information, the Code committee can than decide to limit or not limit the applicable processes. Preliminary proposed requirements are provided in Figure 6.

Figure 6: Minimum Proposed Data Requirements for Weld Metal and Weldment Test Data to Facilitate Analysis for This Project

	Minimum Number of Lots (a,b)	Test type and duration (c, d)		Minimum Number of Temps	Reporting Requirements for Weld / Weldment	Reporting Requirements for Test Results (e)
Weld Metal	**1** - suggest nominally matching filler metal if available	Rupture, Creep-rate	Max rupture time in excess of 6,000 hrs	**3** including 50°C (100°F) above the maximum intended use temperature	BM chemistry, WM chemistry, welding process, joint geometry	Specimen Size, Specimen Orientation to in weld/weldment, test conditions, rupture life, minimum creep rate (weld metal), reduction of area, failure location
Weldments	**3** – suggest lots contain two weld processes and/or two different filler metal heats (chemistries)	Standard cross-weld rupture tests				

a) A lot is defined as a weld or weldment made by a defined process with a defined filler metal heat (chemistries); for example, two weldments made by the same process with the same filler metal heat will count as one lot, but if two different heats of filler metal are utilized for the same process each weldment will count as one lot
b) Weld metal can be removed from a weldment or taken from a weld pad build-up provided specimens are taken such that any chemical dilution in the weld metal is not included in the tests and (if applicable) post-weld heat-treatment is performed
c) Longer test durations are advantageous with the goal of facilitating estimated 100,000 hour life for comparison with base metal dataset
d) Standard cross-weld specimens meet the requirements for base metal specimens tested to a recognized international standard such as ASTM with either the weldment in the center of the gauge or the fusion-line centered in the gauge with weld metal comprising ½ of the specimen length. When the weld is centered in the gauge, to ensure sufficient base metal is present on each side of the weldment, the length of base metal (l) plus the width of the weld metal (w) should meet/exceed the typical ASTM requirement of gauge length (L) equal to four times the specimen gauge diameter as follows: $L = (l + w) \geq 4d$
e) Details on reporting specimen failure location and/or metallographic assessment of failure modes is encouraged

2 APPLICATION TO CHROMIUM-MOLYBDENUM LONGITUDINAL SEAM WELDS

This chapter describes the evaluation of the EPRI Grade 22 weld/weldment database, an analysis of the database, the application of the modeling tool/procedure to evaluate the cross-weld data, a comparison with data on large cross-weld specimens, and implications for WSRFs.

2.1 Step 1: Grade 22 Database & Step 2 Pre-Analysis

The EPRI Grade 22 base metal, weld and cross-weld stress rupture database as described in the Task 1a report [10] was reviewed.

2.1.1 Base Metal

The base metal (BM) stress rupture database includes 354 data points, the majority of which (330) are from ASTM Data Series DS 6S2 that includes data on quenched and tempered, normalized and tempered, and annealed material. Test durations ranged from about 500 hours to 22,000 hours, stress from 3.7 to about 70 ksi, and temperature from 900 to 1200°F. Figure 7 is a representation of the BM data on a Larson-Miller Parameter (LMP = T(deg R).[20+log t(h)]) – Rupture Stress plot. The graphic suggests that the data below a stress of about 20 ksi exhibit far lower scatter than do the data above this stress level. Indeed, below about 20 ksi at the relatively higher LMP values where the effect of prior heat treatment would potentially wash out during testing, there was no obvious effect of heat treatment. For this study and demonstration, no attempt was made to separate the data on the basis of heat treatment. Also, given that data above 20 ksi at low LMP values were likely to be influenced by heat treatment or generated in a stress-temperature regime where lifetime is not creep-governed, a preliminary evaluation suggests a censoring of this data for analysis.

2.1.2 Weld Metal

The weld metal (WM) stress rupture database comprises 842 data points. The vast majority of the tested weld metals were in a post-weld heat treat (PWHT) condition, although the database does include material in the as-welded, subcritically annealed, and normalized & tempered conditions (estimated at < 20%). The data include welds made with the SAW, SMAW, GTAW processes, although no attempt has been made here to separate the data on the basis of weld process. Test durations ranged from less than 10 hours to about 46,000 hours, stress from 4.5 to about 110 ksi, and temperature from 750 to about 1300°F. Figure 8 is a representation of the data on a Larson-Miller Parameter (LMP = T(deg R).[20+log t(h)]) – Rupture Stress plot. As in the case of base metal, the scatter increases with increasing stress. Given the predominance of PWHT weld metal in the database, for this study and demonstration, no attempt has been made to separate data on the basis of heat treatment. Also, for consistency with the base metal database, and given the nature of the scatter, the preliminary evaluation again suggests a censoring of the data above 20 ksi.

2.1.3 Cross-Weld Data

The cross-weld database consists of 243 data points. Test durations ranged from less than 10 hours to about 15,000 hours, stress from 3.4 to about 65 ksi, and temperature from 850 to 1300°F. The reported failure locations were as follows:

- Not reported: 59
- BM: 84
- WM: 80
- WM/FL (weld metal/fusion line): 8
- FL: 3
- HAZ (heat-affected zone): 9

In this particular case of Grade 22 weldments, the service experience provides an indication of the most relevant failure locations, so the data may simply be censored on the basis of failure location. The data of particular relevance to the service application include data where failures have been reported to be in weld metal, at the weld metal/fusion line area, at the fusion line and in the heat-affected zone (HAZ). Figure 9 summarizes the available data on a Larson-Miller Parameter (LMP = T(deg R).[20+log t(h)]) – Rupture Stress plot. While the limited HAZ failure location data appear to be at the higher end of the scatterband, the WM, WM/FL, FL and HAZ failure location taken together appear to exhibit a single trend. The preliminary evaluation indicates that these data with failure locations representative of service experience may be separately analyzed.

With regard to heat treatment, again given the bulk of the data were for material in the PWHT condition, that the database is relatively small, particularly for the service-relevant failure locations, and given the observed trends exhibited in Figure 9, for this study and demonstration no attempt was made to separate the data on the basis of heat treatment.

Test specimen sizes, where reported (80 tests not reported), varied in diameter or equivalent diameter as follows (number of data points in parentheses): 0.12 in. (81); 0.2 in. (6); 0.32 in. (65); 0.38 in. (6); and 0.51in. (1).

Figure 7: Grade 22 Base Metal Stress Rupture Data from EPRI TR-110807 [10]

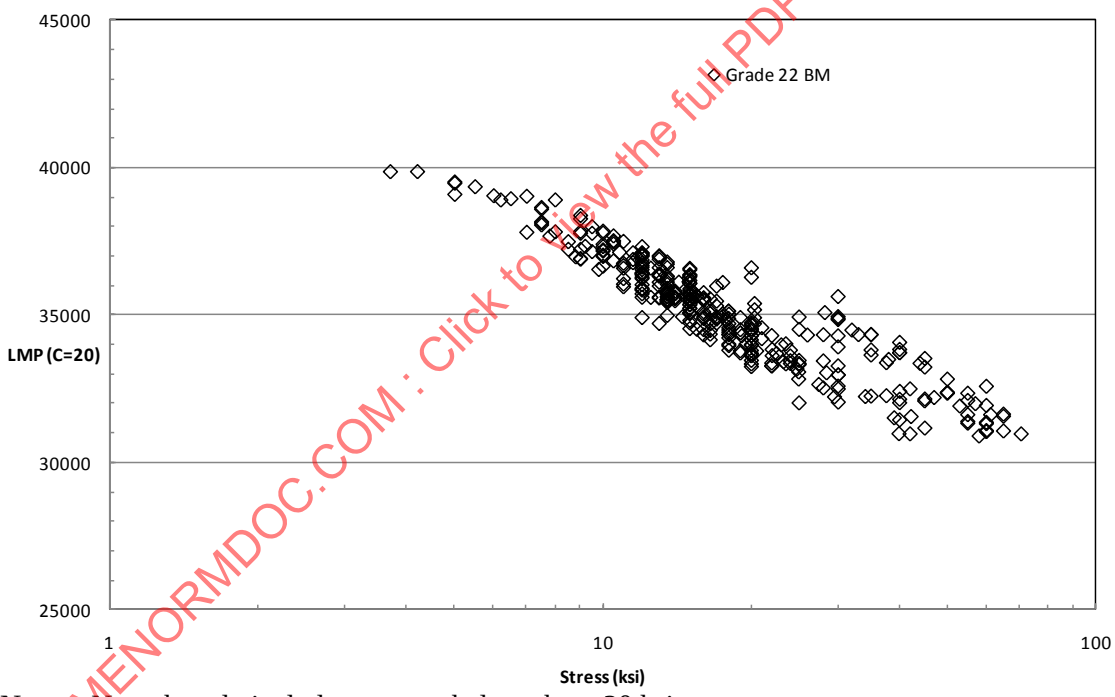

Notes: Note the relatively low scatter below about 20 ksi.

Figure 8: Grade 22 Weld Metal Stress Rupture Data from EPRI TR-110807 [10]

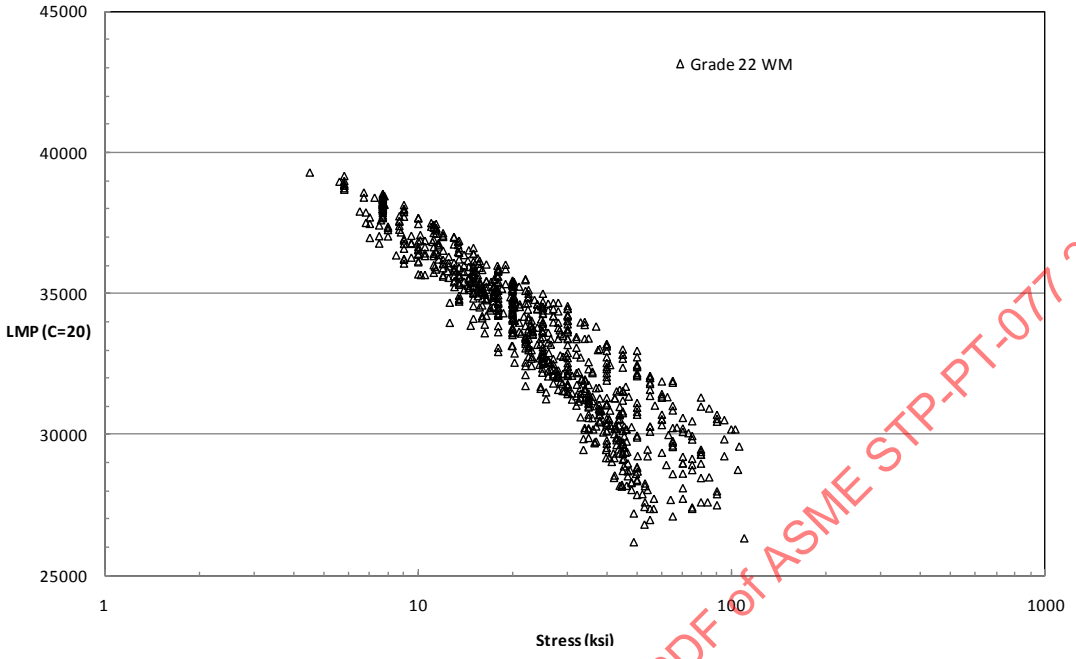

Figure 9: Grade 22 Cross-Weld (X-W) Specimen Stress Rupture Data from EPRI TR-110807 [10]

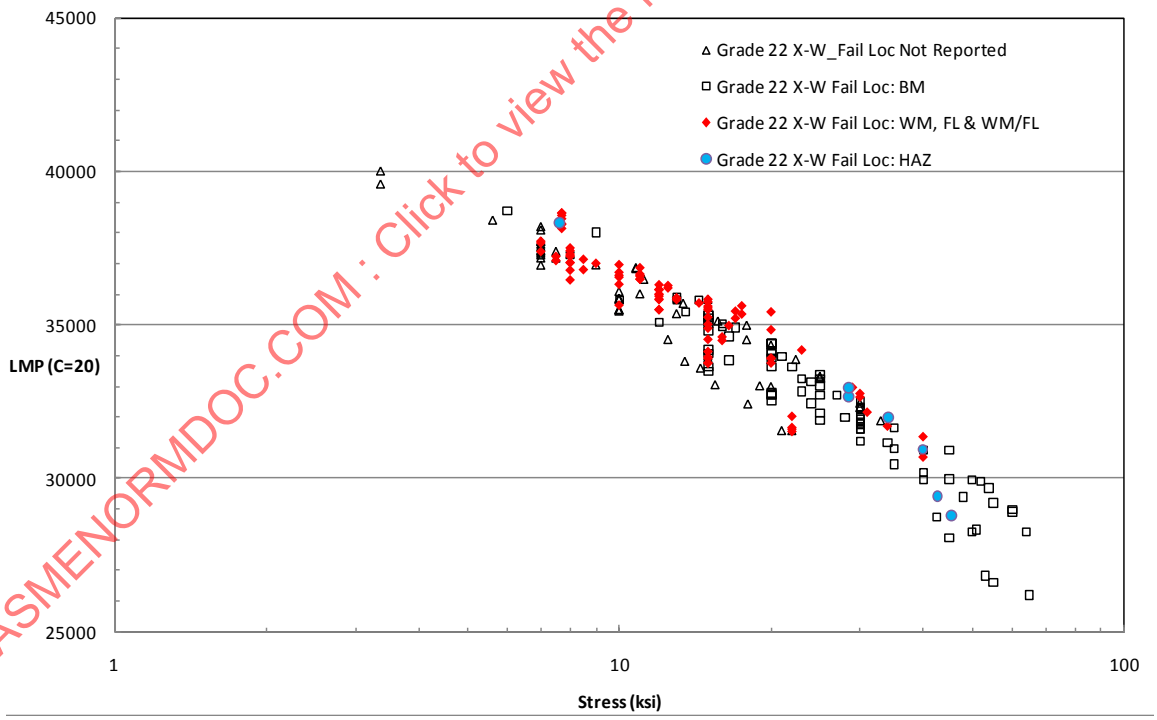

Notes: Note the generally consistent trend exhibited with the service-relevant failure location data (WM, FL, WM/FL and HAZ).

2.2 Step 2: Grade 22 Data Analysis

A preferred analysis method was first developed through exploration of the base metal database. Following this, the same method was employed for the weld metal and the cross-weld databases. The approach and results are briefly summarized below.

2.2.1 Base Metal Data Analysis

First, two fitting functions were explored:

- ASME Code-typical (log stress polynomial) :

$$\log t_R = a_0 + a_1/T + a_2(\log S)/T + a_3(\log S)^2/T + a_4(\log S)^3/T$$

- Spera function, as used in 1990 by the ASME Code for Grade 22 [11]:

$$\log t_R = b_0 + b_1/T + b_2(\log S)/T + b_3(S)/T + b_4(S)^2/T$$

where t_R is the rupture time, T is the test temperature in absolute units, S is the test stress, and the coefficients, a_0 through a_4 and b_0 through b_4 are coefficients determined through a regression curve-fitting procedure.

In each case, in order to examine the behavior in comparison with that expected from experience, a_0 and b_o were allowed to float and their best-fit values checked against the expected LMP constant C=20 value (a_0 and b_0 = -20). The final regression fits used in this study were developed by constraining the a_0 and b_0 to -20.

For a first view of the behavior, all of the data were analyzed. Both curve-fits gave floating a_0 and b_0 values that were significantly lower in magnitude than the expected 20, suggesting that this database exhibits behavior different from that used in development of the ASME Code allowable (b_0 close to -20). However, constraining the fits to a_0=b_0=-20 did not reduce the quality of the fits by much. The Spera function fit gave a lower standard error of the estimate (SEE) for log t_R. Based on the overall fitting capability for the data sets examined here, it was decided to use the Spera function throughout the remainder of this Grade 22 data analysis.

As noted earlier, a case may be made for censoring the data above 20 ksi. Further, a re-analysis of the censored data (245 data points) gave a vastly improved quality of fit, reducing the log t_R SEE from 0.44 to 0.12 for the Spera function fit. Figure 10 shows the data and corresponding curve-fit to the base metal data at 20 ksi and below. The best-fit function is:

$$\log t_R = -20 + 43009.92/T - 2884.39(\log S)/T - 338.394(S)/T + 4.094(S)^2/T \qquad (1)$$

with t_R in hours, T in degree R, S in ksi and a log t_R SEE of 0.118.

2.2.2 Weld Metal Data Analysis

The weld metal data exhibited considerably more scatter than did the base metal data (compare Figs. 8 and 9). As a result, the curve-fits gave significantly higher standard errors. As with the base metal data analysis, the analyzed data were restricted to 20 ksi and below. The data scatter increases with stress, and the extent of scatter above 20 ksi (see Figure 9) is such that restricting the analysis to data at 20 ksi and below significantly improved the curve-fit. As with the base metal, the floating LMP constant fit produced a value for C of about 13, significantly lower than the value of 20 typical and expected for base metal. Constraining the fit to C=20 increased the SEE (from about 0.33 to 0.39). For consistency with the base metal data

analysis, however, and given that the SEE increase was not considerable, the fitting procedure constrained the fit to C=20. Figure 11 illustrates the data and Spera function curve-fit.

$$\log tR = -20 + 43940.61/T - 4962.68(\log S)/T - 271.024(S)/T + 6.2169(S)2/T \quad (2)$$

Figure 10: Grade 22 Base Metal (BM) Specimen Stress Rupture Data at ≤ 20 ksi from EPRI TR-110807 [10] and the Corresponding Spera Function Curve-Fit

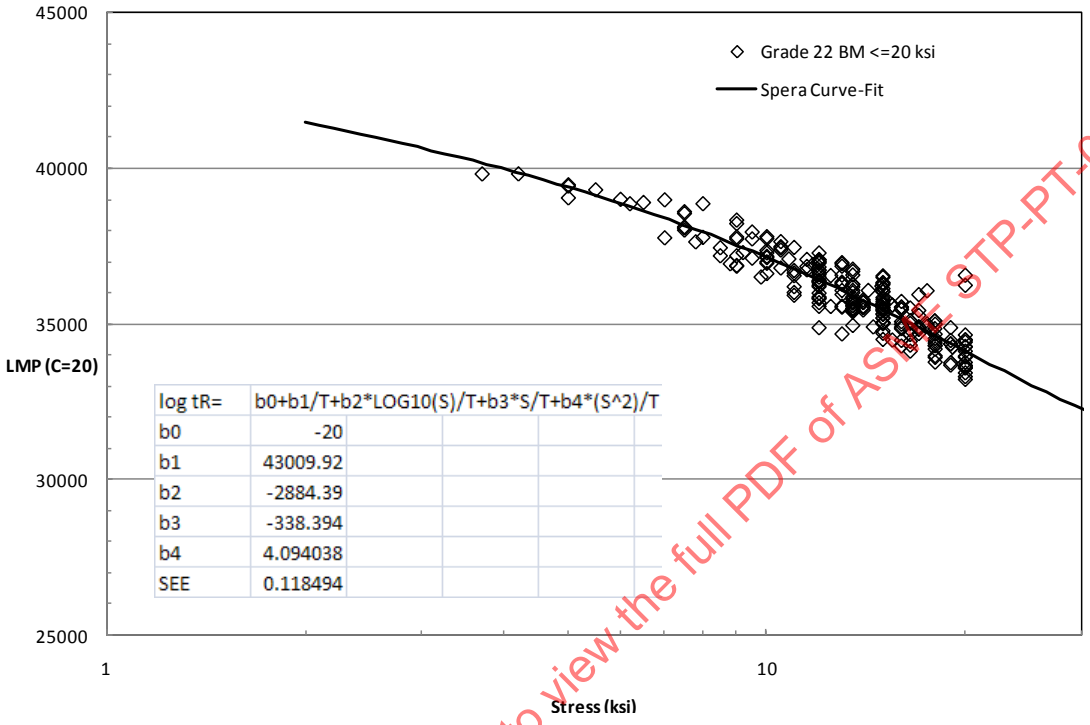

Figure 11: Grade 22 Weld Metal (WM) Specimen Stress Rupture Data at ≤ 20 ksi from EPRI TR-110807 [10] and the Corresponding Spera Function Curve-Fit

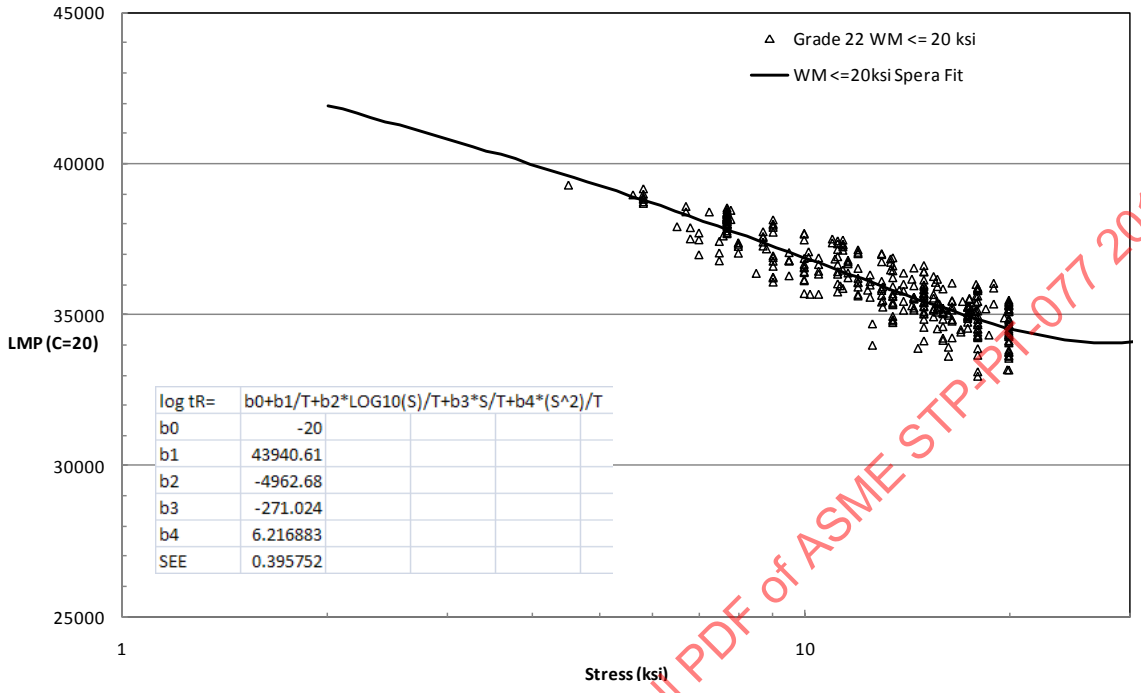

2.2.3 Cross-Weld Specimen Data Analysis

Given the service experience with respect to failure location, only cross-weld specimen data where the failure location was reported as WM, HAZ, FL or WM/FL (100 data points) were analyzed. The data were explored in three ways. First, the data were not censored on the basis of the 20 ksi stress level used for analysis of the base metal and weld metal data. Data above 20 ksi were included here mainly because of the limited size of the database and because the higher stress test specimens failed at locations representative of the service experience. Second, the data were censored as for the base and weld metal analyses (exclusion of data above 20 ksi). Finally, a set of analyses was conducted to examine whether this dataset would show obvious specimen size-dependent trends, recognizing however that nearly all of the tested specimens are of conventional laboratory dimensions and of a small size relative to thick-section structural applications.

All WM, FL, HAZ Failure Location Data

Figure 12 summarizes the data and analysis results for the cross-weld data where test specimens exhibited failure in weld metal (WM), at the fusion line (FL), in weld metal near the fusion line (WM/FL), and the heat-affected zone (HAZ) (100 data points). Also shown is the Spera function curve-fit with the Larson-Miller parameter constant C constrained to 20:

$$\log t_R = -20 + 47571.52/T - 13081.7(\log S)/T + 247.1096(S)/T - 3.7182(S)^2/T \qquad (3)$$

with a log t_R SEE of 0.45.

WM, FL, HAZ Failure Location Data at Stresses ≤ 20 ksi

Figure 13 summarizes the data and analysis results for the cross-weld data where test specimens exhibited failure in weld metal (WM), at the fusion line (FL), in weld metal near the fusion line (WM/FL), and the

heat-affected zone (HAZ) and where the test stresses were ≤ 20 ksi (81 data points). Also shown is the Spera function curve-fit with the Larson-Miller parameter constant C constrained to 20:

$$\log t_R = -20 + 38516.22/T + 8601.43(\log S)/T - 1327.13(S)/T + 28.334(S)^2/T \quad (4)$$

with a log t_R SEE of 0.37

There are two obvious concerns with the data and fit: (1) the fit shows unrealistic behavior in the extrapolated regions outside of the data, a likely consequence of the second concern: (2) sparseness and scatter of the data. For further analyses, the curve-fit to all of the data per Eq. (3) appears to be the preferred choice.

Figure 12: Grade 22 Cross-Weld (X-W) Data and Best-Fit Spera Curve for Specimens Exhibiting Failure in WM, FL, WM/FL and the HAZ

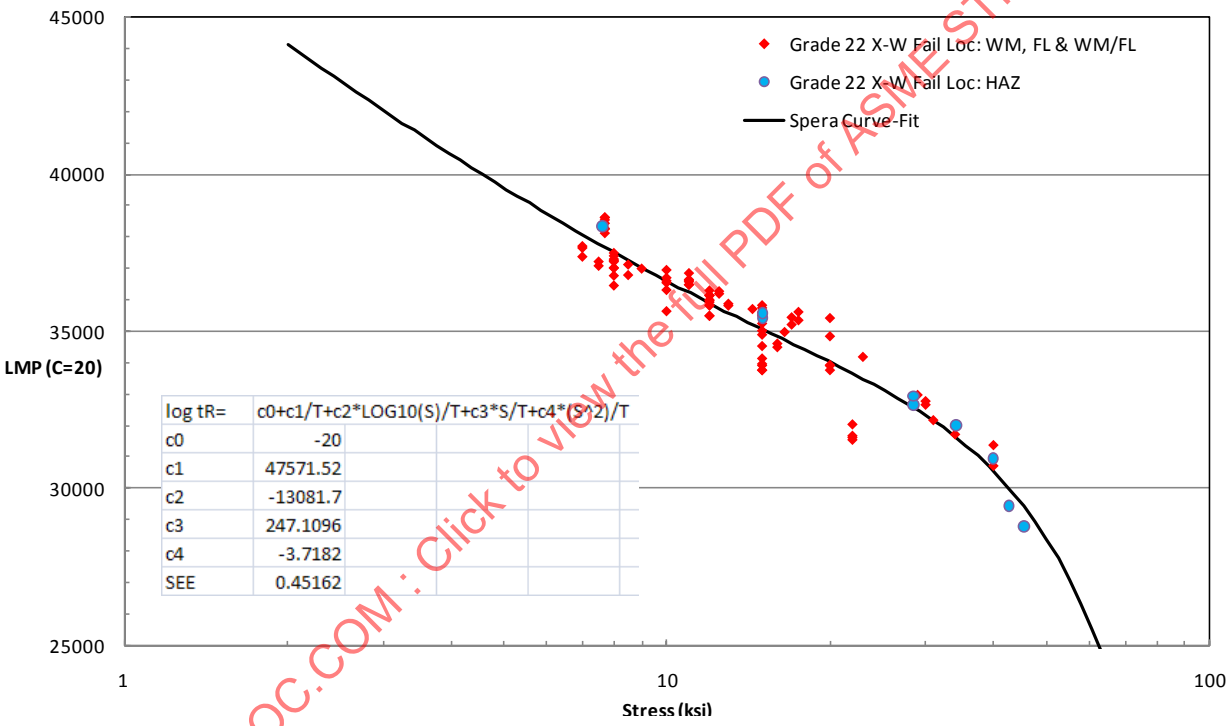

Figure 13: Grade 22 Cross-Weld (X-W) Data and Best-Fit Spera Curve for Specimens Exhibiting Failure in WM, FL, WM/FL and the HAZ and Tested at ≤ 20 ksi

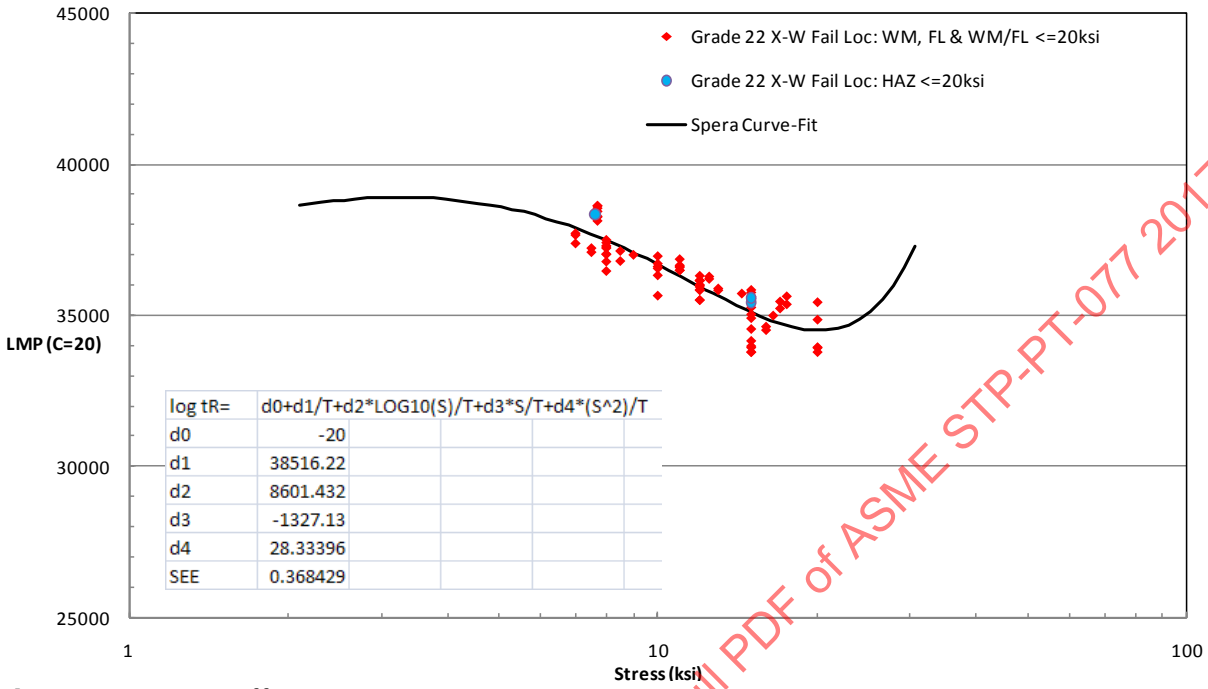

The Specimen Size Effect

A preliminary examination of the data for possible specimen size effects showed that size-splitting the cross-weld WM-HAZ-FL data into two sets - 0.08-0.2 in. dia. (26 data points; SEE=0.38) and 0.32-0.51 in. dia. (62 data points, SEE=0.39) - gave excessively low predictions for the larger size set at ≥ 1000°F. However, the smaller size set behaved very much like the cross-weld data and fit (Eq. (3)). The size effect explored using the two sets of data did not appear reasonable on account of the larger size data fit predicting exceedingly low rupture life. The existing database does not show any evidence of a trend in behavior as a function of specimen size. This is not surprising, given the database consists of test data on specimens of conventional laboratory specimen dimensions and of small size relative to section sizes in thick-section structural applications.

2.2.4 Summary

Figure 14 is a summary of the best-fit curves of Eqs. (1), (2) and (3) for the three cases: BM, WM, and Cross-Weld Behavior, respectively, the last consisting of only data where the failure locations represent those seen in service.

Figure 14: Grade 22 BM, WM and Cross-Weld (X-W) Best-Fit Behavior as Derived from the EPRI Database

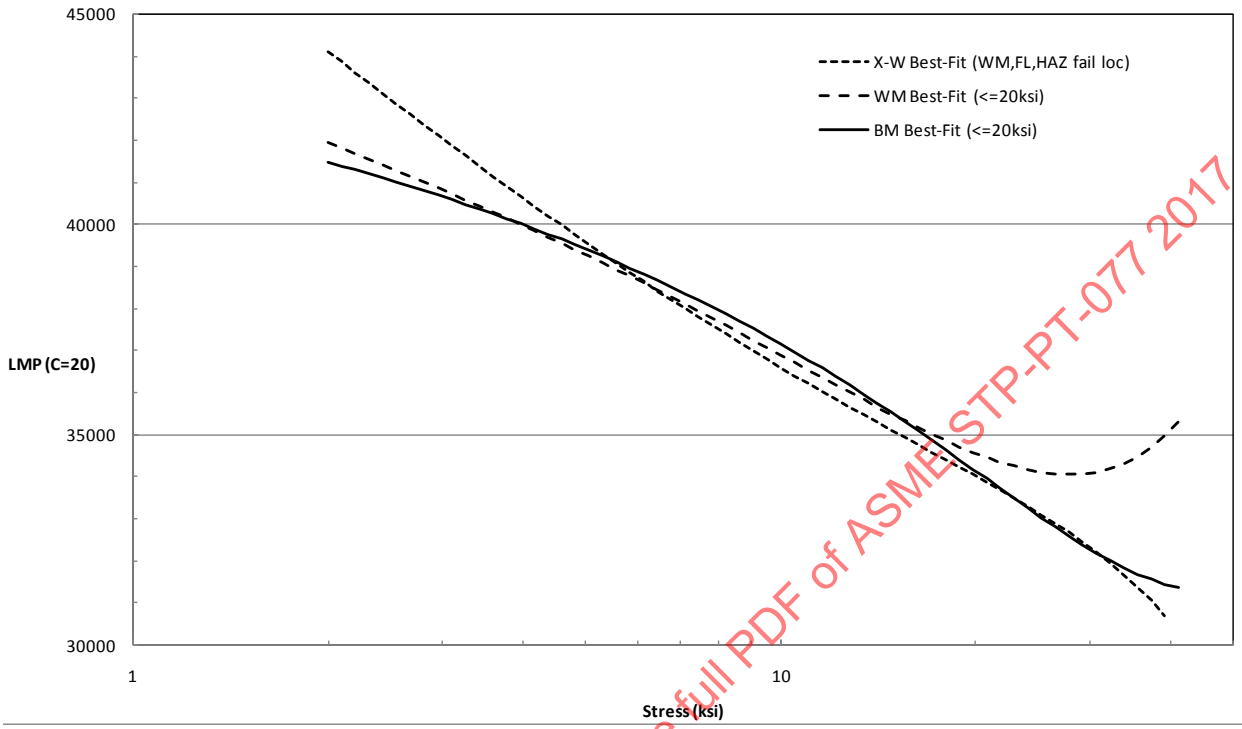

Notes: While the extrapolations to stress levels above about 5 ksi do not appear reasonable, the behavior in the 5 to 15 ksi range may be useful in further analyses.

The extrapolation of the curves to low stresses (below about 5 ksi) provide predictions that do not appear reasonable (cross-weld behavior strengthens significantly compared with both base and weld metal behavior). For the purpose of this investigation into developing suitable interpretations of cross-weld test specimen behavior for structural applications, the data in the 5 to 15 ksi range provide potentially useful information.

2.3 Step 3: Extracting the Base Metal Strength Factor from Cross-Weld Tests

As noted in Chapter 1, we seek to explain the cross-weld trend line in Figure 14 with:
(a) A base material strength factor (BMSF)
(b) A basis for the transition from effective stress behavior to maximum principal stress (MPS) behavior

The method is as follows.

1) Perform a limit analysis of a representative or typical test specimen geometry. The outputs from the analysis for each load step up to the limit are for the point or points with highest MPS:
   a) Maximum principal stress
   b) Effective stress
   c) Inelastic strain
   d) Load
2) Then for a particular sample test stress the following quantities are calculated:
   a) MPS = test stress x limit MPS / limit load
   b) Effective stress = test stress x limit effective stress / limit load

Note: these quantities may depend on which point in 1 is used. It is usually clear which is the region of highest MPS in the limit analysis. The associated plastic strain may be compared with a calculated creep strain at the effective stress. This gives a basis for selecting a particular load step to define the MPS and effective stress to characterize the component or sample.

3) These stresses divided by the base material strength factor (BMSF) may then be used to calculate rupture life to match cross-weld data.
4) If there is an indication that some combination of effective stress and MPS should be used to calculate rupture, then the following procedure is used.
   a) Using ASME FFS-1 [12] data, the ratio (omega/creep exponent, n) is calculated for the effective stress in 2. It is postulated that as this ratio increases, the rupture behavior will be driven increasingly by MPS. Conversely, as it decreases, the rupture behavior will be driven increasingly by effective stress.
   b) The limits of this ratio for the transition from one type of behavior to the other are calculated to match crossweld data.

The key to understanding crossweld tests is to be able to analyze the specimen efficiently, allowing multiple test conditions to be understood in terms of effective stress and maximum principal stress. Limit analysis shows the development of constraint and multiaxial stress with inelastic strain. The results may be used in spreadsheet calculations to derive material strength factors characterizing crossweld sample failure and used to predict weldment failure. Figure 15 and Figure 16 show maximum principal stress (MPS) distributions for minimum and maximum constraint cases of cross-weld geometry.

Figure 15 and Figure 16 show finite element limit analyses of a crossweld specimen with diameter = 0.4”, with different weak zone sizes. Even for the minimum constraint case, the maximum principal stress is greater than the nominal tension stress.

Figure 15: Maximum Principal Stress Distribution for 2:1 Weak Zone : Specimen Diameter Ratio (Assumed Cross-Weld Sample Geometry)

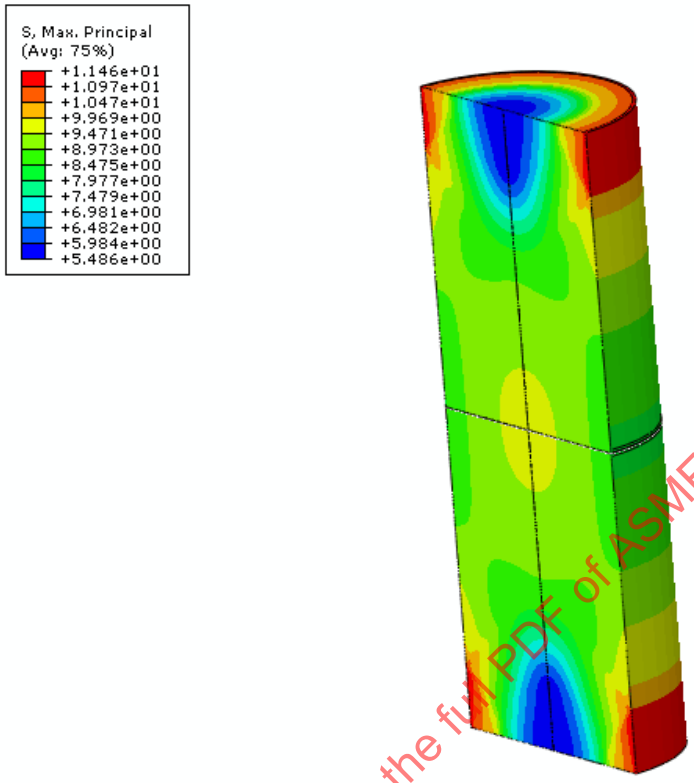

Figure 16: Maximum Principal Stress Distribution for 1:1 Weak Zone : Specimen Diameter Ratio

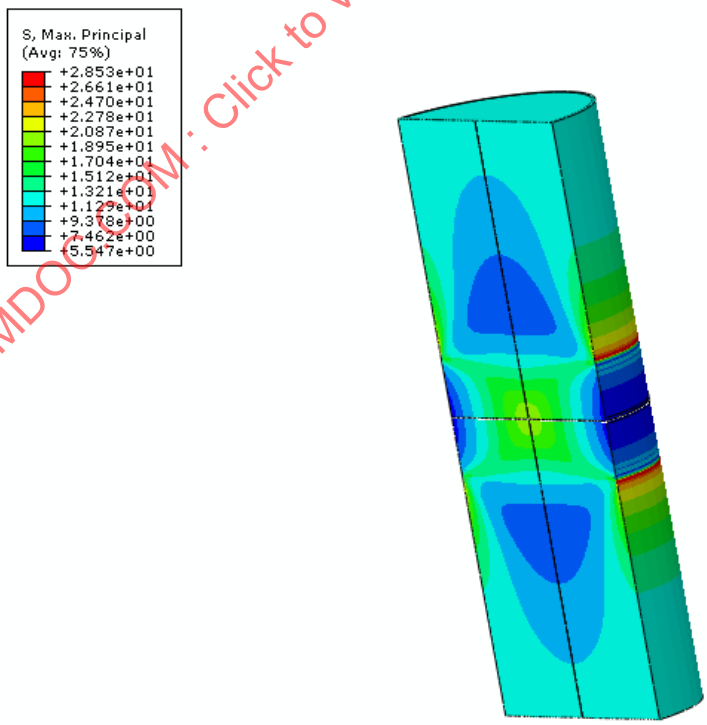

The combinations of von Mises and maximum principal stress in this analysis were used to back out a base material strength factor (BMSF), and the transition from ductile to brittle rupture, which match the crossweld data described in the previous section. Figure 17 shows the trend lines defining the BMSF.

From limit analyses of a series of geometries, and the properties used in Figure 17, it is possible to calculate the effect of specimen size on rupture time. This is shown in Figure 18, where we see that both strengthening and weakening behaviors are possible, depending on stress.

Figure 17: Results of Matching Cross-weld and Base Metal Rupture Data

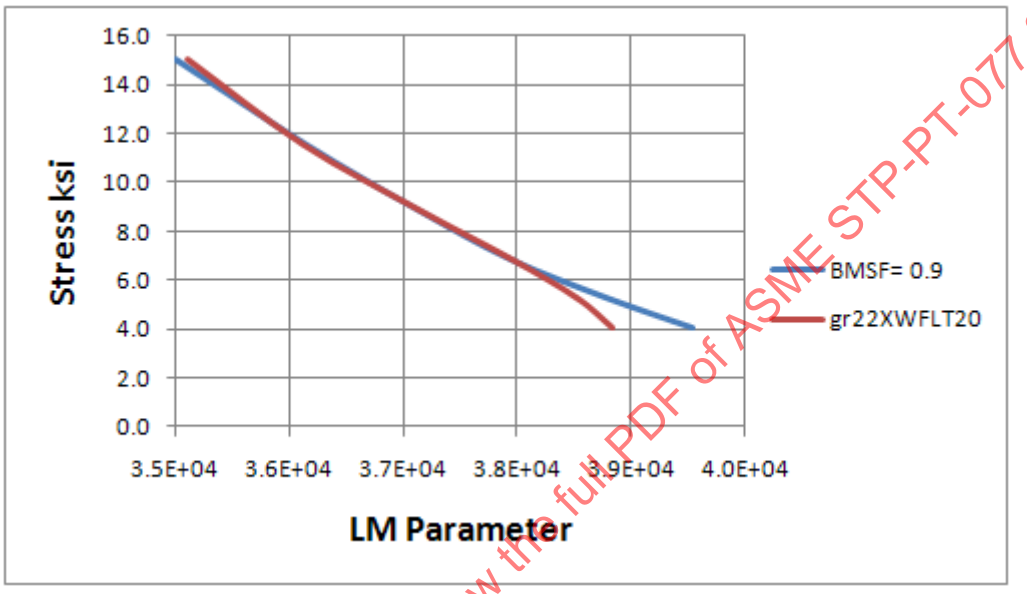

Notes: For Stress in the range 6 – 15 ksi, derived BMSF = 0.9. ratios of "Omega/n" for the ductile/brittle transition are 1 and 4.

Figure 18: Predicted Sample Size Effect Showing Strengthening and Weakening Behavior

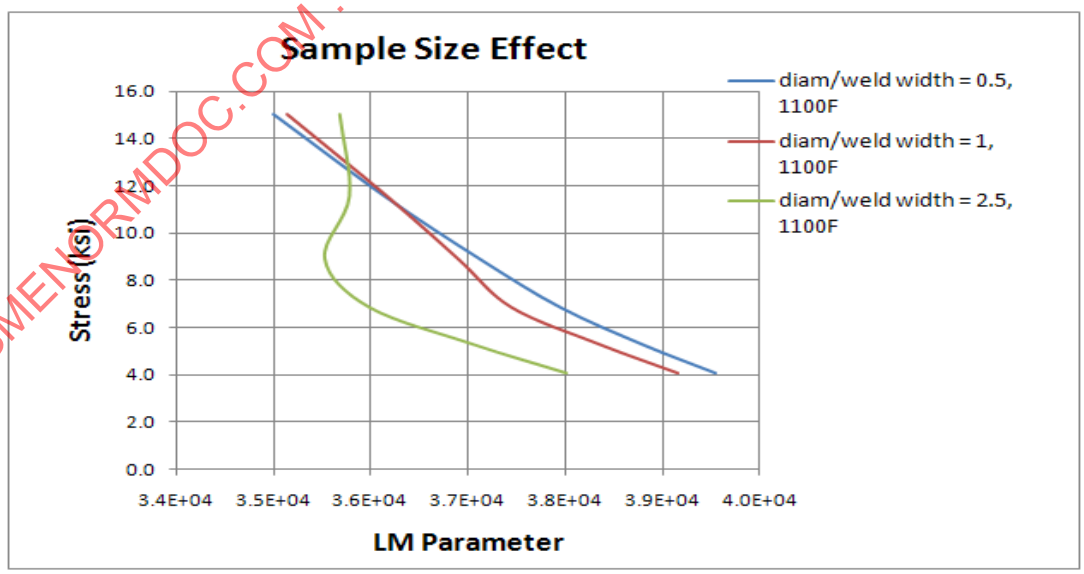

2.4 Step 4: Testing Assumptions

As a check on these calculations, the base metal strength factor (BMSF) calculated from crossweld tests and the ratio of weld metal strength to base metal strength may be compared. Figure 19 shows the factored base metal data, the crossweld data and the weld metal data from the previous section. The weld metal is slightly stronger than the crossweld specimens, suggesting that some crossweld specimens may have had weaker material than the weld metal.

Figure 19: Comparison of Factored Base Metal, Cross-weld and Weld Metal Strength Trend Lines

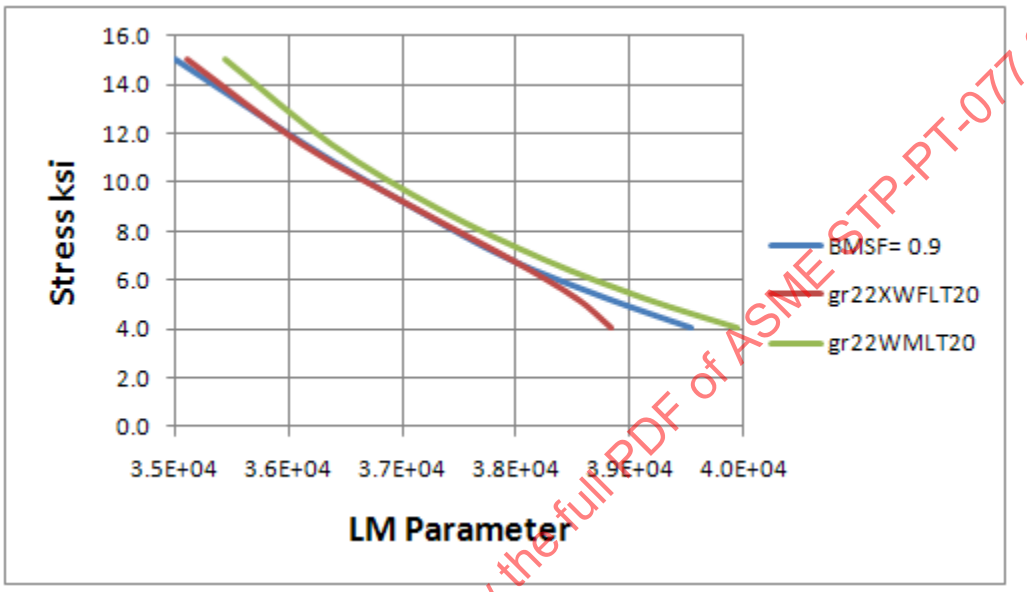

2.5 Step 5: Application to Seam Weld Structure

Seamweld life prediction

The calculation of welded joint life proceeds along the same lines as used to analyze crossweld specimens. The effective stress to maximum principal stress transition may be modeled if there is a basis for the required parameters. If not, it is conservative, and recommended for design, that the maximum principal stress is used. In this section the method is illustrated for a heavy Grade 22 Pipe section with a 50 semi-angle "U" groove weld and a thinner 'hot reheat size' X-groove.

The application of the analysis methods to a heavy walled pipe geometry (shown in Figure 20) is as follows.

Figure 20: Seamweld model: Pipe OD = 762 mm, ID = 457 mm, weld semi-angle = 50

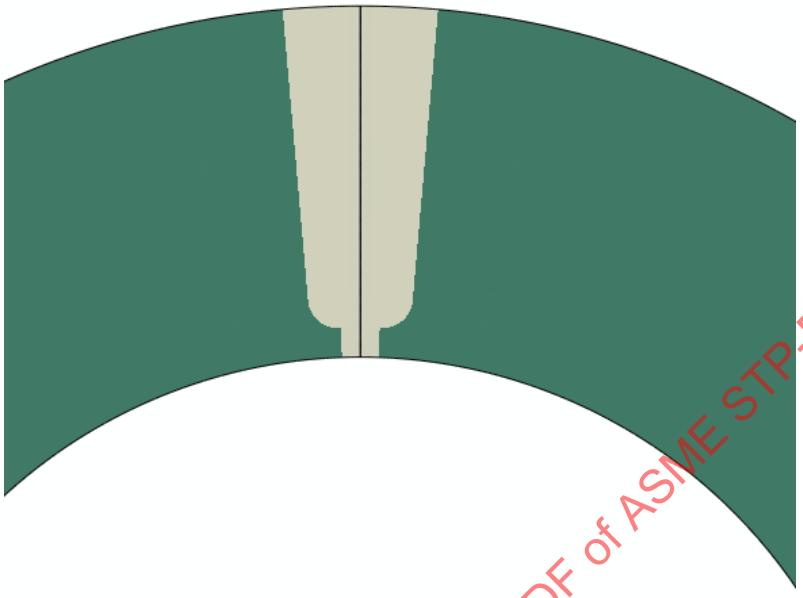

Figure 21 and Figure 23 show the results from the limit analysis. The area of highest maximum principal stress is on the OD, as a result of re-distribution from the bore due to yielding. The value of MPS in the weak zone is no higher than the plain pipe OD value. Maximum inelastic strain occurs in the bore in the weld region. Figure 23 shows the development of OD von Mises and Tresca stresses as yielding occurs.

The weldment design and life predictions are shown in Figure 24. Two approaches are used.

The life assessment calculation follows the description given above. The HAZ maximum principal stress is modified by the BMSF which is the derived material strength factor from crossweld data in Figure 18. For each of the three temperatures, the internal pressure is calculated which leads to a predicted life of 100,000 hours, based on the mean base metal trend lines. These pressures are then used to calculate design stresses using the design calculation S = p/ln(OD/ID), where p = design pressure. (The stresses are clearly higher than realistic design stresses, the use of 100,000 hours to define rupture stress is convenient and typical.) The "design" lives associated with these stresses are then calculated from the design stress, modified by a weldment strength reduction factor (WSRF). In general, these will be different from the BMSF's, depending on the weld joint analysis. In this case it was found the weldment weak zone did not weaken the joint more than the BMSF. This should mean that the design and calculated lives are the same. In this case there is a slight discrepancy due to the calculated MPS being slightly lower than the design calculation. (This may be due to the limit analysis not getting to the theoretical limit pressure. Smaller minimum increments could improve the result).

The conclusion is that for this weldment geometry, WSRF = BMSF.

Figure 21: Distribution of Plastic Strain Prior to Collapse

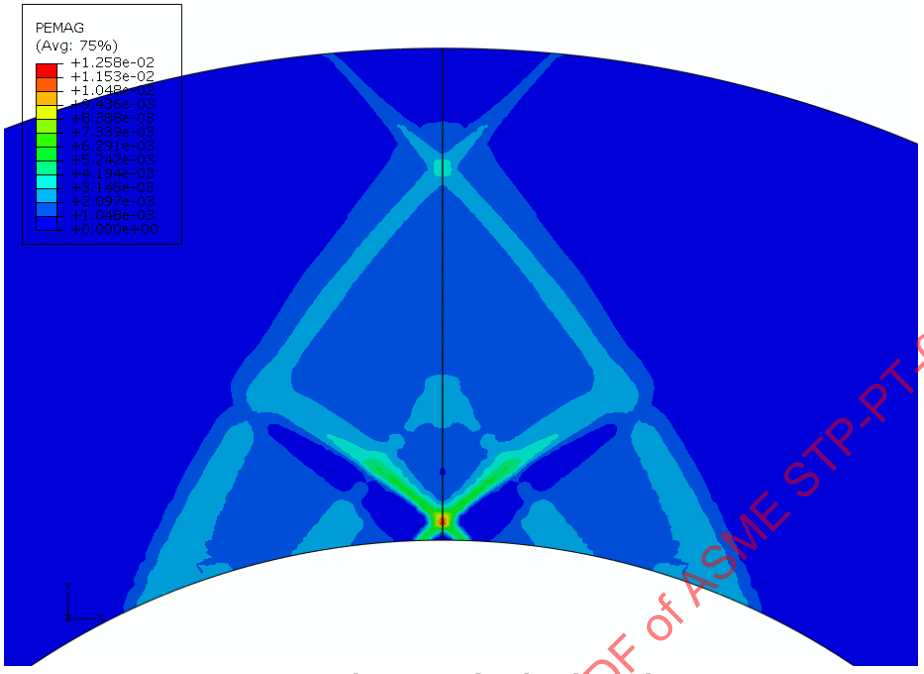

Notes: High strain is localized near bore.

Figure 22: Distribution of MPS Prior to Collapse

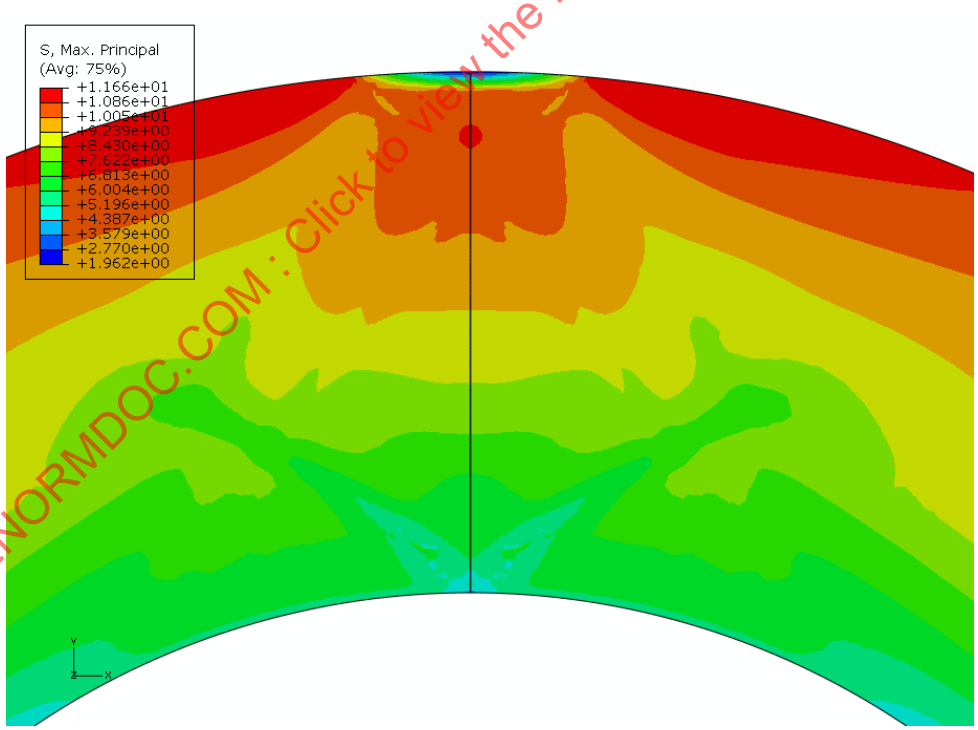

Notes: Max. weld values similar to design OD values.

Figure 23: Development of Max. Weld MPS to OD with Inelastic Strain and Time

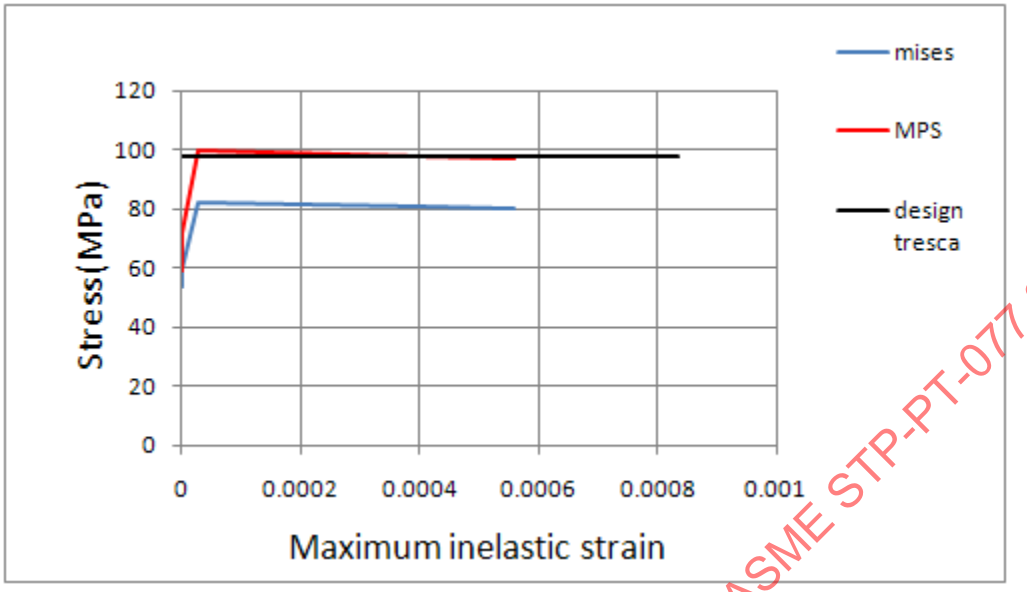

Notes: Redistribution from bore to OD can be seen. Nominal Design Pressure = 50 MPa.

Figure 24: Calculation of Joint WSRF: Single Sided "U" Weld

	Life assessment				Design		
Temp. C	Pressure MPa	MPS	BMSF	Life hours	Tresca stress	WSRF	Life hours
500	55.77	107.8	0.90	100000	109.2	0.91	100000
525	43.46	84.0	0.90	100000	85.1	0.91	100000
550	33.04	63.8	0.90	100000	64.7	0.91	100000

To compare with the 'heavy wall' U-groove pipe section (diameter:thickness ratio of ~4.5), a thinner wall seam-welded pipe with an X-groove configuration (diameter:thickness ration of ~ 26) was modeled in the same manner using the same input data. Figure 25 depicts the geometry of the pipe section and Figure 26 shows the distribution of the MPS. Careful inspection of the results show a high-stress region in the cusp of the fusion line (FL) between the weld and the base metal. Figure 27 provides the weldment design and life prediction calculations for the same three temperatures as in Figure 24.

It can be seen that in this case WSRF ≠ BMSF. Under different conditions, the X-groove weldment is weaker than the weakest material.

Figure 25: "X-Groove" Weld Geometry in 20" OD x 0.76" Thick Pipe

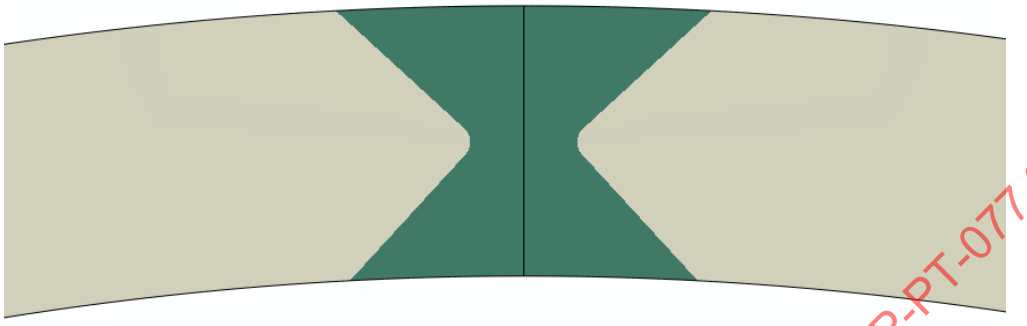

Figure 26: Distribution of Maximum Principal Stress Due to Inelastic Strain in Weld Metal

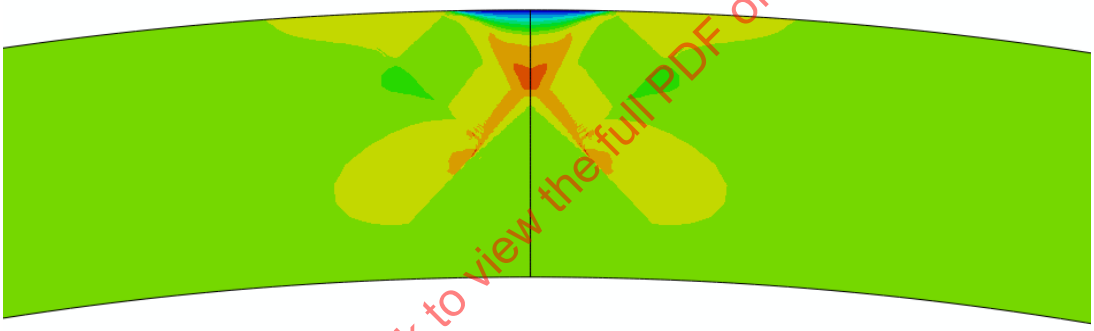

Figure 27: Calculation of Joint WSRF: "X-Groove" Configuration

		Life assessment		Design		
Temperature C	Pressure MPa	BMSF	Life hours	Tresca stress	WSRF	Life hours
520	6.80	0.90	100000	89.7	0.89	100000
550	4.24	0.90	100000	55.9	0.8	100000
580	2.90	0.90	100000	38.2	0.8	100000

In Figure 24 and Figure 27, comparisons are given of life assessment calculations based on finite element limit analysis with the BMSF, and design calculations, where a different WSRF from the BMSF may be necessary. In the case of the single "U" weld, there is no significant difference. In the case of the "X-groove" weld, there is a significant difference. These results show that in order to obtain the design WSRF, an analysis of the weld geometry is important and will, in general, affect the results.

2.6 Step 6: Summary and Implications for WSRFs

- The analysis of the Grade 22 weld/weldment database in this chapter by the methodology proposed in this project produced a BMSF = 0.9 for stress in the range of 6 – 15 ksi. This value was not found to be a function of time and temperature.
- It was also noted from the specimen size effect analyses (Figs. 18-20), that the minimum WSRF is more likely to be seen with tests under accelerated temperature conditions. A general implication of this finding is that accelerated temperature creep testing should be preferred over stress-accelerated testing when evaluating Grade 22 weldment behavior. (Note: Accelerated temperature isostress testing of CrMo boiler tubes and piping has been used for many years as a valid life assessment approach, so such a finding is not surprising but does add to the justification for such an approach with this material class)
- It is also apparent from the size effect analyses, that trends for large specimens versus standard specimens may be a function of testing time (applied stress) and temperature, so that universally opting for, or requiring large specimen weldment test data is not justified and can even lead to non-conservative predictions of component lifetime if applied directly. The findings suggest that using standard specimen data to back-out a base material strength factor and applying this factor to a structural analysis is the preferred method for helping establish WSRFs.
- Examples of seamweld analyses show that WSRF's less than the BMSF are likely for double "X"-groove weldments. Single sided "U"-groove weldments may have WSRF = BMSF.
- In the Task 1 report, a statistical analysis of estimated failure rates in CrMo piping was conducted (based on reported pipe design conditions). Assuming the estimated failure rate could be represented by the same data scatter (statistical distribution) which was found in development of the Grade 22 stress allowables (creep data analysis), the ratio of allowable stress to the failure rate stress was found to be 0.93 for only reported failures and 0.83-0.89 with considerations for estimates of inspections and minor damage. These values are in general agreement with the analysis conducted in this chapter. Thus, this analysis and experience suggest the current ASME Section I/B31.1 WSRFs for CrMo seam welds appear conservative at 1000°F and above (and potentially at lower temperatures).

A summary plot of the current ASME Section I WSRF for CrMo weldments, the findings from the statistical analysis of service failures, the BMSF used in the analysis, and the two weldment geometries is provided in Figure 28 to clarify the points above.

Figure 28: Summary Plot of CrMo Steel Weldment Reduction Factors

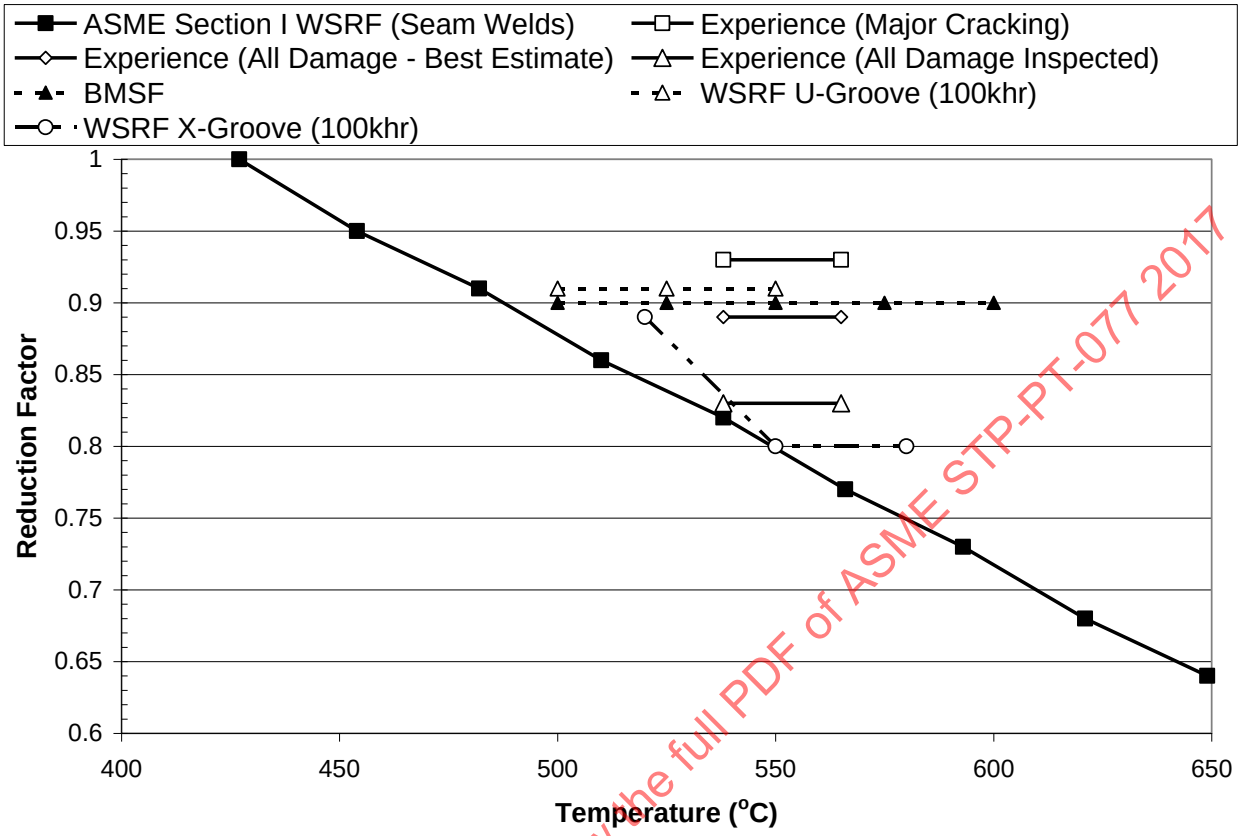

Notes: Including current ASME Section I WSRFs, the findings from Task 1a on a statistical study of failure experience, the BMSF used in this analysis, and the two geometries used for this study

3 APPLICATION TO SUBCRITICALLY HEAT-TREATED GRADE 91 SEAM WELDS

This chapter describes the evaluation of the Grade 91 weld/weldment database, an analysis of the database, the application of the modeling tool/procedure to evaluate the cross-weld data, a comparison with data on large cross-weld specimens, the application to seam-weld geometries, and implications for WSRFs.

3.1 Step 1: (Database) & Step 2 Pre-Analysis (Analyze Data)

The Grade 91 weld/weldment database is described and found in the Task 1a report [13]. The key concern based on the limited failure experience with Grade 91 and from laboratory studies is failure in the heat-affected-zones (HAZ) of weldments, often referred to as Type IV failure. Therefore, the weldment (cross-weld) specimen database (282 data points) was interrogated on the basis of failure mode. Researchers classified failures using differing terminology; thus the data were grouped into four major failure locations. 10 failures were identified as occurring in the *base metal* (base, BM). 59 failures were identified in the *weld metal* (weld, all weld, WM). 51 failures were identified in the *fusion line* locations (FL, FL/HAZ, HAZ/FL, WMFL). 98 failures were in the *Type IV/HAZ* (HAZ, IV, FG-HAZ). In summary, 218 of the 282 data points had reported failure locations.

Figure 29 contains four plots of the failure data as a function of applied test stress and temperature with failure location identified. In each plot, the entire database is plotted with data for one failure mode identified. Failure maps have been proposed as a function of stress and temperature for Grade 91 but inspections of these plots do not show any clear trends. Base metal failures are restricted to higher-stresses, but the data are limited. Weld metal, fusion line, and Type IV/HAZ failures appear to occur over the range of test conditions.

As an alternative, Figure 30 is the same data plotted as a function of temperature and time to rupture. While no obvious failure map is observed for all mechanisms, inspection of the Type IV/HAZ failures show a region at shorter times and lower temperatures where that failure mechanism does not appear. Figure 31 is a plot describing where the suggested Type IV failures are likely or are not likely to occur. The data suggest that at very long-times even at temperatures as low as 550°C, Type IV / HAZ failures are possible and should be considered in any data analysis procedure.

Figure 29: Failure Locations as a Function of Test Stress and Temperature for Grade 91 Weld/Weldment Creep-Rupture Database

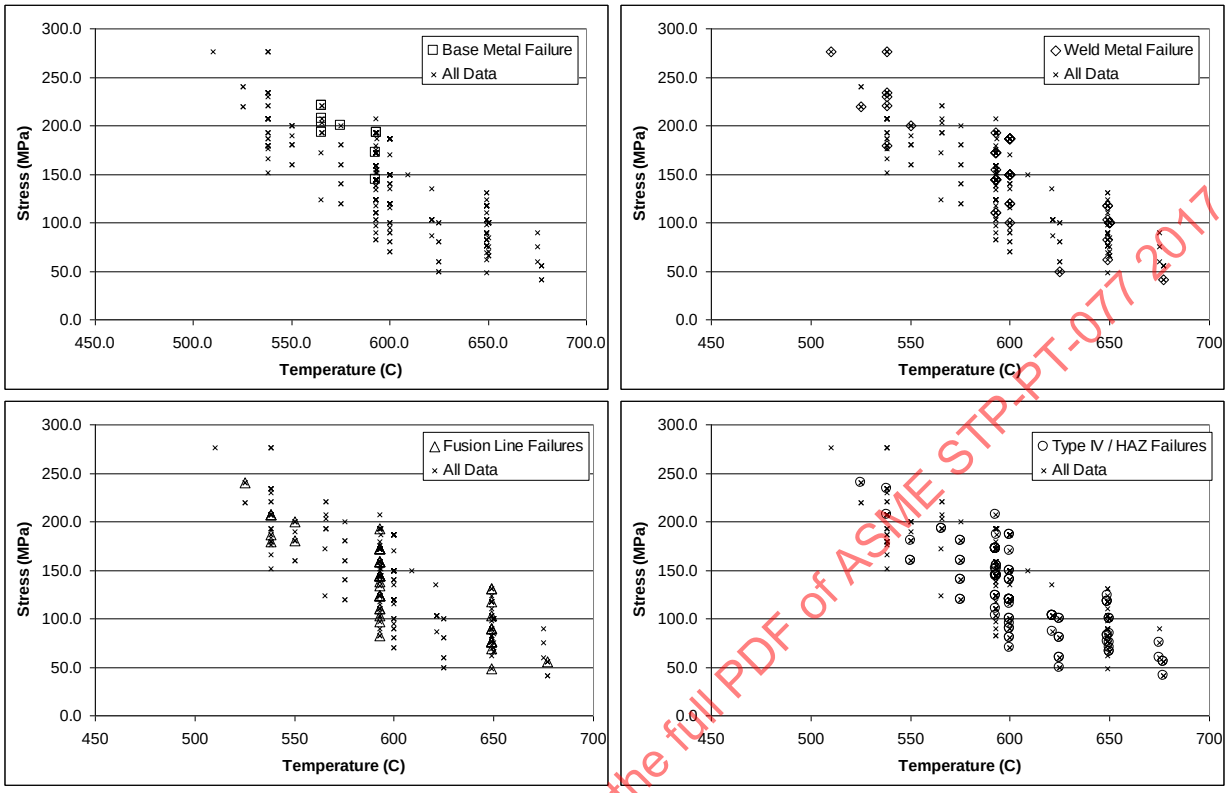

Figure 30: Failure Locations as a Function of Rupture Life and Temperature for Grade 91 Weld/Weldment Creep-Rupture Database

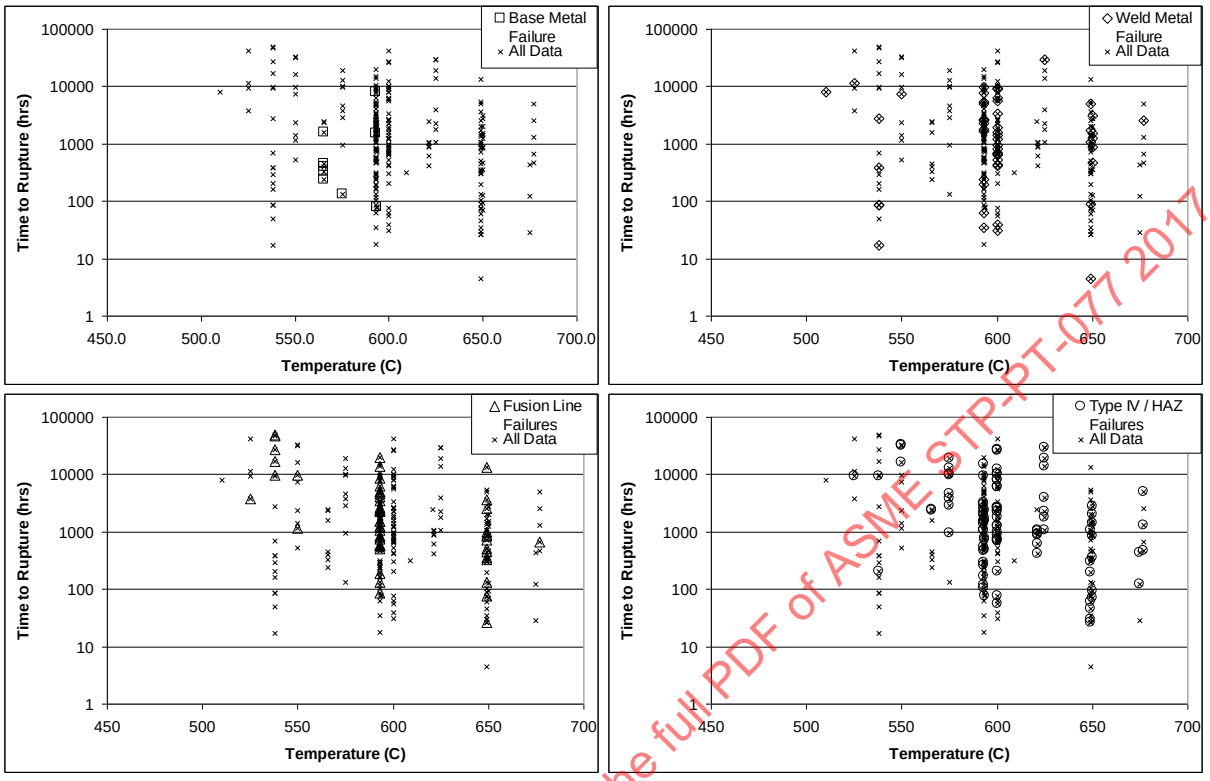

Figure 31: Suggested Regions Where Type IV/HAZ Failures Occur for Grade 91 Weldments

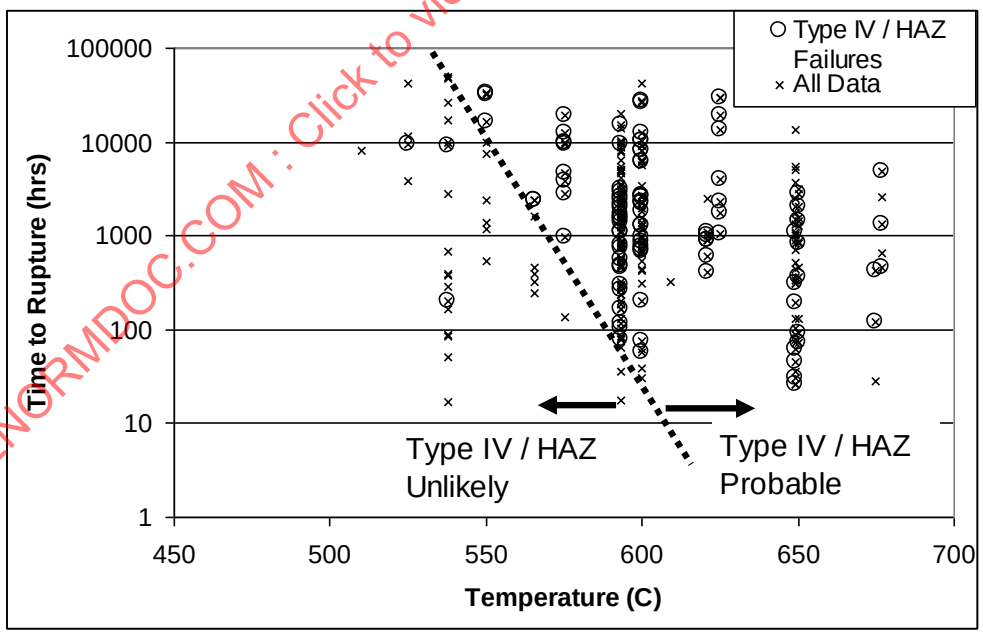

To qualitatively compare the time to rupture data for the various failure locations, the database is plotted using the Larson-Miller Parameter (LMP) with a constant of C=28.944 in Figure 32, Figure 33, Figure 34, and Figure 35. Included on the plot is the Grade 91 base metal average (solid line) and base metal minimum

(dashed line) behavior. The value for the base metal LMP constant, the fit used, and the minimum line (defined as 1.65 standard deviation at 100,000 hours) is based on the findings from a detailed study of a 1700+ base metal data point analysis of Grade 91 (using and evaluating over 15 different modeling methods) conducted by Fishburn as presented to ASME as the preferred fit to the database [14]. The equation is provided in Figure 39 (Chapter 3.2). The limited base metal failures in cross-welds, Figure 32, occur near the Grade 91 average line with no datapoints falling below the minimum, in agreement with the base metal analysis.

Figure 32: Larson-Miller Parameter (C=28.944) Comparison of Grade 91 Base Metal Average and Minimum Curves to Cross-Welds with Base Metal Cross-Weld Failures Identified

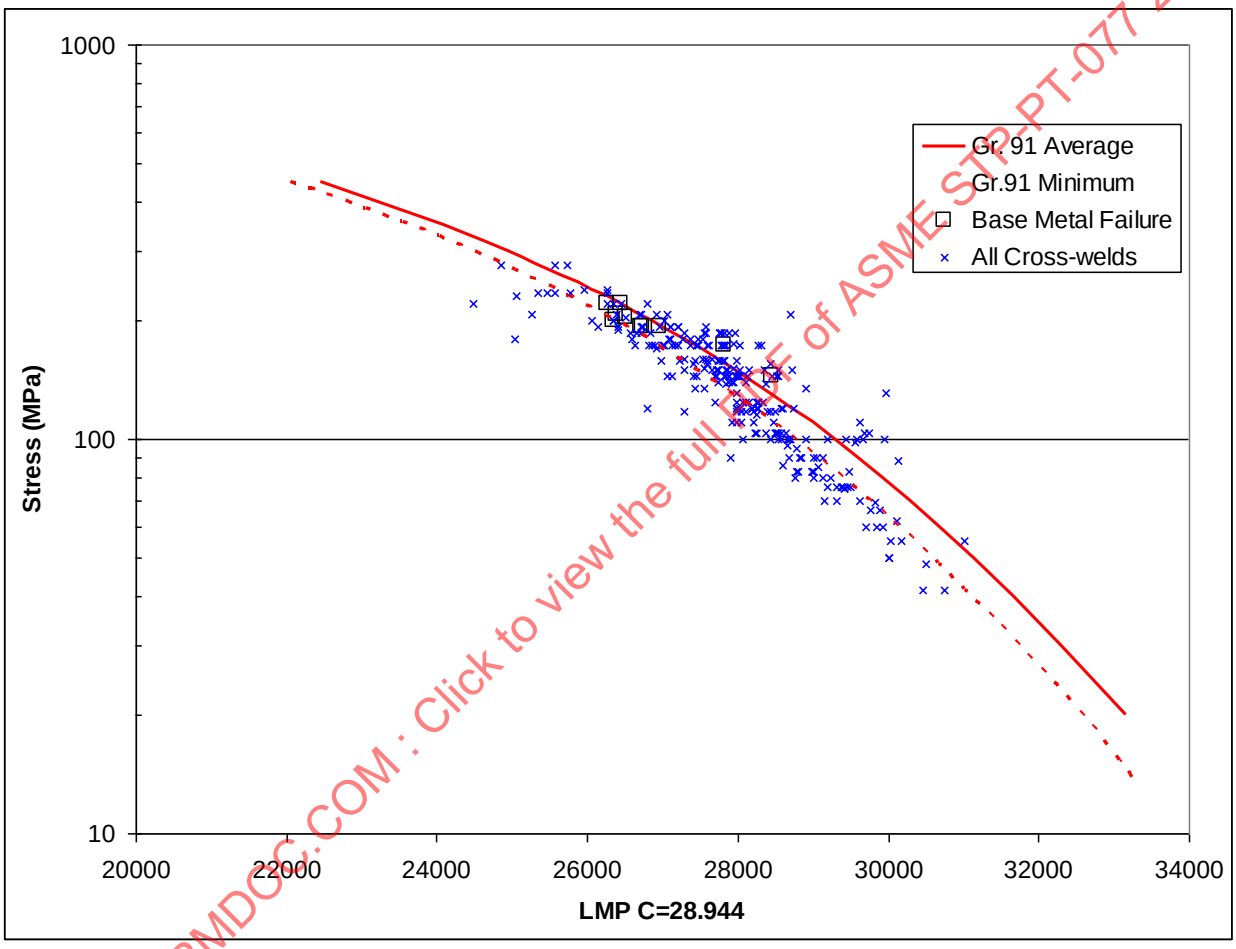

In Figure 33, the weld metal failures are plotted. A wide scatter of data is observed with some ruptures exceeding the expectations of the base metal and some data falling below the minimum. To extend this evaluation, the weld failures identified as weld metal only tests (data taken not from cross-welds but where the entire specimen was weld metal) were identified as solid diamonds in the plot. All of these datapoints fall above the Gr. 91 average suggesting the weld metal (not the weldment) strength slightly exceeds that of the base metal. Data that fell below the Gr. 91 minimum were examined, and in some but not all cases, the failures were in short-times less than 100 hours. Weld defects or sources of failures were not identified, but could not be ruled out as a source of the apparent premature failures. Thus, for modeling exercises relevant to long-term behavior, it appears the Gr. 91 weld metal is generally as strong or stronger than the base metal if good weld quality is assumed.

Figure 33: Larson-Miller Parameter (C=28.944) Comparison of Grade 91 Base Metal Average and Minimum Curves to Cross-Welds with Weld Metal Failures and All Weld Metal Test Data Identified

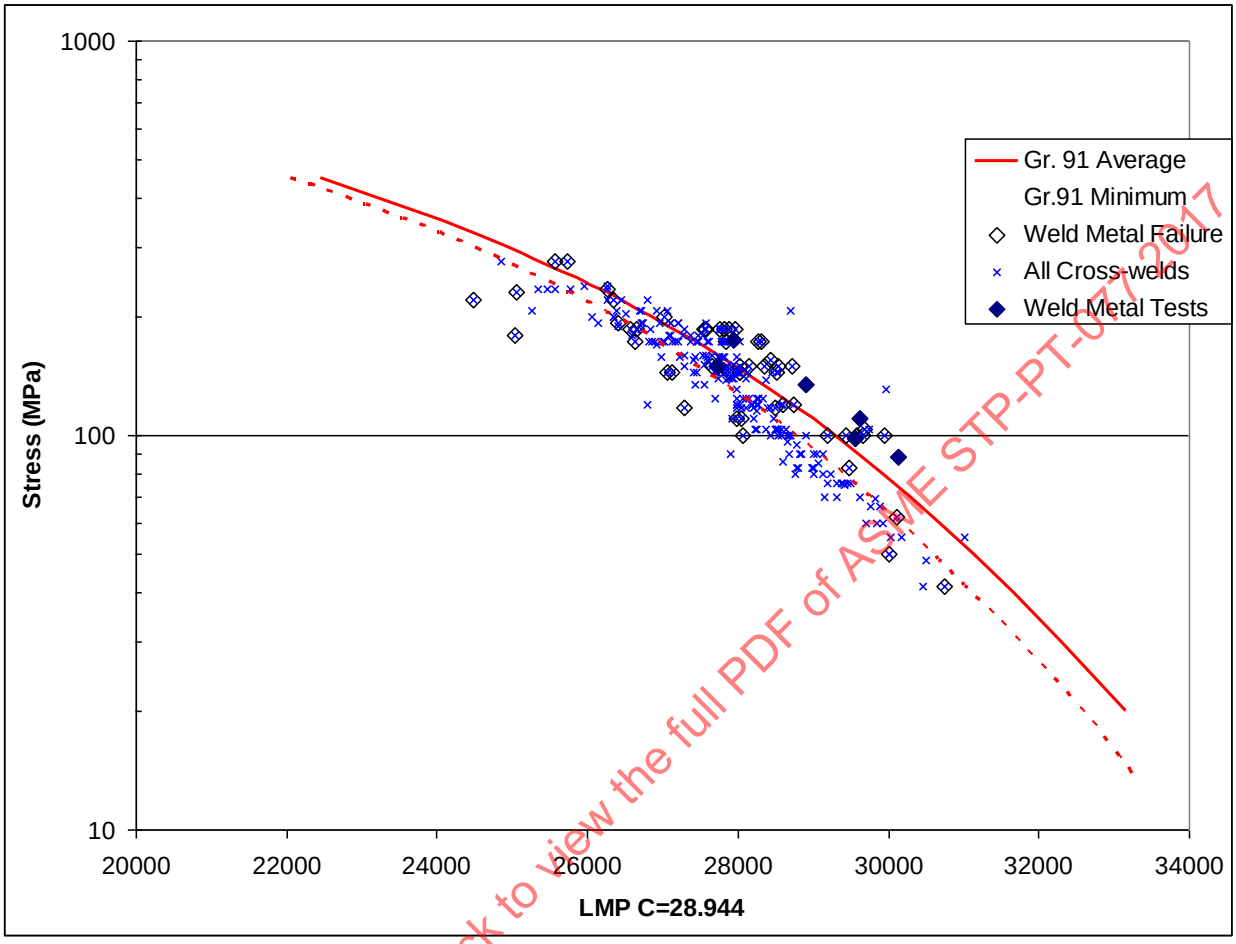

Reported fusion lines failures are plotted in Figure 34. At higher stresses, above ~130MPa, the failures were within the Gr. 91 average to minimum expected behavior. With decreasing stress, the failures tend to shift towards the Gr. 91 minimum and below ~100MPa, most data fall below the Gr. 91 minimum. Some details on fusion line failures are provided in the appendix of the Task 1a report. Generally, the failures macroscopically appear as 'shear' failures without necking. Location is assumed to be on the weld metal and base metal interface, but unless specimens were metallographically prepared, identifying the difference between weld metal, the interface, and the heat-affected zones is 'best guess' in most cases.

Figure 34: Larson-Miller Parameter (C=28.944) Comparison of Grade 91 Base Metal Average and Minimum Curves to Cross-Welds with Fusion Line Failures Identified

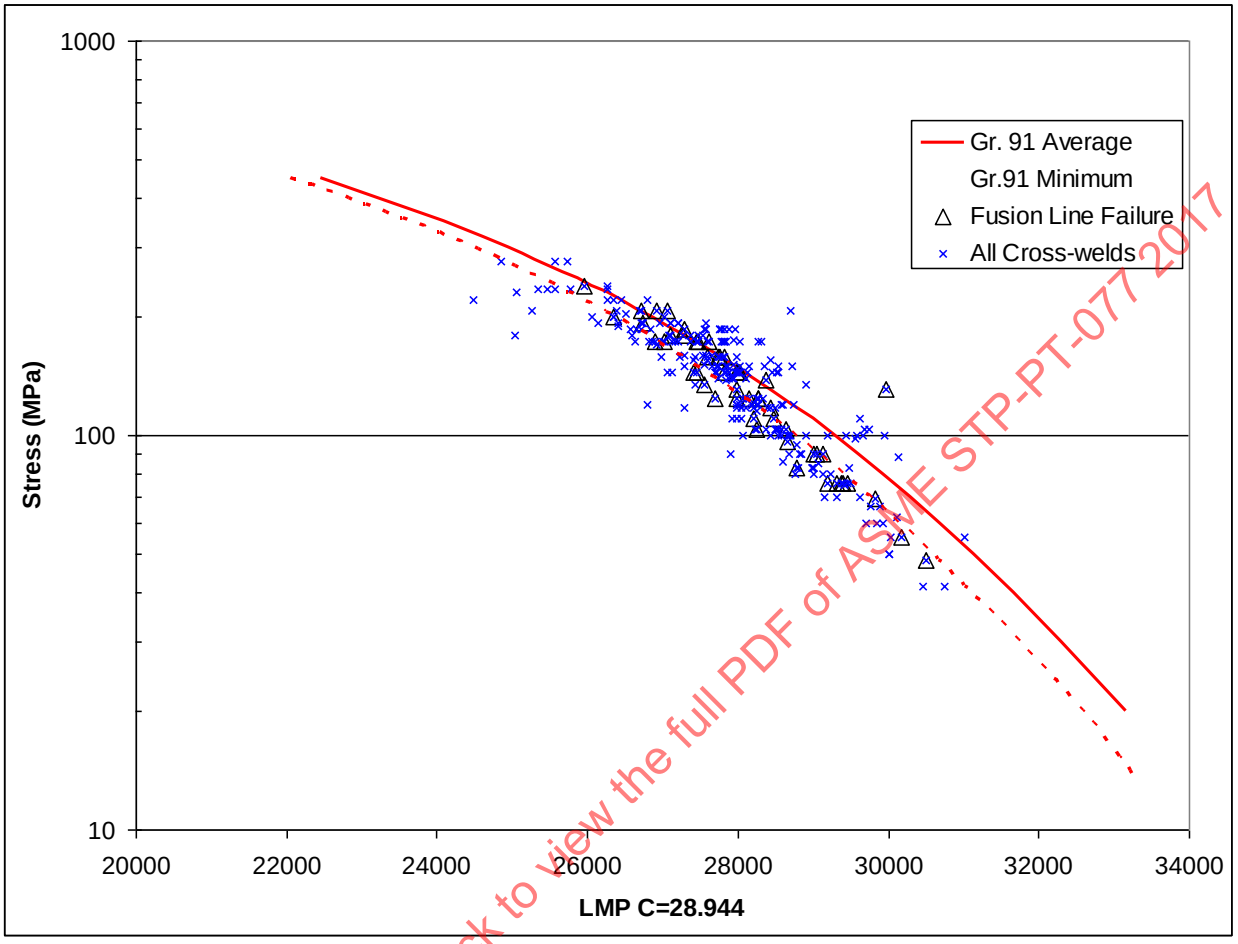

Figure 35 is a plot of the Type IV/HAZ failures for all cross-weld tests. Similar to the fusion line failures, at high stresses, ~130MPa and above, failures fall within the Gr. 91 average to minimum expectations. At lower stresses, the data clearly fall below the minimum expectations. This is consistent with recent research (see [13]) on Type IV failures. Unlike the fusion line failures, examination of the database shows these failures exhibited some degree of necking. Only one datapoint was identified as a shear failure, and in this case, it was the test at 55MPa that fell above the Gr. 91 average curve. Thus, it appears to be an outlier in the dataset. Two other outliers were examined, but no reason for exclusion from the database could be justified. The trend for Type IV/HAZ failures as reported by other researchers is clearly observed in this database. Furthermore, other data that had no failure location identified follow this same trend. Therefore, developing a representation of these cross-weld data on the basis of HAZ/Type IV failure mode should be viewed as an important improvement for evaluating the cross-weld data as compared to almost all other studies that have used full cross-weld databases without detailed examination of failure data.

Figure 35: Larson-Miller Parameter (C=28.944) Comparison of Grade 91 Base Metal Average and Minimum Curves to Cross-Welds with Type IV/HAZ Failures Identified

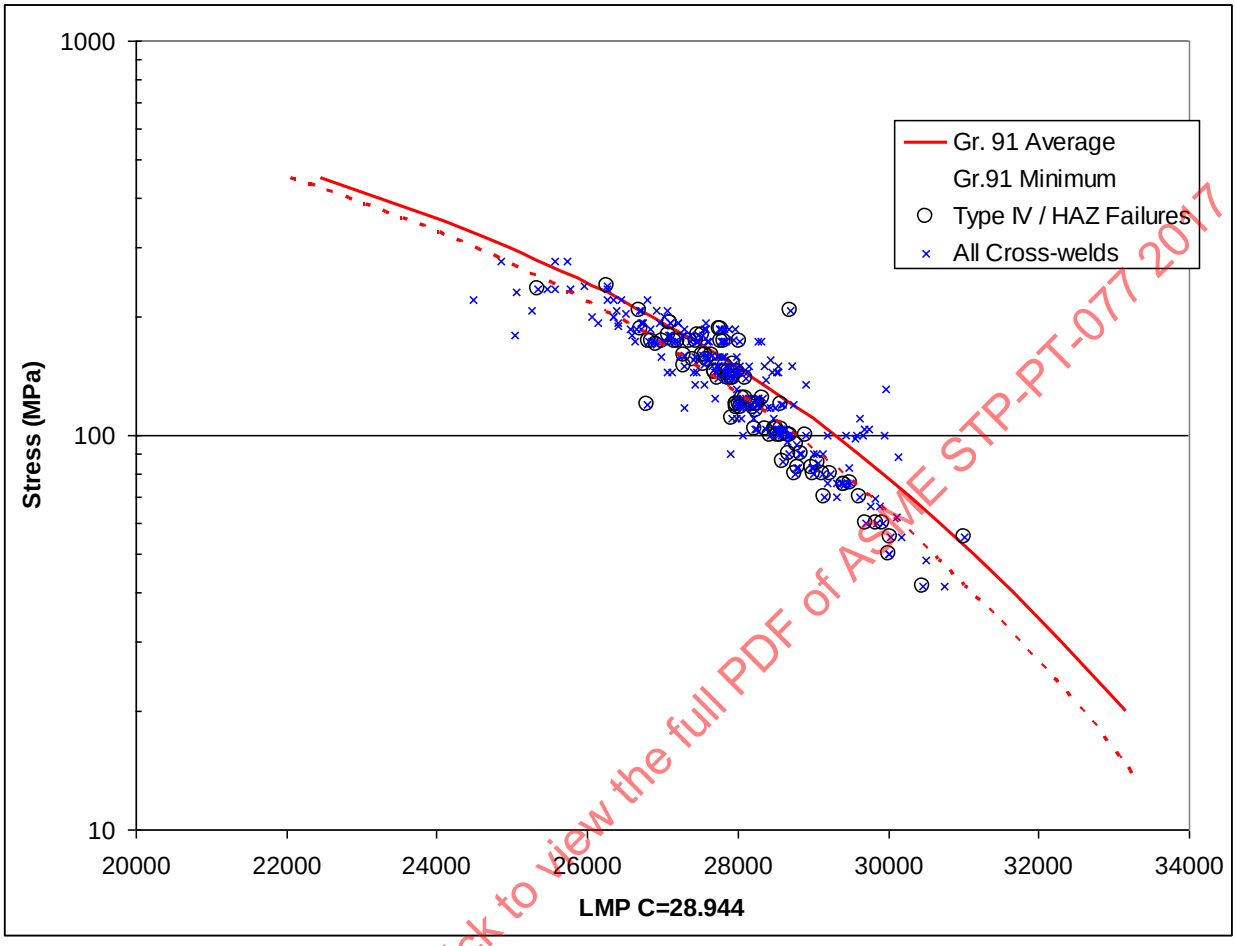

3.2 Step 2: (Analyze Data) Development of Trend Curves

Based on the qualitative assessment of the Gr. 91 weld/weldment database by investigation of failure mode, two assessments of the data appear useful. The first assessment is for the Gr. 91 weld metal. Because weld metal data were limited and generally follow the Gr. 91 database, a regression analysis was performed with the same LMP constant. A log-linear stress fit (Spera fit) was utilized to match the Grade 91 base metal as follows in equation 1:

$$\log(t_r) = A_0 + \frac{A_1}{T} + \frac{A_2 \log(\sigma)}{T} + \frac{A_3 \sigma}{T} \qquad \text{(Eqn. 1)}$$

Where A_0 is the LMP constant, A_1, A_2, *and* A_3 are the regression constants, T is absolute temperature (Kelvin), σ is applied stress (MPa), and t_r is the rupture life. The results of the regression (Weld Metal Fit) are plotted along with the data in Figure 36. Because data were limited, the fit was constrained to the base metal by using the same LMP, A_2, *and* A_3 constants (parallel fit). Because the stress range of interest may extend beyond the limits of the data in an analysis, the weld metal fit is plotted to 30MPa to ensure (visually) that there is not a gross divergence or unanticipated cross-over in the curve fit. The standard error of the estimate (SEE) in $\log(t_r)$ for the fit was calculated and is provided along with the regression constants in Figure 39.

Figure 36: LMP Plot for Grade 91 Base Metal Average and Minimum Curves with the Weld Metal Fit Curve Plotted

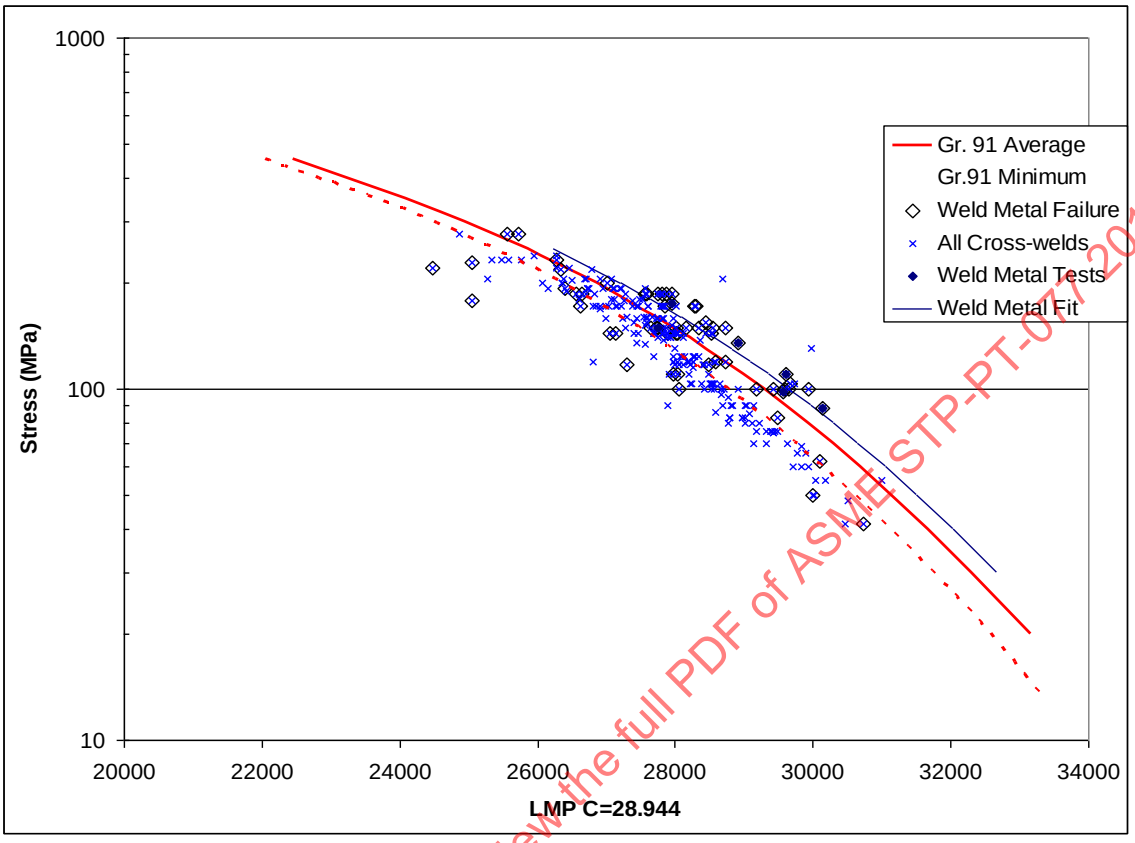

Notes: Including the Cross-Weld Data with Failures Identified in the Weld Metal and the Weld Metal Test Results

A second assessment was conducted on the HAZ/Type IV failure data. As previously described, one datapoint was identified as a 'shear' type failure and was removed from the analysis. The other outlier datapoints were retained as no technical justification was found for their removal. Additionally, two test data on large cross-weld specimens were removed from the analysis so specimen size would not factor into the analysis. Therefore, from the original 282 data collected, the HAZ/Type IV analysis was conducted on 95 cross-weld datapoints representing specimen diameters from 0.236-0.315" and weld angles from 30 to 45 degrees. Various welding processes were represented, but since all failures that were located in the fusion line, weld metal, base metal, and those not reported were censored, the weld metal was not used to limit the database. Maximum test durations exceeded 10,000 hours at multiple temperatures.

A regression was performed to minimize the error in log (t_r) for equation 1. A plot of the expected and measured rupture lives based on the regression analysis is shown in Figure 37. Three datapoints are clearly outliers and are identified by circles. From the remaining data, all but one data fall within +/- 5X on life (solid line). The slope of the data is 0.72 where unity is an ideal prediction. The low slope suggests a conservative prediction, but further inspection of the data show that the main reason for the low slope is the short-term data less than 200 hour, most of which fall above the unity line. For long-term data beyond 8,000 hour test duration, all but one datapoint fall within a +/- 2X on rupture life (shaded area), suggesting very good prediction for long-term data analysis. The SEE, found in Figure 39 along with the regression constants, is 0.409. Segmenting short-term data or using an alternate stress function to equation (1) was explored to improve the goodness of fit, but based on the predictive capability for long-term data and realizing the variation in the data (high SEE), the fit was judged acceptable for further study. To check the

applicability of using a different LMP constant from the base and weld metal, an additional assessment was performed using the same LMP constant as the base metal, but when the fit was plotted by the same method as Figure 37, the number of outlying datapoints increased. A LMP plot of the fit, the data used in the analysis, and the two large cross-weld tests (which failed in the Type IV FG-HAZ) are plotted in Figure 38.

Figure 37: Comparison of Expected and Measured Rupture Life for Fit of HAZ/Type IV Failures

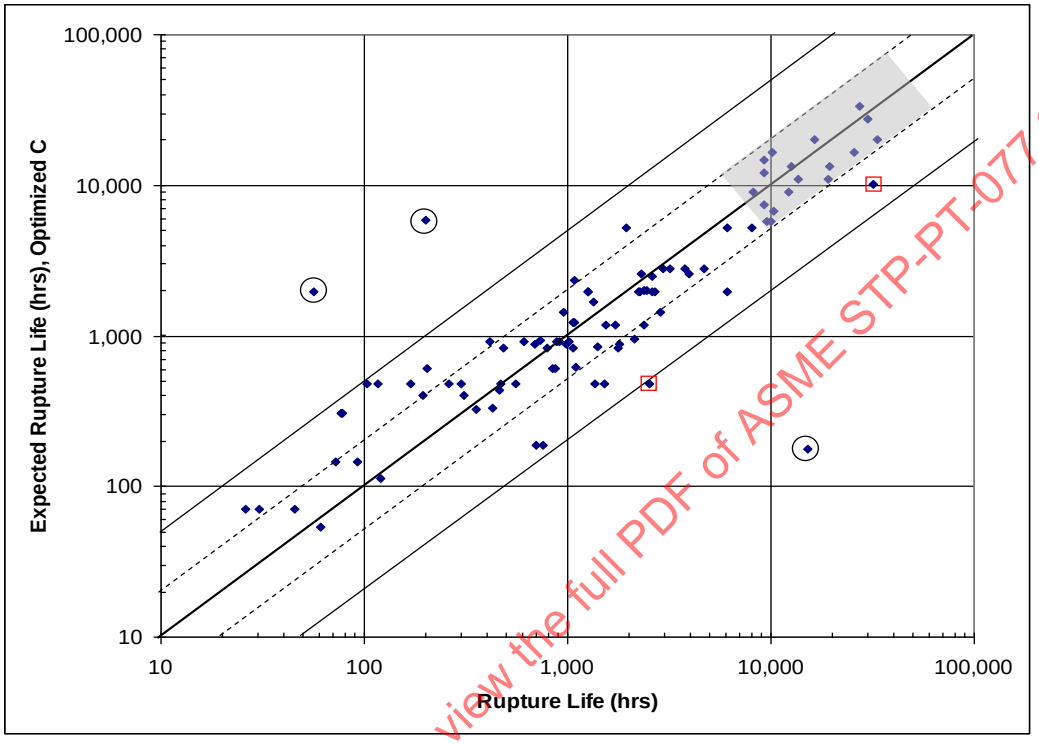

Figure 38: LMP Plot (Optimized C=24.859) of the HAZ/Type IV Data Curve-Fit Result

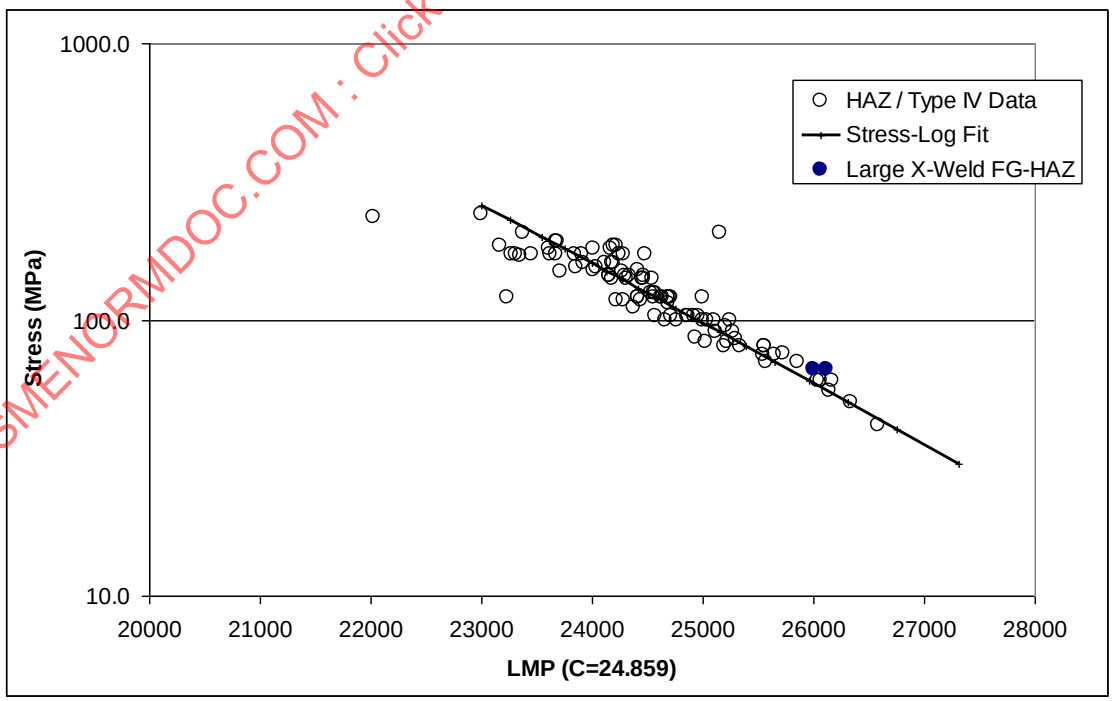

Notes: Includes the censored dataset used in the analysis and two test results on large cross-welds (X-Weld) that failed in the Fine-Grained Heat-Affected-Zone (FG-HAZ) not used in the data analysis

Figure 39: Regression Constants for Equation (1) Time-Temperature Analysis for Grade 91 Developed by Evaluation of the Database

	Base Metal (1)	Weld Metal (2)	HAZ-Type IV (3)
A_0	-2.8944469E+01	-2.8944000E+01	-2.4859059E+01
A_1	3.8871568E+04	3.9235093E+04	3.3892627E+04
A_2	-4.2069257E+03	-4.2069257E+03	-4.4428451E+03
A_3	-1.1664457E+01	-1.1664457E+01	-6.3124865E-01
SEE	0.351	0.364	0.409

(1) Equivalent to Fishburn Analysis to ASME [14]
(2) Based on weld metal only tests (not cross-weld failures)
(3) Analysis of cross-welds with reported HAZ and/or Type IV failures: diameter = 0.236-0.315", fusion-line angle = 30-45deg

To further examine the goodness of the datafits, Figure 40 through Figure 43 are isothermal plots of the predicted base metal averages, base metal minimum (1.65 standard deviations), the weld metal (WM) average prediction (Figure 39), and the HAZ-Type IV average predictions (Figure 39). For each plot, the data with failure location is plotted. Additionally, weld metal test data (weld metal only) and the large cross-weld specimen (Large X-Weld Type IV) data are plotted where applicable.

Figure 40 is the isothermal plot at 550°C. The divergence of the HAZ-Type IV prediction with decreasing stress is observed at long-times. In general, all of the observed failures, whether HAZ-Type IV, weld metal, or fusion line all fall within the scatterband for the Gr. 91 base metal as expected by the prediction.

Figure 41 is the isothermal plot at 593°C. Again, the divergence of the HAZ-Type IV prediction with decreasing stress is observed. The short-term data fall within the base metal scatterband. The weld metal failures are generally above the Gr. 91 average as predicted by the WM-Average curve. At long-times, the fusion line failures trend with the HAZ-Type IV failures. Because the fusion line failures were not included in the analysis of the data, this suggests that the fusion line failures may be the result of the same failure mechanism observed in the HAZ-Type IV failures, that some fusion line failures may in fact be located in the HAZ, or the life of the weldments may be reduced due to a difference in strength between the base metal and weld metal where damage is preferentially located at the fusion line. In any case, the HAZ-Type IV failure prediction appears to work well to describe the fusion line failures.

Figure 40: Comparison of Predictions in Figure 39 Plotted with Data at 550°C

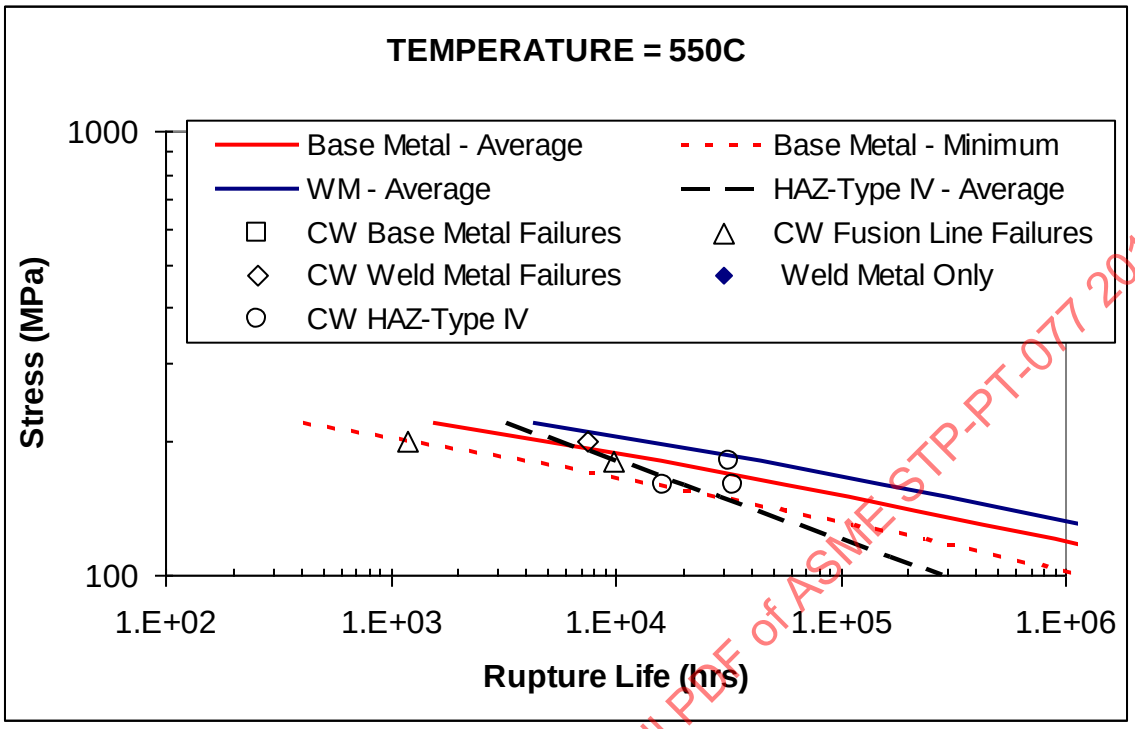

Figure 41: Comparison of Predictions in Figure 39 Plotted with Data at 593°C

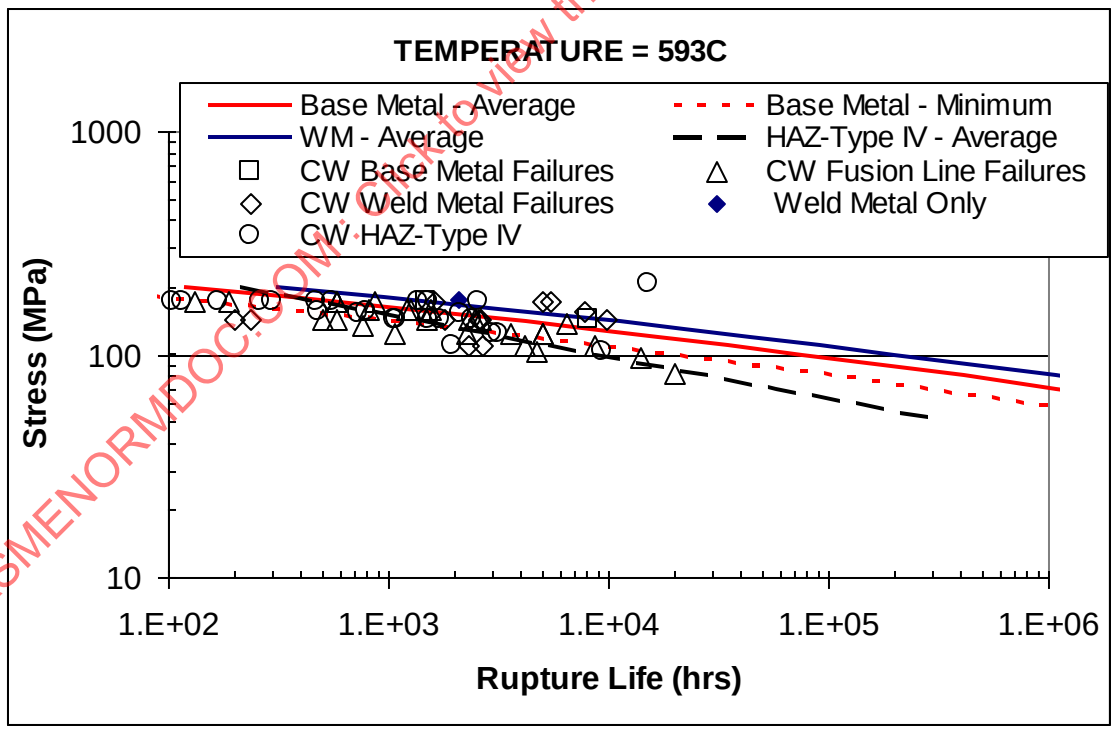

Figure 42 is the isothermal plot at 600°C. The failure data strongly support the predictions at these temperatures. Weld metal failures, with only a few exceptions, trend with the WM-average line above the

Gr. 91 base metal average. Type IV failures clearly diverge with decreasing stress, with the HAZ-Type IV trendline intersecting the observed failures.

Figure 43 is the isothermal plot at 650°C. Data from tests conducted at 649°C are also included in the plot. The weld metal data meet the expectations of the WM-average curve. Both the HAZ-Type IV failures and the fusion line failures are in good agreement with the HAZ-Type IV trendline. The large specimen cross-weld data are slightly higher than the expected HAZ-Type IV trendline, but below the base metal minimum.

Overall, Figure 40 through Figure 43 show that the analysis and trendline found in Figure 39, which are based on data censored by failure location and specimen size/configuration, well describe the entire database of Gr. 91 weld/weldments. Figure 44 is a comparison of the predicted stress for rupture in 100,000 hours for the base metal average and HAZ-Type IV average expected stresses at the temperatures in the previous figures. The ratio between these stress levels is also calculated. Compared to WSRFs proposed in other research [13], most notably Japan, they are more pessimistic. This may be because they are based on an optimized assessment of a database censored on the basis of failure location. It should be noted that these ratios are not WSRFs because specimen size and application to seam weld geometries are not included in this comparison. Analysis of these data will be provided in the later sections.

Figure 42: Comparison of Predictions in Figure 39 Plotted with Data at 600°C

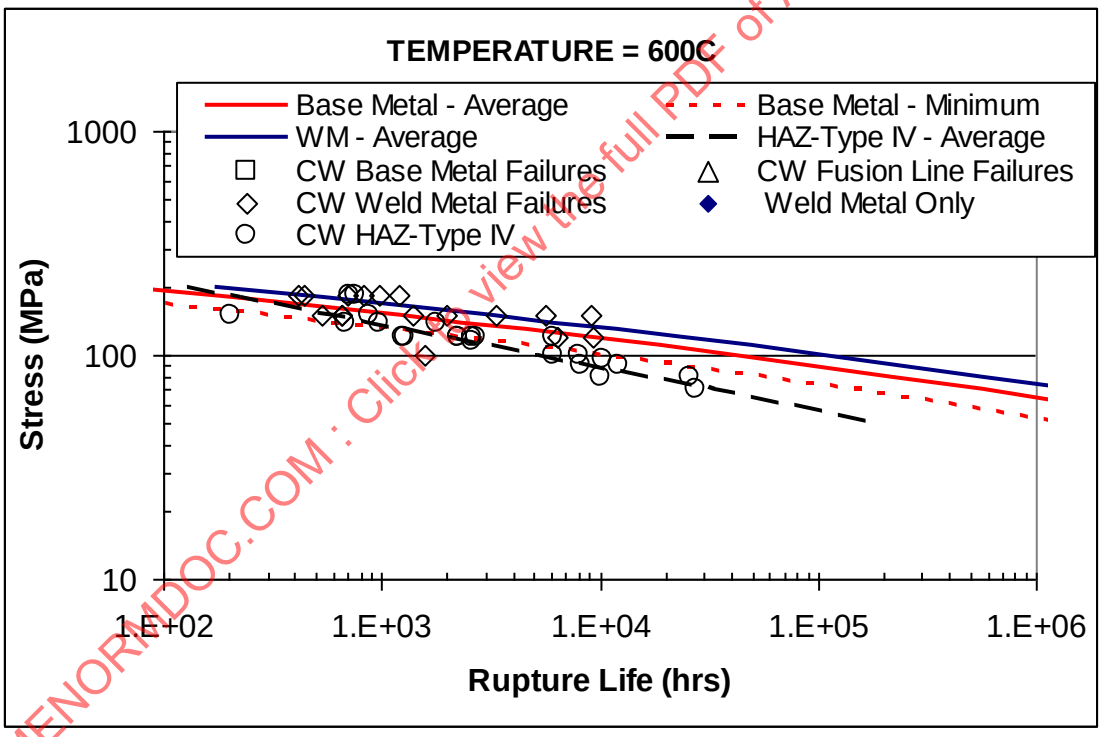

Figure 43: Comparison of Predictions in Figure 39 Plotted with Data at 649/650°C

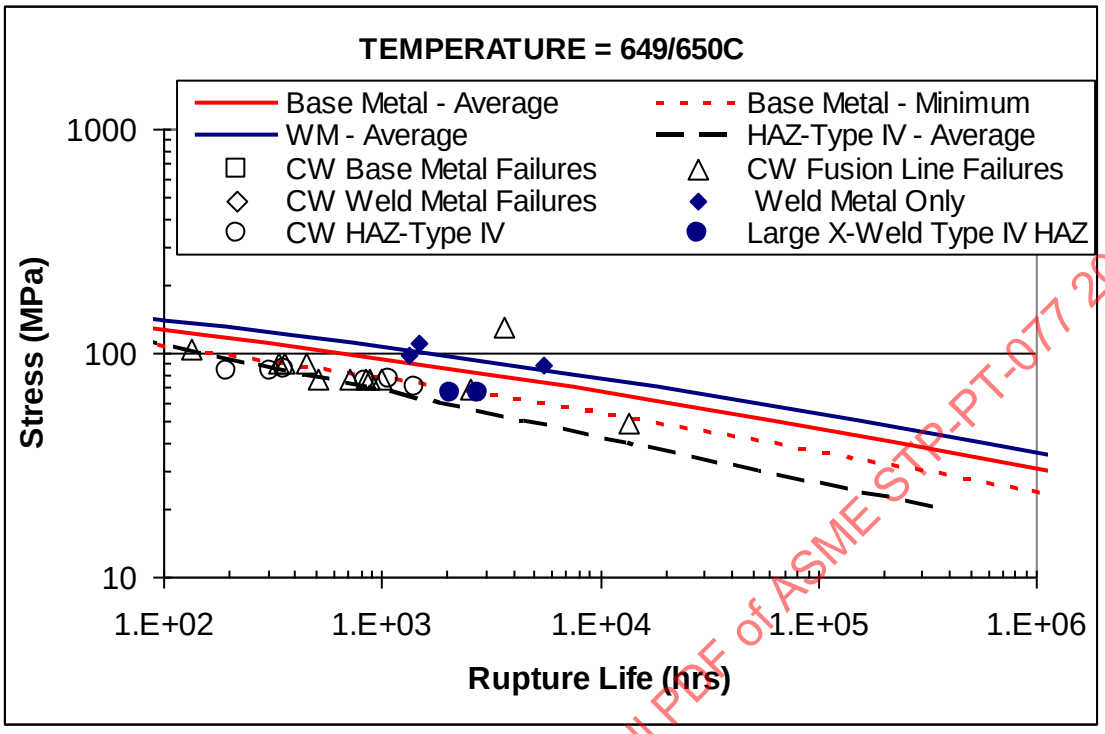

Figure 44: Stress (MPa) for 100,000 Hour Predicted Average Rupture Life for Grade 91 Base Metal and HAZ-Type IV Failures

Temperature (°C)	550	593	600	650
BM - Average	151.3	96.8	89.0	46.2
HAZ-Type IV - Average	120.3	63.0	56.7	26.4
Ratio:	*0.80*	*0.65*	*0.64*	*0.57*

3.3 Step 3: Extracting the Base Material Strength Factor

As noted in Chapter 1, we seek to explain the cross-weld trend lines in Figure 40 through Figure 43 with:

(a) A base material strength factor (BMSF)
(b) A basis for the transition from effective stress behavior to MPS behavior.

The method is as follows:

(a) Perform a limit analysis of a representative or typical cross-weld test specimen geometry. In this case we consider a 0.25" diameter specimen with a 0.08" wide weak HAZ at 35° to the transverse cross section. Figure 45 shows the maximum principal stress distribution at the maximum load before the limit analysis failed to converge. The outputs from the analysis for each load step up to the limit are for the point or points with highest MPS:
  (1) Maximum principal stress
  (2) Effective stress
  (3) Plastic strain
  (4) Load
(b) Then for a particular sample test stress the following quantities are calculated:
  (1) MPS = test stress x limit MPS / limit load
  (2) Effective stress = test stress x limit effective stress / limit load.

(3) Note: these quantities may depend on which point in 1 is used. It is usually clear which is the region of highest MPS in the limit analysis. The associated plastic strain may be compared with a calculated creep strain at the effective stress. This gives a basis for selecting a particular load step to define the MPS and effective stress to characterize the component or sample.

(c) These stresses divided by the base material strength factor (BMSF) may then be used to calculate rupture life to match cross-weld data.

(d) If there is an indication that some combination of effective stress and MPS should be used to calculate rupture, then the following procedure is used.

(1) Using ASME FFS-1 data [15], [16], the ratio (omega/creep exponent) is calculated for the effective stress in 2. It is postulated that as this ratio increases, the rupture behavior will be driven increasingly by MPS. Conversely, as it decreases, the rupture behavior will be driven increasingly by effective stress.

(2) The limits of this ratio for the transition from one type of behavior to the other are calculated to match cross-weld data.

(3) It may be seen that the change in slope of the crossweld rupture, which is clear in the Grade 91 data and trend plots, is associated with this transition. The implication is that if lower stress cross-weld data existed, it would indicate a second change in slope, returning to the slope of the base metal or weld metal trends.

(e) A confirmation of the limit analysis prediction should be made with a creep analysis. This turned out to be more difficult with the ASME FFS-1/API 579 Grade 91 data than for Grade 11 and Grade 22 data, for reasons that are not clear, but the significant discrepancies between it and the ASME III NH data may be associated with the problem.

Figure 45 shows maximum principal stress distributions in the standard crossweld specimen, indicating finite internal volumes over which maximum principal stress driven damage is expected to initiate. Internal/subsurface damage initiation in the HAZ of Grade 91 is an observed failure mode. Figure 46 through Figure 48 show the results of the strength factor calculations. The conclusion is that the base metal strength factor (strength of the weak Type IV region) accounting for cross-weld behavior depends on temperature, with the value being 0.95, 0.85, and 0.82 for 550°C, 600°C, and 650°C, respectively.

Figure 45: Distribution of Maximum Principal Stress (MPS) in the Weak HAZ of the 0.25”Diameter Cross-weld Tensile Specimen for 66 MPa Tension

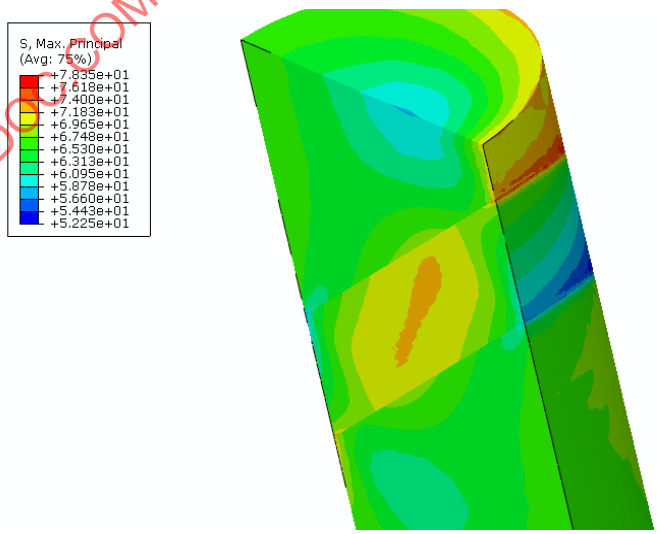

Notes: Note the predicted initial failure locations on specimen center and HAZ edges

Figure 46: Comparison of Average HAZ and Other Trendlines with Predicted Cross-weld Behavior (550°C) Using a Base Metal Strength Factor =0.95

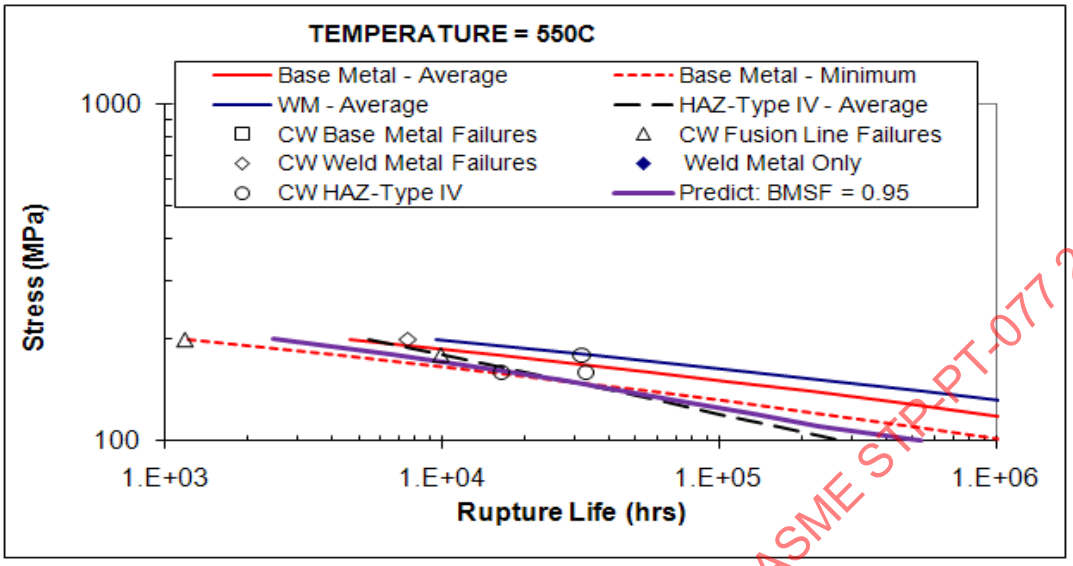

Figure 47: Comparison of Average HAZ and Other Trendlines with Predicted Cross-weld Behavior (600°c) Using a Base Metal Strength Factor =0.85.

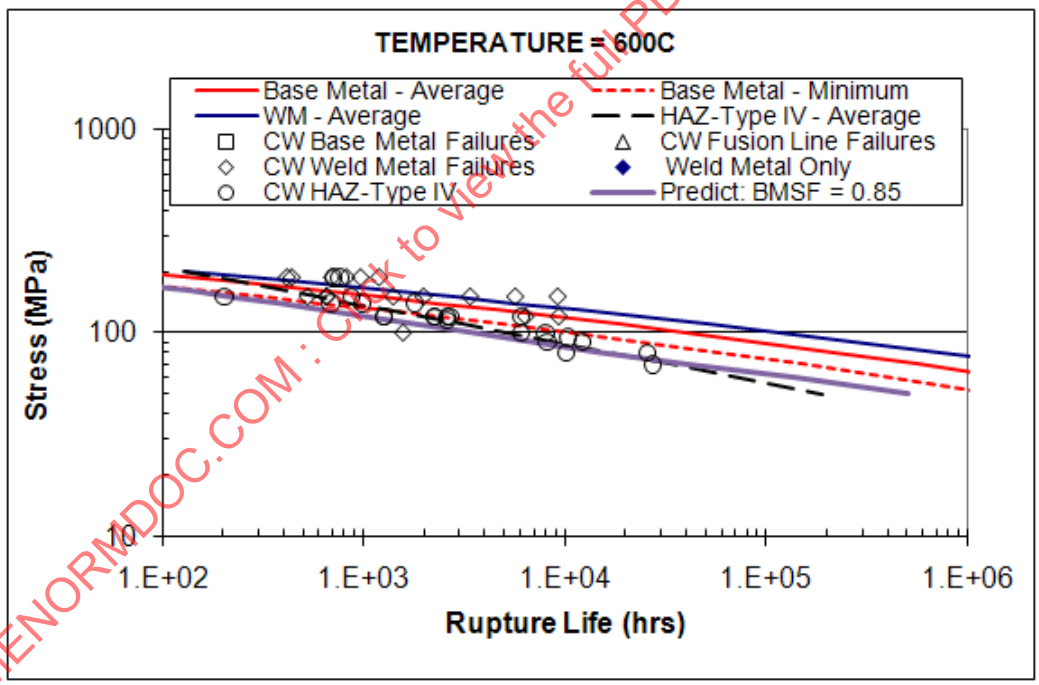

Figure 48: Comparison Of Average HAZ And Other Trendlines With Predicted Cross-weld Behavior (650°C) Using A Base Metal Strength Factor =0.82

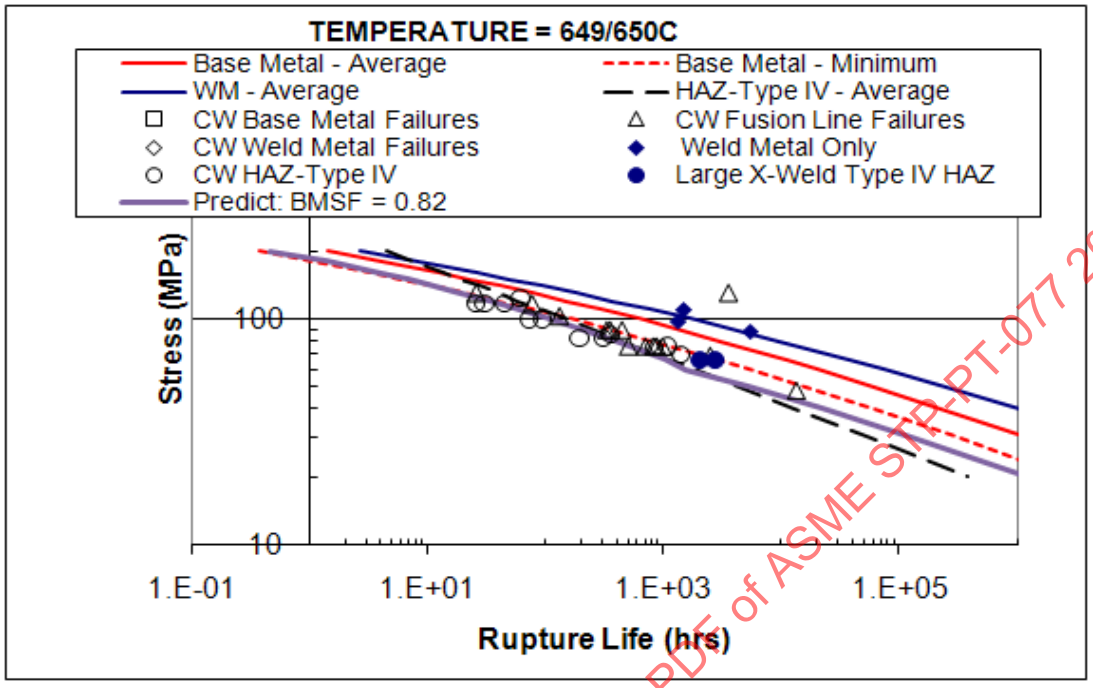

3.4 Step 4: Testing Assumptions Against Non-Standard Specimens

Two non-standard uniaxial cross-weld tests were identified to test the base material strength factor. Some description of the specimens and test results is provided in the following sections.

3.4.1 Masuyama Specimens

Masuyama [17] tested large specimens 40mm x 32mm with two different weld geometries (U & X groove) as shown in Figure 49. The test condition was 650°C-66MPa and the results are given in Figure 53. The U groove had slightly longer rupture life compared to the X groove which was slightly longer than the estimated life from standard specimen tests. The rupture times were relatively short, less than 3,000 hours, and the estimated Type IV life from the equation in Figure 39 was 1,142 hours (Figure 44). Figure 50 contains post-test metallographic assessment of the specimens. Failure was confirmed in the Type IV HAZ region, but interestingly, the side of the weldment that did not fail, showed cracks originating from the surface. Typical long-term Type IV failures in Grade 91 generally manifest themselves as subsurface cracks.

This contradiction in failure mode supports a transition in failure mode from effective stress to maximum principal stress.

Figure 49: Large U and X-Groove Specimens Evaluated by Masuyama [17]

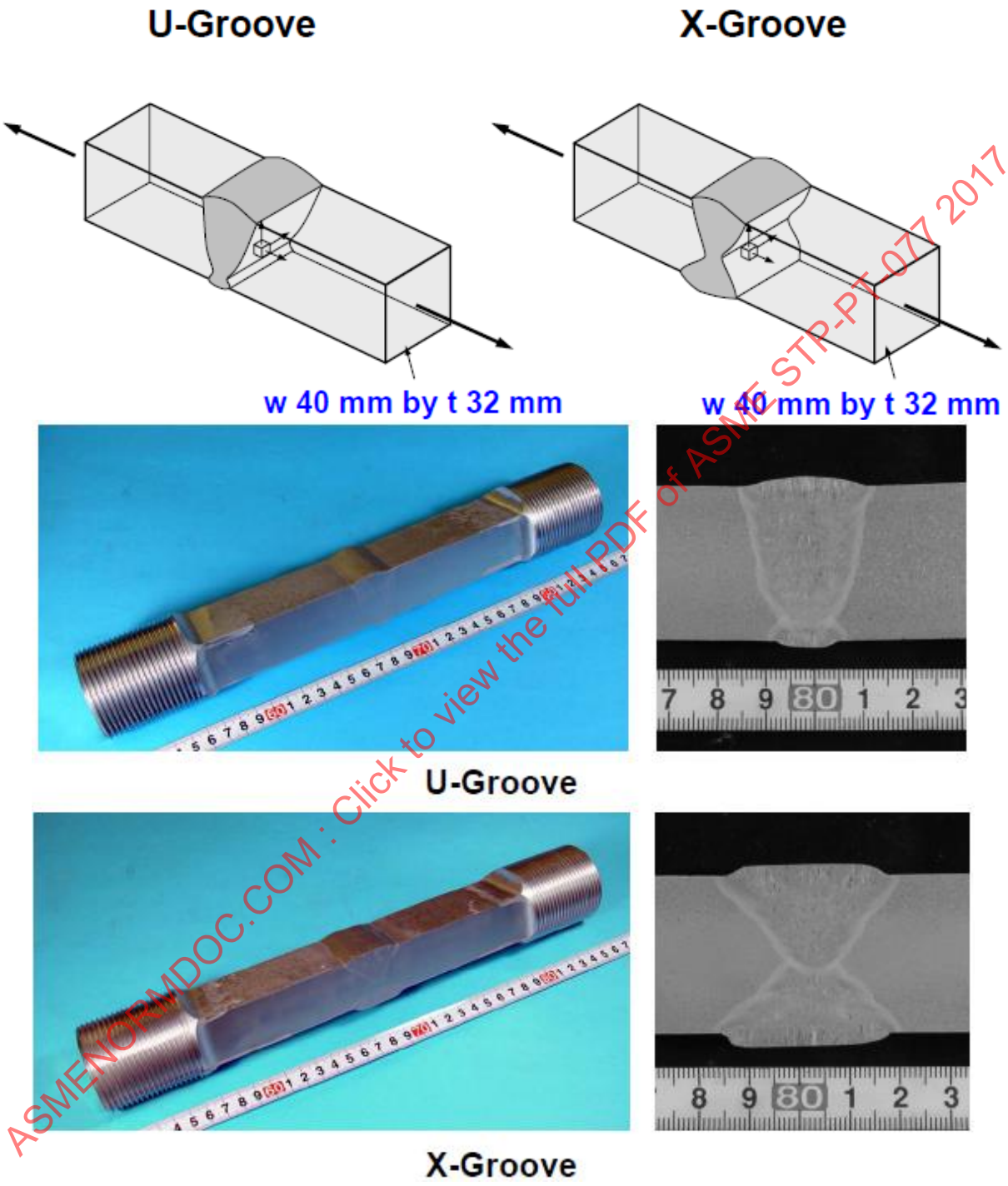

Figure 50: Test Results for Large Cross-Weld Specimens Tested at 650°C-66MPa [17]

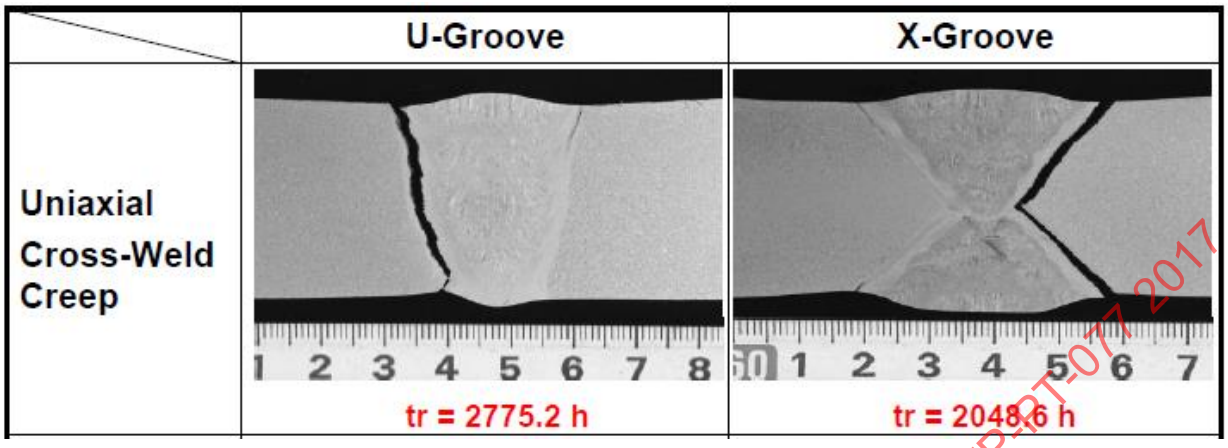

Figure 51: Limit Analysis of Masuyama 32 mm x 40 mm Tensile Specimen Showing the Predicted Weak Zone MPS Failure Location on the Center (Symmetry) Plane

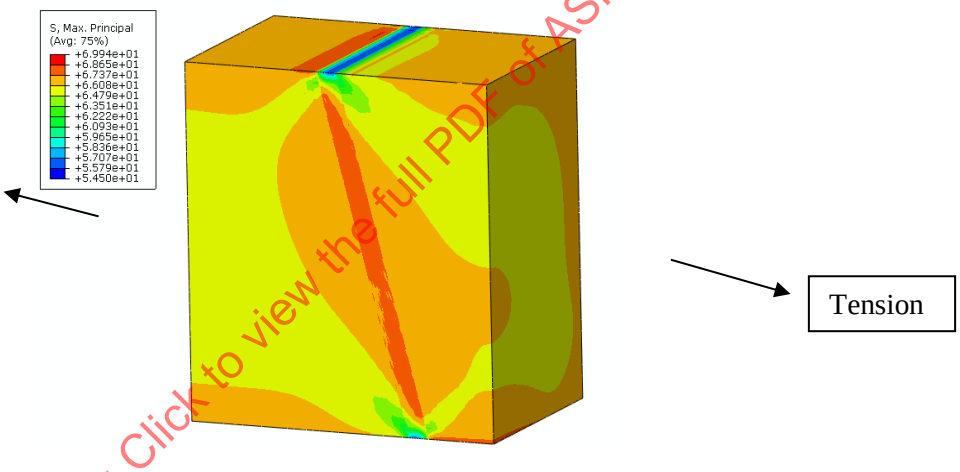

Figure 51 shows maximum principal stress distributions in the Masuyama specimen, indicating finite internal volumes over which maximum principal stress-driven damage is expected to initiate. The time to rupture results for the modeled Masuyama specimen are provided in Figure 53. The value for the BMSF was 0.82. For the test conditions, the model predicts the Masuyama specimen will have an ~2X improvement in life compared to a standard specimen, which is in very good agreement with the experimental data.

Figure 52 illustrates the key differences between the 0.25" diameter (standard) cross-weld and Masuyama specimens that as inelastic strain accumulates, effective stress and maximum principal stress change different ways. The nominal (loading) stress is 66 MPa. As creep strain accumulates, maximum principal stress increases from 66 MPa to 80 MPa. The effective stress decreases from 66MPa, to 60 MPa for the standard specimen, and to 40 MPa for the Masuyama specimen. Therefore, depending on whether the controlling rupture stress is effective stress, maximum principal stress or a combination, the different specimens could exhibit strengthening or weakening. A second implication of these stress histories is that, with the reduced effective stress, creep strain rates will be correspondingly reduced, and when the failure surfaces are examined, they will appear to have reduced ductility compared with less constrained failures. Therefore, the observed low ductility in multiaxial conditions may be at least partially due to the relatively low effective stress, rather than a material degradation. Section 3.4.2 shows the size and constraint effects

on life for the tensile cross-weld specimens, the Masuyama 32 x 40 mm specimen, and two EPRI specimens with different weld angles.

Figure 52: Calculated Changes in Stress for the Two Cross-weld Specimens Considered

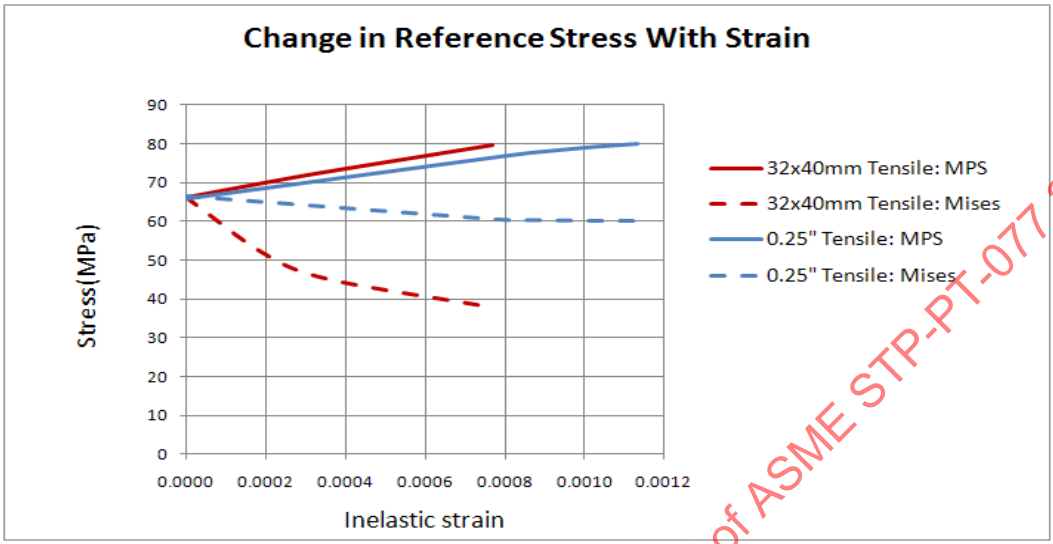

Notes: Note the significant reduction in effective stress predicted for the 32 x 40 mm (Masuyama) specimen (Section 3.4.1).

Figure 53: Table of Comparison of Time to Rupture and Estimated Time to Rupture for Grade 91 Large Specimen Cross-Weld Tests

650°C-66MPa	Time to Rupture (hrs)
Grade 91 Base Metal - Average	11029.6
HAZ-Type IV (analysis of std. specimen size cross-welds – Figure 39)	1141.6
Masuyama Large X-Groove	2048.6
Masuyama Large U-Groove	2775.2
Prediction (This work) U-Groove (BMSF = 0.82)	1600 - 2800

3.4.2 EPRI Large Specimens

EPRI is currently conducting a research program on Grade 91. Data from this project have not been made available in this publication or in the database, but some non-standard cross-weld tests are being conducted [18]. The results for one such test are given in Figure 56. Figure 54 is a sketch of two Grade 91 cross-weld specimens made with typical B-9 filler metal using identical welding processes with the only variable changed as the joint angle. The results in Figure 56 show the joint with a 10 degree angle had over two times the life of the same weld with a 37.5 degree angle. The HAZ equation for standard cross-welds gives a life of ~2,500 hours for the test condition, which is just shy of the measured life of the 37.5 degree sample. Using the same methodology and data as described previously, life estimates were performed for Grade 91 material and welds. Figure 55 shows the MPS distribution calculated for these specimens. Results for time to rupture (initiation) are given in Figure 56, which are in excellent agreement with experimental measurements. To illustrate the effect of specimen size and geometry, Figure 57 plots the calculated time to rupture as a function of applied stress for the standard specimen, Masuyama single-V specimen, and the EPRI specimens.

Figure 54: Sketch of Cross-Weld Specimen Configuration for EPRI Tests [18]

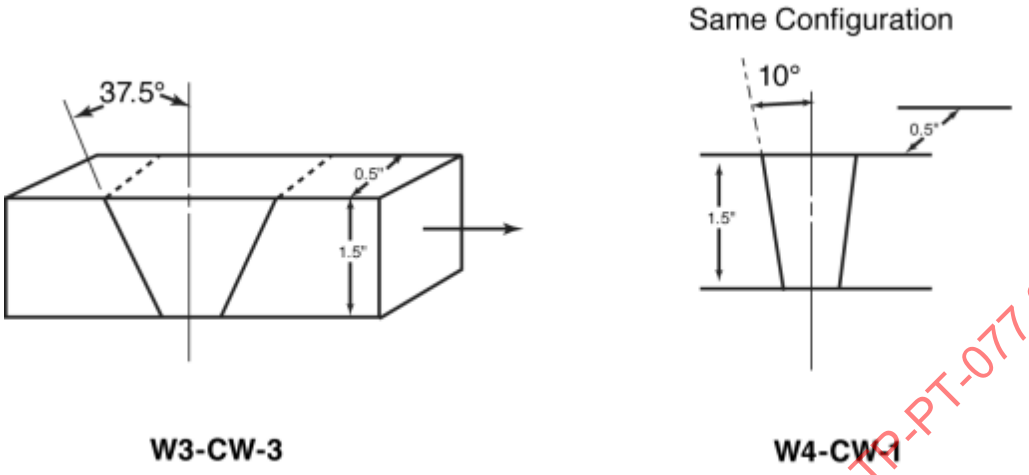

Figure 55: Limit Analysis Maximum Principal Stress Plots on Symmetry Planes of EPRI 37.5^0 and 10^0 Samples

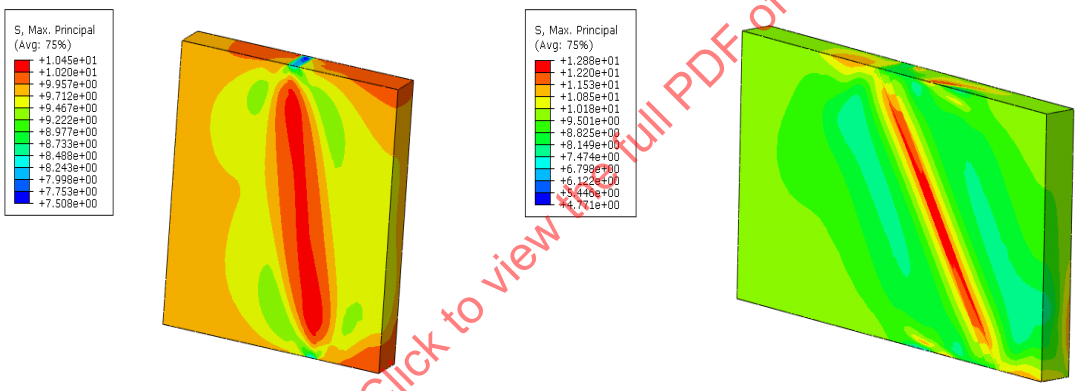

Figure 56: Comparison of Time to Rupture and Estimated Time to Rupture for EPRI Grade 91 Cross-Weld Tests [18]

625°C-80MPa	(Estimated) Time to Rupture (hrs)
Grade 91 Base Metal - Average	24,415
HAZ-Type IV (analysis of std. specimen size cross-welds – Figure 39)	2579.5
EPRI 37.5° angle (75°V – 1.5" thick) W3-CW-3	2850
EPRI 10° angle (20°J – 1.5" thick) W4-CW-1	6250
Prediction 37.5^0	2410
Prediction 10^0	6580

Figure 57: Predictions of Grade 91 Cross-weld Tests Show Strengthening Effect of Constraint for a Wide Range of Stress for Both Sets of Non-Standard Samples Analyzed

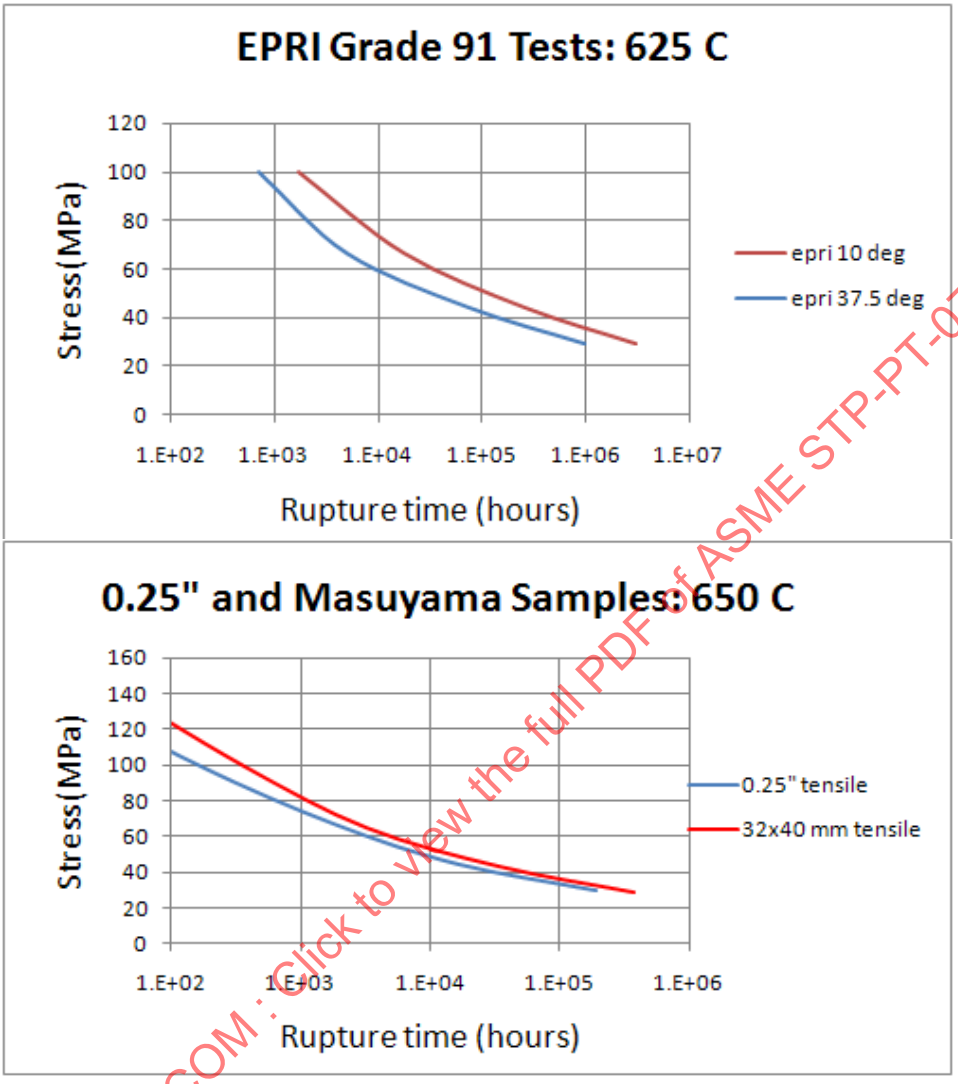

3.5 Step 5: Application to Welded Structures

Seamweld life prediction

The calculation of welded joint life proceeds along the same lines as used to analyze cross-weld specimens. The effective stress to maximum principal stress transition may be modeled if there is a basis for the required parameters. If not, it is conservative, and recommended for design, that the maximum principal stress is used. In this section, the method is illustrated for a heavy Grade 91 pipe section with a 10^0 "U" groove weld and a thinner 'hot reheat size' X-groove.

The application of the analysis methods to a heavy walled pipe geometry (shown in Figure 58) is as follows.

Figure 58: Seamweld HAZ Model Pipe OD = 762 mm, ID = 427 mm, Weak HAZ Width = 2 mm, Weld Semi-Angle = 10^0

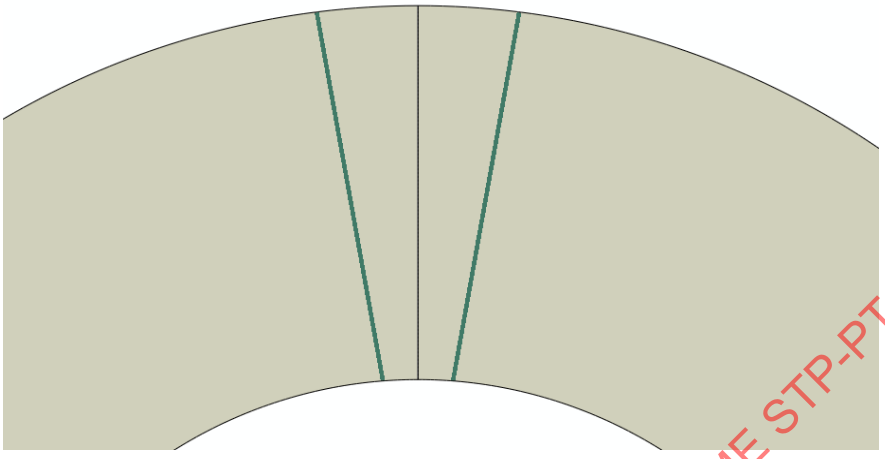

Figure 59 and Figure 60 show the results from the limit analysis. The area of highest maximum principal stress is on the OD, as a result of re-distribution from the bore due to yielding. The value of MPS in the weak zone is no higher than the plain pipe OD value. Maximum inelastic strain occurs in the bore in the weld region. Figure 61 shows the development of OD von Mises and Tresca stresses as yielding occurs.

The weldment design and life predictions are shown in Figure 56. Two approaches are used.

The life assessment calculation follows the description given above. The HAZ maximum principal stress is modified by the BMSF, which is the derived material strength factor from cross-weld data in Figure 46 through Figure 48. For each of the three temperatures, the internal pressure is calculated which gives a predicted life of 100,000 hours, based on the mean base metal trend lines. These pressures are then used to calculate design stresses using the design calculation S = p/ln(OD/ID), where p = design pressure. (The stresses are clearly higher than realistic design stresses; the use of 100,000 hours to define rupture stress is convenient and typical.) The "design" lives associated with these stresses are then calculated from the design stress, modified by a weldment strength reduction factor (WSRF). In general, these will be different from the BMSF's, depending on the weld joint analysis. In this case it was found that the weldment weak zone did not weaken the joint more than the BMSF. This should mean that the design and calculated lives are the same. In this case there is a slight discrepancy due to the calculated MPS being slightly lower than the design calculation. (This may be due to the limit analysis not getting to the theoretical limit pressure. Smaller minimum increments could improve the result).

The conclusion is that for this weldment geometry, WSRF = BMSF.

Figure 59: Distribution of Inelastic Strain Prior to Collapse. High Strain is Localized in Bore

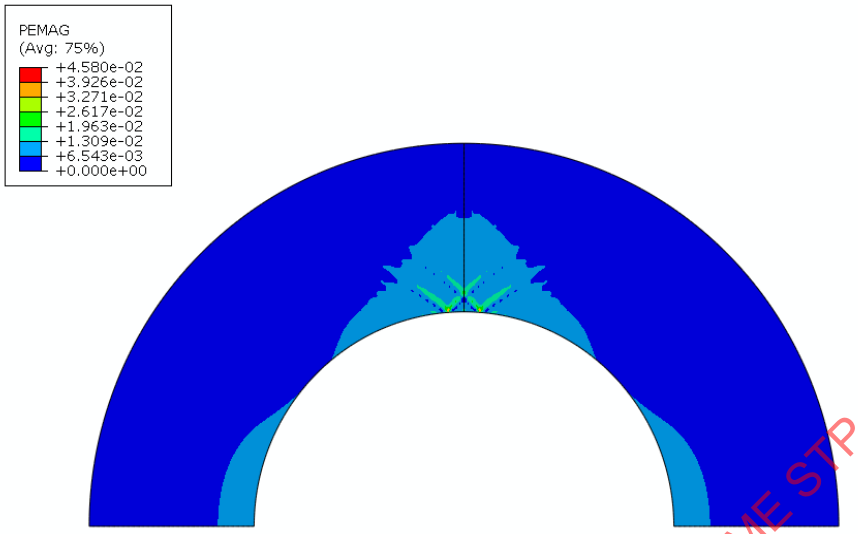

Figure 60: Distribution of MPS Prior to Collapse

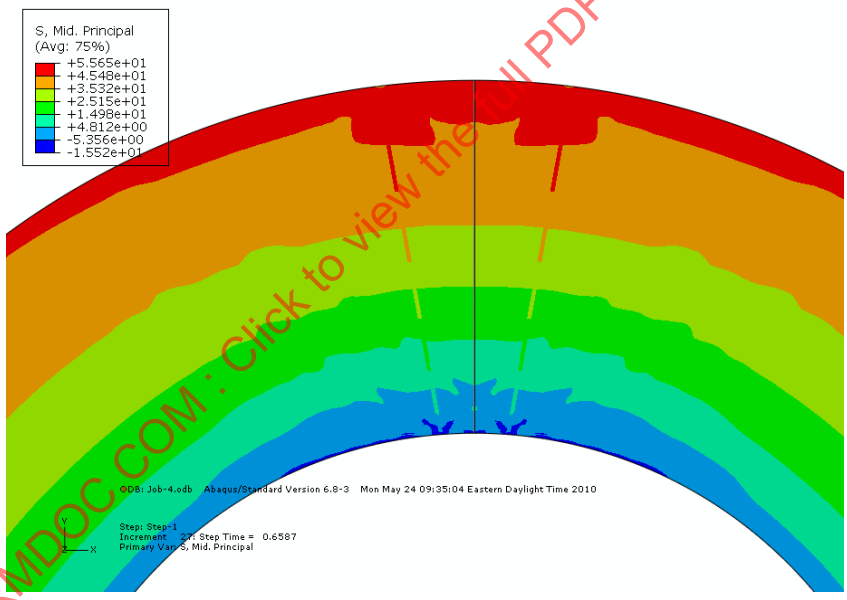

Notes: HAZ values similar to general OD values.

Figure 61: Development of HAZ Stress Near OD with Creep Strain and Time

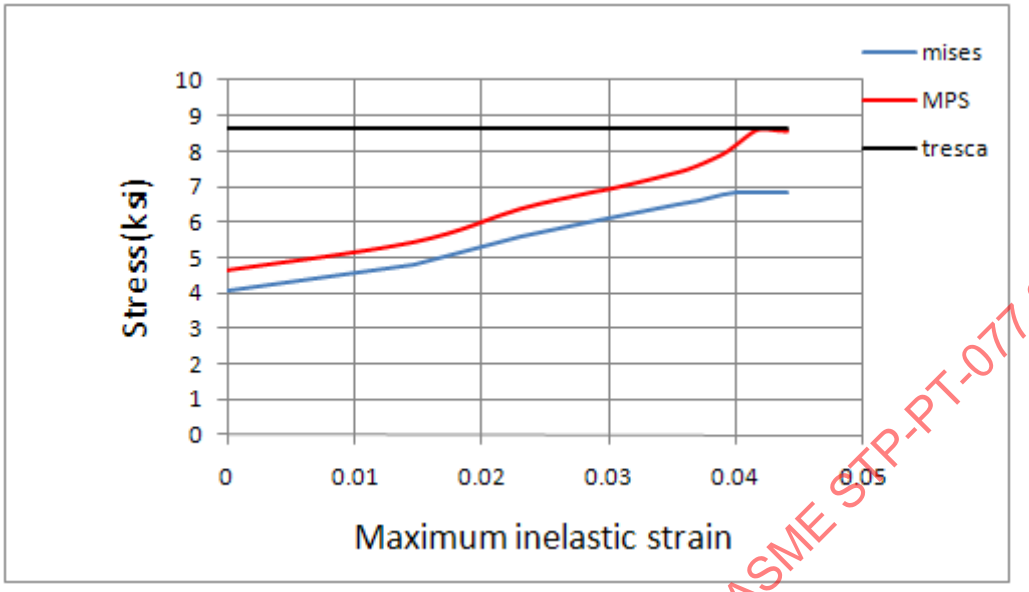

Notes: Redistribution from bore to OD and effects of constraint can be seen.

Figure 62: Calculation of Joint WSRF: Single Sided "U" Weld

		Life assessment		Design			
Temperature C	Pressure MPa	MPS	BMSF	Life hours	Tresca stress	WSRF	Life hours
550	10.44	140.7	0.95	100000	137.7	0.91	99999
600	5.61	75.6	0.85	100000	74.0	0.83	100000
650	2.81	37.9	0.82	100000	37.1	0.80	100000

To compare the 'heavy wall' U-groove pipe section (diameter:thickness ratio of ~4.5), a thinner wall seam-welded pipe with an X-groove configuration (diameter:thickness ration of ~ 26) was modeled in the same manner using the same input data. Figure 63 depicts the geometry of the pipe section and Figure 64 shows the distribution of the MPS. Careful inspection of the results show a high-stress region in the cusp of the HAZ. Figure 65 provides the model results for the same three temperatures.

Figure 63: "X-groove" Weld Geometry in 20" OD x 0.76" Thick Pipe

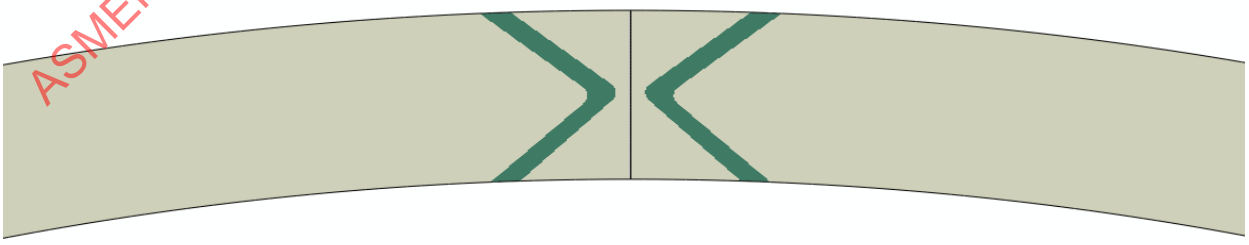

Figure 64: Position of Maximum HAZ Maximum Principal Stress

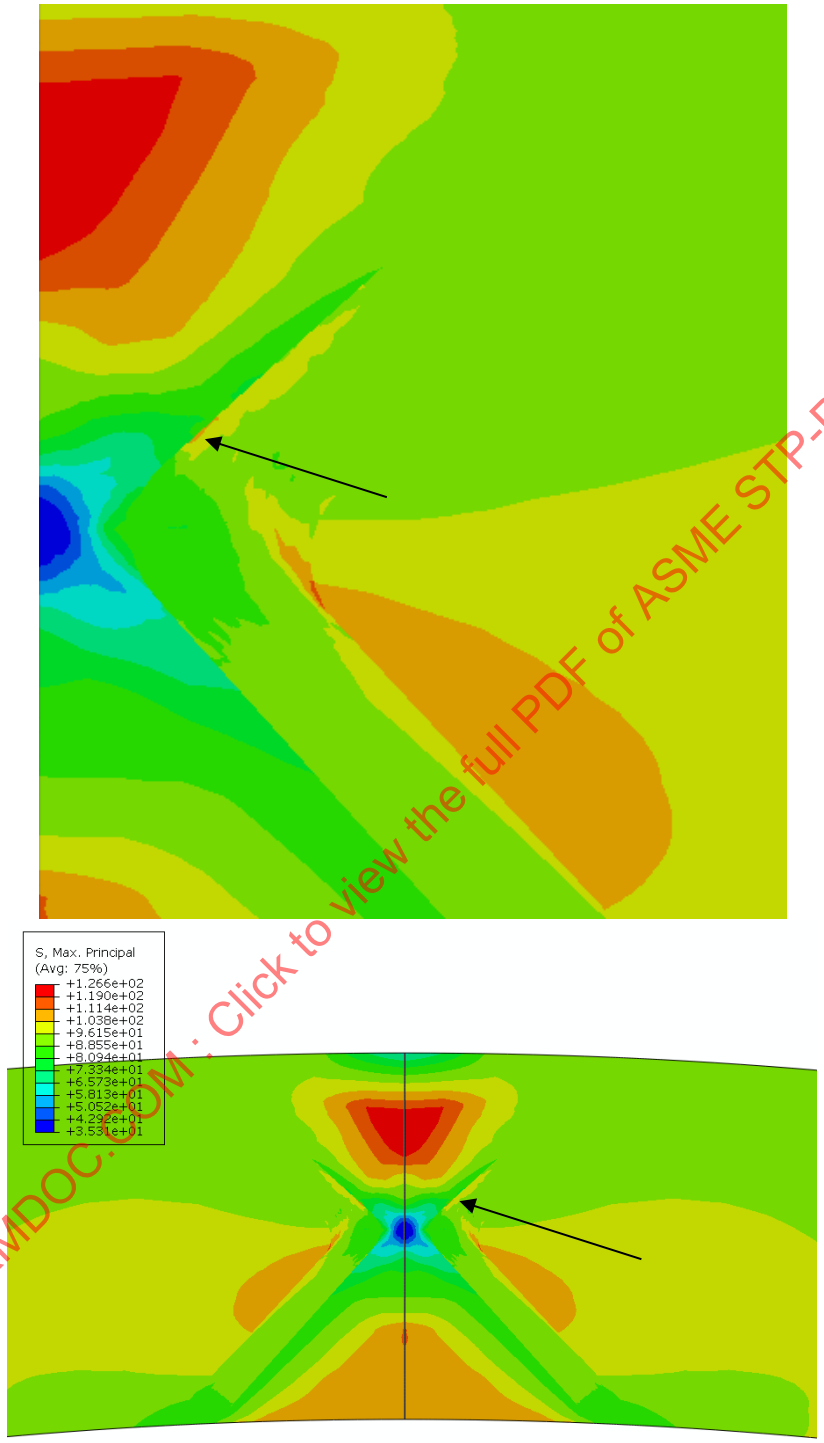

Figure 65: Calculation of Joint WSRF: "X-Groove" Configuration

		Life assessment		Design			
Temperature C	Pressure MPa	MPS	BMSF	Life hours	Tresca stress	WSRF	Life hours
550	10.44	140.7	0.95	100000	137.7	0.91	99999
600	5.61	75.6	0.85	100000	74.0	0.83	100000
650	2.81	37.9	0.82	100000	37.1	0.80	100000

In Figure 56 and Figure 62, comparisons are given of life assessment calculations based on finite element limit analysis with the BMSF, and design calculations, where a different WSRF from the BMSF may be necessary. In the case of the single "U" weld, there is no significant difference. In the case of the "X-groove" weld, there is a minor difference. These results show that in order to obtain the design WSRF, an analysis of the weld geometry is important and will affect results.

3.6 Step 6: (Design Strength Ratio) Summary & Implications for WSRFs

In this chapter a critical assessment of the Grade 91 weld/weldment database was conducted. The analysis showed the behavior of standard cross-weld failures identified as Type IV-HAZ resulted in strength factors as a function of time and temperature. Applying the methodology developed on this project, the BMSF was found to be a function of temperature. Effects in non-standard large specimens from two independent studies with different weldment configurations were captured by the model even though the data were not used in the initial data analysis. Plots of changes in effective stress states as a function of specimen size, test time, and strain helped explain the experimental observations from these tests. The model and inputs were then applied at three temperatures to two seam-weld pipe geometries representing two piping extremes: a thick-walled U-groove 'main-steam' pipe and a thin-wall X-groove 'hot-reheat' pipe geometry. These two geometries, using the same input data and BMSFs, produced differing WSRFs at 100,000 hours. For the thick-section weld, time to damage initiation was essentially the same as the calculated BMSFs, but for the thin-section X-groove, damage initiation was predicted at slightly shorter-times (or higher-stresses) leading to WSRFs lower than the BMSFs.

A comparison of the standard cross-weld analysis, the determined BMSF, the 100,000 hour U-groove pipe WSRF, the 100,000 hour X-Groove WSRF, the current ASME Section I WSRFs, and a Japanese analysis from the Task 1 report is shown in Figure 66. Clearly, the ASME Section I/B31.1 WSRF's are conservative compared to any other analysis. The analysis of the standard cross-welds in this work are in generally good agreement with other studies such as those in the UK (Task 1 report) which suggest the data trending to a WSRF of 0.60 at higher-temperatures and longer times. The ratio results for the cross-welds in this work are lower than the Japanese values. This is most likely due to the fact that in this analysis, only the Type IV-HAZ reported failures were considered, whereas the Japanese did the regression on all the cross-weld data irrespective of failure mode. The BMSF obtained from analysis of the cross-welds was higher than has generally been reported for WSRFs. When the BMSF and the approach developed in this project was applied to the pipe geometries, a narrow range of WSRFs at 100,000 hours were obtained at or slightly below the BMSF. One conclusion from these findings could be that WSRFs will have to be developed for a range of materials and geometries. However, it is also clear that the ratio obtained from the standard cross-welds were conservative compared to the model predictions for pipes using the data. Therefore, in the absence of modeling a range of geometries, careful long-term analysis of standard cross-welds, segmented by failure mode and/or failure location appear to provide a lower bound for development of WSRFs.

The following summary observations are made:

- The analysis of the Grade 91 weld/weldment database in this chapter by the methodology proposed in this project produced a BMSF that decreased with increasing temperature. The application of this BMSF to welded structures is expected to produce a similar temperature-varying WSRF.
- It was also noted from the specimen size effect analyses that the minimum WSRF is more likely to be seen with tests under accelerated temperature conditions.
- It is also apparent from the size effect analyses that trends for large specimens versus standard specimens may be a function of testing time (applied stress) and temperature, so that universally opting for, or requiring large specimen weldment test data is not justified and can even lead to non-conservative predictions of component lifetime if applied directly. The findings suggest that using standard specimen data to back-out a base material strength factor and applying this factor to a structural analysis is the preferred method for helping establish WSRFs.
- For the seam weld cases considered, the WSRFs obtained for subcritically heat-treated grade 91 were at or slightly below the obtained BMSF results.
- The database analysis showed the behavior of standard cross-weld failures identified as Type IV-HAZ resulted in strength factors as a function of time and temperature. The magnitude of the observed reduction was higher than some global cross-weld data analyses of Grade 91. This was most likely due to this analysis segmenting data by failure modes as opposed to grouping all cross-welds together. However, final magnitudes were consistent with studies suggesting a long-time high-temperature reduction 'floor' of 0.60.

Figure 66: Comparison of Reduction Factors Calculated From This Work (Ratio Between Standard Specimen Type IV-HAZ and BM Curves, BMSF, and WSRFs Calculated for Two Pipe Geometries) Compared to ASME Section I/B31.1 Seam-Weld WSRFs, and Japanese (Yoshida et al.) Analysis

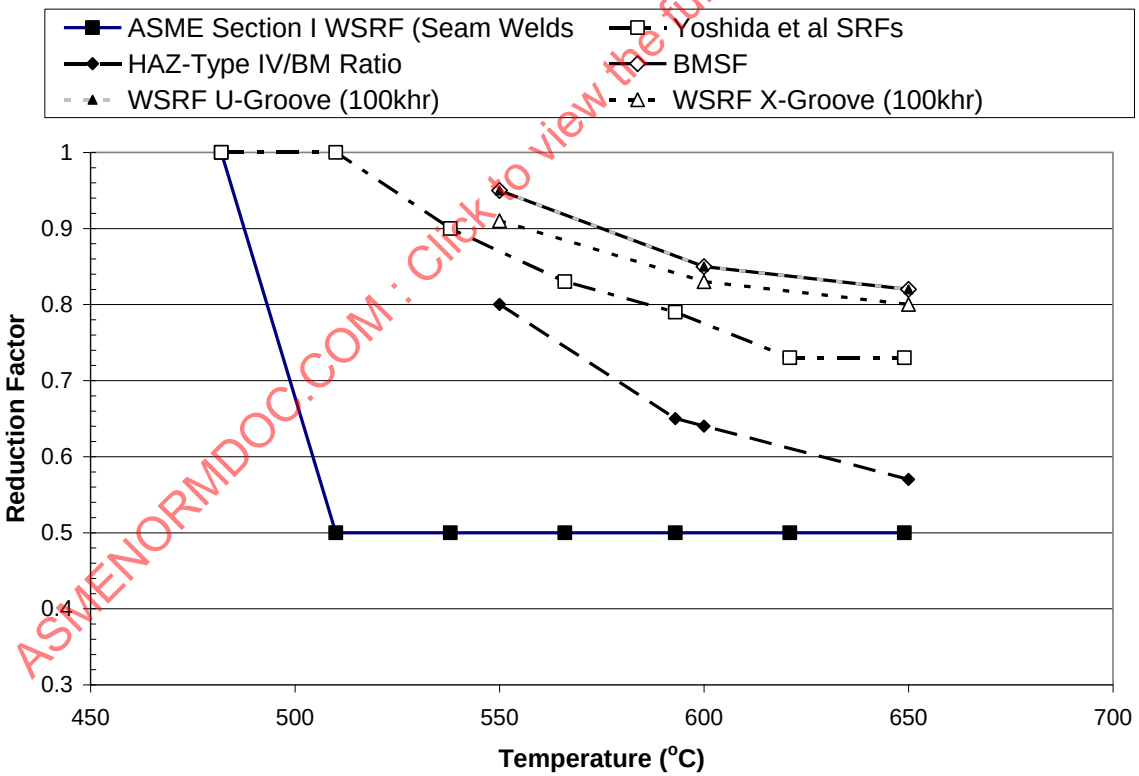

4 OVERALL PROJECT SUMMARY AND FINDINGS

The purpose of the ASME-EPRI research project was to develop the methodology and data to help establish weld strength reduction factors (WSRF) for service in the creep regime for a wide range of materials with applicability to various sections of ASME Boiler & Pressure Vessel Codes. As noted earlier, the reports of the various project tasks that are discussed below have been reproduced for this publication: Part 1-Tasks 1b and 3; Part 2-Task 1a; Part 3-Task 2. The Task 1a report includes: an extensive weld/weldment database covering 6 materials/material classes including reviews of each database and research performed, a review of seam weld failures, a first-of-a-kind global statistical analysis of CrMo seam weld failure rates, and a comparison of various methods used around the world for design rules of welded structures operating in the creep regime. The Task 2 report covers the model development and the research completed to assess the use of simplified methods for the purpose of design. The methodology that was developed by this research (Task 1b) and its reasoning is provided in the first chapter of this report. Special attention is given in this chapter to specimen size and data requirements. The methodology has been applied to two datasets (developed as part of a larger Task 1a database effort) in Chapters 2 and 3 of this publication. From this body of research, a summary of key findings and conclusions is as follows:

- **Task 1a**
  - Experience:
    - Reported experience shows seam-weld failures in CrMo piping (primarily in power generation applications) have occurred at a rate higher than would be expected based on the design allowable and statistical distribution of base metal creep rupture data.
    - The best-estimate CrMo seam-weld field failure rate corresponds to a failure rate that would be expected in base metal (per the laboratory base metal data) with the stress elevated above the design allowable by a factor of about 1.12. For perspective on WSRFs, the field failure rate therefore suggests a desired reduction of the allowable by a factor of about 0.9 (=1/1.12).
    - Limited CrMo low alloy seam-weld failures have been reported for piping in petrochemical applications and some operation-related factors have been suggested for this apparent discrepancy with the power generation experience, but additional work is warranted for improved understanding.
    - Failures in creep-strength enhanced ferritic steels (CSEF) seam welds have been reported. Various studies have shown subcritically heat-treated seam-welds have significantly reduced strength due to a weak fine-grained heat-affected-zone (FG-HAZ) with failures in the Type IV region of weldments.
    - Research shows that the service experience with carbon steel weldments does not exhibit evidence of premature failures of the kind seen with the low alloy CrMo steels.
  - Codes
    - Codified approaches around the world for weldment strength reductions for service in the creep regime vary substantially. ASME, particularly ASME Section III-NH, has one of the more developed methodologies. However, some data and analysis are not available, including the origins and data used in the development of the 2 1/4Cr-1Mo weldment values.
  - Database development
    - A detailed review and analysis of the carbon steel weldment data was conducted. Most data were from serviced exposed materials. No deficiencies were found to support the need for WSRFs for carbon steel.
    - Databases for 6 materials/material classes were assembled for use in this project and future ASME projects.

- **Task 2**
  - A brief review of modeling methods for creep of welded structures was conducted which concluded that although sophisticated continuum damage mechanics (CDM) approaches are now available, their application, in light of the broad goals for this project, was limited.
  - A simplified approach (analysis tool/methodology) was developed to evaluate the creep rupture strength of a weldment relative to that of a base metal.
  - The approach was benchmarked against selected high-temperature, long seam weldment piping failures, full CDM models, and component testing experience.
  - The approach has good technical basis as similar research around the world has shown it applicable for design purposes without over conservatism.
  - The approach has been used to develop a simplified methodology to enable quick and computational economical methods for evaluating WSRFs which, in Task 2, were applied to a range of geometries and loading conditions to demonstrate the usefulness of the approach
- **Task 1b**
  - An application guideline for developing WSRFs was developed on the basis of available input data, the Task 2 modeling approach, and perceived needs for design codes.
  - A 5-step process was outlined:
    - Develop Database
    - Analyze Data
    - Base Material Strength Factor(s)
    - Application to Welded Structures
    - Design Strength Ratios
  - A key feature of this process is the development of Base Material Strength Factors (BMSF) extracted from standard size cross-weld creep-rupture tests.
  - Non-standard or 'large' cross-weld specimen data are not necessary but are useful in testing out model assumptions.
  - Critical input data for this approach are details on specimen geometry and failure location in cross-weld specimens.
  - A general outline for data requirements is provided as part of the task.
- **Task 3**
  - Grade 22 analysis
    - Segmenting the database to less than 20ksi was required to provide meaningful datafits for WSRF analysis
    - Cross-weld data were used to develop a BMSF of 0.94 where the model predicted failure in the weld metal at the fusion line between the weld metal and the base metal which is consistent with a large percentage of field failures
    - Developed behavior from cross-welds suggested slightly weaker weld metal compared to the overall rupture behavior of the weld metal
    - The BMSF and WSRFs for two weldment geometries are in general agreement with the statistical treatment of service experience (Task 1a report)
    - Accelerated temperature creep testing will be useful for evaluating Gr. 22 welded material behavior.
    - Based on the Gr. 22 analysis and experience, it is suggested the current ASME Section I/B31.1 WSRFs for CrMo seam welds are conservative at temperatures greater than 1000F (and potentially at lower temperatures as well).
  - Subcritically heat-treated Grade 91
    - A clear trend in changing failure mode was not observed for the developed database, but the qualitative analysis suggested Type IV FG-HAZ failures can occur at long times at 550°C.

- The database analysis showed the behavior of standard cross-weld failures identified as Type IV-HAZ resulted in strength factors as a function of time and temperature. The magnitude of the observed reduction was higher than some global cross-weld analyses of Grade 91. This was most likely due to this analysis segmenting data by failure modes as opposed to grouping all cross-welds together. However, final magnitudes were consistent with studies suggesting a long-time high-temperature reduction 'floor' of 0.60.
- Applying the methodology developed on this project, the BMSF was found to be a function of temperature with the value being 0.95, 0.85, and 0.82 for 550°C, 600°C, and 650°C, respectively.
- The model and inputs where applied at three temperatures to two seam-weld pipe geometries representing two piping extremes: a thick-walled U-groove 'main-steam' pipe and a thin-wall X-groove 'hot-reheat' pipe geometry. These two geometries, using the same input data and BMSFs, produced differing WSRFs at 100,000 hours. For the thick-section weld, time to damage initiation was essentially the same as the calculated BMSFs, but for the thin-section X-groove, damage initiation was predicted at slightly shorter-times (or higher-stresses) leading to WSRFs lower than the BMSFs.
- For Grade 91, the importance of weldment configuration of the WSRF was demonstrated.
- In the absence of modeling a range of geometries, careful long-term analysis of standard cross-welds segmented by failure mode and/or failure location appear to provide a lower bound for development of WSRFs.

- From the size effect analyses, it was found that trends for large specimens versus standard specimens may be a function of testing time (applied stress) and temperature, so that universally opting for, or requiring large specimen weldment test data is not justified and can even lead to non-conservative predictions of component lifetime if applied directly. The findings suggest that using standard specimen data to back-out a base material strength factor and applying this factor to a structural analysis is the preferred method for helping establish WSRFs.

In summary, this research represents an effort to evaluate material behavior and component performance (and their interaction) for application in the safe design of weldments operating in the creep regime. These three reports provide the roadmap (Task 1b: Application Guideline), the methodology (Task 2), and the data (Task 1a) to develop WSRFs. The process has been demonstrated for two materials (Task 3). In the course of this research, new insights were gained on field failure rates in CrMo seam welds, the behavior and usefulness of standard and non-standard cross-weld specimens was investigated, data and analysis was provided in support of needs on C-steels weldments, critical analyses and comparisons were developed for Grade 22 and Grade 91 weldments, and information to guide data requirements was provided.

REFERENCES – PART 1

[1] Development of Weld Strength Reduction Factors and Weld Joint Influence Factors for Service in the Creep Regime and Application to ASME Codes: Task 1a Report: Experience Review and Data. ASME Standards Technology, LLC Project #3052, New York, NY – EPRI, Palo Alto, CA: May 2010.

[2] J. M. Corum, "Evaluation of Weldment Creep and Fatigue Strength-Reduction Factors for Elevated-Temperature Design," pp. 9-17 in Structural Design for Elevated Temperature Environments- Creep, Ratchet, Fatigue, and Fracture, PVP-Vol. 163, American Society of Mechanical Engineers, New York, NY, July 1989.

[3] Development of Weld Strength Reduction Factors and Weld Joint Influence Factors for Service in the Creep Regime and Application to ASME Codes: Task 2 Report: Development of Weld Joint Influence Factors. ASME Standards Technology, LLC Project #3052, New York, NY – EPRI, Palo Alto, CA: December 2009.

[4] Prager, M. "Issues in Life Assessment of Chrome-Moly Welds." PVP-Vol. 239/MPC-Vol. 33, Serviceability of Petroleum, Process, and Power Equipment, ASME 1992.

[5] Masuyama, F. "Effect of Specimen Size and Shape on Creep-Rupture Behavior of Creep Strength Enhanced Ferritic Steel Welds." Proceeding to the International Conference WELDS 2009, June 24-26, 2009, Fort Myers, FL © EPRI, 2009.

[6] Ellis, F.V., Viswanathan, R. "Review of Type IV Cracking." PVP-Vol. 380, Fitness-for-Service Evaluations in Petroleum and Fossil Power Plants. ASME 1998. 59-76.

[7] Wakai, T. et al. "Creep Strength Evaluation of Welded Joint Made of Modified 9Cr-1Mo Steel for Japanese Sodium Cooled Fast Reactor (JSFR). Proceeding of PVP 2010 July 18-22, Bellevue, Washington, USA. PVP2010-26014 © 2010 ASME.

[8] Fujibayashi, S. et al. "Cross-weld Creep Behavior and Life Prediction of Low Alloy Ferritic Steels." ISIJ International, Vol. 44 (2004), N. 10, pp. 1753-1761.

[9] 2007 ASME Boiler & Pressure Vessel Code, 2007 Edition. © 2007 The American Society of Mechanical Engineers.

[10] "A Review of High Temperature Performance Trends and Design Rules for Cr-Mo Steel Weldments," EPRI TR-110807, EPRI, Palo Alto, CA: 1998; also in Task 1 report of this project – ASME Standards Technology, LLC Project # 3052.

[11] B. Roberts, "Review of Allowable stresses for Wrought 21/4Cr-1Mo, 11/4C-1/2Mo-Si, and 1Cr-1/2Mo Steel," Box No. SCP-85-29, Reference No. BC-85-491, updated to BC 90-471, ASME Boiler and Pressure Vessel Code data package, ASME, New York, NY, September 10, 1990

[12] API 579/ASME FFS Fitness-For-Service ASME New York 2007

[13] Development of Weld Strength Reduction Factors and Weld Joint Influence Factors for Service in the Creep Regime and Application to ASME Codes: Task 1a Report: Experience Review and Data. ASME Standards Technology, LLC Project #3052, New York, NY – EPRI, Palo Alto, CA: May 2010.

[14] J.D. Fishburn, presentations to ASME Section II, 2007.

[15] API 579/ASME FFS Fitness-For-Service ASME New York 2007

[16] ASME Section III Division 1 Subsection NH, 2007.

[17] Masuyama, F. "Effect of Specimen Size and Shape on Creep-Rupture Behavior of Creep Strength Enhanced Ferritic Steel Welds." Proceeding to the International Conference WELDS 2009, June 24-26, 2009, Fort Myers, FL © EPRI, 2009.

[18] Coleman, K. EPRI unpublished research, personal communication May 2010.

PART 2: LITERATURE REVIEW, INDUSTRY APPROACH, AND DATA COMPILATION IN SUPPORT OF WSRF DEVELOPMENT

1 INTRODUCTION

This report represents part of a larger research project aimed at developing weld strength reduction factors (WSRF) and weld joint influence factors (WJIF) for service in the creep regime. The project is sponsored by ASME Standards and Technology, LLC (project # 3052) with co-funding from the Electric Power Research Institute. The overall objective of the project is to provide materials data and a methodology for addressing weldments in ASME codes and design allowable stresses. This report covers Task 1a of the work which is a literature review of creep failures in welded components, approaches to weld strength reduction factors, and a compilation of creep-rupture data on welds and weldments. A review of creep modeling of weldments and structures is included in the Task 2 report.

Chapter 2 covers a detailed review of the service experience with chromium-molybdenum seam-welds and provides context for the industry failures in terms of the 'survivor' population. By comparing the statistical distribution for base metal creep data and design, a unique perspective is gained on the overall issue. Experience with creep strength enhanced ferritic steels are also provided in chapter 2, suggesting concern for Type IV fine-grained heat-affected zone failures in these materials. Some discussion on service experience differences between industry design practice is also discussed.

Chapter 3 reviews current design practices for weld strength reduction factors within ASME and other codes. A historical review of the current ASME rules is provided along with equations used to develop the rules. A number of different European practices are presented. Overall, there exist considerable differences between approaches around the world.

Chapter 4 describes the development of the weld and weldment database for this project. Tabular data are contained within the appendices. Some limited analyses were conducted on the carbon steel data that were mostly limited to ex-service materials as part of this exercise. Additional work was undertaken to revisit old data and tested specimens from Grade 91 studies to develop additional data on failure modes that may be critical to analyzing the data. A review is also included on the numerous studies that have suggested weld strength reduction factors for Grade 91.

2 CREEP FAILURES IN SEAM-WELDED COMPONENTS

This chapter summarizes experience with welded steel components operating at elevated temperatures. The focus is on long seam-welded pressure boundary equipment for which designs may be directly impacted by ASME Code rules involving weld strength reduction factors (WSRF) [1], [2]. Concerns for the integrity of long seam-welded components operating at elevated temperature have stemmed from several failures, some catastrophic, of low alloy CrMo steel piping in fossil-fueled electric power plants. As a result, the vast majority of available data on failure experience and operational factors, and on research into the behavior of high-temperature weldments has been related to power plant piping. Following is a description of the experience with power plant long seam-welded piping, summary of some relatively recent experience with the creep strength enhanced ferritic (CSEF) steels, results of a limited review into comparable piping in the process (refinery and petrochemical) industry, and implications of the assessment of the power plant piping experience with respect to WSRFs. This summary of experience is intended to provide global perspective on failure and damage rates of high-temperature long seam-welded piping with consideration of the miles of piping that have evidently performed satisfactorily for decades. No attempt is made here to provide or explain the possible root cause(s) of any of the failures. As such, the failures are listed and examined only within the context of reported design parameters.

2.1 CrMo Power Plant Seam-Welded Piping Experience

Following the catastrophic failure of a hot reheat pipe long seam weld at the Mohave power station in 1985, the Electric Power Research Institute (EPRI) has been actively engaged in documenting experience with use of long seam-welded piping at elevated temperatures, and in developing and helping implement guidelines for the evaluation of such piping in service. This section focuses on summarizing the body of experience that EPRI has documented on fossil power plant long seam-welded high-temperature piping. The experience includes failures (ruptures and leaks), cases where damage in the form of cracking has been found, and an estimation of the overall population of fossil plant long seam-welded piping that has been in service. The population estimate, that includes the "survivors" and approximate duration of service, helps put the documented cases of damage and failure into perspective and provides additional general insight into what WSRFs may be suitable for design of low alloy CrMo long seam-welded equipment.

Much of the damage and failure experience summarized here has been taken from EPRI's 4th edition of Guidelines for the Evaluation of Seam-Welded High-Energy Piping [3]. This edition, an update of the 1996 EPRI Guidelines [4], includes experience accumulated through to 2003. In addition, the 2003 edition documented instances of damage detected using an advanced ultrasonic test method or the specific seam weldment inspection procedure developed and recommended by EPRI in 1996. Prior to establishing the need for an enhanced damage detection procedure over that previously used (per ASME Boiler & Pressure Vessel Code, Section V) and the development of the EPRI procedure, field inspections were generally inadequate for detection of such damage. This summary therefore includes inspection-based information generated only after 1996. Over the last decade, there has been a significant reduction in the frequency of long seam-welded high-temperature failures in the power industry, perhaps partly due to the progressive replacement of seamed piping with seamless product and the increased frequency and enhanced quality of in-service inspections of seamed piping. The extent of seam-welded piping replacement is not precisely known, so assumptions have been made in estimating the "survivor" population and duration of exposure.

2.1.1 Failures and Major Cracking

EPRI has documented 27 cases of failure and major cracking (near- or imminent failures) in high-temperature seam-welded piping of fossil plants [3]. Of these, 20 cases have reported steam design temperature and pressure, and pipe diameter and wall thickness information. These cases have been used to illustrate where these worst-case instances of performance sit with respect to design pressure stresses as compared against the ASME Code allowable stress for the material at the design temperature.Figure 67 is

a summary of the 20 failure and major cracking cases, as prepared primarily from the data in Refs. [3] and [4]. In three instances, as referenced in the table, other published data [5], [6] were used to infer the exposure time and the operating temperature and pressure. In one case where operating hours were not available, these have been estimated assuming 7000 operating hours per year of service. The table provides the reported nominal design-type information (pressure, temperature, pipe dimensions, component type, weld configuration) in each case. Also included in the table are the results of calculations made to help provide a stress-based, WSRF-relevant perspective on these worst-case failures. Recognize that these cases represent extreme lower-bound experience and involve a multitude of fabrication and operating factors contributing to damage, some possibly extreme, and cannot therefore be used in isolation to help establish or evaluate WSRFs for design. However, they provide a conservative rough first cut in any use of experience toward helping evaluate WSRFs for future design. Note that this chapter also includes a first, albeit coarse, semi-quantitative assessment of the many miles of long seam-welded high-temperature piping that have not failed, for a more balanced view of the issue.

For perspective on the negative margins against failure in terms of the ASME Code base metal design expectations, in each of these cases, the nominal operating primary pressure hoop stress was calculated per the ASME Code design rule (Boiler and Pressure Vessel Code, Section I and Power Piping Code, B31.1) for the reported pressure and pipe dimensions. This "design" stress was then compared against an estimate of the stress that would be required to produce failure in the lifetime observed, assuming base metal rupture strength properties. Two estimates of base metal rupture strength were used – a mean stress that represents expected average rupture behavior, and a lower-bound "minimum" stress that represents highly pessimistic rupture strength properties. The comparison was made in the form of ratios – (operating) hoop stress/mean stress and (operating) hoop stress/minimum stress. For Grade 22, the as-analyzed ASME Code data and data package on annealed Grade 22 [7] was used to estimate the mean and minimum stress for rupture in the observed lifetime and at the reported temperature. For Grade 11, a database comprising EPRI-archived data and the Japanese NIMS (National institute of Materials Science, formerly NRIM) database on Grade 11 was analyzed using a Spera function and a Larson-Miller polynomial. In addition, the ASTM Data Series DS 50 Larson-Miller rupture behavior average and minimum curves for wrought 1-1/4Cr-1/2Mo-Si were used. The "EPRI-NIMS" database analysis results provided average and minimum strength estimates comparable to the ASTM DS 50 graphic predictions. Mean and minimum stress estimates from this analysis were used in Figure 67. For both Grade 11 and 22, the lower-bound minimum properties used were 95% statistical lower-bound values as reported (in case of Grade 22) or as determined from the standard error on stress via analysis of the data (Grade 11).

The following observations are made from Figure 67 and from the EPRI failures and major cracking database:

- The experience suggests that both Grade 11 and Grade 22 long seam weldments are susceptible to premature failure with no distinguishable preference between the two.
- Failure lifetimes in these documented cases represent a fraction of the expected lifetime of base metal (<15%); the failure lifetimes varied from 88,000 to about 300,000 hours, with a mean of about 186,400 hours.
- None of the documented instances of failure and major cracking have been explained on the basis of abnormal operating conditions or cycling.
- While inferior weld metal creep rupture properties due to high oxygen, high inclusion producing acid flux use in submerged arc welds could be a contributing factor in some cases [8], this by itself does not explain all of the failures and the many miles of long seam-welded "survivor" piping.
- The failed thicker-section main steam line weldments generally endured longer exposure times than did the failed thinner section hot reheat pipe weldments.
- The thicker-section main steam weldment failures were consistently Type IV failures in the fine grain HAZ in base metal or in weld metal at the centerline or associated with a repair weld.

- The thinner section hot reheat line weldment failures were predominantly fusion line failures (weld metal very near fusion line) typical of the breadth of experience with this class of components.
- Indications are that the thinner section hot reheat weldments can also experience Type IV fine grain HAZ cracking and failure over longer exposure durations.
- The database does not conclusively illustrate what determines the "winner" of the apparent competition between fusion line and Type IV cracking. Damage is potentially driven by the stress (and strain gradients) associated with section thickness and the relative width of the heat-affected zone, by the geometry of the weld (thinner section double-V versus thick-section single-U), and by the post-weld heat treatment (subcritical versus normalized and tempered).
- Except for one case that appears to be an outlier, the ratio of the nominal operating pressure stress to the mean rupture strength of base metal for the duration of service at operating temperature varies between about 0.5 and 0.7; and the ratio of the nominal operating pressure stress to the minimum rupture strength of base metal for the duration of service varies between about 0.65 and 0.85.
- From a WSRF perspective (discussed in some detail later in this chapter), these worst-case incidents may be considered to reflect an average inferiority in weldment rupture strength of 50-70% to that of base metal.

Figure 67: Table of EPRI Database of Select Incidents of Major Cracking and Failure of Long Seam-Welded Piping

Plant Unit	MW	Vintage	Pipe Type[a]	Weld Geometry	Exposure time, t, Hrs	T(F)	P(psig)	OD (in)	Min. Wall (in.)	Hoop stress[b], σ (ksi)	ASME Allow[c] σ (ksi)	Min[d] σ (ksi)	Mean[d] σ (ksi)	Hoop σ /Min σ	Hoop σ /Mean σ	Mode	Location[e]
S1	220	62-79	HRH Bend(11)	Double-V	120000	1000	488	20	0.74	6.25	6.3	8	10.3	0.75	0.61	Rupture	FL
S2	220	62-92	HRH Bend (11)	Double-V	212000	1000	488	20	0.74	6.25	6.3	7.2	9.4	0.84	0.69	Leak	FL
M2	750	71-85	HRH Straight (11)	Double-V	88000	1000	597	30	1.313	6.40	6.3	8.4	10.8	0.72	0.59	Rupture	FL
P1*	326	60-85	HRH Straight (11)		175000	1000	484	17.75	0.81	4.96	6.3	7.4	9.6	0.64	0.52	Maj Cracking	NR
F	745	70-86	HRH Clamshell Elb (11)	Double-V	101000	1000	600	30	1.4	6.01	6.3	8.3	10.75	0.69	0.57	Maj Cracking	FL
U	NR	??-'97	HRH Clamshell Elb (11)		152341	955	575	27	0.9	8.33	9	10.7	14	0.72	0.59	Rupture	NR
MS3	570	65-93	MS Header Out-Lead (11)	U-Groove	172000	1000	2640	20	3.375	5.97	6.3	7.5	9.5	0.77	0.63	Maj Cracking	Type IV
SB1	147	60-95	MS Clamshell Elb (11)		278500	1000	2000	14	2	5.69	6.3	7	9.1	0.80	0.65	Leak	FG-HAZ of Repair Weld
ECG4	250	62-01	HRH Bend (11)	Double-V	160000	1000	465	20	0.832	5.26	6.3	7.6	9.8	0.67	0.55	Rupture	FL
M1	760	70-86	HRH Straight (22)	Double-V	97000	1000	730	32	1.505	7.25	8	9.94	12.05	0.73	0.60	Rupture	FL
J	200	57-85	HRH Straight (22)	Double-V	184000	1050	360	18	0.75	4.07	5.7	6.03	7.31	0.67	0.56	Maj Cracking	FL(HAZ of Repair)
G2**	250	57-85	HRH Straight (22)	U-Groove	174000	1050	390	27.5	1.125	4.49	5.7	6.05	7.33	0.74	0.61	Maj Cracking	FL
B	1120	75-87	HRH Straight (22)	Double-V	80000	1000	720	36	2.25	5.26	8	10.35	12.59	0.51	0.42	Maj Cracking	FL
C	NR	65-93	HRH Straight (22)	U-Groove	150000	1050	515	27.64	1.44	4.58	5.7	6.31	7.59	0.73	0.60	Maj Cracking	FL & Type IV
MS1	570	65-90	MS Link (22)	U-Groove	152000	1000	2640	16	2.75	5.83	8	9.2	11.22	0.63	0.52	Maj Cracking	FG-HAZ (W Center)
MS2	570	65-92	MS Link (22)	U-Groove	168000	1000	2640	16	2.75	5.83	8	8.91	10.72	0.65	0.54	Leak	FG-HAZ (W Center)
G1	880	74-93	MS Header Out-Lead (22)	U-Groove	156000	1000	3600	18	3.625	6.42	8	9.33	11.48	0.69	0.56	Leak	Type IV
C1	552	72-99	MS Link (22)	NR	198000	1000	2500	20	3.032	6.50	7.77	8.6	10.23	0.76	0.63	Leak	NR
H5***	500	67-98	MS Straight Vert (22)	J-Groove	200000	1005	2500	18	2.75	6.79	8	8.3	10.7	0.82	0.63	Rupture	ID-to-OD
S1A***	565	65-96	MS Straight (22)	NR	190000	1000	2640	20	3.5	5.69	7.77	8.5	10.1	0.67	0.56	Rupture	NR

a: HRH: Hot Reheat; MS: Main Steam; Elb: elbow; Vert.: Vertical pipe run

b: ASME I/B31.1-calculated stress

c: Current ASME Section I Allowable Stress for SA-335 (Grades 11 and 22)

d: Mean and Minimum (Min) rupture stress for observed failure time determined from analysis of EPRI & NIMS database for N&T Grade 11 (curve-fit comparable to ASTM DS50) and ASME Code Data ("Annealed" Grade 22) [7] (minimum curve used is the 95% lower-bound on log [rupture time])

e: NR: Not Reported; FL: Fusion Line; HAZ: Heat-Affected Zone; FG: Fine Grain; W: Weld

* Estimated hours at 7,000/year

** Exposure time inferred from other published data [5]

*** Exposure time and operating temperature & pressure inferred from other published data [6]

2.1.2 Cracking and Damage from Inspections

In addition to the 27 cases of major cracking and failure, EPRI has also documented instances of minor cracking and has surveyed fossil power plant owner-operators for their findings from in-service inspections [3]. The survey findings briefly summarized here include only the results of in-service inspections reportedly performed using advanced ultrasonic methods or the specific EPRI-recommended procedure published in 1996 [4]. For reasons having to do with the inadequacy of inspections performed prior to 1996 and a consequent underestimation of the extent of damaged equipment, the results of the first EPRI survey immediately following the Mohave failure (1985-86) have been excluded from this summary.

2.1.2.1 Minor Cracking

Sixteen cases of minor cracking in long seam-welded CrMo piping have been summarized [3]. These cases include 7 base-loaded, hot reheat pipe weldments, and 9 thick-section main steam pipe weldments, 5 of that were reportedly in cycling or peaking service. Reported operating steam temperature was 1000°-1005°F (538°-540°C), except in one case of a hot reheat unit with temperature of 950°F (510°C) and one main steam unit with a temperature of 900°F (482°C). The nominal margin on the design pressure stress is not known in most cases. The operating hours were estimated from the reported service duration using 7000 hours of operation per year, and the estimated operating hours varied from a low of about 147,000 to a high of 343,000 hours with a mean of about 232,000 hours.

2.1.2.2 Inspections Survey

Following development of its 1996 Guidelines [4], EPRI completed a survey of seam-welded piping inspections. Reportedly, these inspections were conducted using advanced ultrasonic procedures or followed the procedures put forth in the 1996 Guidelines [4]. This survey covered 162 units with 47,000 feet (14,000 m) of seam-welded high-energy piping. The reported inspection results were from inspection of 30,000 feet (9,000 m) of in-service seam weld.

The reported flaws included:

- 37 flaws that were >0.2 inch (5 mm) deep
- 23 flaws that were 0.1–0.2 inch (2–5 mm) deep with a continuous or intermittent length (parallel to seam) >2 ft (0.6 m)
- Hundreds of short flaws, 0.1–0.2 inch (2–5 mm) deep

Results of this survey suggested a significant fraction of reported flaws were non-propagating.

2.2 Creep Strength Enhanced Ferritic Steels Long-Seam Experience

This section summarizes some of the published experience with long seam weldments of the relatively new class of creep strength-enhanced ferritic (CSEF) steels that are subject to WSRFs via ASME Section I and B31.

While the focus of this chapter is on the low alloy CrMo steel long seam-welded piping for which there has been a great deal of documented experience, it is appropriate to briefly mention the creep strength enhanced ferritic steels (CSEFs) in current use. These steels include Grades 91, 911, 92, 122 and 23, although long seam-welded 92 would not currently be ASME Code-compliant (the plate form is not ASME Code-listed). Except for Grade 91, the relevant thick-section welded component experience with these steels is relatively limited.

Many of the CSEF steels have shown a susceptibility to premature weldment cracking and failure in the creep temperature range, and are potentially subject to long seam weldment WSRFs as are the low alloy CrMo materials.

Grade 91, for which considerable experience has been gained since its commercial use began in the 1980s, has experienced a multitude of thick-section weldment cracks and failures (e.g., [9], [10], [11], [12], [13], [14]), including a few failures associated with long seam weldments ([13], [14]). The vast majority of the Grade 91 in-service weldment failures have been of the Type IV kind with damage in the fine grain or intercritical region of the heat-affected zone (HAZ). In one long seam-welded pipe case where nominal operating and design information were reported, the failure occurred, May 2001, in the intrados seam weld of a hot reheat pipe clamshell elbow after about 65,000 hours of operation at a maximum temperature of 1105°F (596°C). The failure was predominantly associated with Type IV cracking apparently initiated at the cusp location (near the ID) of an asymmetric (cusp near ID) of a double-V weld.

Nominal pressure stress levels appeared to have been less than 50% of the base material expected minimum and average rupture strength. The failure was attributed to stress intensification at the elbow intrados, local stress concentration at the double-V cusp, and excessive weld heat input rate that produced hot cracking in the weld metal and reduced the strength of the joint [14]. Regardless of the relative contribution of the many possible factors, the nature and location of the failure indicates that damage drivers operative in this case are similar to those seen with the low alloy CrMo weldments experiencing the Type IV problem, albeit on a different time and stress scale.

Regarding Grade 122, there have been published reports of at least one long seam-welded Grade 122 piping failure in Japan (noted in Refs. [14], [15]), and unpublished reports of at least two such failures. Reportedly [14], one of the failures (June 2004) occurred in the long seam weldment of a hot reheat pipe after about 33,000 hours of operation at a maximum temperature of 1121°F (605°C). In this case, the reported nominal pressure stress was about 10% higher than what is currently permitted by Code Case 2180 of the ASME Boiler and Pressure Vessel Code, but still less than about 75% of the expected base metal average rupture strength. This failure occurred in the Type IV region [15], although details are not known. It is generally acknowledged that many of the CSEF steels are susceptible to the Type IV HAZ damage phenomenon (e.g., [16]). At the present time, however, there is insufficient detail available on the weldment cracking and field use and failure experience with these steels to help provide a perspective on WSRFs.

There exists some laboratory cross-weld data that allows for a preliminary assessment of weldment penalties associated with this form of cracking in case of some of the 9-12%Cr steels. While the laboratory data need not reflect field behavior, a few comments are in order. Following the Grade 91 and 122 long seam weldment failure experience in Japan, the Japanese Nuclear and Industrial Safety Agency conducted a review of laboratory cross-weld data for several CSEF steels (91, 92, 122 and 23) [15]. A review [17] of the published Grades 91, 92, 122 and 23 lumped Larson-Miller parametric analysis of Yoshida et al. [15] suggests various reduction factors on rupture strength as shown in Figure 68 below. The reduction factors were estimated as a ratio of the Yoshida et al. average curve-fit-calculated 100,000-hour cross-weld rupture strength to 1.5 times the listed ASME Code allowable stress for pipe. Yoshida et al. used a split-region analysis for Grades 92, 122 and 23, and in these cases, the long-term behavior has been used for the reduction factor estimation.

Figure 68: Table of Estimates of Strength Reduction Factors Reflected in the Best-Fit Average Larson-Miller Behavior of Laboratory Cross-Weld Data of Yoshida et al. [15] Compared with Approximate Average Behavior of Base Metal*

Material	900°F (482°C)	950°F (510°C)	1000°F (538°C)	1050°F (566°C)	1100°F (593°C)	1150°F (621°C)	1200°F (649°C)
91	1.0[a]	1.0	0.90	0.83	0.79	0.73	0.73
92	1.0	1.0	1.0	0.82	0.69	0.57	0.45
122	1.0	1.0	1.0	0.84	0.73	0.64	0.53
23	1.0	1.0	1.0	0.84	0.64	0.63	1.0[b]

*Average base metal rupture strength taken as 1.5xASME Code allowable
a: Calculated factors >1.0 have been truncated at 1.0
b: Calculated weldment strength exceeds "ASME average" base metal

The calculated reduction factors of Figure 68 are based on limited laboratory data and presented only for preliminary perspective on the CSEF steels. Other laboratory test-based findings give similar results. For example, Abson et al. [18] have reported comparable 100 khr rupture strength reduction factors on tests of Grade 122 cross welds. The UK Fourcrack program concluded, in a study of Grades 911, 91, 92, and 122 weldments, that the weldment creep rupture strength falls toward a floor value of about 60% of the base metal strength in the longer term [19]. A key aspect of the UK perspective is that the WSRF gets lower with increasing creep exposure time.

In summary, at a minimum, the CSEF steels should be considered susceptible to premature Type IV HAZ damage and failure, although the field experience is currently insufficient to help provide full perspective on WSRFs for these alloys. The laboratory cross-weld specimen data for these steels, while not necessarily directly reflecting expected in-service behavior, provide a means of inferring in-service behavior via suitable stress and data analyses. This issue has been examined as part of a separate task in this project.

2.3 Process Plant Long-Seam Experience

Briefly included in this section are comments on the experience with long seam-welded piping in process plants primarily in the refining and petrochemical industries.

The long seam-welded component experience in process plants contrasts with that in the electric power industry in that there have reportedly been very few failures. The American Petroleum Institute (API) reports in its API Recommended Practice 571 [20] that cracking has been found at long seam welds in some high temperature piping and in reactors on catalytic reformers. A detailed search and review of the available published information on the subject, however, revealed only one fully documented instance of a long seam-welded Grade 11 pipe having failed in a refinery catalytic reforming unit [21], [22]. As reported by Buchheim et al. in describing this failure [22], there were two other low alloy steel seam weld pipe failures in catalytic reformer units. However, the details on these failures are not available, except that as indicated, one failure was attributed to a poor factory repair of the weld seam, and the other to severe mismatch at the weld.

2.3.1 Refinery Catalytic Reformer Piping Failure

This documented failure [21], [22] occurred in a vertical section of thin-wall, large diameter pipe (36 in. OD, ½ in. thickness). The failure occurred at the weldment with the predominant cracking having occurred at the fusion line, a location common to the thin-wall reheat piping failures in fossil plants (Figure 67). Reportedly, the pipe had been in service for approximately 100 khr with operating conditions varying between 970°-1000°F (521°-538°C) and 150-170 psig (1034-1172 kPa) temperature and pressure,

respectively. For the range of operating conditions, a set of nominal calculations were made as were done in developing Figure 67.

The ratio of the nominal operating pressure stress to the mean rupture strength of base metal for the duration of service at operating temperature is estimated at about 0.4 to 0.6; the ratio of the nominal operating pressure stress to the minimum rupture strength of base metal for the duration of service is about 0.5 to 0.7. Failure lifetime in this case represents a very small fraction of the expected lifetime of base metal (1 to 6 %). These ratios are lower than what has been generally observed with the power plant long seam-welded piping failures, indicating that the failure was even more premature than what has been seen with the power plant piping incidents. There is at least one reason for this: as explained in the failure investigation [22], the pipe had a significant weld peak profile (0.31 in. maximum radial deviation from circular or about a 5° deviation) that elevated the maximum effective stress by nearly a factor of 4 as elastically determined, persisting even with relaxation to about 1.4 in 100 khr. The apparent crack initiation location at the weld toe at the pipe ID is consistent with the peaking effect.

The design parameters for the failed pipe were not reported, but the operating conditions reflect a significant margin on lifetime with estimated expected average base metal lifetime well above one million hours and as high as six million hours for the lowest temperature and pressure condition. Put in terms of stress and temperature: (1) at the reported maximum operating temperature of 1000°F (538°C), the Code-calculate pressure stress has about a 5 to 15% margin on the allowable; (2) at the reported lowest operating temperature of 970°F (521°C), the Code-calculate pressure stress has about a 25 to 35% margin on the allowable; (3) depending on the operating conditions, the calculated Code-allowed temperature margin can be as high as about 55°F (31°C) above the operating condition.

2.3.2 Comment

This review did not include a survey of the design, construction and operating conditions of long seam-welded high-temperature components in the process industry. As a result, the contrast in failure experience between the electric power and the process industry cannot be fully explained.

It is possible that the difference in experience in the two sets of industries relate to differences in design margins. Preliminary indications are that design temperatures may be 25°-50°F (14°-28°C) higher than the maximum operating temperature (e.g., [23]) in case of refinery/petrochemical component designs. The need to accommodate variations in pressure and temperature beyond the normal operating conditions may, in some process industry environments, drive piping designs toward higher margins. In addition, while the permissible variations in short-term pressure and temperature excursions beyond design are greater in case of ASME B31.3 process piping than are those for ASME B31.1 power piping, the requirement on the B31.3 designer to determine that such variations do not impact safety can also drive the design toward higher margins. The relatively high margins (compared with typical power plant piping) associated with the one documented refinery piping failure is one illustration of the design difference.

In summary, proper understanding of the process industry experience will require a survey of that industry for details on its use (design, fabrication and operation) of high-temperature long seam-welded components.

2.4 Implications to WSRF

The low alloy steel long seam weldment piping damage and failure experience documented by EPRI for fossil power plants has potentially quantifiable implications with regard to what weld strength reduction factors (WSRFs) may be appropriate for this class of weldments. The database of experience in case of other materials such as the CSEF steels, however, is currently too limited to permit any quantification. This section is therefore restricted to an evaluation of the low alloy CrMo long seam weldment experience.

Given (a) that there have been numerous cases of long seam-welded piping failures that have occurred in a fraction of the lifetime that is expected for all-base metal piping (<15%); (b) that these failures have occurred at nominal operating pressure stress levels well below a level that would be expected to cause failure in all-base metal piping in these service durations (50-70% of expected stress); and (c) that the mode of failure can be catastrophic, an immediate inference drawn is that these failures reflect a need for imposition of a WSRF in this class of components. However, since the documented cases of failure and damage represent a very small fraction of the population of relevant components, it is important that the overall experience, including the "survivor" population, be considered in assessing the implications to WSRFs. This section focuses on an aggregate, global, semi-quantitative evaluation of the damage and failure experience in fossil plant low alloy steel long seam-welded piping in terms of a rate of failure measured against the performance of the overall population. The evaluation is a coarse, approximate one that required making a set of assumptions in order to estimate the extent of seam-welded piping and associated operating hours for the population of such piping, data that are not available.

2.4.1 Damage and Failure Rate

Since any quantitative assessment of experience requires knowledge of the operating time and the length of seam weld, an "exposure" parameter has been defined and used, represented by the arithmetic product of the length of weld and the operating time. The exposure is defined as:

Exposure (ft-hrs) = Length of long seam-welded piping (ft) x Operating time (hrs)

A *Damage* or *Failure Rate* can then be defined as the *Exposure* associated with damaged or failed piping divided by the *Exposure* associated with the overall population of long seam-welded piping of this class; i.e.,

$$\textit{Damage} \text{ or } \textit{Failure Rate} = \frac{\textit{Exposure} \text{ of Damaged or Failed Seam-Welded Piping}}{\textit{Exposure} \text{ of Population of Seam-Welded Piping}}$$

Estimates of rates were made for the 27 cases of major cracking and failure, and also for the damage represented by the minor cracking cases and the inspection survey results. The minor cracking cases and the number of potentially significant flaws of the inspection survey total 76 (16 cases of minor cracking and 60 reported inspection flaws). The number of units represented in this database of failures, minor cracking, and surveys is 204. For perspective on the size of this sample, the United States EIA (Energy Information Administration) 2006 database indicates a total of 2157 fossil units of size >30 MW operating in the US. Thus, the sample size used here is roughly 9.5% of the total number of units, but would be considerably higher if only units with long seam-welded piping are considered. The same EIA database allowed for an estimation of the average age of these fossil units as 34 years, the number used in estimation of operating hours.

Calculation of *Exposure* requires knowing the length of piping of concern and the operating hours, both of which may not be reported or easily available. In order to conduct this assessment and utilize the data, several assumptions were made:

- Average susceptible seam-welded piping per unit is 290 feet (based on survey reporting 47,000 feet for 162 units)
- For survey data, assumed 10 ft of affected or damaged piping in each instance of reported flaw
- For EPRI-tabulated data on failures and major cracking, assumed 20 ft of damaged/failed pipe length in each case, except for S1 and S2 where specific inspection data and damaged pipe lengths were reported
- Where exposure time is not known, assumed 7,000 operating hours per year of service

- Assumed that on average, 50% of all fossil units had seam-welded HRH piping until 2003; this assumption is intended to partly account for post-1986 long seam-welded piping replacement with seamless piping and the mix of inventory of seamless and seam-welded piping in fossil plants

Figure 69 summarizes the *Exposure* parameters derived for the overall population of long seam-welded piping and the subsets of piping that experienced major cracking or failure, piping that exhibited minor cracking and damage from the inspection survey, and the subset of the seam-welded piping population that included only units that had failures and reported cracking.

Figure 69: Table of Exposure Parameters Estimated for Long Seam-Welded Piping in Fossil Power Plants

	Relevant Piping Length (ft)	Average Operating Hours	*Exposure* (ft-hrs)
Failures & Major Cracking (27 cases)	533	161,370	8.6 E+07
All Damage[a] (103 cases)	1,453	208,530	3.03 E+08
Entire Population	312,765	238,000	7.44 E+10
Only Units Inspected / Affected (204)	59,160	220,080	1.30 E+10

a: Includes failures, major cracking, minor cracking and inspections survey

Figure 70 is a summary of the result of a set of *Failure Rate* calculations using the *Exposure* parameter values of Figure 69. The table includes several measures of *Failure Rate*:

- Only the cases of major cracking and failures measured against the *Exposure* of the entire population. This is assuredly non-conservative since it excludes the minor cracking and results of the inspections survey that include numerous instances of damage.
- All of the damage cases that include failures, major cracking, minor cracking, and the results of the inspections survey measured against the *Exposure* of the entire population. This estimate may be considered a best-estimate, but since it excludes unreported data, it is possibly non-conservative.
- All of the damage cases, but measured against only the units that were inspected or that were associated with failures or cracking. In this case, the denominator excludes the majority of the population for which there is no reported data or failures. As such, this estimate is believed to be conservative.

Figure 70: Table of Estimation of Failure Rates

Case	*Failure Rate* %	Comments
Failures & Major Cracking/Entire Population	0.11	Non-conservative; excludes inspection survey and minor cracking
All Damage/Entire Population	0.41	Best-estimate, but potentially non-conservative
All Damage/Only Inspected or Affected Units	2.3	Considered conservative; large fraction of population excluded in denominator

The estimated failure rates provide semi-quantitative support for WSRFs, given that for this class of CrMo seam-welded piping, the experienced rates have been >0.4% and can conservatively be put at 2.3%. As described below, for perspective, these rates were compared against corresponding percentiles of the statistical distribution of rupture strength for a base metal data set.

2.4.2 Perspective on CrMo Failure Experience

One way to gain perspective on the estimated failure rates of CrMo long seam-welded piping is to look at what these failure rates correspond to in a typical distribution of rupture strength properties. This may be done by considering the estimated failure rates to be equivalent to the probability of failure in a statistical distribution of rupture strength. A review was conducted of the statistical distribution of the laboratory data used in developing the ASME Code allowable stresses for Grade 22 (2-1/4Cr1Mo) steel [24]. That ASME data package includes a description of the as-analyzed normal distribution on both log (rupture time) and on log (rupture strength or stress). The distribution on log (rupture strength) for annealed Grade 22 was used for this exercise.

Ref. [24] lists the standard error of the estimate (SEE) of the log normal distribution of rupture strength, σ, as 0.0474526. The SEE can be easily used to determine the statistical lower-bound percentile or probability of failure for any selected stress level (area under the standard normal curve below the selected stress) where the ratio of the rupture strength to the estimated mean strength of the distribution is known. Conversely, the stress-to-mean rupture strength ratio corresponding to any lower-bound percentile can be determined. Figure 70 illustrates points of interest in the Grade 22 rupture strength distribution of Ref. [24]. Note that Ref. [24] indicates that the minimum stress was defined to be at the 4.95% lower-bound percentile.

Figure 71: Table of Points of Interest on the Grade 22 Statistical Rupture Strength Distribution of Ref. [24]

	σ/σ_{ave} [a]	Lower-bound percentile or P_f [b]
Minimum stress	0.835	4.95%
Allowable stress	0.667	0.011%

a: σ_{ave}= average stress in the distribution; b: P_f = Probability of Failure or Failure Rate

By comparing the failure rate (i.e., probability of failure) estimates in Figure 70 with the numbers represented by the minimum and allowable stress levels of the selected Grade 22 base metal distribution in Figure 71, it can be seen that while the estimated seam-welded piping failure rates are well below the failure probability of Grade 22 base metal at the minimum rupture strength, they are, not surprisingly, significantly greater than what may be expected for base metal at stress levels at and below the Code allowable. The question that remains then is what relative base metal design stress levels would the estimated failure rates correspond to for this specific Grade 22 distribution of rupture strength?

Figure 72 illustrates what each of the estimated failure rates of Figure 70 correspond to by way of stress level, σ, in the distribution of rupture strength. The stresses are presented as ratios to the average stress, σ_{ave}, and to the allowable stress, σ_{allow} of the distribution. The σ_{allow}/σ ratio reflects a multiplier on the failure rate-corresponding stress level needed to bring the failure rates down to that represented by the allowable stress for this distribution. As such, this exercise and the σ_{allow}/σ ratio provide a general failure rate-based perspective on a WSRF.

Figure 72: Table of Stress Level, σ, in the Distribution of Grade 22 Rupture Strength, Corresponding to the Estimated Failure Rates of Figure 70

Case	Failure Rate %	σ_{ave}/σ	σ_{allow}/σ	Comments
Failures & Major Cracking/Entire Population	0.11	1.40	0.93	Failure rate is non-conservative
All Damage/Entire Population	0.41	1.33	0.89	Best-estimate failure rate, but potentially non-conservative
All Damage/Only Inspected or Affected Units	2.3	1.24	0.83	Considered a conservative estimate of failure rate

Since the evaluation included consideration of the survivor population of long seam-welded piping, it provides a more balanced view on the margins against failure in this class of welded CrMo piping, absent the imposition of any design WSRFs. To be clear, there is no specific recommendation intended here with regard to application to design, although this preliminary quantification of experience, heretofore unknown, is a useful benchmark for the development of WSRFs.

3 CURRENT DESIGN PRACTICES FOR WELD STRENGTH REDUCTION FACTORS

3.1 ASME Approach: Section III N-H

3.1.1 Section III N-H

The history of construction rules for high-temperature nuclear components was summarized by Snow and Jakub in 1982 [25] and Dhalla in 1991 [26]. Although the rules for welded construction were central to the early codes, which considered materials such as 304H and 316H stainless steels in Code Case 1331-5 (1971), no mention was made of stress factors for welds for creep or fatigue until the 1980s. Minutes from BPV code committees show that consideration of weld metal strength for use in the high-temperature nuclear code began in the BPV SG-Elevated Temperature Construction and the SG-Strength of Weldments in the early 1980s and was based on research undertaken in the 1970s to support the design and construction rules for the Fast Flux Test Facility (FFTF) at Hanford [27] and the Fast Breeder Reactor programs at Oak Ridge [28]. By 1984, correlations for the stress-rupture strength of the filler metals for 304H and 316H stainless steels appeared [29], [30], [31]. For the 304H stainless steel filler metal, namely 308 stainless steel, the specific model used to represent the rupture life, t_r, was as follows [29]:

$$\log t_r = C_h - 0.01573\ S - 0.02043\ T - 0.002185\ T \log S,$$

where t_r is the life in hours, C_h is the average "lot Constant," T is temperature in Kelvin, and S is stress in MPa. The value for the average C_h is given as 27.862.

The specific model used to represent the rupture life, t_r, for one of the 316H stainless steel filler metals, namely 16-8-2 stainless steel, was as follows [30]:

$$\log t_r = C_h - 0.01044\ S - 0.01702\ T - 0.005687\ T \log S,$$

where t_r is the life in hours, C_h is the average "lot Constant," T is temperature in Kelvin, and S is stress in MPa. The value for the average C_h was given as 31.525.

The specific model used to represent the stress-rupture life, tr, for 316 stainless steel filler metal was as follows [30]:

$$\log t_r = C_h - 0.0102\ S - 0.01387\ T - 0.002668\ T \log S,$$

where again t_r is the life in hours, C_h is the average "lot Constant," T is temperature in Kelvin, and S is stress in MPa. The value for the average C_h is given as 22.483.

The specific models used to determine the stress-rupture life relationship with stress and temperature for the filler metals for alloy 800H and 2 1/4Cr-1Mo steel and were not found in the minutes and other records that were available. However, the data that formed the basis for the stress-rupture models used for the alloy 800H filler metal, namely alloy A (ENiCrFe-2) and alloy 82 (ERNiCr-3), are reviewed in another section of this report.

The Stress Rupture Factors for weld metals were proposed for CC N-47 in the mid 1980s. The Stress Rupture Factor, *R*, was defined as the average rupture strength of the deposited filler metal to the average rupture strength of the base metal. The limits for load controlled stresses, currently covered in NH-3221 for weldments, made use of the Stress Rupture Factor, *R*, in two ways. First, the allowable limit of the general primary membrane stress intensity, S_{mt}, had to be taken as the lower of S_{mt} or

$$0.8\ S_r \times R.$$

where S_r was the expected minimum stress-to-rupture strength. Second, the temperature and time-dependent stress intensity limit, S_t, had to be the lower of S_t or

$$0.8\ S_r \times R.$$

Thus, it was necessary to provide the minimum stress-to-rupture strength correlations with time and temperature as well as the *R* values to make use of the Stress Rupture Factors in design.

Further modifications of the Stress Rupture Factor values were undertaken in the ensuing years and an additional material, 9Cr-1Mo-V steel, was included. In the case of the 9Cr-1Mo-V steel, however, the Stress Rupture Factor was based on the results of cross weld tested specimens rather than deposited weld metal specimens. The correlation for the stress-rupture of 9Cr-1Mo-V steel was developed by Brinkman and co-workers [32], [33] and the specific model was as follows:

$$\log t_r = C_h - 0.0231\ S - 2.385 \log S, - 0.01387\ T + 31080/T,$$

where again t_r is the life in hours, C_h is the average "lot Constant," T is temperature in Kelvin, and S is stress in MPa. The value for the average C_h was given as 24.257. The model was numerically identical to the base metal, except for the value of the average lot constant. The effect of the model was to produce values for *R* that were not time-dependent.

By 1986, "reduction factors" for weld metal were proposed for use in CC N-253. Included were fillers for 304H, 316H, alloy 800H, 2-1/4Cr-1Mo steel, and 9Cr-1Mo-V steel. Values that appeared in Table C 1.3 of CC N-253 were based on the stress factors for 100,000 hours. Finally, in 1987, creep and fatigue reduction factors appeared in CC N-47-26. Corum [34] published the technical justification for the factors that were the same as those that appear in III-NH today. Other weldment issues addressed by BPV III-NH were briefly covered by Jetter [35].

Griffin summarized a number of weldment issues related to safety [36]. The concerns of the Nuclear Regulatory Commission were identified as follows: a) early crack initiation near the inside wall of weld HAZs; b) deleterious effects associated with large variations in the materials properties within the weld zone that could lead to creep-fatigue or creep-rupture damage; and c) the damaging effect of time rate, cycle rate, and hold time on the propagation of long shallow cracks in the HAZ of the weldment. No issues specific to the use of the stress factors were identified but a "confirmatory program" to address several other important issues was outlined [36].

3.2 ASME Approach: Section I and B31

3.2.1 Background on Universal 'Presumptive' Factor

In 2007, ASME took broad action to adopted weld strength reduction factors (WSRF) for longitudinal seam welds operating in the creep regime. The actions focused on Section I, B31.1, and B31.3. The impetus for this work was a concern that various studies have shown reduced creep life for weldments compared to base metal, and the failures of seam welded components in the fossil power industry (already discussed in detail in chapter 2). The initial proposal was based on work conducted within B31.3 for a 'presumptive' weld strength factor [37]. In the absence of specific data, the developed weld strength reduction factors in ASME Section III-NH at 100,000 hours were plotted and a universal factor was fit to the data that varied

from 1.0 at 950°F (510°C) to 0.5 at 1500°F (816°C). Figure 73 is a plot of the 100,000 hour reduction factors taken from ASME Section III-NH along with the proposed 'presumptive' weld factor (factor).

Figure 73: Basis for Universal 'Presumptive' Weld Factor from [37]

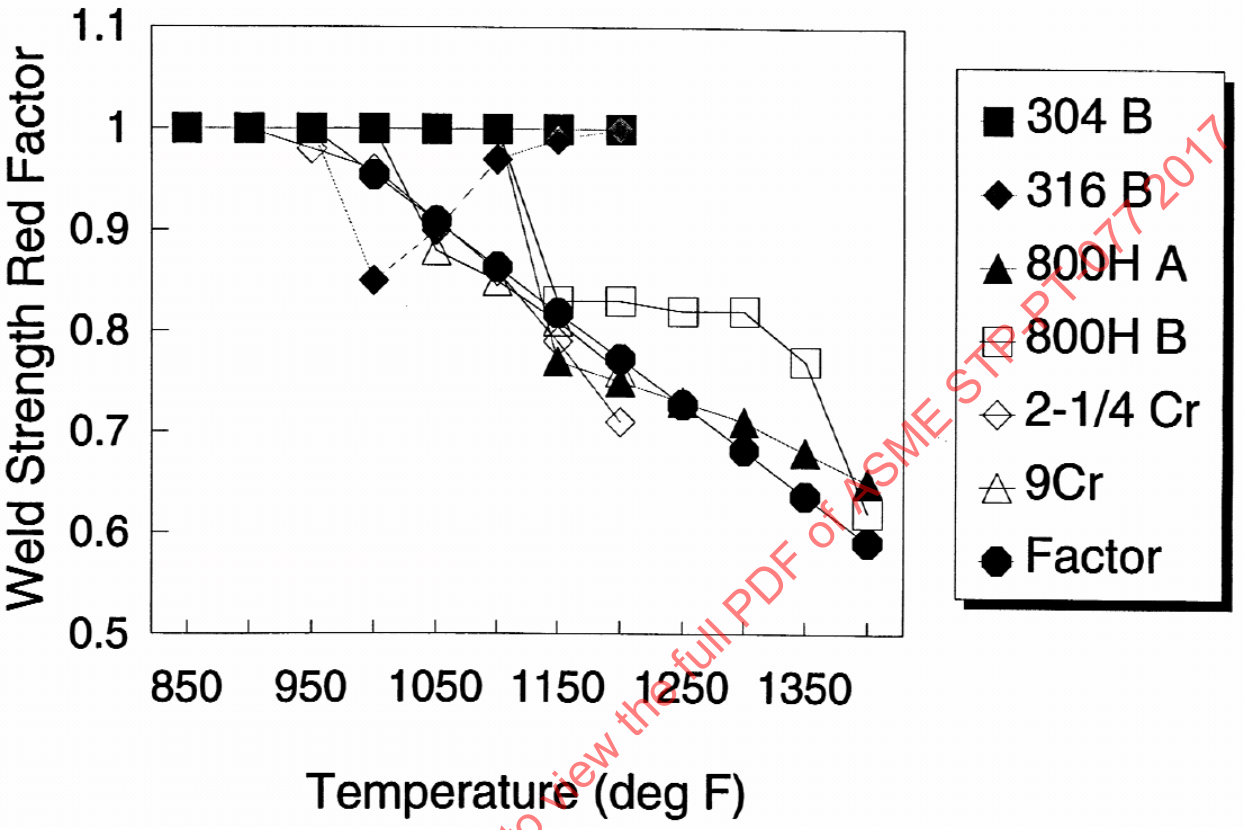

3.2.2 Development of WSRFs for Section I, B31.1, and B31.3

This universal 'presumptive' weld factor was further developed by an ASME standards committee to develop factors that were adopted in ASME Section I, B31.1, and B31.3 in 2008. Numerous changes were made to the original factor proposal. First, the factor was only applied to components fabricated with a longitudinal seam weld (girth welds for example were not addressed). Second, the slope of the universal 'presumptive' weld factor was maintained for Chromium-Molybdenum steels (Cr-Mo), creep strength enhanced ferritic (CSEF) steels in the normalized and tempered condition (N+T), and austenitic stainless steels and alloys 800H and 800HT, but the minimum temperature of application was tied to the start of the material's creep regime, that was defined as 50°F (25°C) lower than t-note temperature. For Cr-Mo this was 800°F, and for CSEF (N+T) steel and for the austenitic stainless steels and alloys this was 950°F. Due in part to 'good service experience' with cabon steel pipes (primarily in B31.3 application), no WSRF was applied to carbon steel pipes and tubes.

Additionally, CSEF steels subjected to a subcritical post-weld heat-treatment (subcrit.) were given a universal WSRF of 0.50 at 950°F and above due to concerns over very short-term type IV failures and numerous studies suggesting the WSRF for welded joints of 91, 92, and 122 were approaching 0.5 at long-times and high-temperatures (see chapter 2.2 and 4.6.3). Autogenously welded austenitic stainless steels were exempted from a WSRF, provided that solution annealing and non-destructive evaluation are conducted. Additionally, for type 304 and 316 stainless steels welded with 16-8-2 chemistries, relief from austenitic stainless steel WSRFs can be obtained with use of proper filler metals and solution heat-

treatment. Finally, welding process and flux acidity are restricted for CrMo and CSEF steels based on service experience with these alloys. Figure 74 is a reproduction of ASME Section I Table PG-26 which was developed by the committee. Similar tables are found in B31.1 and B31.3.

For Section I, *w* is defined as the weld joint strength reduction factor. It is applied by multiplying the maximum allowable stress value at the design temperature of the metal (*S*) by *w* in the PG-27 calculations for minimum required thickness (*t*) or maximum allowable working pressure (*P*). The user is cautioned that 'there are many factors that may affect the life of a welded joint at elevated temperature and all those factors cannot be addressed in the table of WSRFs' [38].

Figure 74: Weld Strength Reduction Factors and Applicable Notes for ASME Section I PG-26 [38]

Temperature, °F Temperature, °C	700 371	750 399	800 427	850 454	900 482	950 510	1,000 538	1,050 566	1,100 593	1,150 621	1,200 649	1,250 677	1,300 704	1,350 732	1,400 760	1,450 788	1,500 816
Steel Group	Weld Strength Reduction Factor [Notes (1)–(6)]																
Cr-Mo [Notes (7)–(9)]	...	...	1.00	0.95	0.91	0.86	0.82	0.77	0.73	0.68	0.64	NP	NP	NP	NP	NP	NP
CSEF (N+T) [Notes (9)–(11)]	...	...	...	...	...	1.00	0.95	0.91	0.86	0.82	0.77	NP	NP	NP	NP	NP	NP
CSEF (subcrit.) [Notes (9), (12)]	...	...	...	...	1.00	0.50	0.50	0.50	0.50	0.50	0.50	NP	NP	NP	NP	NP	NP
Austenitic stainless steels and alloys 800H (N08800) and 800HT (N08810) [Notes (13), (14)]	...	...	...	...	...	1.00	0.95	0.91	0.86	0.82	0.77	0.73	0.68	0.64	0.59	0.55	0.50
Autogenously welded austenitic stainless [Note (15)]	...	...	...	...	...	1.00	1.00	1.00	1.00	1.00	1.00	1.00	1.00	1.00	1.00	1.00	1.00

GENERAL NOTE: Nothing in this table shall be construed to permit materials that are not permitted by PG-5 through PG-9 of this Section or to permit use of materials at temperatures beyond limitations established by this Section. Several materials covered by this table are currently permitted for Section I application only via code case.

NOTES:

(1) Cautionary Note: There are many factors that may affect the life of a welded joint at elevated temperature, and all of those factors cannot be addressed in a table of weld strength reduction factors. For example, fabrication issues such as the deviation from a true circular form in pipe (e.g., "peaking" at longitudinal weld seams) or offset at the weld joint can cause an increase in stress that may result in reduced service life, and control of these deviations is recommended.

(2) NP = not permitted.

(3) Carbon steel pipes and tubes are exempt from the requirements of PG-26 and Table PG-26.

(4) Longitudinal seam welds in pipe for materials not covered in this table operating in the creep regime are not permitted. For the purposes of this table, the creep regime temperature range is defined to begin at a temperature 50°F (25°C) below the T-note temperature listed in Section II, Part D design property tables for the base material involved.

(5) All weld filler metal shall have a minimum carbon content of 0.05% for the Cr-Mo and CSEF materials and a minimum carbon content of 0.04% for the austenitic stainless steels.

(6) At temperatures below those where WSRFs are tabulated, a value of 1.0 shall be used for the factor *w* where required by the rules of this Section; however, the additional rules of this table and notes do not apply.

(7) The Cr-Mo steels include ½Cr-½Mo, 1Cr-½Mo, 1¼Cr-½Mo-Si, 2¼Cr-1Mo, 3Cr-1Mo, and 5Cr-½Mo. Longitudinal welds shall either be normalized, normalized and tempered, or subjected to proper subcritical PWHT for the alloy.

(8) Longitudinal seam fusion welded construction is not permitted for C-½Mo steel.

(9) Basicity index of SAW flux ≥ 1.0.

(10) N + T = normalizing + tempering PWHT.

(11) The CSEF (creep strength enhanced ferritic) steels include Grades 91, 92, 911, 122, and 23.

(12) subcrit. = subcritical PWHT is required. No exemptions from PWHT are permitted. The PWHT time and temperature shall meet the requirements of Table PW-39; the alternative PWHT requirements of Table PW-39.1 are not permitted.

(13) Certain heats of the austenitic stainless steels, particularly for those grades whose creep strength is enhanced by the precipitation of temper-resistant carbides and carbo-nitrides, can suffer from an embrittlement condition in the weld heat-affected zone that can lead to premature failure of welded components operating at elevated temperatures. A solution annealing heat treatment of the weld area mitigates this susceptibility.

(14) Alternatively, the following factors may be used as the weld joint strength reduction factor for the materials and welding consumables specified, provided the weldment is solution annealed after welding.

Temperature, °F Temperature, °C	950 510	1,000 538	1,050 566	1,100 593	1,150 621	1,200 649	1,250 677	1,300 704	1,350 732	1,400 760	1,450 788	1,500 816
Materials	Weld Strength Reduction Factor											
Type 304 stainless steel welded with SFA-5.22 EXXXT-G (16-8-2 chemistry), SFA 5.4E 16-8-2, and SFA-5.9 ER 16-8-2	1.00	1.00	1.00	1.00	1.00	1.00						
Type 316 stainless steel welded with SFA-5.22 EXXXT-G (16-8-2 chemistry), SFA 5.4 E 16-8-2, and SFA-5.9 ER 16-8-2	1.00	0.85	0.90	0.97	0.99	1.00						

(15) Autogenous welds (without weld filler metal) in austenitic SS materials have been assigned a WSRF of 1.00 up 1,500°F (816°C), provided that the product is solution annealed after welding and receives nondestructive electric examination, in accordance with the material specification.

3.3 European Practices

3.3.1 Practices of Determination and Use of WSRF in European Countries

In the European approach, all factors that in some sense are related to the weakening effect of weldments in high temperature applications are regarded as weldment reduction (sometimes called adjustment) factors. Therefore, for some of the design codes or assessment procedures, the weldment reduction factor is not a factor directly applied to the allowable stress, or strain, but a factor which, for example, enhances the stress level in the weldment region in order to account for the deficiency of the weldment.

In the German AD-Merkblatt and French RCC-MR, the weldment reduction factors are used to reduce the allowable stress level. The AD-Merkblatt uses the most simplified approach that can be used for an arbitrary weld system, while RCC-MR base reduction factors on results from tests of actual welded components with well-known, pre-specified weld systems.

In British PD6539 and R5, and French PODIS, factors are instead applied to different stress measures or similar, in order to take account of the weldment weakening effect. Among these procedures, R5 is the most comprehensive one.

Only two assessment procedures, i.e. PD6539 and R5, consider the influence of the weldment high temperature response in the assessment of weldments containing cracks. The approach used in PD6539 is a simplification of what is done in the R5 procedures.

The Italian approach is similar to the ASME approach.

3.3.1.1 Practices of Use of WSRF in Germany

The need for higher performance of power generation plants requires higher steam temperature which in turn requires use of welded larger piping. The German approach is that the creep failure of welded ferritic steel pipes can be prevented by modified design and/or production methods. The German high temperature design procedure is TRD 300/301 and assessment procedure is TRD 508, VGB-R509L.

In these procedures it is noted that the creep failure of ferritic weld steels is affected by base metal and constraint effect in loading and temperature. It is noted that at maximum service temperature, the strength ratio of weld metal to base metal, named “weldfactor”, is close to 0.5. The failure will also be effected by additional design-related loading such as bending moments and loading in pipe length direction that increase the “weldfactor” further.

In order to prevent creep failure of welded steels, designers consider creep “weld reduction factor” as a material specific property. It is also noted that in welded components of ferritic-martensitic steels, the failure in heat affected zone (HAZ) is confined to a narrow zone, and the criteria used for base metal, such as 1% or 2% strain, is not applicable. Hence, DIN EN 13480-3, Section 5.3.1, introduced an additional requirement of 20% strain on base metal data if creep rupture data is not available for weld-metal. A similar approach is taken in Draft European Norms EN 13445-2:20002/prA1:2006.7 as well as EN 13445-3:2002/prA1:2006.9.

Thus, defined “weld factor”, z, is multiplied with “weld creep strength reduction factor (WCSRF), c_z, which takes the value of:

- c_z,=1: when experimental data determined following Annex C EN13445-2:2002/prA1:2006.7 is available and meet the conditions in Annex C for the value of 1.

- c_z,<1: when experimental data following Annex C EN13445-2:2002/prA1:2006.7 is available but does not meet the conditions in Annex C for the value of 1.
- c_z,=0.8: when there is no experimental data determined following Annex C EN13445-2:2002/prA1:2006.7 is available.

The material data showed a reduced base metal average value of 50% for high alloyed steels at higher temperatures. This has a consequence on the codes that DIN EN 13480-3 as well as EN 13445-3:2002/prA1:2006.9 are not conservative. A further gap in assessment of weldments is the availability of long time weld metal creep data and extrapolation of weld creep data. State–of-the-art extrapolation allows a factor of 3 on rupture time of base metal data.

3.3.1.2 Practices of Use of WSRF in Italy: ISPESL P.T. 15/92

Life assessment of welded components requires creep rupture data of base and weld metal of a welded joint. The creep rupture data may be taken from national or international standards, or from tests performed in certified laboratories. If the required data is not available, the original material design data shall be used, such that:

- Considering a WCSRF (weld creep strength reduction factor), considering welding joint characteristics, base material behaviour, etc..
- Considering half of maximum cycle foreseen for base material low cycle for creep-fatigue calculation.

The typical WSRF values used are 0,7-0,85-1, according to NDE level. In case information about welds are missing, WSRF of 0,9 shall be adopted.

A WCSRF is mandatory in case of longitudinal joints, while it may be avoided in case of circumferential joints. In case of welds located on shell openings, there is a special evaluation of the joint which includes considering the real direction of the main stress. However, it is left to the responsibility of the user. The procedure of life expectancy of pressure components is the same as of EN 12952-4, including mandatory NDE tests.

3.3.1.3 Practices of Use of WSRF in UK: R5

The British Energy code R5 is a comprehensive creep assessment document. The development specifically addressed weldments and defects so that R5 goes beyond the scope of existing design codes to defect assessment procedure. The R5 document consists of 5 volumes:

- Volume 1: The Overview
- Volume 2/3: Creep-Fatigue Crack Initiation Procedure for Defect-Free Structures
- Volume 4/5: Procedure for Assessing Defects Under Creep and Creep-Fatigue Loading
- Volume 6: Assessment Procedure for Dissimilar Metal Welds
- Volume 7: Behaviour of Similar Weldments: Guidance for Steady Creep Loading of Ferritic Pipework Components

The general procedures are given in Volumes 2/3 and 4/5. Volumes 6 and 7 are applications of the creep-fatigue damage calculations of Volume 2/3 and the creep crack growth calculations of Volume 4/5, respectively, to particular weldments and operating conditions found in UK Advanced Gas Cooled Reactors.

The current approaches to calculation of both creep-fatigue damage and creep-fatigue crack growth use adjustment (reduction) factors applied to methods for homogeneous components. Such adjustment factors have been used for many years and were developed at a time when inelastic analysis of multi-material

components was difficult if not impossible. Materials testing to obtain the properties of the individual regions of a weldment was also difficult. The adjustment factors are successful when they are based on test data collected under conditions that closely match those in the component being assessed. However, they are less successful in describing, for example, creep-fatigue interactions under a wide range of conditions from creep-dominated to fatigue-dominated cycles. Developments in computational modelling and improvements in miniaturized testing and material descriptions are now allowing more detailed assessments to be made. Hence, it is now possible to refine procedures for assessing weldments in order to obtain greater accuracy. The developing refinements to the R5 procedures are described in Sections 4 and 5 for creep-fatigue initiation and creep-fatigue crack growth, respectively.

3.3.1.3.1 R5: Modifications for Weldments

In R5, the procedures of Volume 2/3 are set out as step-by-step instructions. The weldment is modelled as a single material for elastic analysis (Step 2). For dressed weldments, an accurate representation of the weld profile is used, so that the elastic analysis includes peak stresses due to local weld geometry. For undressed welds, the nominal geometry of the weldment, excluding the detail of the weld profile, is modelled.

In Step 5, the limit load given in Equation (1) to assess creep rupture using a rupture reference stress, which is calculated using the primary load reference stress, σ^{p}_{ref} , which may be calculated from

$$\sigma^{p}_{ref} = P\sigma_y / P_L \quad (1)$$

where P represents the magnitude of the primary loads and P_L is the corresponding value at plastic collapse for a rigid plastic material with yield stress σ_y .

It is replaced by a so-called mismatch limit load, P_{Lmis}, derived for the component where the yield stress is assumed to vary with position x in the structure as

$$\sigma_y(x) \propto S_R[M(x), T(x), t] \quad (2)$$

where S_R is the rupture strength for material M at temperature T (which may also vary with position) for the time at temperature or desired service life, t. Although there is a single value of P_{Lmis}, Equation (1) leads to a reference stress that differs in the different material zones because of the spatial variation of yield stress. However, these all lead to the same increment of creep usage because the corresponding variation in rupture strength is the same as the variation in yield stress.

In the shakedown analysis of Step 6, the geometrical modelling in Step 2 leads to peak stresses being included in the calculations for dressed weldments but not for undressed welds.

In Step 8, the start-of-dwell stress for dressed welds is calculated from a standard shakedown analysis using the elastic stresses from the single material analysis. If the position where creep damage is being calculated is in weld metal and the yield stress of the weld metal is higher than that of the parent, then the calculated start-of-dwell stress is multiplied by the ratio of the weld to parent yield stresses to account approximately for the effect of the increased strength of the weld. The increased stress is then used in Step 15 in conjunction with the creep ductility of the weld metal to calculate the creep damage. More generally, the creep ductility to be used is that of the material at the location being assessed.

3.3.1.3.1 R5: Procedure for Dissimilar Metal Welds

The procedures of R5 Volume 6 follow the principles of Volume 2/3 as described above, but differ in some details particularly in the use of weldment specific data.

The rupture reference stress is defined for the specific circumferentially welded geometry in terms of mid-wall hoop, radial and axial stresses and a multiaxial factor. This may be considered as a specific definition of limit load in Equation (1) incorporating the stress concentration effects of Equation (3).

For creep ductile materials the rupture reference stress is then calculated from:

$$\sigma_{ref}^{R} = \{1 + 0.13[\chi - 1]\}\sigma_{ref}^{p} \quad (3)$$

where the stress concentration factor χ is calculated from:

$$\chi = \bar{\sigma}_{el,max} / \sigma_{ref}^{p} \quad (4)$$

where $\bar{\sigma}_{el,max}$ is the maximum elastically calculated value of equivalent stress, at the chosen section.

Creep damage for the conditions dominated by primary loading in British Energy plant is due to the primary loading and this is evaluated as in Equation (5).

The increment of creep usage factor, dU, in a cycle of duration t is then

$$dU = \frac{t}{t_f(\sigma_{ref}^{R}, T_{ref})} \quad (5)$$

where t_f is the allowable time, from the creep rupture curve at the rupture reference stress σ_{ref}^{R}, at the reference temperature T_{ref}.

Thus, a mismatch limit load is not used and so the effects of material differences are included in the rupture data used in Equation (5), which are derived from cross-weld samples of the specific weldments of interest.

3.3.2 The ECCC Approach on Determination of WSRF

Within the European Creep Collaborative Committee, an evaluation of the influence of welding on creep resistance was performed 1993. The test results from cross-weld and parent metal creep testing were compiled for ferritic, martensitic and austenitic creep resistant materials. The concept of strength reduction factors and life reduction factors are discussed, the former for design purposes and the latter for judging the lifetime of welded components at normal design stresses. Strength reduction factors for weldments subjected to creep are suggested for a number of weld systems. For P91, in the temperature range of 600 to 650ºC, a strength reduction factor of 0.7 is suggested. The risk of determining non-conservative strength reduction factors, when performing accelerated cross-weld creep tests, is also addressed.

The importance of considering the influence of the multiaxial stress state in the weldment region when assessing weldments subjected to creep is also addressed. A semi analytical approach in determining weldment creep strength reduction factors is described. This approach has sufficient accuracy to a low cost. It is suggested that the spatial distribution of constitutive parameters is determined by uniaxial testing while the creep response of components is simulated by numerical methods. By considering the stress multiaxiality and the corresponding stress redistribution process, weldment creep reduction factors are then derived. The use of simple weld reduction factors (0.8 with respect to creep rupture, 0.5 with respect to cyclic life) in the life prediction procedure for welds may risk being nonconservative.

3.3.3 WSRF in European Codes

3.3.3.1 French Code: RCC-MR

The French RCC-MR Code for Fast Reactors (FRs), which includes design rules for elevated temperatures (> 425°C), was issued by AFCEN (French Society for Design and Construction Rules for Nuclear Island Components) in 2007. However, the rules and requirements provided by this Code are not limited to FRs, and RCC-MR is therefore the most consistent set of rules applicable in the high temperature domain.

The modifications to RCC-MR and subsections are made in the 2007 edition (which is available in French and English) and include:

- Improvement of sets of material properties for base metal and associated **welded joints** taking into account the latest test results from R&D European activities
- Larger use of references to European standards
- Modification of design rules taking into account the feedback from design studies and recent improvements resulting from R&D work
- Extension of the scope of the RCC-MR by the introduction of a guide for Leak Before Break analysis (Subsection Z, Appendix A16)

The RCC-MR code provides in Section 1, Subsection Z, Appendix A3: General, consistent sets of material properties that are needed for the application of the design rules of Section I. Appendix A3 covers in particular the following groups of materials:

- Austenitic stainless steels: 316 or 316L(N), 304, 316L, 304L
- Nickel Iron alloy (alloy 800)
- Carbon manganese steels
- Chromium molybdenum steels: 2.25 Cr 1 Mo and 9 Cr 1 Mo V Nb grades
- Precipitation hardened austenitic steel for bolting (25 Ni 15 Cr Mo V Ti Al)

The material properties of Appendix A3 are applicable to the base material. The allowable stresses of the welded joints depend on the quality of the weld (type of joint, extent of control) and on the material properties of the base and weld metal. Subsection Z, Appendix A9: Characteristics of Welded Joints, provides **weld joint factors** that can be used to determine the material properties of the welded joints on the basis of the properties of the base material. The allowable stresses for base metal, S_m, S_t, S_r. are presented in Annex 9.

The general rules for use of the base metal properties are given in Section 1, Subsection RB3252: Rules for prevention of type P damage in case of significant creep, and Subsection RB3260: Rules for prevention of type S damage in case of significant creep.

The rules for use of weld joint coefficients, J_m, J_r, J_t, J_f are given in Section 1, Subsection RB3290, where;

- J_m is the characteristic coefficient for the weld
- J_t is the characteristic coefficient for the weld at flow
- J_r is the characteristic coefficient for the weld at rupture

The allowable stresses in the weld are directly deduced from those of the base metal by multiplying allowable stresses for base metal by characteristic coefficients. The coefficients J_m, J_r, J_t, J_f are given in tables in Appendix 9, although for limited number of materials. The work is in progress on other materials which is expected to be published in the next edition of the RCC-MRx in 2010.

The WSRF is named in RCC-MR as Jr coefficient which is defined above. Its application involves materials data provided in Appendix A9, and creep damage, W, is calculated from

$$W = \int_0^{t_r} \frac{dt}{t_r\left(\frac{1.35\sigma}{nJ_r}\right)} \tag{6}$$

Unlike the ASME Section III-NH, where WSRF is defined as the uniaxial creep rupture strength ratio of weld metal to base metal (for stainless steel), the RCC-MR defines WSRF as the ratio of the strength of the weld joint to the strength of the base metal. The RCC-MR definition of WSRF does not provide any recommendation for the size effect.

To handle multiaxial stresses, RCC-MR allows the use of either the maximum shear theory (Tresca) or octahedral shear theory to compute stress intensities or stress range intensities.

The average stress to rupture values for the weld joint are obtained by multiplying the average stress to rupture values for the base metal given in the RCC-MR code with the corresponding weld strength reduction factors given in Figure 75 below.

Figure 75: Table of Weld Strength Reduction Factors for 316L(N) SS as Recommended by RCC-MR Code

Time (h)	873 K	923 K
1	0.99	0.92
10	0.99	0.92
30	0.99	0.92
100	0.94	0.85
300	0.86	0.78
1000	0.78	0.76
3000	0.76	0.73
10000	0.74	0.70
30000	0.72	0.66
100000	0.70	0.63
300000	0.66	0.58

3.3.3.2 European Norm: EN 13480-3:2002 and EN 12952-3:2001

The approach taken in EN is briefly mentioned in section 3.3.1.1.

The design stress for welded connections operating under creep conditions

When the creep properties of the welded connection are known, the smallest of the design strengths of the welded connection and the two joined materials shall be used for loading at the weld seam.

When the creep properties of the welded connection are not known, but those of the filler material are known, the design strength for this loading shall be reduced by 20% from the smaller of the design strengths of the joined materials.

When the creep strength of the filler metal is not known, the joint strength shall be reduced by a further 20%.

In the case of austenitic steels, the following shall be used:

- if its elongation after rupture exceeds 30%, 2/3 of R_{et}.
- or, alternatively, and if its elongation after rupture exceeds 35%, 5/3 of R_{et} and 1/3 of R_{m20}.

Weld Joint Coefficient

The joint coefficient z shall be used in the calculation of the thicknesses of components which include one or several butt welds, other than circumferential, and shall not exceed the following values:

- for equipment subject to destructive and non-destructive testing which confirms that the whole series of joints show no significant imperfections: 1;
- for equipment subject to random non-destructive testing: 0,85;
- for equipment not subject to non-destructive testing other than visual inspection: 0,7.

For the calculation of the strength of butt welded assemblies under exceptional operating conditions or under test conditions, it shall not be necessary to take a joint coefficient into account.

For the calculation of the required thickness of certain welded components (e.g. cylinders, cones and spheres), the design formulae contain z, which is the weld joint coefficient of the governing welded joint(s) of the component.

Examples of governing welded joints are:

- longitudinal or helical welds in a cylindrical shell;
- longitudinal welds in a conical shell;
- any main weld in a spherical shell/head;
- main welds in a dished head fabricated from two or more plates.

The following welded joints are not governing welded joints:

- circumferential weld between a cylindrical or conical shell and a cylinder, cone, flange or end other than hemispherical;
- welds attaching nozzles to shells;
- welds subjected exclusively to compressive stress.

NOTE: Circumferential joints may become governing joints due to external loads.

For the normal operating load cases, the value of z is given in Figure 76 (original Table 5.6-1). It is related to the testing group of the governing welded joints. Testing groups are specified in EN 13445-5:2002, Clause 6.

Figure 76: Table of Weld Joint Coefficient and Corresponding Testing Group

z	1	0,85	0.7
Testing Group	1, 2	3	4

Note: In parent material, away from governing joints, z = 1.

For exceptional and testing conditions, a value of 1 shall be used, irrespective of the testing group.

3.3.3.3 British Standards: BS 7910

There is no explicit coverage of creep assessment of high temperature welds in BS7910.

3.3.3.4 British Energy Code: R5

R5 does not use WSRF for creep assessment of welds. In predominantly load controlled situations where rupture strength is used in the procedure, the rupture data for different weldment zones is used. In the case of narrow Type IV zones in CMV welds, these data are obtained from multi-zone cross-weld tests. For creep-fatigue and strain controlled situations, R5 uses ductility exhaustion.

3.3.3.5 Swedish Pressure Vessel Code: TKN87, Tryckkarlskommissionen, 1987

The Swedish Code TKN87 use a Weld Reduction Factor only related to NDE after manufacturing, with no other allowance for weldments operating in creep regime.

4 DATABASE OF WELD AND WELDMENT CREEP-RUPTURE PROPERTIES

4.1 Carbon Steel

A literature search and review was conducted for information on the creep rupture behavior of C-steel weldments. The search produced a very limited number of published papers on the subject. The most relevant papers describe creep rupture testing of weldments and base metal sample material removed from in-service petro-chemical plant equipment. The test durations were nearly always less than 10,000 hours and typical test durations did not exceed 4000 hours. Additional stress-rupture data were also supplied on carbon steel filler metal by a boiler OEM. Appendix A contains the tabular data. The limitations of the data notwithstanding, the review and analysis yielded some preliminary findings as summarized below.

4.1.1 Summary of Data

The available cross-weld data were reviewed and evaluated against (a) base metal data from the same source, and (b) the plate base metal data of ASTM DS 11S1 [39]. Figure 77 is a summary of the published data analyzed. The following relevant features of the data sets are noted:

- All of the tested materials were ex-service, removed from petro-chemical plants. As such, a direct comparison of the ex-service cross-weld (X-W) behavior against unexposed base metal would likely be conservative.
- Some of the data sets include tests on ex-service base metal, so that to the extent possible, comparisons may be made between cross-weld and base metal behavior removed from the same piece of equipment.
- The creep rupture test durations are generally short (well below 10,000 hours and typically less than 4,000 hours) and extrapolations to typical service conditions are uncertain. In any case, the Larson-Miller time-temperature parameter has been used for the comparative analysis.
- In the majority of cross-weld cases, the rupture test specimen failure occurred in the fine grain material of the heat-affected zone (HAZ). In the remaining cases, the failure locations appeared to be evenly split between the base metal (BM) and the weld metal (WM).

Figure 77: Summary Table of Published Data Analyzed

Reference	Material	Service Conditions	Creep Rupture Test Conditions	Comments
Ellis et al. (1993) [40]	Ex-service, mitered C-steel elbow (long seam and girth weld) in transfer line of petro-chemical plant	26 yrs., Temperature conditions not reported. Future operation at 1.45 ksi and 1022F.	BM: 1.75-3.5 ksi, 1150°-1300°F, 80-4400 h. X-W: 2.7, 3.75 ksi, 1100°-1300°F, 66-10080 h.	All X-W specimens failed in the FG HAZ
McLaughlin et al. (1994) [41]	Ex-service C-steel petro-chemical plant reactor	Approximately 40 yrs., Maximum temperature of 970°F	Only X-W tests. All at 3 ksi. 1125°, 1175°F, 908-4167 h.	All X-W specimens failed in the FG HAZ
Moss & Davidson (1993) [42]	Ex-service material from three FCCU reactor vessels, A 201 Grade A or B	27, 33 and 36 yrs, at 932°, 970° and 973°F, respectively.	X-W: 2.6 – 7.0 ksi, 1074°-1238°F, 132-1635 h.	X-W specimens failed in the FG Wm and the FG HAZ. Plotted BM data appeared to be in error and not used.

Reference	Material	Service Conditions	Creep Rupture Test Conditions	Comments
Ray et al. (2000) [43]	Ex-service material from FCCU reactor vessel, A 201 Grade A	Approximately 32 yrs. at 900°F	BM: 10.15-17.4 ksi, 842°, 887°, 932°F, 360-2370 h. X-W: 10.15-24.66 ksi, 842°, 887°, 932°F, 4-2496h.	All X-W specimens failed in the BM. As analyzed, the X-W and BM data were indistinguishable.
Wilson, WRC 32 (1957) [44]	Ex-service petroleum refining equipment from 3 plants (C,D,F). Plates are A 201 (C,D: Grade A and FD: Grade unknown)	C: 80khr, 925°F D: 88khr, 890°F F: 25khr, 913°-930°F	C: 9-18 ksi, 5-750 h D: 9-14 ksi, 7-900 h F: 9-14 ksi, 25-1200 h All tests at 1000°F.	Failure locations varied: FG HAZ for C, BM for D, and WM for F

4.1.2 Qualitative Observations

With regard to the relative performance of cross-welds (weldments) compared with base metal, the following general observations are made:

- The data of Ellis et al. [40] on ex-service material indicate the weld metal rupture strength to be the highest, followed by that of the base metal, and the cross-weld configuration in that order.
- In the absence of creep rate data, no firm conclusions can be made regarding the relative creep resistance of weld metal and weldments compared with base metal. However, the majority of the documented laboratory and in-service instances of cracking and failure occurred in the fine grain HAZ, and the weak weld-driven fusion line failure problem of the low alloy CrMo steels is evidently absent.
- In the case of C-steels, weld metal creep and creep rupture strength may be assumed to be comparable to, or better than base metal. This is discussed below.
- The HAZ region of cross-weld specimens was observed to undergo greater creep deformation than the adjacent base and weld metal [41].
- The reported service experience did not show the kind of premature weldment failures seen with the low alloy CrMo steels, consistent with a relatively minimal mismatch effect.
- In three of the four ex-service material test cases where base metal and cross-weld test data were obtained [40], [42], [44] the cross-weld rupture strength was reportedly somewhat lower than that of the base metal. In one case [40], the investigators report Manson-Succop parametric parallel, heat-centered (base metal and cross-weld treated as heats) analysis constants that suggest a cross-weld to base metal rupture strength ratio of about 0.9. In the fourth case, the base metal and cross-weld rupture data were comparable.
- The reported cross-weld tested specimen ductility, while typically lower than that in base metal specimens, remained substantial – 20-27% elongation.

4.1.3 Analysis of Data

All of the published creep rupture data from the references of Figure 77 were represented on a Larson-Miller parametric plot, along with the ASTM DS 11S1 plate data, and third-order logarithmic stress best-fit and minimum (90% normal distribution lower statistical bound) curves representing the ASTM data. All of this is shown in Figure 78. For clarity, the figure is reproduced without the ASTM data as Figure 79.

The noteworthy aspects of the data as presented in the figures are:

- The ex-service cross-weld and base metal test data at the lower stresses (and higher temperatures – Ellis et al. [40], McLaughlin et al. [41], and Moss & Davidson [42]) are well within the band of the ASTM data and not distinguishable from the unexposed base metal data. Test temperatures for the data ranged from 1100° to 1238°F.
- The ex-service cross-weld and base metal test data at the higher stresses (test temperature was 1000°F for the Wilson WRC 32 data [44] and ranged from about 840° to 940°F for the Ray et al. [43] data) appeared to fall at the low end of or below the ASTM data. This is likely due to the effect of in-service aging which is not reflected in the unexposed base metal data in this stress range.
- Of the three cases where there were cross-weld data and base metal data generated on material from the same source and ex-service equipment sample [40], [43], [44], it qualitatively appears that the cross-weld data were slightly inferior to that of the base metal in two cases (Ellis et al. [40] and Wilson WRC 32 [44] and nearly identical to that of the base metal in the third case (Ray et al. [43]).

The ex-service data of Ray et al. [43] and Wilson WRC 32 [44]) were separately reviewed and analyzed to examine the difference between base metal and cross-weld behavior. The data of Ellis et al. [40] could not be analyzed due to the limited data and spread across the test stresses. Given the limited nature of the data sets, a simple first order log stress LMP fit was made to the base metal data. Following this, a similar, but parallel fit was made to the cross-weld data in each case. Figure 80 illustrates these curve-fits. The cross-weld and base metal data best-fits of Ray et al. are indistinguishable. The fits to the Wilson WRC 32 data showed a stress offset or cross-weld to base metal best-fit stress ratio of 0.94. Given the statistical scatterband for the data, the base metal and cross-weld data for these two sets are not statistically distinguishable.

Figure 78: As-Reported C-Steel Weldment and Base Metal Rupture Data [40], [41], [42], [43], [44] on a Larson-Miller Parameter (LMP) Plot Along with the ASTM DS 11S1 Plate [39] and the Curve-Fits to That Data

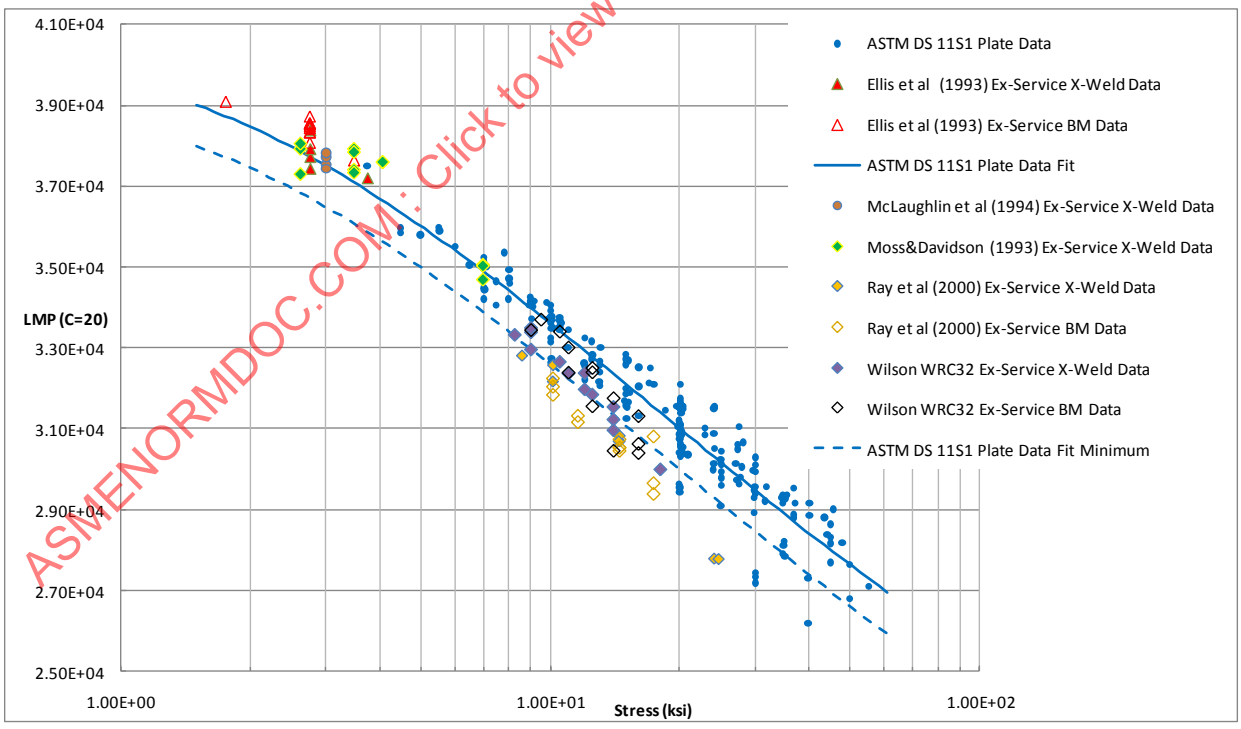

Figure 79: Reproduction of Figure 78 Without the ASTM Data

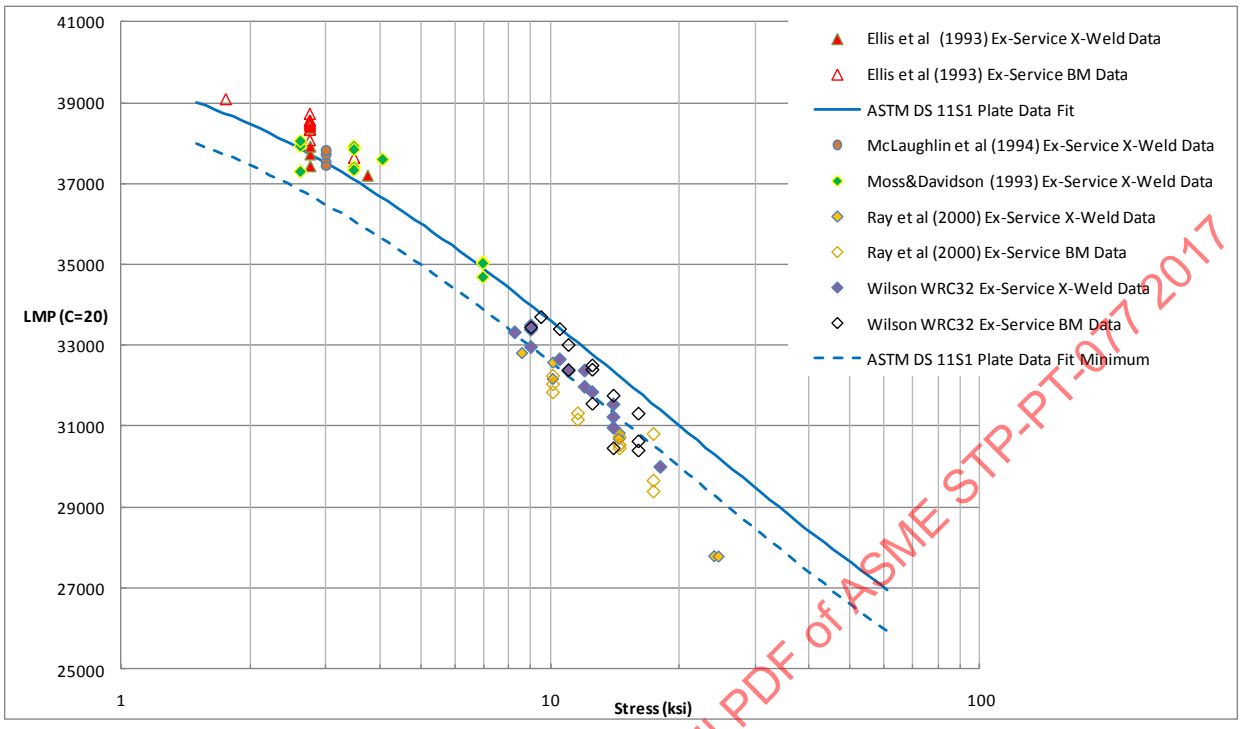

While a similar exercise could not be conducted for the data from Ellis et al. [40], as noted earlier, the investigators reported heat-specific (base metal and cross-weld considered as heats) Manson-Succop heat constants that translate to an approximate stress ratio (cross-weld to base metal rupture strength) of 0.9. What is perhaps more important is that all of the data are well within the unexposed base metal data band and some data are above the ASTM data best-fit curve (Figure 78 and Figure 79).

The ex-service cross-weld data from Refs. [41], [42] similarly are well within the ASTM data scatterband and some data are above the ASTM data best-fit curve.

Figure 80: Base Metal and Cross-Weld Test Data Linear Fits Compared for Ex-Service Material Rupture Tests from Ray et al. [43] and Wilson WRC 32 [44]

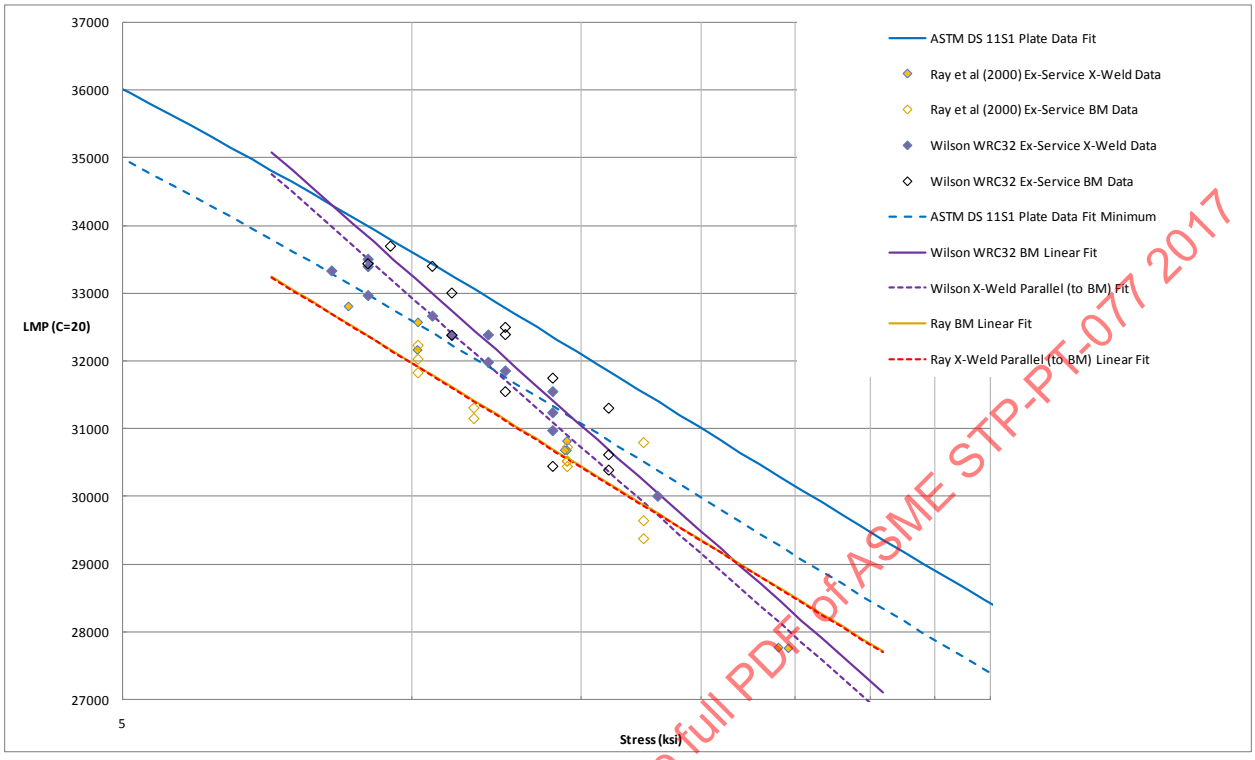

4.1.4 Weld Metal Behavior

This review focused on comparing cross-weld/weldment behavior against base metal, and no effort has been made to examine the relative behavior of weld metal. However, given that weldment creep rupture behavior may be affected and predicted by the relative difference in performance of base metal and weld metal separately, a review was conducted of the all weld metal (E7018 filler) stress rupture data provided by Babcock & Wilcox Co. (B&W) to EPRI [45]. In addition, the limited ex-service weld metal data of Ellis et al. [40] was reviewed along with the B&W data set.

The B&W stress rupture data consisted of tests on E7018 filler weld metal of three carbon content levels (nominally 0.05, 0.1 and 0.15 weight %, henceforth referred to as low, medium and high carbon, respectively) with tests at 800° and 950°F and with a maximum duration of about 4,400 hours. Tests were mostly conducted with specimens oriented longitudinal to the weld with a limited number of tests transverse to the weld. The weld material was tested in both the as-welded and in the stress-relieved condition (1125°F/8 hours).

B&W concluded that all of its tested weld metal stress rupture data were above the average ASTM DS 11S1 base metal properties. The comparison was made isothermally, apparently using pipe/tube base metal data. B&W also observed for the two higher carbon weld deposits that there appeared to be a change in slope of the isothermal rupture behavior at 950°F occurring at 1000 hours, such that the weld metal data would be projected to cross-over the ASTM average behavior at 10,000-20,000 hours.

For this review, the data were, as for the cross-weld cases described earlier, presented on a LMP plot illustrating the ASTM DS 11S1 plate data and curve-fits (Figure 81). Also included on the plot are the ex-service weld metal data of Ellis et al. [40] It can be seen from the graphic that:

- Except for some of the B&W stress-relieved weld metal data and one as-welded test data point at 800°F, all of the weld metal data are above the ASTM DS 11S1 base metal data.
- The effect of stress-relief is not seen at 950°F, indicating that the suggested possibly inferior (to base metal) behavior at 800°F is due to "accelerated" aging of the stress-relief, and would likely not persist to longer test durations.
- While not illustrated in the figure and as mentioned earlier, the ex-service weld metal data of Ellis et al. exhibited superior rupture strength to the base metal and cross-weld material from the same sample.
- The reviewed weld metal test data do not indicate significant evidence of a relative (to base metal) weak weld. Indications are that in case of C-steel, the weld metal may have a rupture strength comparable to, or even slightly higher than base metal.

Figure 81: All Weld Metal Data from B&W [45] and the Ex-Service Weld Metal Data of Ellis et al. [40] in Comparison with the ASTM DS 11S1 Plate Data and Curve-Fits on a Larson-Miller Parametric Plot, SR: Stress-Relieved

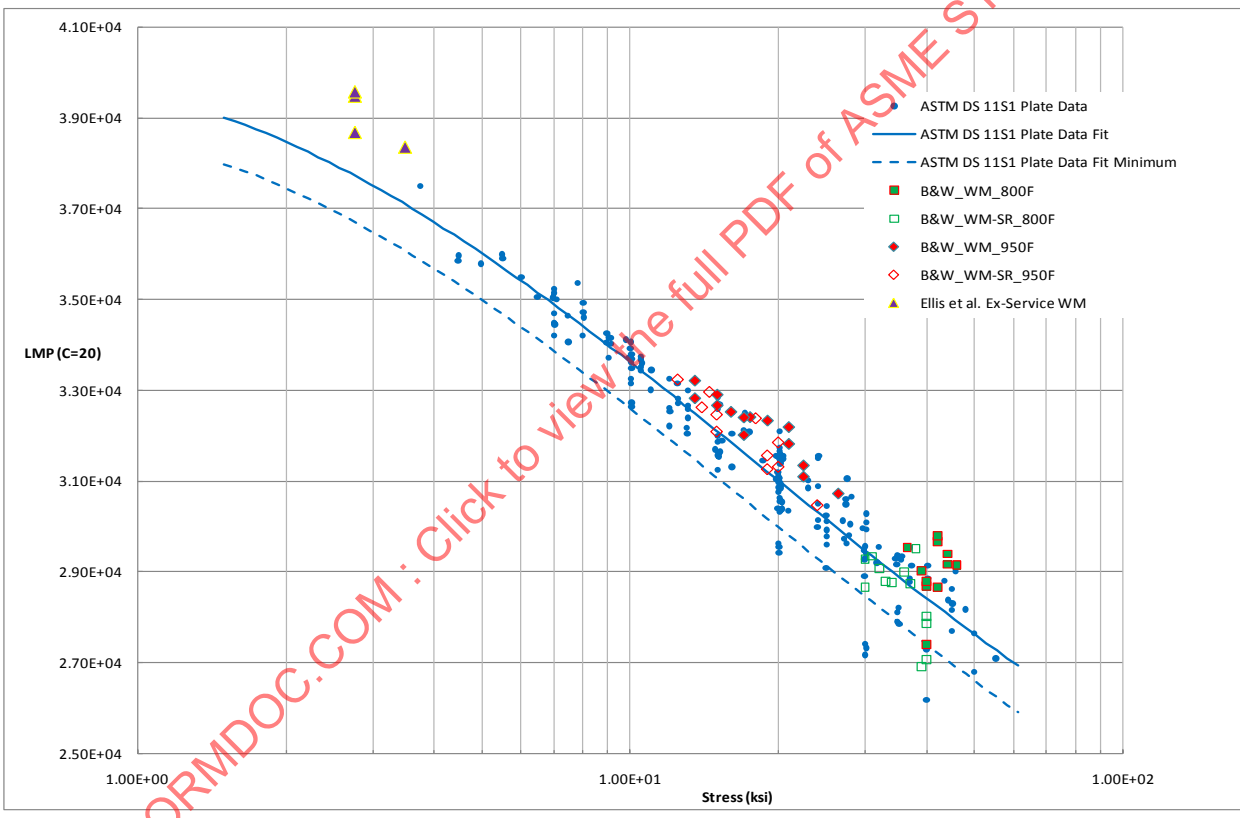

4.1.5 Summary

This investigation into the creep rupture behavior of C-steel weldments resulted in the following findings to date:

- The broad search for C-steel weldment creep rupture data resulted in very limited published information. This may well be because the service experience with C-steel weldments has not shown evidence of premature failures of the kind seen with the low alloy CrMo steels.
- Indications are that C-steel weldments do not suffer from the weak weld mismatch effect that drives near-fusion line failures in the low alloy CrMo steel. C-steel weldments appear to have weld metal rupture strength that is comparable to or slightly superior to that of base metal.

- The limited published laboratory cross-weld data reviewed showed that the fine grain heat-affected zone of C-steel weldments is the prominent creep rupture failure location in cross-weld tests, although the data show no evidence that this failure mode results in a significant decrease in rupture life compared with base metal.
- In a qualitative comparison of the available ex-service cross-weld data with unexposed plate base metal data, the higher temperature, lower stress test data lie well within the scatterband of the base metal data and show no evidence of significantly lower rupture life.
- Ex-service weldment cross-weld tests at the higher stress and lower temperatures show rupture lives that appear shorter than that of unexposed base metal, likely a consequence of the in-service aging effect. However, a direct comparison of the cross-weld rupture data against the base metal data within each data set showed that the cross-welds were not significantly inferior to the base metal.
- Stress-rupture data on carbon steel weld metals with various levels of carbon all met or exceeded the expected creep strength of C-steel base metal.
- The review did not produce substantive evidence that weldments of C-steel are susceptible to premature failure.

4.2 Chromium-Molybdenum Steels (Gr. 11 & 22)

4.2.1 Database

The Electric Power Research Institute (EPRI) conducted a detailed review of available data on Chromium-Molybdenum (Cr-Mo) steels in 1998 [46]. The report, "A Review of High Temperature Performance Trends and Design Rules for Cr-Mo Steel Weldments, TR-110807," is found in Appendix B. The tabular database are included in this report and covering a total of ~1400 weld metal or weldment creep test data and another ~1600 base metal data primarily on Grades 11 (1-1/4Cr-1/2Mo) and 22 (2-1/4Cr-1Mo). Figure 82 and Figure 83 contain a summary of the spread of data obtained from this work which covered a wide range of welding processes and chemistries from 33 references. As is evident by inspection of these tables, the Grade 11 database contains relatively shorter duration tests and few datapoints.

Figure 82: Summary Table of Grade 11 Weld and Weldment Data from Ref [46]

Grade 11	All	CW	Weld Metal	Other
Datapoints:	**138**	37	101	
Failure Location		9	n/a	
Creep Strain		No	No	
Temperature °F (°C)	900-1229 (482-665)	1000-1229 (540-665)	900-1200 (482-649)	
Approximate Max Test Time (hrs)	12,000	6,000	12,000	

Figure 83: Summary Table of Grade 22 Weld and Weldment Data from Ref [46]

Grade 22	All	CW	Weld Metal	Other
Datapoints:	**1174**	258	900	16 (HAZ)
Failure Location		188	n/a	
Creep Strain		Yes	Yes	Yes
Temperature °F (°C)	750-1319 (400-715)	850-1300 (454-704)	900-1292 (482-700)	1022-1319 (550-715)
Approximate Max Test Time (hrs)	46,000	25,000	46,000	1650

4.2.2 Summary of Observations

As part of the database development effort, the weldment data were qualitatively compared to base metal rupture data and design curves in a series of isothermal and time-temperature-parameter plots. Trends in the data suggested some systematic influences on performance including: post-weld heat-treatment, weld metal carbon content, and fabrication. Trends were examined for welding process, specimen type, and weld fusion angle boundary, but trends were either non-existent, unclear, or inconsistent. Overall, the study found, based on the data examined, that combining the weld strength reduction factors for 2-1/4Cr-1Mo as prescribed in ASME Code Case N-47 (now ASME Section III-NH) to the maximum allowable stresses in ASME Section I, VIII, and B31.1 would be 'excessively' conservative. It should be noted the report also suggests that the use of standard specimens may not reflect the crack initiation and growth behavior of long-term failure modes, but the report did not interrogate the database on the basis of failure mode; so no supporting evidence was presented for this statement.

In summary, the report found for Grades 11 and 22:

- In terms of currently available creep-rupture data, combining the weld reduction factors given in Code Case N-47 with maximum allowable stresses prescribed by ASME Sections I and VII and B31.1 represents an unwarranted level of conservatism for inspected weldments.
- In comparison with design practices in Europe, the practice of Code Case N-47 is less conservative under 1000°F but is substantially more conservative above 1000°F.
- There appear to be the following systematic creep-rupture performance trends based on a qualitative assessment of the data:
    - For service temperatures at or below 1000°F, minimizing PWHT and tempering temperatures should be advantageous, but for service above 1000°F, PWHT condition has little effect on weldment life.
    - In some (but not all) cases, annealed and tempered microstructures were found to be superior to PWHTed material above 1000°F.
    - Excessively long (greater than 12 hours) heating times should be avoided at PWHT temperatures above 1250°F.
    - For service temperatures at or below 1050°F, the higher (>0.05%) carbon versions of Gr 11 and 22 weld metals are advantageous. Above 1050°F, weld metal carbon content has a negligible effect between 0.02 and 0.15%.
- Creep-rupture performance trends associated with welding process, specimen type, and fusion boundary angle are unclear or inconsistent and require further study.

Finally, the report suggests an effort to evaluate industry experience with weldment creep performance through computational and/or experimental studies is necessary, including an understanding of standard and full-size specimen behavior.

4.3 308 Stainless Steel Weld Metal and 304/308 Stainless Steel Weldment Stress-Rupture Data

4.3.1 Review of Studies

In 1954, Wylie, Corey, and Leyda [47] reported results of stress-rupture tests on "eleven compositions of commercial stainless steel weld deposits." Weld pads were produced using the shielded metal arc process (SMA), and these pads were of sufficient thickness to produce all-weld-metal specimens parallel and transverse to the welding direction. Three carbon levels (0.09, 0.07, and 0.03%) for 308 filler metal were examined. Specimens were 0.252 and .505-in. diameter. Stress-rupture tests were performed at 1050°F (566°C) and 1200°F (650°C). Rupture strengths were tabulated for 100, 1000, and 10,000 h. Wylie, Corey,

and Leyda provided stress-rupture plots. Hardness and magnetic permeability measurements were taken on aged specimens, and changes were reported.

In 1958, Voorhees and Freeman [48] produced a compilation of weldment data published by the American Society for Testing and Materials. Stress-rupture data for three lots of "18-9" stainless steel weld metal were included in the database. All welds were produced by the SMA process, and one filler metal was a low-carbon composition. Reported data included stress, life, and elongation at 1050 and 1200°F (566 and 649°C).

In 1966, Canonico and Swindeman [49] performed exploratory fatigue, tensile, and stress-rupture tests on specimens machined from 304/308 weldments. Butt welds were made in 5/8-in. (16-mm) plate by the gas tungsten arc (GTA) process, and 1/4-in. (6.3-mm) diam. gage specimens were machined transverse to the weld. Some specimens were tested in the as-welded condition. Other specimens were annealed at 1850°F (1010°C) prior to testing. All failures were in the base metal.

Davis and Cullen [50] examined the influence of nitrogen on the strength of 308 stainless steel weldments in 1968. Three nitrogen levels (0.053, 0.14, and 0.29% N) were introduced by adding nitrogen to the argon cover gas during the butt welding of 347 stainless steel tubes by the gas-metal-arc (GMA) process. Weldments were annealed prior to testing, which was performed in the temperature range of 1200 to 1500°F (649 to 815°C). All failures occurred in the 308 weld metal.

In the late 1960's, the Department of Energy (DOE), then the U. S. Atomic Energy Commission and later the Energy Research and Development Agency, initiated a major research and development program on austenitic stainless steel weld metals. Research included the evaluation of existing filler metals, the development of filler metals with improved strength and ductility, and the development of a design methodology for use in nuclear construction. A very large number of papers and reports were issued during the program which lasted more than 15 years. Research on filler metals started with an examination of the effect of ferrite content on microstructure and properties summarized by Edmonds, Vandergriff, and Gray [51]. Electrodes with different coatings were produced by Combustion Engineering, Inc. and butt welds were made in 304 stainless steel plates by the shielded metal arc (SMA) process. Button-head specimens were machined parallel to the welds and having 1/8-in. (3.2-mm) gage diam. These specimens were tested in the as-welded condition at 1200°F (649°C). Summary reports and papers included those by Berggren, et al. 1977 and 1978 [52], [53]. Most of the original data have been destroyed, but minimum creep rate and rupture life data for a few weld metals remain.

From the work of Edmonds, et al. [51], Berggren, et al. [52], [53], King, et al. [54], and Stiegler, et al. [55] came a coated electrode that produced a deposit with controlled residual elements (CRE) - titanium, phosphorus, and boron. Typically, titanium was around 0.06%, phosphorus was around 0.04%, and boron was around 0.007%. The 308CRE stainless steel electrode was used to produce welds in 2 3/8-in.(60-mm) 304H stainless steel plates that were ordered for the fabrication of the pressure vessel in Fast Test Flux Facility (FFTF) at Hanford, WA. Two heats of 304H stainless steel base plates were used for the experimental program, and more than fourteen heats of 308CRE stainless steel filler metal were consumed in welding the test plates with a double-U groove configuration. The plates were sawed to make over one hundred blocks, each 8x12x2-3/8 inches (200x300x60 mm). Testing of specimens machined from the blocks included physical properties, tensile, creep, fatigue, crack-growth, and aging studies. Several testing laboratories were involved in the evaluations [56], [57], [58]. Most of the elevated-temperature testing was in the temperature range of 900 to 1200°F (482 to 649°C), although some testing was performed as high as 1600°F (871°C) and the creep and stress-rupture testing at the Oak Ridge National Laboratory (ORNL) involved three filler metals. Specimens from three locations through the thickness were tested, and it was found that the specimens closest to the crown of the weld were weaker than specimens whose locations

were toward the root. The weld metal was found to be substantially stronger and more ductile than weld-deposited 308 stainless steel.

As part of the research sponsored by the DOE, a testing program was initiated at the Hanford Engineering Development Laboratory (HEDL) to determine the strength and ductility of austenitic stainless steel weldments in the irradiated and aged conditions [57], [58]. Similar and dissimilar welded joints were produced at HEDL and ORNL, and testing on weld metal, HAZ metal, and base metal was performed at both laboratories. Filler metals included 308 and 308CRE stainless steels. Welding processes included gas-tungsten-arc (GTA), shielded-metal-arc (SMA), and submerged-arc (SA). Tests included tensile, creep, and stress-rupture at temperatures as high as 1200°F (649°C). The data produced by HEDL and ORNL were used in establishing Stress Reduction Factors for various combinations of base metals and filler metals.

In the mid-1970's Edmonds and Bolling [59], Klueh and Edmonds [60], and others started a study to examine the effect of controlled residual elements on the stress-rupture properties of 308 stainless steel deposited by the gas-tungsten-arc (GTA) process. As with the 308CRE electrodes for the SMA process described above, the residual elements of interest for the GTA welds were titanium, phosphorus, and boron. Laboratory heats and commercial heats of filler metal were produced as wire. Butt welds were made in 1/2-in (13-mm plate), and button-head specimens with 1/8-in. (3.2-mm) diam gage sections were machined parallel to the welding direction. All testing was performed at 1200°F (649°C). The research showed that titanium was effective in improving the strength and ductility of GTA weld metal. A combination of titanium, phosphorus, and boron was found that enhanced properties over titanium additions alone. Efforts were made by Edmonds and coworkers [61] to develop a submerged arc (SA) welding technology that would deposit 308 stainless steel filler metal with improved strength and ductility.

Again, titanium, phosphorus, and boron were added to the 308 composition. Small and large experimental heats of weld wire were produced, and SA welds were made in 1-in. (25-mm) plate with a single V-groove and a 3/4-in. (75-mm) root opening. The backing strip was the same material as the base metal plate (304H stainless steel). Specimens were machined from the plate parallel to the welding direction. Gage diameters were 1/4-in. (6.3-mm). Creep tests were performed at 1200°F (649°C). Generally, the rupture strength of the SA welds from the 308CRE stainless steel wire exhibited about the same strength level as conventional 308 stainless steel welds. Data trends suggested that extrapolated long-time strength was better. Conventional SA welds of 308 stainless steel in pipes were also examined by Edmonds and coworkers, and stress rupture data were collected.

Klueh and Canonico [62], [63] examined the microstructure and mechanical properties of a 304H stainless steel forging overlay clad with 308 stainless steel weld. The 30-in. (760-mm) diameter forging was similar to the tubesheet procured for the FFTF intermediate heat exchanger. Six layers of 308 stainless steel filler metal were deposited by the submerged-arc process. Specimens were machined in the radial, tangential, and axial directions of the cladding and the base metal near the cladding. Tensile, creep, and stress rupture tests were performed at temperatures in the range of 900 to 1100°F (482 to 649°C). The 308 weld metal was observed to be weaker than the forging steel near the fusion line and away from the fusion line. Cross-weld specimens failed in the 308 stainless steel weld metal.

In 1977 and 1981, McAfee, Richardson, and Sartory [64], [65] reported the results of a series of experiments on 304H stainless steel tubes [4-in. (100-mm) diameter] containing 308 stainless steel welds. These pipes contained girth welds and end cap welds. The tubes were pressurized at 1100°F (593°C). Both deformation and rupture life data were collected for eleven experiments covering the time range from 35 to 9712 hours. McAfee, et al. [64] concluded that the lives of the tubes were controlled by the base metal properties and rupture lives correlated best with uniaxial base metal data through the maximum principal stress criterion. Although all failures were in the base metal, some cracking was observed near or in the weld region of the end caps. Cracking was attributed to the high discontinuity stresses that existed in those locations.

In 1978, the Metals Properties Council, Inc. sponsored a symposium on the properties of steel weldments for elevated temperature [66], [67]. Hauser and VanEcho [67] reported the results of creep-rupture tests on shielded metal arc weld metals with varying ferrite contents. Four levels of ferrite content were produced in weld pads, and the microstructures were fully characterized. Specimens having 0.505-in. (12.5-mm) diam. were machined from the pads for tensile and creep-rupture testing. Creep tests were performed at temperatures in the range of 1000 to 1200°F (538 to 649°C). Results of the experimental work suggested that the high-ferrite weld possessed the best short-time strength and ductilities, while the low and extra-low ferrite welds possessed the best long-time strength.

Leyda, et al. [68] reported stress-rupture data for 304H stainless steel plates butt-welded with 308 stainless steel by the SMA welding process. Testing temperatures were 1050, 1100, and 1200°F (566, 593, and 649°C). Most failures occurred in the weld metal. Strengths were compared to the database for 304H stainless steel, and it was found that weldment strength decreased, relative to base metal, with increasing temperature. A need for a strength reduction factor at 1200°F (649°C) was suggested.

In 1978, White and LeMay [69], [70] published results of creep-rupture tests on composite specimens in which 308L stainless steel was used to join 316 stainless steel bar. Cross-weld specimens were machined and tested at temperatures in the range of 1065 to 1697°F (575 to 925°C). All failures were in the 308L stainless steel filler metal.

Swindeman, Bolling, and King [71] performed tensile and creep-rupture tests on weldments of 308CRE stainless steel to assist the study of weldment behavior by Manjoine [72], [73], [74], [75], [76]. Butt welds were produced in 1/2-in (13-mm) 304 stainless steel plates using 308CRE stainless steel electrodes. Samples were machined from various sections parallel to the weld and in the weld, heat affected zone, and base metal. Transverse specimens were machined. Tensile and creep tests were performed at 1100°F (593°C). It was found the 308CRE stainless steel weld metal was substantially stronger than the 304H stainless steel base metal. A creep law was formulated for the weld metal. Manjoine reported results from a series of tests on 304H stainless steel plates and bars containing welds and notches [72], [73], [74], [75], [76]. Both deformation and rupture life data were collected at 1100°F (593°C) over the time period from 50 to 20,000 hours. Manjoine observed that the strength of axial and transverse weldments exceeded that of all-base metal plates. Such performance was expected for the 308CRE filler metal.

Van der Schaaf, de Vries, and Elen [77], [78] provided creep-rupture data for weldments extracted from GTA welds in 20-mm (0.79-in.) thick plates of 304H (DIN 1.4849) stainless steel. The weld configuration was a double “V.” The root pass was by GTA and the finishing passes by SMA. All samples were cross welds 8.8 mm (0.35-in.). They tested at 1022°F (550°C) for times to 10,000 hours, and all failures were in the weld metal.

In 1981, an effort began at ORNL to expand the database for "commercial" heats of 308CRE stainless steel filler metal [79]. Butt welds were made in 1/2-in (13-mm) stainless steel plate using the GTA process and commercial 308CRE stainless steel wire. Button-head specimens were machined along the center line of the weld and transverse to the weld. Long-time testing at temperatures in the range of 1000 to 1200°F (538 to 649°C) were planned, but the program was canceled before full testing was begun. A few high-temperature tests on transverse specimens were completed.

Swindeman and Williams [80] performed tensile and creep tests on specimens machined from a 304H/308 stainless steel weldment that simulated the weld joint between a dummy nozzle skirt and a cylindrical vessel being used for structural testing under creep-ratcheting conditions [35], [36]. Weld metal, HAZ metal, and weld metal specimens were tested at 1100°F (593°C). Creep rates for the 308 stainless steel were much below those for base metal, and trends suggested that the weld metal would be stronger than the base metal for times to at least 10,000 h.

Padden [80], in 1983, and Dhalla [81], in 1991, reported the results of tests on a vessel that included 308 stainless steel weld joints between a 304 stainless steel nozzles and a 304H stainless steel shell. The vessel was a test configuration intended to examine ratcheting mechanisms. The nominal peak temperature was 1050°F (566°C) and total testing time was less than 2000 hours. Cracking was observed in the heat affect zones of three nozzles. The weld metal did not appear to be the initiation site. Failures appeared to be similar to creep rupture. A possible mechanism is relaxation cracking due to the cold work in the nozzle skirt. Whatever the cause, the vessel operated under conditions where the SRF for the weldment would be close to 1.0.

Also in the early 1980's, McAfee, et al. [82] performed creep-rupture tests on 304 stainless steel plates with longitudinal and transverse welds of 308CRE stainless steel. Specimens were cut from identical welds for control data. Tensile and creep tests were performed on 1/4-in. (6.3-mm) diam. specimens machined parallel to the welding direction in the base metal, HAZ, fusion line region, and weld metal. Data of tests at 1100°F (593°C) indicated that the 308CRE weld metal was stronger than the 304H base metal. McAfee, Battiste, and Swindeman reported the results of tests on welded plates in 1984 [83]. Plate specimens contained longitudinal welds produced by GTA welding with 308CRE wire. Testing was at 1100°F (593°C) with time extended to 6400 hours. Results were similar to those produced by Manjoine. Cracking initiated at the fusion line and extended into the base metal and weld metal. Again, the SRF for the 304H/308CRE was expected to be 1.0.

A major testing program on 308 stainless steel was undertaken by the National Research Institute for Metals (NRIM) in the 1980s [84], [85], [86]. Four heats of controlled-chemistry filler metal were used to butt-welded 304H stainless steel plates of two heats by the submerged-arc process. Filler metals contained titanium and niobium at low levels, and very detailed descriptions of the welding conditions were provided. Specimens were machined that were centered on the “center” and “quarter” locations. Base metal, weld metal, and cross metal specimens were tested over a broad range of temperatures and stresses. Testing temperatures ranged from to 887 to 1292°F (475 to 700°C) and times extended to 100,000 h. Creep data were obtained for two of the weld metals. The results of the testing program were described by Monma, et al [85], [86]. Depending on the combination of materials and test conditions, failures were observed in either base metal or weld metal of cross-weld specimens. Generally, the strength of the weld metals was greater than standard 308 stainless steel but less than the strength of the 308CRE deposited by the SMA process.

In 1983, Huthman and Borgsted [87] published results from tests of cross-weld (GTA) specimens taken from butt-welded plate specimens. These stress-rupture data plots were provided for 1022°F (550°C). Other work in Europe on the effects of residual elements were reported in this time period [88].

Lin and Battistte evaluated the creep and cyclic behavior of a welded-beam at 593°C (1100°F) [89]. Although the beam test was not taken to failure, a deformation model based on a multiple material zone (weld metal, HAZ, heat affected base metal, and base metal) was used in the elastic-plastic-creep analysis that yielded “excellent agreement.”

Beggs and Iberra [90] reported results of all-weld metal tests on 308 and 308L stainless steel filler metals deposited by the SMA process. Their work was intended to examine the influence of ferrite content on stress-rupture. All testing was performed at 1250°F (677°C). They found that weld deposits with high ferrite numbers were weaker than base metal while welds with ferrite numbers of 5 and lower exhibited similar or better strength than 304H stainless steel base metal.

Vitek, David, and Sikka re-examined the effect of the residual elements in improving the strength and ductility of 308 stainless steel weld metal [91]. To provide samples for detailed metallurgical studies, conventional 308 stainless steel and 308CRE stainless steel welds were produced by the GTA process and

samples were tested at 1200°F (649°C). Creep data were gathered and creep tests were interrupted for metallurgical studies. It was observed that the 308CRE weld metal did not form embrittling carbide networks under the testing conditions that were examined, and the improved creep ductility of the CRE stainless steel was attributed to this characteristic.

A report by Etienne and Heerings in 1993 cited two European references to stress-rupture testing of weldments in 304H (DIN 1.4948) at temperatures in the range of 550 to 650°C (1022 to 1202°F) [92]. The "Stress Reduction Factor" for times less than 10,000 hours were reported to be less than 0.9.

As part of a project to examine improved materials for superheater tubing, Swindeman initiated testing of 304 stainless steel tubing butt-welded with 308 stainless steel filler metal [93]. Welds were produced by the GTA process, and cross weld specimens were machined from the tubing for testing at temperatures in the range of 1000 to 1800°F (538 to 982°C). Failures occurred in the filler metal.

Finally, the NIMS report on long-time stress-rupture testing of 304H/308 weld metal and weldments was issued in 1995 [94].

4.3.2 Summary of the Database on the Stress-Rupture of 304H/308 Stainless Steel Filler Metals and Weldments

A listing of data sources extracted from the research effort summarized above is provided in Figure 84 and Figure 85. Information in Figure 84 includes the type of filler metal, the type of base metal, the welding process, the maximum temperature of testing, and one or two references for the source of the information. Often, the references include more than one filler metal, as described above.

Figure 85 provides more detail on the available data. Categories are listed under the ITEM column that include the welding process, the product form being welded, the thickness of the product, the filler metal "composition", the make-up of the testing specimens, the condition of the testing coupons, the coupon location within the weldment, the type of time-dependent data, the number of lots, and the number of time-dependent tests in each data file.

Weld processes include SMA, GTA, and SA. Weld configurations include butt-welded plates, girth welds in pipes and tubes, overlay (pad) depositions on plates and forgings, longitudinal welds in large diameter pipes, and nozzle skirts to shells. Product thicknesses range from 0.3 to over 2 in (7.6 to 50 mm). Weld preps include single V, double V, single U, and double U.

Filler metals include "standard" 308 filler (wire, coated electrodes, and cored wire), low-carbon grades (generally, dilution increases the carbon level in the deposited weld metal), and controlled residual element (CRE) additives (either in the metal or in the coating). Composition and deposition procedures for the standard 308 filler metal range sufficiently to examine ferrite effects, nitrogen effects, and titanium effects (from the electrode coating). Controlled residual elements additions include titanium, niobium, phosphorus, nitrogen, and boron.

Post weld conditions include as-welded, post-weld heat treatments, solution anneals, and some aging.

Test coupon locations include near root, quarter thickness, centerline, and near crown. Microstructures represent all-weld metal, HAZ base metal, and cross-weld. Test sections in the coupons cover diameters from 1/8 to ½ inch (3.2 to 13 mm). Data from a few "full section" tubes, pipes, and plates are included.

All references include stress-rupture data, and many references include minimum creep rate (mcr) data. Lambda values may be obtained from files that provide mcr, rupture-life, and elongation data. Data are provided in Appendix C.

Figure 84: Summary Table of 304H/308 Filler Metal & Weldment Creep-Rupture Data Sources

File Number	Filler Metal	Base Metal	Type Weld	Temperature Maximum (°F)	Reference	Date
1	308L	316	GTA	1562	White & Le May	1978, 1980
2	308		SMA	1200	Voorhees & Freeman	1958
2	308L		SMA	1200	Voorhees & Freeman	1958
2	308		SMA	1200	Voorhees & Freeman	1958
3	308L	304	SMA	1200	Wylie, Corey, & Leyda	1954
3	308	304	SMA	1200	Wylie, Corey, & Leyda	1954
3	308L	304	SMA	1200	Wylie, Corey, & Leyda	1954
4	308CRE	304	SMA	1200	King, Stiegler, & Goodwin	1973
5	308CRE	304	SMA	1600	King, Stiegler, & Goodwin	1973
6	308CRE	304	SMA	1200	King, Stiegler, & Goodwin	1973
7	308CRE	304	GTA	1100	McAfee, Battiste, & Swindeman	1984
8	308CRE	304	SMA	1100	Swindeman, Bolling, & King	1980
9	308	304	GTA	1100	Ward, et al., Ward	1971, 1974
10	308	304	SA	1100	Ward, et al., Ward	1971, 1974
11	308L	304L	GMA	1100	Ward, et al., Ward	1971, 1974
12	308L	304L	SA	1100	Ward, et al., Ward	1971, 1974
13	308	304	SA	1100	Ward, et al., Ward	1971, 1974
14	308CRE	304	SMA	1000	Ward, et al., Ward	1971, 1974
15	308CRE	304	SMA	1000	Ward, et al., Ward	1971, 1974
16	308CRE	304	SMA	1000	Ward, et al., Ward	1971, 1974
17	308CRE	304	SMA	1000	Ward, et al., Ward	1971, 1974
18	308	304L	SMA	1200	Ward, et al., Ward	1971, 1974
19	308CRE	304	GTA	1200	Edmonds & Bolling, Klueh & Edmonds	1975, 1982
20	308	304	SA	1200	Edmonds, King, et al.	1975
21	308	304	SMA	1100	Hauser & Van Echo	1978
22	308	304	SMA	1100	Hauser & Van Echo	1978
23	308	304	SMA	1100	Hauser & Van Echo	1978
24	308	304	SMA	1100	Hauser & Van Echo	1978
25	308		SMA	1200	Leyda, Katz, Gold, & Snyder	1978
26	308	304	GTA	1500	Swindeman & Canonico	1966
27	308L	304	GTA	1800	Swindeman	1995
28	308L	304	GTA	1400	Bolling & Swindeman	1980
29	308	304	SMA	1200	Swindeman & Williams	1980
30	308	304	SA	1292	Monma, Yokoi, & Yamazaki, NRIM	1984, 1995
31	308	304	SA	1292	Monma, Yokoi, & Yamazaki, NRIM	1984, 1995
32	308	304	SA	1292	Monma, Yokoi, & Yamazaki, NRIM	1984, 1995
33	308	304	SA	1292	Monma, Yokoi, & Yamazaki, NRIM	1984, 1995
34	308	347	GMA	1500	Davis & Cullen	1968
35	308	304	GTA	1200	Edmonds & Bolling	1975

File Number	Filler Metal	Base Metal	Type Weld	Temperature Maximum (°F)	Reference	Date
36	308CRE	304	GTA	1200	Edmonds & Bolling, Klueh & Edmonds	1975, 1982
37	308CRE	304	GTA	1200	Edmonds & Bolling, Klueh & Edmonds	1975, 1982
38	308CRE	304	SA	1200	Edmonds & Bolling, Klueh & Edmonds	1975, 1982
39	308CRE	304	SA	1200	Edmonds & Bolling, Klueh & Edmonds	1975, 1982
40	308	304	SA	1100	Klueh & Canonico	1976
41	308	304	SA	1200	Bolling & King	1976
42	308	304	SMA	1200	Bolling & King	1976
43	308CRE	304	GTA	1200	Vitek, David, & Sikka	1992
44	308	304	SMA	1200	Breggren, et al.	1977
45	308CRE	304	SMA	1200	Cole, Goodwin, & Bolling	1973
46	308CRE	304	SMA	1200	Cole, Goodwin, & Bolling	1973
47	308		SMA	1200	Booker	1984
48	308		SA	1200	Booker	1984
49	308	304	GTA	1022	Huthman & Borgstedt	1983
50	308		SMA	1250	Beggs & Ibarra	1991
51	308CRE	304	SMA	1350	Combustion Engineering	Unpublished
52	308	304	SMA	1350	Combustion Engineering	Unpublished
53	308CRE	304	SMA	1350	Combustion Engineering	Unpublished
54	308CRE	304	SMA	1350	Combustion Engineering	Unpublished
55	308	304	SMA	1200	Combustion Engineering	Unpublished
56	308CRE	304	SMA	1350	Combustion Engineering	Unpublished
57	308CRE	304	SMA	1350	Combustion Engineering	Unpublished
58	308CRE	304	SMA	1350	Combustion Engineering	Unpublished
59	308CRE	304	SMA	1350	Combustion Engineering	Unpublished
60	308CRE	304	SMA	1350	Combustion Engineering	Unpublished
61	308CRE	304	SMA	1350	Combustion Engineering	Unpublished
62	308	304	SA	1350	Combustion Engineering	Unpublished
63	308	304	SMA	1022	van der Schaaf, de Vries, & Elen	1979

Note: File for same reference may include cross welds, different heats, different ferrite numbers, ...

Figure 85: Summary Table of 304H/308 Filler Metal & Weldment Creep-Rupture Data

		DATA FILE NUMBER								
ITEM		1	2	3	4	5	6	7	8	9
Welding Process		GTA	SMA	SMA	SMA	SMA	SMA	GTA	SMA	GTA
Product Form		B	PLT	PAD	PLT	PLT	PLT	PLT	PLT	PLT
Thickness	(inch)	1		1	2	2	2	0.5	0.5	1
Filler Metal	Std		STD	STD						STD
Composition	LC	LC	LC	LC						
	CRE				CRE	CRE	CRE	CRE	CRE	
No. Chem		1	3	3	1	1	1	1	1	1
Orientation	All-weld		W	W	W	W	W	W	W	W
	Cross	C				C	C		C	
Specimen	As-welded	AW	AW	AW	AW	AW	AW	AW	AW	AW
Condition	annealed									ANN
	Aged					AGE				
Specimen	Root	R			R	R	R			
Location	Quarter		Q	Q	Q	Q	Q	Q	Q	Q
	Crown				C	C	C			
Size	(8th inch)	2		2,4	2	1,2	2	2	1	1
Data	Rupture	R	R	R	R	R	R	R	R	R
Available	MCR	MCR				MCR	MCR	MCR	MCR	MCR
	Creep					C		C	C	
	Lambda					L	L	L	L	L
No. Lots		1	3	3	1	1	1	1	1	1
No. Data	1106	26	24	20	8	116	17	14	12	5
NOTES:	GTA = Gas Tungste-Arc				SA = Submerged-Arc					
	SMA = Shielded Metal-Arc				GMA = Gas Metal-Arc					
	PP = pipe product				LC = low carbon in filler metal					
	B = bar product				CRE = Controlled residual elements					
	F = ferrite content variation				Crown = crown of the weld					
	N = nitrogen content variation				Quarter =half-way between root & crown					
	Ti = titanium effect				Root = toward the root pass					
	MCR = minimum creep rate									
	Creep = some measure of deformation versus time beyond the mcr.									

		DATA FILE NUMBER								
ITEM		10	11	12	13	14	15	16	17	18
Welding Process		SA	GMA	SA	SA	SMA	SMA	SMA	SMA	SMA
Product Form		PLT	PLT	PLT	PLT	PLT	PLT	PLT	PLT	PLT
Thickness	(inch)	1	1	2	2	1		2	2	1
Filler Metal	Std	STD			STD					
Composition	LC		LC	LC						LC
	CRE					CRE	CRE	CRE	CRE	
No. Chem		1	1	1	1	1	1	1	1	1
Orientation	All-weld	W	W	W	W	W	W	W	W	W
	Cross							C		
Specimen	As-welded	AW	AW	AW	AW	AW	AW	AW	AW	AW
Condition	annealed			ANN						
	Aged						AGE			
Specimen	Root									
Location	Quarter	Q	Q			Q				Q
	Crown									
Size	(8th inch)	1	1	1	1	1	1	1	1	1
Data	Rupture	R	R	R	R	R	R	R	R	R
Available	MCR	MCR	MCR	MCR	MCR	MCR	MCR	MCR	MCR	MCR
	Creep	C	C	C	C	C	C	C	C	C
	Lambda	L	L	L	L	L	L	L	L	L
No. Lots		1	1	1	1	1	1	1	1	1
No. Data	1106	9	5	36	6	1	3	7	5	10
NOTES:	GTA = Gas Tungste-Arc				SA = Submerged-Arc					
	SMA = Shielded Metal-Arc				GMA = Gas Metal-Arc					
	PP = pipe product				LC = low carbon in filler metal					
	B = bar product				CRE = Controlled residual elements					
	F = ferrite content variation				Crown = crown of the weld					
	N = nitrogen content variation				Quarter =half-way between root & crown					
	Ti = titanium effect				Root = toward the root pass					
	MCR = minimum creep rate									
	Creep = some measure of deformation versus time beyond the mcr.									
	Lambda = ratio of total creep strain to linear creep strain (after the									
	loading strain and the transient strain are extracted from the creep curve)									

		DATA FILE NUMBER								
ITEM		19	20	21	22	23	24	25	26	27
Welding Process		GTA	SA	SMA	SMA	SMA	SMA	SMA	GTA	GTA
Product Form		PLT	PP	PAD	PAD	PAD	PAD	PLT	PLT	Tube
Thickness	(inch)	0.5	1						0.5	0.3
Filler Metal	Std		STD	F	F	F	F		STD	
Composition	LC									LC
	CRE	CRE								
No. Chem		10	1	1	1	1	1			1
Orientation	All-weld	W	W	W	W	W	W	W		
	Cross		C						C	C
Specimen	As-welded	AW	AW	AW	AW	AW	AW	AW	AW	AW
Condition	annealed								ANN	
	Aged									
Specimen	Root								R	
Location	Quarter	Q	Q	Q	Q	Q	Q			Q
	Crown									
Size	(8th inch)	1	2	4	4	4	4		2	2
Data	Rupture	R	R	R	R	R	R	R	R	R
Available	MCR			MCR	MCR	MCR	MCR			
	Creep			C	C	C	C			
	Lambda			L	L	L				
No. Lots		10	1	1	1	1	1	1	2	1
No. Data	1106	26	10	11	13	12	11	19	7	10

NOTES:	GTA = Gas Tungste-Arc	SA = Submerged-Arc
	SMA = Shielded Metal-Arc	GMA = Gas Metal-Arc
	PP = pipe product	LC = low carbon in filler metal
	B = bar product	CRE = Controlled residual elements
	F = ferrite content variation	Crown = crown of the weld
	N = nitrogen content variation	Quarter =half-way between root & crown
	Ti = titanium effect	Root = toward the root pass
	MCR = minimum creep rate	
	Creep = some measure of deformation versus time beyond the mcr.	
	Lambda = ratio of total creep strain to linear creep strain (after the	
	loading strain and the transient strain are extracted from the creep curve)	

		DATA FILE NUMBER								
ITEM		28	29	30	31	32	33	34	35	36
Welding Process		GTA	SMA	SA	SA	SA	SA	GMA	GTA	GTA
Product Form		PLT	PLT	PLT	PLT	PLT	PLT	TUBE	PLT	PLT
Thickness	(inch)	0.5	1	1	1	1	1	1	0.5	0.5
Filler Metal	Std		STD					N		
Composition	LC	LC							LC	
	CRE			CRE	CRE	CRE	CRE			CRE
No. Chem		1	1	1	1	1	1	3	2	5
Orientation	All-weld	W	W	W	W	W	W		W	W
	Cross		C	C	C	C	C	C		
Specimen	As-welded	AW	AW	AW	AW	AW	AW		AW	AW
Condition	annealed							ANN		
	Aged									
Specimen	Root			R	R	R	R			
Location	Quarter	Q	Q	Q	Q	Q	Q		Q	Q
	Crown									
Size	(8th inch)	2	2	2	3	3	2	2	1	1
Data	Rupture	R	R	R	R	R	R	R	R	R
Available	MCR	MCR	MCR	MCR			MCR		MCR	MCR
	Creep		C	C			C			
	Lambda			L			L		L	L
No. Lots		1	1	1	1	1	1	4	2	5
No. Data	1106	3	8	32	30	34	32	36	8	16

NOTES:	GTA = Gas Tungste-Arc	SA = Submerged-Arc
	SMA = Shielded Metal-Arc	GMA = Gas Metal-Arc
	PP = pipe product	LC = low carbon in filler metal
	B = bar product	CRE = Controlled residual elements
	F = ferrite content variation	Crown = crown of the weld
	N = nitrogen content variation	Quarter =half-way between root & crown
	Ti = titanium effect	Root = toward the root pass
	MCR = minimum creep rate	
	Creep = some measure of deformation versus time beyond the mcr.	
	Lambda = ratio of total creep strain to linear creep strain (after the	
	loading strain and the transient strain are extracted from the creep curve)	

		DATA FILE NUMBER								
ITEM		37	38	39	40	41	42	43	44	45
Welding Process		GTA	SA	SA	SA	SA	SMA	GTA	SMA	SMA
Product Form		PLT	PLT	PLT	PAD	PLT	PLT	PLT	PLT	PLT
Thickness	(inch)	0.5	1	1	0.7	2	2	0.5	0.5	0.5
Filler Metal	Std				STD	STD	STD	STD	F	
Composition	LC									
	CRE	CRE	CRE	CRE				CRE		CRE
No. Chem		5	4	5	1		1	4	6	1
Orientation	All-weld	W	W	W	W	W	W	W	W	W
	Cross				C					
Specimen	As-welded	AW	AW	AW	AW	AW	AW	AW	AW	AW
Condition	annealed					ANN		ANN		
	Aged					AGE				
Specimen	Root					R	R			
Location	Quarter	Q	Q	Q	Q	Q	Q	Q	Q	Q
	Crown					C	C			
Size	(8th inch)	1	1	1	2	2	2	2	1	1
Data	Rupture	R	R	R	R	R	R	R	R	R
Available	MCR	MCR	MCR	MCR	MCR	MCR	MCR	MCR	MCR	MCR
	Creep	C			C	C		C		C
	Lambda	L	L	L	L	L		L	L	
No. Lots		5	4	5	1	1	1	4	5	1
No. Data	1106	16	13	15	41	18	8	18	16	3

NOTES:	GTA = Gas Tungste-Arc	SA = Submerged-Arc
	SMA = Shielded Metal-Arc	GMA = Gas Metal-Arc
	PP = pipe product	LC = low carbon in filler metal
	B = bar product	CRE = Controlled residual elements
	F = ferrite content variation	Crown = crown of the weld
	N = nitrogen content variation	Quarter =half-way between root & crown
	Ti = titanium effect	Root = toward the root pass
	MCR = minimum creep rate	
	Creep = some measure of deformation versus time beyond the mcr.	
	Lambda = ratio of total creep strain to linear creep strain (after the	
	loading strain and the transient strain are extracted from the creep curve)	

		DATA FILE NUMBER								
ITEM		46	47	48	49	50	51	52	53	54
Welding Process		SMA	SMA	SA	GTA	SMA	SMA	SMA	SMA	SMA
Product Form		PLT	PLT	PLT	PLT	PLT	PLT	PLT	PLT	PLT
Thickness	(inch)	0.5			0.75	2.5	0.5	2	2	2
Filler Metal	Std	Ti	STD	STD	STD	STD				
Composition	LC					LC				
	CRE	CRE					CRE	CRE	CRE	CRE
No. Chem		3			1	1	1	1	1	1
Orientation	All-weld	W	W	W		W	W	W	W	W
	Cross				C					
Specimen	As-welded	AW	AW	AW	AW	AW	AW	AW	AW	AW
Condition	annealed									
	Aged									
Specimen	Root				R		R	R	R	R
Location	Quarter	Q				Q	Q		Q	Q
	Crown						C	C	C	C
Size	(8th inch)	1	1	1	1,2	2	2	2	2	2
Data	Rupture	R	R	R	R	R	R	R	R	R
Available	MCR	MCR	MCR	MCR						
	Creep	C								
	Lambda		L	L						
No. Lots		3	18	10	1	2	1	1	1	1
No. Data	1106	6	67	50	10	9	27	4	9	21
NOTES:	GTA = Gas Tungste-Arc				SA = Submerged-Arc					
	SMA = Shielded Metal-Arc				GMA = Gas Metal-Arc					
	PP = pipe product				LC = low carbon in filler metal					
	B = bar product				CRE = Controlled residual elements					
	F = ferrite content variation				Crown = crown of the weld					
	N = nitrogen content variation				Quarter =half-way between root & crown					
	Ti = titanium effect				Root = toward the root pass					
	MCR = minimum creep rate									
	Creep = some measure of deformation versus time beyond the mcr.									
	Lambda = ratio of total creep strain to linear creep strain (after the									
	loading strain and the transient strain are extracted from the creep curve)									

		DATA FILE NUMBER								
ITEM		55	56	57	58	59	60	61	62	63
Welding Process		SMA	SMA	SMA	SMA	SMA	SMA	SMA	SA	SMA
Product Form		PLT	PLT	PLT	PLT	PLT	PLT	PLT	PLT	PLT
Thickness	(inch)					2	2	2		0.75
Filler Metal	Std								STD	STD
Composition	LC									
	CRE	CRE	CRE	CRE	CRE	CRE	CRE	CRE		
No. Chem		2	1	2	1	2	2	2	3	1
Orientation	All-weld	W	W	W	W	W	W	W	W	
	Cross									C
Specimen	As-welded	AW	AW	AW	AW	AW	AW	AW	AW	AW
Condition	annealed									PWHT
	Aged									
Specimen	Root				R	R	R			
Location	Quarter				Q					Q
	Crown				C	C	C			
Size	(8th inch)	2	2	2	4	2	2	4	2	
Data	Rupture	R	R	R	R	R	R	R	R	R
Available	MCR									MCR
	Creep									C
	Lambda									
No. Lots		2	1	2	2	2	2	2	3	1
No. Data	113	13	17	23	17	4	4	2	21	12

NOTES:	GTA = Gas Tungste-Arc	SA = Submerged-Arc
	SMA = Shielded Metal-Arc	GMA = Gas Metal-Arc
	PP = pipe product	LC = low carbon in filler metal
	B = bar product	CRE = Controlled residual elements
	F = ferrite content variation	Crown = crown of the weld
	N = nitrogen content variation	Quarter =half-way between root & crown
	Ti = titanium effect	Root = toward the root pass
	MCR = minimum creep rate	
	Creep = some measure of deformation versus time beyond the mcr.	
	Lambda = ratio of total creep strain to linear creep strain (after the loading strain and the transient strain are extracted from the creep curve)	

4.4 316H & 16-8-2 Weld Metal

4.4.1 Review of Research on the Stress-Rupture of 316 and 16-8-2 Stainless Steel Filler Metals and Weldments

Guarnieri evaluated autogenous welds in 316 stainless steel in 1951 [95] and found that the creep-rupture strength of the weldment specimens was lower than the base metal at 1200, 1500, and 1800°F (649, 816, and 982°C). Depending on the temperature and time, the weldments exhibited strength from 70 to 90% of the base metal. All failures were in the weld metal.

In 1954, Wylie, Corey, and Leyda [96] reported results of stress-rupture tests on "eleven compositions of commercial stainless steel weld deposits." Weld pads were produced using the shielded metal arc process (SMA), and these pads were of sufficient thickness to produce all-weld-metal specimens parallel and transverse to the welding direction. Two carbon levels (0.10 and 0.03%) for 18Cr-12Ni-Mo filler metal were examined. Specimens were ¼- and 1/2-in. (6.3- and 13-mm) diameter. Stress-rupture tests were performed at 1200, 1350, and 1500°F (649, 732, and 816°C). Rupture times extended to beyond 10,000 h. Hardness and magnetic permeability measurements were taken on aged specimens, and changes were reported. The investigators found that the weld metal specimens had lower strength than expected for base metal. Depending on the temperature and time, the weld metal exhibited strengths from 55 to 95% of the base metal. In the discussion of the paper Thomas provided additional stress-rupture data for 316 stainless steel weld metal that indicated slightly lower strength at 1200°F (649°C) [96].

In 1958, Voorhees and Freeman [97] produced a compilation of weldment data published by the American Society for Testing and Materials. Stress-rupture data for several lots of "316" stainless steel weld metal were included in the database. All welds were produced by the SMA process, and one filler metal was a low-carbon composition.

Rowe and Stewart reported the "weld efficiency" for rupture strength of weld metal relative to base metal for temperatures of 1350, 1500, and 1650°F (732, 816, and 900°C) in 1962 [98]. Welds were made by the GTA process in ½-in. (13-mm) plates that were cut from 6 ½-in. (165-mm) bar and prepared with a double "V" configuration. They tested cross-weld specimens in the as-welded, 1600°F (871°C) stress-relieved, and 1950°F (1038°C) annealed conditions. All samples failed in the "weld bead." They found the weld efficiency decreased with increasing rupture time and observed values as low as 50%.

Christoffel reported on the notch sensitivity of the heat-affected zone of welds in 316 stainless steel using 16-8-2 filler metal [99]. All specimens were tested at 1100°F (593°C) and included both as-welded and solution-annealed conditions for times to 10,000 hours. The solution-annealed specimens lasted longer than as-welded specimens at the lower stresses. All notched specimens exhibited greater lives than smooth base metal specimens.

Truman and Hardwick reported on the rupture life of solution-treated weldment specimens in 316 stainless steel at 1100, 1200, and 1300°F (593, 649. and 704°C) [100]. All failures occurred in the weld metal.

In the late 1960's, the Department of Energy (then the U. S. Atomic Energy Commission and later the Energy Research and Development Agency) initiated a major research and development program on austenitic stainless steel weld metals [101], [102], [103], [104], [105], [106], [107], [108]. Research included the evaluation of filler metals and weld processes to determine the performance of candidate materials for liquid metal fast breeder reactor components. Filler metals of interest included 308, 308L, and 16-8-2 stainless steels. Welds were made in 1-in. (25-mm) thick plate by shielded metal arc (SMA), gas-tungsten arc (GTA), and submerged arc (SA) processes. Button-head specimens having 1/8-in and ¼-in. (3.2- and 6.3-mm) gage diameters were machined as weld-metal and cross-weld specimens. These

specimens were tested in the as-welded condition at temperatures from 900 to 1200°F (482 to 649°C). Aging effects and irradiation effects studies were included [106]. Generally, it was found that the stress-rupture data for weld metal and weldments fell within the range of scatter for 316H stainless steel base metal. No effort was made to determine stress-rupture factors.

In 1977 and 1978, White and LeMay [109], [110] published results of creep-rupture tests on 316/316L stainless steel weld joints. Cross-weld specimens were machined and tested at temperatures in the range of 1065 to 1697°F (575 to 925°C). All failures were in the 316L stainless steel filler metal.

In the mid and late 1970s, development work was undertaken to understand and improve the performance of filler metals for 316 stainless steel components needed for the fast breeder reactor concepts [111], [112], [113], [114], [115]. A number of different electrodes were examined for 316 and 16-8-2 stainless steel filler metals. Material from longitudinal welds in formed-and-welded pipe was examined as well as girth welds in large diameter piping. Creep and stress-rupture testing covered temperatures from 900 to 1200°F (482 to 649°C). Generally, the weld metal and weldments were weaker than the base metal at high stress and short times but tended to converge with the strength of the base metal at long times.

In 1980, Etienne and co-workers reported on their studies of 316 stainless steel weld metal and weldments in ~2-in (50-mm) thick plate under creep conditions [116], [117]. They tested specimens extracted from four zones through the weld (weld, HAZ, near-weld base metal, and away from the weld) at temperatures from 1022 to 1202°F (550 t0 650°C). They found the weld metal (deposited from "coated electrodes") to be weak relative to the base metal and the HAZ material to be strong [116]. An analysis was undertaken for creep and plasticity of a "thick" section weldment using the data from the coupons extracted from the four zones [117]. The analysis was consistent with the test on the composite but showed that testing cross-weld specimens led to a very conservative prediction of life.

In 1981, weld Stress Rupture Factors were approved by the code Working Group on the Strength of Weldments for weldments designed to the rules of ASME Section III Code Case N-47. These were based on early work at the Hanford Engineering Development Laboratory for Code Case 1592. However, approval for incorporation into CC N-47 did not occur for several years afterward.

In early 1980s, an effort was undertaken by Edmonds and co-workers to develop Controlled Residual Element (CRE) additions to 316 and 16-8-2 stainless steel filler metals for improved creep strength and ductility [118], [119]. Titanium, boron, and phosphorous additions were introduced. The GTA and SA processes were employed using both "experimental" and "commercial" heats of filler wire. Deposited chemistries of several CRE weld metals were within the chemistry limitations of straight 316 stainless steel weld metal. Creep and stress-rupture testing of weld metals was limited to 1200°F (649°C) but some testing extended to 20,000 hours. Some success was achieved in improving ductility, but optimized compositional ranges for the filler metals were not established.

Sikka and co-workers examined stress-rupture behavior of 16-8-2 stainless steel GTA weldments at several temperatures [120], [121]. Some weldment specimens were extracted from girth welds in large diameter piping. Aged materials were included. Weldment specimens exhibited lower rupture strength that base metal at 10,000 hr.

In the mid 1980s, the Stress Rupture Factors for 316 and 16-8-2 stainless steel weldments were developed from the criteria established earlier. One of the criteria was the ratio of the average stress-to-rupture for the deposited filler metal to the average time to failure for the base metal (316 stainless steel) for a specified time. Confirmatory testing was initiated that involved stress-rupture testing of "special welded structures" that included beams, plates, pipes and tubes. Corum and coworkers produced a series of reports and papers that covered the results of testing of 316 stainless steel configurations that contained welds [122], [123],

[124], [125], [126], [127]. Corum compared the ratio of the life of welded 316 stainless steel components to the N-47 minimum life for 316 stainless steel for 14 structural weldments and found ratios in the range of 1 to 4, with an average of 2.3. Typically, testing temperatures were in the range of 1000 to 1100°F (538 to 593°C) and lives extended to 10,000 hr. Several of the tests included the evaluation of the cracking characteristics near the fusion line.

The IIW Cie IX Working Group Creep reviewed work on Strength Reduction Factors (SRFs) and Lifetime Reduction Factors (LRFs) for weldments in 1993 [128]. They provided only one reference for work on 316H stainless steel weldments and cited values of 0.95 for 1202°F (650°C) and 1.0 for 1292°F (700°C) [129].

Hsiao, Zhang, and Daehn examined the distribution of stresses and creep damage in 316 stainless steel joined by 316 and 16-8-2 filler metals at 1202°F (650°C) [130]. They found failures to occur in the weaker weld metal, although analysis showed the stress to be significantly higher in the base metal.

4.4.2 Review of the Database on the Stress-Rupture of 316 and 16-8-2 Stainless Steel Filler Metals and Weldments

A listing of data sources extracted from the research effort summarized above is provided in Figure 86 for the 16-8-2 stainless steel filler metal and Figure 87 for the 316 stainless steel filler metal. Information in both tables includes the type of filler metal, the type of base metal, the welding process, the maximum temperature of testing, and one or two references for the source of the information.

The database for the 16-8-2 filler metal consists of results from about 300 tests. Weld processes include SMA, GTA, and SA. Weld configurations include butt-welded plates, girth welds in pipes and tubes, overlay (pad) depositions on plates and forgings, and longitudinal welds in large diameter pipes. Product thicknesses range from 0.3 to over 2 in (7.6 to 50 mm). Weld preps include single V, double V, single U, and double U. Appendix D contains the chemistries and creep-rupture data.

Filler metals include “standard” 16-8-2 stainless steel and controlled residual element compositions. Controlled residual elements additions include titanium, niobium, phosphorus, nitrogen, and boron.

Some data are available that relate to post weld heat treatment, solution annealing, and some aging.

Test coupon locations include near root, quarter thickness, centerline, and near crown. Microstructures represent all-weld metal, HAZ base metal, and cross-weld. Test sections in the coupons cover diameters from 1/8 to ½ inch (3.2 to 13 mm). Data from a few “full section” tubes, pipes, and plates referenced above are not included.

The database for 316 stainless steel filler metal is smaller than that for the 16-8-2 stainless steel filler metal and consist of only 160 entries. Most of the data for the controlled residual element weldments have been omitted but, even so, the scope of the testing program on the 316 stainless steel weldments was not as broad.

Figure 86: Summary Table of 16-8-2 Filler Metal Data

File Number	Filler Metal	Base Metal	Type Weld	Temperature Maximum (°F)	Reference
w1-3 to w1-4	16-8-2	316	GTA	1100	HEDL TME 74-25
w4-1 to w4-6	16-8-2	316	GTA	1200	ORNL 5107
13-4	16-8-2	316	SMA	1100	Booker Note

File Number	Filler Metal	Base Metal	Type Weld	Temperature Maximum (°F)	Reference
17-1	16-8-2	316	GTA	1200	ORNL 5107
18-1	16-8-2	316	GTA	1200	Booker Note
18-2, 18-3	16-8-2	316	SMA	1200	Booker Note
18-4	16-8-2	316	GTA	1200	Booker Note
16-5	16-8-2	316	GTA	1200	Booker Note
22-3	16-8-2	316	SA	1200	Booker Note
22-4, 22-5	16-8-2	316	SA	1200	ORNL 5218
24-1, 24-2	16-8-2	316	GTA	1200	Booker Note
24-5	16-8-2	316	SA	1200	Booker Note
FFTF-1	16-8-2	316	GTA	1200	ORNL 5594
FFTF-1CW	16-8-2	316	GTA	1200	ORNL 5594
FFTF-2	16-8-2	316	GTA	1200	ORNL 5594
2546	16-8-2	316	GTA	1200	ORNL 5945
35047	16-8-2	316	SA	1200	ORNL 5945
9236sa, 9206sa	16-8-2	316	SA	1200	ORNL 5945
9213sa, 9234sa	16-8-2	316	SA	1200	ORNL 5945
9235sa	16-8-2	316	SA	1200	ORNL 5945
9213gta, 9234gta	16-8-2	316	GTA	1200	ORNL 5945
9235gta, 9236gta	16-8-2	316	GTA	1200	ORNL 5945
77-15, 77-16	16-8-2	316	SA	1200	ORNL 5594
77-17	16-8-2	316	SA	1200	ORNL 5594
E-13, F-14	16-8-2	316	SA	1200	ORNL/TM-7394
H-22	16-8-2	316	SA	1200	ORNL/TM-7394

Booker Note: Data with these IDs were included in the evaluation of SRFs for BPV III-NH.
Booker Note Sources include TME 74-25, and TME 71-118.

Figure 87: Summary Table of 316 Filler Metal Data

File Number	Filler Metal	Base Metal	Type Weld	Temperature Maximum (°F)	Reference
w1-2	316	316	GTA	1100	HEDL TME 74-25
w9-4 to w9-9	316	316	SMA	1500	Booker Note
w19-3	316	316	GTA	1200	0RNL 5105
w19-6	316	316	SMA	1200	Booker Note
w24-3, W24-3cw	316	316	SA	1200	ORNL-7394
w24-4, w24-4CW	316	316	GTA	1200	ORNL-7394
w9-8, w19-11, w19-2	316	316	SMA	1350	Booker Note
ERR, ERR-CW	316	316	SMA	1202	Etienne, et al.
W-M-CW	316L	316	GTA	1200	White & Le May
R-S-CW	316	316	GTA	1200	Rowe & Stewart
WD	316	316	GTA	1650	Ward

Booker Note: Data with these IDs were included in the evaluation of SRFs for BPV III-NH.
Booker Note Sources include TME 74-25, and TME 71-118.

4.4.3 A Brief Review of the Determination of Stress Rupture Factors for 316 and 16-8-2

The Stress Rupture Factors in BPV III-NH Table I-14.10 B-1 and B-2 are mostly based on the collection of data from the references listed above for the years up to 1980 and analysis methods described by Booker and Booker [131]. The specific model used to represent the rupture life, t_r, for 16-8-2 stainless steel filler metal was as follows:

$$\log tr = Ch - 0.01044\ S - 0.01702\ T - 0.005687\ T \log S,$$

where t_r is the life in hours, C_h is the average "lot Constant," T is temperature in Kelvin, and S is stress in MPa. The value for the average C_h is given as 31.525. The Lot Constant used to determine the minimum life is 30.756. The database used to develop the model consisted of 109 lives obtained at temperatures from 900 to 1200°F (482 to 649°C) and time in the range of 20 to 9000 hours. Data from GTA, SMA, and SA weld deposits were included.

The specific model used to represent the rupture life, tr, for 316 stainless steel filler metal was as follows:

$$\log tr = Ch - 0.0102\ S - 0.01387\ T - 0.002668\ T \log S,$$

where again tr is the life in hours, Ch is the average "lot Constant," T is temperature in Kelvin, and S is stress in MPa. The value for the average Ch is given as 22.483. The Lot Constant used to determine the minimum life is 21.630. The database used to develop the model consisted of 82 lives obtained at temperatures from 1000 to 1500°F (538 to 816°C) and time in the range of 10 to 11000 hours. Data from GTA, SMA, and SA weld deposits were included.

4.5 Alloy 800/800H

4.5.1 Identification of Alloy 800/800H Filler Metals and Weldment Stress-Rupture Data

Alloy 800H is one of three classes (or "grades") of 33Ni-42Fe-21Cr alloy that are listed in ASME Section II and approved for construction of pressure boundary components. The three grades are identified as UNS

N08800, UNS N08810, and UNS N08811 for alloy 800, alloy 800H, and alloy 800HT, respectively. Alloy 800 (N0880) corresponds to a relatively fine-grained annealed condition normally used at lower temperatures where creep strength is not an important consideration. Alloy 800H (N08810) corresponds to a relatively coarse-grained material (ASTM grain size number 5 or greater) with a carbon range of 0.05 to 0.10% which is typically annealed around 1150°C (2175°F). This material is approved for construction to 982°C (1800°F) under the rules of ASME Section VIII.

Alloy 800HT (N08811) requires carbon to be at least 0.06%, the aluminum plus titanium to be in the range of 0.85 to 1.2%, and the annealing temperature to be at least 1149°C (2150°F). This stronger version of alloy 800H is used when creep strength is important and relaxation cracking is not of great concern. Only alloy 800H is permitted under the rules in ASME III-NH and an additional restriction requires the Al+Ti content to be in the range of 0.4 to 1.2%. The specific grade of base metal and its associated properties are important considerations in this review which includes the data produced on weldments that may rupture in the base metal heat affected zone or the base metal itself. Since the three grades have different strengths, one might expect that the SRFs would have a different value for each grade.

A number of filler metals have been used for joining similar and dissimilar metal welds with alloy 800H. Some compositions are listed in Figure 88 for coated electrodes for shielded metal arc welding (SMAW) included in the AWS 5.11 specification. Only one of these filler metals, alloy A (ENiCrFe-2), is permitted in ASME III-NH, according to Table I-14.1(b), and Table I-14.10 C-1 provides stress factors for the bare electrode equivalent (ENiCrFe-2, see Figure 89) used for SMAW. The database reviewed here includes alloy 132, alloy A, alloy 617, and 21/33/Nb which is considered to be a matching filler metal for alloy 800H.

Figure 88: Comparison Table of Chemistries for Coated Filler Metal Electrodes Used to Join the Three Grades of Alloy 800

Element	alloy 132	alloy A	alloy 182	alloy 617	21/33/Nb
ENiCrFe-1	ENiCrFe-2 (W86132)	ENiCrFe-3 (W86133)	ENiCrCoMo-1 (W86182)	(W86117)	
C	0.08 max	0.10 max	0.10 max	0.05-0.15	0.06-0.12
Mn	3.5 max	1.0-3.5	5.0-9.5	0.3-2.3	1.6-4.0
Fe	11.0 max	12.0 max	10.0 max	5.0 max	Rem
P	0.03 max	0.03 max	0.03 max	0.03 max	0.03 max
S	0.015 max	0.02 max	0.015 max	0.015 max	0.02 max
Si	0.75 max	0.75 max	1.0 max	0.75 max	0.6 max
Cu	0.50 max	0.50 max	0.50 max	0.50 max	-
Ni	62.0 min	62.0 min	59.0 min	Rem	30.0-35.0
Co	-	0.12 max*	0.12 max*	9.0-15.0	-
Ti	-	-	1.0 max-	-	-
Cr	13.0-17.0	13.0-17.0	13.0-17.0	21.0-26.0	19.0-23.0
Nb	1.5-4.0	0.5-3.0	1.0-2.5	1.0 max	0.08-1.5
Mo	-	0.5-2.5	-	8.0-10.0	0.5 max

Notes: * Co 0.12 max when specified by purchaser; max for other elements is 0.50.

Compositions for bare filler metal electrodes (SFA-5.14) are listed in Figure 89. Only ERNiCr-3 (alloy 82) is permitted for use by ASME III-NH, according to Table I-14.1(b), and Table I-14.10 C-2 provides stress factors for joints with this alloy.

Figure 89: Comparison Table of Chemistries for Bare Filler Metal Electrodes Used to Join Three Grades of Alloy 800

Element	alloy 82 ERNiCr-3 (N06082)	alloy 617 ERNiCrCoMo-1 (N06617)
C	0.10 max	0.05-0.15
Mn	2.5-3.5	0.3-2.3
Fe	3.0 max	5.0 max
P	0.03 max	0.03 max
S	0.015 max	0.015 max
Si	0.50 max	0.75 max
Cu	0.50 max	0.50 max
Ni	67.0 min	Rem
Co	0.12 max*	9.0-15.0
Ti	0.75 max	-
Cr	18.0-22.0	21.0-26.0
Nb	2.0-3.0	1.0 max
Mo	-	8.0-10.0

Notes: * Co 0.12 max when specified by purchaser; max for other elements is 0.50.

4.5.2 Review of Research on the Stress-Rupture of Filler Metals and Weldments

Early data on filler metals and weldments used for alloy 800 and nickel base alloys were summarized in *The Elevated-Temperature Properties of Weld-Deposited Metal and Weldments* (ASTM STP No. 226) [132]. Pages 154 to 170 of the report provided McBee-type data sheets for a number of filler metals. Two data sheets were provided for alloy 132 deposited filler metal. Two data sheets were provided for alloy 132 filler metal in alloy 800H plates. Most weldment ruptures occurred in the weldment fusion line.

York and Flury performed a literature search for suitable filler metals for alloy 800 and selected Incoloy 88 & 182 filler metals for joining alloy 800 [133]. It was reported that weldments from the two filler metals exhibited similar tensile and creep-rupture properties for temperatures less than 649°C (1200°F). This work was in support of the fast-breeder reactor (FBR) program which had a need for a steam generator operating at less than 649°C (1200°F).

Studies by Klueh and King in support of the FBR program were published in 1978 and 1979 and included creep and stress-rupture behavior of ERNiCr-3 weld metal [134], [135], [136], [137]. Data for deposited alloy 82 filler metal were reported to 732°C (1350°F).

Sartory required a creep law for an inelastic ratcheting analysis of a 2 ¼Cr-1 Mo steel pipe joined to type 316H stainless steel using alloy 82 filler metal [138], [139]. The creep law was developed and revised from test data on coupons machined from a dissimilar metal weld test article. Data were in the range of 510 to 566°C (950 to 1050°F).

Booker and Strizak produced cyclic data on weld-deposited alloy 82 at 649°C (1200°F) [140]. Hold times at constant stress were introduced in tensile or compression and strains were reversed by strain-rate control to produced creep reversed by plasticity or plasticity reversed by creep. Tests were also performed with creep reversals in both tension and compression. No effort was made to develop expressions for the creep behavior.

Klueh and King examined the thermal aging behavior of alloy 82 weld metal and weldments [141]. Aging was performed at 510 and 566°C (950 and 1050F). Tensile testing was performed to 677°C (1250°F) and creep-rupture tests to 566°C (1050°F).

Nippon-Kokan (NKK) reported the properties of Tempaloy 800H tubes welded with matching filler metal and alloy 82 [142]. Information included composition, microstructures, cross weld hardness, and tensile properties for as-welded and solution-annealed weldments in 11-mm plates. The tensile data indicated higher yield strengths than for base metal for the as-welded cross-weld samples for temperatures to 1000°C (1832°F) but the same ultimate strength. No stress-rupture data for weldments were provided.

Data for pressurized alloy 800H tubes containing butt welds were reported by Stannett and Wickens [143]. Alloy 82 and 182 fillers were used. Testing was at 550 and 700°C (1022 to 1292°F). All tube burst failures occurred in the base metal.

In 1982, Klueh and J. F. King examined the elevated-temperature tensile and creep-rupture behavior of alloy 800H/ERNiCr-3 Weld Metal/2 ¼Cr-1Mo steel dissimilar-metal weldments [144]. Creep-rupture data extended to 732°C (1350°F).

McCoy and King investigated the tensile and creep-rupture properties of weld-deposited alloy A (EniCrFe-2) and alloy 82 filler metal and weldments including alloy 800H and Hastelloy X [145]. Tensile data on deposited alloy A weld metal went from 23 to 871°C (70 to 1600°F) and creep rupture data were gathered from 482 to 760°C (900 to 1400°F). Tensile and creep-rupture data for weldments were produced to 649°C (1200°F) for both filler metals. Testing data for aged weldments were included. They also investigated the mechanical properties of weld-clad alloy 800H tubesheet forgings [146].

Lindgren, Thurgood, Ryder, and Li reviewed the mechanical properties of welds in commercial alloys for high-temperature gas-cooled reactor components in 1984 [147]. They presented creep-rupture data for several filler metals and weldments used for joining alloy 800H and dissimilar metal tubes or pipes. Included were alloy 88 and alloy 188, alloy 82 and alloy 182. Plots of stress-rupture behavior were shown for temperatures to 760°C (1400°F).

In the same issue of *Nuclear Technology*, Bassford and Hosier discussed the production and welding technology of some high-temperature nickel alloys and provided guidance and data for welding alloy 800H for applications up to 790°C (1450°F) [148]. Stress-rupture data for all-weld metal were tabulated for alloy A and alloy 82 to 982°C (1800°F).

Schubert, Bruch, Cook, Diehl, Ennis, Jakobeit, Penkalla, te Heesen, and Ullrich reviewed the creep-rupture behavior of candidate materials for nuclear process heat applications [149]. The paper provided one figure that plotted stress versus rupture life for alloy 82 and a 21/33/Nb at 850 and 950°C (1575 and.1650°F) The alloy 82 weld metal was weaker than average strength alloy 800H while the 21/33Nb matching filler metal appeared to have strength comparable to the base metal.

In 1986, an INCO brochure provided a table for the stress-rupture for strength of alloy A and alloy 82 for temperatures in the range of 538 to 982°C (1000 to 1800°F) and times to 10,000 hours [150]. Also, a figure was provided for the stress-rupture of deposits from welding electrode 117 in comparison to alloy 800HT for temperatures in the range of 649 to 982°C (1200 to 1800°F) and time to 10,000 hours. About the same time, Bassford, provided tensile and stress-rupture data for alloy 117 and alloy 112 deposited weld metal and cross welds in alloy 800H [151]. Temperatures ranged to 1093°C (2000°F).

A *Survey and Guidelines for High Strength Superheater Materials- Alloy 800H* was compiled for the Electric Power Research Institute in 1987 [152]. This report included a "steel maker's search on alloy

800H" by three participants: Sumitomo Metal Industries, Ltd., Nippon Steel Corp., and Nippon Kokan K. K (NKK). The reviews drew heavily from the studies of alloy 800H that were performed in support of the high-temperature gas-cooled reactor programs (in the US, UK, and Germany) and the fast breeder reactor programs in the US. In the summary section, plots for tensile data were supplied that were constructed from seven sources and ranged to 1100°C (2000°F). Several filler metals including alloys 82 and 182 were listed and both deposited metal and joint configurations were included. Stress-rupture data were provided as a stress versus Larson Miller parameter plots. Again, both deposited metal and joint data were included. However, the data did not appear to be original data but rather were derived from processed curves or tables. The review by Sumitomo Metal Industries, Ltd. was the most extensive with respect to filler metals. Of the 193 references, there were 32 references that addressed weld metal and weldment issues. About 14 of these references reported mechanical behavior such as tensile or creep-rupture properties. About half of these were of Japanese origin. Figures were provided that were reproduced from many of these references.

McCoy produced tensile and creep test data for a heat of alloy 800H in 1993. Data for deposited alloy 82 weld metal and weldments were provided [153], [154]. Tensile data ranged to 871°C (1600°F) and creep-rupture data ranged to 816°C (1500°F).

4.5.3 Assembly of the Stress-Rupture Database

The bulk of the stress-rupture data for deposited weld metals and weldments data for various grades of alloy 800 was produced by programs focused on components intended for operation below 750°C (1382°F). These data were used to develop the Stress Rupture Factors (SRFs) in ASME Section III-NH Tables I-14-10 C-1 and C-2. Although meager, some data exist for higher temperatures. A summary of available data sources outlined above is provided in Figure 90 and actual data are provided in the Appendix E.

The tabulated data were extracted from tables in reports, when possible, but some data were extracted from plots in papers and reports. These data lacked the precision and accuracy that was desired, but considering the overall lot-to-lot variability were considered to be better than no data at all. Since ASME III-NH only provides SRFs that are based on stress-rupture behavior, data bearing on other aspects of the time-dependent behavior of filler metals, such as time to 1% creep and the time to the initiation of tertiary creep, were not collected. Data for several types of filler metals were included. These filler metals are listed in Figure 88 and Figure 89 of this report. Alloy 132 (ENiCrFe-1) was an exception, and data for this filler metal were not included in Figure 90 and the appendix.

Figure 90: Summary Table of 800H Weld and Weldment Data

Number	Metal	Metal	Weld	Maximum (°C)	
INCO-1	A		SMA	982	INCO
M-K-1, M-K-1-CW	A	800H		760	McCoy & King TM-8728
BMI-CW	A			927	
33431	21-33Nb	800H		850	Schubert, et al.
19424	21-33Nb	800H		950	Schubert, et al.
SHINO, SHINO-CW	182	800H	SMA	927	Shino
INCO-2	82	800H	GTA	982	INCO
K-K-1	82	800H	GTA	732	Klueh & King TM-5404
K-K-2	82	800H	GTA	732	Klueh & King TM-5783
HEM-1-CW	82	800H	GTA	732	McCoy TM-7399
SCH	82	800H	GTA	950	Schubert, et al.

Number	Metal	Metal	Weld	Maximum (°C)	
HEM-2-CW	82	800H	GTA	816	McCoy TM-12438
K-M, K-M-CW	82	800H	GTA	649	King & McCoy TM-9108
M-K-CW	82	800H	GTA	482	McCoy & King TM-8728
82-13	82	800H	GTA	1000	EPRI 82-13

4.6 Review of 9Cr-1Mo-V (Grade 91) Steel Weld Metal and Weldments Creep-Rupture Data and Weld Strength Reduction Factors

4.6.1 Background and Data Sources

A developmental program on 9Cr-1Mo-V steel was undertaken by Combustion Engineering, Inc. in 1975 to meet the property goals identified by Patriarca, et al. in 1976 [155]. A screening program was undertaken to reach these goals [156] that included weld filler metal development. The emphasis was on the Shielded Metal Arc (SMA) process, and batches were produced with 127 different compositions. The SMA wires with the best impact properties were selected for production of larger batches of wire to be used for both the SMA and Gas Tungsten Arc (GTA) welding processes. Creep-rupture testing at 538, 593, and 649°C (1000, 1100, and 1200°F) was undertaken on two filler metals that were judged to be the best based on toughness. Of these, one proved to be superior in stress-rupture to the reference base metal and the other inferior. The chemistry of the undiluted weld pad for the best wire was 0.064% C; 0.64% Mn; 0.01% P; 0.011% S; 0.20% Si; 0.02% Ni; 9.15% Cr; 1.03% Mo; 0.04% Cb; 0.053% N, 0.001% Al; 0.16% V; and 0.03% Cu. Work on the poorer performing weld filler metal was discontinued.

From 1975 to the mid-1990s, the U.S. Department of Energy (DOE) supported further mechanical testing of weldments in Gr 91, and the Oak Ridge National Laboratory (ORNL) assumed the management of the technology program. By 1982, when data packages were prepared for submission to ASME Section I and Section VIII for code approval, the available creep-rupture data were from weldments fabricated using both standard 9Cr-1Mo filler and matching 9Cr-1Mo-V filler. Except for the developmental work of Bodine, et al., all welds were produced by the gas tungsten arc (GTA) process. Further development by Sikka and coworkers produced weldments by the submerged arc (SA) and shielded metal arc (SMA) processes [157], [158], [159], [160]. The filler metal most often used was the standard 9Cr-1Mo (Gr 9) steel. By 1987 it became clear that weldments in Gr 91 were significantly weaker than the base metal with the relative weakness increasing with increasing temperature [161], [162]. Various welding procedures and post weld heat treatments were examined, but the lower strength associated with a weakness in the fine-grained region of the heat affected zone (HAZ) persisted [163], [164], [165]. These observations were confirmed by intensive investigations of weldment performance undertaken in Europe and Asia to qualify the material and components for usage in power-generating applications for the temperature range from 550 to 650°C (1020 to 1200°F) [166], [167], [168], [169].

The DOE-sponsored programs produced virtually all of the information that led to the development of stress rupture factors for Gr 91 weldments, similar to those in ASME III-NH Table 1-14.10 for other materials. These factors were based on the ratio of the average strength of the weldment (for the ferritics) to the base metal [163]. In the subsequent revisions of ASME III Code Case N-47 that led to ASME III-NH, the material specifications for the Gr 91 filler metals that were addressed by the original code case submission were altered from SFA 5.4 (E505) to those mentioned earlier in this report, namely SFA-5.28 ER 90S-B9, SFA-5.5 E90XX, and SFA-E.23 EB9. Since the HAZ in the base metal was thought to control the stress factor for weldments, the filler metal was not of primary concern and the stress rupture factors were not changed. The stress rupture factors for Gr 91 were found to be relatively time independent but decreased with increasing temperatures. Since 1990, procedures and estimates of weld strength reduction factors were

developed in Europe and Asia, and several papers relating to their development have been published. Generally speaking, weld metal and weldment test data have not been available for inclusion in the database available for the re-assessment of Stress-Rupture Factors (section 4.5.3 reviews these studies). However, in addition to the data gathered in the original compilation used for development of Stress-Rupture Factors in ASME BPV III-NH, new data were obtained and are reported in Appendix F as follows:

- Test data from Oak Ridge National Laboratory since the original ASME code case including a re-evaluation of specimen failure modes which was not generally reported [170]
- Data from research supported by the Electric Power Research Institute on the effect of tempering temperature on the performance of Gr. 91 SMA welds [171], [172]
- Reported European test results from Jandova et al. [173], including test data in excess of 40,000 hours at lower stress including failure mode investigation
- Results on Grade 91 cross-weld creep from a Japanese study by Masuyama et al. [174], [175], including limited data on weldment configuration and specimen size effect
- Rupture data on Grade 91 filler metal made by GTAW with ER90S-B9 filler metal [176]

4.6.2 Characteristics of the Gr. 91 Weld and Weldment Database

The original database for Gr 91 weldments in ASME III-NH was focused on the stress-rupture behavior. However, some data on creep behavior and ductility were produced and reported. There were a number of significant factors that were considered and evaluated with respect to the stress-rupture for weldments. These included:

- Base metal composition and product thickness
- Filler metal composition and flux or coating, if used
- Welding process and process variables
- Weld configuration and number of passes
- Preheat temperature, interpass temperature, and hold/drop preheat prior to PWHT
- Post weld heat treat temperature and time
- Test specimen location (all-weld or cross weld) and size
- Failure location (weld, fusion line, HAZ, base metal away from weld)

Appendix F.1 is a listing of chemistry information on approximately 75 weldments and Appendix F.2 provides information on the weld and specimen configurations. Appendix F.3 provides drawings for many of these welds as listed in F.2. Products included plates, tubes, and pipes of Gr 91 with thicknesses in the range of 9 to 200 mm (3/8 to 8 in.). Filler metals included both standard 9Cr-1Mo steel and 9C-1Mo-V steel deposited by SMA, GTA, SA, and flux core arc (FCA) welding processes. Not all 75 welded products were tested in creep-rupture. Some were used for toughness testing, bend testing, aging studies, tensile tests, fatigue tests, crack growth studies, and the like. Some weldments were tested in the as-welded condition, but most were post weld heat treated (PWHT) in the temperature range of 705 to 785°C (1300 to 1450°F). Emphasis was placed on PWHT at 730 and 760°C (1350 and 1400°F) with times being one hour or longer for products of 25-mm (1-in.) or more thickness. Some weldments were re-normalized and tempered (NT).

Stress-rupture data for weld and weldment specimens are listed in Appendix F.4. There are approximately 270 entries representing about 45 welds and weldments. The table includes temperature, stress, rupture life, elongation, reduction of area, and information on failure location. The failure location information for the ORNL data was obtained by inspecting more than 150 specimens recovered from archival storage. Typically, failures identified as “shear” were in the fine-grained HAZ of the base metal. When the weld HAZ was more normal to the specimen axis, necking was sometimes observed. The failure locations in the database include 85 failures classified as heat affected zone (HAZ) and/or Type IV failures, 60 weld metal failures (including both weld metal and cross-weld tests), and the rest being classified as base metal, fusion line (FL), or not reported failure locations.

The distribution of testing times with filler metals, weld process, PWHT temperature, and test temperatures are shown in Figure 91 for the ORNL data. About the same number of tests were performed on weldments from standard Gr 9 and Gr 91 filler metals, but the testing times for the standard filler metal were longer. Several of the longer times represent discontinued creep-rupture tests, so most of the data pertain to times less than 10,000 hours. The longer time tests were mostly from the GTA weldment, although a few of the SA welds exceeded 10,000 hours. Most of the testing was performed at 538 and 593°C (1000 and 1100°F). There were no data below 538°C (1000°F). Finally, the number of tests on material with the 732°C (1350°F) PWHT was about the same as for the 760°C (1400°F) PWHT. The data not related to the ORNL dataset (originally used for development of the ASME Section III-NH factors) generally contains tests at higher temperatures, lower stresses, and longer times.

Figure 91: The Distribution of the ORNL Rupture Data for Filler Metal (a), Weld Process (b), Test Temperature (c) and PWHT Temperature (d)

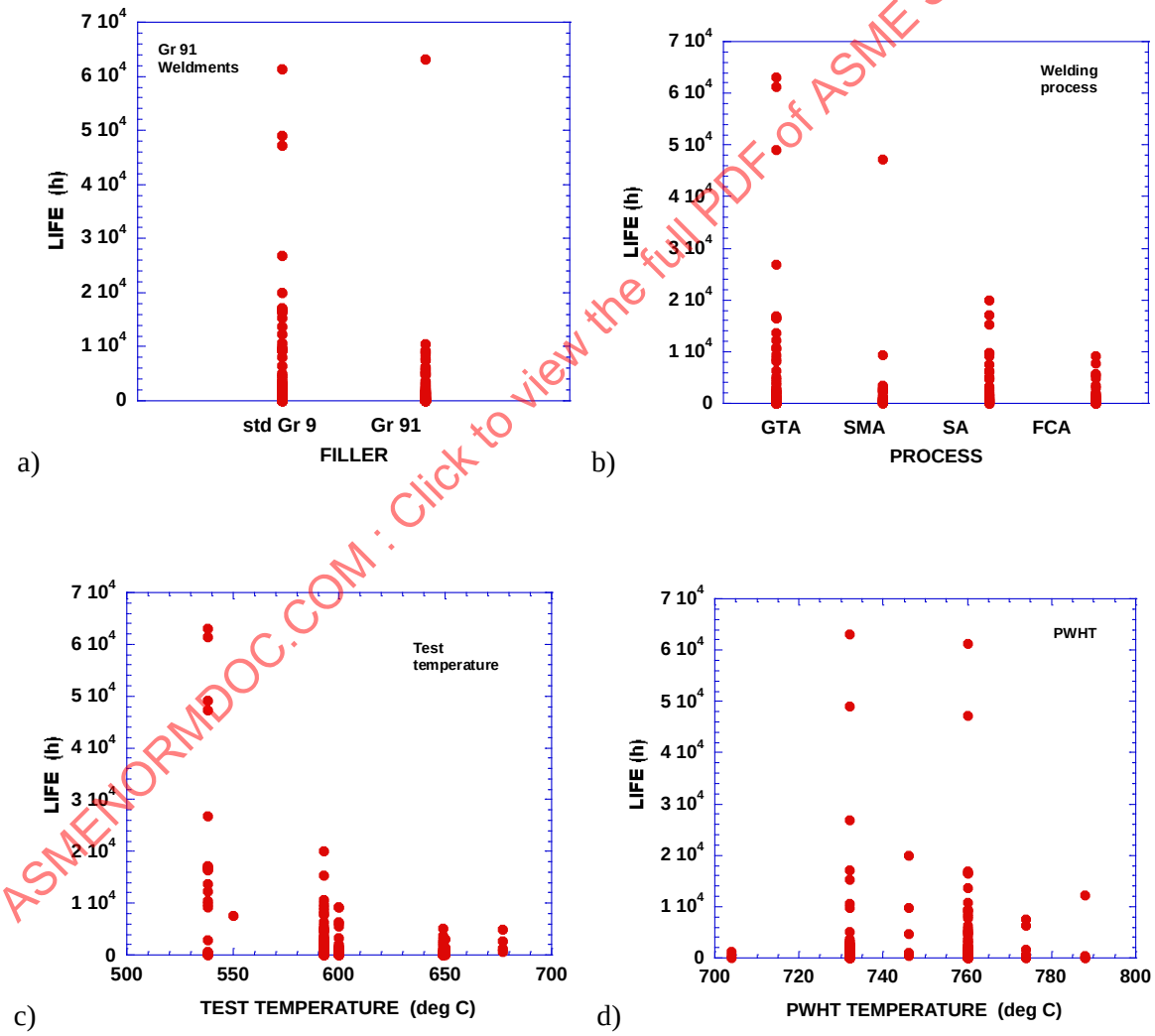

4.6.3 Review of Reports and Papers on WSRFs for Grade 91

In the service experience portion of this report, limited failures in grade 91 and creep strength enhanced ferritic steels were enumerated (chapter 2). Additionally, some research on WSRFs for CSEF was reviewed. In this section, a more in-depth review of grade 91 studies related to development of WSRFs for this alloy is presented.

Early work in Japan revealed low rupture strengths in the fine-grained region of the HAZ. Significant differences between base metal and weldments were observed by Sakaguchi for times to beyond 1000 h at 550, 600, and 650°C (1020, 1110, and 1200°F) with rupture strength ratios as low as 0.60 [167]. A recommendation was made by Sakaguchi to lower the tempering temperature of the base metal to below 700°C (1290°F) but increase the PWHT at 760°C (1400°F). This procedure improved the relative strength of the weldment. About the same time, Toyoda et al. performed stress-rupture tests on weldments with PWHT at 750°C (1380°F) and observed very little reduction in strength for times to 10,000 h [168]. Similar results were obtained by Taguchi, et al. [169]. They provided stress-rupture curves to 10,000 h for welded joints in plates, forgings, and tubes. At 500 and 550°C (930 and 1020°F) the weldment strengths were close to base metal strengths while at 650°C (1200°F).

Studies were undertaken of the all-weld metal properties and the re-normalized and tempered properties of weld metal and weldments [156], [170], [178], [179], [180], [181]. These studies generally showed improved strength relative to the PWHT weldments.

Middleton et al. performed extensive evaluations of data from laboratory weldment tests, HAZ simulated material tests, and field in-service ruptures to establish the conditions that produced Type IV cracking in Gr 91 weldments [181]. They defined the temperature-life regions for parent metal failures and for Type IV HAZ failures and made estimates of a weld strength reduction factor. Masuyama and Askins published their test results of butt welds in tubes welded to headers and found significant early failures in Gr 91 weldments at 655°C (1210°F) due to Type IV cracking [183]. Tanoue et al. evaluated damage in thick-section Gr 91 weldments tested at 650°C (1200°F) [184]. They observed Type IV cracking and failure of the HAZ after 6000 h at 58.8 MPa. Based on the average strength of base metal determined in Part 1 of this report, the SRF from the work of Tanoue et al. would be around 0.81.

Nonaka and coworkers examined stress-rupture behavior of welded P91 piping and elbows at 650°C (1200°F) [184], [185]. They tested full-thickness specimens extracted from the piping and elbows in addition to the pressurized pipes and elbows. Results showed similar failure modes and similar stress-rupture behavior in extracted samples and full section components when stress was based on the maximum principal stress. Although no SRFs were provided, it was clear that test data based on full-section, cross weld samples were a reliable indication of pressurized welded piping behavior.

Masuyama and Komai published results on continued testing in Japan of thick-section weldments and butt-welded tubes of Gr 91 [186]. They compared thick-section cross weld specimen data to base metal and included some results on pressurized vessels. One comparison was on the basis of the Larson Miller parameter in which a parametric constant of 36 for both the base metal and weldments was used. The stress functions were found to differ, and the trends suggested that the SRFs decreased with increasing temperature and time. Interpolation of the LMP curves for 10^5 h at 500°C (930°F) indicated an SRF around 0.91 or 0.92. At the other extreme, it was possible to estimate the SRF for 10^4 h at 650°C (1200°F) to be around 0.77. These SRF values were consistent with values in ASME III-NH. In a later paper, Masuyama re-plotted the LMP curves using a parametric constant of 20 [187]. In this interpretation, the SRF at 650°C (1200°F) decreased to near 0.64. Comparison of the LMP curves for the two parametric constants, however, showed that the higher value for the parametric constant (C=36) was a better choice in fitting the data.

Cohn and Coleman reviewed work on the cross weld testing of Gr 91 and considered the effect of the PWHT temperature [188]. They found better strength when the PWHT was at 649°C (1200°F) rather than 704 or 760°C (1300 to 1400°F). They estimated some SRFs and observed that they decreased with decreasing stress and increasing time. They mentioned SRF values of 0.76 at 621°C (1150°F) and 0.8 at 607°C (1125°F). Most testing involved relatively short times, so decreases in the SRFs below the estimates provided by Cohn and Coleman were judged to be likely for longer times.

Brett and co-workers examined service failures in Gr 91 components and found that materials with high aluminum and low nitrogen were susceptible to premature rupture [189], [190], [181]. The HAZ of weldments in such lots exhibited low rupture strength relative to average strength material. Again, the relative strength decreased with increasing time and increasing temperature. The SRF values at 1000 h were around 0.75 for both 600 and 650°C (1110 and 1200°F). They suggested that SRFs could decrease to a "floor value" near 0.60.

Schubert, Klenk, and Maile studied weldment behavior in several Cr-Mo-V steels for times to beyond 20,000 h [191]. They found that at high stresses and short time, failures occurred in the base metals away from the welds. With decreasing stresses and increasing time, HAZ ruptures were encountered, the stress-rupture curves for weldment data diverged from the base metal curves, and life asymptotically approached stress-rupture curves representing 100% simulated HAZ materials. For the class of steels that includes Gr 91, they suggested the SRF should be around 0.95 at 550°C (1020°F) and 0.65 at 600°C (1110°F) for 100,000 h. The value at 550°C (1020°F) is higher than that in ASME III-NH while the value at 650°C (1200°F) is much lower.

The SRFs in ASME III-NH formed the basis for the weld joint strength reduction factors (WSRFs) adopted for use with ASME B31.3 piping rules. The rationale for the WSRF values was provided by Becht [192], who recognized that the criteria for setting stress intensities in ASME III-NH differed from the criteria for setting allowable stresses for B31.1 Table A-1. For temperatures of 566°C (1050°F) and above, the WSRFs for Gr 91 were essentially identical to the SRFs in ASME III-NH.

Tabuchi and Takahashi provided a very comprehensive evaluation of WSRFs for Gr 91 based on a collection of 370 welded joint data [193]. Joining processes included SA, SMA, GTA, and metal active gas (MAG) welds and testing times extended to well beyond 20,000 h at 550°C (1020°F). They used the Larson Miller parameter in combination with a second order polynomial log-stress function to represent the base metal and weldment data. Comparisons with the model used by Brinkman [163] to develop the SRFs for ASME III-NH revealed a very similar fit and prediction of stresses. Tabuchi and Takahashi also examined subsets of data that included (a) only tests that failed in the HAZ of the base metal and (b) only tests on thicker products that had specimen locations, groove angles, and HAZs typical of components. The model was based on 141 data from specimens that qualified, with respect to HAZ width and groove angle, as typical of a structural component. The WSRFs recommended by Tabuchi and Takahashi were based on 80% of the minimum strength of the weldment for 100,000 h life divided by the allowable stress for the base metal for that same life. The minimum strength corresponded to the stress for a rupture curve that was displaced to shorter times by 1.65 multiples of the SEE of the model. This criterion for estimating the WSRF was different than the criterion used by Brinkman for estimating the SRFs for ASME III-NH, so a direct comparison of the SRFs and WSRFs was not possible.

Further work on Gr 91 weldments was published in 2007. Tabuchi et al. investigated GTA weldments with a "high" Ni filler metal for times to 10,000 h [194]. Again, Type IV failures occurred in the fine-grained HAZ of the base metal. At 600°C (1110°F), the slope of the log stress-log life curve for weldments between 1000 and 10,000 h was near -4. The estimated SRFs for 10,000 h at 550, 600, and 650°C (1020, 1110, and 1200°F) were 0.83, 0.65, and 0.58, respectively. Yamazaki, Hongo, and Watanabe examined the creep behavior of thick section Gr 91 GTA weldments for times to 10,000 h [195]. Their findings differed slightly

from Tabuchi et al. [194] in that ruptures at 550°C (1020°F) and times to 1000 h at higher temperatures occurred in the weld metal. At 10,000 h the estimated SRFs at 550, 600, and 650°C (1020, 1110, and 1200°F) were 0.87, 0.67, and 0.67, respectively.

Product thickness could be important since the base metal properties are known to be sensitive to thickness. In ASME Section II Part D, products thicker than 75 mm (3 in.) have lower allowable stresses than thinner products for some temperatures. Thus, depending on the thickness, one might observe different SRFs for the same temperature-time conditions. The database considered here included only one thick product, and only five data at 593°C (1100°F) were produced on the thick material. European and Asian researchers undertook more testing of weldments from thick products but no clear pattern emerged. However, it is significant that Tabuchi and Takahashi did not consider thin products in their development of WSRFs [193]. The filler metal composition could be important. Sometimes, Ni is added to filler metal for improved toughness. When the Ni + Mn exceed 1.2%, the A_{c1}, martensite start, and martensite finish temperatures are lowered. The creep strength of the weld metal may be affected by untempered martensite produced from the retained austenite after tempering [196], [197]. This will extend the region of failures in the weld metal, which normally occur at short times and high stresses. A few data from high Ni + Mn welds were included in the database. Half of the welds in the database were standard 9Cr-1Mo steel. This weld metal is expected to be weaker than 9Cr-1Mo-V.

Most of the test results included in the database were produced on 6.3-mm (1/4-in) diameter specimens. Some testing of full-thickness weldments is considered to be important to capture the effect of geometric restraint on the stress state in the HAZ. A few multiaxial tests were performed of the type described by Corum [198], and these generally supported the usefulness of the small specimen test results. Fortunately, testing of full-section weldments was undertaken by the Japanese [185], [186], [193], [194].

5 SUMMARY

In this report, a wealth of information is provided on the performance of welds and weldments in service and laboratory tests. A review and statistical analysis of CrMo seam-weld failure rates in fossil piping application was conducted. Since the evaluation included consideration of the survivor population of long seam-welded piping, it provides a more balanced view on the margins against failure in this class of welded CrMo piping, absent the imposition of any design WSRFs. The analysis is provided as a useful benchmark when considering the development of WSRFs. Discussions are also presented on the potential differences in design/operation practices between various industry applications. Limited failures in creep strength enhanced ferritic steels are also presented.

A review of the origins of ASME code rules for the imposition of WSRFs was also conducted. Some comparisons were made with other codified approaches to welded structures in the creep regime. While some international codes provide more rigorous rules for the creep analysis of welds, many codes have no approach beyond 'good engineering practice.' As the ASME rules have evolved, it is clear that the performance of weldments, not only weld metal, is critical to developing WSRFs. To complete this report, a large body of creep-rupture data on welds and weldments was assembled. Some preliminary assessments of the data were conducted and all data are tabulated in the appendix, allowing access for future codes and standards activities as needed.

Additional work was conducted on critical materials, such as grade 91, to identify failure locations and gather data from various researchers/organizations to be representative of the worldwide experience and research on these alloys. A review of service exposed carbon steel material showed no systematic deficiencies in the creep-rupture performance of this class of materials. These data will be used in Task 3 on the development of WSRFs.

APPENDIX A: CARBON STEEL

A.1 Ex-Service Weldment Data

F. Ellis, S. Ibarra and N. Mack, "Remaining Creep Life Estimation for Carbon Steel Mitered Elbow," Proc., ASME PVP 1993, PVP-Vol. 261, pp213-220

Material: C-Steel mitered elbow with long seam and girth welds. 26 years of service. Operating temperature not reported.

All test specimens transverse to pipe axis. All X-weld specimens failed in the FG HAZ.

Stress (MPa)	Temp. (C)	Rupture Time (Hours)	Elong. (%)	Reduction In Area (%)
		Base Material - Conventional		6.4 mm dia.
19	621	4404.4	23	52
12.1	649	3459.9	16	43
19	649	1210.5	23	--
24.1	649	459.8	38	57
19	677	291.2	30	46
19	704	81.9	55	72
		Base Material - Miniature		5 mm dia.
19	649	1199.4	48	65
19	677	332.1	52	58
19	677	312.0	58	73
19	704	81.3	63	80
19	704	101.6	62	75
		Girth Butt Weld Metal		6.4 mm dia.
19	649	1986.0	23	42
24.1	649	1265.3	23	--
19	677	1196.6	25	20
19	704	312.2	25	38
		Longitudinal Seam Weldment		9.5 mm dia.
19	593	10079.8	16	20
19	621	2718.8	22	36
19	649	691.7	23	68
25.9	649	254.2	25	48
19	704	66.0	50	71

J.E. McLaughlin, G.G. Karcher and P. Barnes, "Life Assessment of Carbon Steel Vessel with Cracks Operating in the Creep Range," Proc., ASME PVP 1994, PVP-Vol. 288, pp 351-361

Material: C-Steel of petro-chemical plant reactor. Sample contained weld. Approximately 40 years of service. Operating temperature: 970°F maximum.

All test specimens were cross-weld containing the entire weld within the gage, and failed in the FG HAZ.

Sample Type	Temperature °F (°C)	Stress ksi (MPa)	Rupture Time (hours)	Minimum Creep Rate (%)
1) 0.252" 0 by 1.0" gage	1175 (635)	3 (20.69)	908.2	0.0073
2) 0.252" 0 by 1.0" gage	1175 (635)	3 (20.69)	1185.5	0.0050
3) 0.252" 0 by 1.0" gage	1175 (635)	3 (20.69)	1343.3	0.0060
4) 0.505" 0 by 2.0" gage	1125 (607)	3 (20.69)	4166.8	0.0017
5) 0.505" 0 by 2.0" gage	1075 (580)	3 (20.69)	*	0.0063

* Test interrupted

C.J. Moss and J.L. Davidson, "Graphitisation in Type 201 Carbon Steel in Petro-Chemical Plant after Long Term Service," Materials Forum, v. 17, 1993, pp 35-359

Material: A 201 Grade A or B from three FCCU reactor vessels, 27, 33 and 36 yrs, at 932°, 970° and 973°F, respectively.

Data digitized from as-reported plots of cross-weld specimen rupture time. Cross-weld specimens failed in the FG WM and the FG HAZ. Plotted BM data appeared to be in error and not used.

Reactor	Test Temperature, deg C	Test Stress (MPa)	Rupture Time (h)
A	630	28.00	1326
A	650	28.00	420
B	619	18.00	1634
B	639	18.00	1215
B	644	18.00	1076
C	648	24.00	366
C	648	24.00	331
C	677	24.00	147
C	677	24.00	132
C	579	48.00	425
C	605	48.00	148
C	606	48.00	140

A.K. Ray et al., "Prediction of Remaining Life of a FCCU Reactor Plate," Engineering Failure Analysis, vol. 7, no.2, 2000, pp 75-86

Material: A 201 Grade A from FCCU reactor vessel after approximately 32 years at 900°F. Sample material from head (dome)-to-shell weld.

The weld, axial specimens identified in the table are cross-weld specimens with the weld metal at the center of the gage. Specimens were of rectangular cross-section, 6.25 mm x 4 mm, and reportedly failed in BM.

Creep rupture test results[a]

Test mark	Temperature, °C	Stress, MPa	Rupture, h	% elongation
WA	450	166	21	18
WA	475	170	4	18
WA	475	100	594	26
WA	500	100	137	20
WA	500	70	2496	16
BAS	450	100	2370	30
BAS	450	120	360	38
BAS	475	80	1320	32
BAS	475	100	450	37
BAS	500	70	1008	24
BAD	475	120	720	40
BAD	475	100	640	31
BAD	500	70	722	23
BCS	450	120	576	32
BCS	475	80	1728	
BCS	475	100	450	37
BCS	500	70	1416	31

[a] WA weld, axial; BAD base metal, axial, dome; BAS base metal, axial, shell; BCS base metal, circumferential, shell.

Three additional cross-weld data points (1985 study of same reactor) digitized from the reported Stress (MPa) versus T(20+logtr) plot:

Stress (MPa)	T(K)[20+log t(h)]
59.3	1.82E+04
69.9	1.79E+04
99.5	1.70E+04

J.G. Wilson, "Graphitization of Steel in Petroleum Refining Equipment" and "The Effect of Graphitization of Steel on Stress Rupture Properties," Welding Research Council (WRC) Bulletin 32, WRC, New York, NY, 1957

Material: Ex-service petroleum refining equipment from 3 plants (C, D, F). Plates are A 201 (C, D: Grade A, and F: Grade unknown)

Failure locations varied: FG HAZ for C, BM for D, and WM for F.

Specimen	T(F)	S (ksi)	tR(h)	Specimen	T(F)	S (ksi)	tR(h)
BM C4A	1000	16	6.5	X-W C1	1000	18	3.5
BM C5A	1000	16	9.3	X-W C3	1000	14	40.3
BM C1A	1000	14	55.7	X-W C8	1000	12	151.3
BM C2A	1000	12.5	153.9	X-W C5	1000	9	746.6
BM C3A	1000	10.5	757.6	X-W F3	1000	14	24.6
BM F2B	1000	16	27.6	X-W F1	1000	12.5	65.3
BM F1B	1000	12.5	182.2	X-W F4	1000	11	149
BM F3B	1000	11	406.1	X-W F5	1000	9	380
BM F4B	1000	9.5	1211.7	X-W F2	1000	8.25	674.9
BM D1B	1000	14	7.1	X-W D3	1000	14	16.2
BM D2B	1000	12.5	40.6	X-W D1	1000	12	80
BM D4B	1000	11	151.7	X-W D5	1000	10.5	235
BM D4B	1000	9	805	X-W D4	1000	9	886.4

A.2 Weld Metal Stress-Rupture

E-7018 Weld Metal

Carbon Content: 0.155%

Specimen No.	Condition	Test Temp., °F	Stress, psi	Hours	Elongation % 2"	Reduction of Area, %
9RA	AW	800	42,000	559	22.5	80.8
10RA	AW	800	39,000	1,076	21.0	81.0
11RA	AW	800	36,500	2789	21.5	80.0
13RA	AW	950	21,000	365	26.0	87.6
14RA	AW	950	19,000	845	29.5	87.2
15RA	AW	950	16,000	1158	55.0	89.0
16RA	AW	950	15,000	1462	45.0	88.5
17RA	AW	950	13,500	1891	60.0	89.6
18RA	AW	950	11,500	4273*		

*Test Stopped- Specimen Not Ruptured

Carbon Content: 0.089%

Specimen No.	Condition	Test Temp., °F	Stress, psi	Hours	Elongation % 2"	Reduction of Area, %
9RC	AW	800	42,000	3449	40.0	70.4
11RC	AW	800	44,000	1386	14.0	77.1
12RC	AW	800	46,000	1344	12.0	76.0
14RC	AW	950	26,500	61	22.5	84.9
15RC	AW	950	21,000	669	17.0	84.7
16RC	AW	950	17,500	959	28.5	86.8
17RC	AW	950	15,000	2150	28.0	41.0
18RC	AW	950	13,500	3564	38.0	87.0

Carbon Content: 0.051%

Specimen No.	Condition	Test Temp., °F	Stress, psi	Hours	Elongation % 2"	Reduction of Area, %
5RB	AW	800	42,000	4367	18.0	76.9
6RB	AW	800	44,000	2141	11.0	60.0
7RB	AW	800	46,000	1357	13.0	73.2

E-7018
Weld Metal

Carbon Content: 0.155%

Specimen No.	Condition	Test Temp., °F	Stress, psi	Hours	Elongation % 2"	Reduction of Area, %
1RA	AW + SR	800	40,000	174	27.5	72.4
2RA	AW + SR	800	37,000	645	28.0	81.0
3RA	AW + SR	800	34,000	672	32.0	83.0
4RA	AW + SR	800	31,000	1930	28.5	83.0
5RA	AW + SR	950	18,000	920	27.5	85.7
6RA	AW + SR	950	20,000	388	28.0	87.5
7RA	AW + SR	950	14,500	2365	41.5	86.4

Carbon Content: 0.089%

Specimen No.	Condition	Test Temp., °F	Stress, psi	Hours	Elongation % 2"	Reduction of Area, %
1RC	AW + SR	800	36,000	1026	36.5	81.0
2RC	AW + SR	800	40,000	129	33.5	80.8
3RC	AW + SR	800	33,000	711	32.5	82.0
4RC	AW + SR	800	30,000	1710	53.0	79.0
5RC	AW + SR	950	24,000	41	41.5	86.0
6RC	AW + SR	950	20,000	162	53.5	88.4
7RC	AW + SR	950	15,000	1050	49.5	85.8
8RC	AW + SR	950	12,500	3685	37.0	84.0

Carbon Content: 0.051%

Specimen No.	Condition	Test Temp., °F	Stress, psi	Hours	Elongation % 2"	Reduction of Area, %
1RB	AW + SR	800	30,000	6424*		
2RB	AW + SR	800	38,000	2625	46.0	78.4
3RB	AW + SR	800	40,000	30	25.5	78.0
4RB	AW + SR	800	39,000	23	26.0	19.9

*Test Stopped- Specimen Not Ruptured

Stress Relief: 1125°F + 25°F/8 hrs

E-7018
Weld Metal
Specimens Transverse to Weld Direction

Carbon Content: 0.051%

Specimen No.	Condition	Test Temp., °F	Stress, psi	Hours	Elongation % 2"	Reduction of Area, %
1469-1TRB	AW + SR	800	30,000	556	6.0	44.0
1469-2TRB	AW + SR	800	25,000	1819*		
1469-3TRB	AW + SR	800	37,500	4.5**		

Carbon Content: 0.089%

Specimen No.	Condition	Test Temp., °F	Stress, psi	Hours	Elongation % 2"	Reduction of Area, %
1469-1TRC	AW + SR	950	19,000	149	24.0	73.8
1469-2TRC	AW + SR	950	15,000	571	15.5	80.6

Carbon Content: 0.155%

Specimen No.	Condition	Test Temp., °F	Stress, psi	Hours	Elongation % 2"	Reduction of Area, %
1469-1TRA	AW + SR	950	19,000	243	26.0	88.0
1469-2TRA	AW + SR	950	14,000	1363	17.0	68.0
1469-3TRA	AW + SR	800	32,000	1169	16.0	54.0

Carbon Content: 0.051%

Specimen No.	Condition	Test Temp., °F	Stress, psi	Hours	Elongation % 2"	Reduction of Area, %
1469-4TRB	AW	800	40,000	55	17.5	79.0
1469-5TRB	AW	800	30,000	1988*		

Carbon Content: 0.089%

Specimen No.	Condition	Test Temp., °F	Stress, psi	Hours	Elongation % 2"	Reduction of Area, %
1469-4TRC	AW	950	22,500	168	15.5	80.6
1469-5TRC	AW	950	17,000	946	19.0	87.0
1469-6TRC	AW	800	40,000	592	19.0	81.0

Carbon Content: 0.155%

Specimen No.	Condition	Test Temp., °F	Stress, psi	Hours	Elongation % 2"	Reduction of Area, %
1RB	AW	950	22,500	112	24.5	43.0
2RB	AW	950	17,000	503	16.5	70.0
3RB	AW	800	40,000	703	25.5	81.0

*Test Stopped- Specimen Not Ruptured
**Failed at flaw in weld metal- not a valid point
Stress Relief: 1125°F ± 25°F/8 hrs

APPENDIX B: CARBON STEEL

See EPRI report, provided separately:

A Review of High Temperature Performance Trends and Design Rules for Cr-Mo Steel Weldments, EPRI, Palo Alto, CA: 1998. TR-110807.

APPENDIX C: 308 STAINLESS STEEL WELD METAL AND 304/308 STAINLESS STEEL WELDMENT STRESS-RUPTURE DATA

FILE #	Weld Metal	Specimen Type	Welding Process	Temp. (F)	Stress (ksi)	Rupture Life (hrs)	Min. Creep Rate (%/hr)	Elong. (%)	Red. Of Area (%)	Reference	Comments
1B	308L	CROSS	GTA	1697	6.72	3.72	3.44E+00			1B, White & le May	butt wld in bar
1B	308L	CROSS	GTA	1562	6.72	58.9	1.80E-01			1B, White & le May	butt wld in bar
1B	308L	CROSS	GTA	1474	6.72	207	3.00E-02			1B, White & le May	butt wld in bar
1B	308L	CROSS	GTA	1411	6.72	1032	4.80E-03			1B, White & le May	butt wld in bar
1B	308L	CROSS	GTA	1612	8.96	3.1	3.55E+00			1B, White & le May	butt wld in bar
1B	308L	CROSS	GTA	1472	8.96	34.5	2.15E-01			1B, White & le May	butt wld in bar
1B	308L	CROSS	GTA	1382	9.96	439.8	1.73E-02			1B, White & le May	butt wld in bar
1B	308L	CROSS	GTA	1335	8.96	1085	5.90E-03			1B, White & le May	butt wld in bar
1B	308L	CROSS	GTA	1384	11.59	130.8	1.02E-01			1B, White & le May	butt wld in bar
1B	308L	CROSS	GTA	1474	11.59	13.9	8.79E-01			1B, White & le May	butt wld in bar
1B	308L	CROSS	GTA	1382	15.15	25.05	4.30E-01			1B, White & le May	butt wld in bar
1B	308L	CROSS	GTA	1472	15.15	2.43	4.49E+00			1B, White & le May	butt wld in bar
1B	308L	CROSS	GTA	1382	17.92	12.05	1.22E+00			1B, White & le May	butt wld in bar
1B	308L	CROSS	GTA	1292	17.92	72.4	9.40E-02			1B, White & le May	butt wld in bar
1B	308L	CROSS	GTA	1474	17.92	0.69	1.58E+01			1B, White & le May	butt wld in bar
1B	308L	CROSS	GTA	1247	17.92	350.1	1.90E-02			1B, White & le May	butt wld in bar
1B	308L	CROSS	GTA	1202	17.92	1409.8	3.10E-03			1B, White & le May	butt wld in bar
1B	308L	CROSS	GTA	1292	21.39	19.6	3.54E-01			1B, White & le May	butt wld in bar
1B	308L	CROSS	GTA	1292	24.96	9.1	1.46E+00			1B, White & le May	butt wld in bar
1B	308L	CROSS	GTA	1202	24.98	149.7	5.30E-02			1B, White & le May	butt wld in bar
1B	308L	CROSS	GTA	1206	30.3	15.95	4.67E-01			1B, White & le May	butt wld in bar
1B	308L	CROSS	GTA	1202	35.84	0.75	4.63E+00			1B, White & le May	butt wld in bar
1B	308L	CROSS	GTA	1137	35.84	21.75	1.55E-01			1B, White & le May	butt wld in bar
1B	308L	CROSS	GTA	1108	35.84	78.1	5.07E-02			1B, White & le May	butt wld in bar
1B	308L	CROSS	GTA	1065	35.84	361	7.07E-03			1B, White & le May	butt wld in bar

FILE #	Weld Metal	Specimen Type	Welding Process	Temp. (F)	Stress (ksi)	Rupture Life (hrs)	Min. Creep Rate (%/hr)	Elong. (%)	Red. Of Area (%)	Reference	Comments
2B-Lot 1	308	WELD	SMA	1200	25	76		23.6		2B, Voorhees & Freeman	
2B-Lot 1	308	WELD	SMA	1200	22	174		19		2B, Voorhees & Freeman	
2B-Lot 1	308	WELD	SMA	1200	20	250		1.7		2B, Voorhees & Freeman	
2B-Lot 1	308	WELD	SMA	1200	18	1112		18.1		2B, Voorhees & Freeman	
2B-Lot 1	308	WELD	SMA	1200	15	3537		12		2B, Voorhees & Freeman	
2B-Lot 2	308L	WELD	SMA	1200	28	8		26		2B, Voorhees & Freeman	
2B-Lot 2	308L	WELD	SMA	1200	14	1071		4.5		2B, Voorhees & Freeman	
2B-Lot 2	308L	WELD	SMA	1200	12	2728		0.5		2B, Voorhees & Freeman	
2B-Lot 2	308L	WELD	SMA	1200	10	6037		3		2B, Voorhees & Freeman	
2B-Lot 2	308L	WELD	SMA	1200	8	11250		6		2B, Voorhees & Freeman	
2B-Lot 2	308L	WELD	SMA	1050	40	41		17		2B, Voorhees & Freeman	
2B-Lot 2	308L	WELD	SMA	1050	35	260		15		2B, Voorhees & Freeman	
2B-Lot 2	308L	WELD	SMA	1050	30	466		5.5		2B, Voorhees & Freeman	
2B-Lot 2	308L	WELD	SMA	1050	22	6934		4		2B, Voorhees & Freeman	
2B-Lot 2	308L	WELD	SMA	1050	22	6146		3.5		2B, Voorhees & Freeman	
2B-Lot 3	308	WELD	SMA	1050	35	155		15		2B, Voorhees & Freeman	
2B-Lot 3	308	WELD	SMA	1050	30	699		7		2B, Voorhees & Freeman	
2B-Lot 3	308	WELD	SMA	1050	25	2289		4.5		2B, Voorhees & Freeman	
2B-Lot 3	308	WELD	SMA	1050	22	5336		0.5		2B, Voorhees & Freeman	
2B-Lot 3	308	WELD	SMA	1200	25	34		17		2B, Voorhees & Freeman	
2B-Lot 3	308	WELD	SMA	1200	15	779		6		2B, Voorhees & Freeman	
2B-Lot 3	308	WELD	SMA	1200	11	3087		2		2B, Voorhees & Freeman	
2B-Lot 3	308	WELD	SMA	1200	9	5929				2B, Voorhees & Freeman	
2B-Lot 3	308	WELD	SMA	1200	7.5	11299		2		2B, Voorhees & Freeman	

FILE #	Weld Metal	Specimen Type	Welding Process	Temp. (F)	Stress (ksi)	Rupture Life (hrs)	Min. Creep Rate (%/hr)	Elong. (%)	Red. Of Area (%)	Reference	Comments
3B-Lot A	308	WELD	SMA	1050	40	150				3B, Wylie et al.	weld pad
3B-Lot A	308	WELD	SMA	1050	32	600				3B, Wylie et al.	weld pad
3B-Lot A	308	WELD	SMA	1050	26	2100				3B, Wylie et al.	weld pad
3B-Lot A	308	WELD	SMA	1050	20	5400				3B, Wylie et al.	weld pad
3B-Lot A	308	WELD	SMA	1200	28	40				3B, Wylie et al.	weld pad
3B-Lot A	308	WELD	SMA	1200	15	800				3B, Wylie et al.	weld pad
3B-Lot A	308	WELD	SMA	1200	11	3200				3B, Wylie et al.	weld pad
3B-Lot A	308	WELD	SMA	1200	9	5930				3B, Wylie et al.	weld pad
3B-Lot B	308	WELD	SMA	1200	28	80				3B, Wylie et al.	weld pad
3B-Lot B	308	WELD	SMA	1200	20	250				3B, Wylie et al.	weld pad
3B-Lot B	308	WELD	SMA	1200	19	1050				3B, Wylie et al.	weld pad
3B-Lot B	308	WELD	SMA	1200	15	3900				3B, Wylie et al.	weld pad
3B-Lot-C	308L	WELD	SMA	1050	42	43				3B, Wylie et al.	weld pad
3B-Lot-C	308L	WELD	SMA	1050	40	280				3B, Wylie et al.	weld pad
3B-Lot-C	308L	WELD	SMA	1050	31	490				3B, Wylie et al.	weld pad
3B-Lot-C	308L	WELD	SMA	1050	20	6200				3B, Wylie et al.	weld pad
3B-Lot-C	308L	WELD	SMA	1050	20	7000				3B, Wylie et al.	weld pad
3B-Lot-C	308L	WELD	SMA	1200	14	1100				3B, Wylie et al.	weld pad
3B-Lot-C	308L	WELD	SMA	1200	12.5	3100				3B, Wylie et al.	weld pad
3B-Lot-C	308L	WELD	SMA	1200	10	6000				3B, Wylie et al.	weld pad

FILE #	Weld Metal	Specimen Type	Welding Process	Temp. (F)	Stress (ksi)	Rupture Life (hrs)	Min. Creep Rate (%/hr)	Elong. (%)	Red. Of Area (%)	Reference	Comments
4B	308CRE	WELD	SMA	1100	30	74.2		55.2		King et al. 1973	Lot IDCA crown
4B	308CRE	WELD	SMA	1100	25	521.2		22.1		King et al. 1973	Lot IDCA crown
4B	308CRE	WELD	SMA	1200	22.5	56.5		54		King et al. 1973	Lot IDCA crown
4B	308CRE	WELD	SMA	1200	17.5	712.3		42.6		King et al. 1973	Lot IDCA crown
4B	308CRE	WELD	SMA	1200	15	5309.7		11.4		King et al. 1973	Lot IDCA crown
4B	308CRE	WELD	SMA	1200	22.5	168.2		29.7		King et al. 1973	Lot IDCA crown
4B	308CRE	WELD	SMA	1200	17	2979.9		2.2		King et al. 1973	Lot IDCA crown
4B	308CRE	WELD	SMA	1200	17.5	3816.1		4.7		King et al. 1973	Lot IDCA crown
5B-1	308CRE	WELD	SMA	1100	35	267.1		9.1		King, et al. 1973	Lot HBEA 1/8 sps. Various locations
5B-1	308CRE	WELD	SMA	1100	35	12.2		26		King, et al. 1973	Lot HBEA 1/8 sps. Various locations
5B-1	308CRE	WELD	SMA	1100	35	24.7		47.7		King, et al. 1973	Lot HBEA 1/8 sps. Various locations
5B-1	308CRE	WELD	SMA	1300	12.5	8993		10.4	21.3	King, et al. 1973	Lot HBEA 1/8 sps. Various locations
5B-1	308CRE	WELD	SMA	1100	35	22.7		18.8		King, et al. 1973	Lot HBEA 1/8 sps. Various locations
5B-1	308CRE	WELD	SMA	1050	37	106.4		18.8		King, et al. 1973	Lot HBEA 1/8 sps. Various locations
5B-1	308CRE	WELD	SMA	1100	35	556		10.2		King, et al. 1973	Lot HBEA 1/8 sps. Various locations
5B-1	308CRE	WELD	SMA	1050	37	1149		15.3		King, et al. 1973	Lot HBEA 1/8 sps. Various locations
5B-1	308CRE	WELD	SMA	1100	35	908.4		6.9		King, et al. 1973	Lot HBEA 1/8 sps. Various locations
5B-1	308CRE	WELD	SMA	1100	35	1231		7.6		King, et al. 1973	Lot HBEA 1/8 sps. Various locations
5B-1	308CRE	WELD	SMA	1100	35	83.8		18.7		King, et al. 1973	Lot HBEA 1/8 sps. Various locations
5B-1	308CRE	WELD	SMA	1050	36			1.26D		King, et al. 1973	Lot HBEA 1/8 sps. Various locations
5B-1	308CRE	WELD	SMA	1500	7.5	1076.1	9.00E-04	1.8		King, et al. 1973	Lot HBEA 1/8 sps. Various locations
5B-1	308CRE	WELD	SMA	1400	12.5	765.2	5.00E-03			King, et al. 1973	Lot HBEA 1/8 sps. Various locations
5B-1	308CRE	WELD	SMA	1600	6	366.6	3.00E-03			King, et al. 1973	Lot HBEA 1/8 sps. Various locations
5B-1	308CRE	WELD	SMA	1600	7.5	101.1	1.00E-02			King, et al. 1973	Lot HBEA 1/8 sps. Various locations

FILE #	Weld Metal	Specimen Type	Welding Process	Temp. (F)	Stress (ksi)	Rupture Life (hrs)	Min. Creep Rate (%/hr)	Elong. (%)	Red. Of Area (%)	Reference	Comments
5B-Base	BASE			1100	35	508.6		16.1		King, et al., 1973	Base near HAZ 1/8 sps
5B-Base	BASE			1100	35	768.7		12.3		King, et al., 1973	Base near HAZ 1/8 sps
5B-Base	BASE			1100	35	713.3		32.8		King, et al., 1973	Base near HAZ 1/8 sps
5B-Base	BASE			1100	35	339.7		20.4		King, et al., 1973	Base near HAZ 1/8 sps
5B-Base	BASE			1600	6	130.4	0.024	45.2	40	King, et al., 1973	Base near HAZ 1/8 sps
5B-Base	BASE			1050	36	1974		10.9		King, et al., 1973	Base near HAZ 1/8 sps
5B-Base	BASE			1100	35	530.5		19.6		King, et al., 1973	Base near HAZ 1/8 sps
5B-Base	BASE			1100	35	350.7		18.5		King, et al., 1973	Base near HAZ 1/8 sps
5B-Base	BASE			1100	35	434.8		22.1		King, et al., 1973	Base near HAZ 1/8 sps
5B-Base	BASE			1100	35	100.2		21.4		King, et al., 1973	Base near HAZ 1/8 sps
5B-Base	BASE			1100	35	327.5		21.4		King, et al., 1973	Base near HAZ 1/8 sps
5B-Base	BASE			1100	35	278.5		18.5		King, et al., 1973	Base near HAZ 1/8 sps
5B-Base	BASE			1100	35	158.1		20.4		King, et al., 1973	Base near HAZ 1/8 sps
5B-Base	BASE			1100	35	251.1		24.3		King, et al., 1973	Base near HAZ 1/8 sps
5B-Base	BASE			1600	7.5	30.1	1	57.9	44.2	King, et al., 1973	Base near HAZ 1/8 sps
5B-2	308CRE	WELD	SMA	900	45	1008D	2.60E-03	6.6		King, et al., 1973	Lot HBEA, crown, 1/4 sps
5B-2	308CRE	WELD	SMA	1050	35	2779	1.80E-03	21.9		King, et al., 1973	Lot HBEA, quarter, 1/4 sps
5B-2	308CRE	WELD	SMA	900	50	2396	1.30E-03	27.9		King, et al., 1973	Lot HBEA, quarter, 1/4 sps
5B-2	308CRE	WELD	SMA	1050	37	67.95	3.40E-01	32.9	65.3	King, et al., 1973	Lot HBEA, crown, 1/4 sps
5B-2	308CRE	WELD	SMA	1100	33	441.9	8.10E-03	21.4	52.2	King, et al., 1973	Lot HBEA, root, 1/4 sps
5B-2	308CRE	WELD	SMA	1100	30	236.4	5.80E-02	26.2	54.6	King, et al., 1973	Lot HBEA, crown, 1/4 sps
5B-2	308CRE	WELD	SMA	1100	33	73.3	2.50E-01	35.8	49.9	King, et al., 1973	Lot HBEA, crown, 1/4 sps
5B-2	308CRE	WELD	SMA	1100	25	3153	3.90E-04	26.1	64	King, et al., 1973	Lot HBEA, crown, 1/4 sps
5B-2	308CRE	WELD	SMA	900	45	6765	9.20E-04	21.6	31.7	King, et al., 1973	Lot HBEA, crown, 1/4 sps
5B-2	308CRE	WELD	SMA	1100	28	36147	2.80E-05	7.2		King, et al., 1973	Lot HBEA, root, 1/4 sps
5B-2	308CRE	WELD	SMA	900	55	873	5.50E-04	36.2	57.7	King, et al., 1973	Lot HBEA, crown, 1/4 sps
5B-2	308CRE	WELD	SMA	1100	28	5284	2.80E-04	22.1	54.8	King, et al., 1973	Lot HBEA, quarter, 1/4 sps
5B-2	308CRE	WELD	SMA	900	45	14529		19.1		King, et al., 1973	Lot HBEA, root, 1/4 sps

FILE #	Weld Metal	Specimen Type	Welding Process	Temp. (F)	Stress (ksi)	Rupture Life (hrs)	Min. Creep Rate (%/hr)	Elong. (%)	Red. Of Area (%)	Reference	Comments
5B-2	308CRE	WELD	SMA	900	50	2417	1.70E-03	15.3	63.6	King, et al., 1973	Lot HBEA, root, 1/4 sps
5B-2	308CRE	WELD	SMA	900	55	913.8	1.50E-04	29.6	41.5	King, et al., 1973	Lot HBEA, crown, 1/4 sps
5B-2	308CRE	WELD	SMA	900	55	353.9	7.30E-03	27	35.9	King, et al., 1973	Lot HBEA, root, 1/4 sps
5B-2	308CRE	WELD	SMA	900	60	0.1		31.3	43.4	King, et al., 1973	Lot HBEA, root, 1/4 sps
5B-2	308CRE	WELD	SMA	900	57.5	341.1	6.00E-03	20.3	15.7	King, et al., 1973	Lot HBEA, quarter, 1/4 sps
5B-2	308CRE	WELD	SMA	900	57.5	0.1		34.5	46.2	King, et al., 1973	Lot HBEA, crown, 1/4 sps
5B-2	308CRE	WELD	SMA	1200	20	3249.4	3.50E-04	20.5	60.5	King, et al., 1973	Lot HBEA, crown, 1/4 sps
5B-2	308CRE	WELD	SMA	900	57.5	0.1		31.6		King, et al., 1973	Lot HBEA, crown, 1/4 sps
5B-2	308CRE	WELD	SMA	1200	25	128.8		52.2		King, et al., 1973	Lot HBEA, crown, 1/4 sps
5B-2	308CRE	WELD	SMA	1100	35	86		25		King, et al., 1973	Lot HBEA, root, 1/4 sps
5B-2	308CRE	WELD	SMA	900	45	1886		40.8		King, et al., 1973	Lot HBEA, crown, 1/4 sps
5B-2	308CRE	WELD	SMA	900	55	19.2		27.8		King, et al., 1973	Lot HBEA, root, 1/4 sps
5B-2	308CRE	WELD	SMA	1050	35	139.6	1.50E-01	30.2	53.7	King, et al., 1973	Lot HBEA?, Block 15 crown, 1/4 sps
5B-2	308CRE	WELD	SMA	1200	28	23.6	1.70E-02	38.1	54.4	King, et al., 1973	Lot HBEA?, Block 15 crown, 1/4 sps
5B-2	308CRE	WELD	SMA	1050	35	7417.9	9.80E-05	13.8	49.6	King, et al., 1973	Lot HBEA?, Block 15 root, 1/4 sps
5B-2	308CRE	WELD	SMA	1050	35	1311.3	2.90E+00	15.7	49.5	King, et al., 1973	Lot HBEA?, Block 15 quarter, 1/4 sps
5B-2	308CRE	WELD	SMA	1050	35	1195.4	4.10E-03	28.2	49.6	King, et al., 1973	Lot HBEA?, Block 15 root, 1/4 sps
5B-2	308CRE	WELD	SMA	1050	37	703.8	7.20E-03	18.8	49.2	King, et al., 1973	Lot HBEA?, Block 15 quarter, 1/4 sps
5B-2	308CRE	WELD	SMA	900	40	26938	2.20E-04	27.1		King, et al., 1973	Lot HBEA?, Block 15 crown, 1/4 sps
5B-2	308CRE	WELD	SMA	900	40	10000D	1.00E-05			King, et al., 1973	Lot HBEA?, Block 15 root, 1/4 sps
5B-2	308CRE	WELD	SMA	1100	30	2791.2	5.20E-04	18.1	47.9	King, et al., 1973	Lot HBEA?, Block 15 root, 1/4 sps
5B-2	308CRE	WELD	SMA	900	55	492.4	7.30E-04	18.7	28.2	King, et al., 1973	Lot HBEA?, Block 15 quarter, 1/4 sps
5B-2	308CRE	WELD	SMA	900	50	1921.9	4.30E-04	24.3	52.3	King, et al., 1973	Lot HBEA?, Block 15 crown, 1/4 sps
5B-2	308CRE	WELD	SMA	1100	35	18.5	2.60E+00	55.3	65.6	King, et al., 1973	Lot HBEA?, Block 15 crown, 1/4 sps
5B-2	308CRE	WELD	SMA	1100	22.5	38739		27.9		King, et al., 1973	Lot HBEA?, Block 15 crown, 1/4 sps
5B-2	308CRE	WELD	SMA	1200	22	785	8.10E-04	43.3		King, et al., 1973	Lot HBEA?, Block 15 crown, 1/4 sps
5B-2	308CRE	WELD	SMA	1100	30	4446.3		27.1	53.1	King, et al., 1973	Lot HBEA?, Block 15 quarter, 1/4 sps
5B-2	308CRE	WELD	SMA	1200	28	97.5		20.8		King, et al., 1973	Lot HBEA?, Block 15 quarter, 1/4 sps
5B-2	308CRE	WELD	SMA	1100	33	610.2	8.80E-03	23.9	35.5	King, et al., 1973	Lot HBEA?, Block 15 quarter, 1/4 sps
5B-2	308CRE	WELD	SMA	1100	35	9.40E-01		30.6	60.3	King, et al., 1973	Lot HBEA?, Block 15 quarter, 1/4 sps

FILE #	Weld Metal	Specimen Type	Welding Process	Temp. (F)	Stress (ksi)	Rupture Life (hrs)	Min. Creep Rate (%/hr)	Elong. (%)	Red. Of Area (%)	Reference	Comments
5B-2	308CRE	WELD	SMA	1100	28	1.50E-03	1873.9	27.7	58.1	King, et al., 1973	Lot HBEA?, Block 15 crown, 1/4 sps
5B-2	308CRE	WELD	SMA	1200	22	6425.1	4.00E-05	20.5	45.8	King, et al., 1973	Lot HBEA?, Block 20 quarter, 1/4 sps
5B-2	308CRE	WELD	SMA	1200	22	360.6		47.2		King, et al., 1973	Lot HBEA?, Block 20 crown, 1/4 sps
5B-2	308CRE	WELD	SMA	1200	22	343		46.9		King, et al., 1973	Lot HBEA?, Block 20 crown, 1/4 sps
5B-2	308CRE	WELD	SMA	1200	28	13510		6.6		King, et al., 1973	Lot HBEA?, Block 20 root, 1/4 sps
5B-2	308CRE	WELD	SMA	1300	15	6320	1.10E-04	8.8	23.5	King, et al., 1973	Lot HBEA?, Block 20 crown, 1/4 sps
5B-2	308CRE	WELD	SMA	1300	10	12000D				King, et al., 1973	Lot HBEA?, Block 20 quarter, 1/4 sps
5B-2	308CRE	WELD	SMA	1100	25	2000D				King, et al., 1973	Lot HBEA?, Block 20 quarter, 1/4 sps
5B-2	308CRE	WELD	SMA	1100	20	1313D				King, et al., 1973	Lot HBEA?, Block 20 quarter, 1/4 sps
5B-2	308CRE	WELD	SMA	1200	22	269		48.2		King, et al., 1973	Lot HBEA?, Block 20 crown, 1/4 sps
5B-2	308CRE	WELD	SMA	1200	30	23.5		44.1		King, et al., 1973	Lot HBEA?, Block 20 root, 1/4 sps
5B-2	308CRE	WELD	SMA	1200	28	191		25.2		King, et al., 1973	Lot HBEA?, Block 20 root, 1/4 sps
5B-2	308CRE	WELD	SMA	1200	28	42.3		49.5		King, et al., 1973	Lot HBEA?, Block 22 quarter, 1/4 sps
5B-2	308CRE	WELD	SMA	1300	20	131	2.00E-02	23.8	41.3	King, et al., 1973	Lot HBEA?, Block 22 crown, 1/4 sps
5B-2	308CRE	WELD	SMA	1400	10	2638	2.60E-04	4.5	6.2	King, et al., 1973	Lot HBEA?, Block 22 crown, 1/4 sps
5B-2	308CRE	WELD	SMA	1100	33	481		29.6		King, et al., 1973	Lot HBEA?, Block 69 quarter, 1/4 sps
5B-2	308CRE	WELD	SMA	1100	28	606.9		63.2		King, et al., 1973	Lot HBEA?, Block 69 crown, 1/4 sps
5B-2	308CRE	WELD	SMA	1100	28	433.5		60.2		King, et al., 1973	Lot HBEA?, Block 69 crown, 1/4 sps
5B-2	308CRE	WELD	SMA	1100	35	197.2		32.8		King, et al., 1973	Lot HBEA?, Block 69 quarter, 1/4 sps
5B-2	308CRE	WELD	SMA	1100	33	235.4		50.4		King, et al., 1973	Lot HBEA?, Block 69 quarter, 1/4 sps
5B-2	308CRE	WELD	SMA	1100	33	621.6		40		King, et al., 1973	Lot HBEA?, Block 69 quarter, 1/4 sps
5B-2	308CRE	WELD	SMA	1100	30	854.4		36.4		King, et al., 1973	Lot HBEA?, Block 69 quarter, 1/4 sps
5B-2	308CRE	WELD	SMA	1100	30	4390		25.7		King, et al., 1973	Lot HBEA?, Block 69 quarter, 1/4 sps
5B-2	308CRE	WELD	SMA	1100	33	265.2		43.2		King, et al., 1973	Lot HBEA?, Block 69 root, 1/4 sps
5B-2	308CRE	WELD	SMA	1100	33	333.6		37.2		King, et al., 1973	Lot HBEA?, Block 69 root, 1/4 sps

FILE #	Weld Metal	Specimen Type	Welding Process	Temp. (F)	Stress (ksi)	Rupture Life (hrs)	Min. Creep Rate (%/hr)	Elong. (%)	Red. Of Area (%)	Reference	Comments
5B-2-4K-age	308CRE	WELD	SMA	1200	28	19.7		59.3		King, et al., 1973	Lot HBEA?, Block 69, 65, 20, aged @ test temp root, 1/4 sps
5B-2-4K-age	308CRE	WELD	SMA	1200	28	40.9		54.1		King, et al., 1973	Lot HBEA?, Block 69, 65, 20, aged @ test temp root, 1/4 sps
5B-2-4K-age	308CRE	WELD	SMA	900	55	0.1		26.8		King, et al., 1973	Lot HBEA?, Block 69, 65, 20, aged @ test temp root, 1/4 sps
5B-2-4K-age	308CRE	WELD	SMA	900	50	630.5		29.6		King, et al., 1973	Lot HBEA?, Block 69, 65, 20, aged @ test temp root, 1/4 sps
5B-2-4K-age	308CRE	WELD	SMA	900	50	284.7		45.3		King, et al., 1973	Lot HBEA?, Block 69, 65, 20, aged @ test temp root, 1/4 sps
5B-2-4K-age	308CRE	WELD	SMA	1100	30	20.2		51.2		King, et al., 1973	Lot HBEA?, Block 69, 65, 20, aged @ test temp root, 1/4 sps
5B-2-4K-age	308CRE	WELD	SMA	1100	35	84.9		46.3		King, et al., 1973	Lot HBEA?, Block 69, 65, 20, aged @ test temp root, 1/4 sps
5B-2-10K-age	308CRE	WELD	SMA	1200	28	19.3		50.9		King, et al., 1973	Lot HBEA?, Block 69, 65, 20, aged @ test temp root, 1/4 sps
5B-2-10K-age	308CRE	WELD	SMA	1200	28	42.6		52.5		King, et al., 1973	Lot HBEA?, Block 69, 65, 20, aged @ test temp root, 1/4 sps
5B-2-10K-age	308CRE	WELD	SMA	900	45	1796		44.2		King, et al., 1973	Lot HBEA?, Block 69, 65, 20, aged @ test temp root, 1/4 sps
5B-2-10K-age	308CRE	WELD	SMA	900	50	438.2		33.2		King, et al., 1973	Lot HBEA?, Block 69, 65, 20, aged @ test temp root, 1/4 sps
5B-2-10K-age	308CRE	WELD	SMA	900	52.5	0.1		40.2		King, et al., 1973	Lot HBEA?, Block 69, 65, 20, aged @ test temp root, 1/4 sps
5B-2-10K-age	308CRE	WELD	SMA	900	50	247		39.8		King, et al., 1973	Lot HBEA?, Block 69, 65, 20, aged @ test temp root, 1/4 sps
5B-2-10K-age	308CRE	WELD	SMA	900	52.5	159		32.4		King, et al., 1973	Lot HBEA?, Block 69, 65, 20, aged @ test temp root, 1/4 sps
5B-2-10K-age	308CRE	WELD	SMA	1200	30	272		66.5		King, et al., 1973	Lot HBEA?, Block 69, 65, 20, aged @ test temp root, 1/4 sps
5B-2	308CRE	WELD	SMA	1200	28	114.4		27.6		King, et al., 1973	Lot HBEA?, Block 83 root, 1/4 sps
5B-2	308CRE	WELD	SMA	1200	22	1910		33.9		King, et al., 1973	Lot HBEA?, Block 83 crown, 1/4 sps
5B-2	308CRE	WELD	SMA	1200	28	201		45.2		King, et al., 1973	Lot HBEA?, Block 83 root, 1/4 sps
5B-2	308CRE	WELD	SMA	1200	30	13.6		45.2		King, et al., 1973	Lot HBEA?, Block 83 root, 1/4 sps
5B-2	308CRE	WELD	SMA	1200	30	14.3		36		King, et al., 1973	Lot HBEA?, Block 83 root, 1/4 sps
5B-2	308CRE	WELD	SMA	1200	22	543		67.4		King, et al., 1973	Lot HBEA?, Block 83 crown, 1/4 sps

FILE #	Weld Metal	Specimen Type	Welding Process	Temp. (F)	Stress (ksi)	Rupture Life (hrs)	Min. Creep Rate (%/hr)	Elong. (%)	Red. Of Area (%)	Reference	Comments
6B-1	308CRE	CROSS	SMA	1100	33	455.8			8.6	King, et al., 1973	Lot JADA, Block 43, crown, 1/4 sps, base or HAZ failures
6B-1	308CRE	CROSS	SMA	1100	33	1861.6			7.9	King, et al., 1973	Lot JADA, Block 43, root, 1/4 sps, base or HAZ failures
6B-1	308CRE	CROSS	SMA	1100	35	798.6			1.2	King, et al., 1973	Lot JADA, Block 43, root, 1/4 sps, base or HAZ failures
6B-1	308CRE	CROSS	SMA	1100	33	771.1			5.9	King, et al., 1973	Lot JADA, Block 43, root, 1/4 sps, base or HAZ failures
6B-1	308CRE	CROSS	SMA	1100	35	673.8			10.2	King, et al., 1973	Lot JADA, Block 43, crown, 1/4 sps, base or HAZ failures
6B-1	308CRE	CROSS	SMA	1100	33	1773.9			5.6	King, et al., 1973	Lot JADA, Block 43, quarter, 1/4 sps, base or HAZ failures
6B-1	308CRE	CROSS	SMA	1100	35	912.5			6.7	King, et al., 1973	Lot JADA, Block 43, quarter, 1/4 sps, base or HAZ failures
6B-2	308CRE	WELD	SMA	1100	37	124.2	7.70E-02	20.6	48.5	King, et al., 1973	Lot JADA, Block 43, crown 1/4 sps
6B-2	308CRE	WELD	SMA	1100	37	954.4	3.20E-03	11.1	42	King, et al., 1973	Lot JADA, Block 43, quarter 1/4 sps
6B-2	308CRE	WELD	SMA	1100	35	1071.3	5.80E-03	11.8	42.5	King, et al., 1973	Lot JADA, Block 43, crown 1/4 sps
6B-2	308CRE	WELD	SMA	1100	37	251	6.70E-03	7.7	33.4	King, et al., 1973	Lot JADA, Block 43, root 1/4 sps
6B-2	308CRE	WELD	SMA	1200	22	3003.6		32.9		King, et al., 1973	Lot JADA, Block 43, quarter 1/4 sps
6B-2	308CRE	WELD	SMA	1100	37	242.5	1.50E-02	14.2	43.8	King, et al., 1973	Lot JADA, Block 43, root 1/4 sps
6B-2	308CRE	WELD	SMA	1100	35	3203.4		12.6		King, et al., 1973	Lot JADA, Block 43, root 1/4 sps
6B-2	308CRE	WELD	SMA	1100	35	2230.3		11.5		King, et al., 1973	Lot JADA, Block 43, quarter 1/4 sps
6B-2	308CRE	WELD	SMA	1100	30	2852.8	6.50E-04	4.8		King, et al., 1973	Lot JADA, Block 43, crown 1/4 sps
6B-2	308CRE	WELD	SMA	1100	30	7097.9		7.9		King, et al., 1973	Lot JADA, Block 43, quarter 1/4 sps

FILE #	Weld Metal	Specimen Type	Welding Process	Temp. (F)	Stress (ksi)	Rupture Life (hrs)	Min. Creep Rate (%/hr)	Elong. (%)	Red. Of Area (%)	Reference	Comments
7B-1	308CRE	WELD	GTA	1100	35	206.8	0.025	7.6		McAfee, et al. 1984	Control for plate test, 1/4 sps
7B-1	308CRE	WELD	GTA	1100	25	2373D	3.00E-04			McAfee, et al. 1984	Control for plate test, 1/4 sps
7B-2	Base	FUSION LINE		1100	35	61.9	0.205	14.9		McAfee, et al. 1984	Control for plate test, 1/4 sps
7B-2	Base	FUSION LINE		1100	25	842.1	0.011	15.7		McAfee, et al. 1984	Control for plate test, 1/4 sps
7B-3	Base	HAZ		1100	35	45.1	0.35	24.1		McAfee, et al. 1984	Control for plate test, 1/4 sps
7B-3	Base	HAZ		1100	25	758.7	0.009	10.9		McAfee, et al. 1984	Control for plate test, 1/4 sps
7B-4	Base			1100	25	901	0.01	16.08		McAfee, et al. 1984	Control for plate test, 1/4 sps
7B-4	Base			1100	25	696	0.012	14.42		McAfee, et al. 1984	Control for plate test, 1/4 sps
7B-4	Base			1100	35	48.9	0.348			McAfee, et al. 1984	Control for plate test, 1/4 sps
7B-4	Base			1100	25	863	0.009	14.35		McAfee, et al. 1984	Control for plate test, 1/4 sps
7B-4	Base			1100	35	44.1	0.338	26.48		McAfee, et al. 1984	Control for plate test, 1/4 sps
7B-4	Base			1100	25	662	0.012	12.31		McAfee, et al. 1984	Control for plate test, 1/4 sps

FILE #	Weld Metal	Specimen Type	Welding Process	Temp. (F)	Stress (ksi)	Rupture Life (hrs)	Min. Creep Rate (%/hr)	Elong. (%)	Red. Of Area (%)	Reference	Comments
8B-1	308CRE	WELD	SMA	1100	35	48.8	0.54	48	57	Swindeman, et al. 1979	Control for plate test, 1/4 sps
8B-1	308CRE	WELD	SMA	1100	32	237.6	0.1	47	55	Swindeman, et al. 1979	Control for plate test, 1/4 sps
8B-1	308CRE	WELD	SMA	1100	30	1850	0.03	46	54	Swindeman, et al. 1979	Control for plate test, 1/4 sps
8B-1	308CRE	WELD	SMA	1100	28	3488	0.002	35	52	Swindeman, et al. 1979	Control for plate test, 1/4 sps
8B-1	308CRE	WELD	SMA	1100	25	12700	0.00045	35		Swindeman, et al. 1979	Control for plate test, 1/4 sps
8B-1	308CRE	WELD	SMA	1100	20		0.00001			Swindeman, et al. 1979	Control for plate test, 1/4 sps
8B-1	308CRE	CROSS	SMA	1100	32	86.4	0.03	21		Swindeman, et al. 1979	Control for plate test, 1/4 sps
8B-1	308CRE	CROSS	SMA	1100	32	85.7	0.082	13	11	Swindeman, et al. 1979	Control for plate test, 1/4 sps
8B-1	308CRE	CROSS	SMA	1100	28	317.2	0.016	10	6	Swindeman, et al. 1979	Control for plate test, 1/4 sps
8B-1	308CRE	CROSS	SMA	1100	25	752.9	0.001	7.1	9	Swindeman, et al. 1979	Control for plate test, 1/4 sps
8B-1	308CRE	CROSS	SMA	1100	20	5731	0.0002			Swindeman, et al. 1979	Control for plate test, 1/4 sps
8B-2	BASE	FUSION LINE		1100	30	312.5	0.04	30.7		Swindeman, et al. 1979	Control for plate test, 1/4 sps
8B-2	BASE	FUSION LINE		1100	20		4.20E-05			Swindeman, et al. 1979	Control for plate test, 1/4 sps
8B-3	BASE			1100	35	0.5	60	31		Swindeman, et al. 1979	Control for plate test, 1/4 sps
8B-3	BASE			1100	30	0.065	257.9	25		Swindeman, et al. 1979	Control for plate test, 1/4 sps
8B-3	BASE			1100	18	0.00007				Swindeman, et al. 1979	Control for plate test, 1/4 sps
9B-1	308	CROSS	GTA	1100	40	4.4	1.19	14.7		Ward, 1971	1/8 sps
9B-1	308	CROSS	GTA	1100	35	73.3	0.61	12.2		Ward, 1971	1/8 sps
9B-1	308	CROSS	GTA	1100	30	196.9	0.016	10		Ward, 1971	1/8 sps
9B-2 aged	308	CROSS	GTA	1100	25	14.6	0.0005	2.3		Ward, 1971	1200 h at 1100F 1/8 sps
9B-1	308	CROSS	GTA	1100	25	1526	0.0006	1.9		Ward, 1971	1/8 sps

FILE #	Weld Metal	Specimen Type	Welding Process	Temp. (F)	Stress (ksi)	Rupture Life (hrs)	Min. Creep Rate (%/hr)	Elong. (%)	Red. Of Area (%)	Reference	Comments
10B-1	308	CROSS	SA	1100	45	0.3	23.3	21.3		Ward, 1974	1/8 sps
10B-1	308	CROSS	SA	1100	40	1	11.4	28.4		Ward, 1974	1/8 sps
10B-1	308	CROSS	SA	1100	30	48.8	0.213	15.2		Ward, 1974	1/8 sps
10B-1	308	CROSS	SA	1100	25	286	0.021	10.6		Ward, 1974	1/8 sps
10B-1	308	CROSS	SA	1100	23	589	0.0061	4.8		Ward, 1974	1/8 sps
10B-1	308	CROSS	SA	1100	21	1144.8	0.0004	8.4		Ward, 1974	1/8 sps
10B-1	308	CROSS	SA	1000	45	35.5	0.274	20.4		Ward, 1974	1/8 sps
10B-1	308	CROSS	SA	1000	33	435.5	0.0153	11.6		Ward, 1974	1/8 sps
10B-1	308	CROSS	SA	1000	28	2498	0.0014	7.6		Ward, 1974	1/8 sps
11B-1	308L	CROSS	GMA	1100	40	3.2	3.88	25.1		Ward, 1974	1/8 sps
11B-1	308L	CROSS	GMA	1100	30	38.1	0.174	10.3		Ward, 1974	1/8 sps
11B-1	308L	CROSS	GMA	1100	25	275	0.0147	10.7		Ward, 1974	1/8 sps
11B-1	308L	CROSS	GMA	1100	21	6030	0.0056	6.9		Ward, 1974	1/8 sps
11B-1	308L	CROSS	GMA	1100	18	1099	0.0027	4.8		Ward, 1974	1/8 sps
12B-1	308L	WELD	SA	1000	45	4.1	3.12E+00	32.4		Ward, 1974	1/8 sps
12B-1	308L	WELD	SA	1000	39	49.3	3.62E-01	29		Ward, 1974	1/8 sps
12B-1	308L	WELD	SA	1000	35	230.7	4.81E-02	23		Ward, 1974	1/8 sps
12B-1	308L	WELD	SA	1000	30	2113.5	2.08E-03	10.2		Ward, 1974	1/8 sps
12B-1	308L	WELD	SA	1000	28	3943.4	1.14E-03	9.4		Ward, 1974	1/8 sps
12B-1	308L	WELD	SA	1100	35	9	2.20E+00	29.5		Ward, 1974	1/8 sps
12B-1	308L	WELD	SA	1100	28	94.9	1.13E-01	26.2		Ward, 1974	1/8 sps
12B-1	308L	WELD	SA	1100	28	124				Ward, 1974	1/8 sps
12B-1	308L	WELD	SA	1100	25	268				Ward, 1974	1/8 sps
12B-1	308L	WELD	SA	1200	25	13				Ward, 1974	1/8 sps
12B-1	308L	WELD	SA	1200	18	121				Ward, 1974	1/8 sps
12B-1	308L	WELD	SA	1200	15	610				Ward, 1974	1/8 sps
12B-2 ann	308L	WELD	SA	1000	45	16	8.23E-01	36.8		Ward, 1974	annealed 1950F, 1/8 sps
12B-2 ann	308L	WELD	SA	1000	40	117	1.40E-01	31.4		Ward, 1974	annealed 1950F, 1/8 sps
12B-2 ann	308L	WELD	SA	1000	35	257	5.13E-02	26		Ward, 1974	annealed 1950F, 1/8 sps
12B-2 ann	308L	WELD	SA	1000	31	2165	6.07E-03	25		Ward, 1974	annealed 1950F, 1/8 sps
12B-2 ann	308L	WELD	SA	1100	35	8.8	1.93E+00	33		Ward, 1974	annealed 1950F, 1/8 sps
12B-2 ann	308L	WELD	SA	1100	28	84.4	2.80E-01	35.6		Ward, 1974	annealed 1950F, 1/8 sps

FILE #	Weld Metal	Specimen Type	Welding Process	Temp. (F)	Stress (ksi)	Rupture Life (hrs)	Min. Creep Rate (%/hr)	Elong. (%)	Red. Of Area (%)	Reference	Comments
13B	308	WELD	SA	1000	45	40.1	3.69E-01	28.8		Ward, 1974	1/8 sps
13B	308	WELD	SA	1000	39	215.1	6.80E-02	22.3		Ward, 1974	1/8 sps
13B	308	WELD	SA	1000	35	1472.3	3.87E-03	8.2		Ward, 1974	1/8 sps
13B	308	WELD	SA	1000	31	2540.5	2.43E-03	15.7		Ward, 1974	1/8 sps
13B	308	WELD	SA	1100	28	103.9	1.29E-01	21		Ward, 1974	1/8 sps
13B	308	WELD	SA	1100	22	632.6	5.00E-03	5.7		Ward, 1974	1/8 sps
14B	308CRE	WELD	SMA	1000	35	2015.2	0.0017	18.6		Ward, 1974	1/8 sps
15B-1	308CRE	CROSS	SMA	1000	50	55.6	0.084	21.6		Ward, 1974	1/8 sps
15B-1	308CRE	CROSS	SMA	1000	35		0.0001			Ward, 1974	1/8 sps
15B-1-10Kage	308CRE	CROSS	SMA	1000	43	349.2	0.0143	15.4		Ward, 1974	aged 10K at 1000F 1/8 sps
16B-1	308CRE	WELD	SA	1000	45	217.9	3.60E-02	22.8		Ward, 1974	1/8 sps
16B-1	308CRE	WELD	SA	1000	43	350.9	2.30E-02	18.4		Ward, 1974	1/8 sps
16B-1	308CRE	WELD	SA	1000	40	9761.9	2.40E-04	13.3		Ward, 1974	1/8 sps
16B-2	308CRE	CROSS	SA	1000	55	18	1.50E-01	14		Ward, 1974	1/8 sps
16B-2	308CRE	CROSS	SA	1000	45	649.9	3.90E-03	8.4		Ward, 1974	1/8 sps
16B-2	308CRE	CROSS	SA	1000	40	2010.9	1.10E-03	6.7		Ward, 1974	1/8 sps
16B-2	308CRE	CROSS	SA	1000	38		1.60E-04			Ward, 1974	1/8 sps
17B	308CRE	WELD	SMA	1000	2.62	152.1	4.70E-02	17.9		Ward, 1974	1/8 sps
17B	308CRE	WELD	SMA	1000	45	127.3	7.80E-02	25.4		Ward, 1974	1/8 sps
17B	308CRE	WELD	SMA	1000	40	3061.9	8.80E-04	10.2		Ward, 1974	1/8 sps
17B	308CRE	WELD	SMA	1000	45	77.4	8.80E-02	20.3		Ward, 1974	1/8 sps
17B	308CRE	WELD	SMA	1000	45	1232	1.60E-03	10		Ward, 1974	1/8 sps

FILE #	Weld Metal	Specimen Type	Welding Process	Temp. (F)	Stress (ksi)	Rupture Life (hrs)	Min. Creep Rate (%/hr)	Elong. (%)	Red. Of Area (%)	Reference	Comments
18B	308	WELD	SMA or SA?	1200	30	10.4	1.73E-01	13.4		Ward, 1974	deposit chem shows 0.5%C, 1/8 sps
18B	308	WELD	SMA or SA?	1200	27	23.8	8.20E-02	14.4		Ward, 1974	deposit chem shows 0.5%C, 1/8 sps
18B	308	WELD	SMA or SA?	1200	25	32.2	5.30E-02	10		Ward, 1974	deposit chem shows 0.5%C, 1/8 sps
18B	308	WELD	SMA or SA?	1200	23	53.1	2.84E-02	11.5		Ward, 1974	deposit chem shows 0.5%C, 1/8 sps
18B	308	WELD	SMA or SA?	1200	22	67.4	2.10E-02	8.4		Ward, 1974	deposit chem shows 0.5%C, 1/8 sps
18B	308	WELD	SMA or SA?	1200	21	171.5	4.57E-03	4		Ward, 1974	deposit chem shows 0.5%C, 1/8 sps
18B	308	WELD	SMA or SA?	1200	16	1391	1.80E-04	1		Ward, 1974	deposit chem shows 0.5%C, 1/8 sps
18B	308	WELD	SMA or SA?	1200	14.5	1201	2.47E-04	1.2		Ward, 1974	deposit chem shows 0.5%C, 1/8 sps
18B	308	WELD	SMA or SA?	1200	11		8.00E-05			Ward, 1974	deposit chem shows 0.5%C, 1/8 sps
18B	308	WELD	SMA or SA?	1200	11		7.60E-05			Ward, 1974	deposit chem shows 0.5%C, 1/8 sps
19B-V-8	308CRE	WELD	GTA	1200	25	40.2		39.1	47.5	Edmonds, Klueh,..	experimental CRE Lots
19B-V-8	308CRE	WELD	GTA	1200	20	262.2		18.8	24.1	Edmonds, Klueh,..	experimental CRE Lots
19B-V-8	308CRE	WELD	GTA	1200	16	1198		4.6	11.2	Edmonds, Klueh,..	experimental CRE Lots
19B-V-8	308CRE	WELD	GTA	1200	25	26.5		28.2	42.6	Edmonds, Klueh,..	experimental CRE Lots
19B-V-8	308CRE	WELD	GTA	1200	20	190.4		13.4	22.4	Edmonds, Klueh,..	experimental CRE Lots
19B-V-8	308CRE	WELD	GTA	1200	16	1091.7		6.4	6.7	Edmonds, Klueh,..	experimental CRE Lots
19B-V-8	308CRE	WELD	GTA	1200	25	11.4		37.5	80.7	Edmonds, Klueh,..	experimental CRE Lots
19B-V-8	308CRE	WELD	GTA	1200	20	25		13.6	40.4	Edmonds, Klueh,..	experimental CRE Lots
19B-V-8	308CRE	WELD	GTA	1200	14	936.7		25.4	36.6	Edmonds, Klueh,..	experimental CRE Lots
19B-V-11	308CRE	WELD	GTA	1200	25	15.7		32.7	62.1	Edmonds, Klueh,..	experimental CRE Lots
19B-V-11	308CRE	WELD	GTA	1200	16	357.4		33.1	50.8	Edmonds, Klueh,..	experimental CRE Lots
19B-V-11	308CRE	WELD	GTA	1200	14	1496.6		15.4	44.7	Edmonds, Klueh,..	experimental CRE Lots
19B-V-12	308CRE	WELD	GTA	1200	20	215.2		10	21.7	Edmonds, Klueh,..	experimental CRE Lots
19B-V-12	308CRE	WELD	GTA	1200	16	922		4.3	9.2	Edmonds, Klueh,..	experimental CRE Lots
19B-V-13	308CRE	WELD	GTA	1200	20	495.1		6.3	15.3	Edmonds, Klueh,..	experimental CRE Lots
19B-V-13	308CRE	WELD	GTA	1200	16	1634.5		5.5	8.4	Edmonds, Klueh,..	experimental CRE Lots
19B-V-15	308CRE	WELD	GTA	1200	25	100.3		28.8	94.6	Edmonds, Klueh,..	experimental CRE Lots

FILE #	Weld Metal	Specimen Type	Welding Process	Temp. (F)	Stress (ksi)	Rupture Life (hrs)	Min. Creep Rate (%/hr)	Elong. (%)	Red. Of Area (%)	Reference	Comments
19B-V-15	308CRE	WELD	GTA	1200	20	991		35.8	66.1	Edmonds, Klueh,..	experimental CRE Lots
19B-V-15	308CRE	WELD	GTA	1200	18	2083		37.1	63.4	Edmonds, Klueh,..	experimental CRE Lots
19B-V-16	308CRE	WELD	GTA	1200	20	432.4		12.1	21.1	Edmonds, Klueh,..	experimental CRE Lots
19B-V-16	308CRE	WELD	GTA	1200	16	1980		6.3	13	Edmonds, Klueh,..	experimental CRE Lots
19B-V-16	308CRE	WELD	GTA	1200	16	1980		6.3	13	Edmonds, Klueh,..	experimental CRE Lots
19B-V-130	308CRE	WELD	GTA	1200	30	59.1		42.5	64.5	Edmonds, Klueh,..	experimental CRE Lots
19B-V-130	308CRE	WELD	GTA	1200	28	74.2		46.6	70.5	Edmonds, Klueh,..	experimental CRE Lots
19B-V-130	308CRE	WELD	GTA	1200	25	422.4		29.4	60.9	Edmonds, Klueh,..	experimental CRE Lots
19B-V-130	308CRE	WELD	GTA	1200	22	1168.9		34.3	66.8	Edmonds, Klueh,..	experimental CRE Lots
19B-V-130	308CRE	WELD	GTA	1200	18	3001.9		11.41		Edmonds, Klueh,..	experimental CRE Lots
20B-1	308	WELD	SA	1200	25	35.5		62.2	55.2	King, 1975	welded pipe, 1/4 sps
20B-1	308	WELD	SA	1200	25	24.5		59.5	57.3	King, 1975	welded pipe, 1/4 sps
20B-1	308	WELD	SA	1200	20	831.4		30.8		King, 1975	welded pipe, 1/4 sps
20B-1	308	WELD	SA	1200	18	1798.3		17.9	14.8	King, 1975	welded pipe, 1/4 sps
20B-1	308	WELD	SA	1200	18	1568.5		16.7	14.8	King, 1975	welded pipe, 1/4 sps
20B-2	308	CROSS	SA	1200	25	126		14.8	21.1	King, 1975	welded pipe, 1/4 sps, weld metal failures
20B-2	308	CROSS	SA	1200	22	547.9		9.1	8.9	King, 1975	welded pipe, 1/4 sps, weld metal failures
20B-2	308	CROSS	SA	1200	20	1324.3		3.9	5	King, 1975	welded pipe, 1/4 sps, weld metal failures
20B-2	308	CROSS	SA	1200	18	2169.4		3.5		King, 1975	welded pipe, 1/4 sps, weld metal failures
20B-2	308	CROSS	SA	1200	18	2167.1		9.8		King, 1975	welded pipe, 1/4 sps, weld metal failures

FILE #	Weld Metal	Specimen Type	Welding Process	Temp. (F)	Stress (ksi)	Rupture Life (hrs)	Min. Creep Rate (%/hr)	Elong. (%)	Red. Of Area (%)	Reference	Comments
21B	308	WELD	SMA	1100	45	10	8.00E-01	28.9	57.3	Hauser & Van Echo, 1978	weld pad, low ferrite, 1/2 sps
21B	308	WELD	SMA	1100	40	81.6	7.50E-02	26.4	53.9	Hauser & Van Echo, 1978	weld pad, low ferrite, 1/2 sps
21B	308	WELD	SMA	1100	35	615	5.00E-03	23.3	41.2	Hauser & Van Echo, 1978	weld pad, low ferrite, 1/2 sps
21B	308	WELD	SMA	1100	33	1513.6	1.40E-03	12.8	35.7	Hauser & Van Echo, 1978	weld pad, low ferrite, 1/2 sps
21B	308	WELD	SMA	1100	30	5470.2	1.20E-04	4.2	5.1	Hauser & Van Echo, 1978	weld pad, low ferrite, 1/2 sps
21B	308	WELD	SMA	1100	28.5	10756	4.80E-05	4.7	6.8	Hauser & Van Echo, 1978	weld pad, low ferrite, 1/2 sps
21B	308	WELD	SMA	1000	54	9.8	2.00E-02	15.6	40.5	Hauser & Van Echo, 1978	weld pad, low ferrite, 1/2 sps
21B	308	WELD	SMA	1000	47	283	3.20E-02	19.2	33.7	Hauser & Van Echo, 1978	weld pad, low ferrite, 1/2 sps
21B	308	WELD	SMA	1000	42.5	1769	2.90E-03	12.8	30.7	Hauser & Van Echo, 1978	weld pad, low ferrite, 1/2 sps
21B	308	WELD	SMA	1200	31.5	34	1.10E-02	27.9	47.6	Hauser & Van Echo, 1978	weld pad, low ferrite, 1/2 sps
21B	308	WELD	SMA	1200	22	2748	9.00E-05	5.9	10.9	Hauser & Van Echo, 1978	weld pad, low ferrite, 1/2 sps
22B	308	WELD	SMA	1100	45	1.3	1.00E+01	28.1	60.3	Hauser & Van Echo, 1978	weld pad, medium ferrite, 1/2 sps
22B	308	WELD	SMA	1100	40	30.8	5.00E-01	29.3	49.9	Hauser & Van Echo, 1978	weld pad, medium ferrite, 1/2 sps
22B	308	WELD	SMA	1100	37	52.3	2.50E-01	41.2	60.3	Hauser & Van Echo, 1978	weld pad, medium ferrite, 1/2 sps
22B	308	WELD	SMA	1100	33	229.6	2.20E-02	33.6	56.7	Hauser & Van Echo, 1978	weld pad, medium ferrite, 1/2 sps
22B	308	WELD	SMA	1100	31	1220	2.50E-03	9.8	21.7	Hauser & Van Echo, 1978	weld pad, medium ferrite, 1/2 sps
22B	308	WELD	SMA	1100	29	2301.1	8.50E-04	13.6	24.1	Hauser & Van Echo, 1978	weld pad, medium ferrite, 1/2 sps
22B	308	WELD	SMA	1100	27	6126.6	1.10E-04	4.3	7.9	Hauser & Van Echo, 1978	weld pad, medium ferrite, 1/2 sps
22B	308	WELD	SMA	1100	25.5	7797.2	6.40E-05	4.1	4.3	Hauser & Van Echo, 1978	weld pad, medium ferrite, 1/2 sps
22B	308	WELD	SMA	1000	41	9.8	2.00E-02	15.6	40.5	Hauser & Van Echo, 1978	weld pad, medium ferrite, 1/2 sps
22B	308	WELD	SMA	1000	43	283.5	3.20E-02	19.2	33.7	Hauser & Van Echo, 1978	weld pad, medium ferrite, 1/2 sps
22B	308	WELD	SMA	1000	50	1769.2	2.90E-03	12.8	30.7	Hauser & Van Echo, 1978	weld pad, medium ferrite, 1/2 sps
22B	308	WELD	SMA	1200	27.5	122.8	2.70E-02	20	38.6	Hauser & Van Echo, 1978	weld pad, medium ferrite, 1/2 sps
22B	308	WELD	SMA	1200	20.5	2.03E+03	1.70E-04	5.1	12.7	Hauser & Van Echo, 1978	weld pad, medium ferrite, 1/2 sps

FILE #	Weld Metal	Specimen Type	Welding Process	Temp. (F)	Stress (ksi)	Rupture Life (hrs)	Min. Creep Rate (%/hr)	Elong. (%)	Red. Of Area (%)	Reference	Comments
23B	308	WELD	SMA	1100	45.0	7.6	2.00E+0	30.2	39.3	Hauser & Van Echo, 1978	weld pad, high ferrite, 1/2 sps
23B	308	WELD	SMA	1100	40.0	55.7	2.00E-1	26.8	37.2	Hauser & Van Echo, 1978	weld pad, high ferrite, 1/2 sps
23B	308	WELD	SMA	1100	35.0	207.5	3.00E-2	17.0	31.3	Hauser & Van Echo, 1978	weld pad, high ferrite, 1/2 sps
23B	308	WELD	SMA	1100	30.0	1413.5	1.70E-3	06.1	13.7	Hauser & Van Echo, 1978	weld pad, high ferrite, 1/2 sps
23B	308	WELD	SMA	1100	27.5	3375.6	4.20E-4	04.2	11.3	Hauser & Van Echo, 1978	weld pad, high ferrite, 1/2 sps
23B	308	WELD	SMA	1100	26.0	4889.7	2.00E-4	02.5	03.3	Hauser & Van Echo, 1978	weld pad, high ferrite, 1/2 sps
23B	308	WELD	SMA	1100	24.0	7562.6	7.00E-5	03.4	03.7	Hauser & Van Echo, 1978	weld pad, high ferrite, 1/2 sps
23B	308	WELD	SMA	1000	53.0	35.8	2.00E-1	14.9	37.2	Hauser & Van Echo, 1978	weld pad, high ferrite, 1/2 sps
23B	308	WELD	SMA	1000	47.0	430.2	2.10E-2	19.0	29.3	Hauser & Van Echo, 1978	weld pad, high ferrite, 1/2 sps
23B	308	WELD	SMA	1000	43.5	871.2	7.70E-3	14.0	25.4	Hauser & Van Echo, 1978	weld pad, high ferrite, 1/2 sps
23B	308	WELD	SMA	1200	26.5	153.8	3.30E-2	14.1	27.9	Hauser & Van Echo, 1978	weld pad, high ferrite, 1/2 sps
23B	308	WELD	SMA	1200	17.5	2267.6	2.20E-4	03.4	6.0	Hauser & Van Echo, 1978	weld pad, high ferrite, 1/2 sps
24B	308	WELD	SMA	1100	45	10.7	1.20E+00	28.5	57.2	Hauser & Van Echo, 1978	weld pad, low ferrite, 1/2 sps
24B	308	WELD	SMA	1100	40	61	7.00E-02	10.6	20.4	Hauser & Van Echo, 1978	weld pad, low ferrite, 1/2 sps
24B	308	WELD	SMA	1100	35	626.1	3.20E-03	10.2	27.5	Hauser & Van Echo, 1978	weld pad, low ferrite, 1/2 sps
24B	308	WELD	SMA	1100	33	1148.5	1.00E-03	5.1	24	Hauser & Van Echo, 1978	weld pad, low ferrite, 1/2 sps
24B	308	WELD	SMA	1100	30.5	4961	9.50E-05	3.4	7.4	Hauser & Van Echo, 1978	weld pad, low ferrite, 1/2 sps
24B	308	WELD	SMA	1100	29	3333.2	8.50E-05	3	7.2	Hauser & Van Echo, 1978	weld pad, low ferrite, 1/2 sps
24B	308	WELD	SMA	1000	52	142.6	2.00E-02	15.6	40.5	Hauser & Van Echo, 1978	weld pad, low ferrite, 1/2 sps
24B	308	WELD	SMA	1000	47	400.8	1.20E-02	12.4	20.7	Hauser & Van Echo, 1978	weld pad, low ferrite, 1/2 sps
24B	308	WELD	SMA	1000	42.5	2093.3	9.00E-04	7.7	22.5	Hauser & Van Echo, 1978	weld pad, low ferrite, 1/2 sps
24B	308	WELD	SMA	1200	30	119	2.60E-02	26	27.4	Hauser & Van Echo, 1978	weld pad, low ferrite, 1/2 sps
24B	308	WELD	SMA	1200	23.5	1127.4	2.60E-04	4.1	13.4	Hauser & Van Echo, 1978	weld pad, low ferrite, 1/2 sps

FILE #	Weld Metal	Specimen Type	Welding Process	Temp. (F)	Stress (ksi)	Rupture Life (hrs)	Min. Creep Rate (%/hr)	Elong. (%)	Red. Of Area (%)	Reference	Comments
25B-1	308	CROSS	SMA	1050	35	132		24	45.1	Leyda, 1978	
25B-1	308	CROSS	SMA	1050	32	265		24.9	43.1	Leyda, 1978	
25B-1	308	CROSS	SMA	1050	28	797.7		16.7	40.3	Leyda, 1978	
25B-1	308	CROSS	SMA	1100	25	465		14	26.6	Leyda, 1978	
25B-1	308	CROSS	SMA	1100	22	910		11.3	26.1	Leyda, 1978	
25B-1	308	CROSS	SMA	1200	18	245		10	20.6	Leyda, 1978	
25B-1	308	CROSS	SMA	1200	15	960		5.7	8.5	Leyda, 1978	
25B-2	308	CROSS	SMA	1050	32.4	240.5		6.5	15.3	Leyda, 1978	
25B-2	308	CROSS	SMA	1050	32	260		6.3	19.1	Leyda, 1978	
25B-2	308	CROSS	SMA	1050	28	648.8		5	18.1	Leyda, 1978	
25B-2	308	CROSS	SMA	1050	20	9914		2.2	4.3	Leyda, 1978	
25B-2	308	CROSS	SMA	1100	25	361		4.3	17.3	Leyda, 1978	
25B-2	308	CROSS	SMA	1100	22	995		2.4	14.5	Leyda, 1978	
25B-2	308	CROSS	SMA	1100	18	5273		2.4	6.7	Leyda, 1978	
25B-2	308	CROSS	SMA	1200	20	143		3.7	14.3	Leyda, 1978	
25B-2	308	CROSS	SMA	1200	20	160		4.6	14.8	Leyda, 1978	
25B-2	308	CROSS	SMA	1200	17	378.8		2.5	10.1	Leyda, 1978	
25B-2	308	CROSS	SMA	1200	14	1162		1.8	7.8	Leyda, 1978	
25B-2	308	CROSS	SMA	1200	11	4529		4	2.4	Leyda, 1978	
26B-1	308	CROSS	GTA	1300	15	121.2			42	Canonico & Swindeman, 1966	butt weld in plate, 1/4 sps
26B-1	308	CROSS	GTA	1400	9	390.7			33.4	Canonico & Swindeman, 1966	butt weld in plate, 1/4 sps
26B-1	308	CROSS	GTA	1500	6	305			22.4	Canonico & Swindeman, 1966	butt weld in plate, 1/4 sps
26B-1	308	CROSS	GTA	1500	6	182.8			24.2	Canonico & Swindeman, 1966	butt weld in plate, 1/4 sps
26B-1-ann	308	CROSS	GTA	1300	15	100.9				Canonico & Swindeman, 1966	butt weld in plate, 1/4 sps, 1850F ann
26B-1-ann	308	CROSS	GTA	1300	12.5	422.9			37.6	Canonico & Swindeman, 1966	butt weld in plate, 1/4 sps, 1850F ann
26B-1-ann	308	CROSS	GTA	1500	9	19.4			30.5	Canonico & Swindeman, 1966	butt weld in plate, 1/4 sps, 1850F ann

FILE #	Weld Metal	Specimen Type	Welding Process	Temp. (F)	Stress (ksi)	Rupture Life (hrs)	Min. Creep Rate (%/hr)	Elong. (%)	Red. Of Area (%)	Reference	Comments
27B	308	CROSS	GTA	1100	32	598.8			39.2	Swindeman, not published	butt weld in tube, 3/16 sps, weld metal failures
27B	308	CROSS	GTA	1200	25	292.2			41	Swindeman, not published	butt weld in tube, 3/16 sps, weld metal failures
27B	308	CROSS	GTA	1300	20	69.7			44.9	Swindeman, not published	butt weld in tube, 3/16 sps, weld metal failures
27B	308	CROSS	GTA	1400	12.5	94			37	Swindeman, not published	butt weld in tube, 3/16 sps, weld metal failures
27B	308	CROSS	GTA	1500	10	34.5			36.4	Swindeman, not published	butt weld in tube, 3/16 sps, weld metal failures
27B	308	CROSS	GTA	1500	6	924.7			13.5	Swindeman, not published	butt weld in tube, 3/16 sps, weld metal failures
27B	308	CROSS	GTA	1600	6	226.5			22.4	Swindeman, not published	butt weld in tube, 3/16 sps, weld metal failures
27B	308	CROSS	GTA	1600	4.3	598.8			20	Swindeman, not published	butt weld in tube, 3/16 sps, weld metal failures
27B	308	CROSS	GTA	1700	2.5	655.3			35.2	Swindeman, not published	butt weld in tube, 3/16 sps, weld metal failures
27B	308	CROSS	GTA	1800	2.5	53.8			36.4	Swindeman, not published	butt weld in tube, 3/16 sps, base metal failure
28B	308CRE	CROSS	GTA	1300	15	7855	4.50E-04	19.4	25.9	Bolling & Swindeman, not pub	butt weld in plate, 1/4 sps base metal failure
28B	308CRE	CROSS	GTA	1350	15	1723	1.35E-03	21.6	54.8	Bolling & Swindeman, not pub	butt weld in plate, 1/4 sps base metal failure
28B	308CRE	CROSS	GTA	1400	15	332.8	1.20E-02	18.4	40	Bolling & Swindeman, not pub	butt weld in plate, 1/4 sps base metal failure
29B-2	Base			1100	30	471				Swindeman & Williams, not pub	butt weld in plate, 1/4 sps
29B-2	Base			1100	25	3600				Swindeman & Williams, not pub	butt weld in plate, 1/4 sps
29B-2	Base			1100	20	3052D				Swindeman & Williams, not pub	butt weld in plate, 1/4 sps
29B-2	Base			1100	15	5238D				Swindeman & Williams, not pub	butt weld in plate, 1/4 sps
29B-1	308	CROSS	SMA	1100	30	2375				Swindeman & Williams, not pub	butt weld in plate, 1/4 sps
29B-1	308	CROSS	SMA	1100	25	3027D				Swindeman & Williams, not pub	butt weld in plate, 1/4 sps
29B-1	308	CROSS	SMA	1100	20	3601D				Swindeman & Williams, not pub	butt weld in plate, 1/4 sps
29B-1	308	CROSS	SMA	1100	15	2739D				Swindeman & Williams, not pub	butt weld in plate, 1/4 sps
29B-3	HAZ		HAZ2	1100	30	1423				Swindeman & Williams, not pub	butt weld in plate, 1/4 sps
29B-3	HAZ		HAZ5	1100	25					Swindeman & Williams, not pub	butt weld in plate, 1/4 sps
29B-3	HAZ		HAZ3	1100	20	5122D				Swindeman & Williams, not pub	butt weld in plate, 1/4 sps
29B-3	HAZ		HAZ6	1100	15	5187D				Swindeman & Williams, not pub	butt weld in plate, 1/4 sps

FILE #	Weld Metal	Specimen Type	Welding Process	Temp. (F)	Stress (ksi)	Rupture Life (hrs)	Min. Creep Rate (%/hr)	Elong. (%)	Red. Of Area (%)	Reference	Comments
34B-1	308	CROSS	GMA	1200	35	23.8		7	13	Davis & Cullen, 1968	butt weld 347 tube 2050 ann. 0.053%N
34B-1	308	CROSS	GMA	1200	35	18.3		10	15	Davis & Cullen, 1968	butt weld 347 tube 2050 ann. 0.053%N
34B-1	308	CROSS	GMA	1200	27.5	105.2		7	9	Davis & Cullen, 1968	butt weld 347 tube 2050 ann. 0.053%N
34B-1	308	CROSS	GMA	1350	20	11.9		7	17	Davis & Cullen, 1968	butt weld 347 tube 2050 ann. 0.053%N
34B-1	308	CROSS	GMA	1350	9	1197		4	3	Davis & Cullen, 1968	butt weld 347 tube 2050 ann. 0.053%N
34B-1	308	CROSS	GMA	1400	12	25.2		9	9	Davis & Cullen, 1968	butt weld 347 tube 2050 ann. 0.053%N
34B-1	308	CROSS	GMA	1400	6	1977		2	2	Davis & Cullen, 1968	butt weld 347 tube 2050 ann. 0.053%N
34B-2	308	CROSS	GMA	1200	35	20.5		8	19	Davis & Cullen, 1968	butt weld 347 tube 2150F ann. 0.053%N
34B-2	308	CROSS	GMA	1200	35	15.8		13	20	Davis & Cullen, 1968	butt weld 347 tube 2150F ann. 0.053%N
34B-2	308	CROSS	GMA	1200	27.5	95		10	9	Davis & Cullen, 1968	butt weld 347 tube 2150F ann. 0.053%N
34B-2	308	CROSS	GMA	1350	20	16.3		8	11	Davis & Cullen, 1968	butt weld 347 tube 2150F ann. 0.053%N
34B-2	308	CROSS	GMA	1400	12	61.6		5	16	Davis & Cullen, 1968	butt weld 347 tube 2150F ann. 0.053%N
34B-2	308	CROSS	GMA	1400	9	363.3		4	5	Davis & Cullen, 1968	butt weld 347 tube 2150F ann. 0.053%N
34B-2	308	CROSS	GMA	1450	4.8	839		2	2	Davis & Cullen, 1968	butt weld 347 tube 2150F ann. 0.053%N
34B-3	308	CROSS	GMA	1200	35	47.5		10	17	Davis & Cullen, 1968	butt weld 347 tube 2175F ann. 0.14%N
34B-3	308	CROSS	GMA	1200	27.5	199.1		9	14	Davis & Cullen, 1968	butt weld 347 tube 2175F ann. 0.14%N
34B-3	308	CROSS	GMA	1200	25	223		9	13	Davis & Cullen, 1968	butt weld 347 tube 2175F ann. 0.14%N
34B-3	308	CROSS	GMA	1250	25	95.2		10	13	Davis & Cullen, 1968	butt weld 347 tube 2175F ann. 0.14%N
34B-3	308	CROSS	GMA	1350	20	16.4		3	6	Davis & Cullen, 1968	butt weld 347 tube 2175F ann. 0.14%N
34B-3	308	CROSS	GMA	1350	16	53.7		4	3	Davis & Cullen, 1968	butt weld 347 tube 2175F ann. 0.14%N
34B-3	308	CROSS	GMA	1400	12	61.6		5	16	Davis & Cullen, 1968	butt weld 347 tube 2175F ann. 0.14%N
34B-3	308	CROSS	GMA	1400	9	169.2		4	9	Davis & Cullen, 1968	butt weld 347 tube 2175F ann. 0.14%N
34B-3	308	CROSS	GMA	1400	7	1250.5		3		Davis & Cullen, 1968	butt weld 347 tube 2175F ann. 0.14%N
34B-3	308	CROSS	GMA	1450	6	287.3				Davis & Cullen, 1968	butt weld 347 tube 2175F ann. 0.14%N

FILE #	Weld Metal	Specimen Type	Welding Process	Temp. (F)	Stress (ksi)	Rupture Life (hrs)	Min. Creep Rate (%/hr)	Elong. (%)	Red. Of Area (%)	Reference	Comments
34B-4	308	CROSS	GMA	1200	35	17.2		7	15	Davis & Cullin, 1968	butt weld 347 tube 2175F ann. 0.029%N
34B-4	308	CROSS	GMA	1200	30	75		13	18	Davis & Cullin, 1968	butt weld 347 tube 2175F ann. 0.029%N
34B-4	308	CROSS	GMA	1200	25	223.4		9	13	Davis & Cullin, 1968	butt weld 347 tube 2175F ann. 0.029%N
34B-4	308	CROSS	GMA	1250	20	154.3		10	10	Davis & Cullin, 1968	butt weld 347 tube 2175F ann. 0.029%N
34B-4	308	CROSS	GMA	1350	20	20.6		7	6	Davis & Cullin, 1968	butt weld 347 tube 2175F ann. 0.029%N
34B-4	308	CROSS	GMA	1350	15	111.2		5	4	Davis & Cullin, 1968	butt weld 347 tube 2175F ann. 0.029%N
34B-4	308	CROSS	GMA	1350	13	187		4	2	Davis & Cullin, 1968	butt weld 347 tube 2175F ann. 0.029%N
34B-4	308	CROSS	GMA	1400	13.5	111.3		7	1	Davis & Cullin, 1968	butt weld 347 tube 2175F ann. 0.029%N
34B-4	308	CROSS	GMA	1400	10	174.1		5	2	Davis & Cullin, 1968	butt weld 347 tube 2175F ann. 0.029%N
34B-4	308	CROSS	GMA	1500	10	30.4				Davis & Cullin, 1968	butt weld 347 tube 2175F ann. 0.029%N
34B-4	308	CROSS	GMA	1500	7	119		2	1	Davis & Cullin, 1968	butt weld 347 tube 2175F ann. 0.029%N
34B-4	308	CROSS	GMA	1500	5	209		3	1	Davis & Cullin, 1968	butt weld 347 tube 2175F ann. 0.029%N
35B-1	308	WELD	GTA	1200	25	26.6	2.60E-01	18.8	29.3	Edmonds & Biling, 1975	weld V-5, 1/8 sps
35B-1	308	WELD	GTA	1200	25	24	3.40E-01	20.6	24.4	Edmonds & Biling, 1975	weld V-5, 1/8 sps
35B-1	308	WELD	GTA	1200	20	115.4	4.30E-02	11.6	14.7	Edmonds & Biling, 1975	weld V-5, 1/8 sps
35B-1	308	WELD	GTA	1200	20	143.5	3.00E-02	7.9	20.7	Edmonds & Biling, 1975	weld V-5, 1/8 sps
35B-1	308	WELD	GTA	1200	14	927	1.50E-03	2.7	6.1	Edmonds & Biling, 1975	weld V-5, 1/8 sps
35B-2	308	WELD	GTA	1200	20	164.7	2.40E-02	8.8	14.6	Edmonds & Biling, 1975	weld V-14, 1/8 sps
35B-2	308	WELD	GTA	1200	16	733	2.30E-03	3.6	10	Edmonds & Biling, 1975	weld V-14, 1/8 sps
35B-2	308	WELD	GTA	1200	14	1630	3.70E-04	3.6	4.8	Edmonds & Biling, 1975	weld V-14, 1/8 sps

FILE #	Weld Metal	Specimen Type	Welding Process	Temp. (F)	Stress (ksi)	Rupture Life (hrs)	Min. Creep Rate (%/hr)	Elong. (%)	Red. Of Area (%)	Reference	Comments
36B-1	308CRE	WELD	GTA	1200	18	3116	1.00E-04	32.1	55.9	Edmonds, et al., 1983	lot 9190, 1/8 sps
36B-1	308CRE	WELD	GTA	1200	23	441	3.10E-02	34.6	62.6	Edmonds, et al., 1983	lot 9190, 1/8 sps
36B-1	308CRE	WELD	GTA	1200	28	89	6.60E-02	37.5	64.1	Edmonds, et al., 1983	lot 9190, 1/8 sps
36B-2	308CRE	WELD	GTA	1200	18	2916	2.20E-04	2.9	4.6	Edmonds, et al., 1983	lot 9210
36B-2	308CRE	WELD	GTA	1200	23	746	6.50E-03	3.9	2.4	Edmonds, et al., 1983	lot 9210
36B-2	308CRE	WELD	GTA	1200	28	199	8.50E-03	4.4	9.2	Edmonds, et al., 1983	lot 9210
36B-3	308CRE	WELD	GTA	1200	18	5625	1.00E-05	29.7	69.1	Edmonds, et al., 1983	lot 9219
36B-3	308CRE	WELD	GTA	1200	23	1216	5.80E-03	28.5	71.5	Edmonds, et al., 1983	lot 9219
36B-3	308CRE	WELD	GTA	1200	28	301	3.20E-02	31.8	69.7	Edmonds, et al., 1983	lot 9219
36B-4	308CRE	WELD	GTA	1200	18	5505	2.00E-06	4	3.9	Edmonds, et al., 1983	lot 9220
36B-4	308CRE	WELD	GTA	1200	23	334	6.10E-03	9.9	19.8	Edmonds, et al., 1983	lot 9220
36B-4	308CRE	WELD	GTA	1200	28	32	2.00E-02	25.3	49.3	Edmonds, et al., 1983	lot 9220
36B-5	308CRE	WELD	GTA	1200	18	4505	1.20E-03	33.1	58.2	Edmonds, et al., 1983	lot 9221
36B-5	308CRE	WELD	GTA	1200	23	1176	3.40E-03	13.3	21.5	Edmonds, et al., 1983	lot 9221
36B-5	308CRE	WELD	GTA	1200	35	8	1.28E+00	29.4	52.3	Edmonds, et al., 1983	lot 9221
36B-5	308CRE	WELD	GTA	1200	27.5	147	6.90E-01	22.1	34.3	Edmonds, et al., 1983	lot 9221
37B-1	308CRE	WELD	GTA	1200	30	96	1.80E-01	34.4	63.3	Edmonds, Klueh, 1983	lot 35050
37B-1	308CRE	WELD	GTA	1200	25	714	1.60E-02	41.3	34.2	Edmonds, Klueh, 1983	lot 35050
37B-1	308CRE	WELD	GTA	1200	20	4127	1.30E-03	36.2	72.4	Edmonds, Klueh, 1983	lot 35050
37B-1	308CRE	WELD	GTA	1200	20	4127	1.30E-03	36.2	72.4	Edmonds, Klueh, 1983	lot 35050
37B-2	308CRE	WELD	GTA	1200	18	11590	1.10E-04	13.7	47.8	Edmonds, Klueh, 1983	lot A2283
37B-2	308CRE	WELD	GTA	1200	20	3033	8.30E-04	7.1	12.3	Edmonds, Klueh, 1983	lot A2283
37B-2	308CRE	WELD	GTA	1200	25	524	1.20E-02	11.5	17.4	Edmonds, Klueh, 1983	lot A2283
37B-2	308CRE	WELD	GTA	1200	30	131	7.00E-02	20.5	22.8	Edmonds, Klueh, 1983	lot A2283
37B-3	308CRE	WELD	GTA	1200	15	5814		21.6	50.5	Edmonds, Klueh, 1983	lot 2548
37B-3	308CRE	WELD	GTA	1200	30	308	1.40E-02	16.5	42.9	Edmonds, Klueh, 1983	lot 2548
37B-3	308CRE	WELD	GTA	1200	25	1316	2.50E-03	13.6	41	Edmonds, Klueh, 1983	lot 2548
37B-4	308CRE	WELD	GTA	1200	17	16885	6.00E-05	25	46	Edmonds, Klueh, 1983	lot 11386
37B-4	308CRE	WELD	GTA	1200	22	5814	4.00E-04	21.6	50.5	Edmonds, Klueh, 1983	lot 11386
37B-4	308CRE	WELD	GTA	1200	30	308	1.40E-02	16.5	42.9	Edmonds, Klueh, 1983	lot 11386
37B-5	308CRE	WELD	GTA	1200	20	1408	9.80E-03	44.7	69.1	Edmonds, Klueh, 1983	lot 35046
37B-5	308CRE	WELD	GTA	1200	17	5784	7.00E-04	20.1	43.8	Edmonds, Klueh, 1983	lot 35046
37B-5	308CRE	WELD	GTA	1200	30	15	1.60E+00	55.7	66.9	Edmonds, Klueh, 1983	lot 35046

FILE #	Weld Metal	Specimen Type	Welding Process	Temp. (F)	Stress (ksi)	Rupture Life (hrs)	Min. Creep Rate (%/hr)	Elong. (%)	Red. Of Area (%)	Reference	Comments
			Edmonds, et al, 1983								
			1/8-in. diam. specimens, longitudinal								
			308CRE submerged arc welds large commercial heats								
38B-1	308CRE	WELD	35050	1200	15	7792	8.00E-05	5.2	8.6	Edmonds, Klueh, 1983	lot 25050
38B-1	308CRE	WELD	25050	1200	20	523	4.10E-03	12.7	36.6	Edmonds, Klueh, 1983	lot 25050
38B-1	308CRE	WELD	35050	1200	25	70	1.40E-01	18.6	40.1	Edmonds, Klueh, 1983	lot 25050
39B-1	308CRE	WELD	SA	1200	22.5	65	1.00E-01	24.7	72.8	Edmonds, Klueh, 1983	lot A2284
39B-1	308CRE	WELD	SA	1200	17.5	8247	1.70E-04	7.5	20.6	Edmonds, Klueh, 1983	lot A2284
39B-1	308CRE	WELD	SA	1200	12.5	23303	8.00E-05	5	11	Edmonds, Klueh, 1983	lot A2284
39B-2	308CRE	WELD	SA	1200	15	2210	1.00E-04	28.3	59.4	Edmonds, Klueh, 1983	lot 2548
39B-2	308CRE	WELD	SA	1200	17.5	924	9.30E-03	30.8	48.7	Edmonds, Klueh, 1983	lot 2548
39B-2	308CRE	WELD	SA	1200	22.5	107	1.20E-01	26.6	51.8	Edmonds, Klueh, 1983	lot 2548
39B-3	308CRE	WELD	SA	1200	15	926	1.20E-02	43.5	70.8	Edmonds, Klueh, 1983	lot 11372
39B-3	308CRE	WELD	SA	1200	17.5	247	9.00E-02	32.4		Edmonds, Klueh, 1983	lot 11372
39B-3	308CRE	WELD	SA	1200	22.5	49	1.96E+00	17.2	57.6	Edmonds, Klueh, 1983	lot 11372
39B-4	308CRE	WELD	SA	1200	15	2586	3.40E-04	5.3	14	Edmonds, Klueh, 1983	lot 35046
39B-4	308CRE	WELD	SA	1200	20	352	1.20E-02	18.4	28.5	Edmonds, Klueh, 1983	lot 35046
39B-4	308CRE	WELD	SA	1200	25	22	5.90E-01	26.8	45.5	Edmonds, Klueh, 1983	lot 35046

FILE #	Weld Metal	Specimen Type	Welding Process	Temp. (F)	Stress (ksi)	Rupture Life (hrs)	Min. Creep Rate (%/hr)	Elong. (%)	Red. Of Area (%)	Reference	Comments
			308 weld metal; tangential orientation, 1/4-in. diam. specimens								
40B-1	308	WELD	SA	1100	45	3	6.06E+00	35.9	44.8	Klueh & Canonico, 1974, 1976	overlay cladding, 1/4 sps, tangential
40B-1	308	WELD	SA	1100	40	58.9	1.90E-01	24.6	26	Klueh & Canonico, 1974, 1976	overlay cladding, 1/4 sps, tangential
40B-1	308	WELD	SA	1100	35	151.4	5.30E-02	21.4	23.4	Klueh & Canonico, 1974, 1976	overlay cladding, 1/4 sps, tangential
40B-1	308	WELD	SA	1100	32.5	379.6	1.60E-02	16.2	23.2	Klueh & Canonico, 1974, 1976	overlay cladding, 1/4 sps, tangential
40B-1	308	WELD	SA	1100	30	1030.9	3.00E-03	9.9	8.2	Klueh & Canonico, 1974, 1976	overlay cladding, 1/4 sps, tangential
40B-1	308	WELD	SA	1000	55	4.3	3.27E-01	32.8	59.6	Klueh & Canonico, 1974, 1976	overlay cladding, 1/4 sps, tangential
40B-1	308	WELD	SA	1000	50	100.7	7.50E-02	34.6	34.7	Klueh & Canonico, 1974, 1976	overlay cladding, 1/4 sps, tangential
40B-1	308	WELD	SA	1000	45	303	3.32E-02	21.8	30.6	Klueh & Canonico, 1974, 1976	overlay cladding, 1/4 sps, tangential
40B-1	308	WELD	SA	1000	40	1377	4.87E-03	17.2	26	Klueh & Canonico, 1974, 1976	overlay cladding, 1/4 sps, tangential
40B-1	308	WELD	SA	1000	37.5		9.60E-04			Klueh & Canonico, 1974, 1976	overlay cladding, 1/4 sps, tangential
40B-1	308	WELD	SA	900	62.5	339	2.50E-03	27.3	25.9	Klueh & Canonico, 1974, 1976	overlay cladding, 1/4 sps, tangential
40B-1	308	WELD	SA	1100	45	2.4	5.24E+00	24.7	42.6	Klueh & Canonico, 1974, 1976	overlay cladding, 1/4 sps, radial
40B-1	308	WELD	SA	1100	40	14.1	8.20E-01	22.2	44.6	Klueh & Canonico, 1974, 1976	overlay cladding, 1/4 sps, radial
40B-1	308	WELD	SA	1100	35	95.6	5.20E-02	15.8	24.1	Klueh & Canonico, 1974, 1976	overlay cladding, 1/4 sps, radial
40B-1	308	WELD	SA	1100	30	546.6	4.00E-03	9.9	15.4	Klueh & Canonico, 1974, 1976	overlay cladding, 1/4 sps, radial
40B-1	308	WELD	SA	1100	27.5	1294.1	1.40E-03	5	7.4	Klueh & Canonico, 1974, 1976	overlay cladding, 1/4 sps, radial
40B-1	308	WELD	SA	1100	25	3703.4	1.65E-04	4	3.8	Klueh & Canonico, 1974, 1976	overlay cladding, 1/4 sps, radial
40B-1	308	WELD	SA	1000	55	8.5	2.03E-01	24	35.8	Klueh & Canonico, 1974, 1976	overlay cladding, 1/4 sps, radial
40B-1	308	WELD	SA	1000	50	48.5	8.00E-02	24.8	39.2	Klueh & Canonico, 1974, 1976	overlay cladding, 1/4 sps, radial
40B-1	308	WELD	SA	1000	45	263	4.40E-02	26.2	34.7	Klueh & Canonico, 1974, 1976	overlay cladding, 1/4 sps, radial
40B-1	308	WELD	SA	1000	40	1176	4.90E-03	15.3	25.1	Klueh & Canonico, 1974, 1976	overlay cladding, 1/4 sps, radial
40B-1	308	WELD	SA	1000	37.5	1568	2.67E-03	10.5	21.7	Klueh & Canonico, 1974, 1976	overlay cladding, 1/4 sps, radial
40B-1	308	WELD	SA	1000	37.5	2101	2.41E-03	16.2	25.2	Klueh & Canonico, 1974, 1976	overlay cladding, 1/4 sps, radial
40B-1	308	WELD	SA	900	62.5	499.1	2.10E-03	23.1	27.5	Klueh & Canonico, 1974, 1976	overlay cladding, 1/4 sps, radial
40B-1	308	WELD	SA	900	61	744.3	1.60E-03	21	25.9	Klueh & Canonico, 1974, 1976	overlay cladding, 1/4 sps, radial
40B-1	308	WELD	SA	900	60	1257	1.00E-03	19.3	18.7	Klueh & Canonico, 1974, 1976	overlay cladding, 1/4 sps, radial

FILE #	Weld Metal	Specimen Type	Welding Process	Temp. (F)	Stress (ksi)	Rupture Life (hrs)	Min. Creep Rate (%/hr)	Elong. (%)	Red. Of Area (%)	Reference	Comments
40B-2	308	CROSS	SA	1100	40	66.3	5.33E-02	12.4	37.3	Klueh & Canonico, 1974, 1976	overlay cladding, 1/4 sps, failure @ fusion line into weld
40B-2	308	CROSS	SA	1100	35	333.1	8.50E-03	16.1	44.6	Klueh & Canonico, 1974, 1976	overlay cladding, 1/4 sps, failure @ fusion line into weld
40B-2	308	CROSS	SA	1100	32.5	456.7	6.00E-03	11.9	36.7	Klueh & Canonico, 1974, 1976	overlay cladding, 1/4 sps, failure @ fusion line into weld
40B-2	308	CROSS	SA	1100	32	571.1	1.10E-03	16.5	44.8	Klueh & Canonico, 1974, 1976	overlay cladding, 1/4 sps, failure @ fusion line into weld
40B-2	308	CROSS	SA	1100	30	5551	4.30E-04	7.6	5.4	Klueh & Canonico, 1974, 1976	overlay cladding, 1/4 sps, failure @ fusion line into weld
40B-2	308	CROSS	SA	1100	30	3257	1.80E-04	4.3	21.3	Klueh & Canonico, 1974, 1976	overlay cladding, 1/4 sps, failure @ fusion line into weld
40B-2	308	CROSS	SA	1000	55	36.4	2.08E-01	38.5	60.7	Klueh & Canonico, 1974, 1976	overlay cladding, 1/4 sps, failure @ fusion line into weld
40B-2	308	CROSS	SA	1000	50	114.8	2.75E-02	17.3	17.1	Klueh & Canonico, 1974, 1976	overlay cladding, 1/4 sps, failure @ fusion line into weld
40B-2	308	CROSS	SA	1000	47.5	219	2.00E-02	21.8	54.9	Klueh & Canonico, 1974, 1976	overlay cladding, 1/4 sps, failure @ fusion line into weld
40B-2	308	CROSS	SA	1000	45	617.7	4.10E-03	12.4	10.8	Klueh & Canonico, 1974, 1976	overlay cladding, 1/4 sps, failure @ fusion line into weld
40B-2	308	CROSS	SA	1000	42.5	2210	1.00E-03	10.2	26.5	Klueh & Canonico, 1974, 1976	overlay cladding, 1/4 sps, failure @ fusion line into weld
40B-2	308	CROSS	SA	900	62.5	0.1		30.2	51.2	Klueh & Canonico, 1974, 1976	overlay cladding, 1/4 sps, failure @ fusion line into weld
40B-2	308	CROSS	SA	900	61	891.8	1.00E-03	29.3	38.9	Klueh & Canonico, 1974, 1976	overlay cladding, 1/4 sps, failure @ fusion line into weld
40B-2	308	CROSS	SA	900	60	976.4	8.60E-04	24.6	28.4	Klueh & Canonico, 1974, 1976	overlay cladding, 1/4 sps, failure @ fusion line into weld

FILE #	Weld Metal	Specimen Type	Welding Process	Temp. (F)	Stress (ksi)	Rupture Life (hrs)	Min. Creep Rate (%/hr)	Elong. (%)	Red. Of Area (%)	Reference	Comments
40B-3	BASE			1100	50	47.6	1.62E-01	21.6	21.8	Klueh & Canonico, 1974, 1976	near fusion, tangential
40B-3	BASE			1100	48	121.8	3.90E-02	16.1	16.3	Klueh & Canonico, 1974, 1976	near fusion, tangential
40B-3	BASE			1100	45	186.8	1.90E-02	11.8	13	Klueh & Canonico, 1974, 1976	near fusion, tangential
40B-3	BASE			1100	42.5	654.5	5.70E-03	14.4	17.6	Klueh & Canonico, 1974, 1976	near fusion, tangential
40B-3	BASE			1100	40	1298	2.60E-03	17	23.3	Klueh & Canonico, 1974, 1976	near fusion, tangential
40B-3	BASE			1100	40	1126	3.00E-03	16.9	20.5	Klueh & Canonico, 1974, 1976	near fusion, tangential
40B-3	BASE			1100	37.5	2882	1.40E-03	17.8	23.7	Klueh & Canonico, 1974, 1976	near fusion, tangential
40B-3	BASE			1000	60	82.7	3.30E-02	29.1	27.7	Klueh & Canonico, 1974, 1976	near fusion, tangential
40B-3	BASE			1000	57.5	192.6	8.40E-03	16.2	15.9	Klueh & Canonico, 1974, 1976	near fusion, tangential
40B-3	BASE			1000	55	457.5	4.60E-03	13.8	13.2	Klueh & Canonico, 1974, 1976	near fusion, tangential
40B-3	BASE			1000	53	738.8	6.00E-03	12.9	11.4	Klueh & Canonico, 1974, 1976	near fusion, tangential
40B-3	BASE			1000	50	1136	1.40E-03	10.1	8.9	Klueh & Canonico, 1974, 1976	near fusion, tangential
40B-3	BASE			1000	48	1563.9	6.90E-04	10.6	17.1	Klueh & Canonico, 1974, 1976	near fusion, tangential
40B-3	BASE			900	64	1096	2.90E-04	33.1	32.7	Klueh & Canonico, 1974, 1976	near fusion, tangential
40B-3	BASE			1100	45	174	1.10E-02	8.7	15	Klueh & Canonico, 1974, 1976	near fusion, radial
40B-3	BASE			1100	42.5	727.5	5.30E-03	16.9	24.7	Klueh & Canonico, 1974, 1976	near fusion, radial
40B-3	BASE			1100	42.5	723.2	3.50E-03	11	23.3	Klueh & Canonico, 1974, 1976	near fusion, radial
40B-3	BASE			1100	40	1140	2.00E-03	9.4	15.5	Klueh & Canonico, 1974, 1976	near fusion, radial
40B-3	BASE			1100	35	5331D	2.80E-04			Klueh & Canonico, 1974, 1976	near fusion, radial
40B-3	BASE			1000	60	77.5	2.79E-02	27	23.9	Klueh & Canonico, 1974, 1976	near fusion, radial
40B-3	BASE			1000	55	383.4	4.60E-03	15.4	14.6	Klueh & Canonico, 1974, 1976	near fusion, radial
40B-3	BASE			1000	53	621.5	2.60E-03	14.1	13.7	Klueh & Canonico, 1974, 1976	near fusion, radial
40B-3	BASE			1000	50	1501.7	1.10E-03	10.2	12.3	Klueh & Canonico, 1974, 1976	near fusion, radial
40B-3	BASE			900	64	574	5.60E-04	24.8	23.9	Klueh & Canonico, 1974, 1976	near fusion, radial
40B-3	BASE			900	62	1342	3.40E-04	20.6	20.6	Klueh & Canonico, 1974, 1976	near fusion, radial
40B-4	Base			1100	45	78.1	4.70E-02	19.4	16.6	Klueh & Canonico, 1974, 1976	tangential
40B-4	Base			1100	40	427	6.10E-03	15.2	15.7	Klueh & Canonico, 1974, 1976	tangential
40B-4	Base			1100	37.5	1208	3.00E-03	17.4	19.9	Klueh & Canonico, 1974, 1976	tangential
40B-4	Base			1100	35	2246	1.50E-03	26.9	31.2	Klueh & Canonico, 1974, 1976	tangential
40B-4	Base			1000	58	119.4	1.09E-02	26.4	22.4	Klueh & Canonico, 1974, 1976	tangential
40B-4	Base			1000	55	207.4	5.00E-03	21.9	24.1	Klueh & Canonico, 1974, 1976	tangential
40B-4	Base			1000	48	1197.1	2.00E-03	14.9	16.8	Klueh & Canonico, 1974, 1976	tangential
40B-4	Base			1000	45	1871.1	9.60E-04	14.6	14.3	Klueh & Canonico, 1974, 1976	tangential
40B-4	Base			900	64	2161.5	3.50E-04	30.9	25.5	Klueh & Canonico, 1974, 1976	tangential

FILE #	Weld Metal	Specimen Type	Welding Process	Temp. (F)	Stress (ksi)	Rupture Life (hrs)	Min. Creep Rate (%/hr)	Elong. (%)	Red. Of Area (%)	Reference	Comments
40B-4	Base			1100	45	69	6.60E-02	21.6	19.9	Klueh & Canonico, 1974, 1976	radial
40B-4	Base			1100	40	457.1	5.00E-03	16.5	13.7	Klueh & Canonico, 1974, 1976	radial
40B-4	Base			1100	37.5	1275.2	3.00E-03	23.8	26.9	Klueh & Canonico, 1974, 1976	radial
40B-4	Base			1000	58	105.5	8.30E-03	30.6	21.3	Klueh & Canonico, 1974, 1976	radial
40B-4	Base			1000	55	197.9	5.00E-03	27	21.8	Klueh & Canonico, 1974, 1976	radial
40B-4	Base			1000	48	689.8	1.80E-03	19.1	25.2	Klueh & Canonico, 1974, 1976	radial
40B-4	Base			1000	48	618.8	2.10E-03	17.3	21.3	Klueh & Canonico, 1974, 1976	radial
40B-4	Base			1000	45	1753.1	7.80E-04	17.8	21.7	Klueh & Canonico, 1974, 1976	radial
40B-4	Base			900	64	1164.7	3.50E-04	32.9	28.9	Klueh & Canonico, 1974, 1976	radial
40B-4	Base			1100	45	77.4	5.80E-02	20.7	22.8	Klueh & Canonico, 1974, 1976	axial
40B-4	Base			1100	40	515.9	7.90E-03	20.3	19.7	Klueh & Canonico, 1974, 1976	axial
40B-4	Base			1100	37.5	1125	3.60E-03	23.6	27.1	Klueh & Canonico, 1974, 1976	axial
40B-4	Base			1100	35	2420	1.80E-03	31.4	34.1	Klueh & Canonico, 1974, 1976	axial
40B-4	Base			1100	30	2662D	8.70E-04			Klueh & Canonico, 1974, 1976	axial
40B-4	Base			1000	60	50	3.30E-02	33.7	28.2	Klueh & Canonico, 1974, 1976	axial
40B-4	Base			1000	58	83.6	2.00E-02	31.9	29.1	Klueh & Canonico, 1974, 1976	axial
40B-4	Base			1000	55	193.3	6.90E-03	27	24.5	Klueh & Canonico, 1974, 1976	axial
40B-4	Base			1000	50	964.7	1.50E-03	16.2	16.2	Klueh & Canonico, 1974, 1976	axial
40B-4	Base			1000	48	1009.4	1.40E-03	15.2	13.9	Klueh & Canonico, 1974, 1976	axial
40B-4	Base			900	65	0.1		47.9	65.8	Klueh & Canonico, 1974, 1976	axial
40B-4	Base			900	64	1540.3	2.50E-04	41.4	33	Klueh & Canonico, 1974, 1976	axial
40B-4	Base			900	60	2542	2.00E-04	31.1	25.8	Klueh & Canonico, 1974, 1976	axial
41B-1	308	WELD	SA	1200	25	144.9	3.30E-02	19	26.7	Boling & King, 1976	butt weld 2-in, double U, quarter, 1/4 sps
41B-1	308	WELD	SA	1200	20	786.4	9.60E-04	7.6	7.9	Boling & King, 1976	butt weld 2-in, double U, quarter, 1/4 sps
41B-1	308	WELD	SA	1200	25	69.1	2.00E-01	36.3	29.1	Boling & King, 1976	butt weld 2-in, double U, crown, 1/4 sps
41B-1	308	WELD	SA	1200	20			42.6		Boling & King, 1976	butt weld 2-in, double U, crown, 1/4 sps
41B-2	308	CROSS	SA	1200	25	204.5	9.30E-03	8.4	8	Boling & King, 1976	butt weld 2-in, double U, crown, 1/4 sps
41B-2	308	CROSS	SA	1200	20	623.9	5.70E-04	3.8	2.5	Boling & King, 1976	butt weld 2-in, double U, crown, 1/4 sps

FILE #	Weld Metal	Specimen Type	Welding Process	Temp. (F)	Stress (ksi)	Rupture Life (hrs)	Min. Creep Rate (%/hr)	Elong. (%)	Red. Of Area (%)	Reference	Comments
41B-3-SR	308	WELD	SA	1200	25	147.9	3.90E-02	25.5	25.7	Boling & King, 1976	butt weld 2-in, double U, quarter, 1/4 sps, 1125F-4h
41B-3-SR	308	WELD	SA	1200	20	957	6.90E-04	7.1	5	Boling & King, 1976	butt weld 2-in, double U, quarter, 1/4 sps, 1125F-4h
41B-3-SR	308	WELD	SA	1200	25	71.9		30.3	33.4	Boling & King, 1976	butt weld 2-in, double U, crown, 1/4 sps, 1125F-4h
41B-4-SR	308	CROSS	SA	1200	25	217.1	9.80E-03	9.4	14	Boling & King, 1976	butt weld 2-in, double U, crown, 1/4 sps, 1125F-4h
41B-4-SR	308	CROSS	SA	1200	20	1190				Boling & King, 1976	butt weld 2-in, double U, crown, 1/4 sps, 1125F-4h
41B-5-ann	308	WELD	SA	1200	25	166.2	1.60E-01	57	42.4	Boling & King, 1976	butt weld 2-in, double U, quarter, 1/4 sps, 1800F-2h
41B-5-ann	308	WELD	SA	1200	20	1320		12.6	10.9	Boling & King, 1976	butt weld 2-in, double U, quarter, 1/4 sps, 1800F-2h
41B-5-ann	308	WELD	SA	1200	25	79.2	2.70E-01	42.1	36.5	Boling & King, 1976	butt weld 2-in, double U, crown, 1/4 sps, 1800F-2h
41B-5-ann	308	WELD	SA	1200	20	50D				Boling & King, 1976	butt weld 2-in, double U, crown, 1/4 sps, 1800F-2h
41B-6-ann	308	CROSS	SA	1200	25	211.4	7.50E-02	28	46	Boling & King, 1976	butt weld 2-in, double U, crown, 1/4 sps, 1800F-2h
41B-6-ann	308	CROSS	SA	1200	20	1170D				Boling & King, 1976	butt weld 2-in, double U, crown, 1/4 sps, 1800F-2h
42B-1	308	WELD	L1	1200	22	66.5		63.3		Boling, not published	butt weld, double U, crown
42B-1	308	WELD	L2	1200	22.5	838		71.4		Boling, not published	butt weld, double U, quarter
42B-1	308	WELD	L1	1200	17.5	1810		34.1		Boling, not published	butt weld, double U, crown
42B-1	308	WELD	L2	1200	17	3121		7.6		Boling, not published	butt weld, double U, quarter
42B-1	308	WELD	L3	1200	25	62.2		49.5		Boling, not published	butt weld, double U, root
42B-1	308	WELD	L1	1200	20	206.2		74.1		Boling, not published	butt weld, double U, crown
42B-1	308	WELD	L3	1200	20	1310		25		Boling, not published	butt weld, double U, root
42B-1	308	WELD	L1	1200	20	257.6		52.4		Boling, not published	butt weld, double U, crown

FILE #	Weld Metal	Specimen Type	Welding Process	Temp. (F)	Stress (ksi)	Rupture Life (hrs)	Min. Creep Rate (%/hr)	Elong. (%)	Red. Of Area (%)	Reference	Comments
43B-2	308CRE	WELD	CRE-2	1200	16	550D				Vitek, et al., 1992	
43B-3	308CRE	WELD	CRE-3	1200	16	4059D	3.00E-04			Vitek, et al., 1992	
43B-4	308CRE	WELD	CRE-4	1200	16	7136D	4.60E-04			Vitek, et al., 1992	
43B-5	308CRE	WELD	CRE-1	1200	16	10223	4.40E-04	37.6	60.1	Vitek, et al., 1992	
43B-0	308	WELD	308-3	1200	16	74D				Vitek, et al., 1992	
43B-0	308	WELD	308-2	1200	16	673D	2.70E-03			Vitek, et al., 1992	
43B-0	308	WELD	308-5	1200	16	1605D	1.30E-03			Vitek, et al., 1992	
43B-0	308	WELD	308-4	1200	16	2154D	8.00E-04			Vitek, et al., 1992	
43B-0	308	WELD	308-1	1200	16	3614	1.24E-04	19.2	33.3	Vitek, et al., 1992	
43B-3ann	308CRE	WELD	HCRE-3	1200	16	50D				Vitek, et al., 1992	2155F 1 h after re-melt
43B-2ann	308CRE	WELD	HCRE-2	1200	16	1498D				Vitek, et al., 1992	2155F 1 h after re-melt
43B-4ann	308CRE	WELD	HCRE-4	1200	16	3021D				Vitek, et al., 1992	2155F 1 h after re-melt
43B-1ann	308CRE	WELD	HCRE-1	1200	16	7382		39.2	68	Vitek, et al., 1992	2155F 1 h after re-melt
43B-0ann	308	WELD	H308-3	1200	16	63D				Vitek, et al., 1992	2155F 1 h after re-melt
43B-0ann	308	WELD	H308-4	1200	16	2300D				Vitek, et al., 1992	2155F 1 h after re-melt
43B-0ann	308	WELD	H308-5	1200	16	3494D				Vitek, et al., 1992	2155F 1 h after re-melt
43B-0ann	308	WELD	H308-2	1200	16	4688		54.1	47.3	Vitek, et al., 1992	2155F 1 h after re-melt
43B-0ann	308	WELD	H308-1	1200	13	8415		33.6	36.9	Vitek, et al., 1992	2155F 1 h after re-melt
44B-1	308	WELD	SMA	1200	25	180	2.10E-02	32.5	47	Breggren, et al., 1977	V24, 0.6% ferrite
44B-1	308	WELD	SMA	1200	22	840	6.00E-03	28	47	Breggren, et al., 1977	V24, 0.6% ferrite
44B-1	308	WELD	SMA	1200	20	750		37.5	55	Breggren, et al., 1977	V24, 0.6% ferrite
44B-2	308	WELD	SMA	1200	25	23	2.50E-01	29	63	Breggren, et al., 1977	V24, 0.6% ferrite
44B-2	308	WELD	SMA	1200	22	80	7.00E-02	34	70	Breggren, et al., 1977	V24, 0.6% ferrite
44B-2	308	WELD	SMA	1200	18	520	6.20E-03	36	65	Breggren, et al., 1977	V24, 0.6% ferrite
44B-3	308	WELD	SMA	1200	25	39	1.10E-01	49	52.5	Breggren, et al., 1977	V26, 5.2% ferrite
44B-3	308	WELD	SMA	1200	22	98	3.10E-02	35.5	54	Breggren, et al., 1977	V26, 5.2% ferrite
44B-3	308	WELD	SMA	1200	18	400	9.00E-03	26	45	Breggren, et al., 1977	V26, 5.2% ferrite
44B-4	308	WELD	SMA	1200	25	30	3.20E-01	35.5	55	Breggren, et al., 1977	V27, 6.2% ferrite
44B-4	308	WELD	SMA	1200	18	390	1.20E-02	27	33	Breggren, et al., 1977	V27, 6.2% ferrite
44B-5	308	WELD	SMA	1200	25	28	5.20E-01	38	53	Breggren, et al., 1977	V28, 9.4% ferrite
44B-5	308	WELD	SMA	1200	22	59	1.80E-01	24	43	Breggren, et al., 1977	V28, 9.4% ferrite
44B-5	308	WELD	SMA	1200	16	640	7.40E-03	13.5	23.5	Breggren, et al., 1977	V28, 9.4% ferrite
44B-6	308	WELD	SMA	1200	25	33	4.20E-01	33	36	Breggren, et al., 1977	V29, 11.6% ferrite
44B-6	308	WELD	SMA	1200	22	80	1.40E-01	22.5	30.5	Breggren, et al., 1977	V29, 11.6% ferrite
44B-6	308	WELD	SMA	1200	16	520	3.20E-03	6	10.5	Breggren, et al., 1977	V29, 11.6% ferrite

FILE #	Weld Metal	Specimen Type	Welding Process	Temp. (F)	Stress (ksi)	Rupture Life (hrs)	Min. Creep Rate (%/hr)	Elong. (%)	Red. Of Area (%)	Reference	Comments
45B	308CRE	WELD	SMA	1200	30	964	1.75E-03	8.5		Cole, et al., ORNL 4524, 1973	V136
45B	308CRE	WELD	SMA	1200	28	1784	4.50E-04			Cole, et al., ORNL 4524, 1973	V136
45B	308CRE	WELD	SMA	1200	25	4184	1.00E-04	4.7		Cole, et al., ORNL 4524, 1973	V136
46B-1	308CRE	WELD	SMA	1200	20	569	1.40E-02	21.5		Cole, et al., ORNL 4524, 1973	V148, .1Ti, .006B, .042P
46B-1	308CRE	WELD	SMA	1200	15	7440	7.00E-05	13.7		Cole, et al., ORNL 4524, 1973	V148, .1Ti, .006B, .042P
46B-2	308CRE	WELD	SMA	1200	20	1664.3	6.00E-04	13.88		Cole, et al., ORNL 4524, 1973	V149, 0.6Ti, .006B, .042P
46B-2	308CRE	WELD	SMA	1200	18	7357	4.00E-05	8.53		Cole, et al., ORNL 4524, 1973	V149, 0.6Ti, .006B, .042P
46B-3	308CRE	WELD	SMA	1200	25	6192		5.24		Cole, et al., ORNL 4524, 1973	V150, 1,25Ti, .006B, .042P
46B-3	308CRE	WELD	SMA	1200	20	15330		5.47		Cole, et al., ORNL 4524, 1973	V150, 1,25Ti, .006B, .042P
47B-1-1	308	WELD	SMA	1200	14.5	1201	2.50E-04	1.2		Booker collection, 1984	repeats many other files?
47B-1-1	308	WELD	SMA	1200	16	1391	1.80E-04	1		Booker collection, 1984	repeats many other files?
47B-1-1	308	WELD	SMA	1200	21	171.5	4.60E-03	4		Booker collection, 1984	repeats many other files?
47B-1-1	308	WELD	SMA	1200	22	67.4	2.10E-02	8.4		Booker collection, 1984	repeats many other files?
47B-1-1	308	WELD	SMA	1200	23	53.1	2.80E-02	11.5		Booker collection, 1984	repeats many other files?
47B-1-1	308	WELD	SMA	1200	25	32.2	5.30E-02	10		Booker collection, 1984	repeats many other files?
47B-1-1	308	WELD	SMA	1200	27	23.8	8.20E-02	14.4		Booker collection, 1984	repeats many other files?
47B-1-1	308	WELD	SMA	1200	30	10.4	1.70E-01	13.4		Booker collection, 1984	repeats many other files?
47B-3-6	308	WELD	SMA	1100	25	1212	7.80E-04	2.3	5.2	Booker collection, 1984	repeats many other files?
47B-3-6	308	WELD	SMA	1100	35	43.2	3.40E-01	29.8	25.3	Booker collection, 1984	repeats many other files?
47B-3-6	308	WELD	SMA	1200	18	575.5				Booker collection, 1984	repeats many other files?
47B-3-6	308	WELD	SMA	1200	18	654.9	9.00E-04	0.8	0.6	Booker collection, 1984	repeats many other files?
47B-3-6	308	WELD	SMA	1200	20	362.6	5.00E-04	2	10	Booker collection, 1984	repeats many other files?
47B-3-6	308	WELD	SMA	1200	25	16	3.70E-01	29.6	19.9	Booker collection, 1984	repeats many other files?
47B-3-6	308	WELD	SMA	1200	25	25.7	2.10E-01	23		Booker collection, 1984	repeats many other files?
47B-3-6	308	WELD	SMA	1200	25	44	3.70E-02	10.2		Booker collection, 1984	repeats many other files?
47B-3-7	308	WELD	SMA	1100	25	529	3.70E-03	13.2	11.9	Booker collection, 1984	repeats many other files?
47B-3-7	308	WELD	SMA	1200	18	212	5.60E-03	6	5.6	Booker collection, 1984	repeats many other files?
47B-3-7	308	WELD	SMA	1200	20	135	1.10E-02	11.5	19.9	Booker collection, 1984	repeats many other files?
47B-3-7	308	WELD	SMA	1200	25	26.7	2.50E-01	22.5		Booker collection, 1984	repeats many other files?

FILE #	Weld Metal	Specimen Type	Welding Process	Temp. (F)	Stress (ksi)	Rupture Life (hrs)	Min. Creep Rate (%/hr)	Elong. (%)	Red. Of Area (%)	Reference	Comments
47B-3-8	308	WELD	SMA	1200	18	715	2.20E-04	1.4	2.4	Booker collection, 1984	repeats many other files?
47B-3-8	308	WELD	SMA	1200	20	327	8.00E-04	2.3	7.5	Booker collection, 1984	repeats many other files?
47B-3-8	308	WELD	SMA	1200	25	28.7	1.90E-01	24.3	23.7	Booker collection, 1984	repeats many other files?
47B-3-9	308	WELD	SMA	1200	18	490.3	5.00E-04	4.5	7	Booker collection, 1984	repeats many other files?
47B-3-9	308	WELD	SMA	1200	20	346	5.00E-04	4	19.4	Booker collection, 1984	repeats many other files?
47B-3-9	308	WELD	SMA	1200	25	31.5	1.65E-01	22	23.8	Booker collection, 1984	repeats many other files?
47B-19-4	308	WELD	SMA	1200	20	1859.9	3.00E-05	2.3	6.4	Booker collection, 1984	repeats many other files?
47B-19-4	308	WELD	SMA	1200	20	3177.3	2.00E-06	3.2	3.6	Booker collection, 1984	repeats many other files?
47B-19-4	308	WELD	SMA	1200	22.5	900.3	8.40E-04	9.6	31.1	Booker collection, 1984	repeats many other files?
47B-19-4	308	WELD	SMA	1200	22.5	949.3	5.00E-04	4.7	21.6	Booker collection, 1984	repeats many other files?
47B-19-4	308	WELD	SMA	1200	25	317.8	2.30E-03	9.9	49.5	Booker collection, 1984	repeats many other files?
47B-3-10	308	WELD	SMA	1200	18	591.9	1.00E-03	3.2	10.2	Booker collection, 1984	repeats many other files?
47B-3-10	308	WELD	SMA	1200	20	127	2.80E-02	15.7	13.8	Booker collection, 1984	repeats many other files?
47B-3-10	308	WELD	SMA	1200	25	39.7	1.56E-01	26.7	62	Booker collection, 1984	repeats many other files?
47B-3-11	308	WELD	SMA	1200	18	1654.8	1.00E-04	1		Booker collection, 1984	repeats many other files?
47B-3-11	308	WELD	SMA	1200	20	1329	2.60E-04	4.4	18	Booker collection, 1984	repeats many other files?
47B-3-11	308	WELD	SMA	1200	25	47.4	6.00E-02	15.5	15.1	Booker collection, 1984	repeats many other files?
47H-3-12	308	WELD	SMA	1200	18	710	1.10E-04	1.3		Booker collection, 1984	repeats many other files?
47H-3-12	308	WELD	SMA	1200	20	651	3.00E-04	1.3	4.6	Booker collection, 1984	repeats many other files?
47H-3-12	308	WELD	SMA	1200	25	26.5	1.00E-01	16.3	19.7	Booker collection, 1984	repeats many other files?
47H-3-13	308	WELD	SMA	1200	18	525.9	7.60E-04	0.8	1.1	Booker collection, 1984	repeats many other files?
47H-3-13	308	WELD	SMA	1200	20	333	2.00E-04	2.6	15.6	Booker collection, 1984	repeats many other files?
47H-3-13	308	WELD	SMA	1200	25	47.6	6.00E-02	15.5	15.1	Booker collection, 1984	repeats many other files?
47B-3-14	308	WELD	SMA	1200	18	548	3.00E-04	0.7	1.9	Booker collection, 1984	repeats many other files?
47B-3-14	308	WELD	SMA	1200	20	292	8.00E-03	4	18.8	Booker collection, 1984	repeats many other files?
47B-3-14	308	WELD	SMA	1200	25	31	1.46E-01	31.4	23.1	Booker collection, 1984	repeats many other files?
48B-25-21	308	WELD	SA	1200	14	493	1.70E-02	13.3	8.3	Booker collection, 1984	repeats many other files?
48B-25-21	308	WELD	SA	1200	18	62	1.43E-01	14	18	Booker collection, 1984	repeats many other files?
48B-25-21	308	WELD	SA	1200	25	5	2.92E+00	14.3	15.5	Booker collection, 1984	repeats many other files?
48B-25-22	308	WELD	SA	1100	25	367	3.00E-02	18.5	12	Booker collection, 1984	repeats many other files?
48B-25-22	308	WELD	SA	1100	28	120	1.20E-01	24	22.4	Booker collection, 1984	repeats many other files?
48B-25-22	308	WELD	SA	1200	14	949	3.20E-03	5.9	12	Booker collection, 1984	repeats many other files?
48B-25-22	308	WELD	SA	1200	18	171	5.60E-02	12.4	30	Booker collection, 1984	repeats many other files?
48B-25-22	308	WELD	SA	1200	25	12	9.80E-01	17.9	54	Booker collection, 1984	repeats many other files?
48B-25-22	308	WELD	SA	1100	20	2082	3.20E-03	10	12.2	Booker collection, 1984	repeats many other files?

FILE #	Weld Metal	Specimen Type	Welding Process	Temp. (F)	Stress (ksi)	Rupture Life (hrs)	Min. Creep Rate (%/hr)	Elong. (%)	Red. Of Area (%)	Reference	Comments
48B-25-23	308	WELD	SA	1100	20	1225	5.00E-03	10	40.6	Booker collection, 1984	repeats many other files?
48B-25-23	308	WELD	SA	1100	25	283	5.40E-02	24	16	Booker collection, 1984	repeats many other files?
48B-25-23	308	WELD	SA	1100	28	130	1.20E-01	23.1	26.1	Booker collection, 1984	repeats many other files?
48B-25-23	308	WELD	SA	1200	14	663	1.10E-02	10.3	17	Booker collection, 1984	repeats many other files?
48B-25-23	308	WELD	SA	1200	18	126	1.20E-01	19.9	38	Booker collection, 1984	repeats many other files?
48B-25-23	308	WELD	SA	1200	25	11	1.40E+00	22.8	47	Booker collection, 1984	repeats many other files?
48B-25-23	308	WELD	SA	1200	13	1314	2.70E-03	6.4	14.3	Booker collection, 1984	repeats many other files?
48B-25-24	308	WELD	SA	1100	28	46		15.8	16.3	Booker collection, 1984	repeats many other files?
48B-25-24	308	WELD	SA	1200	16	556	1.70E-02	11.7	18.7	Booker collection, 1984	repeats many other files?
48B-25-24	308	WELD	SA	1200	18	236	6.10E-02	18.4	21.3	Booker collection, 1984	repeats many other files?
48B-25-24	308	WELD	SA	1200	25	9	1.40E+00	17	59.5	Booker collection, 1984	repeats many other files?
48B-25-24	308	WELD	SA	1200	25	9	1.30E+00	18.3	52.5	Booker collection, 1984	repeats many other files?
48B-25-24	308	WELD	SA	1100	25	194	1.80E-03	13.9	62.4	Booker collection, 1984	repeats many other files?
48B-25-24	308	WELD	SA	1100	20	3132	6.20E-03	10.6	24.4	Booker collection, 1984	repeats many other files?
48B-25-24	308	WELD	SA	1200	15	1247	6.00E-02	11.1	18.6	Booker collection, 1984	repeats many other files?
48B-25-25	308	WELD	SA	1100	20	878	1.35E-02	21.2	46.1	Booker collection, 1984	repeats many other files?
48B-25-25	308	WELD	SA	1100	25	128	9.60E-02	19.2	46.1	Booker collection, 1984	repeats many other files?
48B-25-25	308	WELD	SA	1200	14	614	8.10E-03	8.9	6.4	Booker collection, 1984	repeats many other files?
48B-25-25	308	WELD	SA	1200	12.5	1430	3.30E-03	5.5	5.6	Booker collection, 1984	repeats many other files?
48B-25-26	308	WELD	SA	1200	18	170	6.00E-02	18.5	31.2	Booker collection, 1984	repeats many other files?
48B-25-26	308	WELD	SA	1200	14	820	1.30E-02	13.9	22.3	Booker collection, 1984	repeats many other files?
48B-25-27	308	WELD	SA	1100	28	124	9.00E-02	16.4	19.8	Booker collection, 1984	repeats many other files?
48B-25-27	308	WELD	SA	1100	25	268	2.70E-02	11.1	17.3	Booker collection, 1984	repeats many other files?
48B-25-27	308	WELD	SA	1100	20	1166	6.40E-03	10.1	26.2	Booker collection, 1984	repeats many other files?
48B-25-27	308	WELD	SA	1200	25	13	7.50E-01	23.1	36	Booker collection, 1984	repeats many other files?
48B-25-27	308	WELD	SA	1200	18	121	1.00E-01	17.9	33.9	Booker collection, 1984	repeats many other files?
48B-25-27	308	WELD	SA	1200	15	610	1.50E-01	13.9	30.3	Booker collection, 1984	repeats many other files?
48B-25-27	308	WELD	SA	1200	14	1022	7.60E-03	11.7	23.5	Booker collection, 1984	repeats many other files?
48B-25-28	308	WELD	SA	1100	25	79	9.60E-02	20.1	58.9	Booker collection, 1984	repeats many other files?
48B-25-28	308	WELD	SA	1100	20	712	7.80E-03	15.3	55.8	Booker collection, 1984	repeats many other files?
48B-25-28	308	WELD	SA	1200	14	735	1.60E-02	18.6	54	Booker collection, 1984	repeats many other files?
48B-25-28	308	WELD	SA	1200	12.5	1995	2.40E-03	8.8	14.7	Booker collection, 1984	repeats many other files?
48B-25-29	308	WELD	SA	1200	22.5	76.4	2.15E-01	28.7	47.4	Booker collection, 1984	repeats many other files?
48B-25-29	308	WELD	SA	1200	17	774.4	6.60E-03	20	47.6	Booker collection, 1984	repeats many other files?
48B-25-29	308	WELD	SA	1200	12.5	6157.1	1.90E-03	16.1	13.9	Booker collection, 1984	repeats many other files?

FILE #	Weld Metal	Specimen Type	Welding Process	Temp. (F)	Stress (ksi)	Rupture Life (hrs)	Min. Creep Rate (%/hr)	Elong. (%)	Red. Of Area (%)	Reference	Comments
48B-25-30	308	WELD	SA	1200	22.5	75	3.80E-01	44.3	55.6	Booker collection, 1984	repeats many other files?
48B-25-30	308	WELD	SA	1200	17	851.6	1.70E-02	17.8	17	Booker collection, 1984	repeats many other files?
48B-25-30	308	WELD	SA	1200	12.5	5528.7	3.00E-03	6.2	5.7	Booker collection, 1984	repeats many other files?
48B-25-30	308	WELD	SA	1200	22.5	183.6	9.00E-02	33.4	39.4	Booker collection, 1984	repeats many other files?
48B-25-30	308	WELD	SA	1200	17	1035.3	1.00E-02	29	35.1	Booker collection, 1984	repeats many other files?
48B-25-30	308	WELD	SA	1200	12.5	5676.2	1.20E-03	15.6	16.3	Booker collection, 1984	repeats many other files?
49B	308	CROSS	WIG	1022	38.9	95				Huthman, et al., 1983	data scaled from plot
49B	308	CROSS	WIG	1022	38.9	125				Huthman, et al., 1983	data scaled from plot
49B	308	CROSS	WIG	1022	33.6	230				Huthman, et al., 1983	data scaled from plot
49B	308	CROSS	WIG	1022	33.6	320				Huthman, et al., 1983	data scaled from plot
49B	308	CROSS	WIG	1022	32.9	470				Huthman, et al., 1983	data scaled from plot
49B	308	CROSS	WIG	1022	32.9	610				Huthman, et al., 1983	data scaled from plot
49B	308	CROSS	WIG	1022	28.7	1800				Huthman, et al., 1983	data scaled from plot
49B	308	CROSS	WIG	1022	28.7	2200				Huthman, et al., 1983	data scaled from plot
49B	308	CROSS	WIG	1022	25.8	3400				Huthman, et al., 1983	data scaled from plot
49B	308	CROSS	WIG	1022	25.8	3900				Huthman, et al., 1983	data scaled from plot
50B-1	308L	WELD	SMA	1250	20	206				Beggs & Ibarra, 1991	
50B-1	308L	WELD	SMA	1250	18	438				Beggs & Ibarra, 1991	
50B-1	308L	WELD	SMA	1250	17	607				Beggs & Ibarra, 1991	
50B-1	308L	WELD	SMA	1250	17	569				Beggs & Ibarra, 1991	
50B-1	308L	WELD	SMA	1250	16.5	984.1				Beggs & Ibarra, 1991	
50B-2	308	WELD	SMA	1250	20	878.1				Beggs & Ibarra, 1991	
50B-2	308	WELD	SMA	1250	20	1866.5				Beggs & Ibarra, 1991	
50B-2	308	WELD	SMA	1250	18	3641.6				Beggs & Ibarra, 1991	
50B-2	308	WELD	SMA	1250	17	4594.5				Beggs & Ibarra, 1991	

FILE #	Weld Metal	Specimen Type	Welding Process	Temp. (F)	Stress (ksi)	Rupture Life (hrs)	Min. Creep Rate (%/hr)	Elong. (%)	Red. Of Area (%)	Reference	Comments
51B	308CRE	WELD	SMA	1050	41	69.2		31	60.8	C-E Met Lab	root
51B	308CRE	WELD	SMA	1050	39	106.5		30	55.9	C-E Met Lab	quarter
51B	308CRE	WELD	SMA	1050	39	60.4		39	54.4	C-E Met Lab	crown
51B	308CRE	WELD	SMA	1050	37	158.2		36	60.2	C-E Met Lab	crown
51B	308CRE	WELD	SMA	1050	37	456		28	59	C-E Met Lab	quarter
51B	308CRE	WELD	SMA	1050	36	268.8		33	55.1	C-E Met Lab	crown
51B	308CRE	WELD	SMA	1050	36	1658.6		27	52	C-E Met Lab	quarter
51B	308CRE	WELD	SMA	1200	31	30.4		25	64.1	C-E Met Lab	quarter
51B	308CRE	WELD	SMA	1200	30	66.6		25	59.1	C-E Met Lab	quarter
51B	308CRE	WELD	SMA	1200	29	63.9		31	64.1	C-E Met Lab	quarter
51B	308CRE	WELD	SMA	1200	28	162.5		26	65.2	C-E Met Lab	quarter
51B	308CRE	WELD	SMA	1200	27.5	190.4		22	62.8	C-E Met Lab	root
51B	308CRE	WELD	SMA	1200	27	486.9		28	61.3	C-E Met Lab	quarter
51B	308CRE	WELD	SMA	1200	26	226.2		26	67.4	C-E Met Lab	crown
51B	308CRE	WELD	SMA	1200	26	666.9		24	66.5	C-E Met Lab	root
51B	308CRE	WELD	SMA	1200	25	3088.7		21	64.8	C-E Met Lab	quarter
51B	308CRE	WELD	SMA	1200	24	3491		23	63.1	C-E Met Lab	quarter
51B	308CRE	WELD	SMA	1200	23	798.4		30	65.8	C-E Met Lab	crown
51B	308CRE	WELD	SMA	1200	23					C-E Met Lab	root
51B	308CRE	WELD	SMA	1350	21	45.7		24	68.4	C-E Met Lab	quarter
51B	308CRE	WELD	SMA	1350	20	29.2		32	72.9	C-E Met Lab	crown
51B	308CRE	WELD	SMA	1350	19	161		29	71.8	C-E Met Lab	quarter
51B	308CRE	WELD	SMA	1350	18	37.9		39	76.4	C-E Met Lab	crown
51B	308CRE	WELD	SMA	1350	18	198.9		26	66.6	C-E Met Lab	quarter
51B	308CRE	WELD	SMA	1350	17	55.9		34	69.5	C-E Met Lab	crown
51B	308CRE	WELD	SMA	1350	17	152.3		33	72.3	C-E Met Lab	root
51B	308CRE	WELD	SMA	1350	16	705.5		24	59	C-E Met Lab	quarter
51B	308CRE	WELD	SMA	1350	15	503.7		30	57.6	C-E Met Lab	crown

FILE #	Weld Metal	Specimen Type	Welding Process	Temp. (F)	Stress (ksi)	Rupture Life (hrs)	Min. Creep Rate (%/hr)	Elong. (%)	Red. Of Area (%)	Reference	Comments
52B	308	WELD	SMA	1350	17	6.7		54	72.8	C-E Met Lab IBCA	crown
52B	308	WELD	SMA	1350	17	10.9		46	65.8	C-E Met Lab IBCA	root
52B	308	WELD	SMA	1350	13	315		19	36.3	C-E Met Lab IBCA	crown
52B	308	WELD	SMA	1350	13	173.8		22	35	C-E Met Lab IBCA	root
53B	308	WELD	SMA	1350	19	94.4		34	69.8	C-E Met Lab ICJA	root
53B	308	WELD	SMA	1350	18	107.2		30	72.8	C-E Met Lab ICJA	crown
53B	308	WELD	SMA	1350	17.5	57		42	73.8	C-E Met Lab ICJA	crown
53B	308	WELD	SMA	1350	17.5	228.8		25	72.4	C-E Met Lab ICJA	quarter
53B	308	WELD	SMA	1350	16	175.9		38	70.7	C-E Met Lab ICJA	crown
53B	308	WELD	SMA	1350	16	569.2		25	67.1	C-E Met Lab ICJA	quarter
53B	308	WELD	SMA	1350	15	455.8		37	66.7	C-E Met Lab ICJA	crown
53B	308	WELD	SMA	1350	15	2342.8		15	24.4	C-E Met Lab ICJA	root
53B	308	WELD	SMA	1350	14	881		25	64.4	C-E Met Lab ICJA	crown
54B	308CRE	WELD	SMA	1050	39	16.9		51	63.3	C-E Met Lab HBEA	crown
54B	308CRE	WELD	SMA	1050	39	42.8		47	72.3	C-E Met Lab HBEA	quarter
54B	308CRE	WELD	SMA	1050	37	173		32	57.8	C-E Met Lab HBEA	crown
54B	308CRE	WELD	SMA	1050	37	316		33	63.9	C-E Met Lab HBEA	quarter
54B	308CRE	WELD	SMA	1050	35	229.5		51	61.6	C-E Met Lab HBEA	crown
54B	308CRE	WELD	SMA	1050	35	2021.6		28	56.8	C-E Met Lab HBEA	root
54B	308CRE	WELD	SMA	1050	34	445.5		29	67.1	C-E Met Lab HBEA	crown
54B	308CRE	WELD	SMA	1050	34	392.9		32	62.5	C-E Met Lab HBEA	crown
54B	308CRE	WELD	SMA	1350	19	30		43	67.4	C-E Met Lab HBEA	crown
54B	308CRE	WELD	SMA	1350	19	22.8		41	78	C-E Met Lab HBEA	root
54B	308CRE	WELD	SMA	1350	17.5	17.9		44	71.8	C-E Met Lab HBEA	crown
54B	308CRE	WELD	SMA	1350	17.5	134.9		26	70.6	C-E Met Lab HBEA	quarter
54B	308CRE	WELD	SMA	1350	17	101.1		22	72.1	C-E Met Lab HBEA	crown
54B	308CRE	WELD	SMA	1350	17	80		28	71.5	C-E Met Lab HBEA	crown
54B	308CRE	WELD	SMA	1350	17	172.4		29	67.7	C-E Met Lab HBEA	root
54B	308CRE	WELD	SMA	1350	17	473.2		13	46.6	C-E Met Lab HBEA	root
54B	308CRE	WELD	SMA	1350	15	1181		31	53.3	C-E Met Lab HBEA	crown
54B	308CRE	WELD	SMA	1350	15	81		25	54.8	C-E Met Lab HBEA	root
54B	308CRE	WELD	SMA	1350	14	849.5		18	51.6	C-E Met Lab HBEA	crown
54B	308CRE	WELD	SMA	1350	14	1750D				C-E Met Lab HBEA	root
54B	308CRE	WELD	SMA	1350	13	1750D				C-E Met Lab HBEA	crown

FILE #	Weld Metal	Specimen Type	Welding Process	Temp. (F)	Stress (ksi)	Rupture Life (hrs)	Min. Creep Rate (%/hr)	Elong. (%)	Red. Of Area (%)	Reference	Comments
55B-1	308	WELD	SMA	1050	40	24.4		39	67.9	C-E Met Lab	M7692
55B-1	308	WELD	SMA	1050	35	182.1		46	59.2	C-E Met Lab	M7692
55B-1	308	WELD	SMA	1050	35	163.6		44	53.1	C-E Met Lab	M7692
55B-1	308	WELD	SMA	1050	27	2201D				C-E Met Lab	M7692
55B-1	308	WELD	SMA	1200	25	72.6		26	62	C-E Met Lab	M7692
55B-1	308	WELD	SMA	1200	22	886.9		22	47.4	C-E Met Lab	M7692
55B-1	308	WELD	SMA	1200	19	2273D				C-E Met Lab	M7692
55B-2	308	WELD	SMA	1050	40	29.9		40	59.1	C-E Met Lab	M7692
55B-2	308	WELD	SMA	1050	35	138.4		43.5	48.8	C-E Met Lab	M7692
55B-2	308	WELD	SMA	1050	27	2102		7	21	C-E Met Lab	M7692
55B-2	308	WELD	SMA	1200	25	30.4		31	46.7	C-E Met Lab	M7692
55B-2	308	WELD	SMA	1200	21	531		8	16.1	C-E Met Lab	M7692
55B-2	308	WELD	SMA	1200	17	1221D				C-E Met Lab	M7692
56B	308CRE	Weld	SMA	1050	40	21.5		39	63.4	C-E Met Lab M7693	
56B	308CRE	Weld	SMA	1050	36	120		39	63.9	C-E Met Lab M7693	
56B	308CRE	Weld	SMA	1050	35	188.6		40	63.8	C-E Met Lab M7693	
56B	308CRE	Weld	SMA	1050	33	261.7		42	60	C-E Met Lab M7693	
56B	308CRE	Weld	SMA	1050	30	2524		20	50.2	C-E Met Lab M7693	
56B	308CRE	Weld	SMA	1200	33	1.2		45	68.3	C-E Met Lab M7693	
56B	308CRE	Weld	SMA	1200	27	19.8		46	72.3	C-E Met Lab M7693	
56B	308CRE	Weld	SMA	1200	24.6	91.4		32	64.1	C-E Met Lab M7693	
56B	308CRE	Weld	SMA	1200	24	59.9		47	69.1	C-E Met Lab M7693	
56B	308CRE	Weld	SMA	1200	24	198		29	69.1	C-E Met Lab M7693	
56B	308CRE	Weld	SMA	1200	22	278.6		28	63.7	C-E Met Lab M7693	
56B	308CRE	Weld	SMA	1200	19	4001.8		22	30.4	C-E Met Lab M7693	
56B	308CRE	Weld	SMA	1200	18	2615.5		17	47.4	C-E Met Lab M7693	
56B	308CRE	Weld	SMA	1350	20	2.9		47	68.3	C-E Met Lab M7693	
56B	308CRE	Weld	SMA	1350	15	74.9		26	53.2	C-E Met Lab M7693	
56B	308CRE	Weld	SMA	1350	13	78.8		45.6	60.3	C-E Met Lab M7693	
56B	308CRE	Weld	SMA	1350	13	320.4		12	31.9	C-E Met Lab M7693	

FILE #	Weld Metal	Specimen Type	Welding Process	Temp. (F)	Stress (ksi)	Rupture Life (hrs)	Min. Creep Rate (%/hr)	Elong. (%)	Red. Of Area (%)	Reference	Comments
			CE Metallurgical Laboratory								
			308CRE weld metal M7745 & M7871								
			Shielded Metal Arc weld: 1/4-in.-diam. specimens								
57B-1	308CRE	WELD	SMA	1050	36	121.8		32	54.8	C-E Met Lab	M7745
57B-1	308CRE	WELD	SMA	1050	33	294.1		32	48.9	C-E Met Lab	M7745
57B-1	308CRE	WELD	SMA	1050	30	1875.3		23	35.7	C-E Met Lab	M7745
57B-1	308CRE	WELD	SMA	1200	24	102.9		30	51.8	C-E Met Lab	M7745
57B-1	308CRE	WELD	SMA	1200	22	385		22	50	C-E Met Lab	M7745
57B-1	308CRE	WELD	SMA	1200	19	2745.3		8	26.6	C-E Met Lab	M7745
57B-2	308CRE	WELD	SMA	1050	39	53.4		40	62.7	C-E Met Lab	M7871
57B-2	308CRE	WELD	SMA	1050	39	57.5		39	57.5	C-E Met Lab	M7871
57B-2	308CRE	WELD	SMA	1050	38	51.7		40	60.6	C-E Met Lab	M7871
57B-2	308CRE	WELD	SMA	1050	37	71.3		36	53.6	C-E Met Lab	M7871
57B-2	308CRE	WELD	SMA	1050	36	57.6		44	59.2	C-E Met Lab	M7871
57B-2	308CRE	WELD	SMA	1050	35	214.4		30	53.3	C-E Met Lab	M7871
57B-2	308CRE	WELD	SMA	1050	34	368.5		38	52.4	C-E Met Lab	M7871
57B-2	308CRE	WELD	SMA	1200	28	25.4		37	59.2	C-E Met Lab	M7871
57B-2	308CRE	WELD	SMA	1200	26	13.5		35	63.2	C-E Met Lab	M7871
57B-2	308CRE	WELD	SMA	1200	26	41.4		34	68.8	C-E Met Lab	M7871
57B-2	308CRE	WELD	SMA	1200	25	117.7		26	61.7	C-E Met Lab	M7871
57B-2	308CRE	WELD	SMA	1200	23	303.2		28	55.6	C-E Met Lab	M7871
57B-2	308CRE	WELD	SMA	1350	19	15.9		29	64.1	C-E Met Lab	M7871
57B-2	308CRE	WELD	SMA	1350	17	52.6		35	61.1	C-E Met Lab	M7871
57B-2	308CRE	WELD	SMA	1350	16	68.9		34	59.2	C-E Met Lab	M7871
57B-2	308CRE	WELD	SMA	1350	15	191.5		20	42.7	C-E Met Lab	M7871
57B-2	308CRE	WELD	SMA	1350	14	314.3		11	32	C-E Met Lab	M7871

FILE #	Weld Metal	Specimen Type	Welding Process	Temp. (F)	Stress (ksi)	Rupture Life (hrs)	Min. Creep Rate (%/hr)	Elong. (%)	Red. Of Area (%)	Reference	Comments
58B	308CRE	WELD	SMA	1050	40	51		30	55.8	C-E Met Lab, M7898	crown
58B	308CRE	WELD	SMA	1050	39	790		25	57.7	C-E Met Lab, M7898	quarter
58B	308CRE	WELD	SMA	1050	39	197		33	63.9	C-E Met Lab, M7898	quarter
58B	308CRE	WELD	SMA	1050	37	1595.5		26	59.3	C-E Met Lab, M7898	quarter
58B	308CRE	WELD	SMA	1050	37	256.3		32	62	C-E Met Lab, M7898	crown
58B	308CRE	WELD	SMA	1050	36	635.3		29	63.8	C-E Met Lab, M7898	quarter
58B	308CRE	WELD	SMA	1200	23	6743.1		28.5	61.1	C-E Met Lab, M7898	crown
58B	308CRE	WELD	SMA	1350	19	49.1		35.5	78.8	C-E Met Lab, M7898	crown
58B	308CRE	WELD	SMA	1350	19	112.9		28	77	C-E Met Lab, M7898	quarter
58B	308CRE	WELD	SMA	1350	18	104.7		38	72	C-E Met Lab, M7898	root
58B	308CRE	WELD	SMA	1350	17.5	164.5		46	77.9	C-E Met Lab, M7898	crown
58B	308CRE	WELD	SMA	1350	17	351		38	73.4	C-E Met Lab, M7898	root
58B	308CRE	WELD	SMA	1350	16	568.7		33.5	73.5	C-E Met Lab, M7898	root
58B	308CRE	WELD	SMA	1350	16	589		24.5	66	C-E Met Lab, M7898	quarter
58B	308CRE	WELD	SMA	1350	15	490		31.3	74.1	C-E Met Lab, M7898	crown
58B	308CRE	WELD	SMA	1350	14	1095		36	58.5	C-E Met Lab, M7898	crown
58B	308CRE	WELD	SMA	1350	13	2086.5		18.5	45.4	C-E Met Lab, M7898	root
59B-1	308CRE	WELD	SMA	1050	39	64.4		34	63.9	C-E Met Lab EOGA	crown
59B-1	308CRE	WELD	SMA	1050	17.5	406.3		7	20.9	C-E Met Lab EOGA	root
59B-2	308CRE	WELD	SMA	1350	17.5	264.9				C-E Met Lab KAGA	crown
59B-2	308CRE	WELD	SMA	1350	17.5	367.7				C-E Met Lab KAGA	root
60B	308CRE	WELD	SMA	1050	39	268.3		31	54.4	C-E Met Lab CAEA	crown
60B	308CRE	WELD	SMA	1350	19	55		29	72	C-E Met Lab CAEA	crown
60B	308CRE	WELD	SMA	1350	19	520.3				C-E Met Lab CAEA	root

FILE #	Weld Metal	Specimen Type	Welding Process	Temp. (F)	Stress (ksi)	Rupture Life (hrs)	Min. Creep Rate (%/hr)	Elong. (%)	Red. Of Area (%)	Reference	Comments
62B-1	308	WELD	SA	1350	19	2.1		16	27.2	C-E Met Lab HR	
62B-1	308	WELD	SA	1350	15	9.7		12.9	13.1	C-E Met Lab HR	
62B-1	308	WELD	SA	1350	10	176.7		3	3.1	C-E Met Lab HR	
62B-1	308	WELD	SA	1350	8	109.3		2	4.6	C-E Met Lab HR	
62B-1	308	WELD	SA	1350	6	452.4		3	3.1	C-E Met Lab HR	
62B-1	308	WELD	SA	1350	5	1144.5		1	1.6	C-E Met Lab HR	
62B-2	308	WELD	SA	1050	35	110.5		20	24.4	C-E Met Lab TJ	
62B-2	308	WELD	SA	1050	30	460.5		15	19.7	C-E Met Lab TJ	
62B-2	308	WELD	SA	1050	25	2236.8		3	4.7	C-E Met Lab TJ	
62B-2	308	WELD	SA	1200	25	11.6		23	33.8	C-E Met Lab TJ	
62B-2	308	WELD	SA	1200	20	106.5		23	20.5	C-E Met Lab TJ	
62B-2	308	WELD	SA	1200	17	305.1		19	24.6	C-E Met Lab TJ	
62B-2	308	WELD	SA	1200	15	607.5		9	8.7	C-E Met Lab TJ	
62B-2	308	WELD	SA	1200	14	1017.5		10	10.1	C-E Met Lab TJ	
62B-2	308	WELD	SA	1200	12	1387.2		6	4.7	C-E Met Lab TJ	
62B-3	308	WELD	SA	1050	35	126.8		16.9	23.8	C-E Met Lab AP	
62B-3	308	WELD	SA	1050	30	274.3		10	15.9	C-E Met Lab AP	
62B-3	308	WELD	SA	1050	22	2569.4		1	3.1	C-E Met Lab AP	
62B-3	308	WELD	SA	1200	20	41		10	15.3	C-E Met Lab AP	
62B-3	308	WELD	SA	1200	15	247.8		3	6.3	C-E Met Lab AP	
62B-3	308	WELD	SA	1200	12	892.4		1	3.1	C-E Met Lab AP	

APPENDIX D: 316 & 16-8-2

D.1 Chemistry

							Chemistry in wt%													
Heat ID	Reference	Product	Process	Filler	Flux	FN	C	Mn	P	S	Si	Ni	Cr	Mo	V	Nb	Ti	Co	Cu	B	N
77-15	ORNL-5594	Plate	SA	16-8-2	Arcos S-4	7.3	0.048	1.33	0.03	0.016	0.96	9.22	17.11	1.79	0.03		0.01	0.08	0.07	0.002	0.034
77-16	ORNL-5594	Plate	SA	16-8-2	Arcos S-16	7.7	0.055	1.38	0.028	0.017	0.88	8.37	16.8	2.23	0.03			0.07	0.08	0.002	0.034
77-17	ORNL-5594	Plate	SA	16-8-2	Linde 0091	2.3	0.059	0.79	0.026	0.014	0.5	9.33	15.33	1.85	0.04			0.1	0.08	0.002	0.032
S-11	ORNL-5594	Plate	SA	16-8-2	Arcos S-11	1.3	0.047	1.48	0.026	0.012	0.89	10.03	14.85	1.76	0.04		0.01	0.03	0.09		0.028
E-13	ORNL/TM-7394	Pipe	GTA+1060C	16-8-2		1.3	0.053	1.57	0.014	0.014	0.49	9.42	16.18	1.95	0.04		0.01	0.06	0.13	0.001	0.041
F-14	ORNL/TM-7394	Pipe	GTA+1066C	16-8-2		5.8	0.026	1.57	0.02	0.009	0.51	11.62	17.88	2.08	0.08		0.01	0.18	0.17	0.001	0.037
G-15	ORNL/TM-7394	Pipe	GTA+1093C	316		0	0.051	1.5	0.026	0.021	0.53	12.68	16.19	2.17	0.05	0.01	0.02	0.23	0.27	0.002	0.059
G-16	ORNL/TM-7394	Pipe	Auto+1066C	none		0	0.055	1.46	0.027	0.023	0.49	12.67	16.33	2.15	0.05	0.01	0.02	0.22	0.27	0.002	0.062
H-22	ORNL/TM-7394	Pipe	SA+1066C	16-8-2		0	0.055	1.72	0.025	0.021	0.53	9.83	15.14	2.06	0.04		0.01	0.08	0.21	0.002	0.044
9234	ORNL/5945	Wire		16-8-2			0.038	1.86	0.037	0.013	0.45	8.59	15.88	2.05			0.19			0.0052	

Note: FN = Ferrite Number

							Chemistry in wt%													
Heat ID	Reference	Product	Process	Filler	Flux	FN	C	Mn	P	S	Si	Ni	Cr	Mo	V	Nb	Ti	Co	Cu	B	N
9236	ORNL/5945	Wire		16-8-2			0.038	2.07	0.03	0.14	0.48	8.45	16.1	2.03			0.16			0.0036	
9213	ORNL/5945	Plate	GTA	16-8-2			0.016	2.04	0.013	0.016	0.49	9.11	15.59	2.15			0.06			0.002	0.069
9234	ORNL/5945	Plate	GTA	16-8-2			0.02	1.76	0.031	0.014	0.49	9.3	15.43	2.18			0.18			0.002	0.057
9236	ORNL/5945	Plate	GTA	16-8-2			0.027	1.93	0.026	0.015	0.51	9.22	15.77	2.14			0.1			0.002	0.051
9206	ORNL/5945	Plate	SA	16-8-2	Arcos S-11		0.052	1.95	0.036	0.016	1.05	9.4	15.55	2.13			0.07			0.004	0.027
9213	ORNL/5945	Plate	SA	16-8-2	Arcos S-11		0.047	1.88	0.02	0.015	0.94	9.39	14.96	2.15			0.02			0.002	0.035
9234	ORNL/5945	Plate	SA	16-8-2	Arcos S-11		0.046	1.72	0.034	0.014	0.8	9.3	14.86	2.16			0.03			0.003	0.031
9235	ORNL/5945	Plate	SA	16-8-2	Arcos S-11		0.056	1.92	0.032	0.012	1.18	9.35	15.38	2.09			0.16			0.003	0.024
9236	ORNL/5945	Plate	SA	16-8-2	Arcos S-11		0.041	1.9	0.028	0.014	0.92	9.53	14.86	2.16			0.04			0.003	0.037
9237	ORNL/5945	Plate	SA	16-8-2	Arcos S-11		0.051	1.79	0.036	0.014	1.18	9.97	14.86	2.17			0.05			0.003	0.026
35047	ORNL/5945	Plate	SA	16-8-2	Arcos S-11		0.051	1.85	0.022	0.012	0.94	10.26	15.76	2.15			0.13			0.001	0.019
xxxxx	ORNL/5945	Plate	SA	16-8-2	Arcos S-4		0.056	1.95	0.022	0.012	1.4	9.63	16.97	2.09			0.1			0.001	0.019
35049	ORNL/5945	Plate	SA	16-8-2	Arcos S-11		0.054	1.88	0.042	0.01	0.87	9.54	15.71	2.15			0.06			0.001	0.017
2546B	ORNL/5945	Plate	SA	16-8-2	Arcos S-11		0.052	1.88	0.037	0.18	0.95	9.44	15.86	1.95			0.07			0.003	0.026

Note: FN = Ferrite Number

D.2 Data

Notes: C=cross-weld specimen, R=weld metal specimen, T=transverse orientation, L=longitudinal orientation

Heat/ ID No.	Weld No.	Temp (C)	Stress (MPa)	Rupture Life (hrs)	elong (%)	Reduction Area (%)	Min Creep Rate (%/hr)	Process	Filler	Reference	Comments
w1-3		593	207	2866.9	17.9		0.0024			TME 74-25	Booker analysis
w1-3		593	241	605.6	24		0.018			TME 74-25	Booker analysis
w1-3		593	255	251.1	32.7		0.059			TME 74-25	Booker analysis
w1-3		593	276	120.9	30.5		0.12			TME 74-25	Booker analysis
w1-4		593	241	832.6	19.6		0.014			TME 74-25	Booker analysis
w1-4		593	255	384.6	21.4		0.0343			TME 74-25	Booker analysis
w1-4		593	276	220.7	26.6		0.0666			TME 74-25	Booker analysis
w4-1		649	145	1775.4	10.9	27.4	0.0011			ORNL 5107	Booker analysis
w4-1		649	152	817.7	14.9	48.8	0.0029			ORNL 5107	Booker analysis
w4-1		649	162	843.9	27.6	47.2	0.0028			ORNL 5107	Booker analysis
w4-1		649	172	328.5	16.6	64.5	0.00616			ORNL 5107	Booker analysis
w4-1		649	193	126.9	19.6	51.6	0.03			ORNL 5107	Booker analysis
w4-2		649	124	1204	43.7	54.8	0.0518			ORNL 5107	Booker analysis
w4-2		649	172	97.1	25.6	67.8	0.075			ORNL 5107	Booker analysis
w4-2		649	138	431.8	34.4	73	0.016			ORNL 5107	Booker analysis
w4-3		649	138	435	31.7	59	0.013			ORNL 5107	Booker analysis
w4-3		649	138	1339.3	21.7	56.3	0.028			ORNL 5107	Booker analysis
w4-3		649	152	804.2	21.6	53.6	0.003			ORNL 5107	Booker analysis
w4-3		649	172	74.6	20.5	45.7	0.07			ORNL 5107	Booker analysis
w4-3		649	172	190.4	29.6	47.7	0.008			ORNL 5107	Booker analysis
w4-3		649	193	28.4	34.9	68.4	0.33			ORNL 5107	Booker analysis
w4-4		649	152	3204.9	8.2	14.6	0.00046			ORNL 5107	Booker analysis
w4-4		649	172	791.6	11.9	55.6	0.001			ORNL 5107	Booker analysis
w4-4		649	193	358.5	12.5	50.6	0.004			ORNL 5107	Booker analysis
w4-4		649	207	127.2	26.5	44.5	0.021			ORNL 5107	Booker analysis
w4-5		649	172	1630.6	53.3	52.6				ORNL 5107	Booker analysis
w4-5		649	193	396.5	42.5	51.7				ORNL 5107	Booker analysis
w4-5		649	207	171.9	52.1	50.8				ORNL 5107	Booker analysis
w4-6		649	172	767.7	22.2	47.4	0.00085			ORNL 5107	Booker analysis
w4-6		649	193	262.1	28.8	33.8				ORNL 5107	Booker analysis
w4-6		649	207	175.3	24.9	40.3	0.0275			ORNL 5107	Booker analysis

Heat/ ID No.	Weld No.	Temp (C)	Stress (MPa)	Rupture Life (hrs)	elong (%)	Reduction Area (%)	Min Creep Rate (%/hr)	Process	Filler	Reference	Comments
13-4		593	207	728	2.3		0.00073				Booker analysis
13-4		593	241	103.4	11.5		0.041				Booker analysis
13-4		593	276	45.3	6.2		0.091				Booker analysis
13-4		593	310	7.2	18.8		1.25				Booker analysis
17-1		482	379	8261	20.5	19.2	0.000093			ORNL 5107	Booker analysis
17-1		593	207	11896.5	17.9	28				ORNL 5107	Booker analysis
17-1		649	152	3602.4	40.1	63.3				ORNL 5107	Booker analysis
17-1		649	172	513	30.1	70				ORNL 5107	Booker analysis
17-1		649	193	107.1	55	64.5				ORNL 5107	Booker analysis
18-1		482	310	14402.5							Booker analysis
18-1		482	345	18863.5	37.5	51.5					Booker analysis
18-1		482	379	2047.1	40.7	52					Booker analysis
18-1		593	172	5600	10.9	7.1					Booker analysis
18-1		593	207	563.3	42.5	48.5					Booker analysis
18-1		593	241	91.6	60.6	61.8					Booker analysis
18-1		649	110	5671.8	23.7	28.4					Booker analysis
18-1		649	124	1703.2	29.8	41.5					Booker analysis
18-1		649	138	756.6	47.6	44.8					Booker analysis
18-1		649	152	722.6	19.8	31	0.0017				Booker analysis
18-1		649	172	104.3	62.9	52.7					Booker analysis
18-1		649	172	176.8	45.7	50.2					Booker analysis
18-1		649	193	68.6	41	56.6	0.0617				Booker analysis
18-1		649	172	1267.2	17.9	34.6					Booker analysis
18-2		649	152	1485.7	37.6	52.2	0.0017				Booker analysis
18-2		649	172	844.5	43.9	44.9	0.0049				Booker analysis
18-2		649	193	138.5	55.5	50.3					Booker analysis
18-2		649	207	132	39.9	54.7	0.0676				Booker analysis
18-2		649	322	0.4	45.8	55.9					Booker analysis
18-3		649	172	954.6	39.1	56.8					Booker analysis
18-3		649	193	810.6	18.1	44.5	0.0017				Booker analysis
18-3		649	207	81	38.6	49.6	0.055				Booker analysis
18-4		649	138	432.2	9.8	21.3	0.0061				Booker analysis
18-4		649	152	230.5	10.5	29	0.014				Booker analysis
18-4		649	152	406.1	33.2	54.7	0.011				Booker analysis
18-4		649	172	241	27.6	60.4	0.0085				Booker analysis

Heat/ ID No.	Weld No.	Temp (C)	Stress (MPa)	Rupture Life (hrs)	elong (%)	Reduction Area (%)	Min Creep Rate (%/hr)	Process	Filler	Reference	Comments
18-5		649	138	2590.5	27	65.6	0.00026				Booker analysis
18-5		649	152	356.8	36	56.3	0.0102				Booker analysis
18-5		649	152	531.8	25.6	69.7	0.0022				Booker analysis
18-5		649	172	113.2	30	60.7	0.042				Booker analysis
18-5		649	172	114.7	24.9	64.7	0.015				Booker analysis
22-1		566	241	899.2	31	53.1	0.00725				Booker analysis
22-1		566	276	126.5	43.6	63.9	0.068				Booker analysis
22-1		566	276	195.1	35.2	49.8	0.051				Booker analysis
22-1		649	110	1963.5	26.7	29.2	0.00188				Booker analysis
22-1		649	110	2069.6	39	44.8	0.00146				Booker analysis
22-1		649	138	321.2	47.7	63.4	0.00976				Booker analysis
22-1		649	138	326.8	49.3	49.3	0.0211				Booker analysis
22-2		566	221	3022.6	29.3	34.1	0.0015				Booker analysis
22-2		566	241	1182.9	26.2	39.3	0.0043				Booker analysis
22-2		566	241	2338.9	23.7	50.6	0.0015				Booker analysis
22-2		566	276	206.8	32.8	53.6	0.0334				Booker analysis
22-2		566	276	216.5	26.9	35.1	0.0303				Booker analysis
22-2		566	310	66.2	31.6	55.1	0.142				Booker analysis
22-2		566	310	103.2	45.7	32.3	0.105				Booker analysis
22-2		649	110	2574.1	21.4	31.5	0.00204				Booker analysis
22-2		649	110	3969	21.2	29.5	0.00062				Booker analysis
22-2		649	138	618.7	47.8	55	0.0128				Booker analysis
22-2		649	138	728.5	25.4	38.4	0.0105				Booker analysis
22-2		649	172	68.2	43	60	0.0939				Booker analysis
22-2		649	172	109.1	45.3	50	0.119				Booker analysis
22-2		649	221	12.2	87.6	46.2	1.5				Booker analysis
22-3		566	207	3148.4	25.8	39.3	0.00063				Booker analysis
22-3		566	207	3655.4	15.4	24.3	0.00095				Booker analysis
22-3		566	221	545.8	15	21.9	0.0086				Booker analysis
22-3		566	241	429.1	20.9	27.2	0.0207				Booker analysis
22-3		566	241	431.3	24.2	35.9	0.0178				Booker analysis

Heat/ ID No.	Weld No.	Temp (C)	Stress (MPa)	Rupture Life (hrs)	elong (%)	Reduction Area (%)	Min Creep Rate (%/hr)	Process	Filler	Reference	Comments
22-3		566	276	80.3	19.9	27.3	0.069				Booker analysis
22-3		566	276	158.6	23.3	32.1	0.0909				Booker analysis
22-3		649	110	2901.6	41.4	43.3	0.00145				Booker analysis
22-3		649	124	859.9	59.4	67.1	0.00425				Booker analysis
22-3		649	138	325.7	49.5	59.7	0.035				Booker analysis
22-3		649	138	369.6	45.2	61.6	0.011				Booker analysis
22-3		649	172	34.1	53.7	65.8	0.213				Booker analysis
22-3		649	172	70.9	50.4	61.9	0.07				Booker analysis
22-4		566	241	699.8	26.2	62	0.0158			ORNL 5218	Booker analysis
22-4		556	276	174	40.3	38				ORNL 5218	Booker analysis
22-4		566	276	209.3	23.3	29.3	0.1			ORNL 5218	Booker analysis
22-4		566	310	78.8	34.7	36.2	0.088			ORNL 5218	Booker analysis
22-4		649	110	3401.6	39.8	51	0.00105			ORNL 5218	Booker analysis
22-4		649	110	3656	52.4	62.3	0.0026			ORNL 5218	Booker analysis
22-4		649	138	478.5	42.5	54	0.047			ORNL 5218	Booker analysis
22-4		649	138	609.4	44.2	56.1	0.0085			ORNL 5218	Booker analysis
22-5		566	207	6324.8	8.9	10	0.00041				Booker analysis
22-5		566	207	6696	6.2	17.3	0.00022				Booker analysis
22-5		566	241	820.7	25.3	36.3	0.0069				Booker analysis
22-5		566	310	45.8	44.1	45.6	0.296				Booker analysis
22-5		649	172	31.5	44.2	58.3	0.072				Booker analysis
22-5		649	172	73.9	48.5	50.1	0.0822				Booker analysis
23-1		566	207	42500	36	50.4				ORNL 5660	Booker analysis
23-1		566	241	2451.5	45	48.9	0.0062			ORNL 5660	Booker analysis
23-1		566	276	316.7	54.5	41.3	0.0525			ORNL 5660	Booker analysis
23-1		649	124	9208	42.4	59.2	0.0002			ORNL 5660	Booker analysis
23-1		649	138	796	50.8	62.7	0.0211			ORNL 5660	Booker analysis
23-1		649	155	571.9	46.3	77.2	0.0626			ORNL 5660	Booker analysis
23-1		649	172	157.3	53.7	63.7	0.145			ORNL 5660	Booker analysis

Heat/ ID No.	Weld No.	Temp (C)	Stress (MPa)	Rupture Life (hrs)	elong (%)	Reduction Area (%)	Min Creep Rate (%/hr)	Process	Filler	Reference	Comments
23-2		566	241	3408.9	22.4	46.5	0.00177			ORNL 5660	Booker analysis
23-2		566	259	1661.9	31.7	50.3	0.00588			ORNL 5660	Booker analysis
23-2		566	259	13200	33.3	38.7				ORNL 5660	Booker analysis
23-2		566	276	464.6	39.6	58.3	0.0248			ORNL 5660	Booker analysis
23-2		566	276	539.2	41.7	51.6	0.0226			ORNL 5660	Booker analysis
23-2		566	293	294.8	35	47.8	0.037			ORNL 5660	Booker analysis
23-2		649	138	2865.1	30.7	68.8	0.000585			ORNL 5660	Booker analysis
23-2		649	155	1195	38	69.6	0.00455			ORNL 5660	Booker analysis
23-2		649	172	266.7	41	71.2	0.0416			ORNL 5660	Booker analysis
23-2		649	190	86.1	57.2	50.2	0.146			ORNL 5660	Booker analysis
23-2		649	207	42.3	47.1	63.8	0.468			ORNL 5660	Booker analysis
24-1		538	310	1750.9	16	15.6	0.0016				Booker analysis
24-1		538	379	209.4	34	42.9	0.022				Booker analysis
24-1		649	152	854.4	42.8	70.1	0.0103				Booker analysis
24-1		649	207	65.7	46.3	57.3	0.34				Booker analysis
24-2		538	310	649.7	28.2	46.2	0.0087				Booker analysis
24-2		649	125	618.6	62.4	74.8	0.0425				Booker analysis
24-2		649	207	15.9	50.7	71	1.475				Booker analysis
24-5		649	152	247.9	14.4	28.7	0.0254				Booker analysis
24-5		649	207	12.7	16.9	23.9	0.695				Booker analysis
24-5		538	310	464	20	20.9	0.0025				Booker analysis
24-5		538	379	565.8	29.6	33.5	0.00575				Booker analysis

Heat/ ID No.	Weld No.	Temp (C)	Stress (MPa)	Rupture Life (hrs)	elong (%)	Reduction Area (%)	Min Creep Rate (%/hr)	Process	Filler	Reference	Comments
FFTF 1		566	241	2451.5	45	49	0.0062	gta		ORNL-5594	
FFTF 1		566	276	316.7	54.5	41	0.052	gta		ORNL-5594	
FFTF 1		649	124	9208	42	59	0.0002	gta		ORNL-5594	
FFTF 1		649	138	796.7	51	63	0.0211	gta		ORNL-5594	
FFTF 1		649	155	517.9	46	77	0.0626	gta		ORNL-5594	
FFTF 1		649	172	157.3	54	64	0.145	gta		ORNL-5594	
FFTF 1cw		566	241	4666.3	14	45	0.00105	gta		ORNL-5594	cross-weld
FFTF 1cw		566	276	883.1	11.4	50	0.00535	gta		ORNL-5594	cross-weld
FFTF 1cw		566	310	272	10.5	39.5	0.00888	gta		ORNL-5594	cross-weld
FFTF 1cw		566	310	163.6	17	45	0.0223	gta		ORNL-5594	cross-weld
FFTF 1cw		566	345	89.3	20	49	0.0228	gta		ORNL-5594	cross-weld
FFTF 1cw		649	138	2917.9	18	35	0.00276	gta		ORNL-5594	cross-weld
FFTF 1cw		649	138	2938.9	23	57	0.00238	gta		ORNL-5594	cross-weld
FFTF 1cw		649	155	1135.1	19	55	0.0056	gta		ORNL-5594	cross-weld
FFTF 1cw		649	175	397.7	18	47	0.02	gta		ORNL-5594	cross-weld
FFTF 1cw		649	172	272.5	18	74	0.018	gta		ORNL-5594	cross-weld
FFTF 1cw		649	207	48.1	18	61	0.154	gta		ORNL-5594	cross-weld
FFTF 2		566	241	3408.9	22	46.5	0.00177	gta		ORNL-5594	
FFTF 2		566	259	1661.9	32	50	0.00588	gta		ORNL-5594	
FFTF 2		566	276	464.6	40	58	0.0248	gta		ORNL-5594	
FFTF 2		566	276	539.2	42	52	0.0226	gta		ORNL-5594	
FFTF 2		566	293	294.8	35	48	0.037	gta		ORNL-5594	
FFTF 2		649	138	2865.1	31	69	0.000585	gta		ORNL-5594	
FFTF 2		649	155	1195	38	70	0.00455	gta		ORNL-5594	
FFTF 2		649	172	266.7	41	71	0.0416	gta		ORNL-5594	
FFTF 2		649	190	86.1	57	50	0.146	gta		ORNL-5594	
FFTF 2		649	207	42.3	47	64	0.468	gta		ORNL-5594	

Heat/ ID No.	Weld No.	Temp (C)	Stress (MPa)	Rupture Life (hrs)	elong (%)	Reduction Area (%)	Min Creep Rate (%/hr)	Process	Filler	Reference	Comments
2546	v235	649	155.1	13440	13.46	40.98	0.0001	gta		ORNL-5945	
2546	v235-2	649	189.6	3285	10.98	52.15	0.0024	gta		ORNL-5945	
2546	v235-3	649	241.3	363	41.77	15.71	0.0125	gta		ORNL-5945	
35047	v172-1	649	241.3	19	46.22	64.27	0.0428	gta		ORNL-5945	
35047	v172-2	649	172.4	904	25.91	47.13	0.00475	gta		ORNL-5945	
35047	v172-3	649	124.1	8125	32.27	45.02	0.0004	gta		ORNL-5945	
35049	v174-1	649	241.3	81	24.36	39.43	0.0545	gta		ORNL-5945	
35049	v174-2	649	241.3	114	34.62	51.72	0.0475	gta		ORNL-5945	
35049	v174-3	649	155.1	2904	19.84	31.13	0.0017	gta		ORNL-5945	
35047	e13-1	649	172.4	184	23.64	75.7	0.013	sa		ORNL-5945	
35047	e13-2	649	206.8	11	25.09	60.63	0.12	sa		ORNL-5945	
35047	e13-3	649	137.9	1287	31.38	70	0.00081	sa		ORNL-5945	
35047	e13-4	649	103.4	17719	4.98	8.57	0.000032	sa		ORNL-5945	
35047	e14.1	649	172.4	39	34.76	66.09	0.11	sa		ORNL-5945	
35047	e14.2	649	137.9	1157	22.31	33.41	0.00213	sa		ORNL-5945	
35047	e14-3	649	155.1	212	23.66	63.64	0.0084	sa		ORNL-5945	
35047	e14-4	649	103.8	14855	3.4	5.35	0.0001	sa		ORNL-5945	
35049	e18-1	649	172.4	123	27.82	60.14	0.14	sa		ORNL-5945	
35049	e18-2	649	137.9	2661	12.25	25.25	0.0002	sa		ORNL-5945	
35049	e18-3	649	103.4	10409	17.02	41.23	0.000151	sa		ORNL-5945	
9236	e42-1	649	120.7	1330	32.98	76.73	0.014	sa		ORNL-5945	
9236	e42-3	649	103.7	9345	40.13	63.38	0.0001	sa		ORNL-5945	
9236	e42-4	649	137.9	1053	43.9	75.6	0.0223	sa		ORNL-5945	
9236	e42-5	649	172.4	43	29.96	79.73		sa		ORNL-5945	
9237	e43-1	649	120.7	3552	33.88	69.52	0.0013	sa		ORNL-5945	
9237	e43-2	649	144.8	1002	24.8	69.68	0.0982	sa		ORNL-5945	
9237	e43-3	649	172.4	84	23.5	67.63	0.01	sa		ORNL-5945	

Heat/ ID No.	Weld No.	Temp (C)	Stress (MPa)	Rupture Life (hrs)	elong (%)	Reduction Area (%)	Min Creep Rate (%/hr)	Process	Filler	Reference	Comments
9206	e44-1	649	120.7	3437	24.93	69.11	0.0008	sa		ORNL-5945	
9206	e44-2	649	137.9	16242	34.69		0.0002	sa		ORNL-5945	
9206	e44-3	649	179.3	86	27.78	66.93	0.005	sa		ORNL-5945	
9213	e41-2	649	120.7	788	52.3	66.57	0.0261	sa		ORNL-5945	
9213	e41-4	649	96.5	4184	49.53	78.05	0.0046	sa		ORNL-5945	
9213	e41-6	649	137.9	457	30.22	65.35	0.011	sa		ORNL-5945	
9234	e39-1	649	120.7	3242	40.9	73.46	0.0047	sa		ORNL-5945	
9234	e39-2	649	144.8	828	27.39	68.7	0.0183	sa		ORNL-5945	
9234	e39-3	649	172.4	109	30.13	66.79	0.12	sa		ORNL-5945	
9235	e34-2	649	144.8	2036	20.31	46.38	0.0013	sa		ORNL-5945	
9235	e34-3	649	179.3	1999	11.73	47.35	0.001	sa		ORNL-5945	
9235	e34-4	649	120.7	8785	22.49	57.44	0.0003	sa		ORNL-5945	
9235	e34-5	649	206.8	61	19.64	71.71	0.092	sa		ORNL-5945	
9213	v181-1	649	155.1	5542	8.87	37.24	0.00018	gta		ORNL-5945	
9213	v181-2	649	189.6	1369	16.71	48.6		gta		ORNL-5945	
9213	v181-3	649	241.3	50	26.93	58.66	0.09	gta		ORNL-5945	
9234	v180-1	649	155.1	6964	4.31	11.62	0.00019	gta		ORNL-5945	
9234	v180-2	649	189.6	1522	8.8	47.05	0.00032	gta		ORNL-5945	
9234	v180-3	649	241.3	113	10.4	50.45	0.0066	gta		ORNL-5945	
9236	v182-1	649	155.1	3245	8	24.51	0.00023	gta		ORNL-5945	
9236	v182-2	649	189.6	881	11.91	36.48	0.0004	gta		ORNL-5945	
9236	v182-3	649	241.3	23	13.78	50.42	0.0925	gta		ORNL-5945	
9237	v184-1	649	155.1	4518	4.13	4.62	0.00026	gta		ORNL-5945	
9237	v184-2	649	189.6	1598	5.87	6.22	0.00103	gta		ORNL-5945	
9237	v184-3	649	241.3	327	9.51	20.78		gta		ORNL-5945	

Heat/ ID No.	Weld No.	Temp (C)	Stress (MPa)	Rupture Life (hrs)	elong (%)	Reduction Area (%)	Min Creep Rate (%/hr)	Process	Filler	Reference	Comments
77-15		566	207					sa	16-8-2	ORNL-5594	C
77-15		566	241	899.2	31	53.1	0.00725	sa	16-8-2	ORNL-5594	C
77-15		566	276	195.1	35.2	49.8	0.051	sa	16-8-2	ORNL-5594	C
77-15		566	276	126.5	43.6	63.9	0.06795	sa	16-8-2	ORNL-5594	R
77-15		649	110	1963.5	26.7	29.2	0.00188	sa	16-8-2	ORNL-5594	C
77-15		649	138	326.8	49.3	49.3	0.0211	sa	16-8-2	ORNL-5594	C
77-15		649	110	2069.6	39	44.8	0.00146	sa	16-8-2	ORNL-5594	R
77-15		649	138	321.2	47.7	63.4	0.00976	sa	16-8-2	ORNL-5594	R
77-16		566	220	3022.6	29.3	34.1	0.0015	sa	16-8-2	ORNL-5594	C
77-16		566	241	1182.9	26.2	39.3	0.0043	sa	16-8-2	ORNL-5594	C
77-16		566	276	216.5	26.9	35.1	0.0303	sa	16-8-2	ORNL-5594	C
77-16		566	310	103.2	45.7	32.3	0.105	sa	16-8-2	ORNL-5594	C
77-16		566	241	2338.9	23.7	50.6	0.0015	sa	16-8-2	ORNL-5594	R
77-16		566	276	206.8	32.8	53.6	0.0334	sa	16-8-2	ORNL-5594	R
77-16		566	310	66.2	31.6	55.1	0.142	sa	16-8-2	ORNL-5594	R
77-16		649	110	2574.1	21.4	31.5	0.00204	sa	16-8-2	ORNL-5594	C
77-16		649	138	728.5	25.4	38.4	0.0105	sa	16-8-2	ORNL-5594	C
77-16		649	172	109.1	45.3	50	0.119	sa	16-8-2	ORNL-5594	C
77-16		649	220	12.2	87.6	46.2	1.5	sa	16-8-2	ORNL-5594	C
77-16		649	110	3969	21.2	29.2	0.000625	sa	16-8-2	ORNL-5594	R
77-16		649	138	618.7	47.8	58	0.0128	sa	16-8-2	ORNL-5594	R
77-16		649	172	68.2	43	60	0.0939	sa	16-8-2	ORNL-5594	R

Heat/ ID No.	Weld No.	Temp (C)	Stress (MPa)	Rupture Life (hrs)	elong (%)	Reduction Area (%)	Min Creep Rate (%/hr)	Process	Filler	Reference	Comments
77-17		566	207	3148.4	25.8	39.3	0.00063	sa	16-8-2	ORNL-5594	C
77-17		566	221	545.8	15	21.9	0.0086	sa	16-8-2	ORNL-5594	C
77-17		566	241	429.1	20.9	27.2	0.0207	sa	16-8-2	ORNL-5594	C
77-17		566	276	80.3	19.9	27.3	0.069	sa	16-8-2	ORNL-5594	C
77-17		566	207	3655.4	15.4	24.3	0.00095	sa	16-8-2	ORNL-5594	R
77-17		566	241	431.3	24.2	35.9	0.0178	sa	16-8-2	ORNL-5594	R
77-17		566	276	158.6	23.3	32.1	0.0909	sa	16-8-2	ORNL-5594	R
77-17		649	110	2901.6	41.4	43.3	0.00145	sa	16-8-2	ORNL-5594	C
77-17		649	124	859.9	59.4	67.1	0.00425	sa	16-8-2	ORNL-5594	C
77-17		649	138	325.7	49.5	59.7	0.035	sa	16-8-2	ORNL-5594	C
77-17		649	172	34.1	53.7	65.8	0.213	sa	16-8-2	ORNL-5594	C
77-17		649	138	369.9	45.2	61.6	0.011	sa	16-8-2	ORNL-5594	R
77-17		649	172	70.9	50.4	61.9	0.07	sa	16-8-2	ORNL-5594	R
E-13		538	310	1750	16.03	15.56	0.0016	gta	16-8-2	ORNL/TM-7394	L
E-13		538	310	1619.1	14.4	32.64	0.00068	gta	16-8-2	ORNL/TM-7394	T
E-13		538	379	209.4	34.04	42.9	0.022	gta	16-8-2	ORNL/TM-7394	L
E-13		538	379	209.4	21.72	24.98	0.0072	gta	16-8-2	ORNL/TM-7394	T
E-13		649	152	854.4	42.78	70.07	0.0103	gta	16-8-2	ORNL/TM-7394	L
E-13		649	152	1368.9	21.6	56.81	0.0054	gta	16-8-2	ORNL/TM-7394	T
E-13		649	207	65.7	46.27	57.32	0.34	gta	16-8-2	ORNL/TM-7394	L
E-13		649	207	107.1	26.64	54.07	0.1355	gta	16-8-2	ORNL/TM-7394	T
F-14		538	310	649.7	28.18	46.16	0.0087	gta	16-8-2	ORNL/TM-7394	L
F-14		538	310	1164.7	24	47.95	0.0022	gta	16-8-2	ORNL/TM-7394	T
F-14		538	379	42.6	35.05	64.11	0.0266	gta	16-8-2	ORNL/TM-7394	T
F-14		649	152	618.6	62.4	74.78	0.0425	gta	16-8-2	ORNL/TM-7394	L
F-14		649	152	502.5	23.2	75.08	0.016	gta	16-8-2	ORNL/TM-7394	T
F-14		649	207	15.9	50.74	70.98	1.475	gta	16-8-2	ORNL/TM-7394	L

Heat/ ID No.	Weld No.	Temp (C)	Stress (MPa)	Rupture Life (hrs)	elong (%)	Reduction Area (%)	Min Creep Rate (%/hr)	Process	Filler	Reference	Comments
F-14		649	207	24.1	23.04	61.4	0.436	gta	16-8-2	ORNL/TM-7394	T
G-15		538	310	2091.9	15.18	19.52	0.00013	gta	316-SS	ORNL/TM-7394	L
G-15		538	310	1602.3	15.2	28.15	0.00007	gta	316-SS	ORNL/TM-7394	T
G-15		538	379	539.8	29.6	23.9	0.0012	gta	316-SS	ORNL/TM-7394	L
G-15		538	379	444.9	27.2	33.75	0.00075	gta	316-SS	ORNL/TM-7394	T
G-15		649	152	6990.7	25.61	64.82	0.00017	gta	316-SS	ORNL/TM-7394	L
G-15		649	152	6329.1	20.8	48.03	0.00013	gta	316-SS	ORNL/TM-7394	T
G-15		649	207	189.2	4.8	10.74	0.0128	gta	316-SS	ORNL/TM-7394	L
G-15		649	207	117.5	10.4	16.02	0.0233	gta	316-SS	ORNL/TM-7394	T
G-16		538	310	1572.5	20	27.12	0.00018	gta	autogenous	ORNL/TM-7394	L
G-16		538	310	1875.1	16	27.51	0.00005	gta	autogenous	ORNL/TM-7394	T
G-16		538	379	374.8	33.6	34.7	0.00187	gta	autogenous	ORNL/TM-7394	L
G-16		538	379	456.7	26.4	35.62	0.00068	gta	autogenous	ORNL/TM-7394	T
G-16		649	152	6263.9	25.6	54.48	0.0002	gta	autogenous	ORNL/TM-7394	L
G-16		649	152	5700.9	18.4	51.36	0.00022	gta	autogenous	ORNL/TM-7394	T
G-16		649	207	89.8	18.4	22.54	0.054	gta	autogenous	ORNL/TM-7394	L
G-16		649	207	73.3	11.2	28.98	0.0305	gta	autogenous	ORNL/TM-7394	T
H-22		538	310	464	20	20.89	0.0025	sa	16-8-2	ORNL/TM-7394	L
H-22		538	310	660.2	17.18	17.36	0.00073	sa	16-8-2	ORNL/TM-7394	T
H-22		538	379	565.8	29.6	33.48	0.00575	sa	16-8-2	ORNL/TM-7394	L
H-22		538	379	152.6	20.75	24.7	0.0081	sa	16-8-2	ORNL/TM-7394	T
H-22		649	152	247.9	14.4	28.7	0.0254	sa	16-8-2	ORNL/TM-7394	L
H-22		649	152	418.1	9.95	36.33	0.00865	sa	16-8-2	ORNL/TM-7394	T
H-22		649	207	12.7	16.87	23.86	0.695	sa	16-8-2	ORNL/TM-7394	L
H-22		649	207	20.6	10.33	30.67	0.215	sa	16-8-2	ORNL/TM-7394	T

APPENDIX E: 800H

Notes: BMF = Base Metal Failure, D = Discontinued Test Prior to Failure

ITEM	Temperature (C)	Stress (MPa)	Time to Rupture (hrs)	Elong. (%)	Red. Of Area (%)	Min. Creep Rate (%/hr)	Process	Filler Metal	Reference	Specimen Type	Comment
INCO	538	414	100				SMA	ALLOY A	INCO	WELD METAL	
INCO	538	352	1000				SMA	ALLOY A	INCO	WELD METAL	
INCO	538	269	10000				SMA	ALLOY A	INCO	WELD METAL	
INCO	649	241	100				SMA	ALLOY A	INCO	WELD METAL	
INCO	649	169	1000				SMA	ALLOY A	INCO	WELD METAL	
INCO	649	110	10000				SMA	ALLOY A	INCO	WELD METAL	
INCO	760	114	100				SMA	ALLOY A	INCO	WELD METAL	
INCO	760	76	1000				SMA	ALLOY A	INCO	WELD METAL	
INCO	760	49	10000				SMA	ALLOY A	INCO	WELD METAL	
INCO	871	48	100				SMA	ALLOY A	INCO	WELD METAL	
INCO	871	25	1000				SMA	ALLOY A	INCO	WELD METAL	
INCO	871	13	10000				SMA	ALLOY A	INCO	WELD METAL	
INCO	982	16	100				SMA	ALLOY A	INCO	WELD METAL	
INCO	982	6	1000				SMA	ALLOY A	INCO	WELD METAL	
HEM-1	482	482	47	42	39	0.027	SMA	ALLOY A	McCoy & King	WELD METAL	TM-8728
HEM-1	538	414	436	24	29	0.006	SMA	ALLOY A	McCoy & King	WELD METAL	TM-8728
HEM-1	649	241	177	41	58	0.079	SMA	ALLOY A	McCoy & King	WELD METAL	TM-8728
HEM-1	649	172	1675	26	54	0.011	SMA	ALLOY A	McCoy & King	WELD METAL	TM-8728
HEM-1	649	103	16900D			0.0000025	SMA	ALLOY A	McCoy & King	WELD METAL	TM-8728
HEM-1	760	138	27	53	45	0.22	SMA	ALLOY A	McCoy & King	WELD METAL	TM-8728
HEM-1	760	103	139	30	34	0.055	SMA	ALLOY A	McCoy & King	WELD METAL	TM-8728
HEM-1	760	69	1330	2.8	1.9	0.00045	SMA	ALLOY A	McCoy & King	WELD METAL	TM-8728
HEM-1	482	414	15373 BMF 800H				SMA	ALLOY A	McCoy & King	HAST X/A/800H CROSS WELD	TM-8728
HEM-1	538	414	340 BMF 800H				SMA	ALLOY A	McCoy & King	HAST X/A/800H CROSS WELD	TM-8728
HEM-1	538	345	5721 BMF 800H				SMA	ALLOY A	McCoy & King	HAST X/A/800H CROSS WELD	TM-8728
HEM-1	649	241	186 BMF 800H				SMA	ALLOY A	McCoy & King	HAST X/A/800H CROSS WELD	TM-8728
HEM-1	649	172	2189 BMF 800H				SMA	ALLOY A	McCoy & King	HAST X/A/800H CROSS WELD	TM-8728

ITEM	Temperature (C)	Stress (MPa)	Time to Rupture (hrs)	Elong. (%)	Red. Of Area (%)	Min. Creep Rate (%/hr)	Process	Filler Metal	Reference	Specimen Type	Comment
HEM-1	482	414	11555 BMF 800H				GTA	ALLOY 82	McCoy & King	HAST X/82/800H CROSS WELD	TM-8728
HEM-1	538	414	315 BMF 800H				GTA	ALLOY 82	McCoy & King	HAST X/82/800H CROSS WELD	TM-8728
HEM-1	538	345	3266 BMF 800H				GTA	ALLOY 82	McCoy & King	HAST X/82/800H CROSS WELD	TM-8728
HEM-1	649	241	163 BMF 800H				GTA	ALLOY 82	McCoy & King	HAST X/82/800H CROSS WELD	TM-8728
HEM-1	649	172	2318 BMF 800H				GTA	ALLOY 82	McCoy & King	HAST X/82/800H CROSS WELD	TM-8728
BMI-Cross	816	75.8	48				SMA	ALLOY A	BMI	INCO A CROSS WELD	
BMI-Cross	816	54.5	340				SMA	ALLOY A	BMI	INCO A CROSS WELD	
BMI-Cross	816	40.7	1200				SMA	ALLOY A	BMI	INCO A CROSS WELD	
BMI-Cross	816	29	3900				SMA	ALLOY A	BMI	INCO A CROSS WELD	
BMI-Cross	927	27.6	48				SMA	ALLOY A	BMI	INCO A CROSS WELD	
BMI-Cross	927	15.2	400				SMA	ALLOY A	BMI	INCO A CROSS WELD	
BMI-Cross	927	9.7	2500				SMA	ALLOY A	BMI	INCO A CROSS WELD	
BMI-Cross	927	6.8	12000				SMA	ALLOY A	BMI	INCO A CROSS WELD	

ITEM	Temperature (C)	Stress (MPa)	Time to Rupture (hrs)	Elong. (%)	Red. Of Area (%)	Min. Creep Rate (%/hr)	Process	Filler Metal	Reference	Specimen Type	Comment
tm12438	538	345	9690D				GTA	ALLOY 82	McCoy	ALLOY 82 WELD METAL	TM12438
tm12438	538	448	178D				GTA	ALLOY 82	McCoy	ALLOY 82 WELD METAL	TM12438
tm12438	593	207	5505D				GTA	ALLOY 82	McCoy	ALLOY 82 WELD METAL	TM12438
tm12438	593	276	1662D				GTA	ALLOY 82	McCoy	ALLOY 82 WELD METAL	TM12438
tm12438	649	138	1453D				GTA	ALLOY 82	McCoy	ALLOY 82 WELD METAL	TM12438
tm12438	649	207	1069.6	7	15	0.00375	GTA	ALLOY 82	McCoy	ALLOY 82 WELD METAL	TM12438
tm12438	704	103	9767	3.9			GTA	ALLOY 82	McCoy	ALLOY 82 WELD METAL	TM12438
tm12438	704	138	1507D				GTA	ALLOY 82	McCoy	ALLOY 82 WELD METAL	TM12438
tm12438	760	68.9	6840	0.9			GTA	ALLOY 82	McCoy	ALLOY 82 WELD METAL	TM12438
tm12438	760	103	347	20	36	0.0205	GTA	ALLOY 82	McCoy	ALLOY 82 WELD METAL	TM12438
tm12438	816	55	1364				GTA	ALLOY 82	McCoy	ALLOY 82 WELD METAL	TM12438
tm12438	816	68.9	391				GTA	ALLOY 82	McCoy	ALLOY 82 WELD METAL	TM12438
tm12438	538	345	576				GTA	ALLOY 82	McCoy	ALLOY 82 CROSS WELD	tm12438
tm12438	538	345	1332				GTA	ALLOY 82	McCoy	ALLOY 82 CROSS WELD	tm12438
tm12438	538	345	550.3				GTA	ALLOY 82	McCoy	ALLOY 82 CROSS WELD	tm12438
tm12438	593	309	576.6				GTA	ALLOY 82	McCoy	ALLOY 82 CROSS WELD	tm12438
tm12438	593	276	760				GTA	ALLOY 82	McCoy	ALLOY 82 CROSS WELD	tm12438
tm12438	649	138	2420D				GTA	ALLOY 82	McCoy	ALLOY 82 CROSS WELD	tm12438
tm12438	704	103	1399				GTA	ALLOY 82	McCoy	ALLOY 82 CROSS WELD	tm12438
tm12438	704	103	2421D				GTA	ALLOY 82	McCoy	ALLOY 82 CROSS WELD	tm12438
tm12438	760	68.9	3450				GTA	ALLOY 82	McCoy	ALLOY 82 CROSS WELD	tm12438
tm12438	760	103	288				GTA	ALLOY 82	McCoy	ALLOY 82 CROSS WELD	tm12438
tm12438	816	55	1159				GTA	ALLOY 82	McCoy	ALLOY 82 CROSS WELD	tm12438
tm12438	816	55	1082				GTA	ALLOY 82	McCoy	ALLOY 82 CROSS WELD	tm12438

ITEM	Temperature (C)	Stress (MPa)	Time to Rupture (hrs)	Elong. (%)	Red. Of Area (%)	Min. Creep Rate (%/hr)	Process	Filler Metal	Reference	Specimen Type	Comment
TM9108	649	207	1070	24	20	0.011	GTA	ALLOY 82	King & McCOY	ALLOY 82 WELD	TM-9108
TM9108	649	207	930	19	27	0.0082	GTA	ALLOY 82	King & McCOY	ALLOY 82 WELD	TM-9108
TM9108	649	241	802	27	17	0.014	GTA	ALLOY 82	King & McCOY	ALLOY 82 WELD	TM-9108
TM9108	649	241	1032	41	40	0.017	GTA	ALLOY 82	King & McCOY	ALLOY 82 WELD	TM-9108
TM9108	649	241	420	22	24	0.035	GTA	ALLOY 82	King & McCOY	ALLOY 82 WELD	TM-9108
TM9108	649	241	307	18	26	0.041	GTA	ALLOY 82	King & McCOY	ALLOY 82 WELD	TM-9108
tm9108-CW	649	206.85	1695				GTA	ALLOY 82	King & McCOY	ALLOY 82 CROSS WELD	TM-9108
tm9108-CW	649	206.85	27.6				GTA	ALLOY 82	King & McCOY	ALLOY 82 CROSS WELD	TM-9108
tm9108-CW	649	241.32	141				GTA	ALLOY 82	King & McCOY	ALLOY 82 CROSS WELD	TM-9108
tm9108-CW	649	241.32	154				GTA	ALLOY 82	King & McCOY	ALLOY 82 CROSS WELD	TM-9108
tm9108-CW	649	241.32	126				GTA	ALLOY 82	King & McCOY	ALLOY 82 CROSS WELD	TM-9108
tm9108-CW	649	241.32	139				GTA	ALLOY 82	King & McCOY	ALLOY 82 CROSS WELD	TM-9108
tm9108-CW	649	241.32	163				GTA	ALLOY 82	King & McCOY	ALLOY 82 CROSS WELD	TM-9108
tm9108-CW	649	241.32	139				GTA	ALLOY 82	King & McCOY	ALLOY 82 CROSS WELD	TM-9108
tm9108-CW-PWHT	649	241.32	122				GTA	ALLOY 82	King & McCOY	ALLOY 82 CROSS WELD	TM-9108
tm9108-CW-PWHT	649	241.32	155				GTA	ALLOY 82	King & McCOY	ALLOY 82 CROSS WELD	TM-9108
tm9108-CW-ann	649	241.32	157				GTA	ALLOY 82	King & McCOY	ALLOY 82 CROSS WELD	TM-9108
tm9108-CW-ann	649	241.32	126				GTA	ALLOY 82	King & McCOY	ALLOY 82 CROSS WELD	TM-9108

ITEM	Temperature (C)	Stress (MPa)	Time to Rupture (hrs)	Elong. (%)	Red. Of Area (%)	Min. Creep Rate (%/hr)	Process	Filler Metal	Reference	Specimen Type	Comment
epri 82-15	900	40.208	58				GTA	ALLOY 82	EPRI SURVEY	ALLOY 82 CROSS WELD	
epri 82-15	900	33.343	90				GTA	ALLOY 82	EPRI SURVEY	ALLOY 82 CROSS WELD	
epri 82-15	900	26.478	260				GTA	ALLOY 82	EPRI SURVEY	ALLOY 82 CROSS WELD	
epri 82-15	900	17.652	900				GTA	ALLOY 82	EPRI SURVEY	ALLOY 82 CROSS WELD	
epri 82-15	900	13.73	3000				GTA	ALLOY 82	EPRI SURVEY	ALLOY 82 CROSS WELD	
epri 82-13	700	156.91	220				GTA	ALLOY 82	EPRI SURVEY	ALLOY 82 CROSS WELD	
epri 82-13	700	156.91	580				GTA	ALLOY 82	EPRI SURVEY	ALLOY 82 CROSS WELD	
epri 82-13	700	98.068	3500				GTA	ALLOY 82	EPRI SURVEY	ALLOY 82 CROSS WELD	
epri 82-13	700	78.454	19000				GTA	ALLOY 82	EPRI SURVEY	ALLOY 82 CROSS WELD	
epri 82-13	800	88.261	68				GTA	ALLOY 82	EPRI SURVEY	ALLOY 82 CROSS WELD	
epri 82-13	800	83.358	440				GTA	ALLOY 82	EPRI SURVEY	ALLOY 82 CROSS WELD	
epri 82-13	800	39.227	4200				GTA	ALLOY 82	EPRI SURVEY	ALLOY 82 CROSS WELD	
epri 82-13	900	27.459	380				GTA	ALLOY 82	EPRI SURVEY	ALLOY 82 CROSS WELD	
epri 82-13	900	21.575	1900				GTA	ALLOY 82	EPRI SURVEY	ALLOY 82 CROSS WELD	
epri 82-13	900	17.652	7000				GTA	ALLOY 82	EPRI SURVEY	ALLOY 82 CROSS WELD	
epri 82-13	1000	15.691	490				GTA	ALLOY 82	EPRI SURVEY	ALLOY 82 CROSS WELD	
epri 82-13	1000	9.8068	5200				GTA	ALLOY 82	EPRI SURVEY	ALLOY 82 CROSS WELD	
epri 82-13	1000	7.3551	6000				GTA	ALLOY 82	EPRI SURVEY	ALLOY 82 CROSS WELD	
INCO	538	400	100				GTA	ALLOY 82	INCO	ALLOY 82 WELD METAL	
INCO	538	359	1000				GTA	ALLOY 82	INCO	ALLOY 82 WELD METAL	
INCO	538	324	10000				GTA	ALLOY 82	INCO	ALLOY 82 WELD METAL	
INCO	649	252	100				GTA	ALLOY 82	INCO	ALLOY 82 WELD METAL	
INCO	649	190	1000				GTA	ALLOY 82	INCO	ALLOY 82 WELD METAL	
INCO	649	141	10000				GTA	ALLOY 82	INCO	ALLOY 82 WELD METAL	
INCO	760	110	100				GTA	ALLOY 82	INCO	ALLOY 82 WELD METAL	
INCO	760	79	1000				GTA	ALLOY 82	INCO	ALLOY 82 WELD METAL	
INCO	760	57	10000				GTA	ALLOY 82	INCO	ALLOY 82 WELD METAL	
INCO	871	47	100				GTA	ALLOY 82	INCO	ALLOY 82 WELD METAL	
INCO	871	24	1000				GTA	ALLOY 82	INCO	ALLOY 82 WELD METAL	
INCO	871	12	10000				GTA	ALLOY 82	INCO	ALLOY 82 WELD METAL	
INCO	982	19	100				GTA	ALLOY 82	INCO	ALLOY 82 WELD METAL	
INCO	982	9	1000				GTA	ALLOY 82	INCO	ALLOY 82 WELD METAL	
INCO	982	4	10000				GTA	ALLOY 82	INCO	ALLOY 82 WELD METAL	

ITEM	Temperature (C)	Stress (MPa)	Time to Rupture (hrs)	Elong. (%)	Red. Of Area (%)	Min. Creep Rate (%/hr)	Process	Filler Metal	Reference	Specimen Type	Comment
TM5404	454	517.12	3.2				GTA	ALLOY 82	Klueh & King	ALLOY 82 WELD METAL	TM-5404
TM5404	454	510.23	142.3				GTA	ALLOY 82	Klueh & King	ALLOY 82 WELD METAL	TM-5404
TM5404	454	496.44	715.1				GTA	ALLOY 82	Klueh & King	ALLOY 82 WELD METAL	TM-5404
TM5404	454	496.44	1012.6				GTA	ALLOY 82	Klueh & King	ALLOY 82 WELD METAL	TM-5404
TM5404	454	489.55	1075.4				GTA	ALLOY 82	Klueh & King	ALLOY 82 WELD METAL	TM-5404
TM5404	510	482.65	10.9				GTA	ALLOY 82	Klueh & King	ALLOY 82 WELD METAL	TM-5404
TM5404	510	455.07	39.4				GTA	ALLOY 82	Klueh & King	ALLOY 82 WELD METAL	TM-5404
TM5404	510	448.17	357.1				GTA	ALLOY 82	Klueh & King	ALLOY 82 WELD METAL	TM-5404
TM5404	510	434.39	1205.1				GTA	ALLOY 82	Klueh & King	ALLOY 82 WELD METAL	TM-5404
TM5404	510	413.7	1645.4				GTA	ALLOY 82	Klueh & King	ALLOY 82 WELD METAL	TM-5404
TM5404	510	393.02	3255				GTA	ALLOY 82	Klueh & King	ALLOY 82 WELD METAL	TM-5404
TM5404	510	379.23	6770.4				GTA	ALLOY 82	Klueh & King	ALLOY 82 WELD METAL	TM-5404
TM5404	566	434.39	29.5				GTA	ALLOY 82	Klueh & King	ALLOY 82 WELD METAL	TM-5404
TM5404	566	413.7	112.8				GTA	ALLOY 82	Klueh & King	ALLOY 82 WELD METAL	TM-5404
TM5404	566	396.46	448.2				GTA	ALLOY 82	Klueh & King	ALLOY 82 WELD METAL	TM-5404
TM5404	566	379.23	841.1				GTA	ALLOY 82	Klueh & King	ALLOY 82 WELD METAL	TM-5404
TM5404	566	365.43	1087.5				GTA	ALLOY 82	Klueh & King	ALLOY 82 WELD METAL	TM-5404
TM5404	566	344.75	6003.3				GTA	ALLOY 82	Klueh & King	ALLOY 82 WELD METAL	TM-5404
TM5404	621	379.23	21.2				GTA	ALLOY 82	Klueh & King	ALLOY 82 WELD METAL	TM-5404
TM5404	621	310.27	295.1				GTA	ALLOY 82	Klueh & King	ALLOY 82 WELD METAL	TM-5404
TM5404	621	293.04	653.1				GTA	ALLOY 82	Klueh & King	ALLOY 82 WELD METAL	TM-5404
TM5404	621	275.8	1195.9				GTA	ALLOY 82	Klueh & King	ALLOY 82 WELD METAL	TM-5404
TM5404	621	241.32	3109.4				GTA	ALLOY 82	Klueh & King	ALLOY 82 WELD METAL	TM-5404
TM5404	677	275.8	26				GTA	ALLOY 82	Klueh & King	ALLOY 82 WELD METAL	TM-5404
TM5404	677	241.32	89				GTA	ALLOY 82	Klueh & King	ALLOY 82 WELD METAL	TM-5404
TM5404	677	206.85	215				GTA	ALLOY 82	Klueh & King	ALLOY 82 WELD METAL	TM-5404
TM5404	677	172.38	778.5				GTA	ALLOY 82	Klueh & King	ALLOY 82 WELD METAL	TM-5404
TM5404	677	137.9	3590				GTA	ALLOY 82	Klueh & King	ALLOY 82 WELD METAL	TM-5404
TM5404	732	172.38	30.7				GTA	ALLOY 82	Klueh & King	ALLOY 82 WELD METAL	TM-5404
TM5404	732	137.9	103.6				GTA	ALLOY 82	Klueh & King	ALLOY 82 WELD METAL	TM-5404
TM5404	732	103.43	634.4				GTA	ALLOY 82	Klueh & King	ALLOY 82 WELD METAL	TM-5404
TM5404	732	82.74	2792.8				GTA	ALLOY 82	Klueh & King	ALLOY 82 WELD METAL	TM-5404

ITEM	Temperature (C)	Stress (MPa)	Time to Rupture (hrs)	Elong. (%)	Red. Of Area (%)	Min. Creep Rate (%/hr)	Process	Filler Metal	Reference	Specimen Type	Comment
TM5491	454	496.44	1671.2				GTA	ALLOY 82	Klueh & King	ALLOY 82 WELD METAL	TM-5491
TM5491	454	482.65	4228.8				GTA	ALLOY 82	Klueh & King	ALLOY 82 WELD METAL	TM-5491
TM5491	454	455.07	8222.4				GTA	ALLOY 82	Klueh & King	ALLOY 82 WELD METAL	TM-5491
TM5491	510	448.17	106.1				GTA	ALLOY 82	Klueh & King	ALLOY 82 WELD METAL	TM-5491
TM5491	510	434.39	260				GTA	ALLOY 82	Klueh & King	ALLOY 82 WELD METAL	TM-5491
TM5491	510	413.7	1049.7				GTA	ALLOY 82	Klueh & King	ALLOY 82 WELD METAL	TM-5491
TM5491	510	396.46	6637.7				GTA	ALLOY 82	Klueh & King	ALLOY 82 WELD METAL	TM-5491
TM5491	510	241.32	12746				GTA	ALLOY 82	Klueh & King	ALLOY 82 WELD METAL	TM-5491
TM5491	566	379.23	129.8				GTA	ALLOY 82	Klueh & King	ALLOY 82 WELD METAL	TM-5491
TM5491	566	365.43	247.1				GTA	ALLOY 82	Klueh & King	ALLOY 82 WELD METAL	TM-5491
TM5491	566	344.75	432.3				GTA	ALLOY 82	Klueh & King	ALLOY 82 WELD METAL	TM-5491
TM5491	566	327.51	2776.1				GTA	ALLOY 82	Klueh & King	ALLOY 82 WELD METAL	TM-5491
TM5491	621	310.27	204.7				GTA	ALLOY 82	Klueh & King	ALLOY 82 WELD METAL	TM-5491
TM5491	621	275.8	652.9				GTA	ALLOY 82	Klueh & King	ALLOY 82 WELD METAL	TM-5491
TM5491	621	241.32	1401.2				GTA	ALLOY 82	Klueh & King	ALLOY 82 WELD METAL	TM-5491
TM5491	677	206.85	183				GTA	ALLOY 82	Klueh & King	ALLOY 82 WELD METAL	TM-5491
TM5491	677	172.38	546.7				GTA	ALLOY 82	Klueh & King	ALLOY 82 WELD METAL	TM-5491
TM5491	677	172.38	366.8				GTA	ALLOY 82	Klueh & King	ALLOY 82 WELD METAL	TM-5491
TM5491	677	137.9	2263.1				GTA	ALLOY 82	Klueh & King	ALLOY 82 WELD METAL	TM-5491
TM5491	732	82.74	1526.6				GTA	ALLOY 82	Klueh & King	ALLOY 82 WELD METAL	TM-5491
TM5491	732	103.43	459.1				GTA	ALLOY 82	Klueh & King	ALLOY 82 WELD METAL	TM-5491
TM5491	732	137.9	77.2				GTA	ALLOY 82	McCoy	ALLOY 82 WELD METAL	TM-7399
HEM7399	538	344.75					GTA	ALLOY 82	McCoy	ALLOY 82 WELD METAL	TM-7399
HEM7399	538	448.17	178				GTA	ALLOY 82	McCoy	ALLOY 82 WELD METAL	TM-7399
HEM7399	593	206.85					GTA	ALLOY 82	McCoy	ALLOY 82 WELD METAL	TM-7399
HEM7399	593	275.8					GTA	ALLOY 82	McCoy	ALLOY 82 WELD METAL	TM-7399
HEM7399	649	137.9					GTA	ALLOY 82	McCoy	ALLOY 82 WELD METAL	TM-7399
HEM7399	649	206.85	1069.6				GTA	ALLOY 82	McCoy	ALLOY 82 WELD METAL	TM-7399
HEM7399	704	103.43	9767				GTA	ALLOY 82	McCoy	ALLOY 82 WELD METAL	TM-7399
HEM7399	704	137.9					GTA	ALLOY 82	McCoy	ALLOY 82 WELD METAL	TM-7399
HEM7399	760	68.95	6940				GTA	ALLOY 82	McCoy	ALLOY 82 WELD METAL	TM-7399
HEM7399	760	103.43	347				GTA	ALLOY 82	McCoy	ALLOY 82 WELD METAL	TM-7399
HEM7399	816	55.16	1364				GTA	ALLOY 82	McCoy	ALLOY 82 WELD METAL	TM-7399
HEM7399	816	68.95	301				GTA	ALLOY 82	McCoy	ALLOY 82 WELD METAL	TM-7399

ITEM	Temperature (C)	Stress (MPa)	Time to Rupture (hrs)	Elong. (%)	Red. Of Area (%)	Min. Creep Rate (%/hr)	Process	Filler Metal	Reference	Specimen Type	Comment
Schubert	850	35	500				GTA	ALLOY 82	SCHUBERT, ET AL.	ALLOY 82 WELD METAL	
Schubert	850	30	500				GTA	ALLOY 82	SCHUBERT, ET AL.	ALLOY 82 WELD METAL	
Schubert	850	30	600				GTA	ALLOY 82	SCHUBERT, ET AL.	ALLOY 82 WELD METAL	
Schubert	850	35	600				GTA	ALLOY 82	SCHUBERT, ET AL.	ALLOY 82 WELD METAL	
Schubert	850	30	680				GTA	ALLOY 82	SCHUBERT, ET AL.	ALLOY 82 WELD METAL	
Schubert	950	18.5	130				GTA	ALLOY 82	SCHUBERT, ET AL.	ALLOY 82 WELD METAL	
Schubert	950	18.5	145				GTA	ALLOY 82	SCHUBERT, ET AL.	ALLOY 82 WELD METAL	
Schubert	950	14.5	330				GTA	ALLOY 82	SCHUBERT, ET AL.	ALLOY 82 WELD METAL	
Schubert	950	14.5	390				GTA	ALLOY 82	SCHUBERT, ET AL.	ALLOY 82 WELD METAL	
Schubert	950	14.5	600				GTA	ALLOY 82	SCHUBERT, ET AL.	ALLOY 82 WELD METAL	
Schubert	950	12.5	600				GTA	ALLOY 82	SCHUBERT, ET AL.	ALLOY 82 WELD METAL	
Schubert	950	12.5	720				GTA	ALLOY 82	SCHUBERT, ET AL.	ALLOY 82 WELD METAL	
Schubert	950	13	1300				GTA	ALLOY 82	SCHUBERT, ET AL.	ALLOY 82 WELD METAL	
Schubert	950	7.8	4800				GTA	ALLOY 82	SCHUBERT, ET AL.	ALLOY 82 WELD METAL	
Schubert	950	7	4800				GTA	ALLOY 82	SCHUBERT, ET AL.	ALLOY 82 WELD METAL	

APPENDIX F: GRADE 91

F.1 Composition

			Composition (wt%)													
Weld ID	Product	Wire	C	Mn	P	S	Si	Ni	Cr	Mo	V	Cb	Ti	Cu	Al	N2
	1 1/16	F5349-wire chem	0.1	0.43	0.01	0.013	0.36	0.12	8.83	0.94	0.208	0.0588	0.01	0.09	0.001	0.011
PC-2	Plate	std 9CrMo														
PC-4	5/8 Plate	F5349-deposit	0.072	0.41	0.01	0.015	0.36	0.11	8.69	0.95	0.21	0.057	0.007	0.09	0.001	0.012
PC-5	1/2 Tube	F5349														
PC-9	5/8 Plate	F5349														
PC-10	5/8 Plate	std 9CrMo-deposit	0.074	0.49	0.01	0.013	0.41	0.12	9	0.96	0.054	0.019	0.006	0.04	<.001	0.02
PC-13	5/8 Plate	std 9CrMo-Y3738F505														
PC-16	5/8 Plate	std 9CrMo-XA3664														
PC-32	5/8 Plate	30182														
PC-35	5/8 Plate	30182-base metal tube	0.081	0.36	0.013	0.003	0.11	0.09	8.32	0.90	0.208	0.176	0.002	0.04	0.004	0.053
PC-36	1 Plate	30394														
PC-39	1 Plate	30394-base metal plate	0.084	0.46	0.01	0.003	0.4	0.09	8.57	1.02	0.198	0.073	0.005	0.04	0.014	0.053
PC-42	1 Plate	30394														
PC-45	1 Plate	30394														
PC-52	1 1/2 Plate	30383-C2616														
PC-58A	3 OD Tube	std 9CrMo-A1977F505														
PC-58B	3 OD Tube	std 9CrMo-A1977F505														
PC-59	Tube	std 9CrMo-CAOIG														

			Composition (wt%)													
Weld ID	Product	Wire	C	Mn	P	S	Si	Ni	Cr	Mo	V	Cb	Ti	Cu	Al	N2
PC-63	Tube	std 9CrMo-CAOIG-wire chem	0.052	0.62	0.005	0.007	0.14	<.01	9.27	0.87	0.03			0.05		
PC-64		std9CrMo-8N9AMIX19	0.089	0.75	0.011	0.011	0.25	0.06	8.05.	0.97						
PC-65	Tube	std 9CrMo-CAOIG-wire chem	0.052	0.62	0.005	0.007	0.14	<.01	9.27	0.87	0.03			0.05		
PC-67B	1 Plate	std 9CrMo-8N20AMIX24	0.078	0.69	0.006	0.015	0.29	0.07	8.1	0.97						
PC-71	1 Plate	std 9CrM0-E4390-E505	0.08	0.69	0.015	0.006	0.29	0.07	8.1	0.97						
PC-72	2 Plate	std 9CrM0-E4390-E505														
PC-73	2 Plate	std 9CrM0-E4390-E505														
PC-74	1 Plate															
PC-75	1 Plate															
PC-77	2 Plate															
PC- 80	2 Plate		0.089	0.53	0.012	0.003	0.48	0.09	8.25	1.04	0.2	0.071	0.004	0.04	0.007	0.048
PC- 86	1 Plate		0.036	0.45	0.016	0.009	0.34	0.22	8.75	0.98	0.036	0.006	0.004	0.3	0.007	0.012
PC-90																
PC-93	8 Plate		0.076	0.55	0.008	0.007	0.35	0.08	8.38	0.96	0.01	0.007	0.005	0.05	0.012	0.019
PC-94																
PC-95																
PC-98			0.011	0.4	0.016	0.012	0.28	0.2	8.78	1.02	0.051	0.006	0.001	0.18	0.003	0.035
PC-99																
PC-100			0.038	0.5	0.016	0.009	0.38	0.14	8.99	1.08	0.048	0.007	0.002	0.18	0.003	0.052
PC-102																
VS1																
PC-104																
ETEC																
PC-109																
PC-110																
PC-111																
302B																
303B																
SW-1																
SW-2																

			Composition (wt%)													
Weld ID	Product	Wire	C	Mn	P	S	Si	Ni	Cr	Mo	V	Cb	Ti	Cu	Al	N2
PC-129																
PC-132																
PC-150																
PC-156																
LNKS	2 Plate	Thermanit MTS3	0.11	0.57	0.012	0.01	0.15	0.74	9.39	0.9	0.22	0.034	0.002	0.04	0.015	0.051
4R	1 Plate		0.13	0.13	0.012	0.009	0.34	0.3	8.8	1	0.16	0.03		0.01	<.01	0.04
5R	1 Plate		0.13	0.89	0.012	0.008	0.33	1	10	1.1	0.2	0.05		0.01	<.01	0.06
9R	1 Plate		0.1	0.57	0.014	0.008	0.25	0.85	10.25	1.07	0.21	0.04		0.01	0.01	0.04
10R	1 Plate		0.1	0.56	0.014	0.008	0.26	0.82	9.94	1.05	0.22	0.05		0.01	0.01	0.04
Pipe-ECCC2009	GTAW	Thermanit MTS3 (root)	0.126	0.61	0.007	0.002	0.24	0.67	8.93	0.99	0.18	0.069			0.007	0.058
Pipe-ECCC2009	SMAW	Chromo 9V (electrode)	0.1	0.62	0.009	0.006	0.24	0.73	9.05	1.05	0.2	0.05			0.007	0.4
Plate-ECCC2009	GTAW	Thermanit MTS3 (root)	0.126	0.61	0.007	0.002	0.24	0.67	8.93	0.99	0.18	0.069			0.007	0.058
Pipe-ECCC2009	SMAW	Chromo 9V (electrode)	0.1	0.62	0.009	0.006	0.24	0.73	9.05	1.05	0.2	0.05			0.007	0.4
ER90S-B9	weld metal	ER90S-B9	0.113	0.59	0.002	0.004	0.21	0.63	8.93	0.95	0.185	0.05	<.001		<.001	0.056
EPRI1004702+	base metal		0.11	0.48	0.011	0.003	0.27	0.28	8.36	0.98	0.217	0.078		0.13	0.16	0.046
EPRI1004702+	SMAW	ER9015-B9 H4 (root)	0.09	0.73	0.007	0.008	0.24	0.37	8.55	1.05	0.17	0.054		0.03	0.004	0.022
EPRI1004702+	SMAW	ER9015-B9 H4 (fill)	0.08	0.62	0.008	0.007	0.22	0.39	9.14	1.11	0.19	0.05		0.01	0.004	0.033

F.2 Weld Configuration & Details

ID/Ref.	Base Metal Product	Base Metal Heat	Base Metal Condition	Base Metal Thickness	Joint Configuration	Welding Process	Weld Wire std	Weld Wire Heat	Passes	PWHT (deg. F unless noted)	Specimen Blank Length (in) and Orientation	Comment
PC-2	Plate	Quaker	NT	1 1/16	90° V	GTA	9Cr	Y3738F505	37	1450	1.25 TW	DWG W1
PC-4	Plate	F5349Y	NT	5/8"	V	GTA	Gr91	F5349Y	16	1400	1.25 TW	DWG W2
PC-5	Tube	F5349Y	NT	5/8"	75° V	GTA	Gr91	F5349Y	4	1400	1.25 TW	DWG W2
PC-9	Plate	F5349Y	NT	5/8"	90° V	GTA	Gr91	F5349Y	24	1350	1.25 TW	DWG W2
PC-10	Plate	F5349Y	NT	5/8"	90° V	GTA	std 9Cr	Y3738F505	20	1350	1.25 TW	DWG W2
PC-13	Plate	F5349Y	NT	3/4"	V	GTA	std 9Cr	Y3738F505	34		1 1/4 all W	DWG W3
PC-16	Plate	F5349Y	NT	3/4"	V	GTA	*Gr91*	XA3664	20	1350	1 1/4 all W	DWG W3
PC-32	Plate	30182	NT	5/8"	V	GTA	Gr91	30182	9	1350	1.25 TW	DWG W2
PC-35	Plate	30182	NT	5/8"	75° V	GTA	Gr91	30182			2.25 TW	DWG W4
PC-36A 1-8	Plate	30394	NT	1"	60° V	GTA	Gr91	30394	25	as-welded	2.25 TW	DWG W4
PC-36B 9-16	Plate	30394	NT	1"	60° V	GTA	Gr91	30394	25	1350	2.25 TW	DWG W4
PC-39	Plate	30394	1038/677	1"	60° V	GTA	Gr91	30394	17	1400	2.25 TW	DWG W4
PC-42	Plate	30394	1038/704	1"		GTA	Gr91	30394	6		2.25 TW	DWG W4
PC-45	Plate	30394	NT	1"	60° V	GTA	Gr91	30394	9	1400	1.25 TW	DWG W2
PC-52	Plate	30384	NT	1"	V	GTA	Gr91	C2616 (30383)	11	1350	1.25 TW	DWG W1
PC-58A	Tube	30394	NT	3" OD 1/2 wall	60° V	GTA	std 9Cr	A1977F-505	10	1350	1.25 TW	DWG W5
PC-58B	Tube	30394	NT	3" OD 1/2 wall	60° V	GTA	std 9Cr	A1977F-505	10	as-welded	1.25 TW	DWG W5
PC-59	Tube	30394	NT	3" OD 1/2 wall	60° V	SMA	std 9Cr	CAOIG-505	26		1.25 TW	DWG W5
PC-63	Tube	sumitomo	NT	3" OD 1/2 wall	60° V	SMA	std 9Cr	CAOIG-505	26	1350	1.25 TW	DWG W5
PC-65	Tube	sumitomo	NT	3" OD 1/2 wall	60° V	SMA	std 9Cr	CAOIG-505	28	1350	1.25 TW	DWG W5
PC-67B	Plate	30176	NT	1"	75° V	SMA	std 9Cr	8N20AMIX24	31	1350	1.25 TW	DWG W1
PC-71	Plate	30176	NT	1"		SA	std 9Cr	E4390-505	13	1350	1 1/4 all W	DWG W6
PC-72	Plate	30383	NT	2"		SA	std 9Cr	E4390-505	37	1350/2h	1 1/4 all W	DWG W7
PC-73	Plate	30383	NT	2"	3/4 Root-15°	SA	std 9Cr	E4390-505	69	1350/2h	1 1/4 all W	DWG W7

ID/Ref.	Base Metal Product	Base Metal Heat	Base Metal Condition	Base Metal Thickness	Joint Configuration	Welding Process	Weld Wire	Weld Wire Heat	Passes	PWHT (deg. F unless noted)	Specimen Blank Length (in) and Orientation	Comment
PC-73	Plate	30383	NT	2"	3/4 Root-15°	SA	std 9Cr	E4390-505	69	1350/2h	1 1/4 all W	DWG W7
PC-74	Plate	30394	NT	1"	60° V	SMA	std 9Cr	*mix10153R5804*	30	1350	1.25 TW	DWG W2
PC-75	Plate	30394	NT	1"	60° V	SMA	Gr91	*mix10166R5804*	32	1350	1.25 TW	DWG W2
PC-76	Plate	30176	NT	1"	3/4 Root-15°	SA	std9Cr	E4390-505	15	1350		
PC-77	Plate	30383	NT	2"	1 Root-15°	SA	std9Cr	33669-505	63	1350/2h	1 1/4 all W	DWG W7
PC-80A	Plate	30383	NT	2"	3/4 Root-15°	SA	Gr91	C2616 (30383)	50	1350/2h	2.25 TW	DWG W8
PC-80B	Plate	30383	NT	2"	3/4 Root-15°	SA	Gr91	C2616 (30383)	50	1900/1400/2h	2.25 TW	DWG W8
PC-86	Plate	30394	NT	1"	3/4 Root-15°	SA	std9Cr	…. E-505	19	1350	1.25 TW	DWG W1
PC-90	Tube	sumitomo	NT	3" OD 1/2 wall	60° V	SMA	std 9Cr	CEM10292	20	1350	1.25 TW	DWG W5
PC-93	Plate	10148	NT	7.6"	5/8 Root-7 1/2°	SA	std 9Cr	33669-505	145	1350/6h	2.25 TW	DWG W9
PC-93	Plate	10148	NT	7.6"	5/8 Root-7 1/2°	SA	std 9Cr	33669-505	145	1350/6h	1.25 TW	DWG W9
PC-93	Plate	10148	NT	7.6"	5/8 Root-7 1/2°	SA	std 9Cr	33669-505	145	1350/6h	1 1/4 all W	DWG W9
PC-94	Tube	59020	NT	3" OD 1/2 wall	60° V	SMA	std 9Cr	CEM10292	12	1350	1.25 TW	DWG W5
PC-95	Tube	59020	NT	3" OD 1/2 wall	60° V	SMA	std 9Cr	CEM10292	17	1350	1.25 TW	DWG W5
PC-98	Plate	30394	NT	1"	C	SA	std9Cr	…. E-505	20			
PC-99	Plate	30394	NT	1"	V	GTA	std9Cr	E4390-505	30	1350	1.25 TW	DWG W2
PC-100	Plate	30394	NT	1"	60° V	GTA			18			
PC-102	Tube	59020	NT	3" OD 1/2 wall	V	SMA	std 9Cr	CEM10292	10	1350	2.8 TW	DWG W10
VS1	Pipe		NT	1/2" wall		SMA		M9412		1350	2.25 TW	DWG W11
PC-104	Plate	30394	NT	1"	60° V	GTA	std9Cr	A1977F-505	30	1250	2.25 TW	DWG W1
PC-104	Plate	30394	NT	1"	V	*GTA*	std9Cr	A1977F-505	30	1300	2.25 TW	DWG W1

ID/Ref.	Base Metal Product	Base Metal Heat	Base Metal Condition	Base Metal Thickness	Joint Configuration	Welding Process	Weld Wire	Weld Wire Heat	Passes	PWHT (deg. F unless noted)	Specimen Blank Length (in) and Orientation	Comment
ETEC-1	*Pipe?*		NT	*9" OD 1/2 wall*		GTA	ERNiCr-3			1350	2.25 TW	DWG W2
ETEC-2	Pipe		NT	9" OD 1/2 wall		GTA	ERNiCr-3			1350+950/2Kh	2.25 TW	DWG W2
PC-109	Plate	10148	1900/1150	2"	V	SAW	std 9Cr	D3612F505		1400/1.5	**2.5 all W?**	DWG W1
PC-110	Plate	30176	1900/1150	1"	V	GTA	std 9Cr	33669		1400	2.25 TW	DWG W1
PC-111	Plate	30394	1900/1150	1"	V	GTA	std 9Cr	33669		1400/1.5	1.25 TW	DWG W1
302B	Tube		NT	3" OD 1/2 wall	V	SMA	Gr91	M9412		1350		
303B	Tube		NT	3" OD 1/2 wall	V	SMA	std 9Cr	CAOIG		1350		
304B	Tube		NT	3" OD 1/2 wall	V	SMA	Gr22	CAADJ		1350	1.25 TW	DWG W5
SW-1	Plate	10148	NT	2"		SA	std 9Cr	D3612F505		1350/2h	**2.5 TW**	DWG W1
SWM-2	Plate		1900/1400	1"		SMA	std 9Cr			*1400/2h?*	**2.5 TW**	DWG W2
PC-129	Plate	30176	NT	1"		GTA	*Gr91? std*	*21078?*		1350	1 1/4 all W	DWG W12
PC-132	Plate	30176	1900/1400	1"		SMA	*9Cr?*	Kobe		1400	2.25 TW	DWG W1
PC-150	Plate	30176	1900/1150	1"		GTA	*Gr91?*	*21648?*		*1350*	2.25 TW	DWG W1
PC-156	Plate	30176	1900/1400	1 1/8"		SA	std 9Cr	USW-21648	23	1375/1h	2.25 TW	DWG W1
LKNS-1	Plate	Lukens	1900/1400	2"		SA	Gr91	MTS3	44	1425/8h	1.25 TW	DWG 13
LKNS-2	Plate	Lukens	1900/1400	2"		SA	Gr91	MTS3	44	1425/8h	1 1/4 all W	DWG 13
LKNS-3	Plate	Lukens	1900/1400	2"		SA	Gr91	MTS3	44	1904/1364	1.25 TW	DWG 13
LKNS-4	Plate	Lukens	1900/1400	2"		SA	Gr91	MTS3	44	1904/1364	1 1/4 all W	DWG 13
LKNS-5	Plate	Lukens	1900/1400	2"		SA	Gr91	MTS3	44	1904/1436	1.25 TW	DWG 13
LKNS-6	Plate	Lukens	1900/1400	2"		SA	Gr91	MTS3	44	1904/1436	1 1/4 all W	DWG 13

ID/Ref.	Base Metal Product	Base Metal Heat	Base Metal Condition	Base Metal Thickness	Joint Configuration	Welding Process	Weld Wire	Weld Wire Heat	Passes	PWHT (deg. F unless noted)	Specimen Blank Length (in) and Orientation	Comment
9R	Plate	51383	1922/1418	3/4"		FCA	Gr91	25B52-9R		1400/4h	1 1/4 all W	
9R	Plate	51383	1922/1418	3/4"		FCA	Gr91	25B52-9R		1400/4h	1.25 TW	
10R	Plate	51383	1922/1418	3/4"		FCA	Gr91	25B52-10R		1400/4h	1 1/4 all W	
10R	Plate	51383	1922/1418	3/4"		FCA	Gr91	25B52-10R		1400/4h	1.25 TW	
W4R-1	Plate	30394	1900/1400	1"		FCA	Gr91	25B52-4R		1400/4h	1 1/4 all W	
W4R-1	Plate	30394	1900/1400	1"		FCA	Gr91	25B52-4R		1400/4h	1.25 TW	
W4R-2	Plate	30394	1900/1400	1"		FCA	Gr91	25B52-4R		1400/4h	1 1/4 all W	
W4R-2	Plate	30394	1900/1400	1"		FCA	Gr91	25B52-4R		1400/4h	1.25 TW	
W5R-1	Plate	30394	1900/1400	1"		FCA	Gr91	25B52-5R		1400/4h	1 1/4 all W	
W5R-1	Plate	30394	1900/1400	1"		FCA	Gr91	25B52-5R		1400/4h	1.25 TW	
W5R-2	Plate	30394	1900/1400	1"		FCA	Gr91	25B52-5R		1400/4h	1 1/4 all W	
W5R-2	Plate	30394	1900/1400	1"		FCA	Gr91	25B52-5R		1400/4h	1.25 TW	
Pipe-ECCC2009	Pipe		1050C-1.5hrs oil-quench, 750C-3.5hrs	1"		GTAW-root SMAW-Fill	91	Thermanit MTS3		760C/3.5hrs	cross-weld	8mm dia.
Plate-ECCC2009	Plate		1050C-1.5hrs oil-quench, 750C-3.5hrs	1"		GTAW-root SMAW-Fill	91	Chromo 9V		745/2.5hrs	cross-weld	8mm dia.
Masuyama-Std.	Plate						Gr91				cross-weld	6mm dia. + Large CW
EPRI1004702+	Plate	C1472	1038C-62min Air Cool, 788C-109min	1.5"	37.5 deg.	SMA	Gr91	E9015-B9		649-760C/2hrs	cross-weld	0.25" dia.
ER90S-B9	Plate	Mild Steel Buttered with E9018-B9 electrode			45degV	GTA	E90S-B9	121376 (Williams Welding/INE)		745C/3hrs	all weld metal	

F.3 Specimen Drawings (DWG # in Comments Field for F.2)

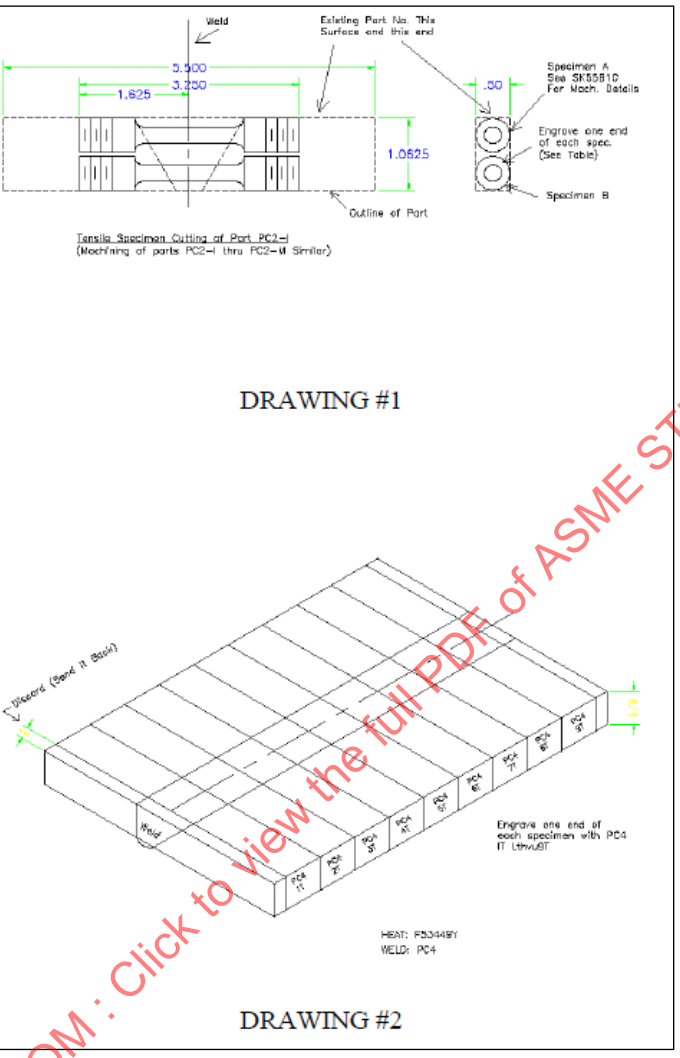

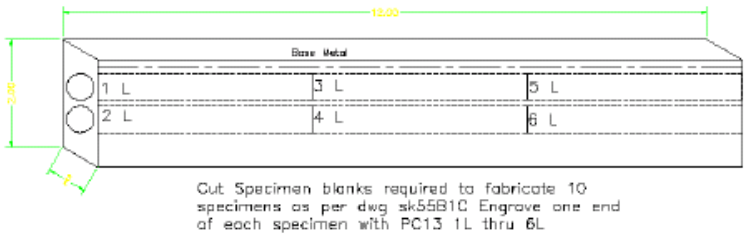

Cut Specimen blanks required to fabricate 10 specimens as per dwg sk55B1C Engrave one end of each specimen with PC13 1L thru 6L

DRAWING #3

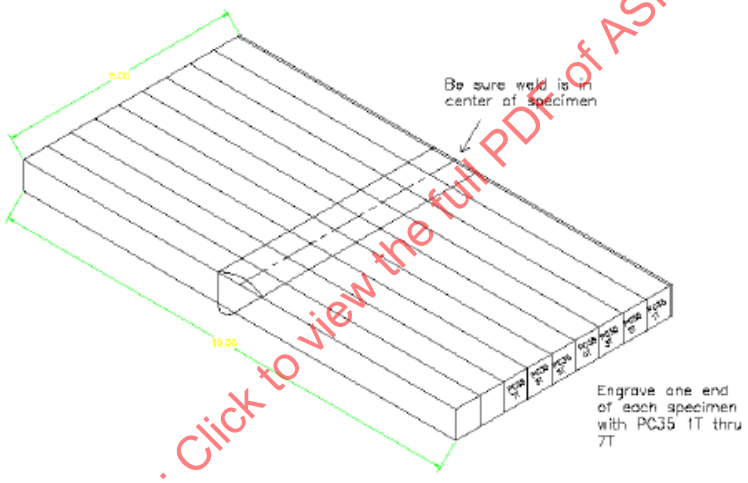

Heat: 30182
Weld: PC35
As Welded

DRAWING #4

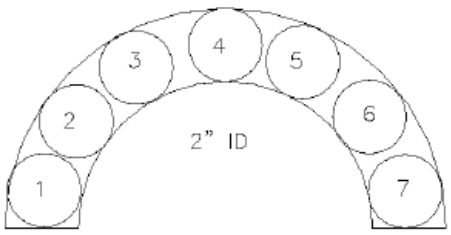

DRAWING #5

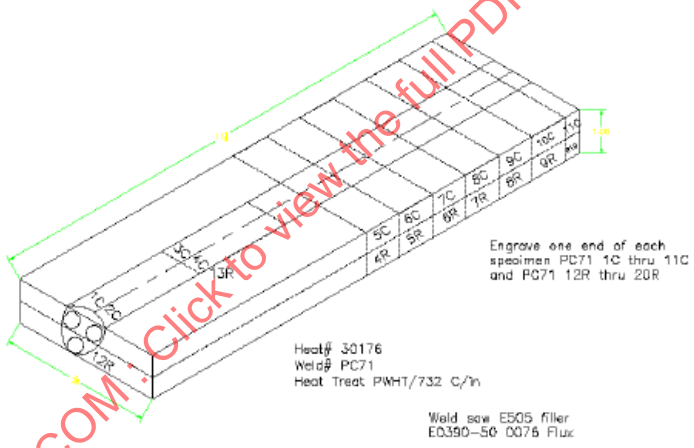

DRAWING #6

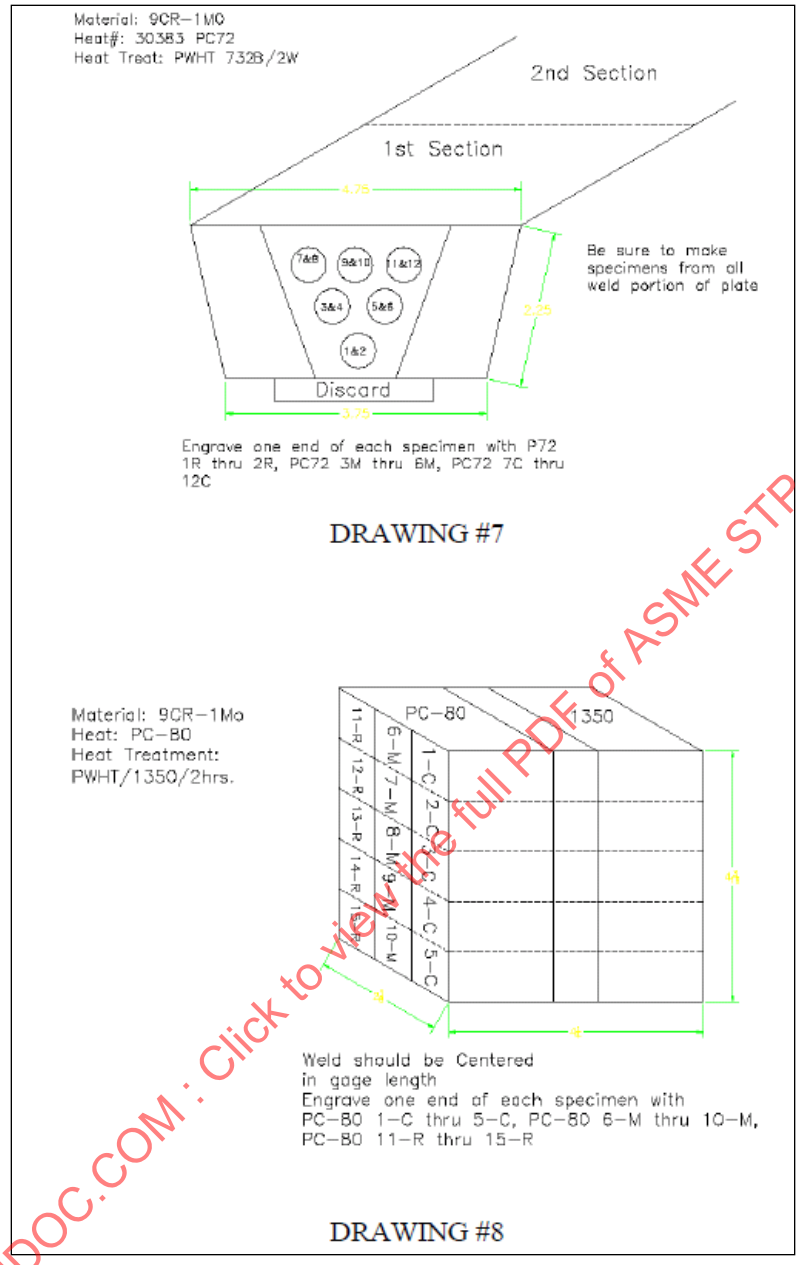

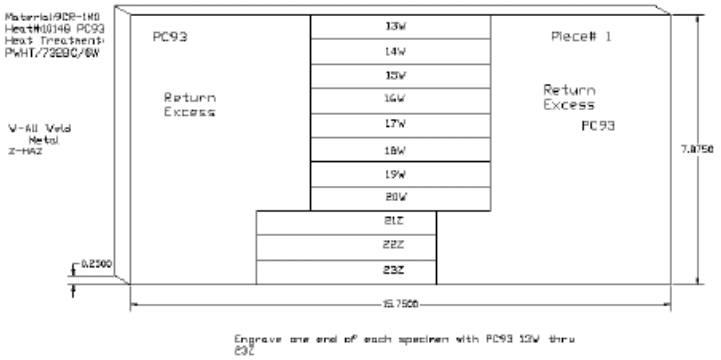

DRAWING #9

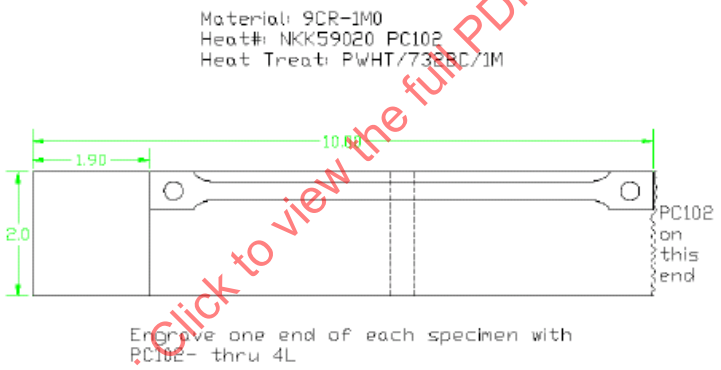

DRAWING #10

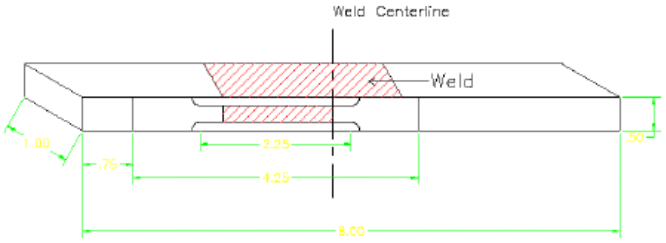

Material– Modified 9C–1M0 steel
Instruction– Make sure that the specimen is cut out as shown in the sketch. If deviated the specimen will be useless.
VSI 1 through VSI 7

VKS–2

DRAWING #11

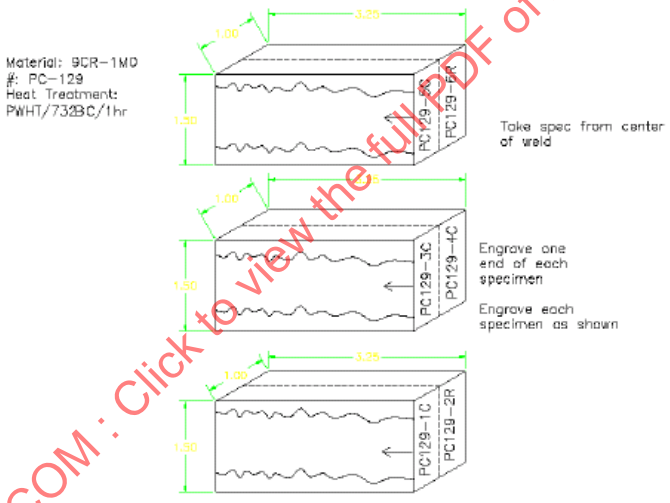

DRAWING #12

F.4 Creep-Rupture Database

Weld ID / Ref	Specimen ID	ORNL TN	Condition	Temp. (C)	Stress (MPa)	Rupture Life (hrs)	Min. Creep Rate (%/hr)	Elong. (%)	Red. Of Area (%)	Failure Location	Comment	Specimen Type	Specimen Dia (inches)
PC-2	1-T	20728	788 pwht	649	117.2	4.5		22.5	91	weld	neck	CW	0.25
PC-2	2-T	20733	788 pwht	649	82.7	336		6.8	36.4			CW	0.25
PC-2	3-T	20744	788 pwht	538	220.6	17.2		20.5	88.3	weld	neck	CW	0.25
PC-2	7-T	20773	788 pwht	538	179.3	85.2		27.1	89.1	weld	neck	CW	0.25
PC-2	8-T	20785	788 pwht	538	151.7	12238D					discontinued	CW	0.25
PC-4	2-T	20991	760 pwht	649	117.2	35.3		18	73.1			CW	0.25
PC-4	3-T	20993	760 pwht	649	82.7	307.2		13.4	49.3			CW	0.25
PC-4	4-T	20997	760 pwht	538	234.4	290		16	75.4			CW	0.25
PC-5	2-T	20998	760 pwht	649	117.2	25.9		13.9	80.7	HAZ	neck	CW	0.25
PC-5	3-T	21003	760 pwht	649	82.7	194.1		13.2	72.5	HAZ	neck	CW	0.25
PC-9	2-L	21215	732 pwht	649	117.2	30.2		19.8	68.3	HAZ	neck	CW	0.25
PC-9	4-L	21225	732 pwht	649	82.7	308.3		14.4	37.9	HAZ	shear	CW	0.25
PC-9	5-L	21236	732 pwht	538	234.4	201		17.2	73.5	HAZ	neck	CW	0.25
PC-10	2-L	21257	732 pwht	649	117.2	45.2		12.4	54.1	HAZ	neck	CW	0.25
PC-10	4-L	**22981**	732 pwht	593	158.6	537.9	0.0053	12.8	54.51			CW	0.25
PC-10	5-L	22995	732 pwht	593	172.4	238.2		12.5	60.3			CW	0.25
PC-13	1-L	21418		649	117.2	89.9		33.4	82.8	weld	neck	CW	0.25
PC-13	2-L	21490		649	82.7	1068.4		32.7	80.1	weld	neck	CW	0.25
PC-13	3-L	21492		538	275.8	379.8		26.4	83.3	weld	neck	CW	0.25
PC-16	1-L	21519	732 pwht	538	275.8	10505D					discontinued	CW	0.25
PC-16	2-L	23233	732 pwht	649	117.2	2834D					discontinued	CW	0.25

Weld ID / Ref	Specimen ID	ORNL TN	Condition	Temp. (C)	Stress (MPa)	Rupture Life (hrs)	Min. Creep Rate (%/hr)	Elong. (%)	Red. Of Area (%)	Failure Location	Comment	Specimen Type	Specimen Dia (inches)
PC-32	3-T	21954	732 pwht	649	103.4	2037.8		19.5	78.3			CW	0.25
PC-32	4-T	22060	732 pwht	593	193.1	35.2		22.1	72.9	weld		CW	0.25
PC-32	5-T	22072	732 pwht	593	158.6	163.7		18.7	77.1			CW	0.25
PC-32	6-T	22086	732 pwht	538	234.4	385.4		18	83.4			CW	0.25
PC-32	7-T	22093	732 pwht	538	275.8	50.4		18.2	84			CW	0.25
PC-32	8-T	22099	732 pwht	538	234.4	682.9		19.8	84.5			CW	0.25
PC-36	3-T	22434	as-welded	593	193.1	770.9		3.2	16.6			CW	0.25
PC-36	13-T	22478	732 pwht	593	193.1	292		5.1	41.3			CW	0.25
PC-39	3-T	22529	760 pwht	649	117.2	72.4		3.7	27.6			CW	0.25
PC-39	4-T	22530	760 pwht	593	193.1	297.4		4.9	20.2			CW	0.25
PC-39	6-T	22534	760 pwht	649	103.4	103.1		3.4	25.2			CW	0.25
PC-36	14-T	22549	732 pwht	593	89.6	1850.1		2.7	6.2			CW	0.25
PC-39	7-T	22550	760 pwht	593	158.6	1447.7		2.6	11.3			CW	0.25
PC-35	7-T	22559	NT	593	179.3	460.8		8.6	9.8			CW	0.25
PC-42	3-T	22596	1038/704/24h	593	193.1	17.7		18.7	84.3			CW	0.25
PC-42	4-T	22609	1038/704/24h	593	158.6	319.8		18.9	86.3			CW	0.25
PC-42	6-T	22627	1038/704/24h	593	144.8	1136		16	85.4			CW	0.25
PC-45	1-T	22836	760 pwht	593	158.6	2317.5		4.1	9.7			CW	0.25
PC-45	2-T	22860	760 pwht	593	124.1	4765.1		3.2	27.6			CW	0.25
PC-52	5-R	22916	732 pwht	593	158.6	813.2		5.3	23.6	FL	shear	CW	0.25
PC-52	5-C	22934	732 pwht	593	158.6	1537.7		2.4	16.8	FL	shear	CW	0.25
PC-52	7-R	22935	732 pwht	593	144.8	2318.9		4.9	22.3	FL	shear	CW	0.25
394L	2-L	22937	as-welded	593	144.8					HAZ	neck	CW	0.25
394L	1-L	22938	as-welded	593	158.6					HAZ	neck	CW	0.25
394L	4-L	22945	as-welded	538	220.6					HAZ	neck	CW	0.25
394L	3-L	22946	as-welded	538	179.3					HAZ	neck	CW	0.25
394L	5-L	22948	as-welded	538	206.9					HAZ/FL	neck	CW	0.25
394L	6-L	22449	as-welded	565	172.4					HAZ	neck	CW	0.25
394L	7-L	22950	as-welded	565	124.1					FL	shear	CW	0.25
394L	11-L	23736	732 pwht	677	41.4	1331.8		12.1	59.1	HAZ	neck	CW	0.25

Weld ID / Ref	Specimen ID	ORNL TN	Condition	Temp. (C)	Stress (MPa)	Rupture Life (hrs)	Min. Creep Rate (%/hr)	Elong. (%)	Red. Of Area (%)	Failure Location	Comment	Specimen Type	Specimen Dia (inches)
PC-58-B	3-L	23022	732 pwht	593	172.4	554.6		15.2	76.2	HAZ	neck	CW	0.25
PC-58-B	4-L	23023	732 pwht	593	158.6	1203.1		9.7	53.2	FL	shear	CW	0.25
PC-58-B	5-L	23025	732 pwht	538	206.9	26800.2		6.3	18.4	FL	shear	CW	0.25
PC-58-B	6-L	23026	732 pwht	538	186.2	49057.6		3.1	7.8	FL	shear	CW	0.25
PC-58-B	7-L	23034	732 pwht	593	144.8	2646.7		7.3	40.5	FL	shear	CW	0.25
PC-59	3-L	23115	as-welded	593	158.6	1268		5.2	19.9	FL	shear	CW	0.25
PC-59	4-L	23116	as-welded	649	103.4	132.8		5.8	16.4	FL	shear	CW	0.25
PC-59	5-L	23124	as-welded	649	89.6	357.4		5.8	11.4	FL	shear	CW	0.25
PC-59	6-L	23161	as-welded	593	172.4	857.7		16.1	43.3	FL	shear	CW	0.25
PC-63	1-L	23236	732 pwht	593	172.4	582.1		8	15.5	FL	shear	CW	0.25
PC-63	5-L	23457	732 pwht	649	89.6	334.1		4.5	16.7	FL	shear	CW	0.25
PC-63	4-L	23295	732 pwht	593	144.8	3363.6		3.6	8.8			CW	0.25
PC-71-TW	7-C	23271	732 pwht	593	172.4	132		9.4	59.4	HAZ/FL	neck	CW	0.25
PC-71-W	2-C	23276	732 pwht	593	172.4	1627.3		13.3	32.3	weld	shear	CW	0.25
PC-71-TW	16-R	23283	732 pwht	593	172.4	185.9		7.8	57.8	HAZ/FL	neck	CW	0.25
PC-71-TW	15-R	23285	732 pwht	538	206.9	17202.9		7	29.5	FL	shear	CW	0.25
PC-71-W	3-C	23430	732 pwht	593	144.8	1784.5		20	36.3	weld	dbl shear	CW	0.25
PC-74	3-T	23366	732 pwht	593	172.4	63.3		18.6	77.2	weld	neck	CW	0.25
PC-74	4-T	23385	732 pwht	593	144.8	197.8		16.9	74.8	weld	neck	CW	0.25
PC-75	4-T	23386	732 pwht	593	144.8	2642.9		2	6.9	weld	neck	CW	0.25
PC-75	3-T	23384	732 pwht	593	172.4	1459.5		2.9	3.3			CW	0.25
PC-80	16-C	23709	760/2h pwht	677	55.2	4923.9		5	25	HAZ	shear	CW	0.25
PC-81	10-C	**23963**	732/40h	593	172.4	297.5	0.0105	24	85.45	HAZ	neck	CW	0.25
PC-81	1-C	**24001**	732/2h	593	172.4	1507	0.000945	15.46	79.82	HAZ	neck	CW	0.25
PC-81	12-C	**24013**	732/40h	649	62.1	5084.5	0.000103	2.66	13.43	weld	brittle	CW	0.25
PC-90	3-L	23485	732 pwht	649	117.2	77.9		4.6	7.2	FL	shear	CW	0.25
PC-90	4-L	23486	732 pwht	649	89.6	450		5.1	15.6	FL	shear	CW	0.25
PC-90	5-L	23489	732 pwht	593	172.4	585.6		9.7	8.6	FL	shear	CW	0.25
PC-90	6-L	23493	732 pwht	593	144.8	2547.8		10.2	48.2	weld	neck	CW	0.25
PC-90	7-L	23497	732 pwht	649	75.8	839.5		3.1	1.2	FL	shear	CW	0.25
PC-90	8-L	23498	732 pwht	649	131.0	26		11.3	16.2	FL	shear	CW	0.25
PC-90	9-L	23501	732 pwht	538	234.4	2783.1		17.1	71.7	weld	neck	CW	0.25
PC-90	10-L	23502	732 pwht	593	193.1	86.2		17.2	61.6	HAZ/FL	neck	CW	0.25
PC-90	11-L	23504	732 pwht	593	206.9	15278.8		18.3	79.7	HAZ	neck	CW	0.25

Weld ID / Ref	Specimen ID	ORNL TN	Condition	Temp. (C)	Stress (MPa)	Rupture Life (hrs)	Min. Creep Rate (%/hr)	Elong. (%)	Red. Of Area (%)	Failure Location	Comment	Specimen Type	Specimen Dia (inches)
PC-93	8-R	23549	732/6h pwht	593	144.8	1070.4		11.4	79.3	HAZ	neck	CW	0.25
PC-93	2-C	23703	732/6h pwht	593	144.8	238.2		14	84.5	weld	neck	CW	0.25
PC-93	29-Z	23771	732/6h pwht	593	124.1	3186.2		18.5	76.9	HAZ	neck	CW	0.25
PC-93	31-Z	23791	732/6h pwht	593	144.8	9835.6		4.4	29	weld	neck	CW	0.25
PC-93	30-Z	23786	732/6h pwht	593	110.3	1949.7		21.1	88.6	HAZ	neck	CW	0.25
PC-94	3-L	23543	732 pwht	649	75.8	881.8		4.4	17.6	FL	shear	CW	0.25
PC-94	4-L	23630	732 pwht	677	41.4	2577.6		13.5	74	weld	neck	CW	0.25
PC-94	5-L	23634	732 pwht	677	55.2	666.8		10.7	34	FL	shear	CW	0.25
PC-95	4-L	23551	732 pwht	649	69.0	2521.3		7.3	13.7	FL	shear	CW	0.25
PC-95	3-L	23540	732 pwht	593	144.8	2223		11.5	52	weld?	neck	CW	0.25
PC-102	3-L	23632	732 pwht	649	75.8	510.4		4.2	48.9	FL	shear	CW	0.25
PC-102	4-L	23644	732 pwht	593	144.8	2468.1		3.7	48.9	FL	shear/neck	CW	0.25
PC-104B	1-C	23812	677 pwht	649	75.8	996.1		4.1	36.2	FL/HAZ	shear/neck	CW	0.25
PC-109	6-R	**25655**	760/1h	593	110.0	2691.6	0.00025	3.8	16.07	weld	0.505 spec	CW	0.505
PC-109	3-C	**25754**	760/1h	538	230.0	87.4	0.025	6.3	7.09	weld	0.505 spec	CW	0.505
PC-109	7-R	**25797**	760/1h	593	110.0	2301.1	0.00034	3.8	5.81	weld	0.505 spec	CW	0.505
PC-110	20-R	**23979**	760/1h	593	172.4	168.1	0.012	8	77.2	HAZ	neck	CW	0.25
PC-110	21-R	**23992**	760/1h	593	144.8	1079.3	0.0012	5.74	63.2	HAZ	neck	CW	0.25
PC-110	19-C	**23997**	760/1h	593	172.4	103.2	0.0235	8.56	71.49	HAZ	neck	CW	0.25
PC-110	22-R	**23999**	760/1h	593	124.1	2277.5	0.00037	4.1	39.47	HAZ/FL	neck/shear	CW	0.25
PC-110	24-T	**24005**	760/1h	593	172.4	1502.9	0.0023	14.95	83.67	base?	neck	CW	0.25
PC-110	25-T	**24006**	760/1h	593	144.8	8086.8	0.00034	13.68	79.41	base?	neck	CW	0.25
PC-110	26-T	**24363**	760/1h	538	179.3	61348D	0.0000086					CW	0.25
PC-110	3-C	25403	760/1h	538	186.2	16746D						CW	0.25
PC-110	11-R	25409	760/1h	538	175.8	16585D					1038/621	CW	0.25
PC-110	4-C	**25411**	760/1h	593	134.5	759.6	0.00029	6.7	88.29	FL	shear	CW	0.25
PC-110	12-R	**25484**	760/1h	593	110.3	4158.7	0.00025	6.3	42.61	HAZ/FL	neck/shear	CW	0.25
PC-110	5-C	**25485**	760/1h	593	103.4	9296.3	0.001	93	53.98	HAZ	neck	CW	0.25
PC-111	3-R	23684	760/1.5 pwht	593	144.8	2304.2		3.8	43.7			CW	0.25
PC-111	1-R	23762	732 pwht	593	172.4	838.2		6.8	69.4			CW	0.25
PC-111	3-C	25401	760/1h	538	193.1	16941D					1038/621	CW	0.25
PC-111	11-R	**25405**	760/1h	593	151.7	2146.6	0.0004	7.6	50.01	HAZ	neck	CW	0.25
PC-111	12-R	25410	760/1h	538	179.3	16439D					10338/621	CW	0.25
PC-111	4-C	**25493**	760/1h	593	137.9	6415.8	0.00016	3.5	7.02	FL	shear	CW	0.25
PC-111	5-C	25535	760/1h	538	165.5	13701D					1038/621	CW	0.25
PC-111	6-C	25604	760/1h	593	117.2	10728D					1038/621	CW	0.25
PC-111	13-C	**25613**	760/1h	593	124.1	2955.3	0.0002	5.7	50.69	HAZ	neck	CW	0.25

Weld ID / Ref	Specimen ID	ORNL TN	Condition	Temp. (C)	Stress (MPa)	Rupture Life (hrs)	Min. Creep Rate (%/hr)	Elong. (%)	Red. Of Area (%)	Failure Location	Comment	Specimen Type	Specimen Dia (inches)
PC-129	1-C	**24163**	732/1h	649	131.0	3615.3	0.000365	8.65	14.52	FL	shear	CW	0.25
PC-129	3-C	24219	as-welded?	593	144.8					weld	brittle	CW	0.25
PC-129	2-R	24279	732/1h	538	206.9	63150D						CW	0.25
PC-132	3-C	**24273**	760/1h	593	172.4	116.3	0.0167	7.84	76.011	HAZ	neck	CW	0.25
PC-132	4-C	**24278**	760/1h	593	144.8	579.9	0.0031	5.8	54.01	FL	shear	CW	0.25
PC-132	5-C	**24285**	760/1h	593	124.1	3568.1	0.000325	4.3	25.88	FL	shear	CW	0.25
PC-132	8-R	**24293**	760/1h	538	206.9	9268.3	0.000272	11.6	80.03	HAZ	neck	CW	0.25
PC-132	9-R	**24376**	760/1h	538	179.3	47271	0.000027	4.25	22.94	FL	shear	CW	0.25
PC-150	1-C	**24545**	732/1h	593	144.8	1503.5	0.00032	1.9	16.94	FL	shear	CW	0.25
PC-150	2-C	**24551**	732/1h	593	124.1	5037.4	0.0000714	1.2	11.98	FL	shear	CW	0.25
PC-150	3-C	**24621**	732/1h	593	110.3	8635.7	0.000044	1.2	9.58	FL	shear	CW	0.25
PC-150	4-C	24625	732/1h	538	193.1					FL	shear	CW	0.25
PC-150	5-C	**24631**	732/1h	649	75.8	711.5	0.00082	1.63	14.67	FL	shear	CW	0.25
PC-156	1-C	**24666**	746/1h	593	144.8	499.4	0.0024	4.3	42.49	FL	shear	CW	0.25
PC-156	4-C	**24962**	746/1h	593	82.7	19972.7	0.000012	2.4	7.45	FL	shear	CW	0.25
PC-156	3-C	**24722**	746/1h	593	103.4	4707.4	0.000125	2.7	24.02	FL	shear	CW	0.25
PC-156	5-C	**24971**	746/1h	538	206.9	9739.4	0.000129	5.7	53.95	FL	shear	CW	0.25
PC-156?	6-C?	24959	746/1h	593	82.7					FL	shear	CW	0.25
PC-156	6-C	24978	746/1h	538	193.1					FL	shear	CW	0.25
PC-158	2-C	24667	746/1h	593	124.1	1075	0.00104	2.8	29.45	FL	shear	CW	0.25
PC-163	CAST?	**24689**	1040/760/1	593	172.4	2540		13.3	83.5	HAZ	neck	CW	0.25
PC-163	CAST?	**24721**	1040/760	593	144.8	10419					NO PLOT	CW	0.25
PC-163	CAST?	**25348**	1040/760	538	206.9	164.2		14	85.6		NO PLOT	CW	0.25
VSI	3	23687	732 pwht	677	55.2	463.9		8.4	71.8	HAZ	neck	CW	0.25
ETEC	4	23718	732 pwht	510	275.8	8046.2		2.6	12.8	weld	DMW	CW	0.25
ETEC	5	23733	1050	593	96.5	14041.7		2	26.8	HAZ/FL	DMW	CW	0.25
ETEC	1	23756	732 pwht	593	172.4	1367.8		5.5	64.1	HAZ	DMW neck	CW	0.25
ETEC	7	23759	732 pwht	649	75.8	1091.7		3.2	53.6	HAZ	DMW neck	CW	0.25
ETEC	15	23769	732 pwht	593	124.1	5013.8		1.4	7.5	FL	DMW interface	CW	0.25
ETEC	16	**24038**	732 pwht	649	48.3	13646.8	0.0000278		3303	FL	DMW shear	CW	0.25

Weld ID / Ref	Specimen ID	ORNL TN	Condition	Temp. (C)	Stress (MPa)	Rupture Life (hrs)	Min. Creep Rate (%/hr)	Elong. (%)	Red. Of Area (%)	Failure Location	Comment	Specimen Type	Specimen Dia (inches)
LNKS	W2(P)	29891	774/8h pwht	600	186.2	38.5	0.15	30.6	44.4	all weld	neck	CW	0.25
LNKS	WA-1	29901	774/8h pwht	600	150.0	660	0.00686	26.2	70.4	all weld	neck	CW	0.25
LNKS	WA-2	29896	774/8h pwht	600	150.0	653	0.007			all weld	neck	CW	0.25
LNKS	WB-1	29911	774/8h pwht	600	120.0	6351	0.00054	14.7	31	all weld	neck	CW	0.25
LNKS	W5	29189	774/8h pwht	593	137.9	1584	0.0017	29.3	72.6			CW	0.25
LNKS	W3(P)	29944	774/8h pwht	650	100.0	468	0.0092	14.5	30.5	all weld	neck	CW	0.25
LNKS	W1(P)	29951	774/8h pwht	550	200.0	7529	0.0004	29.1	73.5	all weld	neck	CW	0.25
LNKS	WA-3	29904	774/8h pwht	600	120.0	56.5				HAZ		CW	0.25
LNKS	W1-1	29879	1040/740 NT	600	186.2	965	0.004	10.1	12.3	all weld		CW	0.25
LNKS	TW1-3	29892	1040/740 NT	600	186.2	706			50.9	HAZ		CW	0.25
LNKS	W1-2	29871	1040/740 NT	600	186.2	760			19.2	HAZ		CW	0.25
LNKS	WE-1	29900	1040/780 NT	600	150.0	1402	0.00346			all weld		CW	0.25
LNKS	WF-1	29918	1040/780 NT	600	120.0	9251	0.00022	7.8	8.2	all weld		CW	0.25
LNKS	WF-3	29928	1040/780 NT	600	150.0	872			76.6	HAZ		CW	0.25
LNKS	WE-3	29918	1040/780 NT	600	120.0	6066			45.4	HAZ		CW	0.25
9R	9AWT	29978	760/4h pwht	593	172.4	4987	0.00045	11.1	18.5	all weld		CW	0.25
9R	9AWC	29981	760/4h pwht	649	103.4	1741	0.001	12.2	21.8	all weld		CW	0.25
9R	9T1	29980	760/4h pwht	593	172.4	468.4			53	HAZ		CW	0.25
10R	10AWC	29975	760/4h pwht	593	172.4	5458	0.00025			all weld		CW	0.25
10R	10AWT	29982	760/4h pwht	593	155.1	7780	0.00019			all weld		CW	0.25
10R	10T1	29979	760/4h pwht	593	172.4	262.5			85.8	HAZ		CW	0.25
10R	10T2	29984	760/4h pwht	649	124.1	61.3			41	HAZ		CW	0.25
W4	W4C-1	29991	760/4h pwht	600	150.0	5632	0.000292	4.8	9	all weld	drop preheat	CW	0.25
W4	W4C-4	30017	760/4h pwht	600	186.2	1193	0.0023	8.3	9.6	all weld	drop preheat	CW	0.25
W4	W4C-3	30052	760/4h pwht	600	100.0	1567	0.001	5.2	6.7	all weld	drop preheat	CW	0.25
W4	W4H-1	29992	hph/760/4h pwht	600	150.0	3373	0.000425	3.5	6.8	all weld	hold preheat	CW	0.25
W4	W4H-3	30019	hph/760/4h pwht	600	186.2	698.4	0.0032	8.4	20.4	all weld	hold preheat	CW	0.25
W4	W4H-2	30055	hph/760/4h pwht	650	100.0	871.2	0.0038	5.1	7.1	all weld	hold preheat	CW	0.25

Weld ID / Ref	Specimen ID	ORNL TN	Condition	Temp. (C)	Stress (MPa)	Rupture Life (hrs)	Min. Creep Rate (%/hr)	Elong. (%)	Red. Of Area (%)	Failure Location	Comment	Specimen Type	Specimen Dia (inches)
W4	W4T-3	29996	hph/760/4h pwht	600	150.0	203			66.8	HAZ	hold preheat	CW	0.25
W4	W4T-4	30027	hph/760/4h pwht	600	120.0	1266			29.3	HAZ	hold preheat	CW	0.25
W4	W4T-2	30064	hph/760/4h pwht	650	100.0	93			45.6	HAZ	hold preheat	CW	0.25
W4	NTW4-2	30132	NT/760/4h	600	150.0	528.1	0.0056	15.3	50.5	all weld	re-NT	CW	0.25
W4	NTW4-5	30135	NT/760/4h	650	100.0	1531				all weld	re-NT	CW	0.25
W4	NTW4-11	30134	NT/760/4h	600	186.2	30.3	0.11	30.3	81.6	all weld	re-NT	CW	0.25
W5	W5C-1	29989	760/4h pwht	600	150.0	1977	0.0019	13.5	28.6	all weld	drop preheat	CW	0.25
W5	W5C-6	30016	760/4h pwht	600	186.2	417	0.0108	18.9	62.8	all weld	drop preheat	CW	0.25
W5	W5C-3	30053	760/4h pwht	650	100.0	1267	0.00193	5.7	27.5	all weld	drop preheat	CW	0.25
W5	W5H-4	29990	hph/760/4h pwht	600	150.0	9152	0.0009	5.3	13.1	all weld	hold preheat	CW	0.25
W5	W5H-3	30018	hph/760/4h pwht	600	186.2	440.8	0.0094	10	23.1	all weld	hold preheat	CW	0.25
W5	W5H-1	30032	hph/760/4h pwht	650	100.0	3106	0.00084	7.7	17.7	all weld	hold preheat	CW	0.25
W5	W5T-2	30028	hph/760/4h pwht	600	186.2	62			82.6		hold preheat	CW	0.25
W5	W5T-3	30000	hph/760/4h pwht	600	150.0	937			22.3		hold preheat	CW	0.25
W5	W5T-4	30065	hph/760/4h pwht	650	100.0	128.6			30.5		hold preheat	CW	0.25
W5	NTW5-2	30133	NT/760/4h	600	186.2	821.8	0.0053	19.9	55.6	all weld	re-NT	CW	0.25
Pipe-ECCC2009	2C1		PWHT 760C-3.5hrs	525	240	3,772		14.6	72.4	WMFL		CW	0.315
Pipe-ECCC2009	3C1		PWHT 760C-3.5hrs	525	220	11,546		9.6	29.7	WM		CW	0.315
Pipe-ECCC2009	6C1		PWHT 760C-3.5hrs	550	200	1,183		14.3	72.4	WMFL		CW	0.315
Pipe-ECCC2009	7C1		PWHT 760C-3.5hrs	550	180	9,853		6.3	14.2	WMFL		CW	0.315
Pipe-ECCC2009	11C1		PWHT 760C-3.5hrs	575	200	134		20.2	84.9	BM		CW	0.315
Pipe-ECCC2009	25C1		PWHT 760C-3.5hrs	575	180	960		15.8	84.9	HAZ		CW	0.315
Pipe-ECCC2009	12C1		PWHT 760C-3.5hrs	575	160	4,704		7.8	37.8	HAZ		CW	0.315
Pipe-ECCC2009	8C1		PWHT 760C-3.5hrs	575	140	9,608		3	18.8	HAZ		CW	0.315
Pipe-ECCC2009	9C1		PWHT 760C-3.5hrs	575	120	12,624		2.1	19	HAZ		CW	0.315

Weld ID / Ref	Specimen ID	ORNL TN	Condition	Temp. (C)	Stress (MPa)	Rupture Life (hrs)	Min. Creep Rate (%/hr)	Elong. (%)	Red. Of Area (%)	Failure Location	Comment	Specimen Type	Specimen Dia (inches)
Pipe-ECCC2009	16C1		PWHT 760C-3.5hrs	600	140	981		20.4	59.3	HAZ		CW	0.315
Pipe-ECCC2009	15C1		PWHT 760C-3.5hrs	600	120	2,242		5	4.9	HAZ		CW	0.315
Pipe-ECCC2009	13C1		PWHT 760C-3.5hrs	600	100	6,080		2.4	12.1	HAZ		CW	0.315
Pipe-ECCC2009	26C1		PWHT 760C-3.5hrs	600	90	8,165		0.5	11.9	HAZ		CW	0.315
Pipe-ECCC2009	14C1		PWHT 760C-3.5hrs	600	80	10,181		2.1	18.8	HAZ		CW	0.315
Pipe-ECCC2009	*24C1		PWHT 760C-3.5hrs	600	70	27,471		1.6	4.9	HAZ		CW	0.315
Pipe-ECCC2009	18C1		PWHT 760C-3.5hrs	625	100	1,777		3.6	18.8	HAZ		CW	0.315
Pipe-ECCC2009	17C1		PWHT 760C-3.5hrs	625	80	3,970		2	16.7	HAZ		CW	0.315
Pipe-ECCC2009	19C1		PWHT 760C-3.5hrs	625	60	13,673		1.8	2.2	HAZ		CW	0.315
Pipe-ECCC2009	*20C1		PWHT 760C-3.5hrs	625	50	29,962		3.4	9.5	HAZ		CW	0.315
Plate-ECCC2009	C16		PWHT 745C-2.5hrs	525	240	9,309		11.9	51	HAZ		CW	0.315
Plate-ECCC2009	C1~		PWHT 745C-2.5hrs	525	220	42,495		?	?	?	in test	CW	0.315
Plate-ECCC2009	C4*		PWHT 745C-2.5hrs	550	180	31,920		2.5	14.4	HAZ		CW	0.315
Plate-ECCC2009	C5*		PWHT 745C-2.5hrs	550	160	33,189		1.6	4.9	HAZ		CW	0.315
Plate-ECCC2009	C6		PWHT 745C-2.5hrs	575	180	2,853		7.6	19.2	HAZ		CW	0.315
Plate-ECCC2009	C15		PWHT 745C-2.5hrs	575	160	3,793		4.3	12.1	HAZ		CW	0.315
Plate-ECCC2009	C7		PWHT 745C-2.5hrs	575	140	10,031		3	4.9	HAZ		CW	0.315
Plate-ECCC2009	C8		PWHT 745C-2.5hrs	575	120	19,289		1.1	7.4	HAZ		CW	0.315
Plate-ECCC2009	C3		PWHT 745C-2.5hrs	600	140	1,797		4.8	12.3	HAZ		CW	0.315
Plate-ECCC2009	C12		PWHT 745C-2.5hrs	600	120	2,610		1.8	14.7	HAZ		CW	0.315
Plate-ECCC2009	C10*		PWHT 745C-2.5hrs	600	80	25,818		1.1	9.8	HAZ		CW	0.315

Weld ID / Ref	Specimen ID	ORNL TN	Condition	Temp. (C)	Stress (MPa)	Rupture Life (hrs)	Min. Creep Rate (%/hr)	Elong. (%)	Red. Of Area (%)	Failure Location	Comment	Specimen Type	Specimen Dia (inches)
Plate-ECCC2009	C11~		PWHT 745C-2.5hrs	600	70	42,632		?	?	?	in test	CW	0.315
Plate-ECCC2009	C2		PWHT 745C-2.5hrs	625	100	1,061		3.2	16.7	HAZ		CW	0.315
Plate-ECCC2009	C9		PWHT 745C-2.5hrs	625	80	2,291		1.1	5.2	HAZ		CW	0.315
Plate-ECCC2009	C13*		PWHT 745C-2.5hrs	625	60	19,210		1.2	7.4	HAZ		CW	0.315
Plate-ECCC2009	C14*		PWHT 745C-2.5hrs	625	50	29,312		9.9	35.2	WM		CW	0.315
Masuyama-Std.			PWHT	550	200.0	530.7		23.5	84			CW	0.236
Masuyama-Std.			PWHT	550	190	1392.6		22.4	82.2			CW	0.236
Masuyama-Std.			PWHT	550	180	2381.6		22.8	78.5			CW	0.236
Masuyama-Std.			PWHT	550	160	16380.1		12.6	40.1			CW	0.236
Masuyama-Std.			PWHT	600	135	305.5		22.5	84.9			CW	0.236
Masuyama-Std.			PWHT	600	120	1262.5		17.9	69.2			CW	0.236
Masuyama-Std.			PWHT	600	115	2605.1		16	54.1			CW	0.236
Masuyama-Std.			PWHT	600	95	10341.3		5.4	35.6			CW	0.236
Masuyama-Std.			PWHT	600	90	12284.7		5.1	30.2			CW	0.236
Masuyama-Std.			PWHT	650	85	357.7		9.9	51			CW	0.236
Masuyama-Std.			PWHT	650	75	839.7		8.7	52.2			CW	0.236
Masuyama-Std.			PWHT	650	70	1412		9.8	50.9			CW	0.236
Masuyama-Std.			PWHT	675	90	28.3		30.9	85.8			CW	0.236
Masuyama-Std.			PWHT	675	75	120.8		19.4	65.4			CW	0.236
Masuyama-Std.			PWHT	675	60	427.2		9.9	47			CW	0.236
Masuyama-Std.			PWHT	650	66	2048.9				FG-HAZ	1.26"x1.575" Specimen	CW - X-groove	
Masuyama-Std.			PWHT	650	66	2775.2				FG-HAZ	1.26"x1.575" Specimen	CW - U-groove	

Weld ID / Ref	Specimen ID	ORNL TN	Condition	Temp. (C)	Stress (MPa)	Rupture Life (hrs)	Min. Creep Rate (%/hr)	Elong. (%)	Red. Of Area (%)	Failure Location	Comment	Specimen Type	Specimen Dia (inches)
EPRI1004702+	1200-1		PWHT 649C-2hrs	565.6	193.1	2363.7				IV		CW	0.25
EPRI1004702+	1200-2		PWHT 649C-2hrs	593.3	144.8	1710.4				IV		CW	0.25
EPRI1004702+	1200-3		PWHT 649C-2hrs	621.1	103.4	885				IV		CW	0.25
EPRI1004702+	1200-4		PWHT 649C-2hrs	565.6	220.6	394.7				base		CW	0.25
EPRI1004702+	1200-5		PWHT 649C-2hrs	593.3	193.1	81				base		CW	0.25
EPRI1004702+	1200-6		PWHT 649C-2hrs	621.1	103.4	1022.7				IV		CW	0.25
EPRI1004702+	1300-1		PWHT 704C-2hrs	565.6	193.1	2436.6				IV		CW	0.25
EPRI1004702+	1300-2		PWHT 704C-2hrs	593.3	144.8	1534.8				IV		CW	0.25
EPRI1004702+	1300-3		PWHT 704C-2hrs	621.1	103.4	413.1				IV		CW	0.25
EPRI1004702+	1300-4		PWHT 704C-2hrs	565.6	220.6	243.1				base		CW	0.25
EPRI1004702+	1300-5		PWHT 704C-2hrs	593.3	193.1	79.4				base		CW	0.25
EPRI1004702+	1300-6		PWHT 704C-2hrs	621.1	86.2	1078.4				IV		CW	0.25
EPRI1004702+	1300-7		PWHT 704C-2hrs	593.3	155.1	787.6				IV		CW	0.25
EPRI1004702+	1300-8		PWHT 704C-2hrs	565.6	203.4	453.9				base		CW	0.25
EPRI1004702+	1400-1		PWHT 760C-2hrs	565.6	193.1	1583.8				base		CW	0.25
EPRI1004702+	1400-2		PWHT 760C-2hrs	593.3	144.8	2387				IV		CW	0.25
EPRI1004702+	1400-3		PWHT 760C-2hrs	621.1	103.4	609.7				IV		CW	0.25
EPRI1004702+	1400-4		PWHT 760C-2hrs	565.6	206.8	324.6				base		CW	0.25
EPRI1004702+	1400-5		PWHT 760C-2hrs	593.3	151.7	732.6				IV		CW	0.25
EPRI1004702+	1400-6		PWHT 760C-2hrs	621.1	103.4	906.3				IV		CW	0.25
EPRI1004702+	1400-7		PWHT 760C-2hrs	593.3	155.1	484.6				IV		CW	0.25
EPRI1004702+	1400-8		PWHT 760C-2hrs	593.3	186.2	77.9				IV		CW	0.25
ER90S-B9	1		PWHT 745C-3hrs	593	175	2092.8		13.5	14.7	weld		All Weld Metal	
ER90S-B9	2		PWHT 745C-3hrs	609	150	322.2		26	70.1	weld		All Weld Metal	
ER90S-B9	3		PWHT 745C-3hrs	621	135	2468.9		12.8	33.2	weld		All Weld Metal	
ER90S-B9	4		PWHT 745C-3hrs	649	110	1488.1		10.5	23.3	weld		All Weld Metal	
ER90S-B9	5		PWHT 745C-3hrs	649	97.9	1334.9		8.9	27.3	weld		All Weld Metal	
ER90S-B9	6		PWHT 745C-3hrs	649	88.3	5479.6		10.1	33.5	weld		All Weld Metal	

Weld ID / Ref	Specimen ID	ORNL TN	Condition	Temp. (C)	Stress (MPa)	Rupture Life (hrs)	Min. Creep Rate (%/hr)	Elong. (%)	Red. Of Area (%)	Failure Location	Comment	Specimen Type	Specimen Dia (inches)
PC-52	8R	30344	PWHT 810C-1hr	600	170	76.7	0.0058	19.7	75.9	HAZ	2.25" GL	CW	0.25
PC-52	6R	30341	PWHT 810C-1hr	650	100	71.9	0.0055	22.4	43.5	HAZ	2.25" GL	CW	0.25
PC-52	9R	30436	PWHT 810C-1hr	600	140	686.2			38.1	HAZ	2.25" GL	CW	0.25
PC-52	11R	30434	PWHT 810C-1hr	600	120	2261.9			24.6	HAZ	2.25" GL	CW	0.25
PC-45	3T	30849	PWHT 760C-1hr	600	120	2685.1		4	17.6	HAZ		CW	0.25
PC-45	4T	30837	PWHT 760C-1hr	600	100	7996.9		2.5	5.2	HAZ		CW	0.25

REFERENCES – PART 2

[1] ASME Boiler and Pressure Vessel Code, Section I: Rules for Construction of Power Boilers, PG-26: Weld Joint Strength Reduction Factor, 2009b Addenda to 2007 Edition, ASME, New York, NY.

[2] ASME Code for Pressure Piping, B31: B31.1 Power Piping and B31.3 Process Piping, 2009.

[3] "Guidelines for the Evaluation of Seam-Welded High-Energy Piping, Fourth Edition," EPRI 1004329, December 2003, EPRI, Palo Alto, CA.

[4] "Guidelines for the Evaluation of Seam-Welded High Energy Piping," EPRI TR-104631, September 1996, EPRI, Palo Alto, CA.

[5] C.D. Lundin et al., "Failure Analysis of a Service-Exposed Hot Reheat Steam Line in a Utility Steam Plant," WRC Bulletin 354, June 1990, WRC/MPC, New York, NY.

[6] M.J. Cohn and S.R. Paterson, "Evaluation of Historical Longitudinal Seam Weld Failures in Grades 11, 12 and 22 Materials," PVP 2008-61245, Proc., ASME Pressure Vessels and Piping Divisions Conference, July 2008, ASME, New York, NY.

[7] ASME Boiler & Pressure Vessel Code archived data as analyzed by B. Roberts, September 10, 1990: Box No. SCP-85-29, Reference No. BC-85-491, updated to BC 90-471.

[8] J.F. Henry, F.V. Ellis and C.D. Lundin, "The Influence of Flux Composition on the Elevated Temperature Properties of Cr-Mo Submerged Arc Weldments," WRC Bulletin 354, June 1990, WRC/MPC, New York, NY.

[9] "Performance Review of P/T91 Steels," 1004516, EPRI, Palo Alto, CA, 2002.

[10] S.J. Brett, "In-service Type IV Cracking in a Modified 9Cr (Grade 91) Header," Proc., ECCC Creep Conference, September 2005, ETD, Ltd., UK.

[11] S.J. Brett, "Service Experience with a Retrofit Modified 9Cr (Grade 91) Steel Header," Proc., EPRI Conference on Advanced Materials, 2007, EPRI, Palo Alto, CA.

[12] A. Shibli and D. Robertson, "Experience with the Use of P91 Steel in Power Plant Boilers and the Development of Tools for Component Integrity/Life Assessment," Proc., EPRI Conference on Advanced Materials, 2007, EPRI, Palo Alto, CA.

[13] J. Parker, "Service Experience for Grade 91 Steel in Boilers and Piping," Presentation, VGB Workshop, Materials and Quality Assurance, Copenhagen, Denmark, May 2009.

[14] IHI, Japan, "Property of Modified 9Cr-1Mo Weld Joint," presentation to ASME Boiler and Pressure Vessel Code Section II and Section IX Subgroup on Strength of Weldments, June 2006.

[15] K. Yoshida, H. Nakai and M. Fukuda, "Regulatory Review Results on Allowable Tensile Stress Values of Creep Strength Enhanced Ferritic Steels," Paper CREEP2007-26512, Proc., Eighth International Conference on Creep and Fatigue at Elevated Temperatures, ASME, New York, NY, 2007.

[16] C. Middleton et al., "An Assessment of the Risk of Type IV Cracking in Welds to Header, Pipework and Turbine Components Constructed from the Advanced Ferritic 8% and 12% Chromium Steels," in Proc. of the 3rd Conference on Advances in Material Technology for Fossil Power Plants, R. Viswanathan et al. Eds., The Institute of Materials, UK, 2001 (also EPRI 1001462), p. 69.

[17] "State-of-Knowledge – Grades 92 and 122 Steel for Fossil Power Plants," 1014929, EPRI, Palo Alto, CA, 2008.

[18] D. Abson, J. Rothwell and B. Cane, "Advances in Weld Creep Resistant 9-12%Cr Steels," Proc., Fifth International Conference on Advances in Materials Technology for Fossil Power Plants, Marco Island, FL, 2007, EPRI, Palo Alto, CA.

[19] "Fourcrack- Advanced Coal-Fired Power Plant Steels -Avoidance of Premature Weld Failure by 'Type IV' Cracking", Project Summary 304, July 2005, Department of Trade and Industry, UK.

[20] "Damage Mechanisms Affecting Fixed Equipment in the Refining Industry," API Recommended Practice 671, First Edition, December 2003, American Petroleum Institute, Washington, DC.

[21] J.D. Dobis et al., "Failure of Seam-Welded Low-Chrome Refinery Piping," Materials Performance, v.34, n. 12, 1995, pp 61-64.

[22] G.M. Buchheim et al., "Failure Investigation of a Low Chrome Long-Seam Weld in a High-Temperature Refinery Piping System," J. Pressure Vessel Technology, v.117, August 1995, ASME, New York, NY.

[23] David A. Hansen and Robert B. Puyear, "Materials Selection for Hydrocarbon and Chemical Plants," Marcel Dekker, New York, NY, 1996, pp 11-12.

[24] B. Roberts, "Review of Allowable stresses for Wrought 21/4Cr-1Mo, 11/4C-1/2Mo-Si, and 1Cr-1/2Mo Steel," Box No. SCP-85-29, Reference No. BC-85-491, updated to BC 90-471, ASME Boiler and Pressure Vessel Code data package, ASME, New York, NY, September 10, 1990.

[25] A. Snow and M. T. Jakub, "Developments in Elevated Temperature Structural Design Criteria," pp. 240-271 in Pressure Vessels and Piping Design Technology- 1882- A Decade of Progress, American Society of Mechanical Engineers, New York, NY, 1982.

[26] A. K. Dhalla, Recommended Practices in Elevated Temperature Design: Compendium of Breeder Reactor Experiences (1970-1987) Volume 1- Current Status and Future Directions, WRC Bulletin 362, Welding Research Council, New York, NY, April, 1991.

[27] A. L. Ward, et al., Preparation, Characterization, and Testing of Austenitic Stainless Steel Weldments, HEDL-TME 71-118, Hanford Engineering Development Laboratory, Richland, WA (August 1971).

[28] G. M. Goodwin, D. G. Harman, and N. C. Cole, pp. 108-109 in Fuels and Materials Development Program Quarterly Progress Report, ORNL-4480, September, 1969.

[29] M. K. Booker & B. P. L. Booker, Unpublished work at the Oak Ridge National Laboratory, Oak Ridge, TN, 1985.

[30] M. K. Booker, Unpublished work at the Oak Ridge National Laboratory, Oak Ridge, TN, 1985.

[31] D. Roberts, Unpublished work at Gulf General Atomics.

[32] C. R. Brinkman, V. K. Sikka, J. A. Horak, and M. L. Santella, Long Term Creep-Rupture Behavior of Modified 9Cr-1Mo Steel Base and Weldment Behavior, ORNL/TM-10504, Oak Ridge National Laboratory, Oak Ridge, TN, November, 1987.

[33] C. R. Brinkman, P. J. Maziasz, B. L. P. Keyes, and H. D. Upton, Development of Stress-Rupture Reduction Factors for Weldments and the Influence of Postest Thermal Aging to 50,000 h on the Microstructural Properties on Modified 9Cr-1Mo Steel, ORNL/TM-11459, Oak Ridge National Laboratory, Oak Ridge, TN, November, 1990.

[34] J. M. Corum, "Evaluation of Weldment Creep and Fatigue Strength-Reduction Factors for Elevated-Temperature Design,' pp. 9-17 in Structural Design for Environments- Creep, Ratchet, Fatigue, and Fracture, PVP- Vol. 163, American Society of Mechanical Engineers, New York, NY, 1989.

[35] R. I. Jetter, "Subsection NH- Class 1 Components in Elevated Temperature Service," pp. 369-404 in Companion Guide to the ASME Boiler & Pressure Vessel Code, Volume, K. R. Rao, editor, American Society of Mechanical Engineers, New York, NY, 2002.

[36] D. S. Griffin, "Elevated-Temperature Structural Design Evaluation Issues in LMFBR Licensing," Nuclear Engineering and Design, Vol. 90, 1985, pp. 299-306.

[37] Charles Becht IV, "New Weld Joint Factors in the Creep Regime for ASME B31.3 Piping." Presentation to: ASME Section II/IX Subgroup Strength of Weldments, November 12, 2007 Dallas, TX.

[38] 2007 ASME Boiler & Pressure Vessel Code, 2008a Addenda; Section I : Rules for Construction of Power Boilers. © 2008 The American Society of Mechanical Engineers, New York, NY.

[39] ASTM Data Series DS 11S1, "An Evaluation of the Elevated Temperature Tensile and Creep Rupture Properties of Wrought Carbon Steel," ASTM, West Conshohocken, PA, 1970.

[40] F. Ellis, S. Ibarra and N. Mack, "Remaining Creep Life Estimation for Carbon Steel Mitered Elbow," Proc., ASME PVP 1993, PVP-Vol. 261, pp213-220.

[41] J.E. McLaughlin, G.G. Karcher and P. Barnes, "Life Assessment of Carbon Steel Vessel with Cracks Operating in the Creep Range," Proc., ASME PVP 1994, PVP-Vol. 288, pp 351-361.

[42] C.J. Moss and J.L. Davidson, "Graphitisation in Type 201 Carbon Steel in Petro-Chemical Plant after Long Term Service," Materials Forum, v. 17, 1993, pp 35-359.

[43] A.K. Ray et al., "Prediction of Remaining Life of a FCCU Reactor Plate," Engineering Failure Analysis, vol. 7, no.2, 2000, pp 75-86.

[44] J.G. Wilson, "Graphitization of Steel in Petroleum Refining Equipment" and "The Effect of Graphitization of Steel on Stress Rupture Properties," Welding Research Council (WRC) Bulletin 32, WRC, New York, NY, 1957.

[45] J.M. Tanzosh and R.H. Emmanuelson to J. Hainsworth, "Final Report – E7018 Weld Metal Properties," Internal Babcock & Wilcox Co. Report, April 27, 1987.

[46] A Review of High Temperature Performance Trends and Design Rules for Cr-Mo Steel Weldments, EPRI, Palo Alto, CA: 1998. TR-110807.

[47] R. D. Wylie, C. L. Corey, and W. E. Leyda, "Stress Rupture Properties of Some Chromium-Nickel Stainless Steel Weld Deposits," Transactions of American Society of Mechanical Engineers, Vol. 76, 1954, pp. 1093-1106.

[48] Voorhees, H. R., and Freeman, J. W., The Elevated-Temperature Properties of Weld-Deposited Metal and Weldments, ASTM STP No. 226, American Society for Testing and Materials, Philadelphia, PA 1958.

[49] D. A. Canonico and R. W. Swindeman, unpublished research, Oak Ridge National Laboratory, 1966.

[50] N. W. Davis and T. M. Cullen, "The Influence of Nitrogen Content on the Rupture Properties of Type 308 Stainless Steel Weldments," pp. 54-65 in Symposium on Properties of Weldments at Elevated Temperature, American Society of Mechanical Engineers, New York, NY, April, 1968.

[51] D. P. Edmonds, D. M. Vandergriff, and R. J. Gray, "Effect of Delta Ferrite Content on the Mechanical Properties of E308-16 Stainless Steel Weld Metal, III. Supplemental Studies," pp. 47 to 62 in Properties of Steel Weldments for Elevated Temperature Pressure Containment Applications, MPC-9, American Society of Mechanical Engineers, New York, NY, April, 1968.

[52] R. G. Berggren, et al., Structure and Elevated Temperature Properties of Type 308 Stainless steel Weld Metal with Varying Ferrite Contents, ORNL-5145, Oak Ridge National Laboratory, Oak Ridge, TN, February, 1977.

[53] R. G. Berggren, et al., "Structure and Elevated Temperature Properties of Type 308 Stainless Steel Weld Metal with Varying Ferrite Contents," Welding Journal Research Supplement, June, 1978.

[54] R. T. King, J. O. Stiegler, and G. M. Goodwin, Creep Properties of a Type 308 Stainless Steel Pressure Vessel Weld with Controlled Residual Elements, ORNL-TM-4131, Oak Ridge National Laboratory, Oak Ridge, TN, May 1973.

[55] J. O Stiegler, R. T. King, and G. M. Goodwin, "Effect of Residual Elements on Fracture Characteristics and Creep Ductility of Type 308 Stainless Steel Weld Metal," Trans. ASME Journal of Engineering Materials and Technology, Vol. 97, 1975, 245-50.

[56] A. L. Ward, Austenitic Stainless Steel Weld Materials A Compilation and Review, HEDL- TME 74-25, Hanford Engineering Development Laboratory, Hanford, WA, May 1974

[57] A. L. Ward, et al., Preparation Characterization and Testing of Austenitic Stainless Steel Weldments, HEDL-TME 71-118, Hanford Engineering Development Laboratory, Hanford, WA, August 1971.

[58] M. W. Williams, Metallographic and Fractographic Observations of Posttest Creep-Fatigue Specimens of Weld-Deposited Type 308 CRE Stainless Steel, ANL-78-74, Argonne National Laboratory, Argonne, IL, August, 1978.

[59] D. P. Edmonds and E. Bolling, "Creep-Rupture Behavior of Gas Tungsten-Arc Types 308, 316, and 16-8-2 Stainless Steel Welds Made with Special Filler Materials," pp. 182 to 187 in Mechanical Properties Test Data for Structural Materials Quarterly Progress Report for Period Ending April 30, 1975, ORNL-5105, Oak Ridge National Laboratory, Oak Ridge TN, 1975.

[60] R, L. Klueh and D. P. Edmonds, Chemical Composition Effects on the Creep of Austenitic Stainless Steel Weld Metals, ORNL-5840, Oak Ridge National Laboratory, Oak Ridge, TN, May 1982.

[61] D. P. Edmonds, et al., Evaluation of Commercial Heats of Stainless Steel Weld Metals with Controlled Residual Elements, ORNL-5945, Oak Ridge National Laboratory, Oak Ridge, TN, December, 1983.

[62] R. L. Klueh and D. A. Canonico, Elevated-Temperature Tensile Strength and Microstructure of a Weld-Overlaid Type 304 Stainless Steel Forging, ORNL-TM-4521, Oak Ridge National Laboratory, Oak Ridge, TN, May, 1974.

[63] R. L. Klueh and D. A. Canonico, The Creep-Rupture Properties of a Weld-Overlaid Type 304 Stainless Steel Forging, ORNL-5085, Oak Ridge National Laboratory, Oak Ridge, TN, February, 1976.

[64] W. J. McAfee and Y. L. Lin, The Effect of Weld-Metal Properties Variations on the Elevated Temperature Deformation and Failure Behavior of Structural Weldments, ORNL/TM-7767, Oak Ridge National Laboratory, Oak Ridge, TN, November, 1981.

[65] W. J. McAfee, M. Richardson, and W. K. Sartory, Creep Deformation and Rupture Behavior of Type 304/308 Stainless Steel Structural Weldments, ORNL-5265, Oak Ridge National Laboratory, Oak Ridge, TN, June, 1977.

[66] R. D. Thomas, Jr., "Effect of Delta Ferrite Content of E308-16 Stainless Steel Weld Metal, I. Weld Metal Preparation," pp. 1 to 16 in Properties of Steel Weldments for Elevated Temperature Pressure Containment Applications, MPC-9, American Society of Mechanical Engineers, New York, NY, April, 1978.

[67] D. Hauser and J. A. VanEcho, "Effect of Delta Ferrite Content of E308-16 Stainless Steel Weld Metal, II. Mechanical Property and Metallographic Studies, pp. 17 to 46 in Properties of Steel Weldments for Elevated Temperature Pressure Containment Applications," MPC-9, American Society of Mechanical Engineers, New York, NY, April, 1978.

[68] W. E. Leyda, L. Katz, M. Gold, and R. L. Snyder, "Stress Rupture Properties of C-Mo, Cr-Mo, Stainless Steel, and Ni-Cr-Fe Welds, pp. 183 to 204 in Properties of Steel Weldments for Elevated Temperature Pressure Containment Applications," MPC-9, American Society of Mechanical Engineers, New York, NY, April, 1978.

[69] W. E. White and I. A. Le May, "On Time-Temperature Parameters for Correlation of Creep-Rupture Data in Stainless Steel Weldments," ASME Journal of Engineering Materials and Technology, Vol. 100, 1978, pp. 319-32.

[70] W. E. White and I. LeMay, "Strain-Time Behavior and Second-Stage Creep Rate Characterization in Stainless Steel Weldments," pp. 89-94 in , International Conference on Engineering Aspects of Creep (Vol. 2), Institute of Mechanical Engineers, London, 1980.

[71] R. W. Swindeman, E. Bolling, and R. T. King, Tensile and Creep Behavior of Type 308 CRE Stainless Steel Joining 13-mm Type 304 Stainless Steel Plate, ORNL/TM-6995, Oak Ridge National Laboratory, Oak Ridge, TN, November, 1979.

[72] M. J. Manjoine, Crack Initiation and Growth in Welds at 593°C, WARD-HT-3045-28, Westinghouse Advanced Reactors Division, Pittsburgh, PA, August, 1977.

[73] M. J. Manjoine, Creep-Rupture Tests of Type 304 Stainless Steel Weldments with Central Axial Welds of Type 308 Stainless Steel at 593°C, WARD-HT-3045-38, Westinghouse Advanced Reactors Division, Pittsburgh, PA, May, 1979.

[74] M. J. Manjoine, Creep-Rupture Tests of Type 304 Stainless Steel Weldments with Central Axial Welds of Type 308 Stainless Steel at 593°C, WARD-HT-94000-3, Westinghouse Advanced Reactors Division, Pittsburgh, PA, September, 1979.

[75] M. J. Manjoine, Creep-Rupture Tests at 593°C (1100°F) of Weldments with Geometric Discontinuities to Produce High Stress and Strain Gradients, WARD-HT-94000-4, Westinghouse Advanced Reactors Division, Pittsburgh, PA, March, 1980.

[76] B. van der Schaaf, M. I. de Vries, and J. D. Elen, Effect of Neutron Irradiation on Creep Properties of 18Cr-11Ni (DIN 1.4948) Stainless Steel Plate and Welded Joints at 823 K, ECN-61, Netherlands Energy Research Foundation, Petten, The Netherlands, May, 1979.

[77] B. van der Schaaf, M. I. de Vries, and J. D. Elen, "Effect of Neutron Irradiation on Creep, Fatigue and Their Interaction of DIN 1.4948 (Type 304) Stainless Steel Plate and Welded Joints at 823 K," pp. 153-158 in , International Conference on Engineering Aspects of Creep (Vol. 1), Institute of Mechanical Engineers, London, 1980.

[78] E. Bolling unpublished research, Oak Ridge National Laboratory, Oak Ridge, TN, 1980.

[79] R. W. Swindeman and W. Williams, unpublished research, Oak Ridge National Laboratory, Oak Ridge, TN, 1980.

[80] T. R. Padden, Metallurgical Characterization of the Creep Ratcheting Test Article Failure, WAESD-HT-94000-28, Westinghouse Electric Company, Madison, PA, June 1983.

[81] A. Dhalla, "Influence of Weld Factors on Creep-Rupture Cracking at Elevated Temperature, J. Pressure Vessel Technology, vol. 113, Mat, 1991, pp. 194-208.

[82] W. J. McAfee and Y. L. Lin, The Effect of Weld-Metal Properties Variations on the Elevated Temperature Deformation and Failure Behavior of Structural Weldments, ORNL/TM-7767, Oak Ridge National Laboratory, Oak Ridge, TN, November, 1981.

[83] W. J. McAfee, R. L. Battiste, and R. W. Swindeman, Elevated Temperature (593°C) Tests and Analysis of Type 304/308-CRE Stainless Steel Plate Weldments, ORNL/TM-9064, Oak Ridge National Laboratory, Oak Ridge, TN, May 1984.

[84] Data Sheets on the Elevated Temperature Properties for Base Metal, Weld Metals, and Welded Joints of 18Cr-8Ni Stainless Steel Plate (SUS 304-HP), NRIM Creep Data Sheet No, 32, National Research Institute for Metals, Tokyo , Japan, 1982.

[85] Y. Monma, S. Yokoi, and M. Yamazaki, "Creep Strain-Time Behavior of 304/308 Weldments for Fast Breeder Reactor Vessel," pp. 1366-92 in Fifth International Conference on Pressure Vessel Technology Vol. II, Materials and Manufacturing, American Society of Mechanical Engineers, New York, NY, 1984.

[86] Y. Monma, M. Yamazaki, and S. Yokoi, "Creep Strain-Time Behavior of 304/308 Steel Welded Joints with Different Specimen Geometries," pp. 33-37 in International Conference on Creep, Japan Institute of Metals, Tokyo, 1986.

[87] H. Huthman, B. Gladbach, and H. U. Borstedt, "Influence of Sodium on the Creep-Rupture Behavior of Steel X 6 CRNI 18 11 (Type 304 SS) at 823 K," pp. 645-72 in Mechanical Properties of Structural Materials Including Environmental Effects, IWGFR-49, International Atomic Energy Agency, 1983.

[88] A. W. Marshall and J. C. M. Farrar, "Influence of Residuals on Properties of Austenitic Stainless Steel Weld Metal with Particular Reference to Energy Industries," pp. 272-85 in Stainless Steels '84, Institute of Metals, London, UK, 1985.

[89] Y. L. Lin and R. L. Battiste, Elevated Temperature Test and Analysis of 304 SS/308 CRE Welded Beam (WB-1), ORNL/TM-10292, Oak Ridge National Laboratory, Oak Ridge, TN, February, 1987.

[90] Beggs, D. V., and Iberra, S., "The Influence of Delta Ferrite Content on the Stress-Rupture Strength of Stainless Steel Welds," pp.117 to 119 in Service Experience in Operating Plants 1991, PVP-Vol. 221, American Society of Mechanical Engineers, New York, NY, 1991.

[91] J. M. Vitek, S. A. David, and V. K. Sikka, "Examination of Types 308 and 308CRE Stainless Steels after Interrupted Creep Testing, Welding Journal-Welding Research Supplement, November 1992, pp. 421s-435s.

[92] C. F. Etienne and J. H. Heerings, Evaluation of the Influence of Welding on Creep Resistance, TNO, Apeldoorn, The Netherland, May, 1993.

[93] R. W. Swindeman, unpublished research, Oak Ridge National Laboratory, Oak Ridge, TN, 1995.

[94] Data Sheets on the Elevated-Temperature Properties for Base Metals, Weld Metals and Welded Joints of 18Cr-8,Ni Stainless Steel Plates (SUS 304-HP), NRIM Creep Data Sheet No. 32A, National Research Institute for Metals, Tokyo, Japan, 1995.

[95] G. J. Guarnieri, Final Report on High Temperature Testing of Type 316 Stainless Steel Sheet, Report No. KB-737-M-3, Cornell Aeronautical Laboratory, Buffalo, NY, June 29, 1951.

[96] R. D. Wylie, C. L. Corey, and W. E. Leyda, "Stress-Rupture of Some Chromium-Nickel Stainless-Steel Weld Deposits, Trans. ASME, Vol. 76 October, 1954, 1093-1106.

[97] H. R. Voorhees and J. W. Freeman, The Elevated-Temperature Properties of Weld-Deposited Metal and Weldments, ASTM STP No. 226, American Society for Testing and Materials, Philadelphia, PA, 1958.

[98] G. H. Rowe and J. R. Stewart, "Creep-Rupture Behavior of Type 316 Stainless Steel Weldments Prepared with and without Restraint," Welding Journal Research Supplement, ASME Paper No. 62-Met-19, December 1962.

[99] R. J. Christoffel, "Notch Sensitivity of the Heat Affected Zone in 316 Materials," Welding Journal, January, 1963, pp. 25s-28s.

[100] R. J. Truman and D. Hardwick, "Some Effects of Heat Treatment and Welding on the Rupture Properties of Three Austenitic Steels," reported in reference 9.

[101] G. M. Goodwin, D. G. Harman, and N. C. Cole, pp. 108-109 in Fuels and Materials Development Program Quarterly Progress Report, ORNL-4480, September, 1969.

[102] A. L. Ward, et al., Preparation, Characterization, and Testing of Austenitic Stainless Steel Weldments, HEDL-TME 71-118, Hanford Engineering Development Laboratory, Richland, WA, August 1971.

[103] R. G. Gilliland, The Behavior of Welded Joints in Stainless and Alloy Steels at Elevated Temperatures, ORNL-4781, Oak Ridge National Laboratory, Oak Ridge, TN, August 1972.

[104] R. A. Moen and L. D. Blackburn, 304 and 316 Stainless Steel - Backup Information for Code Case 1592 Stress Allowables, Hanford Engineering Development Laboratory, Hanford, WA, 1972.

[105] R. G. Berggren, et al., Interim Report on Weldability and Mechanical Properties of 16-8-2 Stainless Steel Filler Metal, ORNL-TM-4365, Oak Ridge National Laboratory, Oak Ridge, TN, November 1973.

[106] A. L. Ward, "Thermal and Irradiation Effects on the Tensile and Creep-Rupture Properties of Weld-Deposited Type 316 Stainless Steel," Nuclear Technology, Vol. 24, November, 1974 pp.201-215.

[107] R. T. King, et al., "Properties and Structure of 16-8-2 Stainless Steel Weld Metal," paper 75-PVP-45, presented at the Second National Conference on Pressure Vessels and Piping, San Francisco, CA, June 23-27, 1975.

[108] R. T. King, G. M. Goodwin, and E. Bolling, "Creep and Creep-Rupture Characterization of Type 16-8-2 Stainless Steel Weld Metal," pp. 174-187 in Mechanical Properties Test Data for Structural Materials Quarterly Progress Report for Period Ending April 30, 1975, ORNL-5105, Oak Ridge National Laboratory, Oak Ridge, TN, 1975.

[109] W. E. White and I. Le May, "On Time-Temperature Parameters for Correlation of Creep-Rupture Data in Stainless Steel Weldments," J. Engineering Materials and Technology, Vol. 100, July 1978, pp. 319-332.

[110] I. Le May and W. E. White, "Creep of Stainless Steel Weldments," pp. 861-870 in Third International Conference on Pressure Vessel Technology, American Society of Mechanical Engineers, New York, NY, 1977.

[111] J. M. Leitnaker, et al., Transformations Occurring on Aging of 16-8-2 Weld Metal, ORNL-5400, Oak Ridge National Laboratory, Oak Ridge, TN, June 1978.

[112] V. K. Sikka and J. W. McEnerney, Use of Ultimate Tensile Strength to Estimate the Creep-Rupture Behavior of Austenitic Weld Metal and Castings, ORNL-6781, Oak Ridge National Laboratory, Oak Ridge, TN, May 1979.

[113] R. L. Klueh and D. P. Edmonds, Mechanical Properties of 16-8-2 Large-Diameter Pipe Girth Welds, ORNL-5660, Oak Ridge National Laboratory, Oak Ridge, TN, September 1980.

[114] R. L. Klueh and D. P. Edmonds, Effects of Different Fluxes on Elevated-Temperature Strength of 16-8-2 Submerged-Arc Welds, ORNL-5594, Oak Ridge National Laboratory, Oak Ridge, TN, February 1980.

[115] J. W. McEnerney and V. K. Sikka, Time-Dependent Properties of Welds in Type 316 Stainless Steel Formed-and-Welded Pipes, ORNL/TM-7394, Oak Ridge National Laboratory, Oak Ridge, TN, September 1980.

[116] C. F. Etienne, and O. van Rossum, "Creep of Welded Joints in AISI 316," paper C328/80 in Engineering Aspects of Creep, Institute of Mechanical Engineers, London UK, 1980.

[117] F. Roode, C. F. Etienne, and O. van Rossum, "Stress and Strain Analysis for Creep and Plasticity of Welded Joints in AISI 316," paper C329/80 in Engineering Aspects of Creep, Institute of Mechanical Engineers, London UK, 1980.

[118] R. L. Klueh and D. P. Edmonds, Chemical Composition Effects on the Creep of Austenitic Stainless Steel Weld Metals, ORNL-5840, Oak Ridge National Laboratory, Oak Ridge, TN (May 1982)

[119] D. P. Edmonds, E. Bolling, M. K. Booker, and R. L. Klueh, Evaluation of Commercial Heats of Stainless Steel Weld Metals with Controlled Residual Elements, ORNL 5945, Oak Ridge National Laboratory, Oak Ridge, TN, December 1983.

[120] V. K. Sikka and K. W. Boling, Design, Assembly, and Initial Results from the Large-Diameter-Pipe Thermal-Aging Test Facility, ORNL/TM-8884, Oak Ridge National Laboratory, Oak Ridge, TN, December 1983.

[121] J. R. Foulds, J. Moteff, V. K. Sikka, and J. W. McEnerney, "Deformation Behavior of a 16-8-2 GTA Weld as Influenced by Its Solidification Substructure," Metallurgical Transactions, Vol. 15A, July 1983, pp. 1357-1366

[122] J. M. Corum, High-Temperature Structural Design Program Semiannual Progress Report for Period Ending June 30, 1982, ORNL-5930, Oak Ridge National Laboratory, Oak Ridge, TN, March 1983.

[123] J. M. Corum and J. J. Blass, Structural Design Technology Annual Progress Report for Period Ending June 30, 1986, ORNL-6341, Oak Ridge National Laboratory, Oak Ridge, TN, March 1987.

[124] J. M. Corum, et al., Experimental and Analytical Evaluation of Weldment Creep Strength Reduction Factors for Elevated-Temperature Structural Design, ORNL-6500, Oak Ridge National Laboratory, Oak Ridge, TN, September, 1988.

[125] J. M. Corum and W. K. Sartory, "Assessment of Current High-Temperature Design Methodology Based on Structural Failure Tests," Journal of Pressure Vessel Technology, Vol. 109, May 1987, pp. 160-168.

[126] J. M. Corum, "Evaluation of Weldment Creep and Fatigue Strength-Reduction Factors for Elevated-Temperature Design," pp. 9-17 in Structural Design for Elevated Temperature Environments- Creep, Ratchet, Fatigue, and Fracture, PVP. Vol. 163, American Society for Mechanical Engineers, New York, NY, 1989.

[127] J. M. Corum and W. K. Sartory, "Assessment of Current High-Temperature Design Methodology Based on Structural Failure Tests," Journal of Pressure Vessel Technology, Vol. 109, May 1997, 160-168.

[128] C. F. Etienne and J. H. Heerings, "Evaluation of the Influence of Welding on Creep Resistance," IIW doc IX-1725-93, paper presented at the meeting of IIW Cie IX Working Group Creep, Copenhagen, 27-28 May, 1993.

[129] B. Lundqvist, T. Andersson, and B. Hallstadt, "Creep Strength of Weld Metal and Weld Metal Joints in Austenitic Cr-Ni Steels and Ni-Alloys," 1985 Sandvik Report presented at Life of Welds at High Temperature, Institute of Mechanical Engineer, London, June 1990.

[130] Y-H Hsiao, H. Zang, and G. S. Daehn, A Study of the Creep Damage Distribution in 316 Stainless Steel Weldments Due to Multiaxial Stresses, EWI MR9507, Edison Welding Institute, Columbus, OH, August 1995.

[131] M. K. Booker and B. P. L. Booker, "New Methods for Analysis of Materials Strength Data for ASME Boiler and Pressure Code," in Use of Computers in Managing Material Property Data, MPC-14, American Society of Mechanical Engineers, New York, NY, 1980.

[132] The Elevated-Temperature Properties of Weld-Deposited Metal and Weldments, ASTM STP No. 226. American Society for Testing and Materials, Philadelphia, PA.

[133] J. W. York and R. L. Flury, Assessment of Candidate Weld Metals for Joining Alloy 800, WNET-119, Westinghouse Electric Corporation Tampa Division, Tampa FL, February 1976.

[134] R. L. Klueh and J. F. King, Elevated Tensile Properties of ERNiCr-3 Weld Metal, ORNL-5354, Oak Ridge National Laboratory, Oak Ridge, TN, December 1977.

[135] J. F. King and R. W. Reed, Jr., Weldability of Alloy 800, ORNL/TM-6276, Oak Ridge National Laboratory, Oak Ridge, TN, April 1978.

[136] R. L. Klueh and J. F. King, Creep and Creep-Rupture Behavior of ERNiCr-3 Weld Metal, ORNL-5404, Oak Ridge National Laboratory, Oak Ridge, TN, June 1978.

[137] R. L. Klueh and J. F. King, Mechanical Properties of ERNiCr-3 Weld Metal Deposited by Gas Tungsten-Arc Process with Hot-Wire Filler Additions, ORNL-5491, Oak Ridge National Laboratory, Oak Ridge, TN, March 1979.

[138] W. K. Sartory, Inelastic Ratchetting Analysis of the 2 1/4Cr-1 Mo Steel to Type 316 Stainless Steel Dissimilar Metal Weldment Region of Specimen TTT-3, ORNL-5512 Oak Ridge National Laboratory, Oak Ridge, TN, March 1979.

[139] W. K. Sartory, Revised Analysis of the Transition Joint Life Test, ORNL/TM-9211, Oak Ridge National Laboratory, Oak Ridge, TN, July 1984.

[140] M. K. Booker and J. P. Strizak, Evaluation of Time-Dependent Fatigue Behavior of ERNiCr-3 Weld Metal by Strain-Range Partitioning, ORNL/TM-7697, Oak Ridge National Laboratory, Oak Ridge, TN, May 1981.

[141] R. L. Klueh and J. F. King, Thermal Aging Behavior of ERNiCr-3 Alloy (Weld and Base Metal), ORNL-5783, Oak Ridge National Laboratory, Oak Ridge, TN, August 1981.

[142] Properties of Heat and Corrosion Resisting High Alloy Steel Tubes- Tempaloy 800H, Nippon Kokan Technical Report Overseas No. 35, Nippon Kokan, Chiyoda-ku, Japan, 1982.

[143] G. Stannett and A. Wickens, "Alloy 800 Tube Welds- Assessment Report," Project 2021; Creep of Steel, ERA Technology Ltd., December 1982.

[144] R. L. Klueh and J. F. King, Elevated-Temperature Tensile and Creep-Rupture Behavior of Alloy 800H/ERNiCr-3 Weld Metal/2 1/4Cr-1Mo Steel Dissimilar-Metal Weldments, ORNL-5899, Oak Ridge National Laboratory, Oak Ridge, TN, November 1982.

[145] H. E. McCoy and J. F. King, Creep and Tensile Properties of Alloy 800H-Hastelloy X Weldments, ORNL/TM-8728, August 1983.

[146] J. F. King and H. E. McCoy, Weldability and Mechanical Property Characterization of Weld Clad Alloy 800H Tubesheet Forging, ORNL/TM-9108, Oak Ridge National Laboratory, Oak Ridge, TN, September 1984.

[147] J. R. Lindgren, B. E. Thurgood, R. H. Ryder, and C-C Li, "Mechanical Properties of Welds in Commercial Alloys for High-Temperature Gas-Cooled Reactor Components," Nuclear Technology, Vol. 66, No. 1, July 1984, pp. 207-213.

[148] T. H. Bassford and J. C. Hosier, "Production and Welding Technology of Some High-Temperature Nickel Alloys in Relation to Their Properties," Nuclear Technology, Vol. 66, No. 1, July 1984, pp. 35-43.

[149] F. Schubert, U. Bruch, R. Cook, H. Diehl, P. J. Ennis, W. Jakobeit, H. J. Penkalla, E. te Heesen, and G. Ullrich, "Creep Rupture Behavior of Candidate Materials for Nuclear Process Heat Applications," Nuclear Technology, Vol. 66, No. 1, July 1984, pp. 227-239.

[150] INCOLOY alloys 800 and 800HT, Inco Alloys International, Huntington, WV, 1986.

[151] T. H. Bassford, Mechanical Properties on Incoloy alloy 800H Weldments Welded with Inconel 117 Welding Electrode, Inco Alloys International, Huntington, WV, February 1986.

[152] Survey and Guidelines for High Strength Superheater Materials- Alloy 800H, EPRI Program RP1403-14 Task 13, November 1987.

[153] H. E. McCoy, Interim Report on Mechanical Properties Data Analysis of Low Carbon Alloy 800 in Support of ASME Code Case N-47 Code Stress Allowables (INCO and ERA Interim Data Sets), unpublished report, Oak Ridge National Laboratory, Oak Ridge, TN, April 1991.

[154] H. E. McCoy, Tensile and Creep Tests on a Single Heat of Alloy 800H, ORNL/TM-12436, Oak Ridge National Laboratory, Oak Ridge, TN, September 1993.

[155] Patriarca, P., Harkness, S. D., Duke, J. M., and Cooper, L. R., "U. S. Advanced Materials Development Program for Steam Generators," Nuclear Technology, Vol. 28, March 1976, 516-536.

[156] Bodine, Jr., G. C., Chakravarti, B., Owens, C. M., Roberts, B. W., Vandergriff, D. M., and Ward, C. T., A Program for the Development of Advanced Ferritic Alloys for LMFBR Structural Applications, TR-MCD-015, Combustion Engineering, Inc., Windsor CT, September 1977.

[157] Sikka V. K., and Patriarca, P., Analysis of Weldment Mechanical Properties of Modified 9Cr-1Mo Steel, ORNL/TM-9045, May 1984.

[158] Sikka, V. K., Cowgill, M. G., and Roberts, B. W., "Creep Properties of Modified 9Cr-1Mo Steel," pp. 413-423 in Proceedings of Topical Conference on Ferritic Alloys for Use in Nuclear Energy Technologies, ASM International, Materials Park, OH, 1985.

[159] King, J. F., Sikka, V. K., Santella, M. L., Turner, J. F., and Pickering, E. W., Weldability of Modified 9Cr-1Mo Steel, ORNL-6299, Oak Ridge National Laboratory, Oak Ridge, TN, September 1986.

[160] DiStefano, J. R., and. Sikka, V. K., Summary of Modified 9Cr-1Mo Steel Development Program : 1975-1985, ORNL-6303, Oak Ridge National Laboratory, Oak Ridge, TN, October 1986.

[161] Brinkman, C. R., Sikka, V. K., Horak, J. A., and Santella, M. L., Long Term Creep-Rupture Behavior of Modified 9Cr-1Mo Steel Base and Weldment Behavior, ORNL/TM-10504, Oak Ridge National Laboratory, Oak Ridge, TN, November 1987.

[162] Haneda, H., Masuyama, F., Kaneko, S., and Toyoda, T., "Fabrication and Characteristic Properties of Modified 9Cr-1Mo Steel for Header and Piping," pp. 231 to 241 in The International Conference on Advances in Materials Technology for Fossil Power Plants, 103 September, 1987, Chicago, IL, ASM International, Materials Park, OH, 1987.

[163] Brinkman, C., R., Maziasz, P. J., Keyes, B. L. P., Upton, H. D., Development of Stress-Rupture Reduction Factors for Weldments and the Influence of Pretest Thermal Aging to 50,000 h on the Microstructural Properties of Modified 9Cr-1Mo Steel, ORNL/TM-11459, Oak Ridge National Laboratory, Oak Ridge, TN, March 1990.

[164] Ellis, F. V., Henry, J. F., and Roberts, B. W., "Welding, Fabrication, and Service Experience with Modified 9Cr-1Mo Steel," pp. 55-63 in New Alloys for Pressure Vessels and Piping, PVP-Vol. 201, ASME, New York, NY, 1990.

[165] Viswanathan, R., Berasi, M., Tanzosh, J., and Thaxton, T., "Ligament Cracking and the Use of Modified 9Cr-1Mo Alloy Steel (P91) for Boiler Headers," pp. 97-104 in New Alloys for Pressure Vessels and Piping, PVP-Vol. 201, ASME, New York, NY, 1990.

[166] Tsuchida, T., et al., "BOP Manufacturing and Properties of ASTM A 387 Grade 91 Steel Plates," pp. 105-114 in New Alloys for Pressure Vessels and Piping, PVP-Vol. 201, ASME, New York, NY, 1990.

[167] Sakaguchi, Y., Babcock-Hitachi K. K., "Creep Rupture Properties of Mod. 9Cr-1Mo Weldment," paper presented at First International Conference on Improved Coal-Fired Power Plants, EPRI, November, Palo Alto, CA, 1987.

[168] Toyoda, T., Haneda, H., Sada, T., and Masuyama, F., "Development of Thick Wall Pipes and Headers of Modified 9Cr Steel (9Cr-1Mo)," pp. 36-1 to 36-19 in Second International Conference on Improved Coal-Fired Power Plants, EPRI, Palo Alto CA, 1989.

[169] Taguchi, K., et al., "Creep. Fatigue, and Creep-Fatigue Properties of Modified 9Cr-1Mo Steel Weldments," pp. 295-301 in Structural Integrity, NDE, Risk and Material Performance for Petroleum, Process and Power, PVP-Vol. 336, ASME, New York, NY, 1996.

[170] Swindeman & Shingledecker, unpublished research 2008-2009.

[171] Optimal Hardness of P91 Weldments, EPRI, Palo Alto, CA: 2003. 1004702.
[172] Coleman, unpublished EPRI research and completed test data from EPRI 1004702.
[173] D. Jandova, J. Kasl, V. Kanta. "Influence of Substructure on Creep Failure of P91 Steel Weld Joints." Proceedings: Creep & Fracture in High Temperature Components, 2nd ECCC Creep Conference, April 21-23, 2009, Zurich, Switzerland. © 2009 DEStech Publication, Inc.177-188.
[174] Masuyama, F, "Effect of Specimen Size and Shape on Creep-Rupture Behavior of Creep Strength Enhanced Ferritic Steel Welds." Proceedings to the EPRI International Conference WELDS 2009, June 24-26, 2009, Fort Myers, FL, USA.
[175] Personal communication with F. Masuyama, 2010.
[176] Personal communication Guiseppe Frasson, 2009 (INE, Italy).
[177] Ellis, F. V. and Zielke, W. H., "Creep-Rupture Properties of Modified 9Cr-1Mo Weld Metal," pp. 121-128 in Service Experience, Fabrication, Residual Stresses and Performance, PVP-Vol. 427, ASME, New York, NY, 2001.
[178] Santella, M. L., Swindeman, R. W., Reed, R. W., and Tanzosh, J. M., "Martensite Formation in 9Cr-1Mo-V Steel Weld Metal and Its Effect on Creep Behavior," paper presented at the EPRI Conference on 9Cr Materials Fabrication and Joining Technologies, Myrtle Beach, SC, July 2001.
[179] Heuser, H., and Jochum, C., "Properties of Matching Filler Metals for P91, E911 and P92," pp. 249-265 in Proceedings of the 3rd Conference on Advances in Material Technology for Fossil Power Plants, The Institute of Materials, London, 2001.
[180] Zang, Z., Marshall, A. W., and Holloway, G. B., "Flux Cored Arc Welding: The High Productivity Welding Process for P91 Steels," pp. 267 to 281 in Proceedings of the 3rd Conference on Advances in Material Technology for Fossil Power Plants, The Institute of Materials, London, 2001.
[181] Allen, D. J., On, E., Harvey, B., and Brett, S. J., "FourCrack-An Investigation of the Creep Performance of Advanced High Alloy Steel Welds," pp. 772-791 in Creep & Fracture in High Temperature Components, ECCC Creep Conference, September 12-14, 2005, DEStech Publications, Inc., Lancaster, PA.
[182] Middleton, C. J., Brear, J. M., Munson, R., and Viswanathan, R., "An Assessment of the Risk of Type IV Cracking in Welds to Header, Pipework and Turbine Components Constructed from the Advanced Ferritic 9% and 12% Chromium Steels," pp. 69 to 78 in Proceedings of the 3rd Conference on Advances in Material Technology for Fossil Power Plants, The Institute of Materials, London, 2001.
[183] Tanoue, T., Nonaka, I., Umaki, H., Susuki, K., and Higuchi, K., "Proposal of Creep Damage Evaluation Procedures for Power Boilers Mod. 9Cr-1Mo Weldments (First Report: Uniaxial Loading), pp. 319 to 328 in Proceedings of the 3rd Conference on Advances in Material Technology for Fossil Power Plants, The Institute of Materials, London, 2001.
[184] Nonaka, I., Ito, T., Takemasa, F., Saito, K., Miachi, Y., and Fujita, A., "Full Size Internal Pressure Creep Tests for Welded P91 Hot Reheat Elbows," pp. 75-83 in Experience with Creep-Strength Enhanced Ferritic Steels and New and Emerging Computational Methods, PVP-Vol. 476, ASME, New York, NY, 2004.
[185] Nonaka, I., Ito, T., Takemasa, F., Saito, K., Miachi, Y., and Fujita, A., "Full Size Internal Pressure Creep Tests for Welded P91 Hot Reheat Piping," pp. 65-74 in Experience with Creep-Strength Enhanced Ferritic Steels and New and Emerging Computational Methods, PVP-Vol. 476, ASME, New York, NY, 2004.
[186] Masuyama, F., and Komai, N., "Creep Failure Behavior of Creep-Strength Enhanced Ferritic Steels," pp. 107 to 114 in Experience with Creep-Strength Enhanced Ferritic Steels and New and Emerging Computational Methods, PVP-Vol. 476, ASME, New York, NY, 2004.
[187] Masuyama, F., "Creep Rupture Life and Design Factors for High Strength Ferritic Steels," pp. 983-996 in Creep & Fracture in High Temperature Components, ECCC Creep Conference, September 12-14, 2005, DEStech Publications, Inc., Lancaster, PA.

[188] Cohn, M. J., Patterson, S. R., and Coleman, K., "Creep Rupture Properties of Grade 91 Weldments," pp. 217-230 in Advances in Materials Technology for Fossil Power Plants, ASM International, Materials Park, OH, 2005.

[189] Brett, S. J., Bartes, J. S., and Thomson, R. C., "Aluminium Nitride Precipitation in Low Strength Grade 91 Power Plant Steels," pp. 1183 to 1197 in Advances in Materials Technology for Fossil Power Plants, ASM International, Materials Park, OH, 2005.

[190] Brett, S. J., Oates, D. L., and Johnston, C., "In-Service Type IV Cracking in a Modified 9Cr (Grade 91) Header," pp. 563 to 572 in Creep & Fracture in High Temperature Components, ECCC Creep Conference, September 12-14, 2005, DEStech Publications, Inc., Lancaster, PA.

[191] Schubert, J., Klenk, A., and Maile, K., "Determination of Weld Strength Factors for the Creep Rupture Strength of Welded Joints," pp. 792-805 in Creep & Fracture in High Temperature Components, ECCC Creep Conference, September 12-14, 2005, DEStech Publications, Inc., Lancaster, PA.

[192] Becht IV, C., "New Weld Joint Strength Reduction Factors in the Creep Regime in ASME B31.3 Piping," paper PVP2005-71016 presented at the ASME Pressure Vessels and Piping Conference, July 17-21, 2005, Denver, CO.

[193] Tabuchi, M., and Takahashi, Y., "Evaluation of Creep Strength Reduction Factors for Welded Joints of Modified 9Cr-1Mo Steel," paper presented at the ASME Pressure Vessels and Piping Division Conference, July 23-27, 2006, Vancouver, BC, Canada.

[194] Tabuchi, M., Hongo, H., Li, Y., Watananbe, T., and Takahashi, Y., "Evaluation of Microstructures and Creep Damages in HAZ of P91 Steel Weldment," paper PVP2007-26495 presented at the ASME Pressure Vessels and Piping Division Conference, July 22-26, 2007, San Antonio, TX.

[195] Yamazaki, M., Hongo, H., Watanabe, T., "Rupture Behavior of Multi-pass Welded Joints of Heat Resistant Steel Subjected to Creep Loading," paper PVP2007-26495 presented at the ASME Pressure Vessels and Piping Division Conference, July 22-26, 2007, San Antonio, TX.

[196] Masuyama, F., and Nishimura, N., "Phase Transformation and Properties of Gr 91 at Around Critical Temperature," pp. 85 to 91 in Experience with Creep-Strength Enhanced Ferritic Steels and New and Emerging Computational Methods, PVP-Vol. 476, ASME, New York, NY, 2004.

[197] Santella, M. L., Swindeman, R. W., Reed, R. W., and Tanzosh, J. M., "Martensite Formation in 9Cr-1Mo-V Steel Weld Metal and Its Effect on Creep Behavior," paper presented at the EPRI Conference on 9Cr Materials Fabrication and Joining Technologies, Myrtle Beach, SC, July 2001.

[198] Corum, J. M., "Evaluation of Weldment Creep and Fatigue Strength-Reduction Factors for Elevated-Temperature Design," Journal of Pressure Vessel Technology, 1990, Vol. 112, No. 4, pp. 333-339.

PART 3: DEVELOPMENT OF WELD JOINT INFLUENCE FACTORS

SUMMARY

This report represents part of a larger research project aimed at developing weld strength reduction factors (WSRF) and weld joint influence factors (WJIF) for service in the creep regime. The project is sponsored by ASME Standards and Technology, LLC (project # 3052) with co-funding from the Electric Power Research Institute. This report covers Task 2 of the work that details the development of structural models to evaluate WJIFs.

The primary objective of Task 2 was to develop an analysis tool to evaluate the creep rupture strength of a weldment relative to that of base metal. The tool is intended to capture the influence of a range of weldment variables relating to configuration, geometry and materials properties. This report summarizes development of the tool and its benchmarking against selected cases of high-temperature, long seam weldment piping field and component testing experience. As part of the Task 2 effort, alternative methods for analysis were compared to detailed methods to evaluate the feasibility of using simplified methods to rapidly characterize a broad range of geometric and materials combinations. These models were compared with structures composed of equivalent parent and weld metal in order to develop factors, referred to as WJIFs, to demonstrate the utility of the model for future use in establishing weldment design rules. To make an accurate prediction of weldment creep failure it is necessary to have certain elements of knowledge and material data available. These are:

(a) Constitutive models for creep deformation of all material components of the weld
(b) A model of creep damage initiation and accumulation to track damage
(c) A suitable finite element program and appropriate models of typical weldments
(d) A simple and economical methodology in order to assess the many possible combinations of materials and geometries likely to be encountered in weldment design
(e) A number of benchmark problems as a check on predictions of simple methods

Having carried out a survey of past efforts in the detailed analysis of weldments, a methodology was developed for calculating WJIFs for any practical combination of materials and weld geometries.

This process involved evaluating a number of well-documented examples of field weldment failures and component tests using relatively complex models of creep deformation and damage accumulation, and developing some simplifying assumptions from the experience to help produce a quick and computationally economical WJIF calculation methodology. As a result of this exercise, it was possible to circumvent use of complex material models and instead use simplified models more routinely available to designers from existing databases.

This methodology has been demonstrated by applying it to a representative set of weldment types. Since the full spectrum of weld geometries and material properties is very large, this study focused on examining the limits of some of the more important variables, such as weld geometry, heat-affected zone (HAZ) property variations, and component configuration of low alloy steel pipe seam and girth welds. The exercise demonstrates the utility of the methodology and tool.

1 INTRODUCTION

This report represents part of a larger research project aimed at developing weld strength reduction factors (WSRF) and weld joint influence factors (WJIF) for service in the creep regime. The project is sponsored by ASME Standards and Technology, LLC (project # 3052) with co-funding from the Electric Power Research Institute. The overall objective of the project is to provide materials data and a methodology for addressing weldments in ASME Codes and design allowable stresses. This report covers Task 2 of the work that details the development of structural models to evaluate structural effects in weldments (WJIFs).

A flow diagram representing the complete project is shown in Figure 92.

Figure 92: Project Outline

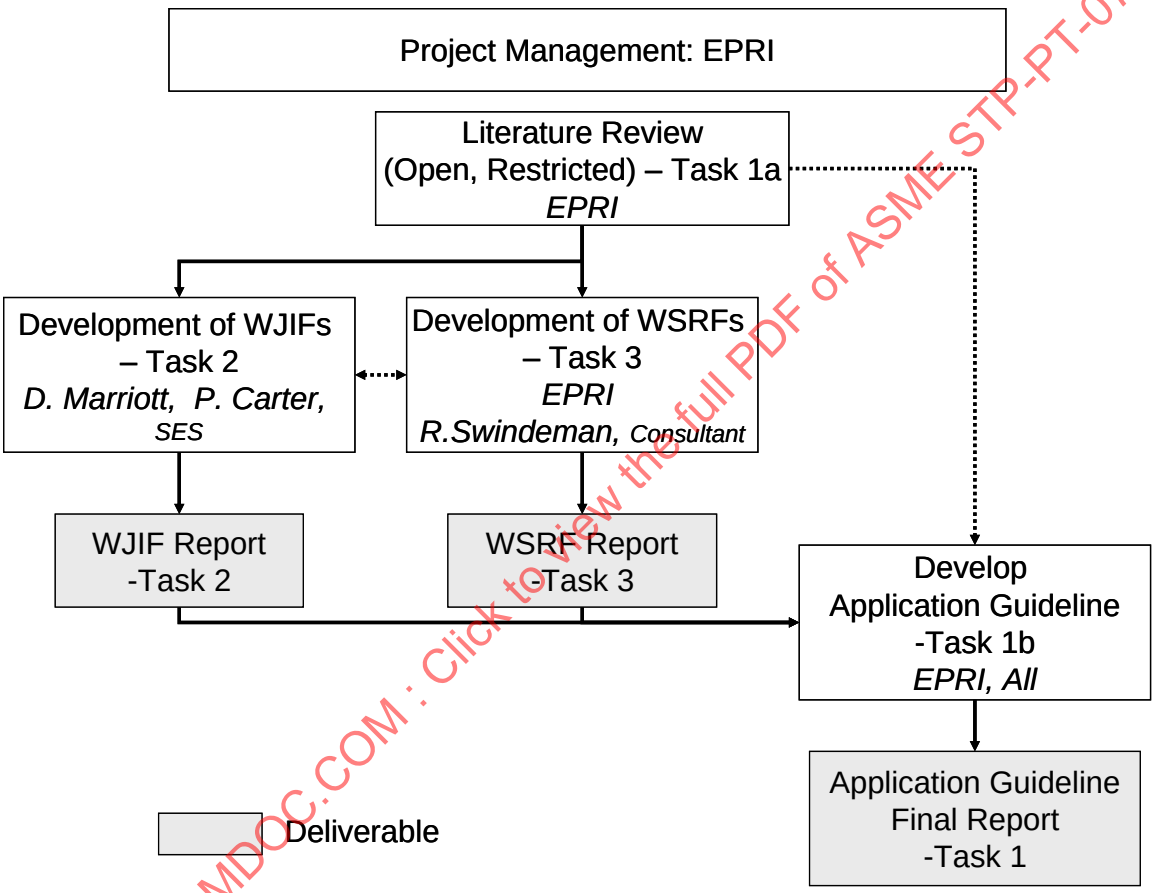

Two parameters were cited in the ASME Standards and Technology, LLC request for proposal (RFP) concerning weld strength. Both are measures of the reduction in creep strength resulting from the insertion of a weld into a structure, and the distinction between them is subtle. According to the RFP, the intent is that "WSRF" should refer to ratio of the strength of the weld material to that of the parent material, whereas the "WJIF" refers to the reduction in strength of the weldment, including all relevant effects such as changes in the heat affected zones (HAZ) and geometric features, such as weld joint configuration, peaking, and misalignment.

Task 2, "Development of WJIFs" was initiated first because the resulting models were judged to be necessary to analyze any cross-weld material data (Task 3), with the eventual output derived from that task to be included in Task 1b as the project reaches completion.

For the purpose of this project therefore, the Task 2 scope focused on:

(a) Developing a systematic, preferably simplified methodology for computing WJIFs that can be applied generally to any combination of geometric and material variations that might be realistically expected in weldments produced by construction in accordance with the rules of the ASME Code [1], and associated Standards of piping construction [2]

(b) Limited benchmarking of the methodology by applications to selected known cases of field long seam weldment piping failures and component tests

(c) Providing proof of concept by applying the methodology to a representative cross section of typical material and weld geometry combinations

(d) As an addendum, such insights as might be gained from the work done in (a) and (b), to make an initial exploration of weld and weldment test sample configurations, and to start looking at the potential value of the commonly performed cross-weld test; results from this effort are being consolidated with the Task 3 activity and will be reported on later.

2 DESCRIPTION OF WORKSCOPE

The first of these Task 2 objectives, involving the construction of a mechanical and material model to theoretically predict failure, comprised the major part of the project task. This was followed by the development of a systematic procedure for computing Weld Joint Influence Factors (WJIF), that can be applied to a wide range of material and geometric variations, as is expected to be found in typical piping weldments. Finally, and to be documented as part of Task 3, as one subset of weld geometries of interest, the behavior of test specimens such as the cross-weld test were explored as a means of obtaining basic properties of the separate material zones found in a weld.

2.1 Weldment Model Development

The first step in the project was to identify a suitable computational model for assessing variations in weld configuration.

A weldment is a complex structure. Geometrically it may be simple, but weldments are made up of several zones with different material mechanical properties, some of which are due to actual material differences, while others, including post-weld heat treatment, are a result of the welding thermal history. The properties of these materials are difficult to measure accurately because they may exist only in thin layers within the weldment, requiring the use of miniature specimens or generation of material via simulated heat treatments.

The work done to develop a suitable model involved several subtasks. These were the following:

(a) Review the prior history on weldment modeling. This review forms Appendix B of this report.
(b) Select suitable generic material constitutive and failure models from among the current candidates available in the technical literature.
(c) Develop a process for quantification of weldment material properties to cope with the lack of direct experimental data for regions such as heat-affected zones (HAZs).
(d) Develop a methodology for the analysis of weldment deformation and failure.
(e) Build Finite Element (FE) models to simulate well-documented examples of weldment failures in the field and in laboratory studies, to validate the proposed methodology.
(f) Examine opportunities for simplification and approximation of the analysis procedures in anticipation of the need to apply the methodology to a wide range of configurations, and test approximations against more detailed computations.

2.2 Computation of Weld Joint Influence Factors

A Weld Joint Influence Factor (WJIF) is defined as the ratio of the creep strength of the welded structure to that of the equivalent structure composed of homogeneous parent (base) material. Since creep deformation and damage are both time dependent, the WJIF should be calculated for a specified time-to-failure.

The standard output of a creep failure assessment is the time-to-failure under a specified load, including both mechanical loading and operating temperature. It is therefore a relatively straightforward matter to calculate the reduction in the life of a structure arising from inserting a weldment. For design purposes however, it is the ratio of the strengths at a specified time that is of interest. Calculation of a WJIF therefore requires some post-analysis evaluation of finite element (FE) predictions in order to arrive at the desired result, since it is not a simple matter to select loads *a priori* that lead directly to the same time-to-failure in both welded and non-welded structures.

As a corollary, WJIF's may also depend on the specified design life over which they are calculated, with the effect generally becoming more significant (i.e. the WJIF typically decreases) with decreasing stress

and increasing life. WJIF's calculated from short-term data may therefore tend to be optimistic when applied to longer service lifetimes.

2.3 Assessment of Test Specimen Geometry

Material properties are a critical path in the quantitative evaluation of weldments because of the difficulty of isolating sufficient material to represent each of the several zones found in a typical weldment. The weldment zones may consist of:

(a) Base, or parent material
(b) Weld material
(c) Several regions in the Heat Affected Zone (HAZ) with properties ranging from typically weak (fine grain (FGHAZ)), to strong (coarse grain (CGHAZ)) relative to the parent material, depending on the welding and post-weld thermal history
(d) Dissimilar metal interfaces that may form very thin layers with distinct properties due to mutual diffusion and dilution

Only the base and weld materials are readily obtainable in quantities large enough to conduct standard specimen creep tests. Properties of the other weldment zones must be obtained by innovative use of miniature specimens, heat treatment of large samples to simulate HAZ microstructures (using a Gleeble machine for example), or by inference from composite specimens cut from weldments, containing all the various microstructures in a single specimen, the latter usually being of the type known as a "cross-weld" specimen.

Miniature and microstructure-simulated specimens have been used successfully in several detailed studies of weldments and it is possible that these techniques may find wider usage in the future [3], [4]. However, data from these sources are unlikely to become generally available for the full spectrum of material of interest to ASME in the foreseeable future, which means that the only current available source of information on weldment properties consists largely of weld metal and cross-weld tests.

3 DETAILS OF WORK PERFORMED

3.1 Weldment Model Development

3.1.1 Subtask 2-1: Review the Prior History on Weldment Modeling

A considerable body of research literature has been generated on the modeling of weldments and prediction of failure by creep at elevated temperature. A more complete summary of the literature survey carried out as part of this project is given in Appendix B of this report.

The salient features of this work are a consensus on the following points.

(a) The creep rupture strength of weldments is governed by the reduced strength of local regions in the weldment due to the presence of dissimilar materials, and microstructural differences due to the welding and post-weld thermal history.

(b) Weakened zones in the weldment fail prematurely in part due to higher creep rates, but also due to the development of complex multiaxial stress states caused by the differential creep rates, which lead to heightened levels of hydrostatic constraint that, in turn, accelerates the rate of creep damage accumulation.

(c) As with homogeneous structures, creep rupture in weldments usually proceeds by the generation of local creep damage progressing into the coalescence of voids. This process leads to local failure that may manifest itself as a cracklike defect or a diffuse region of fissured material with little or no load carrying capacity. Emergence of this zone of local failure is referred to as "initiation". It marks the onset of a period in which the damaged region spreads until the remaining structure is unable to sustain the load, at which time "general structural failure" occurs.

(d) The damage process generally consists of a local "initiation" phase, followed by propagation of damage leading to final structural failure. Prediction of the propagation phase in a structure is a very complex problem. Given (a) the complexity of predicting the creep damage propagation phase, (b) that existing methodologies for developing design allowable stresses do not explicitly consider propagation, and (c) that a method of WJIF development that excludes consideration of propagation is expectedly more reliable and reproducible (more so in cases where propagation represents a relatively small fraction of total lifetime), for this study, local damage initiation is adopted as the definition of weldment failure. This constitutes a major simplification of the WJIF computation.

3.1.2 Subtask 2-2: Selection of Suitable Material Constitutive and Failure Models

The purpose of material modeling in weldment studies is twofold. Firstly, it is necessary to reproduce the inhomogeneous creep deformations leading to development of the localized constraint that drives accelerated creep damage, or the simple failure of the component by excess deformation. This calls for a constitutive model to be used as input to the FE analysis. Secondly, a damage criterion is required for the evaluation of failure in terms of the computed stress and strain histories.

A wide selection of detailed and simplified material models has been used at various times to compute the behavior of weldments. Appendix B provides a brief history of past work in this field. For the present study the decision was made to use the following models.

3.1.2.1 Choice of Constitutive Models

This is the material model defining the relationship between applied loading and the resultant deformations of the component.

The constitutive model selected is based broadly on the MPC Omega model, published in the ASME/API FFS Guideline API 579/2007 [5]. This model provides the essentially tertiary behavior observed in a large

percentage of engineering structural materials. Most importantly, it is linked to a database of material properties covering a wide range of the generic material types approved for use by the ASME Code. This database is understood to have been generated from much of the same material data used in the calculation of design allowables in Section II, Part D of the ASME Code, thereby minimizing the potential confusion that can arise from mixing data from different sources. A summary of the MPC/Omega model is given in Appendix C.

The Omega model, as published in API 579, contains two features aimed at accounting for large deformation and multiaxial effects (see Appendix C). The first of these is the α_Ω factor intended to allow for large deformations leading to ductile instability. The second is the δ_Ω factor, which accounts for the effect of multiaxiality on creep rupture damage accumulation by modifying the parameter, Ω. These phenomena are handled differently in this study.

Ductile instability is automatically accounted for by using the nonlinear geometry feature inherent in the FE code employed in the study (ABAQUS Versions 6.7 and 6.8 [6]). The α_Ω factor is therefore always set to 1.

Damage accumulation is taken into account using an independent damage parameter based on a model of void growth instead of using a single parameter for both deformation and damage as used in the Omega model.

3.1.2.2 Choice of Damage Accumulation Model

The method of calculating damage accumulation used in this study is based on the Rice/Tracey model of void growth that takes the effect of multiaxiality into account by an acceleration factor applied to the effective strain, resulting in a reduction of ductility given by the equation [7] (see Appendix D for a review of the background of multiaxial creep failure),

$$\frac{dD_c}{dt} = \frac{1}{\varepsilon_f}\frac{d\varepsilon_{eff}}{dt}\exp\left[\frac{1}{2}\left(\frac{3\sigma_H}{\sigma_{mises}} - 1\right)\right]$$

where "D_c" is a number representing the fraction of creep damage. According to this equation "damage" in this format grows proportionally to the creep rate, up to the rupture strain, accelerated by the exponential function containing the constraint factor,

$$CT = 3\sigma_H/\sigma_{mises}.$$

By making the assumption that the creep rate is a Bailey/Norton n-power law,

$$\frac{d\varepsilon_c}{dt} = K\sigma^n$$

it is possible to restate this constraint effect as an effective "rupture stress", σ_R, such that

$$\sigma_R = \sigma_{mises}\exp\left[\alpha\left(CT - 1\right)\right]$$

Where "α" is theoretically 1/2n, has been reported to empirically vary from 0 to 0.25, and for this study has been set at 0.2, consistent with what is used for many structural alloys.

This describes the method used to calculate "D_c", the creep damage. When this quantity reaches "1" it is assumed that local rupture occurs. The time to reach this state can be calculated by entering curves of rupture time versus stress at the stress level, σ_R.

The rupture data used in assessing time-to-failure has several sources. It can, for instance, be calculated directly from the Omega model, by using rupture data provided in API 530 in the form of Larson-Miller curves, or from other published models.

The API 530 data are also provided in API 579 as an alternative to the Omega data, primarily for assessment of heater tubes (see Annex F of [5] for details). However, neither of these databases shows the underlying data. In Task 1, data are being assembled for a range of materials and weldments, but for the Task 2 model development, validation, and WJIF study, the API 530 curves were utilized. For Grade 22, the API 530 curve was adopted for damage assessment because it appeared representative of the Grade 22 raw material database from EPRI report TR-110807 [8]. This is also consistent with the findings of Brear who evaluated a number of different rupture models for Grade 22 (including ISO, API 530, BS PD 6525, DIN, Omega, etc.) [9].

3.1.3 Subtask 2-3: Synthesis of Weld Sub-Region Properties

The material regions in a weldment can include:

(a) Parent, or base material
(b) Weld deposit
(c) Coarse Grained HAZ (CGHAZ) (ferritic steels)
(d) Intercritical HAZ (ICHAZ) (ferritic steels)
(e) Fine grain (FGHAZ) (ferritic steels)
(f) Fusion boundaries and mixed composition zones

Only the first two materials on this list are generally available as data collected in conventional creep tests. All others need to be estimated by unconventional or indirect means. This includes testing of miniature specimens or material of simulated microstructures.

This is a task primarily concerned with development of a methodology into which material properties from virtually any source can be inserted. The approach adopted here was to model the different regions of a weldment by an equivalent temperature shift selected to match the creep strength difference compared with the base material. Figure 93 illustrates how, in principle, this shift is translated into “weaker” material properties. This approach is not necessary for eventual implementation of the model, but for this task, the method offers an efficient means of changing material parameters to evaluate effects.

Figure 93: Temperature Shift for Equivalent Material Properties

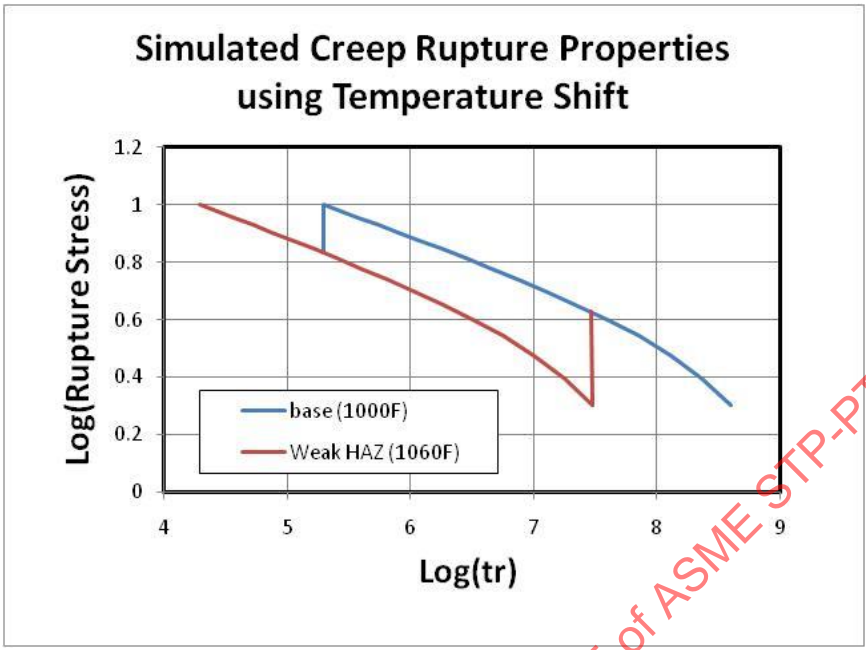

Notes: A 60ºF temperature elevation above 1000°F is equivalent to material with a rupture life approximately 60% of that of the base material.

Rupture data are not sufficient in themselves for the evaluation of welds, because creep rate differentials are a major factor driving the multiaxial damage process. Unfortunately, for many materials of interest, creep rupture data is the only information available, leaving this simple procedure as the sole option. In such instances, it is possible to make use of the Monkman/Grant relationship [10], which states that, for a wide range of material conditions, the time-to-rupture, t_R, and the minimum creep rate, mcr, are linked by the equation,

$$t_R.(mcr)^m = C$$

"m" is close to 1 and, for correlations over small variations, as is the case when comparing different variants of the same material following different heat treatments, can be assumed equal to 1. This establishes the inverse relationship to be used to calculate mcr when no data are directly available.

3.1.4 Subtask 2-4: Methodology for the Analysis of Weldment Deformation and Failure

The detailed evaluation of the creep rupture life of a weldment is a major undertaking. Ideally, it requires an understanding of fundamental failure mechanisms, knowledge of the constitutive relations governing both deformation and damage accumulation, and quantitative material data for a number of material variants caused by the welding process that are difficult to obtain (see examples in Appendix B).

Given that the developed procedure will be expected to be applied to a large population of weldment conditions, it was obvious from the outset of this project that there was a need to search for simplified models that can be run over and over again with reasonable economy of effort and provide answers suitable for practical design purposes.

Therefore, while it is possible to develop highly sophisticated models of welds, and this has been done in isolated cases, the emphasis in this study was on finding simplified methods of analysis that can provide a useful solution with the available information in support of establishing design guidelines.

As a first step, however, a small number of detailed studies were undertaken to determine the key elements of the problem and to provide a baseline for, and benchmarking of the analytical procedures.

For benchmark purposes, three examples were selected:

(a) Test of a low alloy steel welded pressure vessel by the CEGB in the UK. Although constructed of 1¼ Cr ½Mo V steel, which is not listed in Section II Part D of the BPV Code, this vessel test has been documented very thoroughly and has been the focus of several independent studies which include some information on the difficult task of quantifying weldment material properties (partially described in Appendix B and discussed further in Appendix E).

(b) Sabine Grade 11 seamed piping failure. Fusion line failure documented by EPRI involving a relatively thin section, hot reheat pipe bend weldment with no unusual material inhomogeneities and no off-normal operation (Appendix E).

(c) Mt. Storm Grade 22 main steam seamed link piping failure. Weld centerline failure involving a relatively thick-section straight pipe section (Appendix F).

The initial focus for this work concentrated on the ferritic steels because they present a more complex material and structure interaction due to HAZ property variation and because these represent the greatest percentage of interest in piping construction. Because austenitic alloys do not go through a phase transformation during welding, HAZ regions are not reported as having such a wide variation in properties. Thus, any model and procedure developed for the ferritic steels is expected to be applicable by essentially making HAZ regions equivalent to base metal.

Analysis of these cases confirmed the findings of the literature survey concerning the evolution of failure of weldments by creep. This process takes the following steps:

(a) First, loading is carried elastically with little evidence of the presence of the weld, since the only material property in prominent use is the elastic modulus, which is not greatly affected by the material microstructural variations found in a typical weldment.

(b) Creep causes a redistribution of stresses, most importantly leading to the load carried by the weaker regions of the weld being offloaded from shear stress governed by the Mises effective stress, to the hydrostatic stress component. These terms and others are defined in Appendix D, which reviews the stress state effects on failure.

(c) Depending on the type and quality of the material involved, this transfer of load can be beneficial or detrimental. If the material is ductile and resistant to cavitation, increasing the participation of the hydrostatic stress can extend the life by reducing the deformations normally produced by shear. If the material is prone to cavitation, this tendency is accelerated by the increase in hydrostatic stresscc, reducing the rupture life.

(d) Void initiation and growth is the underlying mechanism of creep rupture in typical service conditions of stress and temperature. Failure by void growth is only a matter of generating enough inelastic strain to drive the cavitation process. In many simple tensile tests, it is not possible to generate the necessary strain until well into tertiary creep. The stress state has a strong influence on this growth process (see Appendix D for details). If constraint is added, the strain-to-failure can be significantly reduced, leading potentially to brittle rupture before tertiary creep can become established.

(e) The evolution of creep damage can be tracked as a function of either the accumulating inelastic strain, or the sustained stress state. This state can be represented by a “damage parameter”, D, such that failure occurs by creep rupture in a local volume of material when D = 1. This point in the operating history is designated “initiation”.

(f) Initiation is not necessarily followed immediately by failure of the component, except in simple statically determinate structures. Creep damage does not form a sharp crack in the manner of fatigue, but produces instead a somewhat diffuse region of fissured material whose load transmitting capability has deteriorated to zero. It is true that the cavitated material may, on

> occasion, be channeled by the geometry to form a defect that looks cracklike (see, for instance, the CEGB study described in Appendix E). This form of damage may be treated conservatively as a single crack for purposes of analysis but, generally speaking, the sharp, singularity generating tip of a true crack is not present. As material loses load carrying capacity, load is transferred to adjacent material that eventually fails, passing the load on until there has been sufficient deterioration that the structure collapses. This phase in the life is designated "damage propagation".

In some instances, the damage propagation following initiation can occupy a major part of the total life. In an ASTM sharp notch specimen, for instance, where damage initiates first at a very localized stress/strain concentration, the time spent in propagation can be an order of magnitude greater than the time to initiation.

In many instances of weldments of primary relevance to this project, however, the propagation time is proportionately not large. This is possibly because the stress concentration is usually not large, strength reduction being derived more from discontinuities of creep rate properties from one zone to another. As noted earlier, given (a) the complexity of predicting the creep damage propagation phase, (b) that existing methodologies for developing design allowable stresses do not explicitly consider propagation, and (c) that a method of WJIF development that excludes consideration of propagation is expectedly more reliable and reproducible (more so in cases where propagation represents a relatively small fraction of total lifetime), for this study, local damage initiation is adopted as the definition of weldment failure.

For this reason, the definition of "weld failure" adopted here is *initiation*, i.e. cumulative damage, D = 1 locally. When applied to the extent of damage means a small, but finite volume of affected material, large enough to average out extreme peaks of stress and/or strain but small enough that loss of strength in that volume has no significant effect on the gross structural response. In practical terms, a volume of material of about 10% of the size of the detail causing the local high stresses appears to be an accepted estimate. This is the value used in R5 and the Japanese HT codes to define "local" plastic deformation. As it applies to this case, damage extending 10% of the thickness of the weak layer is considered a plausible definition. Given, e.g. a FGHAZ band 2 mm thick (~ 0.08"), this leads to a definition of "local" of about 0.008". In addition, "damage" was based on the element average rather than the element Gauss point values.

This decision to use the initiation definition of failure is not only driven by the relatively short propagation time experienced in weldments, but also because the process of damage evolution remains an area of research, and no clear consensus has been reached on how to model it. In addition, there are material related phenomena in welding that could have significant effects on the damage propagation process in the weld, as opposed to idealized test conditions. It is beyond the scope of this effort to include a full discussion of all the factors that can complicate the issue, but one obvious one is the potential for local ductility to be degraded due to the introduction of particles and other impurities into the weld, to form sites for premature void initiation. In these circumstances, even if it were possible, in theory, to estimate the propagation phase of creep rupture, it would be imprudent to include this estimate in a procedure intended for design purposes, because of the considerable uncertainty attached to such an estimate.

With weldment failure established for practical purposes as being "initiation", i.e. D = 1 locally, the structural analysis reduces to a much simpler task.

Firstly, it is possible to dispense with complex constitutive models whose primary objective is exactly the prediction of the final, propagation phase of life, and revert to simpler models of the Bailey-Norton form that do not require special programming techniques for their implementation.

Computationally, the consequence of this simplification is that computing stress/strain histories and the creep damage resulting from them can be treated as two separate and sequential steps instead of a single

procedure containing a large amount of interaction. This means that simplifications of both the stress/strain history and the mechanism of damage accumulation can be explored as separate items.

In the case of the stress/strain history, a simplified technique is already known to exist, based on the Reference Stress approach (see Appendix G for explanation). This technique is an approximate one for estimating the stress state in a creep structure from a time independent limit load analysis. A Modified Reference Stress method with application to welds has been in existence for several years and forms part of the British R5 procedures [11].

To avoid confusion, it must be explained here that the Reference Stress technique does not attempt to approximate creep by some form of time-independent plastic deformation. It is purely a technique for approximating the *stress state*. This procedure leads to a further decoupling of the problem, which has already been separated into structural and damage related calculations, by also separating essentially structural behavior from material deformation behavior. In fact, the structural analysis becomes virtually independent of material properties, and material behavior can be provided independently, if necessary, directly from test data.

3.1.5 Methodology Development in Summary

(a) Examine several significant weldment failure case studies in detail, to calibrate and benchmark the analytical methods, and to provide a baseline against which to judge future approximations.
(b) Identify "initiation", being the attainment of D = 1 in a local volume of material, as the definition of weldment failure.
(c) Based on the initiation assumption, separate the assessment procedure into structural analysis and damage calculation steps.
(d) In the structural analysis step, the choice exists to apply a range of analysis methods of varying computational complexity, matched to available resources and data. These can range from a detailed analysis based on a sophisticated constitutive relation, if one is available, through simplifications such as the Reference Stress approach, to hand calculations in simple situations.
(e) The stress/strain history obtained from (d) above is the input to the damage calculation as a sequential step. In this study, for instance, creep damage is assumed to be driven by an equivalent "rupture stress" which includes a correction for the constraint factor, $T = \frac{3\sigma_H}{\sigma_{mises}}$, in the form of the Rice/Tracey factor (see Appendix D).
(f) Life for the weldment is defined by D = 1.

3.2 Computation of Weld Joint Influence Factors

Before going on to describe the work done, it is worth taking time to sketch out briefly the full extent of this task, the reasons for the scope limitations made.

The standard output of a creep failure assessment is the time-to-failure under a specified load including both mechanical loading and operating temperature. It is therefore a relatively straightforward matter to calculate the reduction in the life of a structure arising from inserting a weldment. For design purposes however, it is the ratio of the strengths at a specified time that is of interest. Calculation of a WJIF therefore requires some post-process analyses of FE predictions in order to arrive at the desired result, since it is not a simple matter to select loads *a priori* that lead directly to the same time-to-failure in both welded and non-welded structures.

The definition provided by ASME for a "weld joint influence factor" (WJIF), is that it is the ratio of the creep strength of a weldment to that of the equivalent structure made entirely of base material. A WJIF can include virtually any feature, metallurgical or geometric, that can contribute to a creep strength loss in the welded component. This is a significant computational task even if only one material set and one geometry are involved. In order to provide data to be used in design, many combinations need to be evaluated.

The following is an incomplete list of factors likely to influence WJIFs:

(a) Material grade – There are literally hundreds of materials listed in the ASME Code with possible application to welded pipe construction. Even API 579, which lumps material together into generic groups, lists over 20 materials of interest.

(b) Weld consumables – Every weld has alternative consumables dependent on usage, availability and, often, personal choice.

(c) Heat treat-modified microstructures – Beside the obvious distinction between base and weld material, the typical HAZ is a composite of many microstructures, often having very different creep properties. This in turn can vary depending on whether post-weld heat treatment (PWHT) has been administered or not.

(d) A weld may be a V-groove, X-groove or K-prep (two side weld), J-grove or narrow gap with a range of dimensions and aspect ratios.

(e) Geometry – Welds can be seam or girth welds in pipes, straight welds in flat plate, or complex geometries related to nozzle and attachment welds. Piping welds alone can vary considerably from thin wall, with nearly constant nominal stresses, to thick wall, in which stresses vary significantly through the wall, and the failure site can migrate, e.g. from bore to outside surface, depending on the damage criterion that is considered relevant.

(f) Size effects – Microstructural layers formed in HAZs, for instance, tend not to vary substantially in width. The aspect ratio of the layer, therefore, varies with the component thickness and this, in turn, can have a major effect on the build-up of hydrostatic tension in the weldment.

(g) Structural Loading – Welds can be subjected to transverse (seam weld), in-line (girth weld), pipe section and through thickness bending loads, all of which might be expected to act differently, and therefore require different WJIFs.

(h) Surface Features – Root, toe and reinforcement geometries deviating from the ideal dressed weld profile

(i) Manufacturing defects – Peaking and misalignment

(j) Design Life – WJIFs are not a single number, even for a defined set of material and geometric parameters. It has been observed, for instance, that WJIFs tend to be smaller (more strength reduction) for low stresses and longer lifetimes. Temperature may have an effect as well.

It is impossible to address all these variables in one program. The intent of this project is to develop a methodology that can be applied in a relatively routine fashion to the many welds and configurations that are possible, and to demonstrate the application of the methodology by selective examples. For this purpose, a range of representative weldment geometries have been analyzed as the proof of concept for the methodology.

While the range of materials of potential interest is very large, the data requirements are minimal, at least as far as the simplified method used here is concerned. All that is needed, as a first step, is the rupture data. Ideally, for a more accurate evaluation, the minimum creep rate (mcr) is required as well. However, the mcr is not available for many of the materials of interest, although it does need to be estimated somehow, in order to implement the calculation, using, e.g. the Monkman/Grant relationship [10]. This means that any practical methodology needs to be able to function using the rupture data alone. Given that fact, in reality, it is sufficient to demonstrate the methodology with only one material in order to verify that aspect of the concept. The material chosen for this exercise was Gr22. This is a material for which EPRI has a

large database divided into base, weld, and welded samples of various configurations, and was therefore considered a good starting point (Slide 6 of Appendix H).

The set of weldments used to demonstrate the extraction of WJIFs from FE results explored the following variables:

(a) Material – Gr22 at a fixed nominal temperature of 1000°F
(b) Geometries considered – flat plate, seam weld in pipe, girth weld in pipe
(c) Thickness – Examples considered vary from small simulated crossweld specimens of 0.08" diameter (2 mm) to thick walled pipe 5" thick. Thickness variation was not evaluated systematically, but some trends could be observed given the variations examined.
(d) Weld Profile – V-, X- (K-), J-prep and flat (parallel side) welds
(e) Loading – Mechanical transverse and parallel tension, internal pressure and end loading on piping
(f) Manufacturing Defects – peaking and misalignment

These parameters were not varied individually in great length. This was a sensitivity study intended to identify significant effects and to explore the limits of applicability of the approximations used in the model construction and analysis process. The geometries considered are provided in more detail in Appendix H, which describes the WJIF study in more detail.

Calculation of a WJIF for a given configuration consisted of the following steps:

(a) Calculate the rupture life of the component assuming nominal base material properties throughout.
(b) Define the welded structure by specifying the appropriate properties for each of the zones in the weld and repeat the rupture life calculation using the same loads used on the nominal case.
(c) By reference to Larson-Miller data from API 530, transform the time to failure at the specified load for both geometries, to the loads required to cause failure in a specified time.
(d) The WJIF is the ratio of the load to cause failure in the welded component, to that of the base material component and is particular to a specified time. Figure 93 shows clearly that this ratio increases with increasing time-to-rupture. The only way to define a single valued WJIF is to specify it at a standard time. In the nonnuclear sections of the ASME Code, and in B31, time dependent design criteria are already specified at a nominal 100,000 hours, and this practice could be extended to WJIFs. Otherwise it must include time dependent variation as might be the direction taken in nuclear applications, for instance, where time enters the design procedure explicitly. In the absence of any rule, the practice in this project has been to evaluate the WJIF at the time-to-failure of the welded structure. No restriction on the methodology is incurred by this assumption, and any other convenient time can be used.

3.3 Cross-Weld Tests

The cross-weld test is not universally favored as a data source if considered as a basic material test because the results in the form of rupture times and, occasionally, minimum creep rates, are composites, and do not provide information on the behavior of the separate constituents of the weld. However, for many, if not most of the materials of interest, information on crossweld data is the only information available and a use needs to be found for it if at all possible.

Instead of viewing the crossweld test as a purely material test, it is possible, with some insight into the characteristic behavior of the different microstructures in a weldment, to construct a detailed model of the test specimen and, by reverse engineering, infer material properties from predictions of the overall creep response. In the course of searching for suitable material data to used in WJIF calculations, it became apparent that thought needed to be given to the utilization of crossweld data early on in the proceedings, because this is, and is likely to continue to be, the primary source of weldment property data on a wide front

for the foreseeable future. Finding an acceptable way of making use of it is therefore a problem that will be explored further in the Task 3 workscope.

4 RESULTS

Results of this study come under two basic headings:

- Conceptual ideas for simplified WJIF computation, and
- Numerical predictions of WJIFs for selected examples.

4.1 Concepts

Literature searches, combined with some independent analyses in which attempts were made to follow the damage process all the way to structural collapse, have permitted some useful approximations to be made in preparation for calculating WJIFs on a broad front.

As explained in the preceding section, the practical criterion of creep rupture is taken to be *initiation*, i.e. the time to damage, D = 1 locally.

All the difficulties involved in computing complete structural collapse by creep are bound up with the interaction between evolving damage mechanisms and structural deformation. The ability to halt the analysis at a point where this process is just beginning is a very significant advance, because it allows the deformation of the structure, which drives the damage process, and the damage process itself, to be carried out independently as sequential operations.

Since the deformation and damage calculations have been decoupled, unconnected procedures may now be used, thus opening up the opportunity to utilize approximate methods that can be applied independently of how the remainder of the evaluation is being carried out.

On the negative side of the argument, it is beginning to appear that the desire for a single valued WJIF to fit all occasions may be too simplistic. It has become clear, from examples analyzed in this project, that the WJIF is generally dependent on a large number of geometric and metallurgical features, as well as the time-on-load. As design lives increase, the WJIFs can decrease, i.e. strength loss increases.

On the positive side, it seems that it is possible to deliver an approximate method of weld assessment that is simple enough to permit weld strengths to be calculated directly, on an application-specific basis, as part of the design procedure. In fact, there are a number of different methods with varying degrees of complexity that can be chosen to suit the requirements of the design program. In effect, this means taking the weld out of the material category and placing it with the structural components. Given that case-specific design is normal for such features as nozzles, and welds are both as ubiquitous and possibly even more safety critical than nozzles, this shift would not appear to be a very difficult transformation once the decision is made to do it.

Finally, the findings outlined above have been compiled into a systematic procedure for calculating WJIFs that can be used either to construct design data for inclusion in the ASME Code, or as a procedure to be used directly in design, as proposed.

In summary, the use of simplified de-coupled analysis methods to predict weld life is based on the following:

(a) The approach is a priori plausible because by definition, the stress distribution is predictable with a conventional creep analysis until the first significant damage occurs. In the creep analyses of this report, the API 579 omega creep model is used without multiaxial corrections for this purpose.

(b) The use of a modified reference stress based on a limit analysis is attractive because it does not require a creep analysis and data, and is likely to be useful for materials for which creep data does not exist. Its justification is that the reference stress is an estimate of creep stresses.

(c) In both cases, multiaxiality corrections are made to the stresses calculated in these ways.

(d) The authors have had experience of weld life calculations based on:
  (1) Full continuum damage mechanics models
  (2) Full API 579 analyses
  (3) Decoupled creep and damage analyses.
  (4) Decoupled limit and damage analyses.
(e) The use of decoupled initiation-based weld life calculations is reasonably widespread and accepted, as discussed in the literature survey (Appendix B).
(f) The approach is consistent with the general ASME Design Code approach of considering damage and crack initiation, not propagation.

4.2 Numerical Predictions

4.2.1 WJIF Calculations

Appendix H is a summary of a demonstration of the application of the WJIF methodology to a range of different weldments. Figure 95 summarizes the results.

All the examples assumed the material to be annealed Gr22 base metal with 2¼Cr 1Mo weld consumable at a design temperature of 1000°F.

The weld was modeled in every case as five regions, with the creep properties being simulated by temperature shifts as given in Figure 94 (reproduced here for convenience). The temperature shifts applied do not necessarily represent any weldment or class of weldments, but have been chosen to represent a baseline case for the purpose of demonstrating the methodology and developing an understanding of WJIF's as a function of weld geometry, material zone property differences, and peaking. The selected baseline assumptions matched the assumptions used in the Sabine analysis, which was developed from published Gleeble-simulated material creep rate data on various HAZs of Grade 11 [12], and from the EPRI creep rupture database on Grade 11 weld and base metal [8], since the relative effect of temperature on creep rupture strength is similar for the two alloys.

Figure 94: Table of Temperatures Used to Shift Creep Properties in Gr. 22 Material Zones for the Baseline Case to Demonstrate the Methodology and Sensitivity of Various Parameters to WJIF's

Zone	Equivalent Temperature (°F) (weak weld)	Equivalent Temperature (°F) (strong weld)
Base material	1000	1000
Weld Material	1054	1000
CGHAZ	937	937
ICHAZ	1012	1012
FGHAZ	1046	1046

The problems ranged from a flat plate through a range of seam welded thick pipes under internal pressure, to two types of seamless pipe containing girth welds under internal pressure and an additional system generated axial load.

The effects of weld imperfections were explored by inserting angular and alignment discontinuities in a large diameter pipe.

Figure 95: Summary of WJIF Solutions (Solid Lines) Compared to Relative Strengths of the Weak Zones (Dashed Lines).

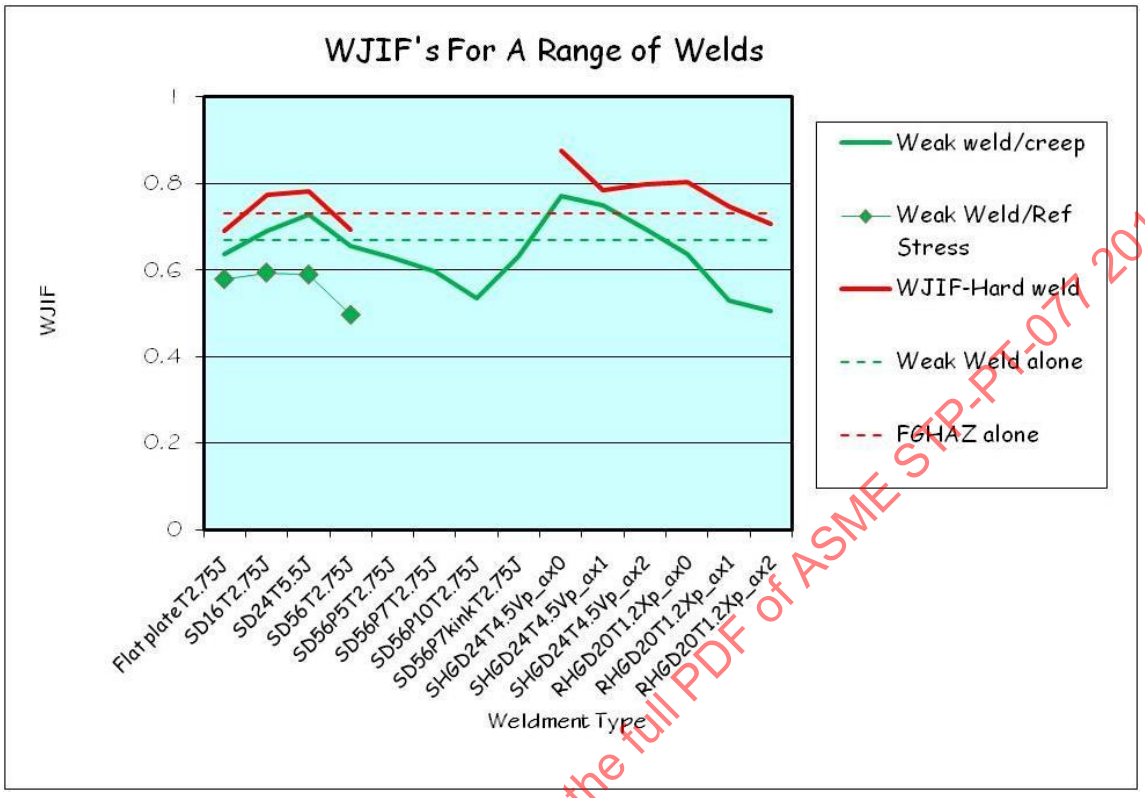

The results summarized in Figure 95 are broken down into more detailed categories in Appendix H. Observations are:

(a) Tubes/pipes with Seam Welds under Internal Pressure – The WJIF does not appear to vary greatly, or with any trend over a significant range of R/t ratios, from a thick tube (R/t = 3.2) to a relatively thin walled pipe (R/t = 11.2). For the conditions chosen for this analysis, the WJIF was, on average, about 0.67 for a "weak" weld, defined as the weld metal having the lowest creep strength. For a "strong weld", defined as the ICHAZ having the lowest strength, the WJIF was about 0.73. Both these values are almost identical to the WSRF for the weak material compared with the base material.

(b) Peaking and Misalignment – The largest pipe used in the pressurized tube study was used for this investigation. A variety of peak angles from 5° to 10° were examined, together with a single example of a misalignment. The WJIF was reduced systematically by the degree of peaking. Specifically, the significant variable is not so much the peaking angle as the offset of the local center surface of the pipe from the nominal diameter. The cause of reduced weld strength in this instance is not a material problem, but is the result of bending of the pipe wall due to out-of-roundness. This may be a problem that is better dealt with by treating the geometric imperfection as a structural problem and calculating the bending stress on the weld section by existing methods contained in the ASME Code.

(c) Girth Welds and Axial Loading – Girth welds show a similar central tendency to seam welds, grouping around the rupture strength of the weakest constituent of the weld. Additional system loading, in the form of axial load over and above end closure reaction has a significant effect on the WJIF. As in the case of weld imperfections, system loading can be estimated by design procedures in the ASME Code, and these can be used to calculate the combined stresses due to pressure and system loading before applying the WJIF.

(d) The feasibility of using the Reference Stress concept (Attachment G) was tested on the sample of seam welded pipes. The method as applied in this study differs in one detail from its application in R5. The difference is that, in this study, the "Reference rupture stress" is corrected for multiaxiality using the Rice/Tracey factor, whereas R5 does not. The predictions made with this approximation were conservative, but not excessively so. The concept therefore offers the prospect of a simple method that can be applied without the need for special purpose user routine, thereby placing it within the reach of a wider constituency of potential users.

5 CONCLUSIONS

In summary:

(a) A simplified approach (analysis tool/methodology) was developed to evaluate the creep rupture strength of a weldment relative to that of base metal.

(b) The tool was benchmarked against selected cases of high-temperature, long seam weldment piping field and component testing experience.

(c) The approach has been used to develop a simplified methodology for quick and computationally economical evaluation of WJIFs, which has been demonstrated by application to a range of representative weldments.

(d) The tool will be used in the next phase of work (Task 3) for the examination of the cross-weld test specimen and data analysis issues.

In this work, the WJIF was defined as the ratio between the strength of a component with a weld compared to the same component without a weld for a given time. Therefore, it includes both material and geometric features. One finding of the project has been that the WJIF parameter depends on so many geometric and material properties, that the aim of representing weld strength by a single number, i.e. a weld strength reduction factor (WSRF), may be too simplistic. On the positive side, simplified methods, such as the Modified Reference Stress approach, have been found that may be directly applicable to design procedures. This could lead to weldments being designed in the future more like other geometric features such as nozzles, on a case-to-case basis. Recommendations for application of this tool will be addressed as part of the final report.

APPENDIX A: SCOPE

STP-PT-077: Development of Weld Strength Reduction Factors and Weld Joint Influence Factors for Service in the Creep Regime and Application to ASME Codes

Except from the Task 2 scope as defined in the original proposal:

The task to develop Weld Joint Influence Factors (WJIFs) will be conducted by D. Marriott (consultant), P. Carter (SES), and EPRI. The WJIF, defined as the ratio of the nominal stress to cause failure of the weld joint to that of a seamless metal with the same strength for the same duration, will be studied for application to piping, components, vessels, and other pressure related equipment operating in the creep regime and subject to ASME B&PV code requirements. This task will develop the data to define WJIFs as a function of weld geometry, weld process (heat input/size of effective HAZ zones), weld technique, alignment, design life, and other geometric factors. The final report for this task is expected to include the following:

- Literature review on methods for determining WJIFs (from Task 1a)
- A comparison of current code methods
- An examination of a modified reference stress method
- FEA and CDM modeling of prototypical weld geometries to calculate WJIFs
- Analysis procedure to determine WJIFs
- Development of WJIFs for seam welded piping and potentially other geometries

APPENDIX B: REVIEW OF SELECTED LITERATURE AND ANALYSIS METHODS

This report focuses on application of efficient methods for weld life prediction, assessment and design. The background and history of the discipline is significant, to which full justice cannot be done in this review. To provide some of this background, and to prevent the impression that this report is isolated from what has gone before, some detail is given of the literature dealing with key issues leading to the present approach. The extensive literature on creep crack growth calculations and high temperature defect assessment has not been included, since the scope of this project excludes it.

The problem of predicting the long-term high temperature strength of welded joints has been an active topic for more than 30 years. Weld strength factor information is now available as in ASME IIINH [1], but practical corresponding design analysis methods are still being developed and tested.

B.1 Summaries of Weld Characteristics

Price and Williams [2] gave (in 1982) a comprehensive description of weld processes, metallurgy, and factors affecting weld strength. Metallurgical implications of the thermal cycle in various zones are described. The intercritical heat affected zone (ICHAZ) region is identified as the source of creep damage for ferritic welded joints (Type IV cracking). Plant failure data (1982) shows that the ranking of the severity (reduction in life) of ferritic weld failure modes is:

(a) Heat affected zone cracking (most severe)
(b) Transverse weld cracking
(c) Type IV cracking

The paper states that (a) and (b) may be eliminated by control of trace elements and correct PWHT. Type IV cracking remains a problem because it is likely that the weld thermal cycle will be unfavorable in some part of the HAZ/parent metal region.

The scope of this paper is extensive, and covers all aspects of the problem of predicting weld properties. Consequences of the weld process such as residual stress, directional properties associated with solidification, solidification cracking and hydrogen cracking are described. Relating critical properties such as grain size, heterogeneous compositions, and residual stress to heat flow and the welding parameters is discussed. Calculations for residual stress and relaxation are given. Mechanical properties of the different zones in ferritic welds are assessed. The complexity of the heterogeneous material is evident in that near the HAZ/parent interface there will exist soft, ductile over-tempered material and coarse-grained bainitic intercritically heated material.

Stress analysis of heterogeneous joints with narrow HAZ's is described. The use of steady state maximum principal stress (MPS) or a combination of maximum principal stress and effective stress to predict crack initiation is discussed. It is concluded that the use a pure MPS criterion should be conservative.

Gooch and Kimmins [3] discussed cross weld tests of 2¼Cr1Mo weld metal - ½Cr½Mo¼V parent metal joints. In addition to observations about hardness, oxidation effects and rupture life, they note that strength mismatch between materials in a welded joint gives hydrostatic stress and loss in ductility. The test specimens used were of variable geometry and intended to re-produce realistic constraint and stress state. The shortcomings of design calculations (too conservative) and of analysis of shear stress (probably unconservative) are pointed out. The report concludes that although weld life reduction factors were ~5 at 40 MPa, the design life of the piping should not be affected due to conservative (small specimen) parent metal rupture data.

The report makes it clear that the mechanical problem associated with weld failures is one of a heterogeneous material, where a region of low strength may have a reduced stress or even an increased stress compared to the nominal (average) value. A life prediction requires information on the weakest

material, and on its operating stress. Obtaining this information from a test program was the objective of the paper.

Cross-weld rupture testing is of particular interest because it tests the weakest link in the parent – HAZ – weld metal sequence. It is an efficient way of characterizing a joint, and any practical weld assessment methodology must be able to use cross-weld rupture data to define uniaxial weld strength. It makes no assumptions about the weld failure mode, possible examples of which are:

(a) *Weld strength mismatch* – A relatively weak weld metal may be deliberate as in Ni-based welds, or accidental
(b) *Cross-weld cracking* – Cracks are perpendicular to weld direction, associated with residual tensile stress
(c) *HAZ cracking* – Associated with low ductility, coarse-grained microstructure
(d) *Fusion boundary failure* – (Type III) Associated with Cr depletion between parent and weld metal
(e) *Type IV cracking* – In spite of the attention it gets in the literature, not all weld strength reduction is due to this phenomenon. The Type IV region may be defined as the weakest condition that can be generated by short-term heat treatments in a ferritic weld.
(f) *Weld defects* – Hot cracking, hydrogen cracking, stress relief cracking, lack-of-penetration, slag entrapment, etc.

Other relevant features of welded joints include transition joint cracking, epitaxial grains and directional strength, geometry of heat and mass flow, leading to segregation perpendicular to tensile stress, and heterogeneous creep properties.

A difficulty with cross-weld testing is dependence on specimen thickness. Constraint and multiaxiality effects associated with heterogeneous properties mean that the weakest uniaxial material properties are difficult to measure with this technique. Use of a realistic cross-section is sometimes recommended so that even if uniaxial properties are not obtained, the joint strength is, which may be used in simple calculations. However, in order to model the weld behavior accurately, individual material and HAZ properties are required.

Although early reviews captured the range of weld behavior, progress was limited by difficulties with analysis. Different approaches have emerged. To understand these, the changes in stress distribution over the life of the component need to be understood.

Stress distributions during weld life. Stress re-distribution occurs continuously. Initially the change is from the elastic to the creep stress distribution. As damage develops, the stress reflects the damaged or rupture stress distribution before final failure. For a homogeneous material, the maximum stress and damage rate in the structure will generally decrease throughout its life. For heterogeneous (weld) materials this is not necessarily the case, and the multiaxial rupture stress can decrease or increase from the elastic to the steady state and then may continue to increase.

Calculation of weld life therefore requires stress analysis that reflects these changes. In the literature, two approaches have emerged. The first is to perform structural analysis as accurately as possible, recognizing that material properties change over time, culminating in failure. This is the continuum damage mechanics (CDM) approach. The second is a simplified approach that seeks to de-couple the stress analysis from the damage (life) calculation. Two forms of simplified method will be described. Use of a creep analysis reflects the change from elastic to steady state. The limit load reference stress typically represents a stress distribution between steady state and rupture. Both approaches assume that:

- The time to re-distribute stress from elastic to creep steady state is small compared to component life.

- Creep strain ductility is sufficient to achieve re-distribution. It is important to note that before full re-distribution is achieved, multiaxial effects are not expected to be significant, and that ductility should not be reduced from uniaxial values.

This is different from the requirement that the tertiary creep ductility is larger than the strains required for re-distribution to the end of life or rupture stress distribution (see R5 procedure [4]). In the R5 procedure, ductility is defined by the ratio of creep ductility to Monkman-Grant strain, which must be > 5 for full stress re-distribution.

Thus the ability of the structure to achieve steady state and full rupture stress distributions depends on creep ductility. In the limit of a very creep brittle material, failure will occur while in the elastic stress distribution. This should not be a realistic possibility for boiler and pressure vessel materials. By definition, a creep ductile material can develop stress distributions so that failure occurs over a volume, for which the limit load reference stress is a good predictor. Intermediate cases could develop steady state stress distributions, but not the full reference stress, before failure. Such cases would have adequate Monkman-Grant strains for initial stress re-distribution, but relatively low values of creep ductility. The limit load calculation can be defined to address this problem, and ensure that the calculation reflects any limited ductility.

B.2 Continuum Damage Mechanics (CDM) Models

The basis for the phenomenological approach to the mechanics of weld failures grew from classical models for creep damage rates and rupture life prediction associated with Kachanov and Rabotnov, and reviewed in [5]. In the finite element models, conventional elastic properties are modified in a similar way to the steady state creep equations to take damage into account. When applied to a welded joint, each of typically four distinct material zones requires a different set of CDM parameters. The first such comprehensive finite element model of a welded joint was by Hall and Hayhurst [6]. This model used a basic continuum damage mechanics (CDM) model for weld and parent material that has been used with variations and developments for all detailed finite element models intending to represent weld and HAZ properties and failure as accurately as possible. A typical uniaxial form of the model is as follows:

$$\dot{\varepsilon}_c = A\exp(-Q_1/RT)\{\sigma/(1-D)/\sigma_D\}^n$$

$$\dot{D} = B\exp(-Q_2/RT)\{\sigma_{rupt}/(1-D)/\sigma_R\}^\chi$$

$$\sigma_{rupt} = \alpha\sigma_I + (\alpha-1)\sigma$$

$$\sigma = E(\varepsilon-\varepsilon_c)/(1-D)$$

In these equations, A, B, Q_1, Q_2, E, s_D, s_R, a, n, and c are material property constants. T is temperature. D is the damage parameter that varies from D = 0 initially to D = 1 when the material test sample has ruptured. s, e and e_c are von Mises effective stress, deviatoric strain and creep strain invariants respectively. Multiaxiality and constraint are described in the equation for s_{rupt}, in this case a linear combination of effective stress and maximum principal stress. This is one form of a three term (effective stress, maximum principal stress, hydrostatic stress) model known as the Leckie-Hayhurst model.

It may be seen that the model consists of a traditional (Norton) equation for creep strain rate modified by a quotient with a "damage" parameter D giving failure (infinite strain rate) in a finite time. The damage rate is given by a similar equation, which may have a different exponent χ. The elastic modulus E is similarly modified, so that elastic strain cannot support load when D = 1.

B.3 Models for Multiaxiality and Ductility Effects

The equation for the rupture stress s_{Rupt} above is given in terms of effective stress and maximum principal stress. The constant a is a material property that defines the effect of stresses other than von Mises effective stress on damage rate. Other formulations are of multiaxial or ductility functions are:

Power law multiaxiality [8] : $\dot{D} = C\dot{\varepsilon}\left\{\frac{\sigma_I}{\sigma_e}\right\}^v \dot{D} = C\dot{\varepsilon}\left(\frac{\sigma_1}{\sigma_e}\right)^v$

This is an alternative to the two term Leckie-Hayhurst model given above, which appears to state the same idea in a different way.

Huddleston (ASME IIIINH [1]): $\sigma_R = \sigma_e \exp C\left[\frac{J_1}{S_S} - 1\right]$

where $S_s = \sqrt{\sigma_1^{\,2} + \sigma_2^{\,2} + \sigma_3^{\,2}}$

Goodall-Ainsworth (R5 [4]): $\sigma_R = \sigma_{ref}\left[1 + \frac{1}{n}(\chi - 1)\right]$

where n = creep index, χ = limit load/yield load.

This is a stress correction for creep steady state. It is used as a ductility limit.

It may be seen that in the CDM models, deformation depends on von Mises (effective) stress, while damage depends on effective stress modified by a multiaxiality or ductility term.

The multiaxiality effect has not received significant attention in the weld analysis literature. This is hard to understand, given the critical role it plays in explaining the difference between homogeneous and heterogeneous materials at high temperature. Without the multiaxiality effect, the observed weakening behavior of welded joints at high temperature would still be a mystery. At present, the maximum principal stress – effective stress alpha model is the most widely used. An alternative to this model is the facet model by Nix et al [7].

In this report, the multiaxiality effect has been calibrated against the use of hoop stress for prediction of long-term creep rupture in tubes. The correlation of long-term tube rupture with average hoop stress was established by Cane [22].

B.4 Weld Assessment Methods

The CDM equations with a multiaxiality correction allow the detailed formation and development of "damage" to be calculated. Subsequent developments have added complexity to the model without changing its basic form. For example, Hayhurst et al in [8] separate the single damage term into hardening, softening and cavitation terms. In this case, temperature dependence was modeled as separate cases, without an explicit temperature dependent function. So for 5 temperatures and 5 material zones, 175 parameters were required.

Hyde et al [9] use the basic CDM model to fit parent, weld and HAZ rupture data for service-exposed 2.25Cr1Mo - 0.5Cr0.5Mo0.25V pipe welds. Properties were obtained from creep tests on samples taken

from the pipe girth welded joints. The paper states that the multiaxiality a varies linearly with failure time. This reflects the known trend of reducing ductility with reducing stress and increasing rupture time.

Although it may be termed a mature technique, at least in its basic form, a significant feature of the CDM models is the complexity and magnitude of the data required. This presents a serious practical problem with the use of such a weld analysis method for component assessment, and for defining weld design factors. It effectively rules out detailed CDM modeling as a general technique for weld assessment and design.

In addition to CDM models, there are several techniques described in the literature for the problem of practical weld assessment, and/or for weld design.

ASME IIINH [1] Provides weld strength reduction factors, but with elastic stress analysis and no explicit representation of the weld, the ability to take full advantage of the data is limited. Elastic analysis does not convincingly capture the differences between girth and seam welds, and between axial and hoop stresses. Further, the problems of stress multiaxiality and weld geometry cannot be considered.

The API 579/ASME FFS document [10] uses the "omega" creep material model that is discussed extensively in the main report. This is a combined deformation and damage model using a specific form for the creep curve defining the material model. Multiaxiality is addressed in a unique approach that is not discussed or identified.

The PD 6539 (British Standards) approach [11] uses the weakest material in a heterogeneous structure to define the structural strength. Therefore no account is taken of stress re-distribution between weak and strong regions.

R5 [4] uses a limit calculation with yield stresses in proportion to rupture strength of the materials. Depending on the structure and load, the weaker material can off-load stress onto the stronger. The results are heterogeneous reference stresses that are in the same proportion as the yield stresses. The interpretation of these reference stresses requires some care. The most accurate value is in the region of failure in the limit analysis. For other regions, the reference stresses are conservative. The reference rupture stress is then modified by

$$\sigma_R = \sigma_{ref}\left[1+\frac{1}{n}(\chi-1)\right]$$, where χ = limit load/load to first yield.

A number of authors have noted that for realistic conditions of life, stress and temperature, weld life is reasonably well characterized by the time to damage initiation. In [11], Molineux et al find that identifiable creep damage appears at a life fraction of 80% - 90% in notched specimens. Similarly Hyde, Sun and Williams [12] found that a life assessment based on steady state creep analysis predicts the failure location and 60% – 80% of weld life. Payten [13] and Hyde, Sun and Becker [14] use a conventional creep analysis and a de-coupled damage calculation conservatively to assess weld creep life. Similarly Hyde, Sun and Williams [15] used full CDM and steady state analyses to evaluate narrow gap and conventional pipe welds. It was found that welded pipe has ~40% of plain pipe rupture life for the case considered.

Hayhurst et al [17] compare standard design methods with de-coupled time-independent R5 calculations for welded pipes, and conclude that the code safety factor is inadequate.

Takemasa [18] proposed that the strength of P91 welded elbows could be predicted using an average weld HAZ stress. Remembering that the multiaxiality parameter a has been observed to increase with rupture time [9], it is possible that this conclusion depends on load and rupture time.

Carter [18] found that, compared to full continuum damage (CDM) calculations, weld life may be reasonably and conservatively estimated using a modified reference stress method, as follows.

As in R5 [4], define limit analysis yield strengths in proportion to creep rupture strength of material (Weld metal, HAZ materials, parent material).

For a particular load case, perform an elastic-plastic limit analysis. If there is concern about the material ductility required to achieve full stress re-distribution, the maximum plastic strain at any stage in the analysis may be used to define the strain-dependent limit load. It is a conservative measure of the creep strain necessary to achieve the stress distribution. Thus the analysis can be curtailed at some plastic strain that is judged to be acceptable. This is a variation on the standard limit load reference stress calculation.

Apply the multiaxiality correction to define the maximum rupture stress obtained in the analysis. Calculate the modified reference stress

$$\sigma_{mod} = \text{operating pressure x limit } \sigma_R \text{ /limit pressure.}$$

The estimated weld (initiation) life is the time to rupture at stress = σ_{mod}.

B.5 Further Examples of Weld Modeling

J. Storesund, K. Borggreen and W. Zang [20] studied creep performance in X20 piping welds using CDM models and replica inspections taken over decades. The model was simplified by considering one HAZ material, parent material and weld metal. Sensitivity analyses were performed on the key parameters for which some uncertainty exists, namely heat affected zone creep rate and the multiaxiality parameter a. The results (weld life) were found to be strongly dependent on these parameters if they were connected, but less so if they are allowed to vary separately. Axial stress was also found to be a significant factor in life reduction. Replica inspection over ~200,000 hours on X20 pipe showed generally low levels of damage, even when high axial stresses are likely as in reheat piping. The report notes differences in safety factors for X20 and for older 2.25Cr1Mo pipes, and concludes that this is responsible for the reliability of the X20 pipes.

G.R. Stevick [21] produced a comprehensive view of high temperature weld life prediction, including initiation and the C* growth of cracks, and significance of inclusions. The difference with the current approach is one of emphasis, which is that weld life may be well and conservatively estimated by the time to significant local creep damage.

B.6 Conclusions

- Due to the data requirements, the use of full CDM methods for weld assessment is primarily limited to research papers and demonstrations of technical capabilities.
- *Steady state creep analysis* and *time-independent reference stress analysis* provide a basis for a decoupled damage/life calculation.
- Time to first significant damage in a decoupled damage calculation is a reasonable and conservative estimate of weld life.

REFERENCES – APPENDIX B

[1] ASME Section III Division 1 Subsection NH, 2007.

[2] A.T. Price and J.A. Williams, "The Influence of Welding on the Creep Properties Of Steel", Recent Advances in Creep and Fracture of Engineering Materials and Structures, Eds. Wilshire and Owen, Pineridge Press, Swansea, 1982.

[3] D.J. Gooch and S.T. Kimmins, "Type IV Cracking in ½Cr½ Mo¼V/ 2¼Cr1Mo Weldments", Proc. 3rd Int. Conf on Creep and Fracture of Engineering Materials and Structures, Eds. Wilshire and Evans, Swansea, 1987.

[4] R5 Assessment Procedure for the High Temperature Response of Structures, Issue 3, British Energy Generation Ltd. 2003.

[5] R.K. Penny and D.L. Marriott, "Design for Creep", Chapman and Hall, Second Edition, 1995.

[6] F.R. Hall and D.R. Hayhurst, "Continuum damage mechanics modeling of high temperature deformation and failure in a pipe weldment", Proc. R. Soc. Lond. (A), 433, 383-403, 1991.

[7] W.D. Nix, J.C. Earthman, G, Eggeler and B. Ilschner. "The principal facet stress as a parameter for predicting creep rupture under multiaxial stress". Acta. Metall, 37, 4, 1067-1077, 1989.

[8] R.J. Hayhurst, F. Vakili-Tahami, R. Mustata and D.R. Hayhurst, "Thickness and multi-axial stress creep rupture criteria of the Type IV component of a ferritic steel weld." J Strain Analysis, 39, 6, 729-743, 2004.

[9] T.H. Hyde, W Sun, A.A. Becker and J.A. Williams, "Creep continuum damage constitutive equations for the base, weld and heat-affected zone materials of a service-aged ½Cr½Mo¼V: 2¼Cr1Mo multipass weld at 640 C, J Strain Analysis, 32, 4 , 1997.

[10] API 579/ASME FFS Fitness-For-Service ASME New York 2007.

[11] PD 6539. Guide to methods for the assessment of the influence of crack growth on the significance of defects in components operating at high temperatures. British Standards Institution, 1994.

[12] E. Molinie, P. Martel, C. Duquenoy, P. Dupas and V. Prunier, " Creep behavior of seam-welded reheat steam pipes in thermal fossil power plant: feedback analysis and life assessment methodology", Materials at High Temperatures, 15, pp 375-384.

[13] T.H. Hyde, W. Sun and J.A. Williams, "Creep analysis of pressurized circumferential pipe weldments – a review" J Strain Analysis, 38, 1, 2003.

[14] W. Payten, "Large scale multi-zone creep finite element modeling of a main steam line branch intersection', Int. J. Press. Vessels and Piping, 83, 359-364, 2006.

[15] T.H. Hyde, W. Sun and A.A. Becker, "Life assessment of weld repairs in ½Cr½Mo¼V main steam pipes using the finite element method." J. Strain Analysis, 35, 5, 359-372, 2000.

[16] T.H. Hyde, J.A. Williams and W. Sun, "Assessment of creep behavior of a narrow gap weld", Int. J. Press. Vessels and Piping, 76, 515-525, 1999.

[17] D.R. Hayhurst, I.W. Goodall, R.J. Hayhurst and D.W. Dean, "Lifetime predictions for high-temperature low-alloy ferritic steel weldments". J. Strain Analysis, 40, 7, 2005.

[18] F. Takemasa et al, "Type IV Creep Damage Analysis for Full Size Component Tests on Welded P91 Boiler Hot Reheat Piping", PVP-Vol 472, Elevated temperature Design and Analysis, San Diego, 2004.

[19] P. Carter, "Simplified methods for high temperature weld design and assessment for steady and cyclic loading", Fifth International Conference on Advances in Materials Technology for Fossil Power Plants, EPRI, San Marco, 2007.

[20] J. Storesund, K, Borggreen and W. Zang. "Creep behavior and lifetime of large welds in X20 CrMoV 12 1 – Results based on simulation and inspection", Int. J. Press. Vessels and Piping, 83, 875-883, 2006.

[21] G.R.Stevick, "Failure of welds at elevated temperatures", WRC Bulletin 390 April 1994.

[22] B.J. Cane, "Present status of predictive methods for remanent life assessment and future developments", ERA report, published in 'Residual Life Prediction' issue of 'Metals Forum', the journal of Australasian Institute of Metals, 1985.

APPENDIX C: DESCRIPTION OF OMEGA

Ref: Prager, M. "Development of the MPC Project Omega Method for Life Assessment in the Creep Range," PVP-Vol. 288, ASME, 1994, pp. 401-421. (Reproduced with permission from ASME)

PVP-Vol. 288, Service Experience and Reliability Improvement: Nuclear, Fossil, and Petrochemical Plants
ASME 1994

DEVELOPMENT OF THE MPC OMEGA METHOD FOR LIFE ASSESSMENT IN THE CREEP RANGE

Martin Prager
Materials Properties Council, Incorporated
New York, New York

ABSTRACT

A methodology for characterizing and assessing the behavior of materials after service in the creep range has been developed and used on a broad range of materials and components. It incorporates the results of relatively short-term tests and improved databases on materials properties. The essence of the method is the definition of a material performance characteristic which the author refers to by the symbol Omega sub p (Ω_p). This coefficient effectively describes the rate at which a material's ability to resist stress is degraded by strain. While Ω_p is a function of stress, temperature and mode of loading, it is amenable to parametric representation and is, therefore, useful in predicting life and strain accumulation. Time to failure and total accumulated strain are shown to be consequences of a characterizing strain rate, as defined herein, and an appropriate Ω_p for the operating conditions and geometry of interest. Accumulated strain, future strain, current creep rate, remaining life, total damage and damage rate are among the quantities which are easily calculated. The development of the method employs and extends the concepts of Larson-Miller, Monkman-Grant, Robinson, Theta Projection, Kachanov and Norton.

INTRODUCTION

Volumes have been written over the past decade regarding life assessment of components in the creep range. Prominently recognizable methods which have been proposed include replication [1], life summation based on Larson-Miller [2] or other [3] parametric concepts, the Kachanov (small omega, ω) approach [4] and isostress testing [5]. While each has been widely used by its advocates, each has its limitations. Evidence of validity is scarce and generalization in terms of useful rules, formulas or correlations has been too slow in coming. Most of the above are employed not because they provide insight into behavior, but because they are likely to be conservative.

Without seeking to be comprehensive here, it should be pointed out that replication is not suitable for most types of materials and components in use in the USA because surface cracking and cavitation are not encountered until too near the end of life or they occur for extraneous reasons. Deficiencies of conventional parameter-based life summation approaches are that the correct constants for ex-service materials may not be the ones found in the handbooks and positioning a component in the scatterband of historical test data is only possible if the prior operating conditions are well known and the evaluator is extremely sophisticated. Alternatively, utilizing the minimum Larson-Miller curve will usually condemn service-worthy components. This is partly the case because handbook reference curves for materials in the creep range are contaminated at design stress levels by test results from badly oxidized specimens which have significantly shortened lives.

Kachanov's concept, as usually presented, is mathematically unwieldy and not necessarily descriptive or insightful into material behavior except to a scant few specialists. Isostress testing is usually marred by the need for long-range extrapolation of short-term stress-rupture test results. Such data are

usually invalid because of microstructural changes (dissolution of phases, recrystallization, etc.) and oxidation of the specimens (which are usually of small size). The requirement for multiple isostress test specimens and problems of data scatter also detract from the appeal of this approach. None of the above methods, except perhaps to a limited extent those based on Kachanov's approach, lead to estimates of strain accumulation (past or future), unambiguous definitions of damage or the rate of damage accumulation in a component. In fact, for many materials, strain accumulation rather than the prospect of failure could lead to retirement.

DEVELOPMENT OF MPC'S OMEGA METHOD

In 1986, MPC's Petroleum and Chemical Committee established a program to examine the above enumerated and other approaches to life assessment. The Group planned and initiated a joint industry supported investigation entitled "A Program to Establish Practical Methods for Determining the Remaining Life of Process Equipment Operating in the Creep Range," Project Omega for short. What evolved was a simple, yet powerful method for dealing with the concepts of creep, remaining life, damage and strain accumulation. A database, methods of testing, and a broad range of specialized computer spreadsheets and graphics tools have been developed under the sponsor committee's direction to support the methodology. The Omega method, which will be described herein has been applied in dozens of applications ranging from process vessels to heater tubes, a few of which are described in this Conference volume [6,7,8,9]. The concept can be incorporated into finite element programs as well as estimating creep crack growth behavior. The activities conducted under Project Omega are too numerous to report here in detail. However, the essence of the evolution of the method will be covered below.

Materials ranging from soft carbon steel to extremely hard (and brittle) 1¼chrome-½moly and rotor-type steels were studied in the course of the research (Figures 1 and 2). Tests were planned to elucidate the meaning and nature of creep damage and to evaluate means of its measurement. The conditions of test used were such that oxidation was not a factor. In the initial phase of the research, conventional size specimens were machined from jumbo size specimens which had been creep damaged by exposure to stress and temperature. This early work led to a number of important observations.

(1) Carbon steel was barely damaged by creep strain under the conditions of exposure (6 ksi and 1060°F (571°C)). That is, material which had been strained even 50% by creep appeared to differ relatively little from unstrained material when both were examined microstructurally or creep-rupture tested at a given stress and temperature (Figure 3).

(2) The creep resistance of the very hard and brittle material studied was significantly altered by small amounts of strain although these changes were not usefully associated with the appearance of creep cavities or cracks (Figure 4).

(3) Laboratory damaged or actual ex-service materials displayed virtually no primary or secondary creep when subsequently creep tested at the stress levels of the prior exposure (Figure 3).

(4) Strain rate increased continuously as a function of strain during tests (Figure 5).

(5) The rate of increase in strain rate with stress (due to cross sectional reduction) during the test generally was much greater than that predicted by Norton's Law (Figure 6).

It was concluded that, under the conditions of test, the time for failure for carbon steel was determined mainly by the strain-rate acceleration due to the substantial increase in stress which was a consequence of cross-sectional area reduction. On the other hand, the stress on the chrome-moly steel increased very little before failure because ductility was so low, but strain rate increased substantially despite the very small amount of strain observed.

These tests led to the concept that strain-rate at the operating stress and temperature might be a direct and useful gauge of the amount of damage in a material. If true, this offered potential for more accurate life assessment because strain rate could be established at relatively lower temperatures and shorter times than are required for a full set of isostress tests. Also, comparing creep rate to rupture testing, the quality of data might be improved, oxida-

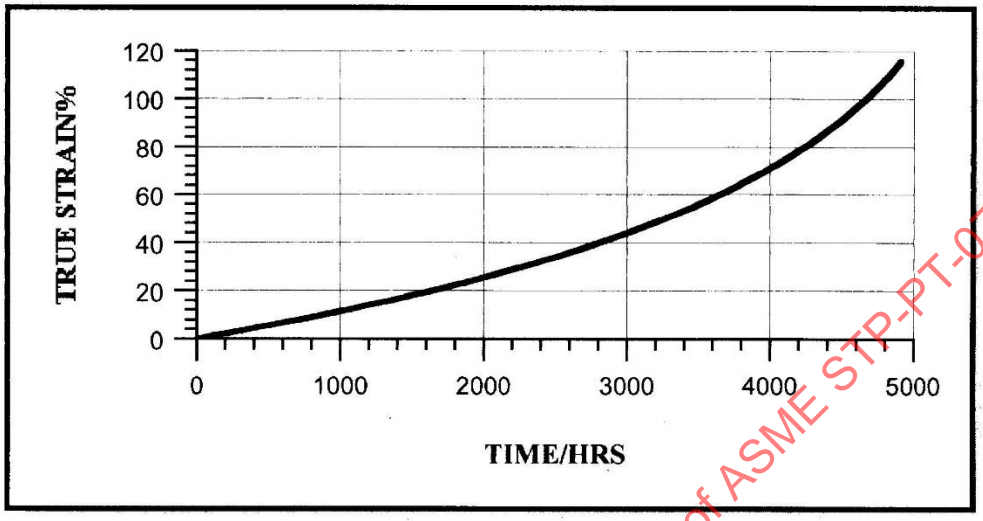

Figure 1. Creep strain of jumbo carbon steel specimen tested under conditions of constant stress.

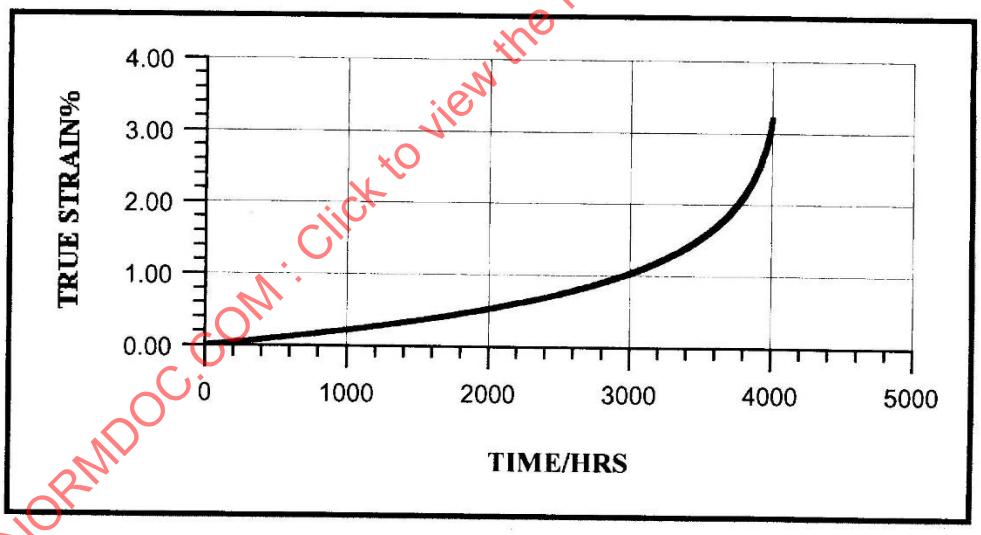

Figure 2. Creep curve for hard 1¼Cr-½Mo steel studied.

403

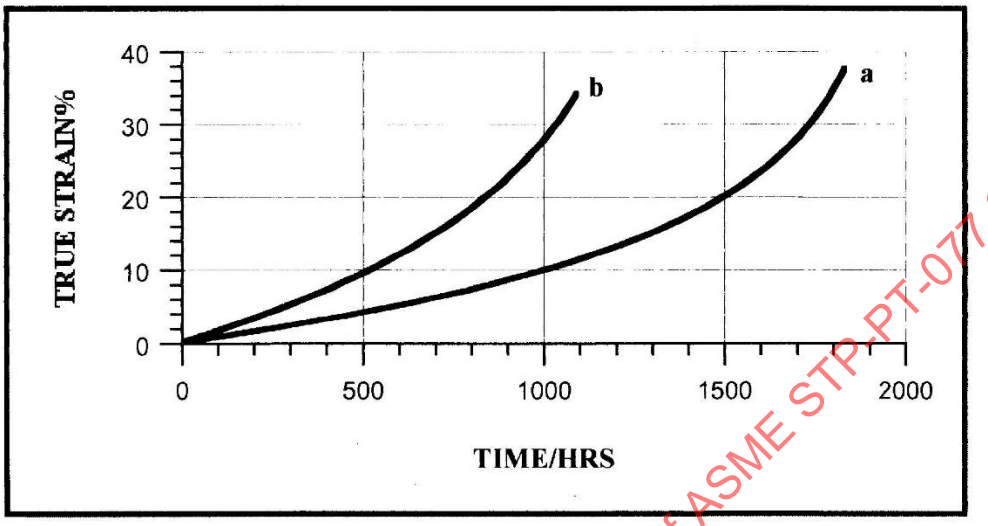

Figure 3. Creep curves for service-exposed carbon steel (a) as received from service, (b) after extensive creep strain under constant stress conditions.

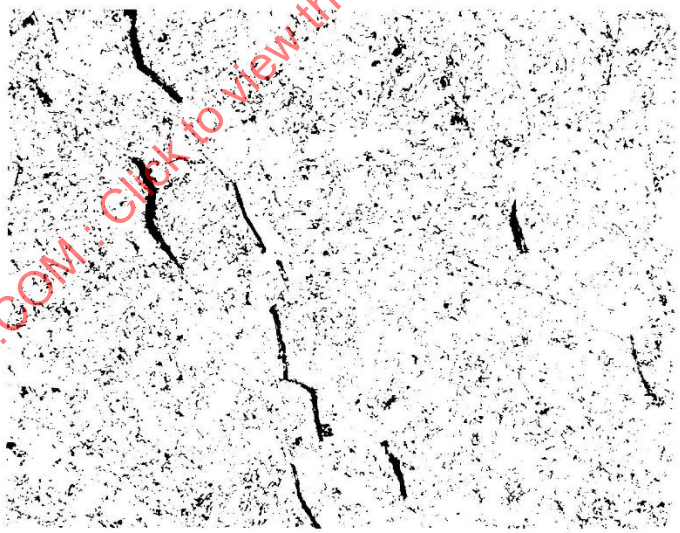

Figure 4. Visible microdamage could not be usefully correlated with prior damage until very late in life.

404

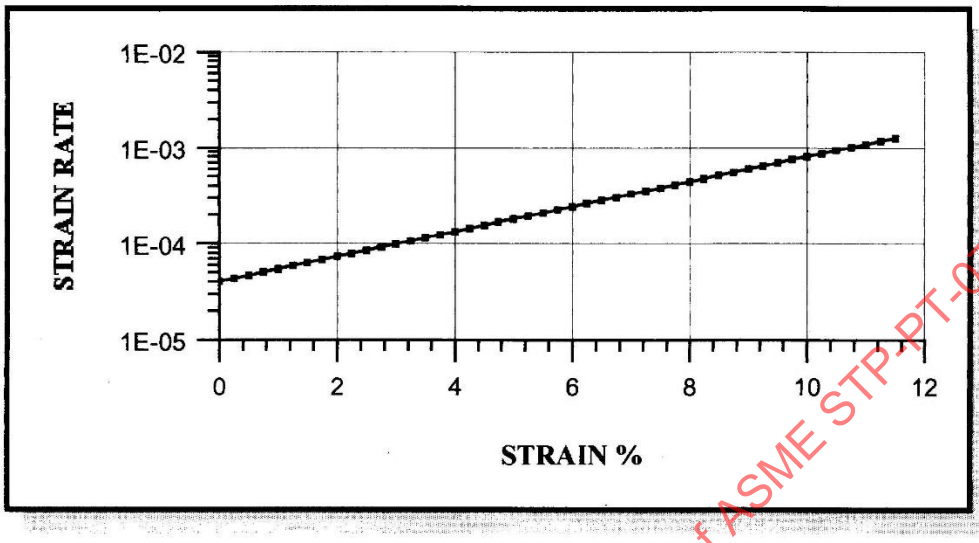

Figure 5. Strain rate as a function of creep strain.

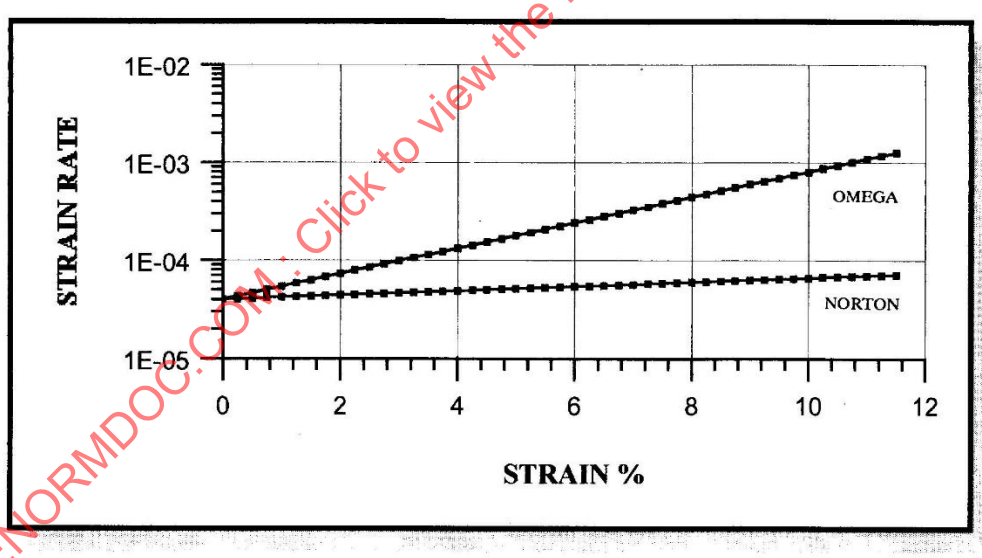

Figure 6. Comparison of strain rate acceleration and Norton's Law prediction.

405

tion effects minimized and uncertainties associated with extrapolation reduced. The author then sought an easily integrated mathematical function and model which would provide relations between strain rate, strain, life consumed, and remaining life. At first, the model was intended to be applied only to materials which had been thermally stabilized by long time in service, i.e., not subject to significant softening or ductility changes under further thermal exposure. In fact, the model has been found to have applicability to a broader range of materials [10, 11].

PROPOSED MODEL FOR ESTIMATION OF LIFE FRACTION CONSUMED AND REMANENT LIFE UNDER DEFINED CONDITIONS

The ultimate objective of Project Omega was to be able to quickly identify during a test those characteristics of the creep curve which would permit estimation of past and/or future creep behavior, with or without explicit knowledge of past operating conditions. It was of interest to determine accumulated strain, future rates, life fraction consumed, damage rate and time to rupture. The problem has been addressed by many, for example, Cane [12] and Leckie [13]. However, the formulations developed were not conveniently used and required assumptions which may differ from fact. Most investigators have started with the equations for strain rate of the Kachanov [4, 13] type

$$\dot{\epsilon} = \dot{\epsilon}_o \left[\frac{\sigma}{\sigma_o} \right]^m \left[\frac{1}{1-\omega} \right]^v \quad (1)$$

where

$\dot{\epsilon}$ = the instantaneous strain rate
$\dot{\epsilon}_o$ = an initial or reference strain rate
σ = the instantaneous value of stress
σ_o = the initial or reference stress
ω = Kachanov's creep damage function

Equation (1) is usually used to model post primary creep rates under constant load conditions wherein the applied stress increases as strain reduces cross sectional area. Obviously, the above equation and the subsequent discussion do not apply to primary creep since the rate calculated increases monotonically with time. However, the reader should understand that primary creep is not usually significant at operating stresses and certainly not in a creep test of a service-exposed material at its prior operating stress and only moderately increased temperatures. In short, in components operating at ASME design level stresses, primary creep should not be a significant contributor to creep damage and certainly may be ignored in post-service testing. Secondary creep may be viewed as a period of constant apparent strain rate brought about by near equality in the rate of decrease in the primary rate and by the rate of increase in the tertiary rate. In fact, experience shows that modeling only tertiary creep for service-exposed materials is quite reasonable.

In order to predict a creep curve of the desired shape, Leckie [13] outlined the development of an integration scheme which led to

$$\dot{\omega} = \frac{K \sigma^v}{(1-\omega)^n} \quad (2)$$

with ω viewed as the microstructural damage parameter, and eventually this leads to

$$\omega(t) = 1 - \left(1 - \frac{\epsilon(t)}{\epsilon_f}\right)^{f\{\epsilon_f/_{MG}\}} \quad (3)$$

where

ϵ_f = the fracture strain
MG = the Monkman-Grant "constant" [14]

Along the way, the exponents for the stress and the damage functions were set equal. The validity of such an assumption has not been demonstrated and, in fact, it is unlikely to hold and certainly does not do so generally. Equation (3) can provide the strongly concave upward tertiary curve which is often observed. However, no guidance has been offered as to how observations can be extrapolated from conditions of test to operating conditions. While this model is not very sensitive to fracture strain, it is necessary to include a value for fracture strain which is generally not known with certainty for reasons which are beyond the scope of this paper.

For the Omega model proposed here, we will start with the following:

ϵ = true strain
E = engineering strain
e = base of natural logarithm

Then, for uniaxial extension at constant volume we have the well-known relation

$$\frac{\sigma}{\sigma_o} = e^{\epsilon} \tag{4}$$

because

$$\epsilon = \ln (1+E)$$

Equation (4) leads to

$$\left[\frac{\sigma}{\sigma_o}\right]^m = e^{m\epsilon} \tag{5}$$

Note, for a tube the exponent would be twice as large due to the diametrical increase associated with wall thinning.

Following the above approach the Kachanov-type expression for uniaxial strain rate becomes

$$\dot{\epsilon} = \dot{\epsilon}_o e^{m\epsilon} \left[\frac{1}{1-\omega}\right]^{\nu} \tag{6}$$

This is still not conveniently integrated.

A general but easily integrated function was sought. It was then proposed that creep rate acceleration during service or during stress-rupture testing could be viewed as a result of the interaction of three separable factors. The three factors proposed were increasing stress, increasing damage and a third for microstructural changes not associated with damage. These factors can be evaluated separately by proper experiments which need not be elaborated upon here. It is possible to include other terms for time-dependent thermal degradation or corrosion, etc., but for simplicity it will be assumed that the materials have been thermally stabilized in service and are not corroding at an important rate. Rather than using Kachanov's power function, the damage may be expressed instead as an exponential function of strain so that the resulting equation can be easily integrated. The exponential was thought to be appropriate at small values of strain. Actually, the exponential approximation was found to hold far out on the strain-time curve, to 20% true strain or more.

Thus:

$$\dot{\epsilon} = \dot{\epsilon}_o e^{m\epsilon} \times \frac{1}{e^{-p\epsilon}} \times \frac{1}{e^{-c\epsilon}} \ldots. \tag{7}$$

where m is assumed to be Norton's exponent to account for the rate increase due to cross section reduction (stress increase), p corresponds to microstructural damage, and c is used to account for deficiencies in Norton's exponent and other microstructural factors associated with the stress change. As noted, the exponential coefficients can be separated by experiment, but for the moment,

$$\dot{\epsilon} = \dot{\epsilon}_o e^{(m+p+c)\epsilon} \tag{8}$$

This expression is easily integrated to give a function containing strain and time, i.e.,

$$\frac{1}{\dot{\epsilon}_o(m+p+c)} (1 - e^{-(m+p+c)\epsilon}) = t \tag{9a}$$

or

$$\epsilon = -\frac{1}{(m+p+c)} \ln (1 - \dot{\epsilon}_o(m+p+c)t) \tag{9b}$$

Similar expressions have been proposed by Sandstrom and Kondyr [15] and by Kussmaul for pipe [16], and Kawasaki and Horiguchi for specific void forming of stainless steels [17] after the minimum creep rate is reached. The last noted investigators started from an atomistic damage model to derive an expression for 347 and 316 stainless steels which includes terms accounting for void formation, dislocation motion and other aspects of the model applied.

For large values of the product of (m+p+c) times ϵ, i.e., greater than 2 or 3, the exponential term in Equation (9a) is negligible and thus at failure

$$\frac{1}{\dot{\epsilon}_o(m+p+c)} = t_r = \frac{1}{\dot{\epsilon}_o \Omega_p} \tag{10}$$

where

$\Omega_p = m+p+c$

At first, Equation (1) appears to be the empirically based Monkman-Grant [14] relation and the sum $(m+p+c)$ or Ω_p can be established simply by determining the reciprocal of the Monkman-Grant "constant." While that may not be a bad approximation in some cases, it is not good in others. This is because here $\dot{\epsilon}_o$ is the "initial creep rate" while Monkman and Grant used the minimum creep rate, usually from tests in which there was considerable primary and secondary behavior. The difference may be small or it may be as much as 50 to 100%. Monkman and Grant did not offer a physical interpretation of their "constant." It will be shown that (because it is similar to Ω_p) it should not necessarily be expected to be a constant over a large range of stress and temperature and it should depend on the geometry of the stressed component. The Monkman-Grant rule works not because the product of the minimum creep rate and time have significance but because creep curves tend to have exponentially shaped tertiary portions which lead to Equation (10). Further comments are made elsewhere [10].

The term Ω_p defined here has both a physical and mathematical significance. Simply put, Ω_p defines the rate at which strain-rate accelerates as a result of creep strain. In effect, it is a total damage coefficient (cross-sectional plus creep damage plus other microstructural effects) for the system. The sum quantitatively describes the ability of a material to tolerate strain. Creep damage is a reduction in the structure's ability to resist stress as measured by the relative increase of strain rate. A material is 50% damaged when its strain rate has doubled and so on.

The definition of Ω_p is expressed mathematically, as follows from Equation (8)

$$\frac{d \ln \dot{\epsilon}}{d\epsilon} = m+p+c = \Omega_p \qquad (11)$$

Equation (11) then suggests one of several convenient means which may be used to determine Ω_p, i.e., plotting the natural log of strain rate versus strain and taking the slope of the straight line (Figure 5).

Alternatively, we see from Equation (9a) that for any time and at fracture

$$\frac{1}{\dot{\epsilon}_o \Omega_p} \left(e^{-\Omega_p \epsilon} - e^{-\Omega_p \epsilon_f}\right) = t_r - t \qquad (12)$$

When the exponential term containing the strain to fracture times Ω_p can be neglected

$$\ln (t_r - t) = \ln \left[\frac{1}{\dot{\epsilon}_o \Omega_p}\right] - \Omega_p \epsilon \qquad (13a)$$

or

$$\epsilon = -\frac{1}{\Omega_p} \ln (t_r - t) + \frac{1}{\Omega_p} \ln \left[\frac{1}{\dot{\epsilon}_o \Omega_p}\right] \qquad (13b)$$

The above expressions suggest a strategy to test the suitability of the model as well as a means of measuring the appropriate initial strain-rate and the damage coefficient Ω_p. The latter is the reciprocal of the slope of the line ϵ vs $\ln (t_r - t)$, which the author refers to as a reverse creep curve. The former can be calculated from the intercept on the strain axis where $(t_r - t) = 1$ (Figure 7). If the reverse creep curve as shown is not linear, the model proposed is not applicable. If there is a primary component the total amount of primary strain (Figure 8) can be extracted by examining the offset from zero at $(t_r - t) = t_r$.

Equation (12) suggests a very important result, that the product of the instantaneous strain rate times the remaining time to failure is constant throughout life. This can be shown as follows:
since

$$\dot{\epsilon} = \dot{\epsilon}_o e^{\Omega_p \epsilon} \qquad (14)$$

When the term containing fracture strain can be neglected, combining Equation (14) and Equation (12) leads to

$$\frac{1}{\dot{\epsilon}_o \Omega_p} \left(e^{-\Omega_p \epsilon} - e^{-\Omega_p \epsilon_f}\right) \approx \frac{1}{\dot{\epsilon} \Omega_p} \approx t_r - t \qquad (15)$$

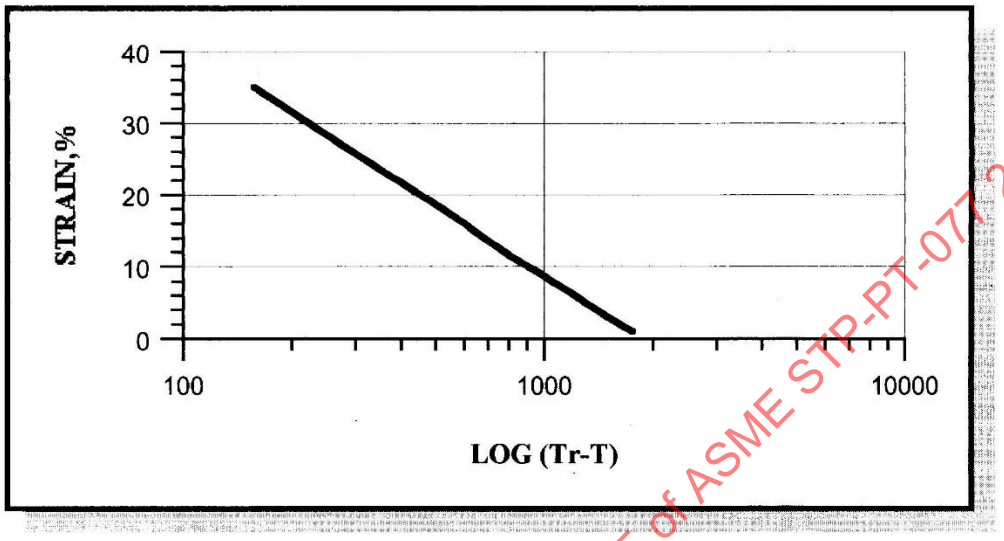

Figure 7. Reverse creep curve plot of strain vs. log (t_R - t). Slope is related to natural log curve by a factor of ln 10.

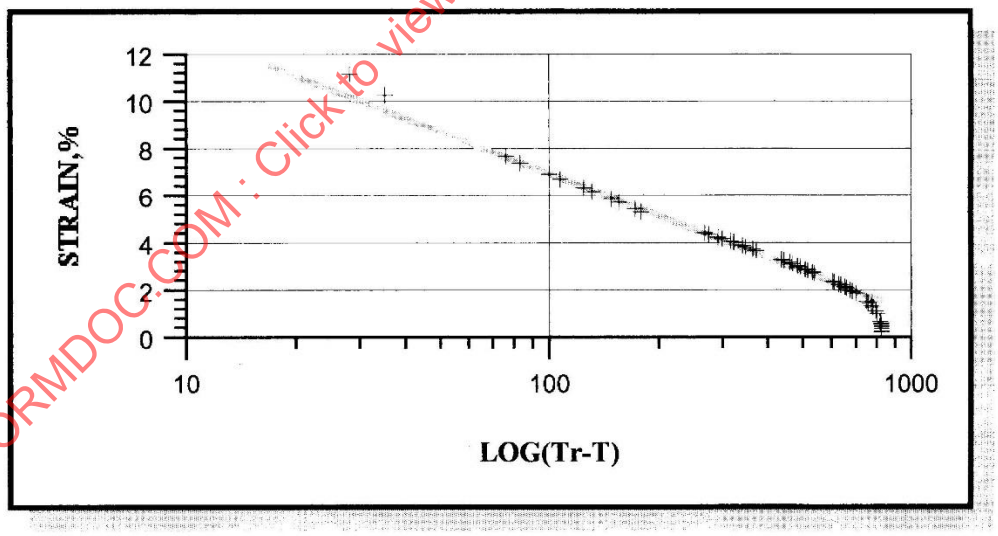

Figure 8. Reverse creep curve displaying primary strain offset.

409

or

$$\frac{1}{\Omega_p} = \dot{\epsilon}(t_r - t) \quad (16)$$

In summary, creep strain versus time curves at a given stress and temperature can be expressed using only two coefficients, an initial rate term $\dot{\epsilon}_o$ and Ω_p. Where the Project Omega model applies, one need only run the test long enough to establish the initial strain rate and the rate of change of strain rate with strain. Hundreds of tests on dozens of ferritic and austenitic materials have shown that the model is broadly applicable (although not universally or always, obviously). Figures 9 and 10 are representative. The model provides a convenient route to many of the quantities needed for life assessment as follows:

Where

t_s = time in service
ϵ_s = strain in service
$\dot{\epsilon}_{os}$ = original strain rate in service

To calculate the original strain rate in service, the life fraction consumed and the accumulated strain in service from an estimate (based on methods described later) of the current in-service strain rate, we start as follows:

$$t_s = \frac{1}{\dot{\epsilon}_{os}\Omega_p}(1 - e^{-\Omega_p\epsilon_s}) \quad (17)$$

and

$$t_r \approx \frac{1}{\dot{\epsilon}_{os}\Omega_p} \quad (18)$$

then

$$\frac{t_s}{t_r} \approx (1 - e^{-\Omega_p\epsilon_s}) \quad (19)$$

but from Equation (8)

$$\dot{\epsilon} = \dot{\epsilon}_{os}e^{-\Omega_p\epsilon_s} \quad \text{or} \quad e^{-\Omega_p\epsilon_s} = \frac{\dot{\epsilon}_{os}}{\dot{\epsilon}} \quad (20)$$

then from Equation (17)

$$(1 - \frac{\dot{\epsilon}_{os}}{\dot{\epsilon}}) = \dot{\epsilon}_{os}t_s\Omega_p \quad (21a)$$

or by transposing terms

$$\dot{\epsilon}_{os} = \frac{\dot{\epsilon}}{t_s\Omega_p\dot{\epsilon} + 1} \quad (21b)$$

then from Equations (18) or (19)

$$\frac{t_s}{t_r} = t_s\dot{\epsilon}_{os}\Omega_p \quad (22)$$

or

$$\frac{t_s}{t_r} = \text{Life Fraction Consumed} = \frac{\dot{\epsilon}t_s\Omega_p}{\dot{\epsilon}t_s\Omega_p + 1} \quad (23)$$

and

$$\epsilon_s = \frac{1}{\Omega_p}\ln(1 + t\dot{\epsilon}\Omega_p) \quad (24)$$

The key point here is that an estimate of the current strain rate in service and of Ω_p which may be obtained with a single test of service-exposed material can give a direct calculation of the life fraction consumed, i.e., fractional damage or accumulated strain. It should be obvious to the reader that life fraction consumed (creep damage) as defined in Equation (23) increases linearly with time at constant stress and temperature. i.e., t_s/t_r is linear with time. Note that the damage rate is simply $1/t_r$.

The closed formed solutions shown here permit calculation of past strain accumulation, future strain accumulation or time to any specific event (strain fracture, strain rate, etc.) for the geometry of interest.

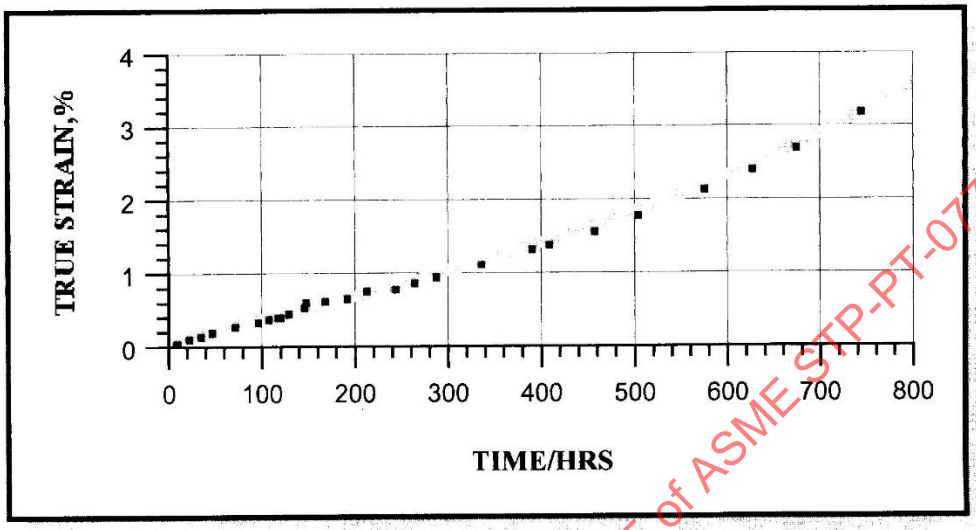

Figure 9. Creep data from service-exposed material specimens.

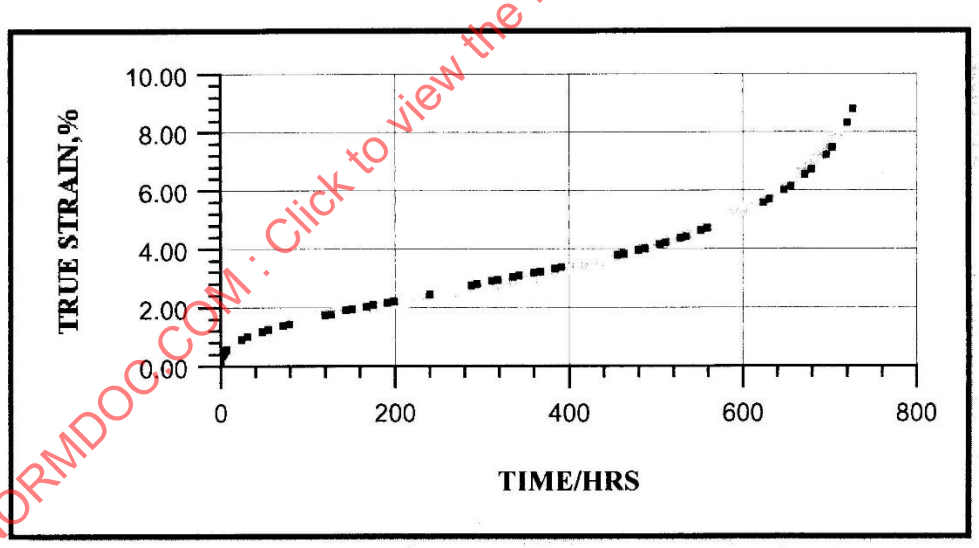

Figure 10. Creep data from virgin material.

411

Example

Say for carbon steel $\Omega_p = 6$ and a creep test at about 100°F (55°C) above the operating temperature on an ex-service sample suggests that the current creep rate in service is 10^{-7}/hr (i.e., 10^{-5}%/hr). If the component has been in service for 200,000 hr, then

$$\text{Life Fraction} = \frac{10^{-7} \times 2 \times 10^{5} \times 6}{10^{-7} \times 2 \times 10^{5} \times 6 + 1} = \frac{.12}{1.12} = 10.7\%$$

or about 11% of rupture life has been consumed.

Since

$$1 - e^{-\Omega_p \epsilon_s} = t\dot{\epsilon}_{os}\Omega_p$$

from Equation (24)

the strain accumulated to date would be

$$\epsilon_s = \frac{1}{6} \ln (1 + 10^{+5} \times 2 \times 10^{-7} \times 6)$$

$$= \frac{1}{6} \times .11 = .0188, \text{ or } 1.88\%$$

and

$$\dot{\epsilon}_{os} = 10^{-7}/_{e} \ln (1.12) \approx 8.93 \times 10^{-8}/\text{hr}$$

or the strain rate has increased only 11% during service

If 3% is the maximum tolerable strain, the time from the start of service to 3% strain is

$$t_{3\%} = \frac{1}{(9 \times 10^{-8}) \times 6} (1 - e^{-6(.03)})$$

$$t_{3\%} = \frac{.1647}{8.93 \times 10^{-8} \times 6} = 307{,}450 \text{ hr}$$

or 3% will be reached in 107,450 additional hours.

IMPLICATIONS FROM THE VALUE OF OMEGA

For some materials, Ω_p is very large, 30, 50 or even 200 or more, and most of service life is spent at very low strains. In the final stages of life, strain rate accelerates rapidly to failure. For such materials, strain at failure or ductility may still be relatively large, leading to the false conclusion that strain measurement during life could give an early warning of failure. This can be misleading as the material's resistance to stress is degraded by small amounts of strain. High Omega behavior may be due to creep softening or brittleness.

A convenient engineering index of total allowable strain is the strain which corresponds to a doubling or tripling of the initial strain rate. The time required would be 50 or 67% of the time to rupture, respectively. This is similar to rules of thumb based on experience. Similarly, the strain equal to the reciprocal of Ω_p, ϵ_m, (approximately the Monkman-Grant strain) is reached at

$$t/_{tr} = (1 - e^{-\Omega_p \epsilon_m}) = (1 - \tfrac{1}{e})$$

or about 62% of life, as is often observed.

IMPLEMENTATION AND COMMENTS

The remarkable feature of the Omega methodology is its prediction that the shape of the creep curve is invariant when plotted as true strain versus time. Thus, the past and the future are calculated with equal ease and testing need be sufficient only to permit estimation of the strain rate at different strains. Strain rate usually may be obtained in tests of only one-tenth the duration required for rupture. This permits testing at 75°F (45°C) lower temperatures then conventional isostress rupture testing and thereby reducing the extent of the extrapolation to predict life by a full order of magnitude.

In the Omega method the physical significance to the creep curve fitting terms is as follows:

$\dot{\epsilon}_o$ is the creep rate corresponding to t = 0 for the given microstructural condition. If part of the creep curve is unavailable or tertiary behavior is combined with primary creep, $\dot{\epsilon}_o$ may still be obtained (Figure 11) graphically or by closed-form calculation (see Equation 21b) from the strain rate at a later time.

Ω_p is the coefficient of the relative (logarithmic) change in strain rate per unit strain. For example, if the creep rate doubles (ln 2 =

Table 1

				OMEGA VALUES FOR CARBON STEEL					
STRESS				TEMPERATURE, F					
KSI	950	975	1000	1025	1050	1075	1100	1125	1150
10.00	7.98	7.40	6.87	6.40	5.97	5.59	5.24	4.92	4.63
9.50	8.17	7.57	7.03	6.54	6.10	5.71	5.35	5.03	4.73
9.00	8.37	7.75	7.20	6.70	6.25	5.84	5.47	5.14	4.83
8.50	8.59	7.95	7.38	6.86	6.40	5.98	5.60	5.26	4.94
8.00	8.83	8.17	7.58	7.04	6.56	6.13	5.74	5.39	5.06
7.50	9.09	8.40	7.79	7.24	6.74	6.30	5.89	5.53	5.19
7.00	9.37	8.66	8.02	7.45	6.94	6.48	6.06	5.68	5.33
6.50	9.68	8.94	8.28	7.69	7.15	6.67	6.24	5.84	5.49
6.00	10.02	9.25	8.56	7.94	7.39	6.89	6.43	6.03	5.65
5.50	10.39	9.59	8.86	8.22	7.64	7.12	6.65	6.22	5.84
5.00	10.80	9.96	9.20	8.53	7.92	7.38	6.89	6.44	6.04
4.50	11.26	10.37	9.58	8.87	8.24	7.67	7.15	6.68	6.26
4.00	11.77	10.83	10.00	9.25	8.58	7.98	7.44	6.95	6.51
3.50	12.33	11.34	10.46	9.67	8.96	8.33	7.76	7.25	6.78
3.00	12.95	11.90	10.96	10.13	9.38	8.71	8.11	7.57	7.08
2.50	13.61	12.50	11.51	10.62	9.83	9.12	8.49	7.91	7.39
2.00	14.29	13.10	12.06	11.12	10.29	9.54	8.87	8.26	7.71

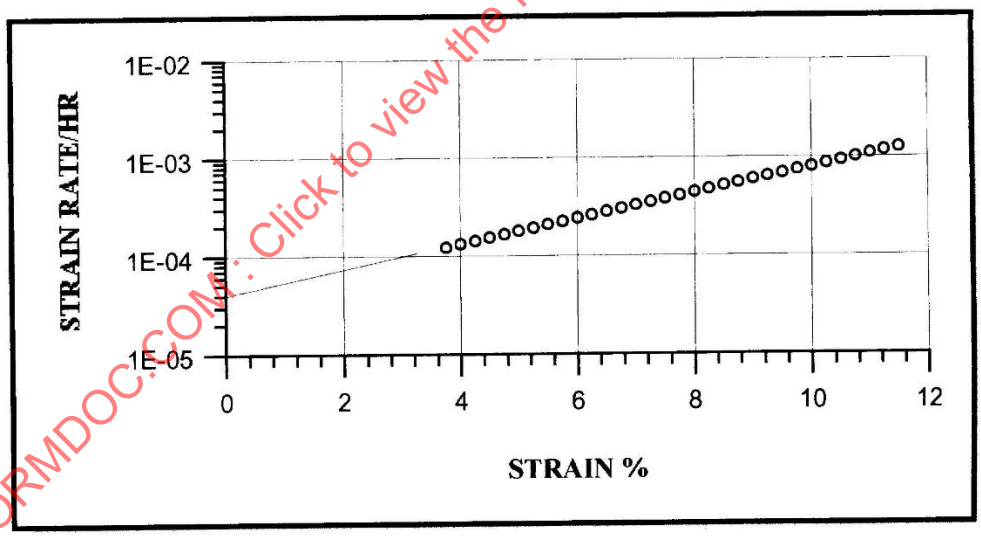

Figure 11. Illustration of the graphical determination of $\dot{\epsilon}_o$ from a partial creep curve.

413

.69) after 3% creep strain, then Ω_p is 23. The value of Ω_p is a direct indication of the concavity of the creep curve. While Ω_p is a function of stress, temperature and geometry (or stress state) a number of trends have emerged. Generally, Ω_p

(a) increases with decreasing stress
(b) increases with decreasing temperature
(c) increases with increasing multiaxiality
(d) is far less sensitive to stress and temperature than strain rate
(e) may be expressed parametrically, say in Larson-Miller or other form to arrive at the stress-temperature dependence as shown in Table 1 and Figure 12.

The initial creep rates used in the Omega method calculations are for given microstructural states (specific amount of damage). As such they might be expected to behave as thermally activated functions of stress and temperature and be amenable to Arrhenius-type (Larson-Miller) correlation with the reciprocal of temperature. The same is not necessarily true of minimum creep rates used in Norton's Law correlations or the coefficients in the Theta projection [18]. Minimum creep rates obtained with the Norton or Theta equations occur at varying amounts of strain (or damage) and the resulting variation in damage state would be expected to corrupt the observed temperature dependence and interfere with correlations of the Arrhenius or Larson-Miller types.

As a practical matter, a single specimen may be used to establish the uniaxial values of strain rate and Omega needed for life assessment. This is accomplished by strain measurements at the operating stress (usually assumed to be the effective stress) and at a temperature of 100 to 150°F (55 to 85°C) above the operating temperature. (For ferrous materials, if higher temperatures are required to measure significant strain rates during the test, it is unlikely there has been any damage in service.) After a small amount of strain is measured, usually only requiring a few hundred hours, stress or temperature may be increased slightly to obtain a creep plot with sufficient curvature to allow determination of Ω_p. While this is not the precise value of Ω_p for the initial conditions, the stress and temperature dependence of Ω_p are relatively small and the difference usually is not important. Creep rate and Omega may be obtained by curve matching rather than regression (Figures 13 and 14). The curve matching method is sufficiently accurate, more rapid, and requires less data. The values obtained are compared to MPC's database to establish whether the material is weak, strong, brittle, or otherwise unusual. The existing database for the material provides the needed function for extrapolation to operating temperature. This is done parametrically as described later. Then the life fraction, % damage, time to future strain, etc., may be calculated using formulas derived herein.

Special care must be exercised in the preparation and testing of creep specimens. Oxidation or lack of precision in measurement will invalidate the data. Special techniques have been developed to overcome these problems without resorting to inert testing atmospheres. While precautions may be taken against oxidation, they sometimes only delay or diminish the effect. Great care must be exercised in interpreting the data. Large specimens oriented in the circumferential stress direction are used to evaluate pipe and tubing (Figure 15)

Tests under moderately variable conditions of temperature and stress suggest that life fractions sum reasonably well (Figures 16 and 17). The rule for life summation under variable operating conditions is that strain rate acceleration results from the total sum of the products of strain and Omega at each condition. This is substantially the equivalent of Robinson's Rule of linear life fraction summation [19]. Over the *i* th interval

$$\epsilon_i = \frac{-1}{\Omega_i} \ln \left(1 - \dot{\epsilon}_{oi}\Omega_i t_i\right)$$

It can be shown that strain rate acceleration in each interval is

$$1/(1 - \dot{\epsilon}_{oi}\Omega_i t_i) \qquad (25)$$

and the product of such terms is the total acceleration. Damage is then simply related to strain rate and fractional remaining life (R.L.) is obviously

R. L. = 1/ (product of all acceleration factors)

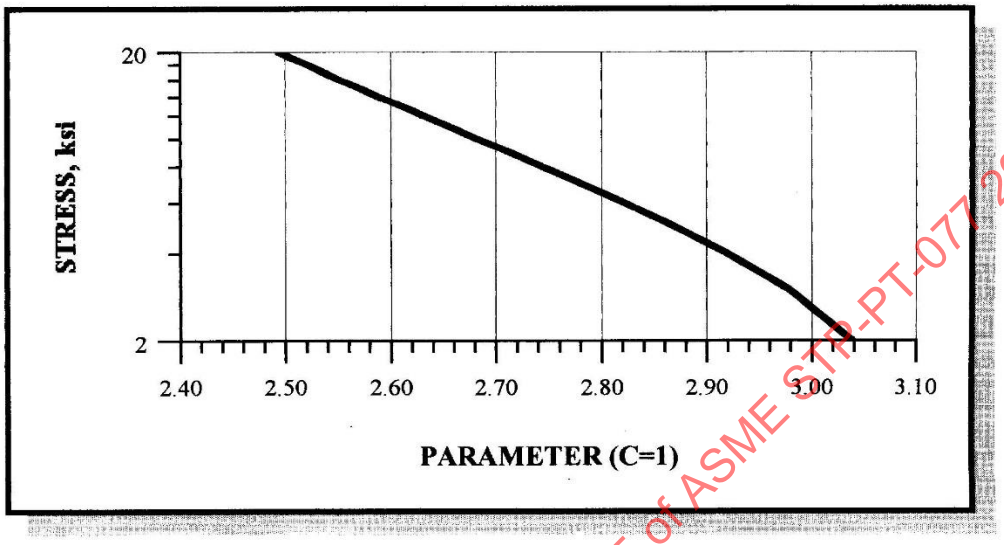

Figure 12. Parametric presentation of stress and temperature dependence of Omega values.

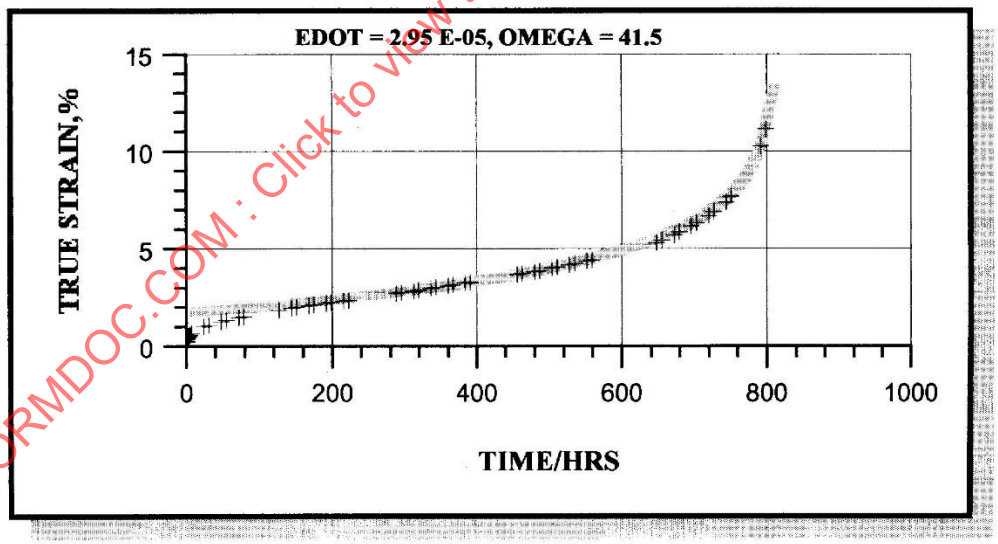

Figure 13. Determination of curve coefficients by matching shadowed curve to data.

415

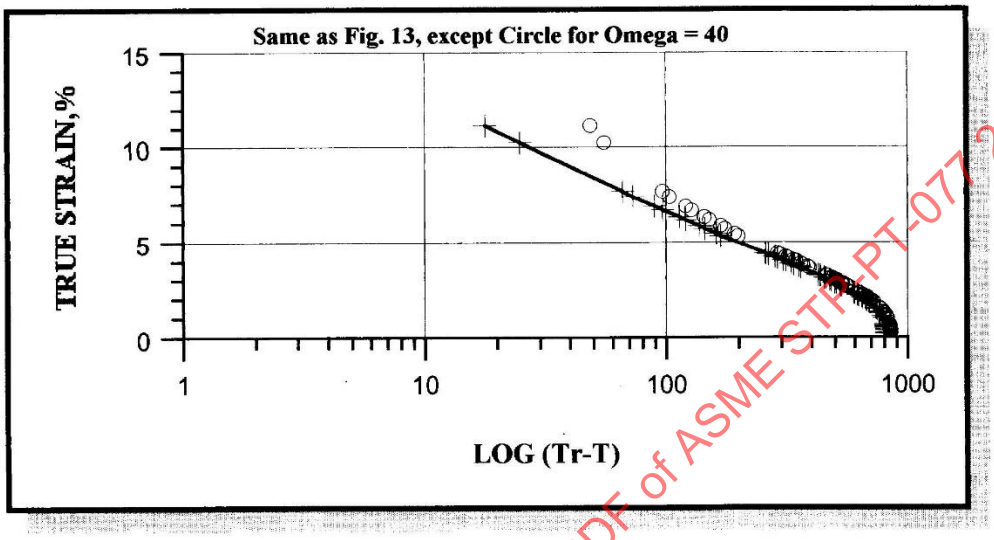

Figure 14. Illustration of sensitivity of curve fitting procedure to small variations in selected coefficients.

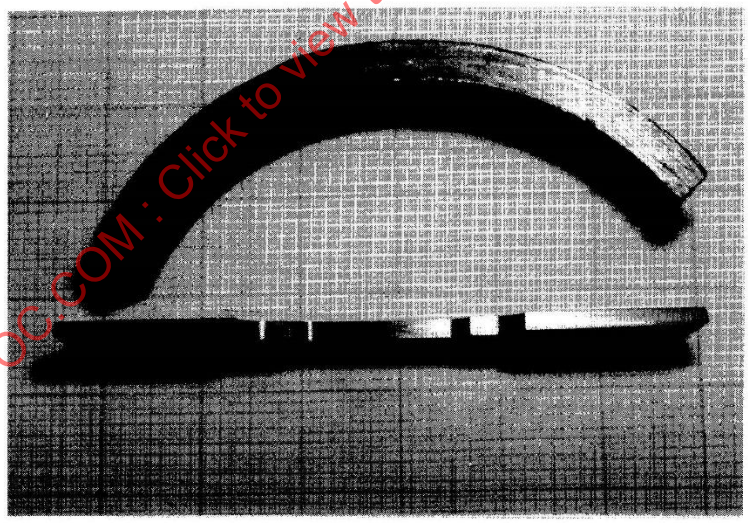

Figure 15. Flat specimen prepared from heater tube.

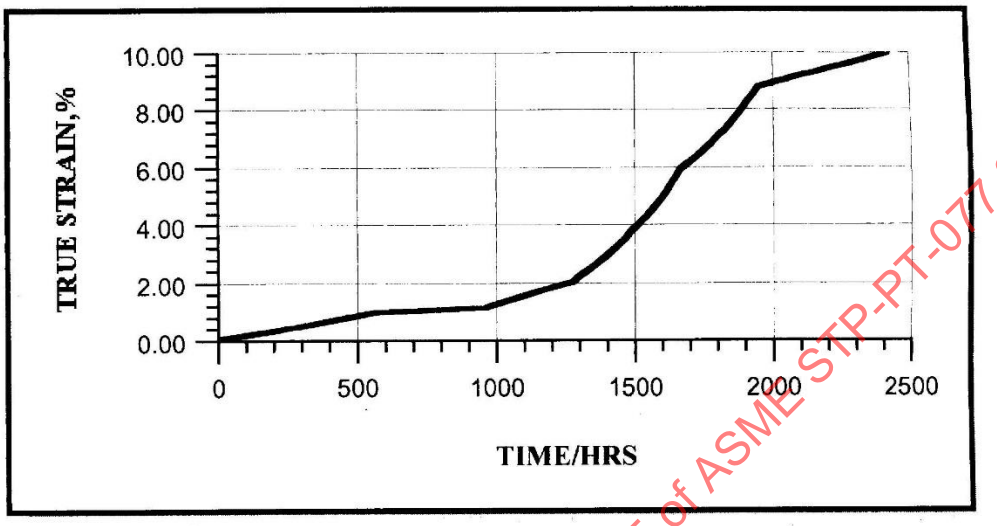

Figure 16. Creep strain observed under variable test conditions.

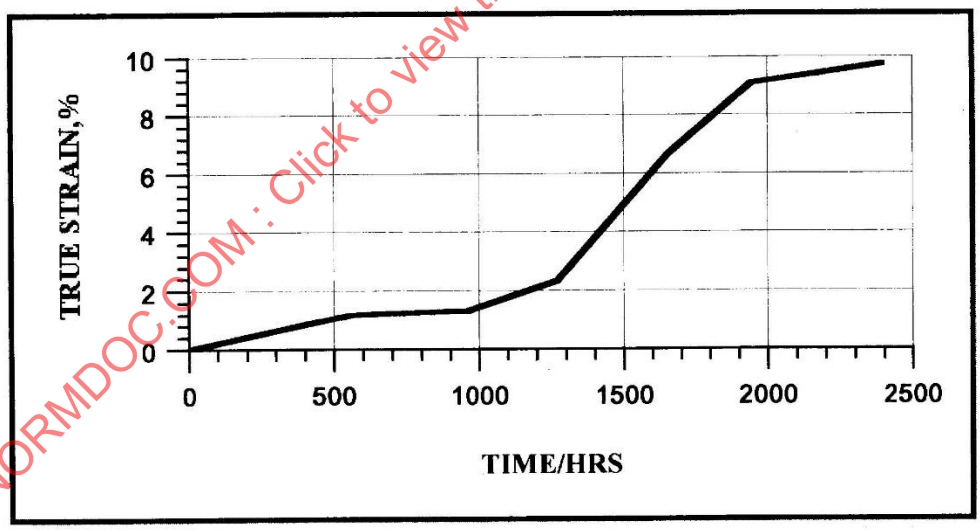

Figure 17. Predicted creep curves based on cumulative life summation rule for the test in Figure 16.

417

For example, if the strain rate is 4 x the initial value then the remaining life is only 25% of the total possible and the life fraction consumed is 75%. Based on these principles, it has been found possible to generate useful data under multiple conditions of stress and temperature with a single specimen. (Note: the sequence must be carefully chosen, stress increases only are allowed.) Curve fitting coefficients have been determined for each segment and creep rates for the undamaged condition at each stress/temperature combination extracted from the data.

The Omega method has led to a number of useful tools for life assessment and to insight into the nature of creep-rupture failure. The suitability of the method is readily verified by plotting strain rate versus strain (Figure 6) or strain versus the logarithm of remaining life (Log (t_r - t)) (Figure 7). The mathematical model described herein may be modified for other than uniaxial constant load stress-rupture testing, e.g., constant stress testing or tubular burst tests. In the case of the former, Omega is less than in the uniaxial case while in the latter is higher. The value of Omega also depends on many microstructural and hardness factors.

Considerable emphasis has been placed on strain rate. Thus, the effective stress which is thought to govern strain rate should be considered as a basis for testing. Inherent ductility is not to be ignored since in some cases it will limit life. For some materials, strain at fracture needs to be included in the life prediction equations enumerated above. It has been found that after only a small amount of strain it is possible to estimate with precision the path of the remainder of the creep curve. However, strain to fracture must be determined empirically, but it is not always critical for estimating test duration.

The concept of Omega as a material property draws attention to differences among materials in their response to creep. Some are highly strain tolerant and fail by plastic collapse after large strains while others lose load carrying capabilities after only small strains, possibly due to microstructural softening or cavitation. If a material is microstructurally unstable, due to precipitation, embrittlement or excessive softening, such behavior can be established from the creep curve [10]. Microstructural issues must be considered in choosing test temperatures and the advisability of applying stabilizing heat treatments prior to tests of virgin materials.

Omega appears to provide a guide to notch sensitivity of materials. Materials displaying high values, in excess of 50 to 100 may display notch sensitivity. Extensive studies of this capability are in progress and useful trends may be established.

DEVELOPMENT OF CONSTITUTIVE EQUATIONS

The need for constitutive equations for strain rate and Omega has stimulated material property data collection at component operating stress levels. While the usual variety of parametric relations have been employed to correlate data, the Larson-Miller parameter has been used mainly because of its compatibility with the concept of activation energy and because it predicts very long lives as temperatures approach the bottom of the creep range.

If we employ the simple relation

$$t_R = \frac{1}{\dot{\epsilon}\Omega_p}$$

then it should be obvious that

$$P_R = P_{(1/\dot{\epsilon})} - P_\Omega$$

where

P = a logarithmic parametric relation. When Larson-Miller parameters are used as all the parameters (not always necessary)

$$C_R = C_{(1/\dot{\epsilon})} - C_\Omega$$

where C is the optimized correlating constant in the logarithmic equation.

In other words, the correlating constant for strain-rate will differ from the value obtained for rupture by the constant which correlates the Omega coefficients. Values of the constants in the strain rate expressions for ferritic steels have been found to range from about 15 to 30 or more depending on alloy content (Figure 18). Since Omega has small temperature sensitivity the correlating constant is usually less than two (Figure 12). The reader is warned that correlating ferritic steel rupture data with